

DISENO SISMICO DE ESTRUCTURAS ESPECIALES

Del 28 de julio al 13 de agosto 1981

Fecha	Horario	Tema	Profesor
Martes 28 de julio	17 a 19 h	Torres y chimeneas	M. en C. Neftalí Rodríguez Cuevas
	19 a 21 h	Tanques	Prof. Arturo Arias Suárez
Jueves 30 de julio	17 a 19 h	Torres y chimeneas	M. en C. Neftalí Rodríguez Cuevas
		Tanques	Prof. Arturo Arias Suárez
Martes 4 de agosto	17 a 19 h	Puentes	Dr. Luis Esteva Maraboto
	19 a 21 h	Estructuras de concreto presforzado	Ing. José Luis Camba Castañeda
Jueves 6 de agosto	17 a 19 h	Puentes	M. en C. Enrique del Valle Calderón
	19 a 21 h	Estructuras de concreto presforzado	Ing. José Luis Camba Castañeda
Martes 11 de agosto	17 a 19 h	Estructuras tipo industrial	M. en C. Enrique Martínez Romero
	19 a 21 h	Tuberías	Dr. Francisco C. Aguilar López de N.
Jueves 13 de agosto	17 a 19 h	Estructuras tipo industrial	M. en C. Mauricio Nanes
	19 a 21 h	Instalaciones especiales	M. en C. Jorge Prince Alfaro



# DISEÑO SISMICO DE ESTRUCTURAS ESPECIALES

1981

## Directorio de Profesores

1. Dr. Francisco Cuauhtémoc Aguilar López de Nava  
Gerente de Ingeniería  
Instituto Mexicano del Petróleo  
Av. Lázaro Cárdenas 152  
México 14, D. F.  
567 82 02
2. Prof. Arturo Arias Suárez  
Investigador de tiempo completo  
Instituto de Ingeniería, UNAM  
Ciudad Universitaria  
México 20, D. F.  
550 52 15 ext. 3629
3. Ing. José Luis Camba Castañeda  
Ingeniero Consultor  
Ometusco 35 desp. 602  
Col. Condesa  
México 11, D. F.  
553 68 80
4. M. en C. Enrique del Valle Calderón  
Profesor titular de tiempo completo  
División de Estudios de Posgrado  
Facultad de Ingeniería, UNAM  
Ciudad Universitaria  
México 20, D. F.  
550 52 15 ext. 4479
5. Dr. Luis Esteva Maraboto  
Investigador de tiempo completo  
Instituto de Ingeniería, UNAM  
Ciudad Universitaria  
México 20, D. F.  
548 97 94
6. M. en C. Enrique Martínez Romero  
Ingeniero Consultor  
Nuevo León 54 - 201  
Col. Hipódromo Condesa  
553 85 68
7. M. en C. Mauricio Nanes  
Bufete Industrial, Diseños y Proyectos  
León Tolstoi 22 9º piso  
Col. Anzures  
México 5, D. F.  
533 15 00

8. M. en C. Jorge Prince Alfaro  
Investigador de tiempo completo  
Instituto de Ingeniería  
Ciudad Universitaria  
México 20, D. F.  
548 11 35
  
9. M. en C. Neftalí Rodríguez Cuevas  
Ingeniero Consultor  
Coordinación de Proyectos de Desarrollo  
de la Presidencia  
Protasio Tagle 95  
Col. Escandón  
México 18, D. F.  
543 96 38



DIVISION DE EDUCACION CONTINUA  
FACULTAD DE INGENIERIA U.N.A.M.

VII CURSO INTERNACIONAL DE INGENIERIA SISMICA

DISEÑO SISMICO DE ESTRUCTURAS ESPECIALES

TORRES Y CHIMENEAS

Profesor: M en I Neftalí Rodríguez Cuevas

Julio, 1981



1. Introducción

Las torres y chimeneas son estructuras esbeltas, de funciones múltiples, que se deben diseñar para soportar la acción de fuerzas horizontales, provocadas por viento o sismo; las cuales inducen efectos dinámicos en las estructuras de soporte.

En las figs. 1 a 5 se muestran algunos de los tipos comunes de torres y chimeneas construidas en diversas partes del mundo.

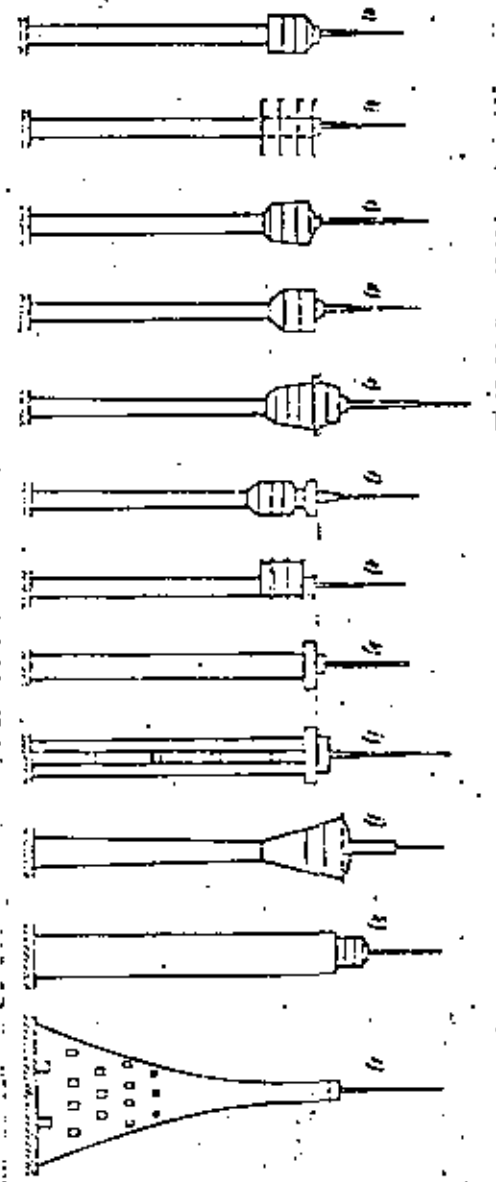
El análisis dinámico de estas estructuras requiere de algunos aspectos que no son comunes a otros tipos de estructuras, y en este trabajo se muestran las consideraciones comunes para su análisis.

2. Idealización para fines de análisis dinámico

Las estructuras de este tipo se idealizan comúnmente como vigas Bernoulli-Euler, y su análisis se realiza en base a la teoría elemental de flexión, la cual implica que las secciones transversales permanecen planas al deformarse bajo la acción de fuerzas normales a su eje medio. Se acepta que los esfuerzos son proporcionales a las deformaciones unitarias, con flexión en un solo plano. Se considera además, que los desplazamientos son pequeños y que la deformación en cortante es pequeña.

Se consideran solo los efectos de inercia provocados por la traslación normal al eje de elementos diferenciales de la viga. No se considera el efecto de la inercia rotacional, igual a  $-I \frac{\partial^3 v}{\partial x \partial t^2}$  por unidad de longitud, provocado

Fig. 1 Algunas tipos de torres construidas en diversas partes del mundo



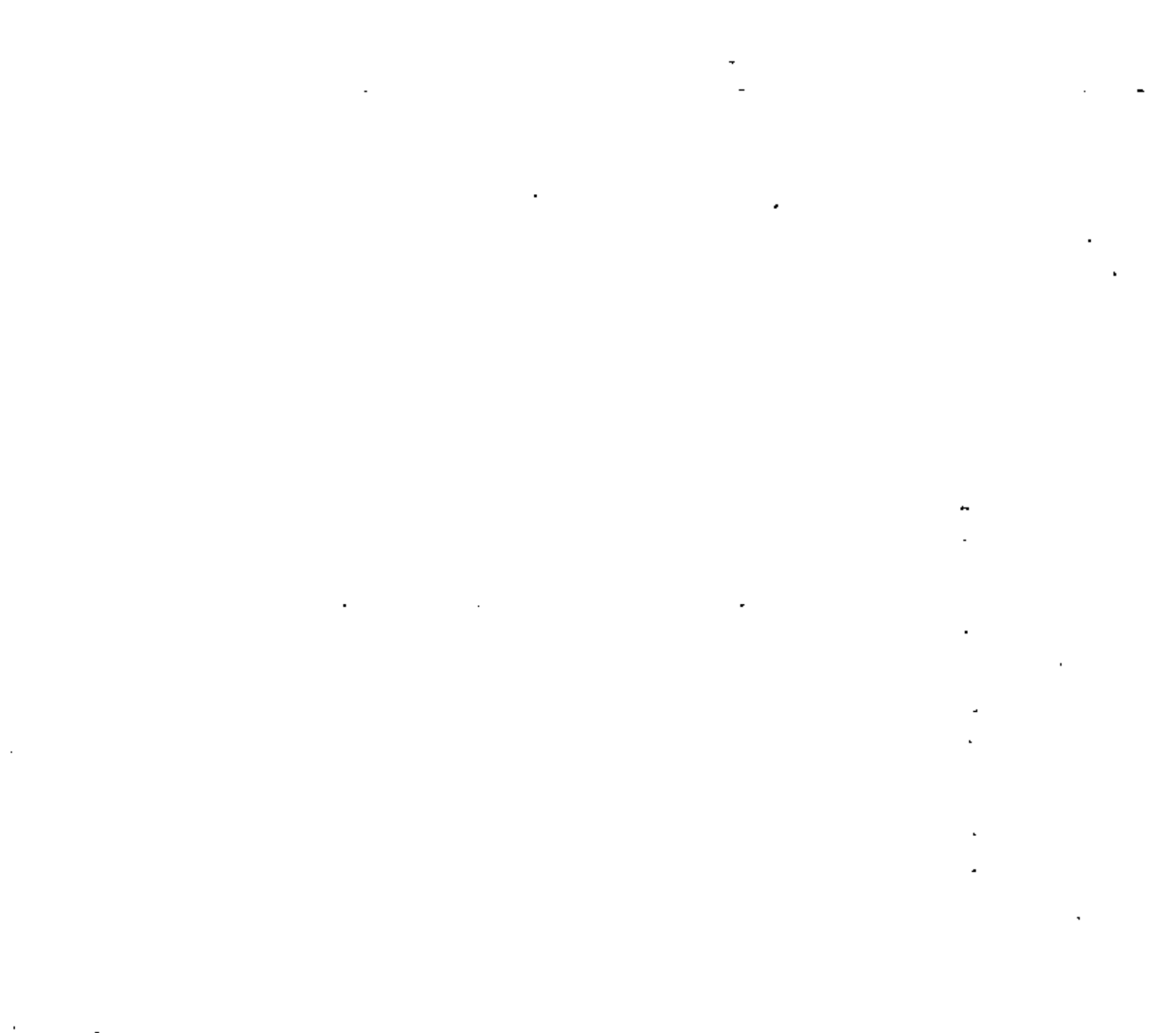


Fig. 3 Características principales de Chimeneas

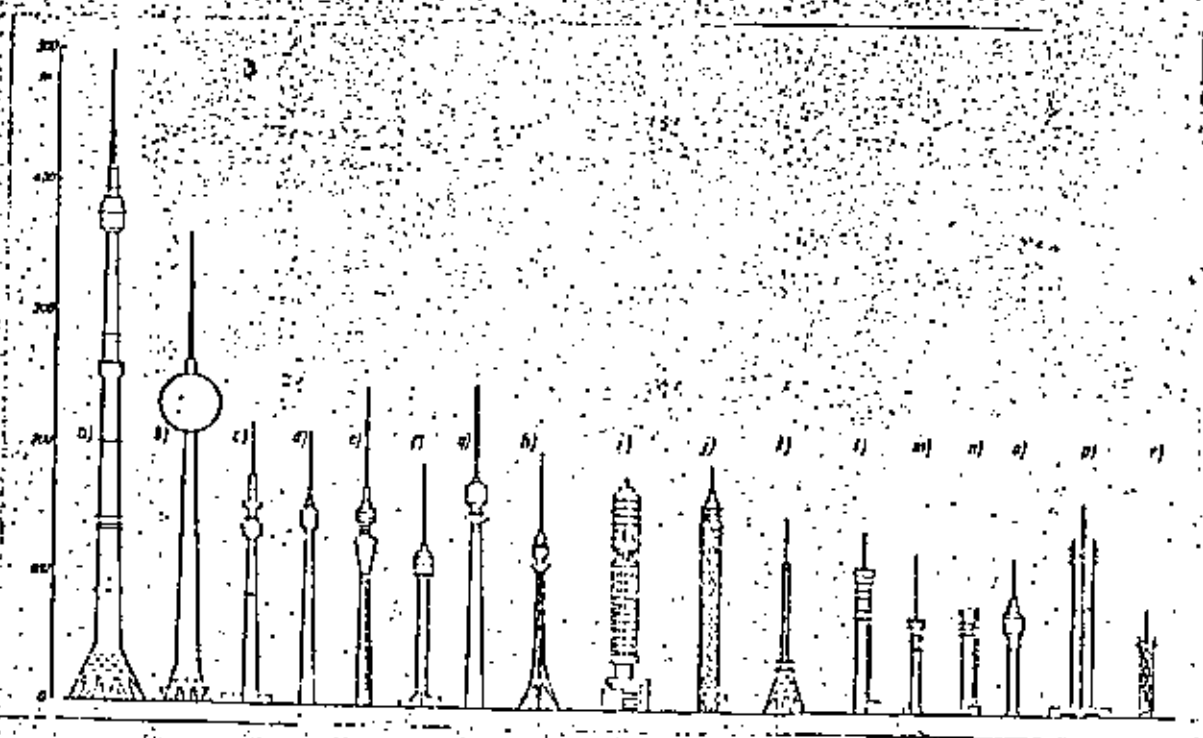
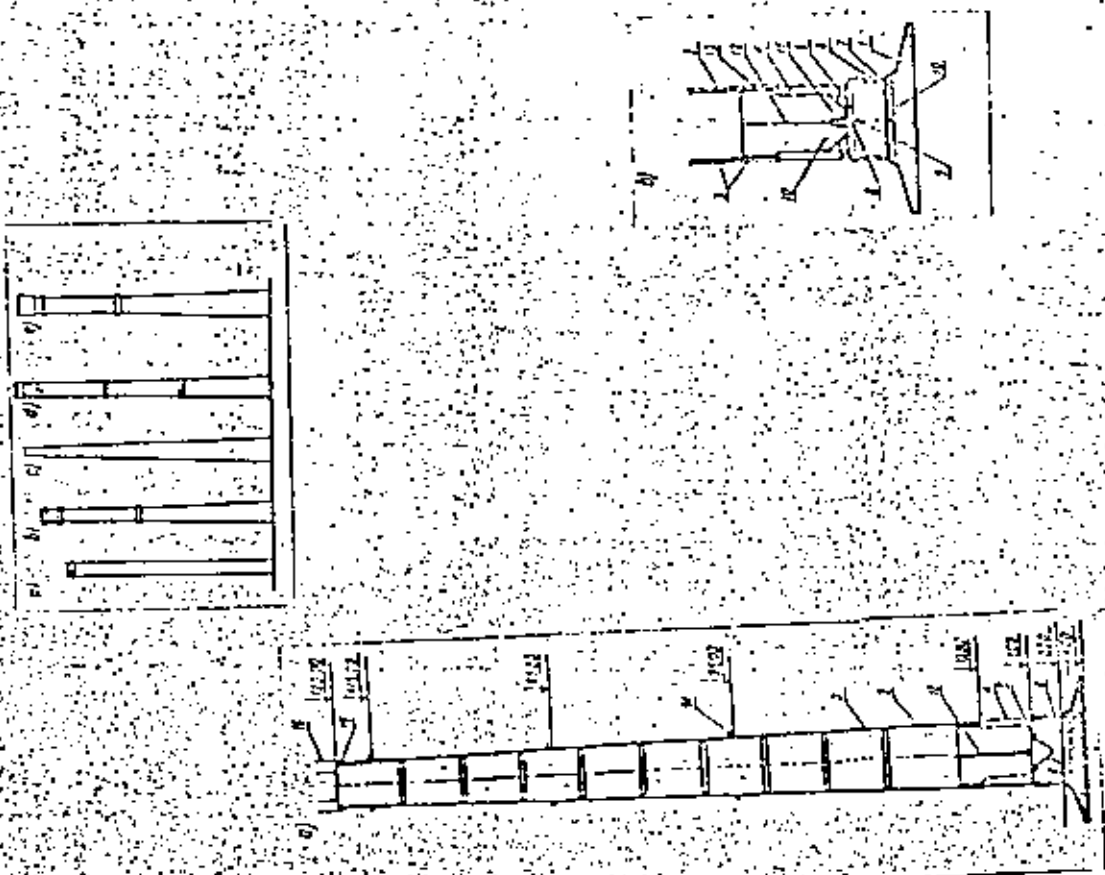


Fig. 2 Características geométricas de torres

- |              |                     |               |               |
|--------------|---------------------|---------------|---------------|
| a) Moscú     | e) Dresden          | i) Londres    | m) Petersberg |
| b) Berlín    | f) Dequeda          | j) Cairo      | n) Rhinow     |
| c) Dortmund  | g) Donauturm, Viena | k) Polonia    | o) Kulpenberg |
| d) Stuttgart | h) Belgrado         | l) Zippendorf | p) Estocolmo  |
|              |                     |               | r) Hannover   |





Fig. 5 Aspectos parciales de chimeneas y torres

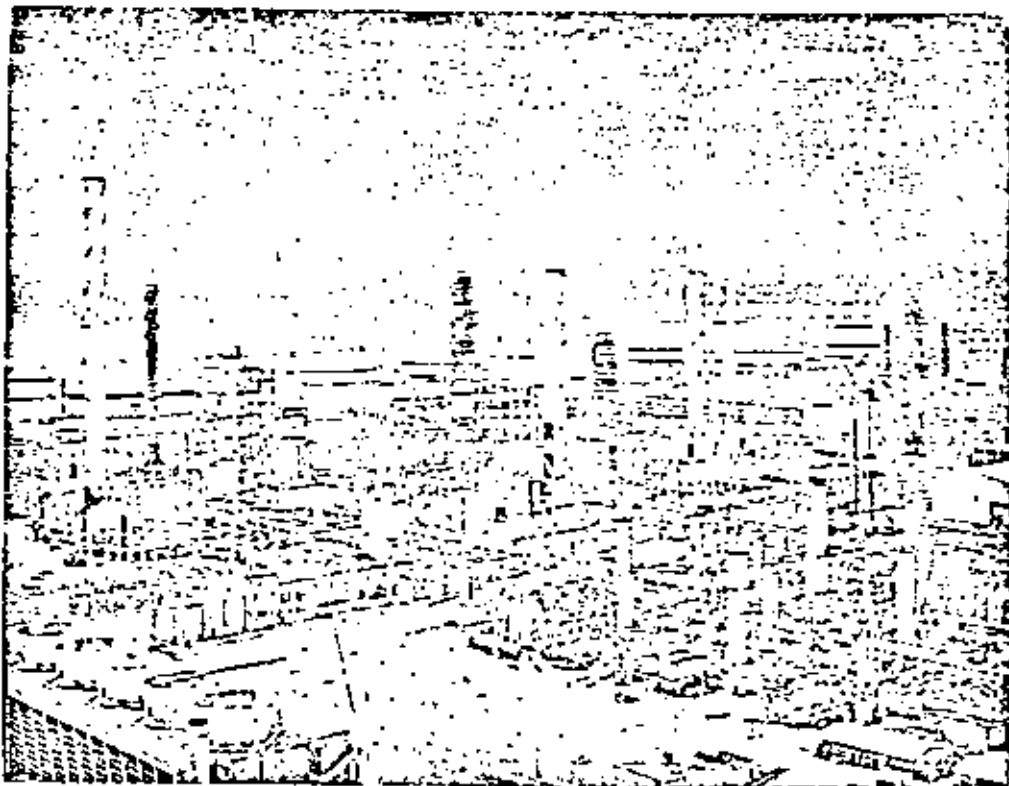
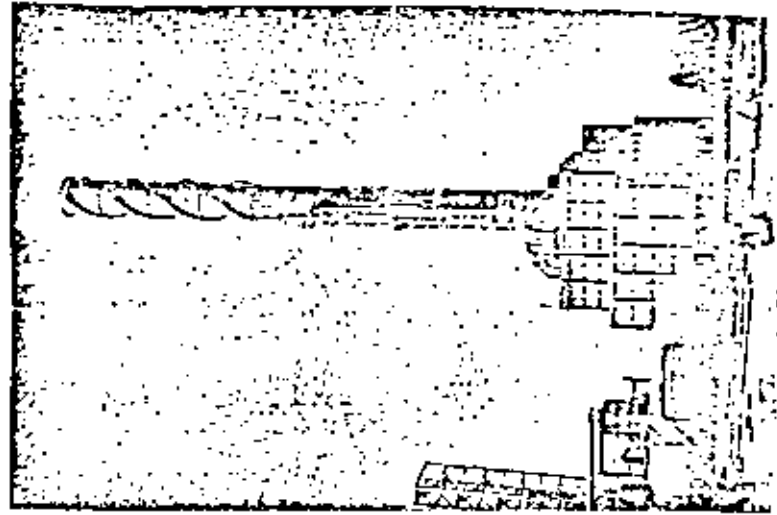
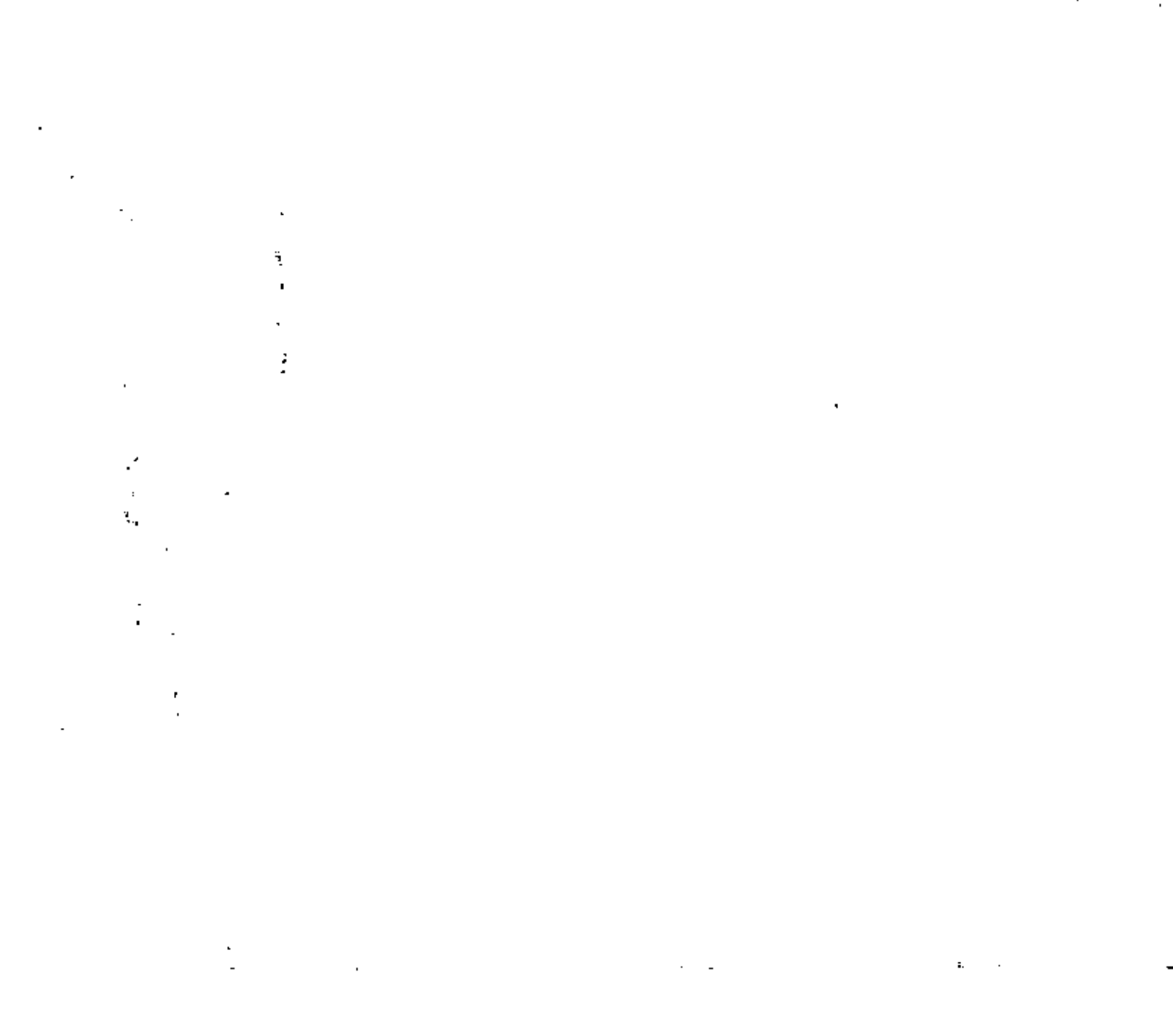


Fig. 4 Refinería en el norte del país, con torres y chimeneas



por el giro angular  $\frac{\partial v}{\partial x}$  de cada elemento, siendo  $v$  la translación normal al eje de la barra.

Cuando las dimensiones de la viga en su sección transversal no son pequeñas en comparación con su longitud, análisis que consideren los efectos de la fuerza cortante y la inercia rotacional se deben llevar a cabo.

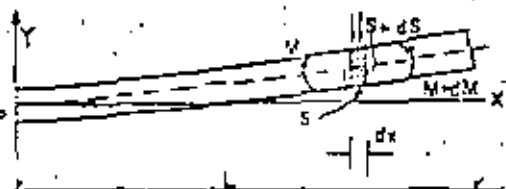
En este escrito se presentan los aspectos sobresalientes del análisis dinámico de este tipo de estructuras, presentando la influencia relativa de la fuerza cortante y la inercia rotacional, así como de la fuerza normal. Cuando se considera que estos efectos no son significativos, se realizan análisis dinámicos simplificados que permiten conocer los desplazamientos y elementos mecánicos que permiten a su vez, revisar el análisis de las características geométricas y del material que forma a estas estructuras.

### 3. Viga Bernoulli-Euler

Al considerar la viga BE, cuyas características se muestran en la fig. 6 sometida a la acción de efectos dinámicos, considérese que  $v = v(x, t)$  sea el desplazamiento transversal del eje neutro y  $\mu(x)$  la masa por unidad de longitud.

Los desplazamientos  $v(x, t)$  producidos por la carga  $p = p(x, t)$  son gobernados por la ecuación diferencial

$$\frac{\partial^2}{\partial x^2} \left( E I \frac{\partial^2 v}{\partial x^2} \right) = - \mu \frac{\partial^2 v}{\partial t^2} + p$$



(3.1)

FIG. 6

Cuando se generan vibraciones libres, es decir  $p = 0$ , aparecen modos normales de vibrar del tipo

$$v(x, t) = \phi(x) \sin(\omega t + \epsilon) \quad (3.2)$$

que al ser sustituidos en (3.1) conducen a la siguiente ecuación diferencial

$$\frac{d^2}{dx^2} \left( E I \frac{d^2 \phi}{dx^2} \right) = \omega^2 \mu \phi \quad (3.3)$$

Esta ecuación, junto con las condiciones de frontera de la viga, constituyen un problema de valores característicos, cuya solución conduce al conocimiento de las frecuencias naturales de cada uno de los  $i$ -ésimos modos de vibrar y a la definición de sus formas características.

Vibraciones libres en piezas de sección constante.

Cuando  $E I = \text{cte.}$  la ecuación 3.3. admite la solución general

$$\phi(x) = C_1 \operatorname{ch} \left( \frac{\lambda x}{L} \right) + C_2 \operatorname{sh} \left( \frac{\lambda x}{L} \right) + C_3 \cos \left( \frac{\lambda x}{L} \right) + C_4 \operatorname{sen} \left( \frac{\lambda x}{L} \right) \quad (3.4)$$

donde

$$\lambda = L \sqrt[4]{\mu \omega^2 / E I}$$

Para torres y chimeneas, las condiciones de frontera resultan ser

$$\phi(0) = \phi'(0) = \phi''(L) = \phi'''(L) = 0$$

a partir de las cuales se obtiene la ecuación característica de frecuencias

$$\cos \lambda \operatorname{ch} \lambda + 1 = 0 \quad (3.5)$$

cuyas raíces resultan ser:

$$\lambda_1 = 1.8751, \quad \lambda_2 = 4.6941, \quad \lambda_3 = 7.8548, \quad \lambda_4 = 10.9955$$

y para valores grandes de  $n$

$$\lambda_n = (2n-1) \pi/4 \quad (3.6)$$

con las formas modales correspondientes

$$\phi(x) = \text{Ch}\left(\frac{\lambda_n x}{L}\right) - \text{Cos}\left(\frac{\lambda_n x}{L}\right) - \frac{\text{Ch}\lambda_n + \text{Cos}\lambda_n}{\text{Sh}\lambda_n + \text{sen}\lambda_n} \left[ \text{Sh}\left(\frac{\lambda_n x}{L}\right) - \text{Sen}\left(\frac{\lambda_n x}{L}\right) \right] \quad (3.7)$$

Las frecuencias naturales resultan ser:

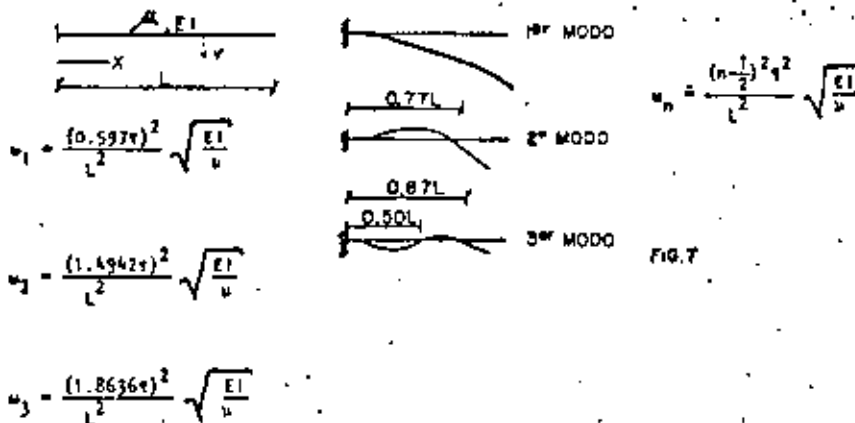


FIG. 7

a partir de los valores anteriores, se definen los períodos correspondientes mediante  $T_n = 2\pi/\omega_n$

Las formas características deben ser funciones que satisfacen las siguientes condiciones de ortogonalidad.

$$\int_0^L v \phi_n \phi_m dx = 0 \quad \text{si } m \neq n$$

$$= \omega_n \quad \text{si } m = n$$

$$\int_0^L EI \phi_n'' \phi_m'' dx = 0 \quad \text{si } m \neq n$$

$$= \omega_n^2 \quad \text{si } m = n$$

(3.8)

donde  $\int_0^L v \phi_n^2 dx = \omega_n$

Vibraciones forzadas sin amortiguamiento

Cuando se considera a la viga sometida a un sistema excitador definido por una carga distribuida  $p = p(x,t)$  y a una ó más fuerzas concentradas  $P_i$  a distancias  $x_i$  del apoyo, la ecuación de Lagrange conduce a la expresión

$$v(x,t) = \sum_{n=1}^{\infty} \phi_n(x) \left[ A_n \text{Cos } \omega_n t + B_n \text{sen } \omega_n t + \frac{1}{\omega_n} \int_0^t Q_n(\tau) \text{sen } \omega_n(t-\tau) d\tau \right] \quad (3.9)$$

donde  $Q_n$  es la fuerza generalizada definida por

$$Q_n(t) = \int_0^L p(x,t) \phi_n(x) dx + \sum_i P_i(t) \phi_n(x_i) \quad (3.10)$$

y los valores de  $A_n$  y  $B_n$  quedan definidos por:

$$A_n = \frac{1}{\omega_n} \int_0^L v_0 \phi_n dx$$

$$B_n = \frac{1}{\omega_n} \int_0^L \dot{v}_0 \phi_n dx$$

(3.11)

Vibraciones forzadas con amortiguamiento

Cuando en la viga (BE) existe una fuerza de amortiguamiento distribuida, igual a  $C(x) \dot{v}$ , donde  $C(x)$  es un coeficiente de amortiguamiento viscoso, variable en  $x$ , definido como  $C(x) = \beta u(x)$  donde  $\beta$  es una constante positiva, el desplazamiento normal  $v$  queda descrito por:

$$v(x,t) = \sum_{n=1}^{\infty} \phi_n(x) \left[ e^{-\frac{\beta t}{2}} (A_n \cos p_n t + B_n \sin p_n t) + \frac{1}{m_n p} \int_0^t Q_n(\tau) e^{-\frac{\beta}{2}(t-\tau)} \sin p_n(t-\tau) d\tau \right] \quad (3.12)$$

donde

$$p_n = \sqrt{\omega_n^2 - \left(\frac{\beta}{2}\right)^2}$$

y

$$A_n = \frac{1}{m_n} \int_0^L v_0 \phi_n dx \quad B_n = \frac{1}{m_n p} \int_0^L \dot{v}_0 \phi_n dx + \frac{\beta A_n}{2 p}$$

4. Influencia de las condiciones de cimentación

En torres y chimeneas las condiciones de cimentación son importantes en su comportamiento bajo la acción dinámica de fuerzas horizontales.

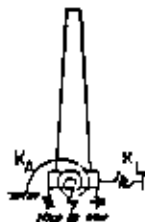


FIG 8

Las propiedades del terreno y el tipo de cimentación seleccionado influyen de manera importante en el análisis dinámico de estas estructuras. Al considerar resortes que definen la acción del suelo sobre la chimenea,

estos alteran los períodos naturales de la estructura y la forma de los modos de vibrar.

La ecuación característica se transforma en

$$\left[ \left( \frac{x^2}{j} - \frac{1}{j} \right) \text{sen } x \text{ Ch } x + x \right] \frac{x^2}{j} + \frac{1}{j} [\cos x \text{ Sh } x - 1] \frac{x^4}{j} + 1 [\cos x \text{ Ch } x + \left( \frac{x^4}{j} - 1 \right)] = 0$$

(4.1)

donde

$$j = \frac{K_L}{EI/L^3}$$

$$l = \frac{K_A}{EI/L}$$

$K_L$  rigidez del resorte horizontal

$K_A$  rigidez angular del resorte que restringe el giro de la cimentación.

$$x = \omega L$$

$\omega$  frecuencia del primero modo

La frecuencia natural de la estructura puede ser escrita como

$$\omega_1 = \frac{A_1}{L^2} \sqrt{\frac{EI}{\mu}} \quad (4.2)$$

Los valores de  $A_1$  dependen de las características de los resortes  $K_A$  y  $K_L$ .

Para estimarlos se puede recurrir a los diagramas siguientes; (ref. 1)

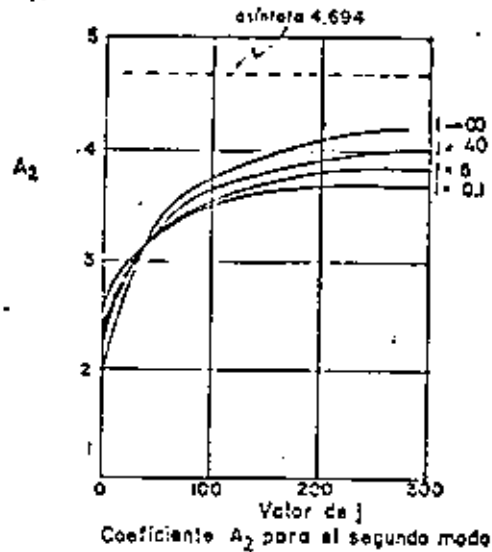
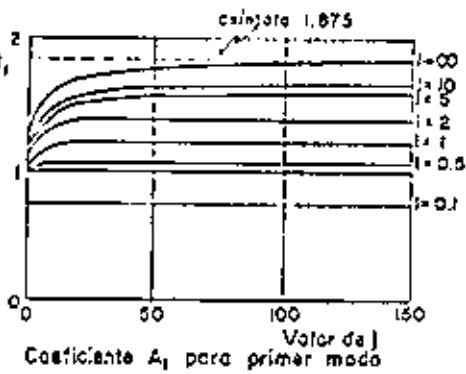


FIG 9

El análisis de este tipo de resultados ha permitido establecer las siguientes condiciones para los análisis dinámicos :

- a) Cuando  $i$  y  $j$  son superiores a 10, para el análisis dinámico se puede recurrir al planteamiento del capítulo 3, a fin de estimar períodos formas características y respuesta dinámica, considerando empotrada la estructura.
- b) Cuando  $0.1 < i < 10$  y  $1 < j < 10$  se deberá considerar la interacción suelo-estructura a fin de efectuar el análisis dinámico.
- c) Si  $i < 0.1$  y  $j < 1$ , se recomienda revisar las condiciones de cimentación para alcanzar valores comprendidos en el inciso a) ó b).

Esta última limitación se debe a que la carga crítica vertical de la estructura es sensible a la rigidez de los resortes  $K_A$  y  $K_L$ ; cuando existe  $K_L \neq 0$  y  $K_A$  resulta inferior a:

$$(K_A)_{crit} = \sqrt{PEI} \tan \sqrt{\frac{PL^2}{EI}} \tag{4.3}$$

donde  $P$  es la carga vertical, la viga BE se vuelve inestable. Así si se establecen las condiciones c) la estructura resulta inestable y tiende a producir desplazamientos grandes al generarse la acción de fuerzas horizontales. Las fuerzas horizontales, al actuar en la sección transversal, y modificar la rigidez, alteran también las frecuencias y modos de la estructura. Para estimar este efecto se utiliza la expresión

$$\omega_p = \frac{A^2}{L^2} \sqrt{\frac{EI}{\mu}} \sqrt{1 - \frac{PL^2}{D^2 EI}} \tag{4.4}$$

donde  $\omega_p$  frecuencia modificada por la fuerza axial  $P$ , coeficiente obtenido la siguiente gráfica.

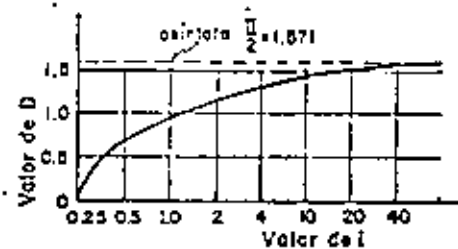


FIG 10

La fuerza axial  $P$  queda definida por el peso por unidad de longitud de la viga (BE), multiplicado por la altura  $L$  de la estructura.

En adición a los análisis previos, se debe revisar la estabilidad contra momento de volteo  $M_v$ , calculado a nivel de la cara inferior de la losa inferior de la subestructura.

En cimentaciones por amplificación de base, en las cuales  $d$  es el diámetro exterior medio de la subestructura, es recomendable lograr que:

a) En suelos con capacidad inferior a  $50 \text{ Kg/cm}^2$

$$M_v \leq 0.3 P_d \text{ para zapata circular u octagonal}$$

$$M_v \leq \text{el menor de } 0.3 \left(1 + \frac{d_2^2}{d_1^2}\right) P_d \text{ ó } 0.375 P_d \text{ para zapatas anulares,}$$

donde  $d_1$  es el diámetro exterior y  $d_2$  el diámetro interior.

b) En suelos con capacidad superior a  $50 \text{ Kg/cm}^2$

$$M_v \leq 0.375 P_d$$

Cuando en la cimentación se recurre a pilotes se buscará evitar la aparición de tensiones en los pilotes, a menos de que se justifique el anclaje adecuado del pilote a la subestructura, y que el refuerzo sea suficiente.

Es recomendable en este último tipo de cimentación que la distribución de pilotes sea óptima a fin de soportar el momento de volteo, considerando la interacción entre los pilotes que forman a la cimentación. Análisis de grupos de pilotes, mediante algoritmos numéricos, debe efectuarse para verificar que las sobrecargas producidas por fuerzas horizontales sean soportadas sin daño, ni pérdida de capacidad.

### 5. Efecto del cortante y la inercia rotacional

El análisis clásico de (BE) es inadecuado para aquellas vigas en las cuales sus dimensiones de la sección transversal sean grandes. Rayleigh (ref. 2) introdujo el efecto de inercia rotacional y Timoshenko (ref. 3 y 4) considerará, en adición, el efecto de la distorsión producida por cortante.

Las ecuaciones acopladas para el desplazamiento total  $v$ , y la pendiente producida por flexión  $\theta$ , desarrolladas por Timoshenko son:

$$EI \frac{\partial^2 \theta}{\partial x^2} + k \left( \frac{\partial v}{\partial x} - \theta \right) AG - \frac{\gamma}{g} \frac{\partial^2 v}{\partial t^2} = 0 \quad (5.1)$$

$$\frac{\gamma A}{g} \frac{\partial^2 v}{\partial t^2} - k \left( \frac{\partial^2 v}{\partial x^2} - \frac{\partial \theta}{\partial x} \right) AG = 0$$

Huang (ref. 5) desacopló las expresiones anteriores, obteniendo

$$EI \frac{\partial^4 v}{\partial x^4} + \frac{\gamma A}{g} \frac{\partial^2 v}{\partial t^2} - \left( \frac{\gamma I}{g} + \frac{EI}{gk} \frac{\gamma}{C} \right) \frac{\partial^4 v}{\partial x^2 \partial t^2} + \frac{\gamma I}{g} \frac{\gamma}{gkC} \frac{\partial^4 v}{\partial t^4} = 0$$

$$EI \frac{\partial^4 \theta}{\partial x^4} + \frac{\gamma A}{g} \frac{\partial^2 \theta}{\partial t^2} - \left( \frac{\gamma I}{g} + \frac{EI}{gk} \frac{\gamma}{C} \right) \frac{\partial^4 \theta}{\partial x^2 \partial t^2} + \frac{\gamma I}{g} \frac{\gamma}{gkC} \frac{\partial^4 \theta}{\partial t^4} = 0 \quad (5.2)$$

donde:

- E módulo de elasticidad
- C módulo de rigidez al cortante
- I momento de inercia de la sección transversal
- A área de la sección transversal
- $\gamma$  peso por unidad de volumen
- k constante del factor de forma de la sección
- g aceleración de la gravedad

Haciendo  $v = T e^{i p t}$   $T, \phi$  formas modales  
 $\phi = \phi e^{i p t}$   $p$  frecuencia angular  
 $\zeta = \kappa / \zeta$   $\kappa = \sqrt{-1}$

Las ecuaciones (5.2) se transforman en:

$$\frac{\partial^4 \zeta}{\partial (\frac{z}{L})^4} + b^2 (r^2 + s^2) \frac{\partial^2 \zeta}{\partial (\frac{z}{L})^2} - b^2 (1 - b^2 r^2 s^2) \zeta = 0$$

$$\frac{\partial^4 \phi}{\partial (\frac{z}{L})^4} + b^2 (r^2 + s^2) \frac{\partial^2 \phi}{\partial (\frac{z}{L})^2} - b^2 (1 - b^2 r^2 s^2) \phi = 0$$

donde  $b^2 = \frac{1}{EI} \frac{\nu A}{g} L^4 p^2$ ;  $r^2 = \frac{1}{AL}$ ;  $s^2 = \frac{EI}{\kappa A g L^2}$

A partir de estas expresiones y al considerar las condiciones de frontera siguientes:

para  $\zeta = 0$   $T(0) = 0$ ,  $\phi(0) = 0$

$\zeta = 1$   $\frac{1}{L} T'(1) = \phi(1) = 0$ ,  $\phi'(1) = 0$

Se obtiene la ecuación característica

$$2 + [b^2 (r^2 + s^2) + 2] \operatorname{Ch} b \zeta \cos b \theta - \frac{b(r^2 + s^2)}{\sqrt{1 - b^2 r^2 s^2}} \operatorname{Sh} b \zeta \operatorname{sen} b \theta = 0$$

donde  $b = \frac{1}{\sqrt{2}} \sqrt{-2(r^2 + s^2) + \sqrt{(r^2 - s^2)^2 + \frac{4}{b^2}}}$  (5.4)

Las formas características de los modos correspondientes quedan descritas

por:

$$\begin{aligned} T &= C [\operatorname{Ch} b \zeta - 1 \cos b \theta - \operatorname{Sh} b \zeta + \operatorname{sen} b \theta] + D [\operatorname{Ch} b \zeta + 1 \cos b \theta + \operatorname{Sh} b \zeta - \operatorname{sen} b \theta] \\ \phi &= H [\operatorname{Ch} b \zeta + \frac{b}{\sqrt{2}} \operatorname{Sh} b \zeta - \cos b \theta + \theta \operatorname{sen} b \theta] \end{aligned} \quad (5.5)$$

donde

$$C = \frac{\frac{1}{\sqrt{2}} \operatorname{Sh} b \zeta - \operatorname{sen} b \theta}{\operatorname{Ch} b \zeta + \cos b \theta} \quad D = \frac{\frac{1}{\sqrt{2}} \operatorname{Sh} b \zeta + \operatorname{sen} b \theta}{\operatorname{Ch} b \zeta + \cos b \theta}$$

$$H = \frac{b}{\sqrt{2}} \quad \zeta = \frac{\alpha^2 + \beta^2}{\alpha^2 - \beta^2} = \frac{\theta^2 - \gamma^2}{\theta^2 + \gamma^2}$$

A partir de los resultados previos se pueden obtener

1o El desplazamiento total  $v = \sum_{i=1}^{\infty} A_i T_i e^{\sqrt{-1} p_i t} + \phi_i$

2o La pendiente generada por flexión  $\phi = \sum_{i=1}^{\infty} \bar{A}_i \phi_i e^{\sqrt{-1} p_i t} + \zeta_i$

3o La pendiente producida por cortante  $\dot{\phi} = \frac{\partial \phi}{\partial \zeta} = \psi$

4o El momento flexionante  $M = -EI \frac{\partial^2 \zeta}{\partial z^2}$

5o La fuerza cortante  $Q = k \phi \zeta$

Las constantes  $A_i, \phi_i, \bar{A}_i, \zeta_i$  se valúan en términos de las condiciones iniciales de las vibraciones libres en estudio

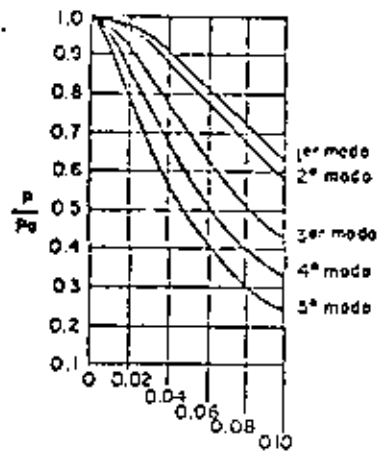


Fig. 11

Relación entre la frecuencia de la viga BE ( $P_0$ ) y la de Timoshenko ( $P$ )

Si  $r = 0.02$  se obtiene

Modo	Primero	Segundo	Tercero	Cuarto	Quinto	notación
$P/P_0$	0.985	0.975	0.930	0.883	0.835	$P$ frecuencia con cortante
% error	2	3	8	13	20	$P_0$ frecuencia (BE)

A fin de ilustrar el efecto de la inercia rotacional y el cortante, a continuación se muestran resultados obtenidos al aceptar

$$\frac{I}{kG} = 4 \quad s = 25 \text{ en piezas de acero } kG$$

en el cálculo de los cinco primeros modos

Por lo que respecta a la forma distorsionada de la estructura, en la figura siguiente se muestra el efecto de la inercia rotacional y el cortante.

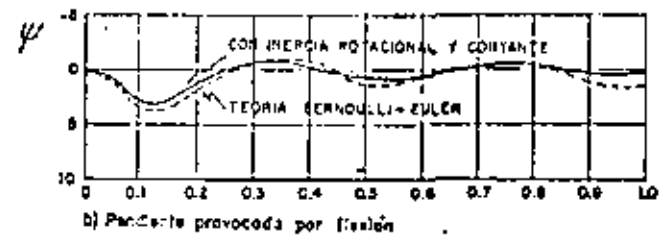
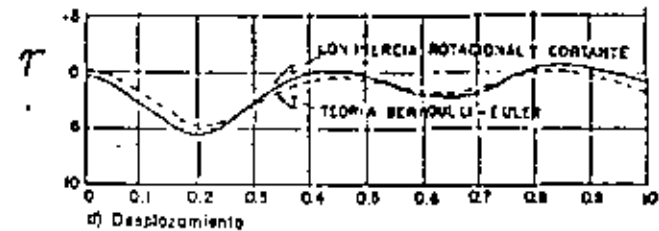


FIG. 12

Planteamientos recientes (ref. 6) en vigas donde se considera la aparición de amortiguamiento de un sólido viscoelástico muestran la posibilidad de incluir estos efectos en el análisis dinámico de estructuras esbeltas.

Influencia del cambio en momento de inercia

En ocasiones las chimeneas y torres se hacen con momento de inercia variable con la altura, ocasionado por el cambio en diámetro y espesor de la pared.

En este caso, el análisis dinámico parte de la ecuación diferencial (3.1), y mediante métodos numéricos se encuentra la solución al problema de definir las frecuencias y formas características

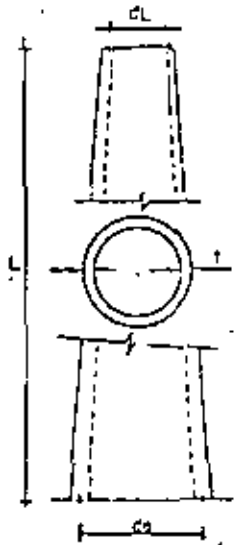
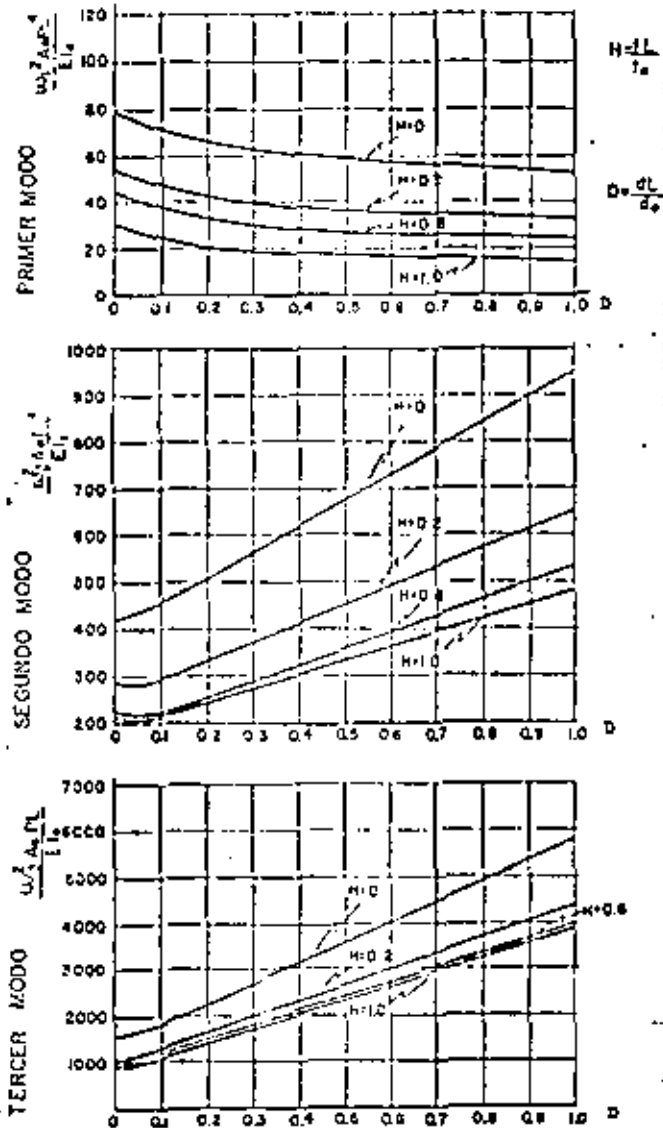


FIG 12  
Curvas para obtener las frecuencias naturales de los modos de vibrar



En la referencia 7 se proporcionan tablas de desplazamientos y sus primeras y segundas derivadas de las formas modales así como las frecuencias correspondientes. En la fig. 13 se condensan los resultados para estructuras cónicas truncadas de espesor linealmente variable, que permiten definir las frecuencias de los tres primeros modos de vibrar.

Para chimeneas con porción cilíndrica y cónica, usualmente se recurre a buscar una chimenea de diámetro constante,  $d_s$ , (igual a) de la porción cilíndrica y se usa una altura equivalente.

$$H_e = H_1 + H_2 \left( \frac{2d_s}{d_s + d_b} \right)^2 \quad (6.1)$$

donde

- $H_e$  altura equivalente
- $H_1$  altura del cono inferior
- $H_2$  altura del cilindro
- $d_s$  diámetro medio de la parte cilíndrica
- $d_b$  diámetro medio en la base de la chimenea

7. Influencia de la distribución de masa

En torres y chimeneas puede suceder que se presenten masas concentradas a lo largo del eje de la chimenea o torre. Esto puede alterar notablemente la idealización de la estructura y conducir a sistemas masa-resorte, en las cuales se acostumbra recurrir a métodos numéricos para resolver el problema de valores característicos. En la fig. 13 se muestra la idealización común de una chimenea con muros de aislamiento sobre ménsulas.

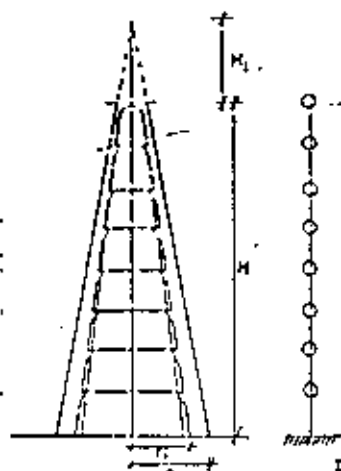


Fig. 13. Chimenea y su idealización en sistema de masas y resortes

$$C_1 = \frac{M_1}{H}$$

$$M = 9.8117 \frac{H^2}{a}$$

$$1.7691M$$

$$2.0560M$$

$$2.3636M$$

$$2.6918M$$

$$3.0407M$$

$$3.4103M$$

$$3.8005M$$

$$IM=20.132M$$

En estos estructuras el análisis se realiza considerando la masa del fuste, el muro de aislamientos y las ménsulas en la posición de estas últimas.

Los tramos de fuste, que funcionan como resortes equivalentes, presentan desplazamientos, rotaciones y momentos flexionantes y fuerzas cortantes que son descritos por las siguientes matrices de transferencia:

a) Vigas Bernoulli-Euler

$$\begin{pmatrix} -v \\ \gamma \\ M \\ T \end{pmatrix}_i = \begin{pmatrix} 0 & 1 & 0 & -\frac{1}{EA} \\ 0 & 0 & \frac{1}{EI} & 0 \\ 0 & -\rho a^2 \omega^2 & 0 & 1 \\ \rho a^2 \omega^2 & 0 & 0 & 0 \end{pmatrix} \begin{pmatrix} -v \\ \gamma \\ M \\ T \end{pmatrix}_{i-1} \quad (7.1)$$

donde

1, sección en la que se valúan los elementos mecánicos

v, γ, M, T desplazamiento, giro, momento y fuerza cortante

p radio de giro de la sección transversal

ω frecuencia circular de vibración

ρ masa por unidad de longitud

b) Vigas de Timoshenko sometidas a fuerza axial

$$\begin{pmatrix} -v \\ \gamma \\ M \\ T \end{pmatrix}_i = \begin{pmatrix} (C_1 - \sigma \tau) C_3 & (C_1 - \sigma \tau) C_3 & \sigma C_2 & \frac{\sigma^2}{\beta^2} [-\sigma C_3 + (\beta^2 + \sigma^2) C_3] \\ \frac{\beta^4}{I} C_3 & C_0 + \tau C_2 & \frac{\beta^2}{I} (C_1 - \tau C_2) & \sigma C_2 \\ \frac{\beta^4}{I} C_2 & \frac{1}{\beta} [-\tau C_1 + (\beta^2 + \tau^2) C_3] & C_2 - \tau C_2 & I [C_1 - (\sigma + \tau) C_3] \\ \frac{\beta^4}{I} (C_1 - \sigma C_2) & \frac{\beta^4}{I} C_2 & \frac{\beta^4}{I} C_3 & C_0 + \sigma C_2 \end{pmatrix} \begin{pmatrix} -v \\ \gamma \\ M \\ T \end{pmatrix}_{i-1}$$

donde

$$\beta = \frac{l^2}{EI} \quad C_0 = A [2 \lambda_2^2 \operatorname{Ch} \lambda_1 + \lambda_1^2 \operatorname{cosh} \lambda_2] \quad (7.2)$$

$$\beta^4 = \frac{\rho a^2 \omega^2}{EI} l^4 \quad C_1 = A \left[ \frac{\lambda_1^2}{\lambda_1} \operatorname{Sh} \lambda_1 + \frac{\lambda_2^2}{\lambda_2} \operatorname{sen} \lambda_2 \right]$$

$$\sigma = \frac{\rho a^2 \omega^2}{EA} l^2 \quad C_2 = A (\operatorname{Ch} \lambda_1 - \operatorname{cosh} \lambda_2)$$

$$\tau = \frac{\rho l^2}{EI} + \frac{\rho^2 a \omega^2}{EI} l^2 \quad C_3 = A \left( \frac{1}{\lambda_1} \operatorname{Sh} \lambda_1 - \frac{1}{\lambda_2} \operatorname{sen} \lambda_2 \right)$$

$$\lambda_1 = \sqrt{\beta^2 + \frac{1}{4} (\sigma - \tau)^2 + \frac{1}{2} (\sigma + \tau)} \quad \lambda_2 = \frac{1}{\lambda_1 + \lambda_2}$$

l es la longitud entre las secciones i y i-1

γ es la fuerza normal media en el tramo

E módulo de rigidez al esfuerzo cortante

A área de la sección transversal

Se observa que el cálculo de las constantes de resorte resulta muy laborioso, cuando se incluye el efecto de inercia rotacional, fuerza cortante y fuerza normal.

Conocidas las masas y las constantes de resorte se plantean las ecuaciones del movimiento reducidas y se obtienen los valores característicos y las formas modales correspondientes.

En la práctica es común recurrir al método de Newmark para valuar las constantes de resorte; para resolver la ecuación de frecuencias y obtener los modos naturales, se recurre a programas que resuelven el problema en ordenadores digitales. Así, para una chimenea de 80m de altura, cuya distribución de masas aparece en la fig. 3, se obtuvieron las frecuencias, períodos y factores de participación de modo que aparecen en la siguiente tabla

Modo	Frecuencia ( $\frac{rad}{seg}$ )	Período (seg)	Coefficiente de participación modo
1*	3.4756	1.807766	0.845940
2*	15.3280	0.409913	-0.028441
3*	38.2289	0.164356	-0.003048
4*	71.8242	0.087482	-0.000645
5*	115.7336	0.054287	+0.000196
6*	168.0762	0.037382	+0.000075
7*	225.5712	0.027854	+0.000035
8*	295.8683	0.021236	-0.000020

Se observa que la participación de los modos superiores es poco significativa en la respuesta, debido a la diferencia notable en los coeficientes de participación modal.

Por ello, en ocasiones para estimar el período del primer modo se recurre al método de Dunkerly en el cual

$$w_1 \approx \frac{1}{\sqrt{\sum_{i=1}^n m_i v_i^2}} \quad (7.3)$$

donde

$m_i$  es la  $i$ -ésima masa

$v_i$  es el desplazamiento de la chimenea, en la  $i$ -ésima masa, al ser sometida a la acción de su peso propio

Estudios en más de 40 chimeneas mostraron que el período natural del primer modo varía linealmente con la altura, una vez que se definen  $M$ ,  $r_0$  y  $C$ , obteniéndose valores comprendidos entre

$$0.003 M < T < 0.020 M \quad (7.4)$$

donde

$T$  período natural en seg.

$M$  altura de la chimenea, en m.

## 8. Consideraciones sobre análisis sísmico

La respuesta de torres y chimeneas es compleja con aspectos dinámicos importantes. Existen demasiadas incógnitas para predecir con certidumbre la respuesta de estas estructuras bajo la acción de sismos futuros.

Se tiene que depender en aspectos cualitativos, en los cuales el buen juicio debe estar presente y de análisis cuantitativos de respuesta en base a sismos registrados en el pasado.

Normalmente el ingeniero recurre a simplificaciones contenidas en reglamentos, como el del diseño en el Distrito Federal, o al SEAOC en los cuales se establecen espectros de diseño en base a los cuales se define la respuesta estructural.

En lo que va sigue se presenta un análisis simplificado y la secuencia de análisis dinámico comúnmente usada en nuestro medio.

Las torres y chimeneas se analizarán de manera independiente en dos direcciones ortogonales, y se verificará que las estructuras sean capaces de resistir cada una de estas condiciones por separado.

En la revisión se deberá buscar los desplazamientos, y elementos mecánicos en diversas secciones transversales, así como las aceleraciones que se presentan en los conos de aislamiento. Se revisarán además las condiciones de estabilidad de la cimentación, para ello se dispone de los siguientes procedimientos.

- Estático equivalente
- Dinámico espectral
- Dinámico bajo la acción de sismos registrados

El primer procedimiento basado en la experiencia obtenida al resolver decenas de chimeneas, es aplicable cuando la cimentación satisface las condiciones descritas en el cap. 4, cuando  $l$  y  $j$  son superiores a 10.

Para fines de diseño inicial, se aceptará la existencia de una carga estática que actúe lateralmente contra la chimenea, con una distribución bilineal definida a continuación:

- En la base, la fuerza será nula. Aumenta linealmente con la altura hasta  $0.3H$ , donde la carga será igual al 15% del valor máximo en la parte superior de la chimenea y es igual, a la altura  $0.3H$ , a  $0.35 C_M W/M$ , siendo  $C_M$  el coeficiente sísmico mínimo,  $W$ , el peso total de la chimenea sobre la cimentación y  $H$  la altura total de la chimenea.
- Desde  $0.3H$  hasta  $H$ , se aceptará otra variación lineal de la fuerza sísmica, con un valor máximo en la parte superior, igual a  $2.35 C_M W/M$ .

La distribución de fuerzas cortantes y momentos flexionantes, así como los desplazamientos horizontales, se estimarán en base a la distribución bilineal antes descrita.

El momento de volteo en la base de la chimenea resulta próximo a  $M_V = C_M W H / \sqrt{2.15}$

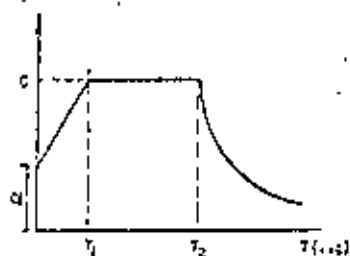
Cuando no exista mejor información, es posible estimar el valor de  $C_M$ , en base a la siguiente tabla, en la que aparecen las cuatro regiones sísmicas en las que se ha dividido el país.

Zona sísmica	A	B	C	D
Coefficiente $C_M$	0.03	0.06	0.09	0.18

El análisis dinámico espectral, considera a las estructuras como sistemas masas-resortes, en los cuales se aplican aceleraciones definidas por espectros de diseño. Este procedimiento es válido cuando las condiciones de cimentación tienen  $l$  y  $j$  mayores a 10, y considera tres tipos de suelos.

- Tipo I: Terreno firme, similar a conglomerados compactos, areniscas medianamente cementadas, o arcillas compactas.
- Tipo II: Suelos de baja rigidez, como arenas sin cementar, limos de mediana o alta compacidad o arcillas de mediana compacidad.
- Tipo III: Arcillas blandas muy compresibles

Los coeficientes de diseño sísmico se definen mediante espectros cuyas características se describen en la tabla siguiente.



Forma del espectro

Fig. 14

Zona Sísmica	Tipo de Suelo	C	$T_1$	$-T_1$	$\alpha$
A	I	0.10	0.40	0.60	0.05
	II	0.16	0.75	1.50	
	III	0.21	1.00	2.50	
B	I	0.21	0.40	0.60	0.10
	II	0.26	0.75	1.50	
	III	0.31	1.00	2.50	
C	I	0.31	0.30	0.50	0.15
	II	0.29	0.60	1.20	
	III	0.47	0.50	2.20	
D	I	0.62	0.20	0.40	0.30
	II	0.73	0.40	1.00	
	III	0.83	0.60	2.00	
			seg	seg.	

Se considera que las zonas del espectro, en cada intervalo, queda definida en forma por las expresiones:

$$c_0 = a + (c - a) \frac{T}{T_1}, \quad \text{si } T < T_1$$

$$c_0 = c \quad \text{si } T_1 < T < T_2$$

$$c_0 = c \left( \frac{T_2}{T} \right)^2 \quad \text{si } T > T_2$$

donde  $T$  es el período natural de alguno de los modos de vibración, en seg.

Ya que en estos espectros se han considerado efectos inelásticos, considerando una ductilidad definida por un factor de ductilidad  $Q = 2$ , solo los momentos flexionantes y fuerzas cortantes se dividirán entre 2 si  $T > T_1$ ,

6 entre  $1 + T/T_1$  en caso contrario.

Finalmente el procedimiento de análisis dinámico bajo la acción de sismos registrados es aconsejable para aquellas estructuras en las cuales debe considerarse la interacción suelo-estructura, como puede verse en la ref. 8.

### 9. Análisis dinámico simplificado

A fin de ilustrar la aplicación del procedimiento espectral simplificado, existe un programa elaborado en el Instituto de Ingeniería, USAM, que permite realizar el análisis dinámico modal de chimeneas, siguiendo la siguiente secuencia:

- Calcula el volumen de fuste y de las ménsulas y lo multiplica por la masa específica para definir la masa asociada a cada ménsula.
- Obtiene la masa de los conos de aislamiento y la agrega a la masa de la estructura en cada ménsula.
- Calcula la matriz de rigideces del sistema de resortes equivalentes, recurriendo al método de Newmark
- Resuelve el problema de valores característicos y define las frecuencias y modos naturales de vibración
- Obtiene la respuesta, a partir de un espectro de diseño, pudiendo seguir cualquiera de los siguientes criterios:

$$R_1 = \sqrt{\sum_{i=1}^n R_i^2} \quad R_2 = \left| \sum_{i=1}^n R_i \right| \quad R_3 = (R_1 + R_2)/2$$

- Calcula momentos flexionantes, fuerzas cortantes y desplazamientos y los grafica automáticamente.

A continuación se muestran los resultados obtenidos en el análisis dinámico modal de una chimenea de concreto de 80 m. de altura, de sección variable, con un radio exterior en la base de 4.625 m y un radio interior en la base igual a 4.125 m. Se considera  $H_1 = 202$  m para el cono exterior y 246.4 m en el cono interior. En el análisis se aceptó  $E = 2.51 \text{ T/m}^2$ ,  $\nu = 0.15$ ; un peso volumétrico del fuste de  $2.4 \text{ T/m}^3$  y una resistencia del concreto igual a  $2500 \text{ T/m}^2$ . Se dividió a la chimenea en 8 tramos de 10 m colocando muros aislantes con un peso de  $2.3 \text{ T/m}^3$  y en el recubrimiento exterior;  $2 \text{ T/m}^3$ . Para el mortero se consideró  $0.55 \text{ T/m}^3$ . El ancho del tubique refractario se consideró de 23 cm; el ancho del recubrimiento adicional de 0.065 m y 0.003 m de mortero. El análisis modal proporcionó los siguientes resultados:

Modo	Frecuencia	Período	Coefficientes de Participación Modal
1	5.4415	1.1547	+ 0.405973
2	25.9263	0.2423	+ 0.0112654
3	61.9485	0.1043	- 0.001378
4	97.8753	0.0842	+ 0.000450
5	116.2222	0.0550	- 0.000072
6	172.5721	0.0487	- 0.000043
7	149.9023	0.0419	- 0.000005
8	189.6007	0.0331	+ 0.0000001

Se seleccionó un espectro de diseño correspondiente a la zona 3, con un suelo tipo II, considerando un valor máximo de  $C = 0.730$  y se empleó un factor de ductilidad igual a 2.

Se hicieron análisis comparativos considerando la participación de 1 hasta 8 modos, y se calcularon las respuestas  $R_1$ ,  $R_2$  y  $R_3$ , las cuales aparecen en las siguientes tablas:

Desplazamientos máximos en las masas

Masa	En solo modo			Los modos		
	$R_1$	$R_2$	$R_3$	$R_1$	$R_2$	$R_3$
1	0.4327	0.4327	0.4327	0.4328	0.4446	0.4307
2	0.3518	0.3518	0.3518	0.7518	0.3568	0.3543
3	0.2723	0.2723	0.2723	0.2723	0.2732	0.2727
4	0.1974	0.1974	0.1974	0.1974	0.2017	0.1996
5	0.1307	0.1307	0.1307	0.1308	0.1361	0.1335
6	0.0755	0.0755	0.0755	0.0756	0.0805	0.0781
7	0.0343	0.0343	0.0343	0.0344	0.0376	0.0360
8	0.0089	0.0089	0.0089	0.0089	0.0100	0.0094

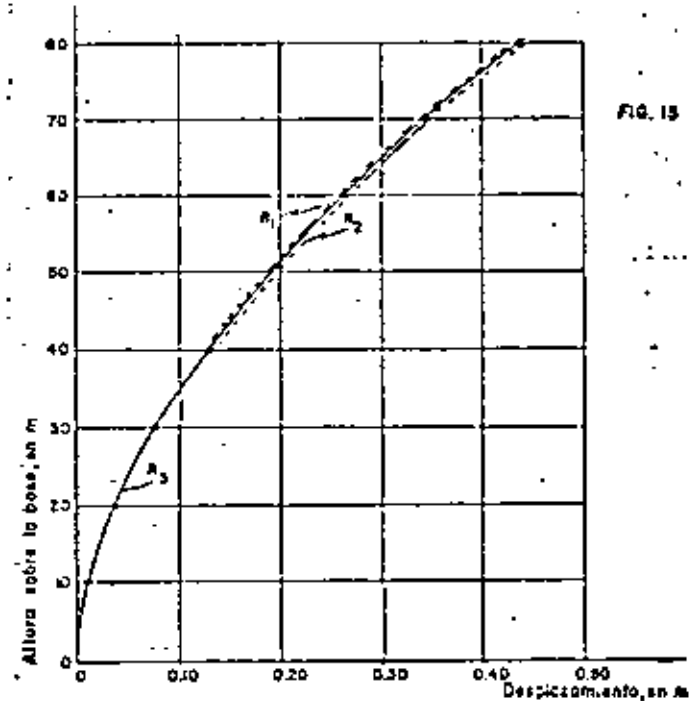


FIG. 15

Variación de los desplazamientos con la altura, con los tres tipos de respuesta.

Fig. 15

Momentos flexionantes en las masas

Masa	Un solo modo			Todos los modos		
	$R_1$	$R_2$	$R_3$	$R_1$	$R_2$	$R_3$
1	0	0	0	0	0	0
2	355.5	355.5	355.5	474.6	909.6	692.1
3	2042	2042	2042	2327	3718	3022
4	4884	4884	4884	5197	7051	6124
5	8660	8660	8660	8078	10960	9319
6	13120	13120	13120	11200	15120	14160
7	18020	18020	18020	15070	20870	18450
8	23130	23130	23130	21200	28220	24230
BASE	28300	28300	28300	28560	33500	31030

En ton-m

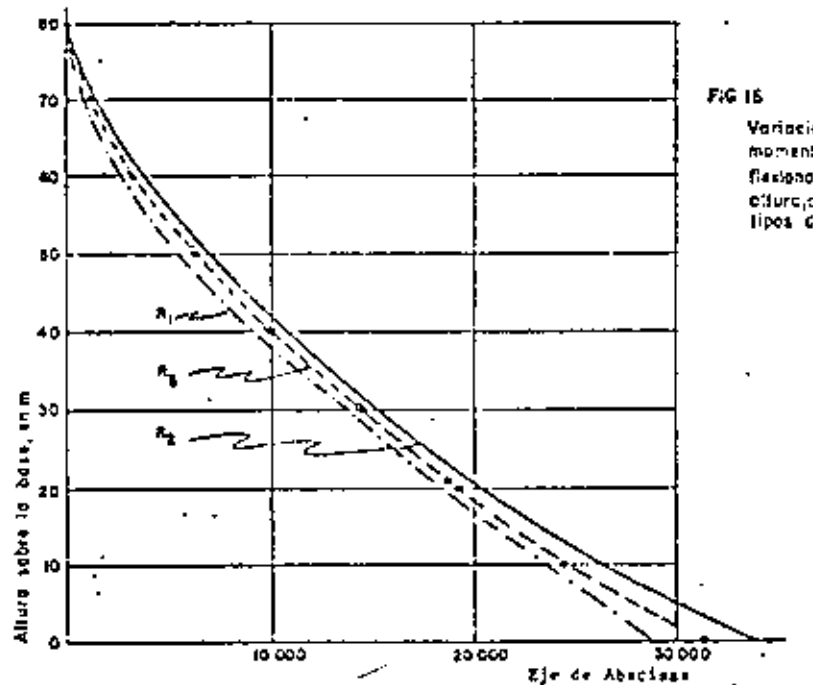


FIG 15

Variación del momento flexionante con la altura, con los tres tipos de respuesta

Finalmente, para la variación de la fuerza cortante se obtuvieron los siguientes resultados, en toneladas.

Masa	Un solo modo			Todos los modos		
	$R_1$	$R_2$	$R_3$	$R_1$	$R_2$	$R_3$
1	0	0	0	0	0	0
2	35.55	35.55	35.55	47.46	90.96	69.21
3	168.7	168.7	168.7	187.4	260.7	215.1
4	284.2	284.2	284.2	274.2	352.0	281.5
5	377.6	377.6	377.6	381.1	464.7	422.6
6	446.0	446.0	446.0	452.1	574.2	513.1
7	489.6	489.6	489.6	507.9	651.1	582.5
8	511.3	511.3	511.3	545.6	700.3	662.9
BASE	517.4	517.4	517.4	583.3	803.3	723.2

## 1. Referencias

1. Ciesielski, A. et alii: "Behälter, Bunker, Silos, Schornsteine, Fernsichttürme und Freileitungsmaste. W. Ernst & Sohn, 1970.
2. Lord Rayleigh: "Theory of Sound". Mc Millan Co. N. Y., pp 293-294
3. Timoshenko, S. P.: "On the Correction for Shear of the Differential equation for transverse vibrations of prismatic bars" Phyl. Mag., Vol 41, 1921.
4. Timoshenko, S. P.: "On the Transverse Vibrations of Bars of Uniform Cross Sections". Phyl. Mag. serie 6, vol 43, 1922, pp 125-131
5. Huang, T. C.: "The Effect of Rotatory Inertia and of Shear Deformation on the frequency and normal mode equations of Uniform Beams with Simple end Conditions". J. Applied Mech. Trans, ASME, Dec. 1961, pp 573.

6. De Silva, C. W.: "Dynamic Beam model with Internal Damping, Rotatory Inertia and Shear Deformation". AIAA Journal, Vol. 14, No. 5, 1978, pp 676-680
7. Housner, G. W., Keightley, W. O.: "Vibrations of linearly tapered Cantilever Beams". Trans. ASCE, 128, 1963, pp 1020-1048.
8. Novak, M: "Effect of Soil on Structural response to Wind and Earthquake" Pub. BLWT-5, 1973. University of Waterloo, Canada.



**DIVISION DE EDUCACION CONTINUA  
FACULTAD DE INGENIERIA U.N.A.M.**

VII CURSO INTERNACIONAL DE INGENIERIA SISMICA

DISEÑO SISMICO DE ESTRUCTURAS ESPECIALES

TANQUES

- \* Análisis Hidrodinámico de tanques
- \*\* -Basis of seismic design-provisions for welded steel oil storage tanks

Profesor: Arturo Arias Suárez

Julio, 1981



## ANÁLISIS HIDRODINÁMICO DE TANQUES

Jesús Iglesias J. (I)  
José de la Cera A. (II)

### RESUMEN

Se presenta la solución matemáticamente rigurosa para el comportamiento hidrodinámico de tanques de paredes rígidas con el objeto de establecer una comparación con el método analógico propuesto por Housner cuyo uso se encuentra ampliamente extendido en la actualidad. Los resultados obtenidos permiten recomendar el uso de la solución rigurosa mediante tablas o gráficas que faciliten su manejo.

### INTRODUCCION

El estudio del comportamiento hidrodinámico de tanques bien puede remontarse a la década de los treinta cuando Hoskins (1) y Ruge (2) realizaron los primeros trabajos de carácter experimental con motivo de las numerosas fallas ocurridas en este tipo de estructuras durante el sismo de 1933 en Long Beach, California. Con estos estudios se evidenció la necesidad de usar criterios de diseño dinámicos en vez de recurrir a la suposición de una carga estática equivalente de diseño actuando en el centro de masa del tanque, tal como se había venido haciendo.

Posteriormente a fines de los años cuarenta, el enfoque analítico del problema recibe un gran impulso con las investigaciones realizadas por Arias (3) y Jacobsen (4), quienes formulan la teoría de la masa reducida que permite llevar a cabo el análisis del tanque modelado por una serie de osciladores hidrodinámicos. Estos conceptos han sido ampliamente desarrollados por Graham (5) y Moran (6) para tanques de forma tanto rectangular como cilíndrica.

En 1957 Housner (7) publica un desarrollo teórico del problema basado en una analogía mecánica que no satisface el equilibrio dinámico en el fluido (8), y que conduce a la obtención de modos senoidales independientemente de la forma del recipiente, todo esto a diferencia de

los trabajos ya mencionados, que parten de la búsqueda del potencial de velocidades del líquido que cumpla con la ecuación de Laplace y las condiciones de frontera.

La presentación eminentemente práctica de los artículos de Housner (7,8) y la gran difusión que han tenido, son la causa de que hayan sido tomados como base para el diseño dinámico de tanques por varias normas (10,11), desechando la aparente complicación que implica el manejo de los modelos matemáticamente rigurosos. Esta situación hace sentir la necesidad de analizar con detenimiento y desde un punto de vista tanto teórico como de aplicación la conveniencia de la elección hecha a favor del método de Housner.

### DETERMINACION DEL POTENCIAL DE VELOCIDADES

La solución del movimiento irrotacional de un fluido homogéneo e incompresible, se reduce a encontrar el potencial de velocidades  $\phi$  que satisfaga la ecuación de continuidad representada por la ecuación de Laplace,

$$\nabla^2 \phi = 0 \quad (1)$$

y las condiciones de frontera correspondientes (12).

Para el caso de un tanque de paredes rígidas, las condiciones de frontera en el fondo y las paredes están dadas por la consideración de que el fluido adyacente sólo tiene respecto a ellas velocidad tangencial. En la superficie libre, si se suponen desplazamientos de oleaje pequeños, la condición de frontera es la de Poisson (12),

$$g \frac{\partial \phi}{\partial z} + \frac{\partial^2 \phi}{\partial t^2} = 0 \quad (2)$$

donde  $g$  es la aceleración de la gravedad,  $t$  la variable temporal y el sistema de referencia es el indicado en las Figs 1 y 3.

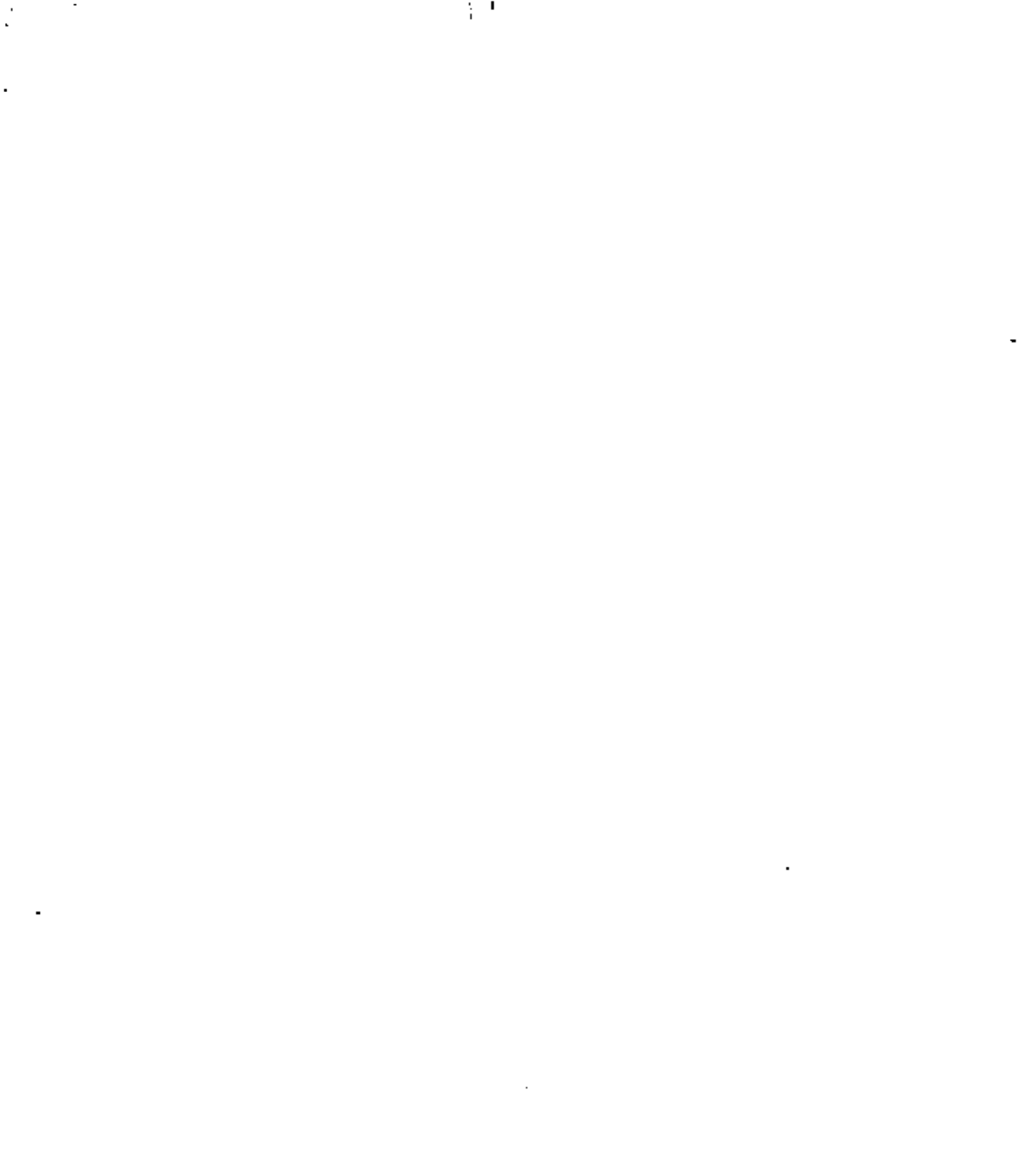
### TANQUE RECTANGULAR

Si se considera que el desplazamiento inicial ocurre en la dirección  $X$  (Fig 1), la ecuación de continuidad será,

$$\frac{\partial^2 \phi}{\partial x^2} + \frac{\partial^2 \phi}{\partial z^2} = 0 \quad (3)$$

(I) Universidad Autónoma Metropolitana, Azcapotzalco, D.F.

(II) Universidad Autónoma Metropolitana, Azcapotzalco, D.F.



las condiciones de frontera en paredes y fondo,

$$\left. \frac{\partial \phi}{\partial x} \right|_{x=0} = 0, \quad \left. \frac{\partial \phi}{\partial z} \right|_{z=h} = 0 \quad (4)$$

y la condición de frontera en la superficie libre

$$g \frac{\partial \phi}{\partial z} + \frac{\partial^2 \phi}{\partial t^2} = 0 \quad (5)$$

Proponiendo un potencial del tipo

$$\phi = A X(x) Z(z) T(t) \quad (6)$$

donde A es una constante, X, Z y T son funciones de x, z y t respectivamente y después de sustituir en la ecuación de Laplace, integrar e introducir las condiciones de frontera, dicho potencial queda definido en función de los n modos del movimiento como

$$\phi = \sum_{n=1}^{\infty} \phi_n = \sum_{n=1}^{\infty} A_n \sin(k_n x) \cosh[k_n(h+z)] \cos(\sigma_n t + \epsilon_n) \quad (7)$$

donde  $A_n$  y  $\epsilon_n$  son constantes y

$$\sigma_n^2 = g k_n \tanh(k_n h) \quad (8)$$

y

$$k_n = \left( \frac{n - 1/2}{a} \right) \pi \quad (9)$$

Puesto que el perfil del líquido en la superficie está definido (12)

por

$$\eta = \frac{1}{g} \frac{\partial \phi}{\partial t} \Big|_{z=0} \quad (10)$$

se observa que la forma de los modos es senoidal (Fig 2)

$$\eta_n = -A_n \sin(k_n x) \cosh(k_n h) \cos(\sigma_n t + \epsilon_n) \quad (11)$$

Esta coincidencia en la forma modal con el método de Housner, no se presenta para otros tipos de tanques como se verá más adelante.

Una vez obtenido  $\phi$ , es posible hallar la energía cinética y el

impulso del fluido para un modo dado (12) mediante

$$T_n = \frac{\rho}{2} \int \bar{v}_n^2 dV, \quad I_n = \rho \int \bar{\eta} dV \quad (12)$$

donde

$$\bar{v}_n = \left\{ \frac{\partial \phi_n}{\partial x}, \frac{\partial \phi_n}{\partial y}, \frac{\partial \phi_n}{\partial z} \right\} \quad (13)$$

Efectuando el cociente

$$\frac{I_n^2}{2T_n} = \frac{(M_n \eta_n)^2}{2 \left( \frac{1}{2} M_n \eta_n^2 \right)} = M_n \quad (14)$$

se obtiene la masa del oscilador hidrodinámico correspondiente al modo n

$$M_n = M \left[ \frac{2 \cosh^2 \left( \frac{\pi_n h}{a} \right)}{\frac{h}{a} \pi_n^2} \right] = M R_n \quad (15)$$

donde M es la masa total del líquido y

$$\pi_n = \pi \left( n - \frac{1}{2} \right) \quad (16)$$

En consecuencia, el factor de masa reducida queda determinado por

$$R_0 = 1 - \sum_{n=1}^{\infty} R_n \quad (17)$$

Graham (5), trabajando el potencial de velocidades a través de la ecuación de presiones llega a obtener los mismos resultados, además de determinar las posiciones de las masas equivalentes y de sus correspondientes resortes (Fig 5)



$$M_n = MR_n \quad ; \quad M_0 = MR_0$$

$$H_n = \left[ 1 - \frac{2 \tan h \left( \frac{\pi_n h}{2a} \right)}{\pi_n \frac{h}{a}} \right] h$$

$$H_0 = \left[ \frac{1}{2} - \frac{1}{h M_0} \sum_{n=1}^{\infty} M_n H_n \right] h \quad (18)$$

$$K_n = \frac{2 M g \tan h^2 \left( \pi_n \frac{h}{a} \right)}{h \pi_n^2}$$

### TANQUE CILINDRICO

En este caso la ecuación de Laplace en coordenadas cilíndricas (Fig 3) es

$$\frac{1}{r^2} \frac{\partial^2 \phi}{\partial \theta^2} + \frac{\partial^2 \phi}{\partial r^2} + \frac{1}{r} \frac{\partial \phi}{\partial r} + \frac{\partial^2 \phi}{\partial z^2} = 0 \quad (19)$$

y las condiciones de frontera son

$$\left. \frac{\partial \phi}{\partial r} \right|_{r=a} = 0 \quad ; \quad \left. \frac{\partial \phi}{\partial z} \right|_{z=h} = 0 \quad ; \quad \left. \frac{\partial \phi}{\partial \theta} \right|_{\theta=0, 2\pi} = 0$$

$$g \frac{\partial \phi}{\partial z} + \frac{\partial^2 \phi}{\partial t^2} = 0 \quad \Big|_{z=0} \quad (20)$$

A partir del potencial

$$\phi = A R(r) \Theta(\theta) Z(z) T(t) \quad (21)$$

sustituyendo en la ecuación de Laplace, integrando e introduciendo las condiciones de frontera, es posible definir dicho potencial como

$$\phi = \sum_{n=1}^{\infty} \phi_n = \sum_{n=1}^{\infty} A_n J_1 \left( \frac{\lambda_n r}{a} \right) \cosh \left( \lambda_n \frac{h+z}{a} \right) \cos(p_n t + \epsilon_n) \cos \theta \quad \dots (22)$$

donde  $J_1$  es la función de Bessel de 1a. especie de orden 1,  $\lambda_n$  son las raíces de  $J_1'$  y

$$p_n^2 = \frac{g}{a} \lambda_n \tan h \left( \lambda_n \frac{h}{a} \right) \quad (23)$$

Ahora los modos ya no son senoidales, sino que adquieren la forma de funciones  $J_1$  de Bessel (Fig 4)

$$\eta_n = -A_n p_n J_1 \left( \lambda_n \frac{r}{a} \right) \cosh \left( \lambda_n \frac{h}{a} \right) \sin(p_n t + \epsilon_n) r \cdot \theta \quad (24)$$

con lo cual surge una diferencia irreconciliable con el método de Housner.

De manera similar al caso anterior es posible obtener las masas equivalentes como

$$M_n = \frac{I_n^2}{T_n} = M \frac{2 \tan h \left( \lambda_n \frac{h}{a} \right)}{\lambda_n (\lambda_n^2 - 1) \frac{h}{a}} = MR_n \quad ; \quad R_0 = 1 - \sum_{n=1}^{\infty} R_n \quad \dots (25)$$

Aunque con un desarrollo más complicado, Moran (8) encuentra también los resultados anteriores e inclusive las expresiones para la posición de las masas y las rigideces de los resortes hidrodinámicos (Fig 5)

$$M_n = MR_n \quad ; \quad M_0 = MR_0$$

$$H_n = \frac{h}{R_n} \left( R_n - S_n + S_n' \right)$$

$$H_0 = \frac{h}{R_0} \left( R_0 + 2S_0 - \frac{1}{2} \right) \quad (26)$$

$$K_n = \frac{2 M g \tan h \left( \lambda_n \frac{h}{a} \right)}{h \lambda_n (\lambda_n^2 - 1)}$$

$$S_n = \frac{2 \left[ 1 - \operatorname{sech} \left( \lambda_n \frac{h}{a} \right) \right]}{\lambda_n^2 (\lambda_n^2 - 1) \left( \frac{h}{a} \right)^2}$$

$$S_n' = \frac{2 \operatorname{sech} \left( \lambda_n \frac{h}{a} \right)}{\lambda_n^2 (\lambda_n^2 - 1) \left( \frac{h}{a} \right)} ; S_0 = \sum_{n=1}^{\infty} S_n$$

#### COMPARACION NUMERICA

Se llevó a cabo un análisis numérico para comparar los resultados obtenidos en  $R_1$  y  $R_0$  tanto con las expresiones de Housner - tomadas de (10), como con las analíticas considerando los primeros 50 modos para el cálculo de  $R_0$ .

Tanque Rectangular. Aquí se aprecia (Fig 6) una pequeña diferencia en cuanto al factor de reducción de masa del primer modo, que se justifica porque en ambos casos es senoidal la forma de los modos, sin embargo en lo que respecta a la masa adherida, su factor de reducción presenta hasta un 10% de diferencia.

Tanque Cilíndrico. Para este tipo de tanque, en el que como se vió anteriormente existe una discrepancia en las formas modales, se presentan diferencias en el cálculo de la masa del oscilador hidrodinámico del primer modo hasta de 17% y en el de la masa adherida hasta de 7%.

#### CONCLUSION

Teniendo en cuenta el aspecto técnico del problema no es difícil aceptar la mayor solidez en el planteamiento riguroso seguido al principio de este trabajo, en relación a la analogía mecánica - propuesta por Housner, hecho que se ve confirmado por el trabajo experimental (13).

En cuanto al aspecto práctico, si bien las expresiones analíticas son complicadas pues el cálculo de  $R_0$  requiere de la evaluación de una serie infinita y en el caso del tanque cilíndrico es necesario trabajar con las funciones de Bessel, el recurso de elaborar tablas o gráficas para obtener los valores requeridos en función de la relación de aspecto del tanque elimina esta dificultad.

En base a lo anterior y teniendo en cuenta que el uso de la analogía de Housner puede conducir a errores de magnitud apreciable, se concluye que es más adecuada e igualmente práctico el uso de los resultados matemáticamente rigurosos.

Agradecimiento. Los autores agradecen al Profesor A. Arias las sugerencias y comentarios al presente trabajo, además de su personal contribución al desarrollo del estudio del comportamiento hidrodinámico de tanques, fruto de una vida ejemplar de dedicación científica.

#### REFERENCIAS

1. L. M. Hoskins y L. S. Jacobson, "Water Pressure in a Tank Caused by a Simulated Earthquake"; Bull. Seism. Soc. Am., 24, 1-32, (1934).
2. A. C. Ruge, "Earthquake Resistance of Elevated Water-Tanks"; Trans. ASCE, 103, 986-999, (1938).
3. A. Arias S., "Oscilaciones de un estanque elevado"; Tesis de Licenciatura en Ingeniería Civil, Universidad de Chile, (1948).
4. L. S. Jacobson, "Impulsive Hydrodynamics of Fluid Inside a Cylindrical Tank and of Fluid Surrounding a Cylindrical Pier"; Bull. Seism. Soc. Am., 39, 189-204, (1949).
5. E. W. Graham y A. M. Rodríguez, "The Characteristics of Fuel Motion Which Affect Airplane Dynamics"; Jour. Applied Mechanics, 19 (3), 381-388, (1952).
6. D. F. Morán, "Respuesta Sísmica en Tanques Elevados de Acero"; Tesis de Licenciatura en Ingeniería Civil, Universidad de Chile, (1963).
7. G. W. Housner, "Dynamic Pressure on Accelerated Fluid Containers"; Bull. Seism. Soc. Am., 47, 18-35, (1957).
8. G. W. Housner, "The Dynamic Behavior of Water Tanks"; Bull. Seism. Soc. Am., 53(2), 381-387, (1963).
9. D. P. Clough, "Experimental Evaluation of Seismic Design Methods for Broad Cylindrical Tanks"; Report No. UCB/EERC-77/10, Univ. of California, (1977).
10. Manual de Diseño de Obras Civiles de la CFE, Sección B: Soluciones, (1963).
11. U. S. Atomic Energy Commission, Division of Reactor Development, "Nuclear Reactors and Earthquakes", (1963).



12. L. M. Milne-Thomson, "Theoretical Hydrodynamics", Mac-Millan Press, 5a. edición, (1930).

13. L. S. Jacobsen y R. S. Ayre, "Hydrodynamic Experiments With Rigid Cylindrical Tanks Subjected to Transient Motions", Bull. Seism. Soc. Am., 41(4), 313-348, (1951).

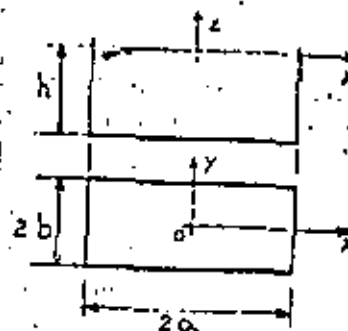


Fig 1. Sistema coordenado del tanque rectangular

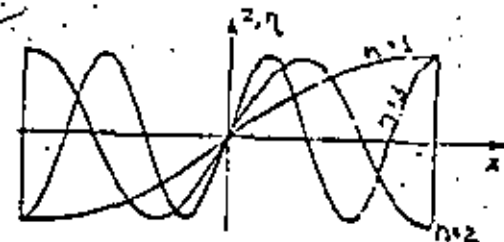


Fig 2. Formas modales en la superficie del tanque rectangular (senoidales).

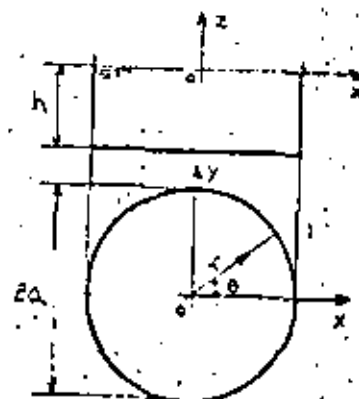


Fig 3. Sistema coordenado del tanque cilindrico

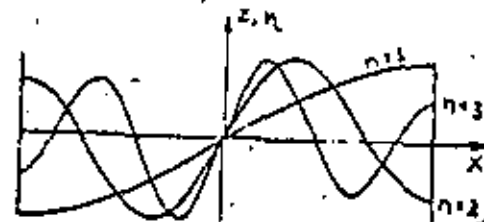


Fig 4. Formas modales en la superficie del tanque cilindrico.

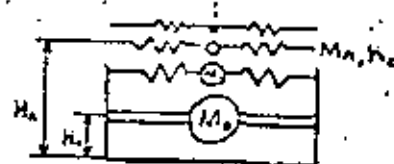


Fig 5. Osciladores hidrodinámicos y masa adherida.

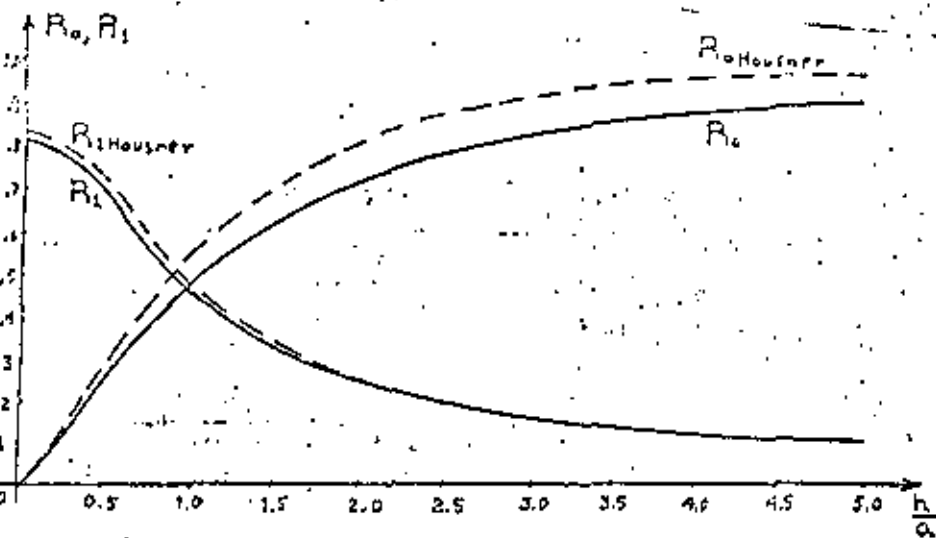


Fig. 6. Factores de reducción de masa del tanque rectangular.

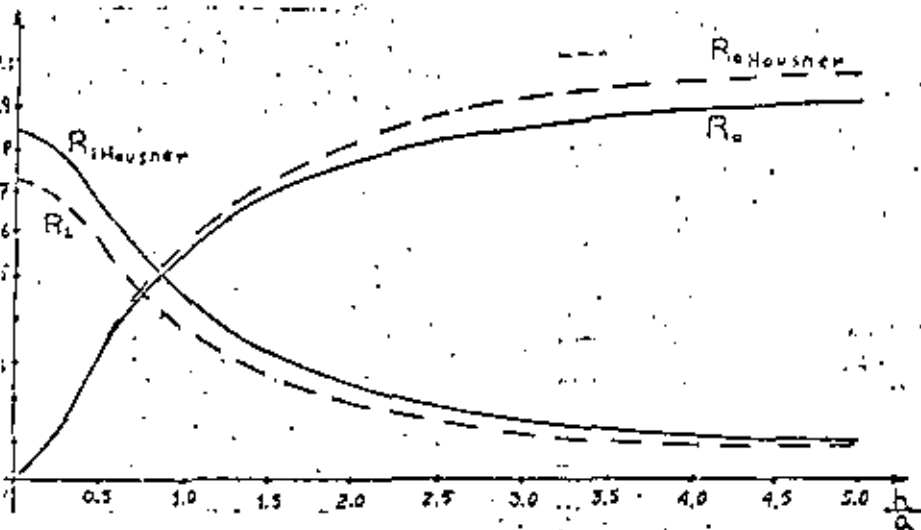


Fig. 7. Factores de reducción de masa del tanque cilíndrico.

PRESENTED AT THE SESSION ON  
 ADVANCES IN STORAGE TANK DESIGN  
 API, REFERING  
 43RD MIDYEAR MEETING  
 SHERATON CENTRE  
 TORONTO, ONTARIO, CANADA  
 TUESDAY, MAY 9, 1978

# BASIS OF SEISMIC DESIGN PROVISIONS FOR WELDED STEEL OIL STORAGE TANKS

SPONSORED BY  
 SIC ON PRESSURE VESSELS AND TANKS  
 MANUFACTURERS SIC ON TANKS AND VESSELS

J.S. Wozniak  
 Chicago Bridge & Iron Company  
 Oak Brook, Illinois  
 and  
 W.W. Mitchell  
 Standard Oil Company of California  
 San Francisco, California

CBT-5359

BASIS OF SEISMIC DESIGN PROVISIONS  
FOR WELDED STEEL OIL STORAGE TANKS

R. S. Hozniak<sup>1</sup> and W. W. Mitchell<sup>2</sup>

ABSTRACT

Recommended design provisions are described for the seismic design of flat bottom storage tanks which are proposed to be included in API Standard 650. The basis for establishing design loads is presented including seismic zone coefficients and the essential facilities factor. The design procedure is based on the approximate method of Professor Housner except that amplification of ground motion is recognized in determining the impulsive response. The derivation of curves is presented which simplify the calculation of the weights of the effective masses of tank contents, their centers of gravity, and the period of vibration of the sloshing mode. The basis of the design lateral force coefficients is given.

Resistance to overturning for unanchored tanks is provided by the tank shell and a portion of the tank contents which depends on the width of bottom annular ring which may lift off the foundation. The basis for determining this width is presented. A curve is included in the provisions for calculating the maximum longitudinal compression force in the shell for unanchored tanks. The derivation of this curve is presented and an approximate formula for the curve given. The formulas for maximum longitudinal compression force in the shell for anchored tanks and required anchorage resistance are explained. The basis is given for establishing the maximum allowable shell compression which takes into account the effect of internal pressure due to the liquid contents.

Supplemental information is presented for calculating the height of sloshing of the liquid contents, for designing roof support columns to resist forces caused by sloshing, and to calculate the increase in hoop tension in the shell due to seismic forces.

INTRODUCTION

Reports of damage from major earthquakes within the last few decades cite cases of damage to flat bottom welded steel storage tanks [1, 2, 3, 4]<sup>3</sup>. Damage to the tanks falls in four general categories:

1. Buckling of the bottom of the tank shell due to longitudinal compressive stresses resulting from overturning forces. This buckling is most frequently in the form of an outward bulge in the bottom foot or two of the tank shell extending partly or completely around the tank termed an "elephant's foot bulge." Damage of this type has generally been limited to unanchored tanks ranging between 10 and 100 feet in diameter. Loss of contents has resulted in some of the more severely buckled tanks.
2. Damage to the roof and upper shell of the tank and to internal roof support columns due to sloshing of the tank contents.
3. Damage to piping and other appurtenances connected to a tank due to movement of the tank.
4. Damage resulting from failure of the supporting ground, notably from liquefaction, washout due to broken piping, and slope failure due to high edge loads.

The damage reports have led to increasing interest in the seismic design of tanks to be located in seismically active areas. Tank builders, owners, and, in some instances, regulatory agencies have developed their own criteria for seismic design. To provide uniform guidelines, recommended design provisions have been prepared which are proposed to be included as an appendix (Appendix P) in API Standard 650, Welded Steel Tanks for Oil Storage. Similar provisions are being developed by the American Water Works Association for water storage tanks.

SCOPE OF DESIGN PROVISIONS

The proposed Appendix P to API Standard 650 covering seismic design of storage tanks is included in Appendix 1 to this paper. Detailed requirements are included to assure

<sup>1</sup> Chicago Bridge & Iron Company, Oak Brook, IL  
<sup>2</sup> Standard Oil Company of California, San Francisco, CA

<sup>3</sup> References are listed at the end of the text.

stability of the tank shell against overturning and to preclude buckling of the tank shell due to longitudinal compression for the level of earthquake ground motion which has a reasonable likelihood of not being exceeded during the life of the tank in the region in which the tank will be located.

A requirement is included to provide suitable flexibility in piping attached to the shell or bottom of the tank. Additional items which the tank purchaser may wish to consider to minimize or avoid overflow and damage to the roof and upper shell and to roof support columns are noted. These latter items normally do not pose a risk to life safety or to the safety of surrounding facilities, but may be considered from the standpoint of economic risk to the tank itself. Guidelines are included later in this paper for the design to accomplish these objectives.

The response of tanks to earthquake ground motion also includes an increase in hoop tension in the shell. This has led to rupture of the shell in the past for riveted tanks. The shells of welded tanks, however, have substantial ductility in hoop tension and can absorb energy resulting from earthquake ground motion through yielding. Current practice for the seismic design of welded steel tanks for hoop tension takes this ductility into account. When this is done, seismic response in hoop tension does not govern the design of the shell for the maximum level of earthquake ground motion proposed for API Standard 650. Consequently, no provisions are included for hoop tension. When tanks are designed for higher levels of earthquake ground motion, increased hoop tension should be investigated. Guidelines for this are included later in this paper.

The proposed Appendix P does not address soil stability since this does not affect the design of the tank. However, it is important that soil conditions at prospective tank sites in seismically active areas be investigated for potential instability including liquefaction during an earthquake.

#### DESIGN LOADING

The Design procedure presented in Appendix P is based on the simplified procedure developed by Professor G. W. Housner [5] and included in Chapter 6 and Appendix F of BSCA TID 7024 [6] with modifications as suggested by Professor A. S. Veletsos [7]. As noted in the Introduction to Appendix P, the procedure considers two response modes of the tank and

its contents: the response of the tank shell and roof together with a portion of the contents which moves in unison with the shell, and the fundamental sloshing mode of the contents. The forces associated with these modes are normally termed the impulsive force and the convective force, respectively. The design overturning moment at the bottom of the shell resulting from these forces is given by the following formula in Section P.3.1:

$$M = 2I(C_1W_1X_1 + C_2W_2X_2) \quad (1)$$

In this formula,  $C_1$  and  $C_2$  are the respective lateral force coefficients for the impulsive and convective forces and  $W_1$  and  $W_2$  are the corresponding weights of the effective masses of the tank contents. Curves for determining  $W_1$  and  $W_2$  as a ratio to the total weight of tank contents,  $W$ , are given in Figure P-2 of Appendix P for various ratios of tank diameter,  $D$ , to maximum filling height,  $H$ . These curves are based on the formulas developed by Housner and presented in TID 7024. For the weight of the liquid contributing to the impulsive force,  $W_1$ , Housner presents the following formula for tanks where the ratio of filling height to radius is less than 1.5 ( $D/H$  greater than 1.333):

$$\frac{W_1}{W} = \frac{\tanh 0.866 \frac{D}{H}}{0.866 \frac{D}{H}} \quad (2a)$$

Where the ratio of filling height to radius is greater than 1.5 ( $D/H$  less than 1.333), Housner's procedure considers the liquid contents in the lower part of the tank below a depth equal to 1.5 times the radius to respond as a rigid body as far as impulsive forces are concerned. The effective weight of the upper portion of the contents is determined from formula (2a) using  $D/H = 1.333$ . The total effective weight is determined by adding the full weight of the lower portion of the contents to the effective weight of the upper portion. This leads to the formula:

$$\frac{W_1}{W} = 1.0 - 0.218 \frac{D}{H} \quad (2b)$$



The formula for the weight of the effective contents used to determine the convective force, which is based on Housner's corrected version of TID 7024, is as follows:

$$\frac{W_2}{W_T} = 0.230 \frac{D}{H} \tanh \left( \frac{3.67}{D/H} \right) \quad (3)$$

The heights  $X_1$  and  $X_2$  from the bottom of the tank shell to the centroids of the lateral seismic forces applied to  $W_1$  and  $W_2$ , respectively, as ratios to the maximum filling height,  $H$ , are given in Figure P-1 of Appendix P for various  $D/H$  ratios. Again, these are based on the work of Housner. For tanks where the ratio of filling height to radius is less than 1.5 ( $D/H$  greater than 1.333), the formula for the height to the centroid of the impulsive force is:

$$\frac{X_1}{H} = 0.375 \quad (4a)$$

Where the ratio of filling height to radius is greater than 1.5 ( $D/H$  less than 1.333):

$$\frac{X_1}{H} = 0.500 - 0.094 \frac{D}{H} \quad (4b)$$

The formula for the height to the centroid of the convective force is:

$$\frac{X_2}{H} = 1.0 - \frac{\cosh \left( \frac{3.67}{D/H} \right) - 1.0}{\frac{3.67}{D/H} \sinh \left( \frac{3.67}{D/H} \right)} \quad (5)$$

As noted at the end of Paragraph P.3.1, the overturning moment calculated in accordance with formula (1) is that applied to the bottom of the shell. The total overturning moment applied to the foundation can be determined by substituting  $X_1$  and  $X_2$  from the following formulas for  $X_1$  and  $X_2$ , respectively, in formula (1):

$$\frac{D}{H} > 1.333:$$

$$\frac{X_1}{H} = 0.375 \left[ 1.0 + 1.333 \left( \frac{0.866 \frac{D}{H}}{\tanh 0.866 \frac{D}{H}} - 1.0 \right) \right] \quad (6a)$$

$$\frac{D}{H} < 1.333:$$

$$\frac{X_1}{H} = 0.500 + 0.060 \frac{D}{H} \quad (6b)$$

$$\frac{X_2}{H} = 1.0 - \frac{\cosh \left( \frac{3.67}{D/H} \right) - 1.937}{\frac{3.67}{D/H} \sinh \left( \frac{3.67}{D/H} \right)} \quad (7)$$

Tanks on the ground are inherently rigid. In his work, Housner considered the tank to be infinitely rigid so that the motion of the tank shell and roof together with that portion of the contents that moves in unison with the shell coincides with ground motion. In reality, tanks are not infinitely rigid. Storage tanks typically have natural periods of vibration in the range of 0.10 to 0.25 seconds. Veletsos, in this study of thin wall flexible tanks, concludes that the impulsive force can be reasonably well estimated from the solutions derived for a rigid tank except replacing the maximum ground acceleration with the spectral value of the pseudo-acceleration corresponding to the fundamental natural frequency of the tank-fluid system. Since the calculation of the fundamental period is complex for tanks which do not experience uplift and unknown for those that do, a constant value is proposed in Appendix P for  $C_1$  which represents the maximum amplified ground motion. The value of 0.24 is consistent with the Uniform Building Code maximum value for structures other than buildings ( $K = 2.0$ ) excluding any soil factor. The soil factor does not appear appropriate for structures with a very low natural period of vibration. The high value of  $C_1$  in comparison with buildings

is appropriate because of the low damping inherent for storage tanks, the lack of nonstructural load bearing elements, and the lack of ductility of the tank shell in longitudinal compression.

For some tanks, taking  $U_1$  as the maximum amplified ground motion may be overconservative. For very rigid tanks which are anchored, it may be desirable to calculate the fundamental period and use a lower spectral acceleration value.

The period of the first sloshing mode is relatively long and the corresponding value of spectral acceleration falls in the region of maximum spectral velocity or displacement. The formula presented for  $C_2$  is based on a maximum spectral velocity of 1.5 to 2.3 ft/sec and a maximum spectral displacement of 1.1 to 1.65 feet, depending on soil type.

The calculation of  $C_2$  requires the determination of the natural period of the first sloshing mode and the site amplification factor,  $S$ . The period can be determined from the expression:

$$T = kD^4 \quad (8)$$

where  $k$  is obtained from Figure P-4 for various  $D/H$  ratios. This comes from the formula:

$$T = \frac{2\pi\sqrt{D}}{3.67g \tanh\left(\frac{3.67}{D/H}\right)} \quad (9)$$

Substituting  $g = 32.2 \text{ ft/sec}^2$ ,  $k$  is then:

$$k = \frac{0.578}{\tanh\left(\frac{1.07}{D/H}\right)} \quad (10)$$

The site amplification factor,  $S$ , is determined from Table P-2 and varies from 1.0 for rock-like soils to 1.5 for soft to medium stiff soils. These amplification factors correspond to those recommended in the Final Review Draft of

Recommended Comprehensive Seismic Design Provisions for Buildings [3] prepared by the Applied Technology Council in a study (Project ATC-3) sponsored by the National Science Foundation and the National Bureau of Standards.

The lateral force coefficients,  $C_1$  and  $C_2$ , are applicable for the areas of highest seismicity and for tanks which are not required to be functional for emergency post earthquake operations. The zone coefficient,  $Z$ , and the essential facilities factor,  $I$ , are included in formula (1) for the design overturning moment to provide an adjustment for tanks located in less seismically active areas and for tanks which are required to be functional for emergency operations after an earthquake. The value of the zone coefficient,  $Z$ , is obtained from Table P-1 for the various zones defined in Figure P-1. The values of  $Z$  correspond to those specified in the Uniform Building Code. The zone maps are based on peak ground motion acceleration contour maps included in the Final Review Draft of the ATC-3 Project. For the 48 contiguous states, the map used is that where the accelerations are a measure of effective peak velocity so to be appropriate for the long period convective force as well as the short period impulsive force. The ATC-3 map depicts contours of approximately equal seismic risk and is considered to be an improvement over the zone map included in the Uniform Building Code which is based on historic earthquake damage levels. The ATC-3 map is for use in establishing ultimate design loads and the acceleration values depicted should be reduced for application in working stress design procedures. The relationships between the zones shown on the maps included in Appendix P and the contour ranges shown on the ATC-3 maps are as follows:

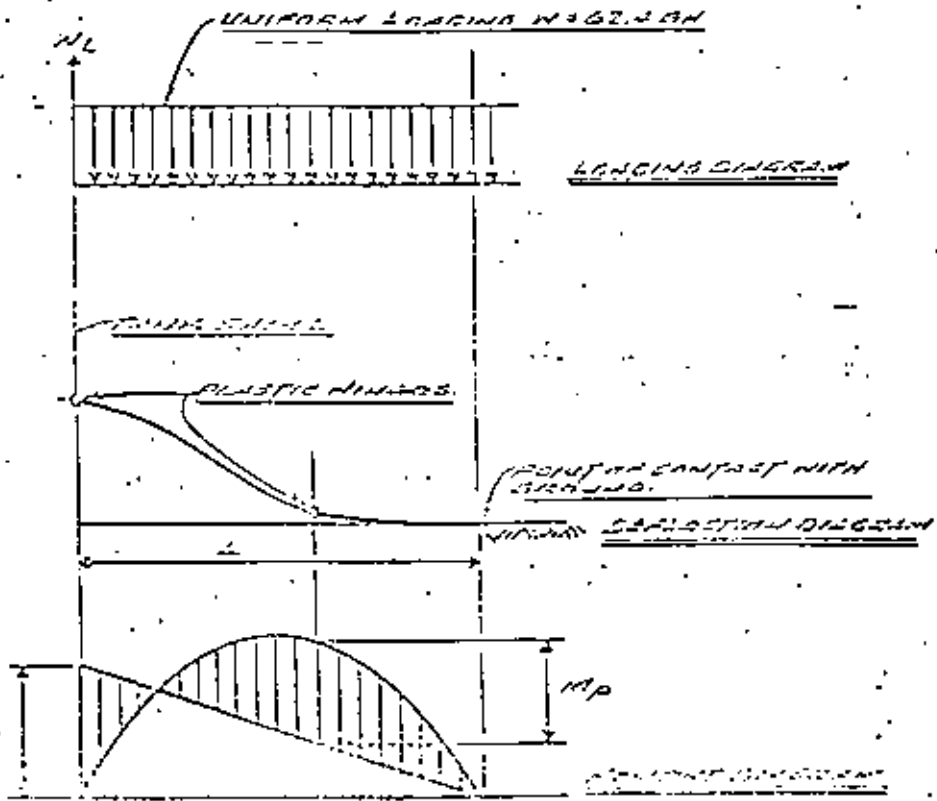
Appendix P Seismic Zone	ATC-3 Map Contour Ranges
4	Over 0.4
3	0.2 to 0.4
2	0.1 to 0.2
1	0.05 to 0.1
0	Under 0.05

The essential facilities factor,  $I$ , corresponds to the Occupancy Importance Factor specified in the Uniform Building Code. The UBC requires that "structures or buildings which must be safe and usable for emergency purposes after an earthquake in order to preserve the health and safety of the general public" be designed for a factor of 1.5. For oil storage, this should apply to tanks such as those storing

fuel for power generating facilities which are essential for emergency postearthquake operations.

RESISTANCE TO OVERTURNING

The factors which may contribute to resistance of the overturning moment are noted in paragraph P.4. The weight of the contents which may be utilized to resist overturning is based on the calculated reaction at the tank shell of an internal strip of the bottom plate perpendicular to the shell which can be lifted off the ground. The calculation is based on small deflection theory and assumes the development of two plastic hinges, one at the junction to the shell and the other at some distance inward from the shell. The assumed loading, deflection and moment diagrams are shown below:



The equilibrium solution leads to the following relationships:

$$w_L = 2\sqrt{wM_p} \tag{11}$$

and

$$L = 1.707 \frac{w_L}{w} \tag{12}$$

Substituting  $M_p = \frac{r_{by}^2}{6}$  and  $w = 62.4GH$ ,

$$w_L = 2.90 r_{by} \sqrt{F_{by} GH} \tag{13}$$

and

$$L = 0.0274 \frac{w_L}{GH} \tag{14}$$

Practice has been to limit the uplift length, L, to 6 to 7 percent of the tank radius [7]. The limitation of  $w_L$  to 1:25 GHD limits L to about 6.8% of the radius. Recent shaking table model tests of tanks [10] show significant changes in the response characteristics which are not accounted for by current design procedures when greater amounts of uplift occur.

The above procedure to establish the maximum resistance of the liquid contents to overturning of the tank is conservative since it does not take into account membrane stresses which will develop in the bottom upon uplift. Further studies need to be undertaken to better determine the uplift resistance and to account for the changes in response when large amounts of uplift occur.

SHELL COMPRESSION

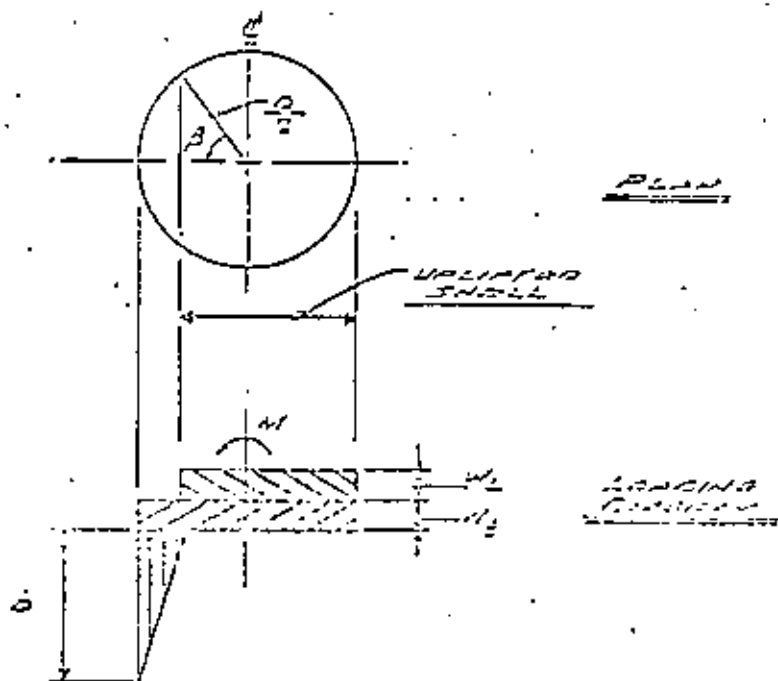
Methods for determining the maximum longitudinal compression force, b, at the bottom of the tank shell are

given in Paragraphs P.5.1 and P.5.2. For unanchored tanks where there is no uplift and for anchored tanks the compression force can be determined readily from the formula:

$$b = w_1 + \frac{4M}{\pi D^2} = w_1 + \frac{1.272M}{D^2} \quad (15)$$

which assumes that the force varies directly with the distance from the centerline of the tank in the direction of the internal loading. For tanks which experience uplift,  $b$  can be determined from the value of the compressive force parameter obtained from Figure P-5 as a function of the overturning moment parameter.

The curve in Figure P-5 is derived from the following assumed load distribution around the shell of the tank:



From the summation of vertical forces and overturning moments, the following expressions are obtained:

$$\frac{b+w}{w_1+w} = \frac{\pi(1-\cos\beta)}{\sin\beta - \beta\cos\beta} \quad (16)$$

$$\frac{M}{D^2(w_1+w)} = \frac{\pi}{8} \frac{2\beta - \sin 2\beta}{\sin 2\beta - \beta\cos\beta} \quad (17)$$

By substituting values of  $\beta$  from 0 to  $\pi$  radians in these expressions, the relationship between the two parameters on the left-hand side of the expressions is obtained. This relationship applies for values of the moment parameter from  $\pi/4$  where uplift commences to  $\pi/2$  where the shell becomes unstable. The relationship may be approximated with good accuracy up to a value of the moment parameter of 1.54 with the following formula:

$$\frac{b+w}{w_1+w} = \frac{1}{0.0212 - 0.1537 \left[ \frac{M}{D^2(w_1+w)} \right]^{2.2}} \quad (18)$$

Formulas for determining the maximum allowable longitudinal compression in the shell are given in paragraph P.5.3. These were established to provide a safety factor against buckling of about 1.5. Excluding the effect of internal pressure, the critical stress for very thin wall shells was established as  $0.125 E/t^2 R$  where  $E$  is the modulus of elasticity,  $t$  the shell thickness, and  $R$  the shell radius. This is based on the work of C. D. Miller [1] of Chicago Bridge & Iron Company. Using  $E = 29,000,000$  psi and a safety factor of about 1.5, this leads to an allowable stress of:

$$\frac{400,000}{D}$$

(19)

where  $t$  is in inches and  $D$  is the diameter in feet.

Lo, Crate and Schwartz (12) determined through theoretical analysis and experimental tests that the critical buckling stress in compression for thin wall cylinders increases with internal pressure. Theoretically, with sufficient internal pressure the critical buckling stress will reach the classical limit of  $0.6 E t / R$ . However, only limited tests have been made to date. The tests made by Lo, Crate and Schwartz showed a doubling of the critical buckling stress as the nondimensional parameter  $\frac{P}{E} \left( \frac{R}{t} \right)^2$  increased from zero (no internal pressure) to a value of 0.1023. This value is reached when the value of  $GHD^2/t^2$  is about 200,000. Based on this, the allowable longitudinal compressive stress for thin wall tanks for values of  $GHD^2/t^2$  greater than 200,000 was established as:

$$F_0 = \frac{800,000}{D} \quad (20)$$

The tests of Lo, Crate and Schwartz showed a nearly linear increase in critical buckling stress with internal pressure up to the limits of their tests. Thus, for values of  $GHD^2/t^2$  less than 200,000 the allowable compressive stress was established as:

$$F_0 = \frac{400,000}{D} + \frac{7SHD}{t} \quad (21)$$

Formula (21) will normally apply only to very small tanks where the shell thickness is established by minimum values rather than by hoop stress.

As the thickness of the shell in proportion to the diameter of the tank becomes relatively large, formulas (20)

and (21) are no longer applicable. Miller presents formulas for critical buckling of shells without internal pressure for intermediate and thick shells leading to a maximum value of critical buckling stress equal to the yield stress. The limit of  $F_0 = 0.5 F_y$  is established in Appendix P to maintain an adequate safety factor throughout the intermediate range of thickness to diameter ratio. This limit will normally apply only to small diameter tanks (under 15 ft diameter).

The longitudinal compressive buckling stress of tank shells is a subject which needs further study. The presence of internal pressure and the radial restraint provided by the bottom leads to a different form of buckling than has been experienced in most experimental work on the buckling of cylinders under axial and bending loads.

#### ANCHORAGE OF TANKS

Generally, tanks need not be anchored when the required resistance to overturning can be provided by the tank shell and internal contents without exceeding the maximum value permitted for  $w_1$ . When anchorage is required, careful attention should be given to the attachment of the anchors to the shell to avoid the possibility of tearing the shell. The specified anchorage resistance given in paragraph P.6 for anchored tanks provides a factor of safety in that the resistance provided by the weight of the tank shell is not considered.

#### SLOSHING WAVE HEIGHT

In some cases it may be desirable to provide freeboard for the tank above the maximum filling height to minimize or avoid overflow and damage to the roof and upper shell due to sloshing of the liquid contents. The height of the sloshing wave may be determined from the following formula based on Housner's corrected version of T19 7024:

$$d = 1.124210_2 T^2 \text{ inch} \left( 4.77 \sqrt{\frac{H}{D}} \right) \quad (22)$$

#### ROOF SUPPORTING COLUMNS

When it is desired to design roof supporting columns to resist the forces caused by the sloshing of the liquid

contents, these forces may be determined as described in Appendix 2 of this paper.

#### HOOP TENSION

When it is desired to analyze the tank shell for increased hoop tension due to earthquake ground motion, the increased hoop tension  $P_2$  per inch of shell height can be obtained from the following expression:

$$P_2 = P_1 + P_2 \quad (23)$$

where  $P_1$  is the tension due to the impulsive force and  $P_2$  is that due to the convective force.

For tanks where  $D/H$  is greater than 1.333,  $P_1$  may be determined from the following formula:

$$P_1 = 4.5 Z I C_1 G C H \left[ \frac{Y}{H} - \frac{1}{2} \left( \frac{Y}{H} \right)^2 \right] \tanh \left( 0.256 \frac{D}{H} \right) \quad (24)$$

where  $Y$  is the distance in feet from the liquid surface to the point under consideration. As can be seen,  $P_1$  is zero at the surface and maximum at the bottom ( $Y = H$ ). Where  $D/H$  is less than 1.333,  $P_1$  may be determined as follows:

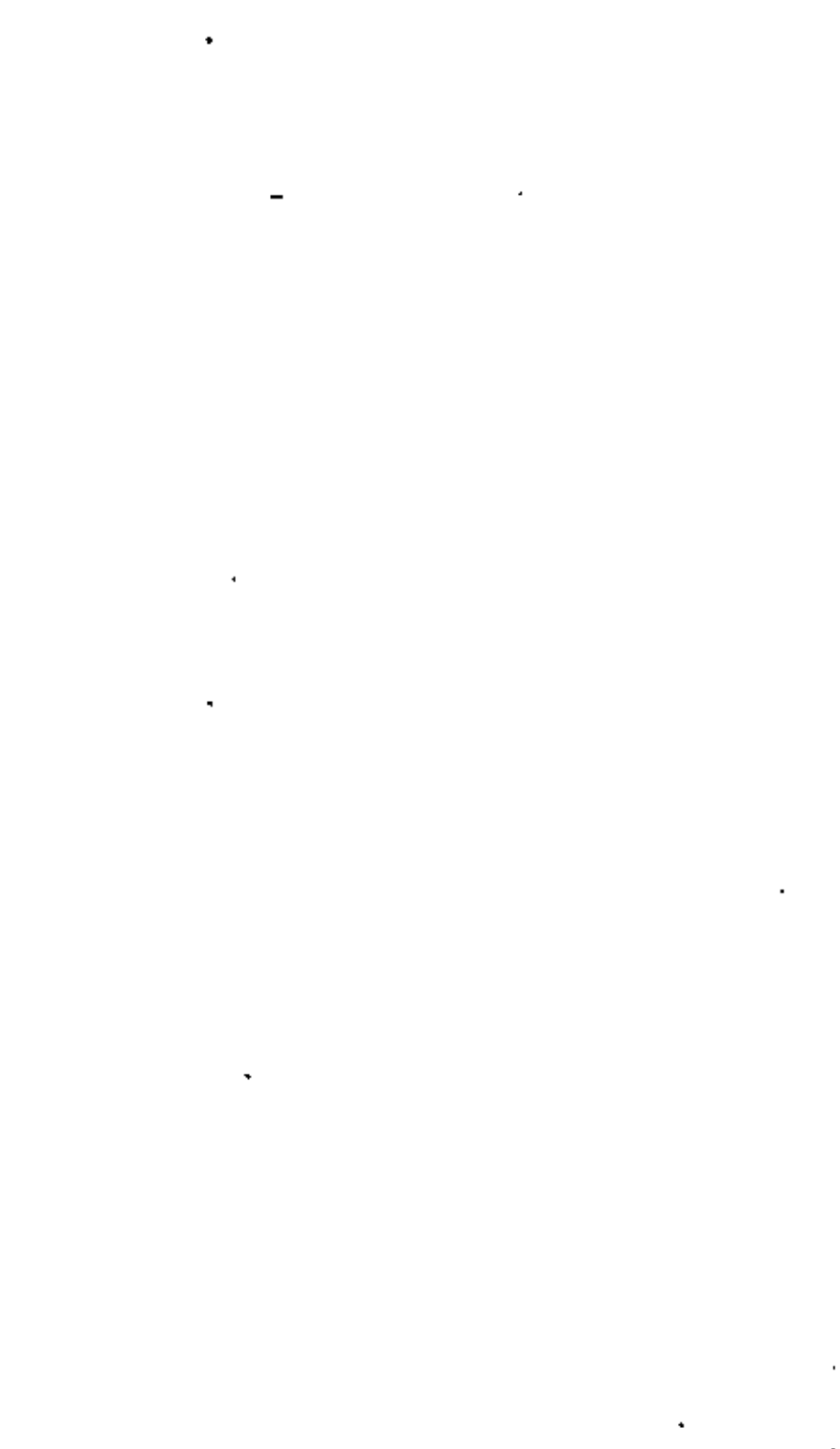
$Y < 0.75D$ :

$$P_1 = 2.77 Z I C_1 G C^2 \left[ \frac{Y}{0.75D} - \frac{1}{2} \left( \frac{Y}{0.75D} \right)^2 \right] \quad (25a)$$

$Y > 0.75D$ :

$$P_1 = 1.384 Z I C_1 G C^2 \quad (25b)$$

The convective hoop tension,  $P_2$  may be determined from the following formula:



NOMENCLATURE

$$P_2 = 0.97521C_2 G_0^2 \frac{\cosh\left(3.68 \frac{H-Y}{D}\right)}{\cosh\left(3.68 \frac{H}{D}\right)} \quad (26)$$

The increased hoop tension due to earthquake ground motion should be added to the hoop tension due to hydrostatic pressure. The hydrodynamic portion of the stress,  $P_2$ , should be divided by a ductility factor of 2.0 for application in the design at normal allowable design tensile stresses.

CONCLUSION

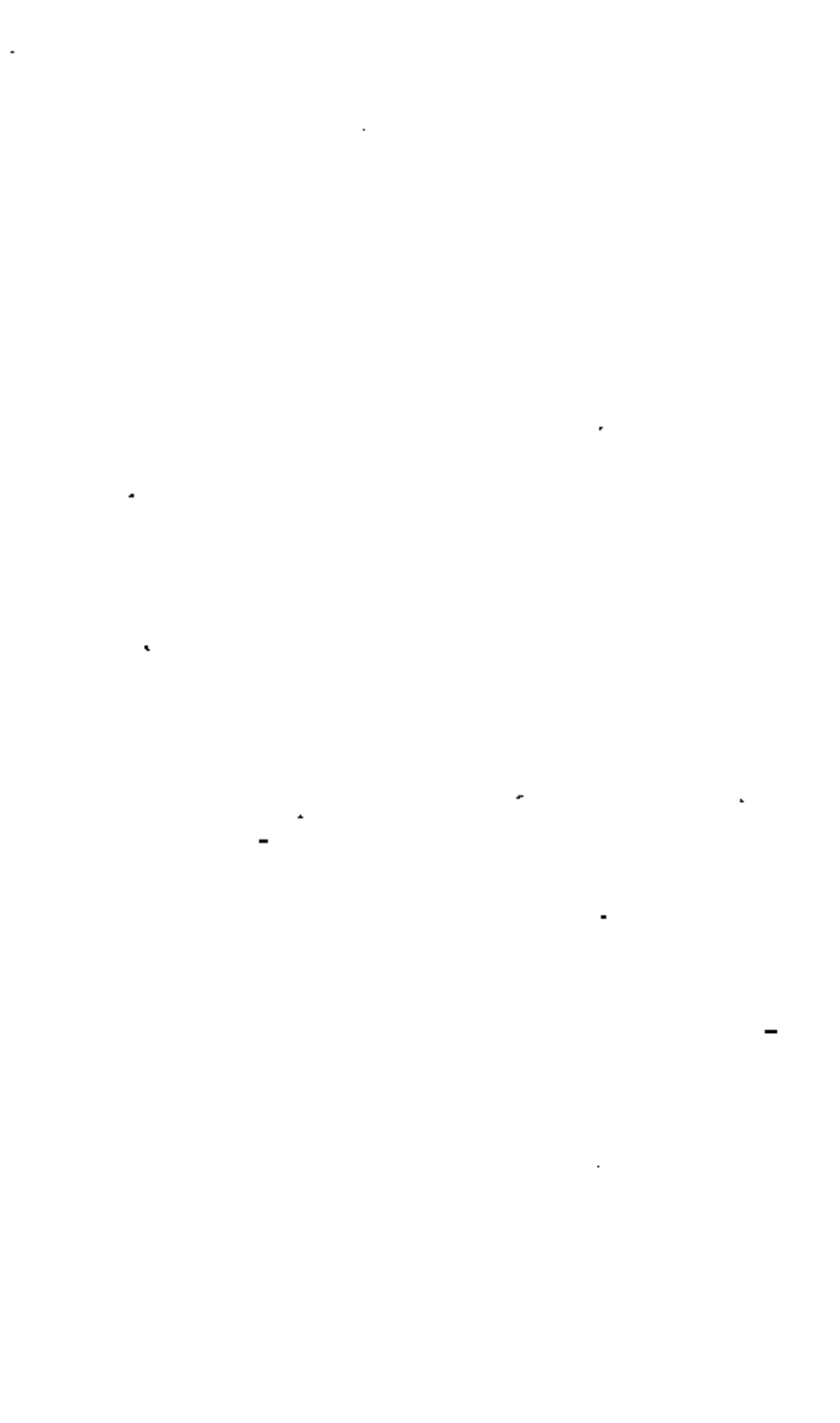
The basis has been presented for the seismic design provisions for oil storage tanks which have been proposed as an appendix (Appendix P) to API Standard 650. The formulas have been given for the curves included in the proposed revision to facilitate design calculations. Supplemental information has been presented to determine the sloshing wave height, the forces on roof supporting columns caused by sloshing and the increased hoop tension due to earthquake ground motion for use when it is desired to take these factors into consideration in the seismic design.

It has been seen that the design provisions are based on the simplified procedure developed by Housner for rigid tanks except that the maximum ground acceleration is replaced with the spectral value of the pseudo-acceleration corresponding to the fundamental natural frequency of the tank-fluid system as suggested by Veletsos. Provisions are included to insure stability of the tank shell against overturning and to preclude buckling of the tank shell due to longitudinal compression; however, further study of these effects are recommended.

- b = maximum longitudinal shell compression force, lbs/ft of shell circumference
- C<sub>1</sub>, C<sub>2</sub> = lateral earthquake coefficients for impulsive and convective forces, respectively
- d = height of sloshing wave above mean depth, ft
- D = tank diameter, ft
- E = modulus of elasticity, psi
- F<sub>a</sub> = maximum allowable longitudinal compressive stress in tank shell, psi
- F<sub>by</sub> and F<sub>ty</sub> = minimum specified yield strength of bottom annular ring and tank shell, respectively, psi
- g = acceleration due to gravity = 32.2 ft/sec<sup>2</sup>
- G = specific gravity (1.0 for water)
- H = maximum filling height of tank, ft
- H<sub>t</sub> = total height of tank shell, ft
- I = essential facilities factor
- k = parameter for calculating T<sub>1</sub> (sec<sup>2</sup>/ft)<sup>1/4</sup>
- L = bottom uplift length, ft
- M = overturning moment applied to bottom of tank shell, ft-lbs
- M<sub>p</sub> = plastic bending moment in bottom annular ring, in.-lbs/in.
- p = internal pressure, psi
- P<sub>1</sub>, P<sub>2</sub>, and P<sub>2</sub> = increased hoop tension in tank shell due to impulsive, convective, and total earthquake force, respectively, lbs/in.
- R = tank radius, in.
- S = site amplification factor

- $t$  = thickness of cylindrical shell, in. when used in the design factor  $K$  applied to thickness of bottom shell, except excluding corrosion allowance.
- $t_b$  = thickness of bottom annular ring, in.
- $T$  = sloshing wave period, sec
- $w$  = unit weight on tank bottom, lbs/sq ft
- $w_L$  = maximum weight of tank contents which may be utilized to resist shell overturning moment, lbs/ft of shell circumference.
- $w_c$  = weight of tank shell, lbs/ft of shell circumference
- $w_g$  = total weight of tank roof plus portion of snow load, if any, lbs
- $w_s$  = total weight of tank shell, lbs
- $w_c$  = total weight of tank contents, lbs
- $w_1$  and  $w_2$  = weight of effective masses of tank contents for determining impulsive and convective lateral earthquake forces, lbs
- $x_s$  = height from bottom of tank shell to center of gravity of shell, ft
- $x_1$  and  $x_2$  = height from bottom of tank shell to centroids of impulsive and convective lateral earthquake forces, respectively, for computing  $M$ , ft
- $x_1'$  and  $x_2'$  = height from bottom of tank shell to centroids of impulsive and convective lateral earthquake forces, respectively, for computing total overturning moment on foundation, ft
- $y$  = vertical distance from liquid surface to point on shell being analyzed for hoop tension, ft
- $Z$  = seismic zone coefficient
- $\theta$  = central angle between axis of tank in the direction of earthquake ground motion and point on circumference where shell uplift commences, radians.

1. J. E. Riene, "Oil Storage Tanks, Alaska Earthquake of 1964," The Prince William Sound, Alaska, Earthquake of 1964, Volume II-7, U.S. Department of Commerce, Coast and Geodetic Survey, 1967.
2. R. D. Hanson, "Behavior of Liquid Storage Tanks," The Great Alaska Earthquake of 1964, Engineering, National Academy of Sciences, Washington, D. C., 1973.
3. P. C. Jennings, "Damage of Storage Tanks," Engineering Features of the San Fernando Earthquake, February 9, 1971, Earthquake Engineering Research Laboratory, Cal. Tech., June 1971.
4. R. Musid, A. F. Espinosa and J. de las Casas, "The Lima Earthquake of October 3, 1974: Damage Distribution," Bulletin of the Seismological Society of America, Volume 67, No. 5, pp. 1441-1472, October 1977.
5. G. W. Housner, "Dynamic Pressures on Accelerated Fluid Containers," Bulletin of the Seismological Society of America, Volume 47, pp. 15-30, January, 1957.
6. Lockheed Aircraft Corporation and Holmes & Narver, Inc., Nuclear Reactors and Earthquakes, Chapter 6 and Appendix F, ERDA TID 7024, pp. 183-195 and 167-199, August 1963.
7. A. S. Veletsos and J. Y. Yang, "Earthquake Response of Liquid-Storage Tanks," Advances in Civil Engineering Through Engineering Mechanics, Proceedings Second Annual Engineering Mechanics Division Specialty Conference, ASCE, pp. 1-24, May 1977.
8. ATC-3-05, "Recommended Comprehensive Seismic Design Provisions for Buildings," Final Review Draft, Applied Technology Council, Palo Alto, California, January 1977.
9. R. S. Hozniak, "Lateral Seismic Loads on Flat Bottomed Tanks," Chicago Bridge & Iron Company, The Water Tower, November 1971.
10. D. P. Clough, "Experimental Evaluation of Seismic Design Methods for Broad Cylindrical Tanks," University of California Earthquake Engineering Research Center Report Number UCB/EEAS-77/10, May 1977.



SEISMIC DESIGN OF STORAGE TANKS

11. C. D. Miller, "Buckling of Axially Compressed Cylinders," Journal of the Structural Division, ASCE, Volume 103, No. ST3, Proc. Paper 12823, pp. 695-721, March 1977.
12. H. Lo, H. Crate and E. B. Schwartz, "Buckling of Thin-Walled Cylinders Under Axial Compression and Internal Pressure," NACA TN 2021, 1950.

P.1 SCOPE

This appendix establishes recommended minimum basic requirements for the design of storage tanks subjected to seismic load as specified by purchaser. These requirements represent accepted practice for application to flat bottom tanks. However, it is recognized that other procedures and applicable factors or additional requirements may be specified by the purchaser or jurisdictional authorities. Any deviation from the requirements herein must be by agreement between purchaser and manufacturer.

P.2 INTRODUCTION

The design procedure considers two response modes of the tank and its contents: (1) the relatively high frequency amplified response to lateral ground motion of the tank shell and roof together with a portion of the liquid contents which moves in unison with the shell, and (2) the relatively low frequency amplified response of a portion of the liquid contents in the fundamental sloshing mode. The design requires the determination of the hydrodynamic seas associated with each mode and the lateral force and overturning moment applied to the shell resulting from the response of the masses to lateral ground motion. Provisions are included to assure stability of the tank shell against overturning and to preclude buckling of the tank shell due to longitudinal compression.

No provisions are included regarding the increase in hoop tension due to seismic forces since this does not affect shell thickness for the lateral force coefficients specified herein taking into account generally accepted increased allowable stress and ductility ratios.

P.3 DESIGN LOADING

P.3.1 Overturning Moment

The overturning moment due to seismic forces applied to the bottom of the shell shall be determined as follows:

$$M = .2I(C_1W_0X_0 + C_1W_rX_r + C_1W_1X_1 + C_2W_2X_2)$$

Where:

- M = Overturning moment in foot pounds applied to bottom of tank shell.
- Z = Zone coefficient from Figure P-1 and Table P-1.
- I = Essential facilities factor. I = 1.5 for tanks which need be functional for emergency post earthquake operations and 1.0 for all other tanks.
- C<sub>1</sub> and C<sub>2</sub> = Lateral earthquake force coefficients determined per paragraph P.3.3.
- W<sub>S</sub> = Total weight in pounds of tank shell.
- X<sub>S</sub> = Height in feet from bottom of tank shell to center of gravity of shell.
- W<sub>T</sub> = Total weight in pounds of tank roof plus portion of snow load, if any, as specified by purchaser.
- H<sub>T</sub> = Total height in feet of tank shell.
- W<sub>1</sub> = Weight in pounds of effective mass of tank contents which moves in unison with tank shell, determined per paragraph P.3.2(a).
- X<sub>1</sub> = Height in feet from bottom of tank shell to centroid of lateral seismic force applied to W<sub>1</sub>, determined per paragraph P.3.2(b).
- W<sub>2</sub> = Weight in pounds of effective mass of first mode sloshing contents of tank, determined per paragraph P.3.2(a).
- X<sub>2</sub> = Height in feet from bottom of tank shell to centroid of lateral seismic force applied to W<sub>2</sub>, determined per paragraph P.3.2(b).

Note: The overturning moment determined per this paragraph is that applied to the bottom of the shell only. The tank foundation is subjected to an additional overturning moment due to lateral displacement of the tank contents which may need to be considered in the design of some foundations such as pile supported concrete mats.

### P.3.2 Effective Mass of Tank Contents

- a. The effective mass W<sub>1</sub> and the effective mass W<sub>2</sub> may be determined by multiplying W<sub>T</sub> by the ratios W<sub>1</sub>/W<sub>T</sub> and W<sub>2</sub>/W<sub>T</sub>, respectively, obtained from Figure P-2 for the ratio D/H.

Where:

W<sub>T</sub> = Total weight in pounds of tank contents (product specific gravity specified by purchaser).

D = Tank diameter in feet.

H = Maximum filling height of tank in feet from bottom of shell to top of top angle or overflow which limits filling height.

- b. The heights from the bottom of the tank shell to the centroids of the lateral seismic forces applied to W<sub>1</sub> and W<sub>2</sub>, X<sub>1</sub> and X<sub>2</sub>, may be determined by multiplying H, by the ratios X<sub>1</sub>/H and X<sub>2</sub>/H, respectively, obtained from Figure P-3 for the ratio of D/H.
- c. The curves in Figures P-2 and P-3 are based on a modification of the equations presented in ERDA Technical Information Document 7024. Alternatively, W<sub>1</sub>, W<sub>2</sub>, X<sub>1</sub> and X<sub>2</sub> may be determined by other analytical procedures based on the dynamic characteristics of the tank.

### P.3.3 Lateral Force Coefficients

- a. The lateral force coefficient C<sub>1</sub> shall be taken as 0.24.

Technical Information Document 7024, Nuclear Reactors and Earthquakes, prepared by Lockheed Aircraft Corporation, and Holmes & Narver, Inc., for the U.S. Atomic Energy Commission, August 1963.

- b. The lateral force coefficient  $C_2$  shall be determined as a function of the natural period of the first mode sloshing,  $T$ , and the soil conditions at the tank site.

When  $T$  is less than 4.5:

$$C_2 = \frac{0.30 S}{T}$$

When  $T$  is greater than 4.5:

$$C_2 = \frac{1.35 S}{T^2}$$

where:

$S$  = Site amplification factor from Table P-2.

$T$  = Natural period in seconds of first mode sloshing.  $T$  may be determined from the following expression:

$$T = \kappa D^3$$

$\kappa$  = Factor obtained from Figure P-4 for the ratio  $D/H$ .

- c. Alternatively,  $C_1$  and  $C_2$  may be determined from response spectra established for the specific site of the tank and for the dynamic characteristics of the tank. The spectrum for  $C_1$  should be established for a damping coefficient of 2% of critical and scaled to a maximum amplified acceleration of 0.24 times the acceleration of gravity. The spectrum for  $C_2$  should correspond to the spectrum for  $C_1$  except modified for a damping coefficient of 0.5% of critical.

#### 4. RESISTANCE TO OVERTURNING

Resistance to the overturning moment at the bottom of the shell may be provided by the weight of the tank shell and by the weight of a portion of the tank contents adjacent to the shell for unanchored tanks or by anchorage of the tank shell. For unanchored tanks, the portion of the contents which may be utilized to resist overturning is

dependent on the width of the bottom annular ring which lifts off the foundation and may be determined as follows:

$$w_L = 7.9 t_b \sqrt{F_{by} G H}$$

except that  $w_L$  shall not exceed 1.25  $GHD$ .

Where:

$w_L$  = Maximum weight of tank contents in pounds per foot of shell circumference which may be utilized to resist the shell overturning moment.

$t_b$  = Thickness of bottom annular ring in inches.

$F_{by}$  = Minimum specified yield strength in pounds per square inch of bottom annular ring.

$G$  = Design specific gravity of contents as specified by purchaser.

- b. The thickness of the bottom annular ring,  $t_b$ , shall not exceed the thickness of the bottom shell course, or 4 inch, whichever is greater. Where the bottom annular ring is thicker than the remainder of the bottom, the width of the annular ring in feet shall be equal to or greater than:

$$0.0274 \frac{w_L}{G H}$$

#### P.5 SHELL COMPRESSION

##### P.5.1 Unanchored Tanks

The maximum longitudinal compression force at the bottom of the shell may be determined as follows:

When  $\frac{M}{G^2(w_L + w_c)}$  is equal to or less than 0.785:

$$b^* = w_L + \frac{1.273 M}{D^2}$$

When  $\frac{M}{D^2(w_L + w_L)}$  is greater than 0.785:

b may be computed from the value of the parameter  $\frac{b+w_L}{w_L+w_L}$  obtained from Figure P-5.

Where:

b = Maximum longitudinal shell compression force in pounds per foot of shell circumference.

w<sub>L</sub> = Weight of tank shell in pounds per foot of shell circumference.

### 5.2 Anchored Tanks

The maximum longitudinal compression force at the bottom of the shell may be determined as follows:

$$b = w_L + \frac{1.273 M}{D^2}$$

### 5.3 Maximum Allowable Shell Compression

The maximum longitudinal compressive stress in the shell,  $\frac{F_A}{t}$ , shall not exceed the maximum allowable stress,  $F_{Ay}$ , determined as follows:

When the value of  $\frac{GH D^2}{t^2}$  is greater than 200,000:

$$F_A = \frac{800,000 t}{D}$$

When the value of  $\frac{GH D^2}{t^2}$  is less than 200,000:

$$F_A = \frac{400,000 t + 2 GH D}{D}$$

Except that in no case shall the value of  $F_A$  exceed  $0.5 F_{Ay}$ .

Where:

t = Thickness in inches, excluding corrosion allowance, of the bottom shell course.

F<sub>A</sub> = Maximum allowable longitudinal compressive stress in the shell in pounds per square inch. The above formulas for F<sub>A</sub> take into account the effect of internal pressure due to the liquid contents.

F<sub>Ay</sub> = Minimum specified yield strength of the shell in pounds per square inch.

### P.6 ANCHORAGE OF TANKS

Anchorage of tanks shall be designed to provide a minimum anchorage resistance in pounds per foot of shell circumference of:

$$\frac{1.273 M}{D^2}$$

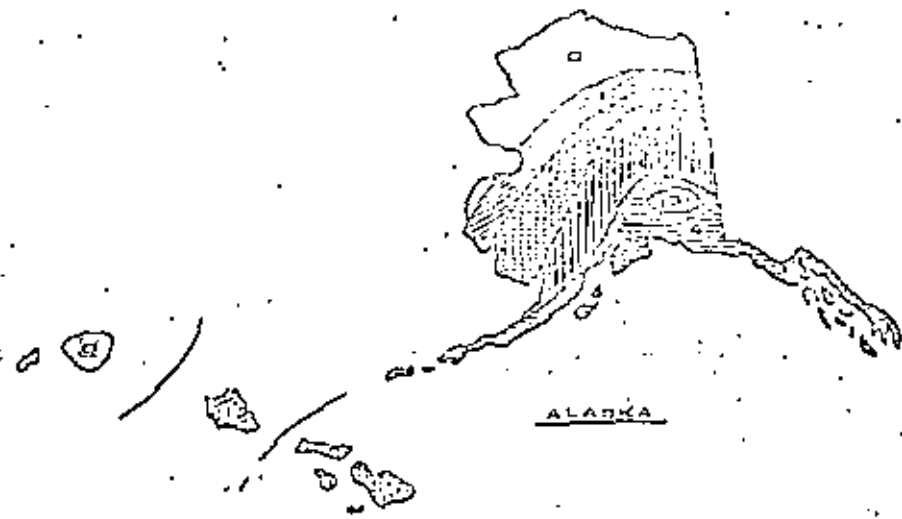
The stresses due to anchor forces in the tank shell at the points of attachment of the anchors shall be investigated.

### P.7 PIPING

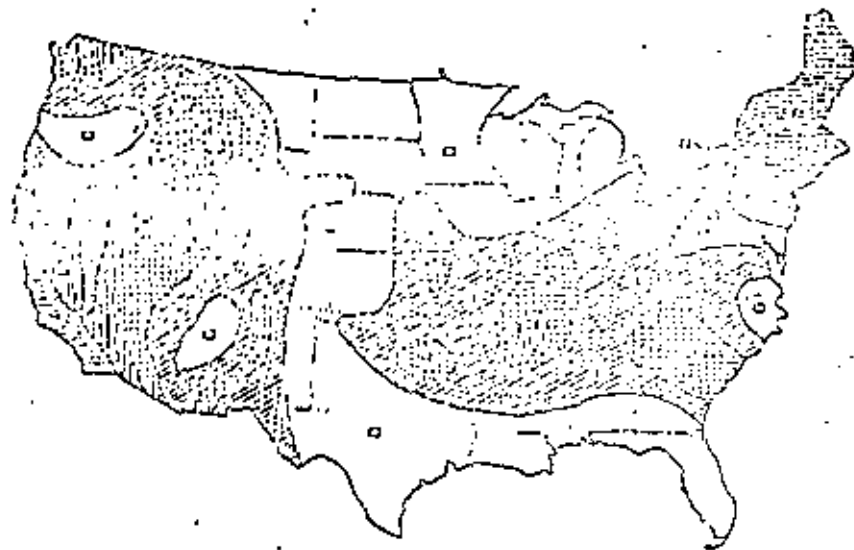
Provisions for suitable flexibility in all piping attached to the shell or bottom of the tank shall be considered. On unanchored tanks subject to bottom uplift, piping connected to the bottom shall be free to lift with the bottom or shall be located so that the horizontal distance measured from the shell to the edge of the connecting reinforcement shall be the width of the bottom hold down as calculated in paragraph P.4(b) plus 12 inches.

### P.8 ADDITIONAL CONSIDERATIONS

- a. The purchaser shall specify any freeboard desired to minimize or avoid overflow and damage to the roof and upper shell due to sloshing of the liquid contents.
- b. The base of the roof supporting column shall be restrained to prevent lateral movement during earthquakes. When specified by the purchaser, the columns shall be designed to resist the forces caused by the sloshing of the liquid contents.



HAWAII



SEISMIC ZONE MAP  
FIGURE P-1

$$\frac{W_2}{W_T} \text{ or } \frac{V_1}{V_T}$$

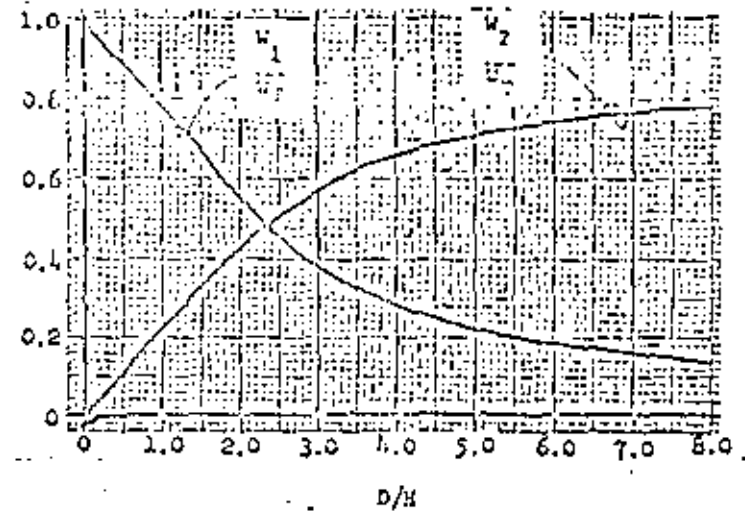


FIGURE P-2

$$\frac{X_1 \text{ or } X_2}{H}$$

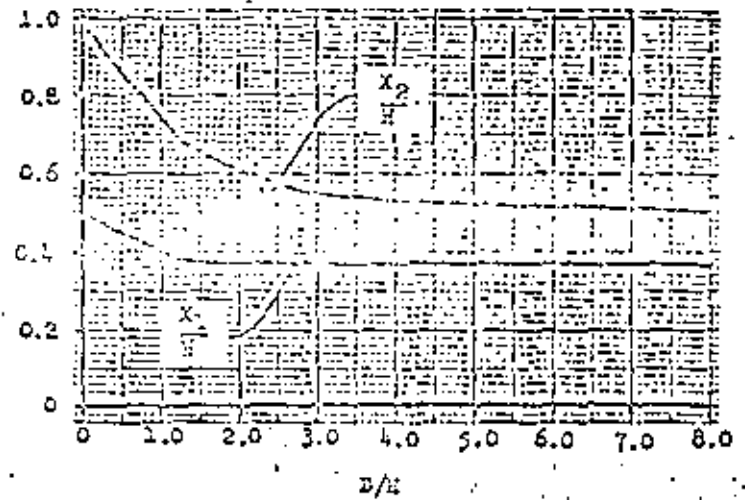


FIGURE P-3



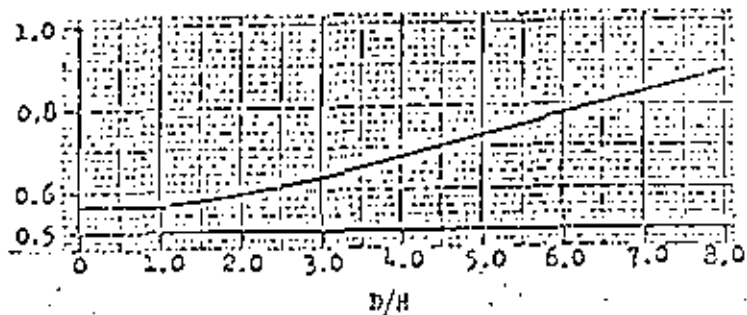


FIGURE P-1

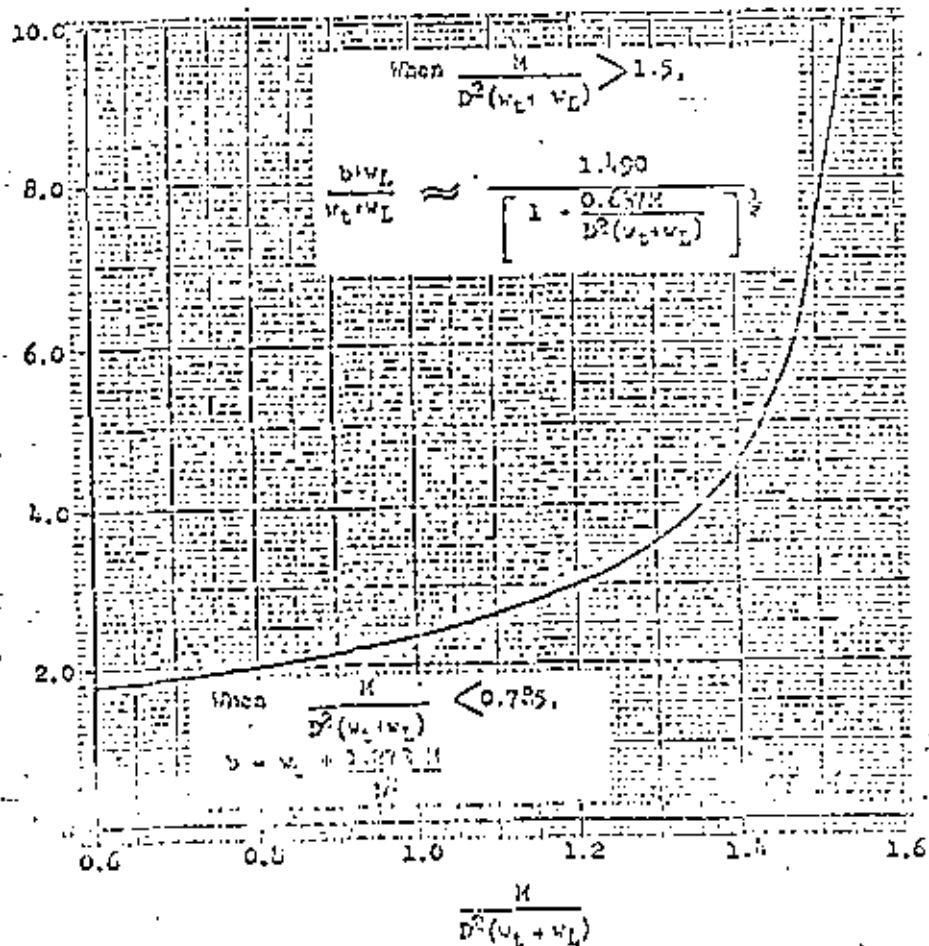


FIGURE P-5

ZONE COEFFICIENT

Seismic Zone Per Figure P-1

	1	2	3	4
Z	0.1875	0.375	0.75	1.0

No earthquake design required for Zone 0.

TABLE P-1

SOIL PROFILE COEFFICIENT

Soil Profile Type

	A	B	C
S	1.0	1.2	1.5

SOIL PROFILE TYPE A is a profile with:

1. Rock of any characteristic, either shale-like or crystalline in nature. Such material may be characterized by a shear wave velocity greater than 2,500 feet per second, or
2. Stiff soil conditions where the soil depth is less than 200 feet and the soil types overlying rock are stable deposits of sands, gravels, or stiff clays.

SOIL PROFILE TYPE B is a profile with deep cohesionless or stiff clay conditions, including sites where the soil depth exceeds 200 feet and the soil types overlying rock are stable deposits of sands, gravels, or stiff clays.

SOIL PROFILE TYPE C is a profile with soft-to-medium-stiff clays and sands, characterized by 30 feet or more of soft-to-medium-stiff clay with or without intervening layers of sand or other cohesionless soils.

In locations where the soil profile type is not known in sufficient detail to determine the soil profile type, Soil Profile C shall be assumed.

TABLE P-2



APPENDIX 2

HORIZONTAL FORCES ON COLUMNS CAUSED BY SLOSHING OF FLUID IN CYLINDRICAL TANKS

The following presentation is considered a reasonable approximation for the determination of seismic induced loads on columns.

The total horizontal force acting per foot of column length includes the drag force, inertial force, acceleration force of the column mass, and the acceleration force of an effective column of water. The acceleration force of the column and its effective water mass are functions of the seismic factor. The drag and inertial forces are functions of the fluid velocity,  $u$ , and acceleration,  $\ddot{u}$ .

$$u = \frac{2d_0 \dot{T}}{D} \frac{\cosh \pi \left( \frac{H-Y}{D} \right) \cos 2\pi \frac{Y}{D} \cos \pi \frac{X}{D}}{\cosh \pi \frac{H}{D}} \quad (1)$$

$$\ddot{u} = \frac{4\pi d_0 \ddot{g}}{D} \frac{\cosh \pi \left( \frac{H-Y}{D} \right) \sin 2\pi \frac{Y}{D} \cos \pi \frac{X}{D}}{\cosh \pi \frac{H}{D}} \quad (2)$$

The average force per foot of column is:

$$\overline{F_T} = \frac{1}{H} \int_0^H dF_d + \frac{1}{H} \int_0^H dF_i + ZIC_1(m_c + m_w)$$

here:  $F_d = C_D \rho D_c \frac{u|u|}{2}$

$$F_i = C_M \rho \frac{\pi D_c^2}{4} \ddot{u}$$

Equation (3) may be applied to circular and rectangular shaped interior columns. For circular columns,  $D_c$  is the maximum dimension of the member cross-section as shown in Figure 1. The analysis for rectangular columns is based on an equivalent circular column with diameter  $D_c$ . The drag factor is corrected for rectangular column to account for the additional resistance to flow.

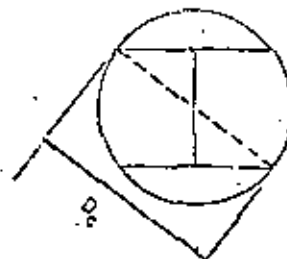


FIG 1

Substituting Equation (1) and (2) into Equation (3) and integrating yields the following average force per foot of column:

$$\overline{F_T} = \frac{C_D \rho D_c \left( \frac{2d_0}{D} \right)^2}{2\pi H D} \frac{\cos 2\pi \frac{Y}{D} \cos \pi \frac{X}{D} \left| \cos 2\pi \frac{Y}{D} \cos \pi \frac{X}{D} \right|}{\cosh^2 \left( \pi \frac{H}{D} \right)} \left( \sinh 2\pi \frac{H}{D} + 2\pi \frac{H}{D} \right) + \frac{\pi C_M \rho D_c^2 d_0}{H} \frac{\sin 2\pi \frac{Y}{D} \cos \pi \frac{X}{D} \sinh \pi \frac{H}{D}}{\cosh \pi \frac{H}{D}} + ZIC_1(m_c + m_w) \quad (4)$$

The solution of Equation (4) is a function of time and location of the column in the tank. An iteration with time over the period of the sloshing wave is necessary to search out the maximum column load.

For simplicity, the design of the column for combined beam-column action is made assuming the seismic load acts uniformly over the full height of the column rather than the fluid height. It is recommended that AISC primary column allowables be used in the beam-column design since secondary



column allowables have safety factors too low to allow an additional increase for the seismic load.

#### NOMENCLATURE FOR APPENDIX 2

The following defines terms used in Appendix 2 only. For other terms, see the Nomenclature following the main body of the paper.

$C_D$  = drag coefficient. A value of 1.0 is recommended for round columns and 1.5 for wide flange structural shapes.

$C_M$  = mass coefficient. A value of 2.0 is recommended.

$D_c$  = maximum cross-section dimension of column, ft.

$F_D$  and  $F_I$  = drag and inertia force on column, lb/ft.

$F_T$  = average total force on column, lb/ft.

$m_c$  = column weight, lb/ft.

$m_w$  = weight of effective column of water, lb/ft.

$$m_w = \frac{\pi D_c^2}{4} \rho_f$$

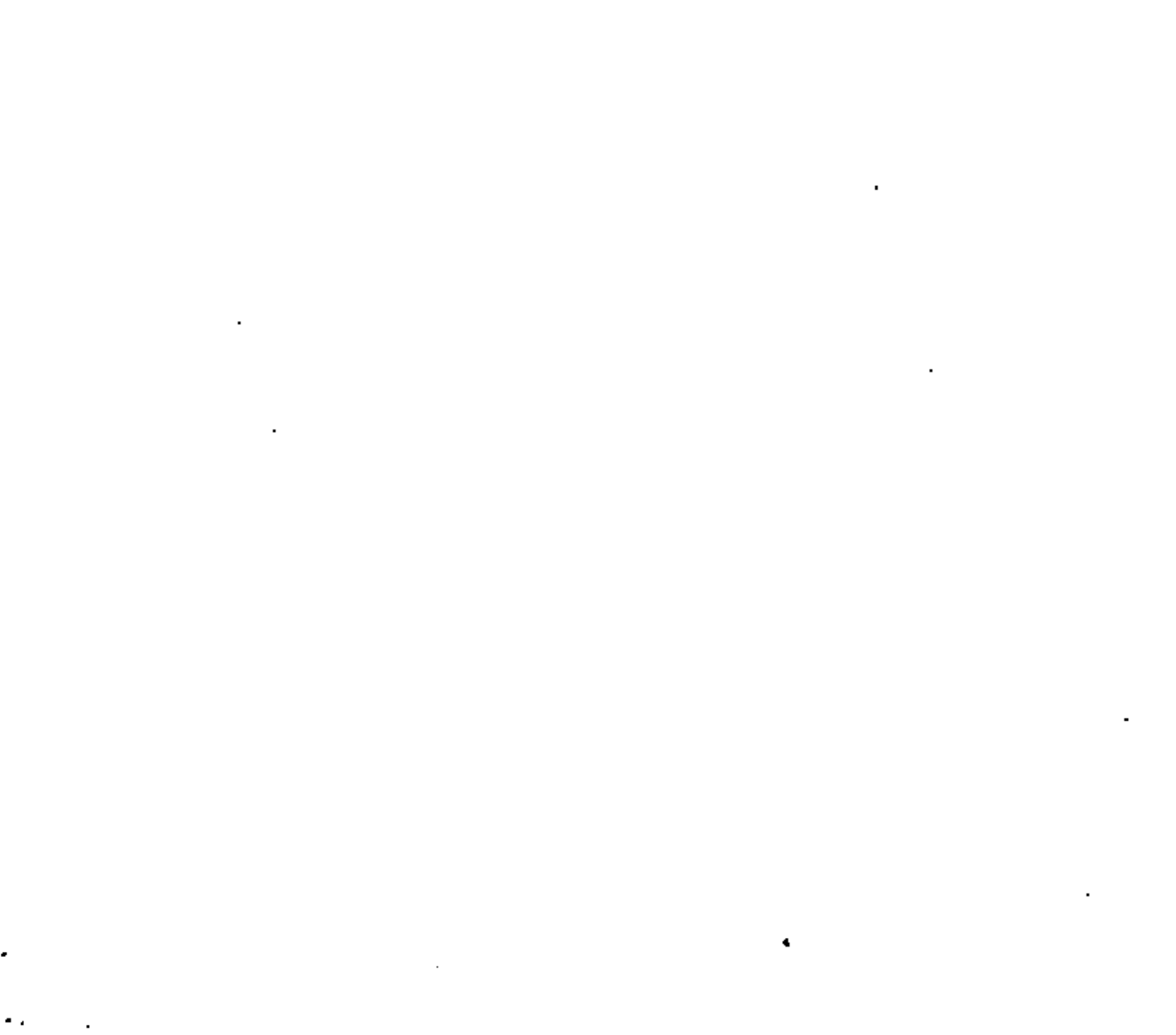
$u$  = fluid particle velocity, ft/sec.

$\dot{u}$  = fluid particle acceleration, ft/sec.<sup>2</sup>

$x$  = horizontal distance in direction of earthquake force from center of tank to center of column, ft.

$\rho$  = mass of fluid, lb-sec<sup>2</sup>/ft.<sup>3</sup>

$\tau$  = time from beginning of wave cycle, sec.  $\tau$  varies from 0 to  $T$ .





DIVISION DE EDUCACION CONTINUA  
FACULTAD DE INGENIERIA U.N.A.M.

VII CURSO INTERNACIONAL DE INGENIERIA SISMICA

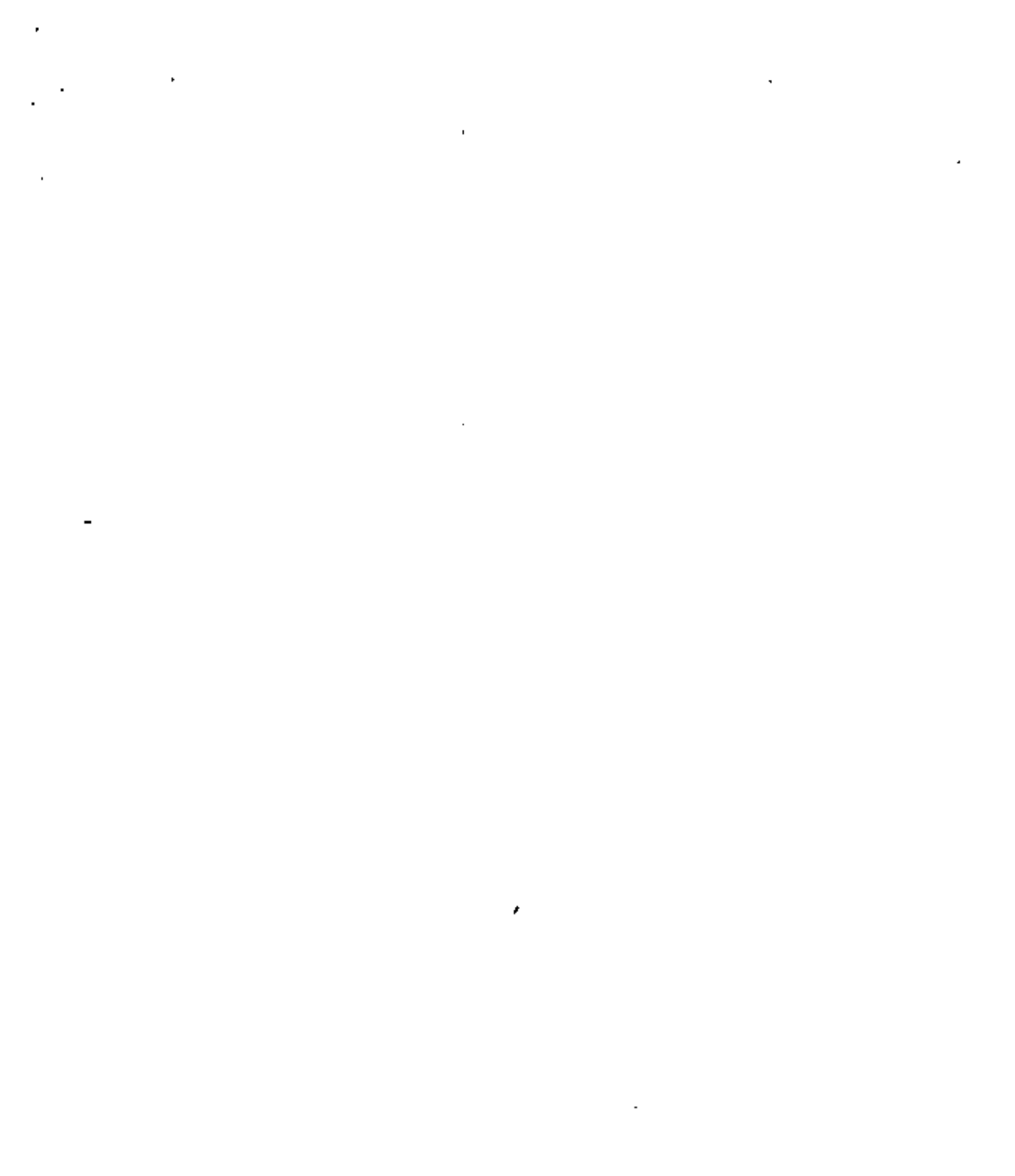
DISEÑO SISMICO DE ESTRUCTURAS ESPECIALES

DISEÑO SISMICO DE CHIMENEA

Ejemplo ilustrado

Por M en I Neftalí Rodríguez Cuevas

Julio, 1981



## EJEMPLO DE ANALISIS DINAMICO DE UNA CHIMENEA

### a) Aspectos generales

Se ilustra a continuación la secuencia de análisis que previamente se discutió, aplicada al cálculo dinámico de una chimenea de concreto de 80 m de altura, construida en la zona del Bajo Río Días, en donde se presentan las condiciones más severas de diseño desde el punto de vista sísmico.

La geometría de la chimenea queda definida por las alturas  $H_1 = 202.4$  m y  $H_2 = 246.40$  m que son las distancias desde la parte superior de la chimenea, hasta el vértice de los conos que definen el manto exterior e interior respectivamente, del fuste de la chimenea.

El radio inferior externo del fuste se consideró igual a  $R_{11} = 4.025$  m, mientras que el radio interior  $R_{12} = 4.125$  m en la sección transversal de la base de la chimenea.

Se consideró que el módulo de elasticidad del concreto era igual a  $2.5 \times 10^6$  ton/m<sup>2</sup> y su resistencia última  $f'_c = 2500$  ton/m<sup>2</sup>, con un peso volumétrico de 2.4 ton/m<sup>3</sup> y un módulo de Poisson igual a 0.15.

Se aceptó la existencia de conos de tabique refractario, con un peso volumétrico de 2.3 ton/m<sup>3</sup>, mortero con peso volumétrico de 0.55 ton/m<sup>3</sup> y recubrimiento de la cámara de ventilación con peso volumétrico de 2 ton/m<sup>3</sup>. Se aceptó que los conos de material refractario tuviesen un espesor de 0.23 m, con capa de mortero de 0.003 m y recubrimiento de 0.065 m. Para todas las cámaras de ventilación, se consideró una separación de 0.07 m entre el fuste y el cono de material refractario.

Se aceptó la existencia de ménsulas rectangulares de soporte de los conos, con dimensiones  $b=0.365$  y  $h=0.40$ , situados a distancias de 10 m. Esto formó la idealización de la chimenea como un sistema de masas concentradas, situadas a 10 m de distancia. En la tabla I se muestran las características geométricas y distribución de masas de la chimenea en estudio.

Para obtener la respuesta del análisis dinámico, se seleccionó un espectro con coeficiente sísmico máximo igual a 0.73, con ordenada al origen igual a 0.30; el período característico inferior se consideró igual a 0.4 seg y el período característico mayor igual a 1 seg; la rama descendente del espectro se consideró representada por un exponente 1.0 y se aceptó un factor de ductilidad igual a 2.0.

La respuesta de la chimenea se analizó tomando en consideración el efecto de la fuerza cortante y de la flexión y se despreció el

Sección	Radio exterior	Radio interior	Volumen	Peso	Masa del fuste	Momento de inercia	Masa de la ménsula	Masa del revestimiento
1	3.3148 3.3957	3.1140 3.1772	45.366	100.079	11.099	24.519	0.727	12.500
2	3.4785 3.5605	3.2403 3.3035	55.432	113.035	13.591	32.674	0.756	13.035
3	3.6424 3.7242	3.3567 3.4299	66.178	159.828	15.190	47.393	0.784	13.569
4	3.8061 3.8880	3.4931 3.5563	77.607	106.257	16.936	53.047	0.812	14.104
5	3.9699 4.0518	3.6195 3.6827	89.713	215.322	21.049	67.220	0.841	14.639
6	4.1337 4.2156	3.7452 3.8081	102.510	243.024	25.079	82.702	0.869	15.174
7	4.2975 4.3793	3.8722 3.9354	115.904	270.351	28.375	100.493	0.897	15.703
8	4.4612 4.5431	3.9926 4.0513	130.140	312.335	31.033	120.302	0.900	16.243

3.

efecto de inercia rotacional. Para el cálculo de las deformaciones de cortante se consideró un factor de forma igual a 1.5.

b) Secuencia de análisis

El análisis fue realizado mediante un ordenador digital que siguió la siguiente secuencia:

1) Cálculo el volumen de concreto del fuste y de las ménsulas de la chimenea, así como del revestimiento interior, mediante el sistema de Pappus, y con estos datos obtiene la masa, a la cual concentra en las ménsulas, seleccionadas como puntos de concentración de las masas de la chimenea.

2) Calcula, en base a métodos de flexibilidades, la matriz de rigideces de la estructura, usando métodos numéricos.

3) Transforma el problema en un problema de valores característicos y define los valores de las frecuencias naturales, las formas características modales y los coeficientes de participación modal mediante el algoritmo de Jacobi.

4) A partir de un espectro de coeficiente sísmico, calcula la respuesta sísmica modal, siguiendo tres criterios diferentes, para el cálculo de la respuesta. En el primer caso, la respuesta se obtiene mediante  $R_1 = \sqrt{\sum_{i=1}^n R_i^2}$  y en el segundo caso  $R_2 = \sqrt{\sum_{i=1}^n R_i}$  y el tercer criterio, resulta ser el valor medio de los dos casos anteriores.

5) Grafica las curvas que definen a la configuración deformada máxima, la representativa del diagrama de fuerza cortante y el diagrama de momento flexionante inducidos por la acción sísmica.

c) Resultados obtenidos

$[R] =$

$+78917E+5$	$-15457E+6$	$+67144E+5$	$+12105E+5$	$-19012E+4$	$-15042E+4$	$-34869E+3$	$-12592E+2$
$-15457E+6$	$+70055E+6$	$-29370E+5$	$+37311E+5$	$+23931E+5$	$+33273E+4$	$-85642E+3$	$-56948E+3$
$+67144E+5$	$-29370E+5$	$+43230E+5$	$-26055E+6$	$+53320E+4$	$+22775E+5$	$+75476E+4$	$+25357E+3$
$+12105E+5$	$+37311E+5$	$-26055E+6$	$+43326E+5$	$-23592E+6$	$-11725E+5$	$+12690E+5$	$+62164E+4$
$-19012E+4$	$+23931E+5$	$+53320E+4$	$-23592E+6$	$+41041E+6$	$-21693E+6$	$-27661E+5$	$+36032E+4$
$-15042E+4$	$+33273E+4$	$+22775E+5$	$-11725E+5$	$-21493E+5$	$+40512E+6$	$-19691E+6$	$-35657E+5$
$-34869E+3$	$-85642E+3$	$+75476E+4$	$+15590E+3$	$-27651E+5$	$-19591E+6$	$+41913E+6$	$-12592E+2$
$-12592E+2$	$-56948E+3$	$+25357E+3$	$+62164E+4$	$+35070E+4$	$-35657E+5$	$-12592E+2$	$+55641E+6$

b) MATRIZ DE MASAS

$[M] =$

$.55494E+1$	0	0	0	0	0	0	0
0	$.25557E+2$	0	0	0	0	0	0
0	0	$.28666E+2$	0	0	0	0	0
0	0	0	$.31942E+2$	0	0	0	0
0	0	0	0	$.35304E+2$	0	0	0
0	0	0	0	0	$.33995E+2$	0	0
0	0	0	0	0	0	$.42770E+2$	0
0	0	0	0	0	0	0	$.46713E+2$

a) Formas características de los modos naturales de vibración

Forma Modo	Primero	Segundo	Tercero	Cuarto	Quinto	Sexto	Séptimo	Octavo
1	$+146226E+0$	$-172315E+0$	$-172782E+0$	$-140679E+0$	$-826670E-1$	$+103981E+0$	$-131317E+0$	$+209272E+0$
2	$+121001E+0$	$-782236E-1$	$-271531E-1$	$-373226E-1$	$-134636E-1$	$-239281E-1$	$-449320E-1$	$-121522E+0$
3	$+936592E-1$	$+540104E-2$	$+709330E-1$	$-215142E-1$	$+799150E-1$	$-644630E-1$	$-360265E-1$	$+105249E+0$
4	$-632957E-1$	$+623951E-1$	$+702543E-1$	$-282544E-1$	$-234922E-1$	$+517343E-1$	$-112399E+0$	$-430010E-1$
5	$+449587E-1$	$+541899E-1$	$-139380E-1$	$-251900E-1$	$-466734E-1$	$+404597E-1$	$-500010E-1$	$+655070E-2$
6	$+759579E-1$	$+733439E-1$	$-699666E-1$	$-319290E-1$	$-313164E+0$	$-104324E+0$	$-423790E-1$	$+371354E-3$
7	$+113912E-1$	$+433300E-1$	$+706561E-1$	$-222947E-1$	$-395514E-1$	$+794502E-1$	$-602372E-2$	$-231745E-1$
8	$+302111E-2$	$+136546E-1$	$-343337E-1$	$-271730E-1$	$-115922E+0$	$-253355E-1$	$-91052E-3$	$-594055E-4$

b) Periodo natural de vibración de cada modo, en seg

$.115463E+1$	$.242343E+0$	$.101426E+0$	$.551930E-1$	$.540310E-1$	$.457174E-1$	$.419152E-1$	$.331541E-1$
--------------	--------------	--------------	--------------	--------------	--------------	--------------	--------------

c) Factores de participación modal

$+405073E+0$	$+112554E-1$	$-132005E-2$	$+442310E-3$	$-223730E-3$	$-605671E-4$	$-464306E-5$	$+132358E-5$
--------------	--------------	--------------	--------------	--------------	--------------	--------------	--------------



SE CALCULAN RESPUESTA PERM PERM EN FUNCION DE 8 MODOS

DESPLAZAMIENTOS

7

DESPLAZAMIENTOS MAXIMOS MODALES

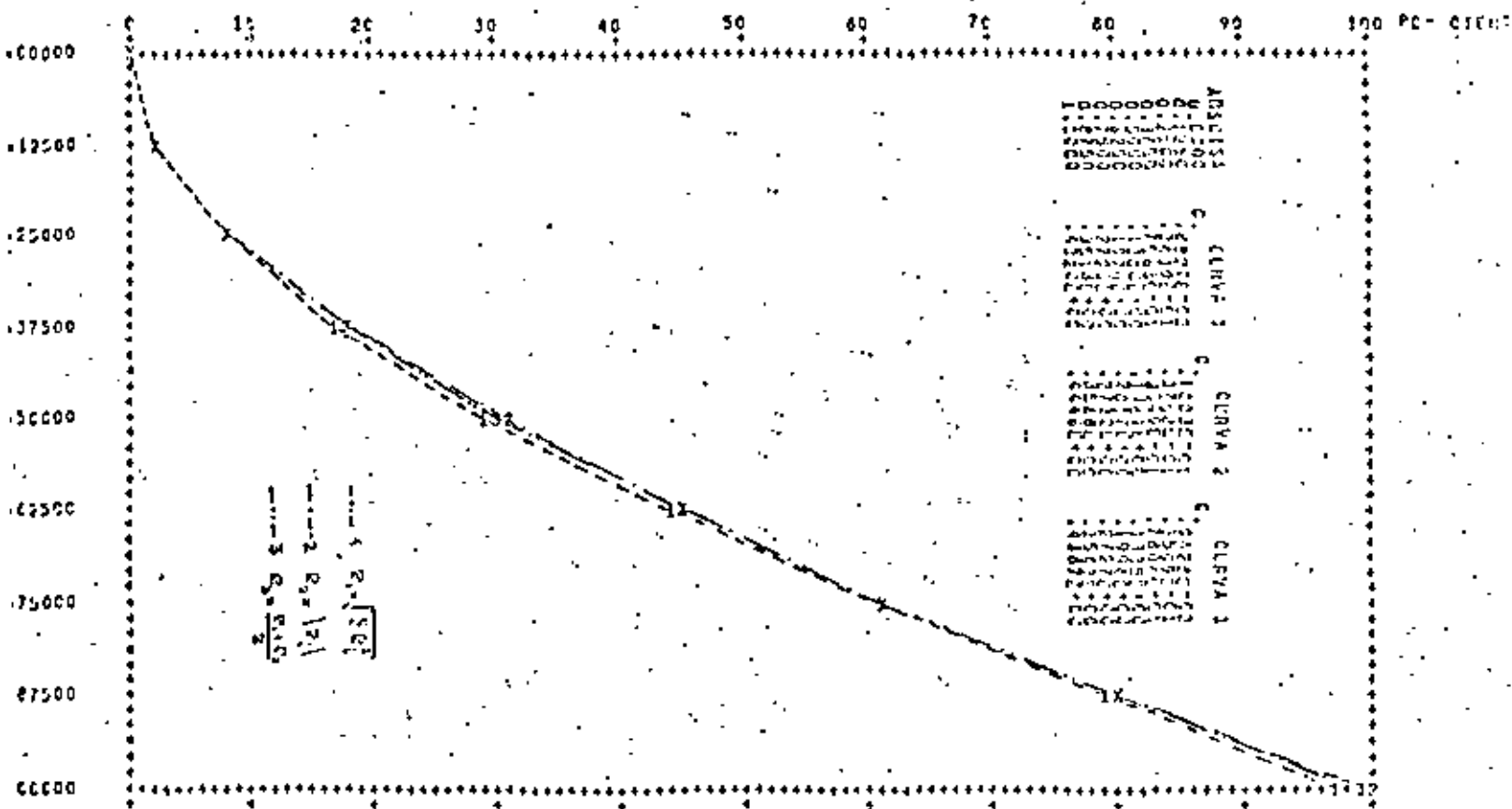
MODO	FASE (1)	FASE (2)	FASE (3)	FASE (4)	FASE (5)	FASE (6)	FASE (7)	FASE (8)
1	0.232200E+00	0.351178E+00	0.400000E+00	0.450000E+00	0.500000E+00	0.550000E+00	0.600000E+00	0.650000E+00
2	0.714400E-01	0.300000E+00	0.400000E+00	0.500000E+00	0.600000E+00	0.700000E+00	0.800000E+00	0.900000E+00
3	0.814400E-01	0.200000E+00	0.300000E+00	0.400000E+00	0.500000E+00	0.600000E+00	0.700000E+00	0.800000E+00
4	0.914400E-01	0.100000E+00	0.200000E+00	0.300000E+00	0.400000E+00	0.500000E+00	0.600000E+00	0.700000E+00
5	0.514400E-01	0.050000E+00	0.100000E+00	0.150000E+00	0.200000E+00	0.250000E+00	0.300000E+00	0.350000E+00
6	0.414400E-01	0.020000E+00	0.040000E+00	0.060000E+00	0.080000E+00	0.100000E+00	0.120000E+00	0.140000E+00
7	0.314400E-01	0.010000E+00	0.020000E+00	0.030000E+00	0.040000E+00	0.050000E+00	0.060000E+00	0.070000E+00
8	0.214400E-01	0.005000E+00	0.010000E+00	0.015000E+00	0.020000E+00	0.025000E+00	0.030000E+00	0.035000E+00

RESPUESTA TOTAL

MAS	R1 = PC(SQ(A*(R+2)))	R2 = ABS(R)	R3 = (R1+R2)/2.0
1	0.314400E+00	0.351178E+00	0.332789E+00
2	0.714400E-01	0.300000E+00	0.507200E-01
3	0.814400E-01	0.400000E+00	0.607200E-01
4	0.914400E-01	0.500000E+00	0.707200E-01
5	0.514400E-01	0.600000E+00	0.807200E-01
6	0.414400E-01	0.700000E+00	0.907200E-01
7	0.314400E-01	0.800000E+00	0.100000E+00
8	0.214400E-01	0.900000E+00	0.200000E+00

8

100 POR CIENTO CORRESPONDE A 444.0000



VALORES NORMALIZADOS DE LA ALTURA -- RELACION DE Z/H



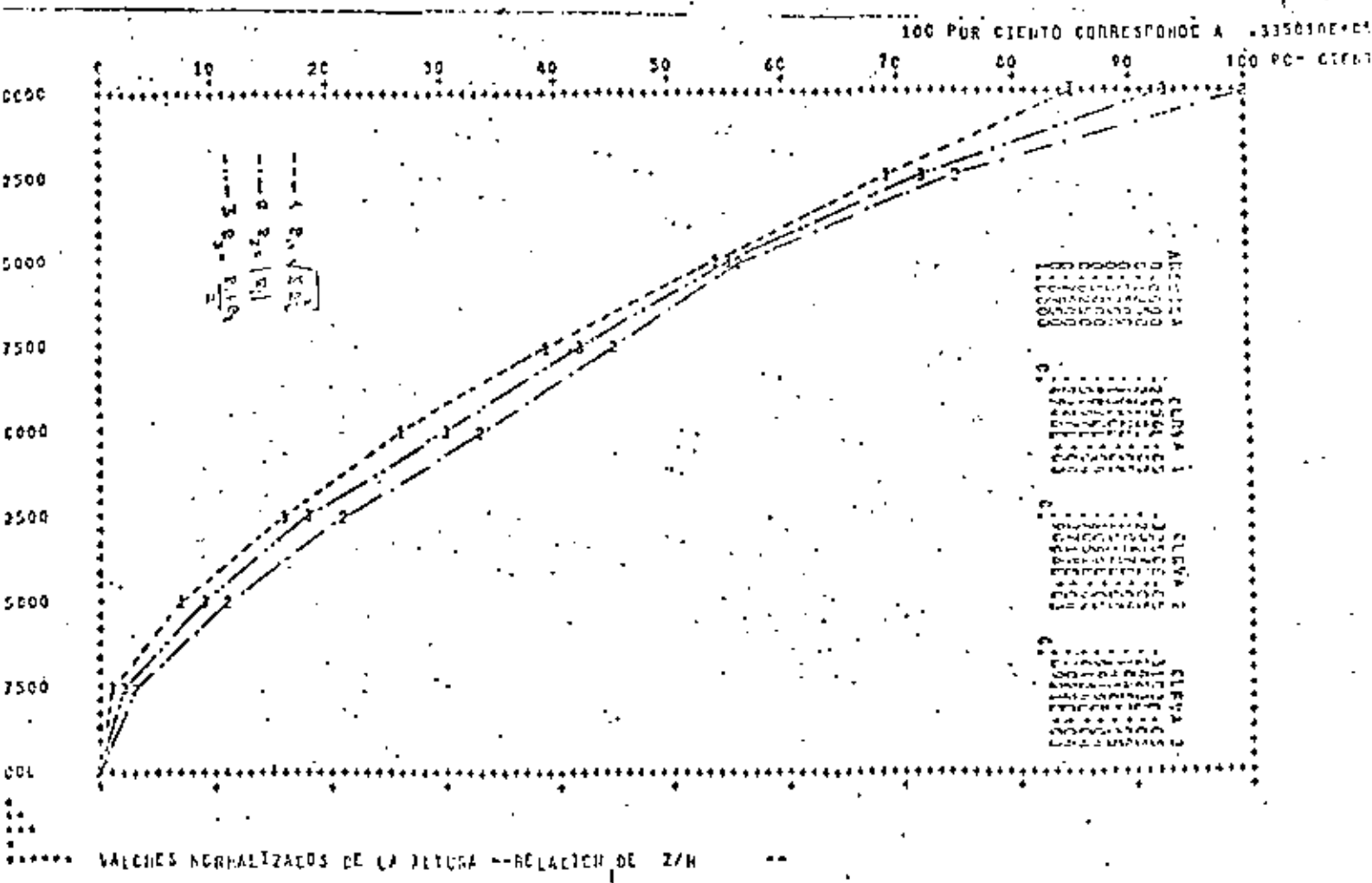


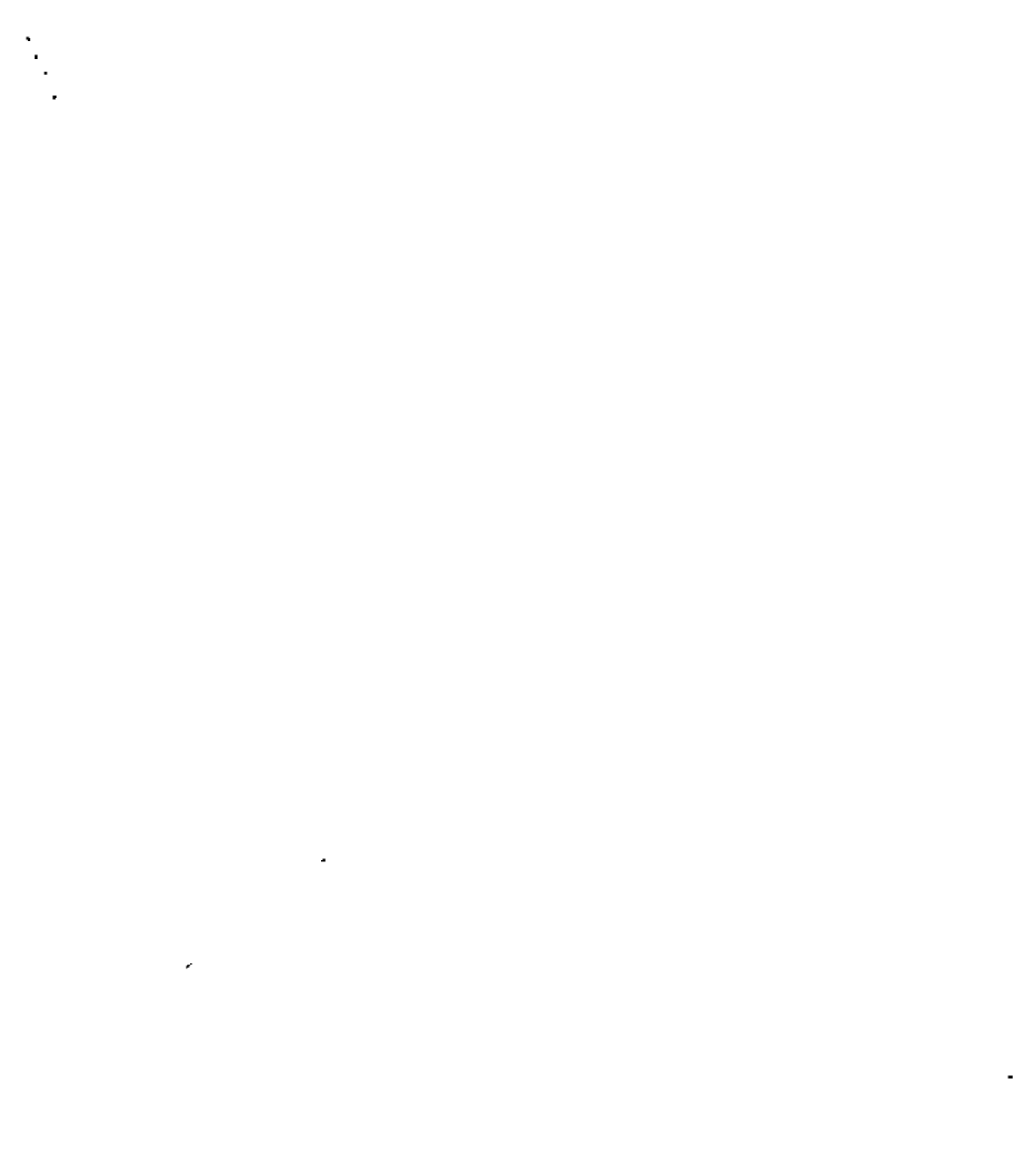
**MOMENTOS FLECTORES MAXIMOS**

MODO	MASA (%)	MASA (K)	MOMENTO MAXIMO (K)	MOMENTO MAXIMO (K)
1	72.00	107.88	173195E+05	262501E+05
2	27.00	39.12	-311472E+04	-215500E+04
3	1.00	1.44	-890151E+02	-616215E+02
4	0.00	0.00	261131E+03	182898E+02
5	0.00	0.00	-768359E+02	-701022E+02
6	0.00	0.00	117026E+01	-376100E+01
7	0.00	0.00	-356805E+00	123576E+00
8	0.00	0.00	255062E-03	-251053E-03

**RESPUESTA MODAL**

MASA	R1=RCOS(LIANG(PI*2))	R2=ABS(S)	R3=(R1+R2)/2.0
1	479120E+03	262810E+03	608000E+03
2	302710E+03	271700E+03	302000E+03
3	110000E+03	100000E+03	100000E+03
4	80770E+02	80770E+02	80770E+02
5	112000E+02	112000E+02	112000E+02
6	170000E+01	170000E+01	170000E+01
7	231000E+01	231000E+01	231000E+01
8	285000E+05	335010E+05	310000E+05







**DIVISION DE EDUCACION CONTINUA  
FACULTAD DE INGENIERIA U.N.A.M.**

VII CURSO INTERNACIONAL DE INGENIERIA SISMICA

DISEÑO SISMICO DE ESTRUCTURAS ESPECIALES

P U E N T E S

Profesores: Dr Luis Esteva Maraboto  
M en C Enrique del Valle Calderón

Julio, 1981

## P U E N T E S

- \* Sesismic analysis of the elevated structure for the México city "metro"
- \*\* Evaluation of analytical procedures used in bridge seismic design practice
- \*\*\* Earthquake-resistant design of bridges
- \*\*\*\* Seismic response of multi-support structures
- \*\*\*\*\* Influencia en la respuesta sísmica del puente Coat-zacoalcos II, de las diferencias de fase en los movimientos de sus apoyos
- \*\*\*\*\* Influencia en la respuesta sísmica del puente Coat-zacoalcos II, de las diferencias de fase en los movimientos de sus apoyos. Segunda Parte

Julio, 1981



## SEISMIC ANALYSIS OF THE ELEVATED STRUCTURE FOR THE MEXICO CITY "METRO"

Enrique del Valle (I)  
 Manuel Díaz-Canales (II)  
 Jorge Prince (III)  
 Alejandro Vázquez (IV)

Summary. Seismic analysis of the elevated structure for the Mexico City Metro is described. The structure was idealized as an inverted pendulum. -- Rotatory inertia and soil structure interaction effects were included in -- the dynamic analyses performed. A comparison with the results of the static analysis is made. Field tests to determine the actual dynamic properties in situ were carried out.

Introduction. An extension of the Metropolitan Transportation System (Metro) of Mexico City is under construction; it will have a new elevated line, 10 km long. Extensive studies were performed to determine the best type of structure, after which it was decided to use prestressed-concrete box-section beams, 8 m wide, cast in place and posttensioned, with spans ranging -- from 25 to 40m supported on a single line of columns with variable cross -- section (fig. 1). The foundation consists of spread footings on friction -- piles.

Beam supports consist of neoprene and steel pads. Different thicknesses were used on each end in order to have a hinged-simple supported beam. Two pads on each side spaced 2.5m transversely to the beam take overturning effects. An extension of the end diaphragms enter a box left in the columns, to transmit all lateral loads to them. To avoid collapse of beams due to excessive movement during strong earthquakes tie-bars were used joining the ends of the two beams resting on each column.

Line loads are of two types: passenger trains with axle loads of 15.9 ton including impact, and a maintenance train, with axle loads of 25.0 ton. Different arrangements were used in order to obtain maximum effects when -- these loads were combined with earthquake.

Seismic analysis. The structure was analyzed using the Mexico City building code which specifies, for the high compressibility clay deposit where most of the line will be located, a seismic coefficient of 0.24 g, which should be increased 30 per cent for the case of special structures. To compute -- forces, this coefficient may be reduced according to ductility characteristics. For the Metro structure the reduction factor is 2; (ref.1).

The Code specifies that analyses may be static or dynamic. For the static analysis of inverted pendulum structures, defined as those having more -- than 50 per cent of the load concentrated at the top, with lateral forces -- resisted by a single element, rotatory inertia should be included using an -- expression given in the Code. An additional reduction of design forces is -- possible using a design spectrum and estimating the fundamental period of vibration. This reduction is generally possible in the case of very rigid -- structures on soft soil or flexible structures on stiff soil. Dynamic analysis may be step by step using four different accelerograms with intensity --

- 
- I. Consultant, ICA Group. Research Professor, National University of Mexico
  - II. Vicepresident, ICA Group
  - III. Subdirector, Institute of Engineering, National University of Mexico
  - IV. Head of Engineering. ISTAC, ICA Group.

compatible with the Code, or a modal analysis using a design spectrum.

To obtain seismic effects the Code specifies that the structure should be analyzed in two orthogonal directions. For the case of inverted pendulum structures, seismic effects in one direction and 50 per cent of the seismic effects on the other direction are combined with gravity loads.

Static Analysis. According to the Code, seismic effects for inverted pendulum structures consist of a horizontal force and a moment applied at the top. The horizontal force is equal to the mass times the seismic coefficient reduced by ductility. An increment of 30% was applied due to the importance of the structure. The moment at the top due to rotatory inertia should be computed as

$$M_0 = 1.5 V_0 r_0^2 \Theta_0 / \delta_0$$

where  $V_0$  is the lateral force;  $r_0$  the radius of gyration of the mass with respect to a horizontal axis at the top of the structure, perpendicular to the direction of analysis;  $\Theta_0$ , the rotation at the upper end due to  $V_0$  and  $\delta_0$  the horizontal displacement of this point due also to  $V_0$ .

As it was mentioned before, additional reductions might be obtained in the case of rigid structures on soft soil, therefore, the fundamental period of vibration was estimated using the following expression, which is a modification of that proposed in the Code to take into account rotational effects:

$$T = 6.3 \left[ (m\delta_0^2 + J\Theta_0^2) / (V_0\delta_0 + M_0\Theta_0) \right]^{1/2}$$

Here  $\delta_0$  and  $\Theta_0$  are total displacements at the upper end due to the combined effect of  $V_0$  and  $M_0$ ,  $m$  is the mass and  $J$  its polar moment of inertia.

Dynamic analysis. Three different models were considered for the dynamic analysis: cantilever column with mass concentrated at the top and perfectly fixed base, column with mass having rotatory inertia at the top and perfectly fixed base and column with mass having rotatory inertia at the top and soil-structure interaction at the base. Linear behavior was assumed using the models proposed in ref.2.

For the first model the moment at the upper end is zero and frequency is equal to the square root of  $m$  over  $k$ . For the second case, the frequencies are given by

$$\omega_{1,2} = \frac{k_r J + mk}{2K m J} \pm \left( \frac{k_r J + mk}{2K m J} - \frac{k_r k}{K^2 m J} \right)^{1/2}$$

where  $k$  is translational stiffness;  $k_r$  rotational stiffness;  $K = 1 - \delta\theta$ ;  $\delta$  is the horizontal displacement at the top due to a moment  $k$ ;  $\theta$  is the rotation at the top due to a horizontal force  $k$ ;  $u = \gamma k$ ,  $\gamma$  is the rotation at the top due to a unit horizontal load or the lateral deformation due to a unit moment applied at the top.

Table 1 summarizes the above elastic properties of the column for both directions of analysis; table 2 shows values of  $m$  and  $J$  corresponding to the most adverse arrangement of live load.

Modal configurations for the second case are given by

$$x_{ij}/\epsilon_{ij} = k\delta / K(k/K - \omega_j^2)$$

where  $x$  and  $\epsilon$  are total displacements and rotations.

The spectrum used corresponds to the soft soil of the city and is described by  $a = (0.06 + 0.225 T) g$  for  $T < 0.8$  sec;  $a = 0.24 g$  for  $0.8 \text{ sec} < T < 3.3 \text{ sec}$ ;  $a = (0.792/T) g$  for  $T > 3.3$  sec. Where  $a$ , the spectral acceleration, may be reduced to compute seismic forces dividing by a ductility reduction factor  $Q = 2$  for  $T > 0.8$  sec or by  $Q' = 1 + 1.25 T$  for  $T < 0.8$  sec.

The fundamental period of the structure is smaller than 0.8 sec, therefore any increase in its value due to soil-structure interaction would increase the response and model 3 was necessary. As the structure is supported on friction piles the dynamic properties of the foundation are difficult to evaluate. As mentioned before the model used is described in ref. 2, it does not include the mass of foundation and adjacent soil. Stiffnesses in translation and rotation of the group of piles were computed using Krennikof's method (ref. 3) Lateral stiffness computed is 21 000 ton/cm and rotational stiffness 3 200 000 ton-m/rad. The mechanical elements obtained by the three dynamic models are presented in table 3 for the least favorable load combination.

Comparison of results. It may be observed in table 3 that the moment computed by the static method is larger than that obtained with dynamic models 1 or 2, however, lateral force is larger in the dynamic model with soil-structure interaction and the moments at the base are larger than those computed statically.

Combination of effects in both directions leads to similar results in the static and dynamic analyses.

Research program and field tests. In order to evaluate the dynamic parameters of the structure a research project is underway at the writing of this paper. It includes free and forced vibration of beams and columns to measure effective modulus of elasticity, periods of vibration and soil-structure interaction effects, as well as theoretical studies to analyze more sophisticated models of soil-structure interaction and step by step analyses with typical accelerograms recorded on the soft-soil of Mexico City. Fig 2 shows a general view of the tests. Due to space limitations results of this research program may be described during the conference.

#### References.

1. Mexico City building code, 1976
2. Rascón, O.A. "Seismic effects on inverted pendulum structures" (in spanish). Rev. Soc. Mex. Ing. Sism., 1965
3. Bowles, J. Foundation Analysis and Design, McGraw Hill Book, Co., 1968.

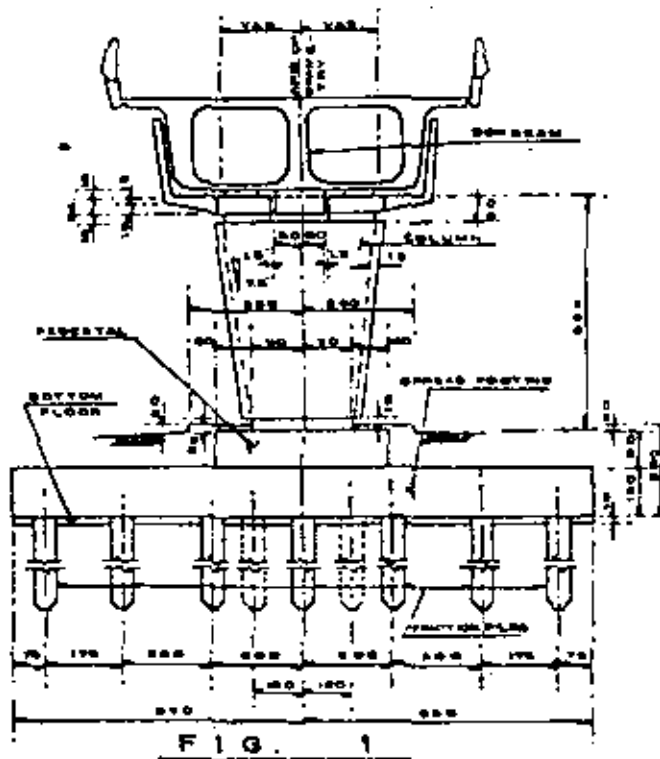


FIG. 1

TABLE 2

m AND J FOR ONE LOADING CONDITION							
EARTHQ. DIR.	MASS (ton.-sec <sup>2</sup> /m)			ROTATORY INERTIA (ton.-m-sec <sup>2</sup> )			
	BINDER + DEADLOAD	COLUMN	LIVE LOAD	TOTAL	BINDER + DEADLOAD	LIVE LOAD	
X	76.48	7.01	22.11	105.60	746.41	1566.83	1812.24
Z	76.48	7.01	20.04	103.51	81.92	17.81	79.83

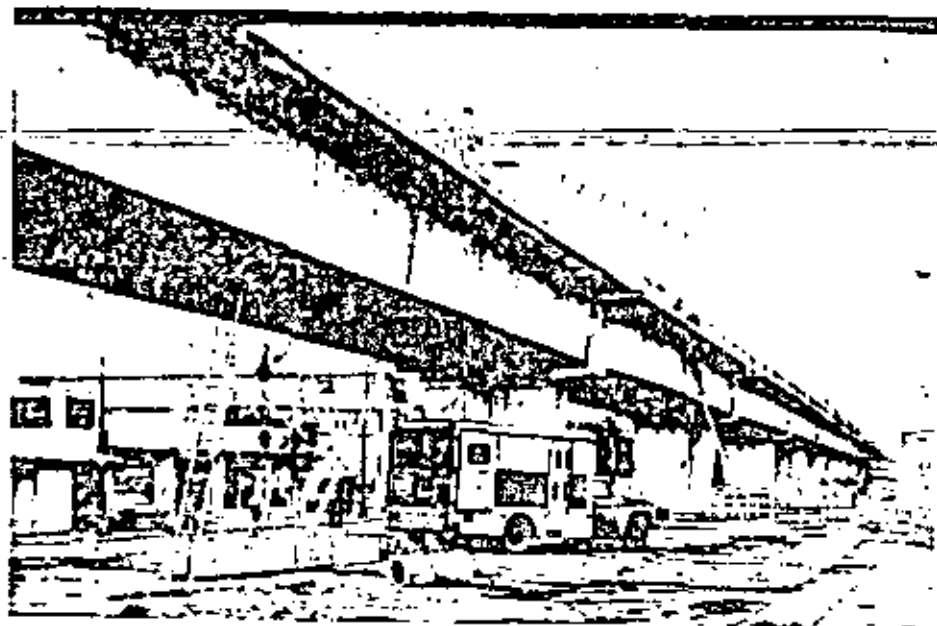
TABLE 1

COLUMN PROPERTIES					
X DIRECTION			Z DIRECTION		
X	73214.37	ton./m	K	70284.7	ton./m
W	448521.35	ton.m/rad	KY	892235.	ton.m/rad
P	3.108x10 <sup>-6</sup>	1/ton.	P	3.515x10 <sup>-6</sup>	1/ton.
Q	0.2311	rad./m	Q	0.24850	rad./m
J	3.63	m/rad.	J	3.14	m/rad.
K	0.180		K	0.220	
V	285760.47	ton.	V	221723.	ton.

TABLE 3

COMPARATIVE RESULTS						
ANALYZED MODEL	EARTHQUAKE DIRECTION	FORCES AND BENDING MOMENTS AT BASE OF COLUMN				
		V (ton.)	%	M (ton.-m)	%	
STATIC ANALYSIS	X	126.27	100.0	1231.13	100.0	
	Z	116.56	100.0	687.60	100.0	
DYNAMIC ANALYSIS	↑	X	117.91	93.4	641.94	52.1
		Z	116.82	99.4	630.08	94.4
	↓	X	81.66	64.8	719.36	58.4
		Z	111.12	95.3	631.17	94.5
	↔	X	138.54	109.7	926.16	75.2
		Z	143.71	123.3	791.63	116.6

FIG. 2



EVALUATION OF ANALYTICAL PROCEDURES  
USED IN BRIDGE SEISMIC DESIGN PRACTICE

by

R. A. Imsen, Vice President  
Engineering Computer Corporation  
R. V. Nutt, Senior Research Engineer  
Engineering Computer Corporation  
J. Peazien, Professor  
University of California, Berkeley

## INTRODUCTION

The accurate prediction of stresses and displacements induced in the various components of a structure during a strong motion earthquake is the key to improved earthquake resistant design. Predicting these stresses and displacements in bridge structures may be divided into the following two general tasks:

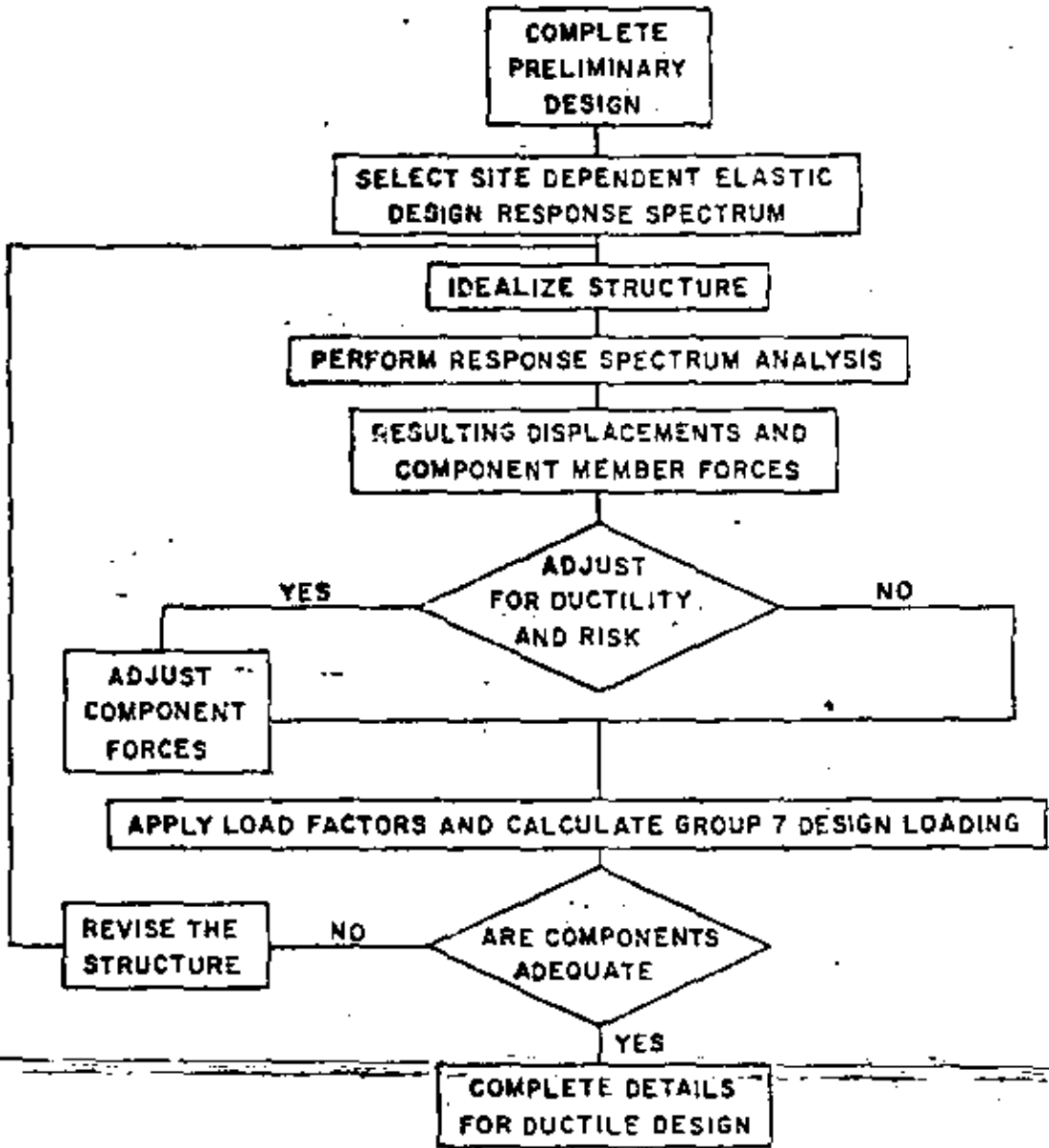
- (1) Determination of the seismic load.
- (2) Determination of the effect of this load on the structure.

These two tasks are typically reflected in current seismic design processes such as the one used at the Office of Structures, California Department of Transportation (CALTRANS). This process is depicted in Figure 1. The seismic load to which a structure will be subjected is determined by selecting the appropriate site dependent design response spectrum. The effect of this loading on the bridge structure is then determined by predicting the elastic response of the structure by any one of several methods, and reducing the elastically determined forces to account for the effects of structure yielding. Elastic displacements are generally considered to be equal to the actual displacements.

With the revolution in structural analysis brought on by the advent of modern digital computers, it may appear to the casual observer unfamiliar with structural dynamics, that the second task (i.e., predicting the effect of a given seismic loading) has evolved to a state which approaches an exact science. However, this is not the case. One of the primary reasons for this is the lack of field data on the actual magnitude of stresses and displacements occurring in bridges during a major earthquake.

In an effort to overcome, at least partially, this absence of data, a model structure was subjected to simulated earthquake loading on the shaking table at the University of California Richmond Field Station. Data gained from this experiment was correlated with results from a sophisticated research oriented computer program developed specifically to predict seismic response of bridge structures. This correlation study resulted in a substantial improvement in the algorithms used to calculate nonlinear response.

Many bridge designers do not have access to computer facilities and those that do must use programs that are less sophisticated than the one mentioned above. In practice, therefore, stresses and displacements are determined by more approximate means which employ several simplifying



CALTRANS  
SEISMIC DESIGN PROCESS

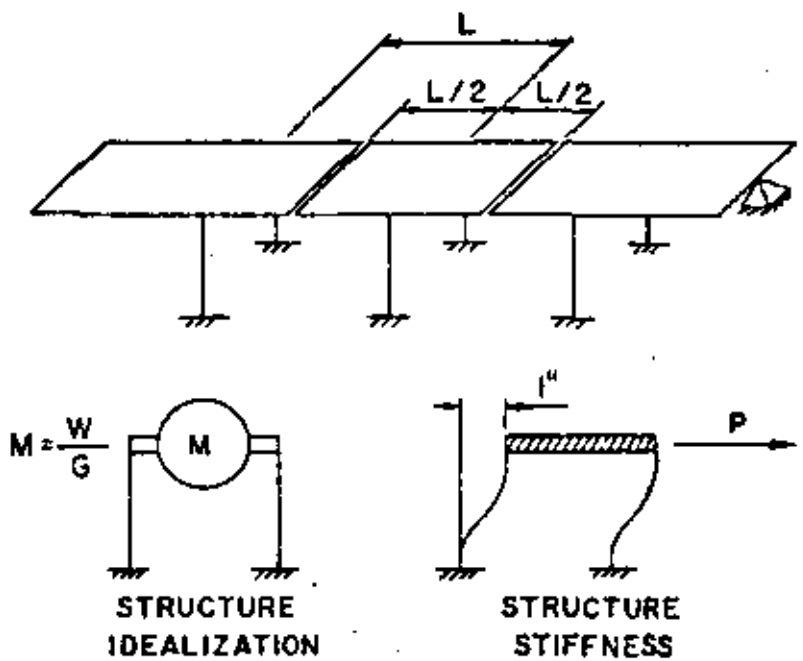
FIGURE 1

assumptions. With the present absence of field data, evaluation of these means can only be done by comparison with more sophisticated analytical approaches which are known to better model reality.

This paper deals with an evaluation of the currently used methods for predicting the response of bridge structures to a given seismic loading. An evaluation of both the equivalent static load and the response spectrum techniques for determining seismic effects on bridge structures is included. The experiences of the authors in their association with the University of California at Berkeley and the California Department of Transportation were drawn on to make this evaluation.

BACKGROUND

Prior to the San Fernando earthquake of 1971, bridges were generally designed for earthquake forces using an equivalent static force-approach known as the Lollipop Method. In other words, the bridge bents were assumed to act independent of one another as single-degree-of-freedom oscillators with a lumped mass equivalent to the tributary deck mass as shown in Figure 2. Both structure period and load distribution were determined using this method.



"Lollipop" Idealization  
Figure 2

Immediately following the earthquake, CALTRANS recognized the need to develop a more rational earthquake design procedure for bridges. Efforts were initiated to develop new earthquake design guidelines that would consider seismicity and the vibrational properties of both the bridge and the underlying soil. There were two basic approaches that evolved regarding the method that should be used to perform the seismic analysis for bridge design. Proponents of the first approach proposed that a simplified technique

for applying equivalent static force be devised that would allow the designer to use his present knowledge of the static behavior of structures to design the bridge. Those who favored the second approach, felt it was more desirable to train the bridge designer to perform more sophisticated analyses which more realistically considered the dynamic behavior of the structure.

The first approach required the development of an improved equivalent static force approach. It became evident to the CALTRANS engineer that the previously used Lollipop Method was not a realistic method of analysis. Efforts to find a simple but realistic method of applying an equivalent static force to a wide range of bridges resulted in the formulation of a uniform lateral load technique, known as the Uniform Load Method. This technique, which was the first attempt to revise the equivalent static force method, is still not totally satisfactory, however, in that it produces accurate results for only a limited number of bridge types.

At CALTRANS there were several factors that have made the second approach involving more sophisticated analysis the most desirable. Some of these factors are as follows:

- (1) The unusual geometric alignments, support conditions, and restraints of many bridge structures on a modern highway system required more sophisticated three-dimensional mathematical idealizations to obtain realistic results.
- (2) Sophisticated in-house computer capabilities were available with the required mathematical idealizations to perform a dynamic analysis.
- (3) It was necessary to use the same computer program to perform a space frame analysis to effectively apply the Uniform Load Method as was required to perform a dynamic analysis. Thus with modest additional training, a more sophisticated analysis was possible at a relatively small additional effort and cost.
- (4) There was a combination of: 1) willingness of management, 2) ability of bridge designers to learn new techniques, and 3) an availability of qualified personnel who were assigned to provide technical support on an ongoing basis.

---

This approach, which has proved successful at CALTRANS, resulted in the implementation of three-dimensional response spectrum modal analysis to determine design seismic forces for bridges on a routine basis.

The AASHTO Specification [1] for Bridges (1977) reflects the two approaches by specifying that the effect of seismic forces on bridges shall be evaluated by considering the dynamic response characteristics of the total bridge using one of the following methods:

- (1) Equivalent static force
- (2) Response spectrum dynamic analysis

For "special cases," the specifications recommended the use of dynamic analysis techniques. Special cases are considered to be structures with one or more of the following characteristics:

- (1) Located adjacent to active fault(s)
- (2) Located in area with unusual geologic conditions
- (3) Unusual geometry, cost, importance, etc.
- (4) Structure period greater than 3 seconds

These specifications were written following the San Fernando earthquake of 1971. They are to a very large degree the reaction of CALTRANS bridge design and research engineers to the failures that occurred during that earthquake.

The San Fernando earthquake also stimulated a renewed enthusiasm for additional theoretical and experimental studies into the seismic behavior of bridges. One of these studies, conducted at the University of California at Berkeley, was designed to investigate the effectiveness of existing bridge design methodology in providing adequate structural resistance to seismic disturbances. This project extended over approximately six years and included the following six phases:

- (1) A review of the world's literature relating to seismic effects on highway bridges [2]
- (2) An analytical investigation of the dynamic response of long, multiple span highway overcrossings [3]
- (3) An analytical investigation of the dynamic response of short, single and multiple span highway overcrossings [4,5]
- (4) Detailed model experiments on a shaking table to provide dynamic response data which could be used to verify theoretical response predictions [6]
- (5) Correlation of experimental and theoretical response, and modification of analytical procedures as necessary [7]
- (6) Preparation of recommendations for changes in seismic design specifications and methodology [8,9].

This project made substantial contributions to the advancement of the state of knowledge regarding the dynamic response analysis of bridge structures subjected to seismic loadings. As part of Phase 6 of this project, case studies were performed to evaluate the accuracy of results obtained from currently available computer analysis techniques. Of primary concern was the response spectrum technique that has gained wide use in bridge design. The results of these case studies provided the basis for the evaluation of response spectrum analysis presented in this paper.

## EQUIVALENT STATIC FORCE METHODS

Introduction

The development of a realistic simplified equivalent static load approach for the dynamic analysis of bridges that would suffice for the final design of simple bridges and could even be used for preliminary design on the more complex bridges, is desirable for the following reasons:

- (1) Simple extensions of what is currently used and would be easy to implement
- (2) Does not require a computer
- (3) Quick and easy to apply

The determination of seismic response by the equivalent static force method basically involves three steps:

- (1) Calculating the period of the first mode of vibration in the direction under consideration.
- (2) Obtaining the corresponding response coefficient "C".
- (3) Distributing the resulting equivalent static earthquake force to the substructure elements.

Lollipop Method

In the past, the determination of the period and distribution of the earthquake force was accomplished by simply applying the formulas in the code. The idealization for the Lollipop Method implied the following simplifying assumptions about the dynamic behavior of a bridge:

- (1) Each bent vibrates in its own natural period, independent of the other bents.
- (2) The transverse bending and torsional stiffness of the superstructure do not contribute to the stiffness of the system.

---

There are several obvious over-simplified assumptions in this approach. Even for bridges of simple geometry, the assumptions were somewhat in error. The inaccuracies that occurred in the calculation of structural period resulted in unrealistic values for the equivalent static earthquake force. In addition, the distribution of this force was in error. The main advantage of this technique was that it was simple and easy to apply.

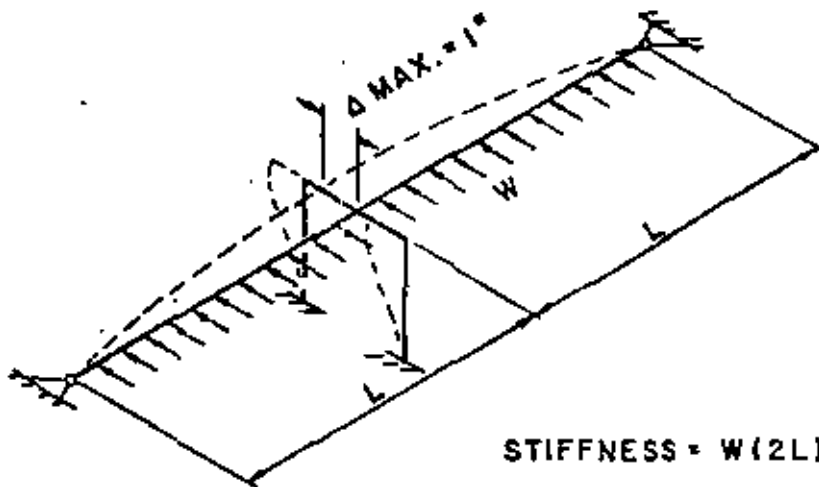
Uniform Load Method

To overcome the deficiencies in the Lollipop Method, an empirical approach, called the Uniform Load Method, was devised with the following objectives:

- (1) Maintain continuity of the superstructure in determining the natural period of the system.
- (2) Distribute the earthquake force to all of the participating elements of the bridge.
- (3) Allow for ease of application using seismic design coefficients and static analysis techniques.

The steps in the Uniform Load Method approach can be summarized as follows:

- (1) Apply a uniform horizontal load (usually taken as unity) to the structure in the direction of vibration as shown in Figure 3.



Uniform Load Idealization  
Figure 3

- (2) Perform a static analysis on the structure to determine the resulting displacements and member forces due to the applied uniform load.
- (3) Adjust the maximum displacement to 1 inch. Using this adjustment factor, adjust the uniform load to correspond to a maximum displacement of 1 inch.
- (4) Multiply the adjusted uniform load by the length of the structure. This is the value for stiffness which, along with the total dead load of the structure, can be used to compute the fundamental transverse period of the structure.

- (5) Having obtained the period, determine the response coefficient "C" from the response curves.
- (6) Determine the total earthquake force acting on the structure by combining the response coefficient with the framing factor and the total dead load.
- (7) Convert the total earthquake force into an equivalent uniform load.
- (8) To determine forces in the members due to this uniform earthquake loading, prorate the forces in the members from the original uniform loading applied to the structure.

The desirability of using a simple approach employing a seismic coefficient in a static analysis, rather than a complex dynamic analysis, has provided the impetus for implementing the Uniform Load Method. Recent experience has shown that this empirical approach gives accurate results for certain types of simple bridges, but it can require more effort than a response spectrum dynamic analysis. This is because the Uniform Load Method requires a space frame analysis for all but very simple structures to properly analyze the transverse stiffness of the columns interacting with the superstructure.

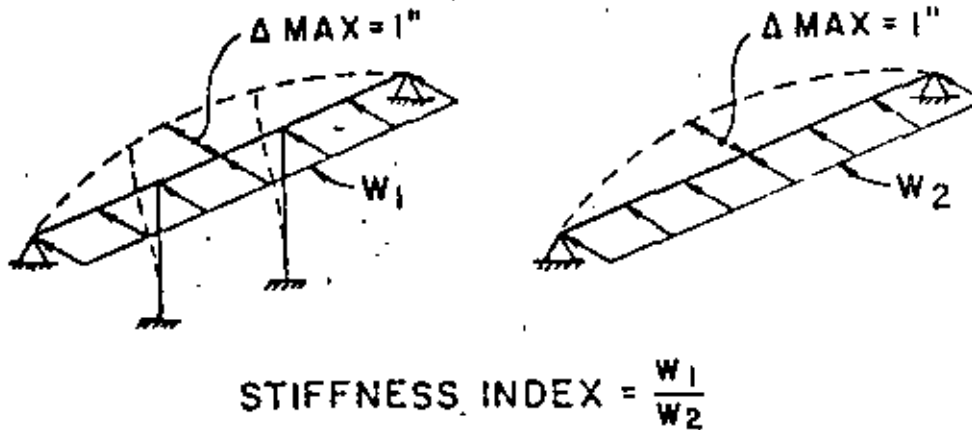
Several case studies [10] were performed to evaluate the accuracy and limitations of the Uniform Load Method as compared to a response spectrum dynamic analysis. For comparison, the Lollipop Method was also included in these case studies. In selecting bridges for these case studies, different structural and geometric characteristics were considered in order to evaluate the effect of the following parameters:

- (1) Number of spans
- (2) Ratio of span lengths
- (3) Number of columns per bent
- (4) Curvature
- (5) Skew
- (6) Structure width
- (7) Column length and fixity

~~An attempt was made to categorize the types of structures which could be accurately analyzed by the Uniform Load Method. It was found that the single most important criterion for categorizing the structure was the relative stiffness between the superstructure and substructure. In order to quantify this criterion, a stiffness index was established.~~

The Stiffness Index relates the relative contribution of the columns to the transverse stiffness of the entire structure. As illustrated in Figure 4, the Index is found by taking the ratio of the transverse stiffness of the entire structure, including the columns, to the stiffness of the superstructure alone, acting as a simple beam.

Based on the cases considered, it was observed that the Uniform Load Method can yield accurate results for structures with certain characteristics. Continuous structures on a straight, non-skewed alignment could generally



Stiffness Index Definition  
Figure 4

be analyzed using this approach provided the stiffness index was 2 or less. However, for structures with a stiffness index greater than 2, only those with balanced span lengths and equal column stiffnesses could be accurately analyzed. This method was not satisfactory for structures with skewed supports, intermediate hinges, or curved alignments.

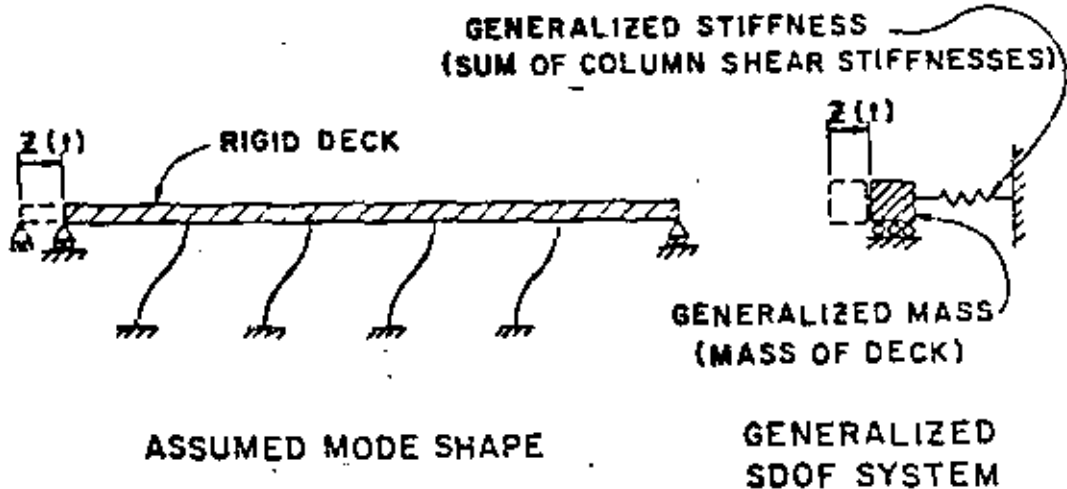
Since there are several limitations to the Uniform Load Method and since it generally requires a space frame analysis, there is a need to develop a simple but effective means for applying the equivalent static force approach to bridge structures.

In the development of an equivalent lateral force analysis procedure, it is necessary to determine the period of a structure and the distribution of the resulting lateral force. A reliable method for calculating the period must include the effective stiffness of the deck, restraining devices and soil springs, and the discontinuity of expansion joints, in addition to the individual column stiffnesses. In short, the true dynamic behavior of the bridge should be considered. The period should, if estimated, be an underestimated value to provide a conservative estimate of the equivalent lateral force. It is unlikely all bridge types will lend themselves to simplified techniques, but a large percentage of common types of bridges should be covered. Both longitudinal and transverse modes should be considered. Above all, the method should not require the use of a computer.

#### Generalized Coordinate Method

Another equivalent static force approach, that shows promise, can also be used to determine the period and earthquake response of certain types of bridges by applying energy principles to a generalized single-degree-of-freedom system. This method is based on the premise that the shape of the vibrating structure can be assumed and expressed mathematically in terms of a single generalized coordinate. The longitudinal and transverse modes of vibration can be separated into two classes of generalized single-degree-of-freedom systems.

For the longitudinal mode of vibration the structural displacement is characterized by the behavior of a rigid deck, limiting all the columns to equal longitudinal displacements as shown in Figure 5. This is the classical approach which has been used in the past to determine the longitudinal earthquake force for design.



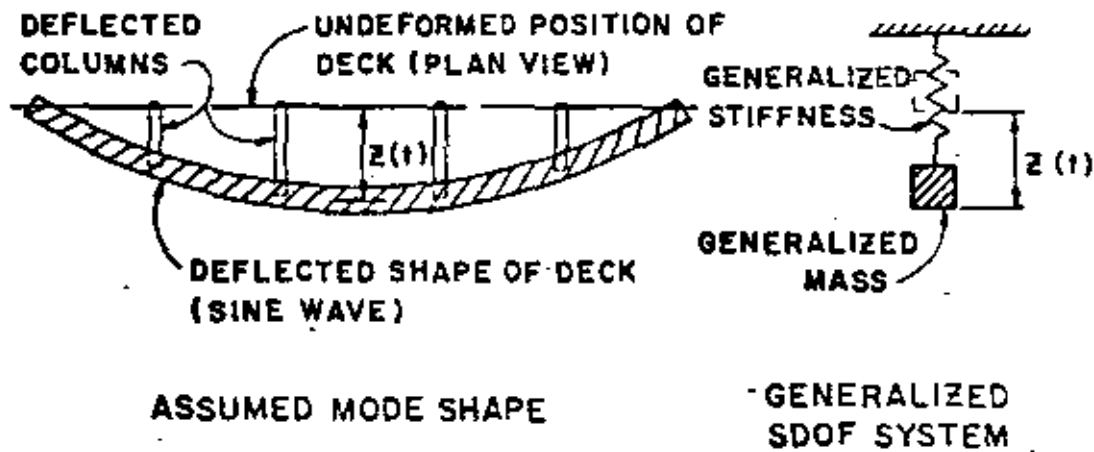
Generalized Coordinate Approach  
Longitudinal Mode  
Figure 5

The transverse mode of vibration is more complex in that the transverse displacement of the columns are not all equal but rather are functions of their position along the superstructure as shown in Figures 6 and 7. In addition to this, the continuous superstructure will undergo bending and will thus make a contribution to the potential energy of the system.

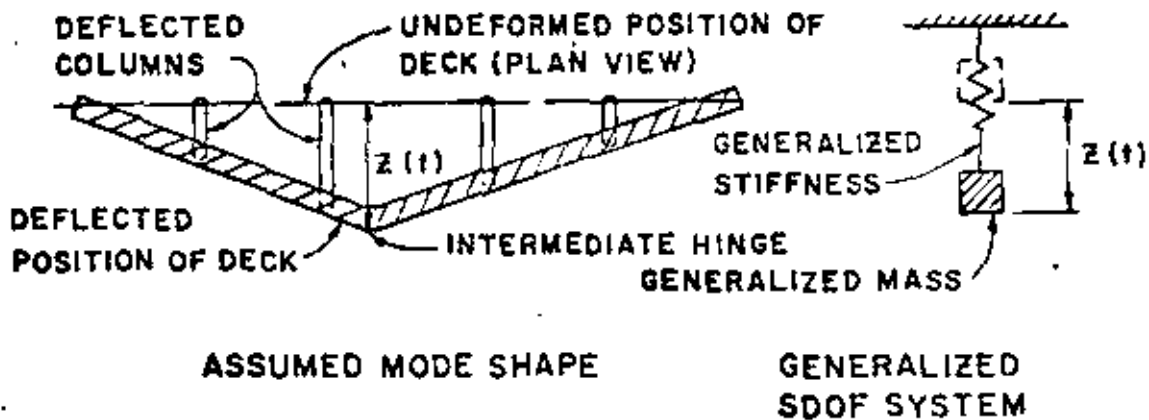
The reliability of this method depends on the ability to predict and define the structure's mode shape. The effective application of this technique also requires that one mode dominate in each direction. Fortunately, many of the simpler bridges being designed today satisfy both of these requirements.

The method may be applied to girder deck bridge with no more than one intermediate hinge and having the following characteristics:

- (1) Tangent or nearly tangent alignment
- (2) Deck length to width ratio less than 15
- (3) Skew angles of the abutments and supports less than twenty degrees
- (4) Approximately uniform span lengths and column stiffness



Generalized Coordinate Approach  
 Transverse Mode (Continuous Deck)  
 Figure 6



Generalized Coordinate Approach  
 Transverse Mode (Intermediate Hinge)  
 Figure 7

The basic approach of the method is outlined in the following steps:

- (1) Assume the predominate mode of vibration and define a generalized coordinate at the location of maximum displacement in the direction under consideration.
- (2) Calculate virtual work done by external forces and internal member forces as the structure vibrates through a unit virtual displacement at the assumed generalized coordinate.
- (3) Equate work to zero and solve for the structure period of the predominate mode in terms of the "Generalized Mass" and the "Generalized Stiffness".
- (4) Determine the seismic coefficient from the appropriate response spectrum chart.
- (5) Determine the earthquake excitation factor and scale the seismic coefficient.
- (6) Determine the maximum generalized displacement.
- (7) Determine the individual column forces using the generalized displacement calculated.
- (8) Calculate member forces, apply ductility factors and design the member.

It should be noted that the first three steps given above are used only in the development of the formulas. The designer need not repeat these steps for each design since they are implied in the use of the formulas.

This approach was tested on several bridges which had previously been analyzed by the response spectrum technique. In most cases where this approach could be applied, the results compared well with those from the response spectrum analysis. In almost all cases, the comparison was better than was obtained using either the Uniform Load Method or the Lollipop Method.

Although the generalized coordinate approach to the equivalent static force method is not widely used, it appears to be a definite improvement over the other two methods.

## THE RESPONSE SPECTRUM TECHNIQUE

### Introduction

The response spectrum dynamic analysis procedure is indeed an improvement over the equivalent static force method. There are limits to its applicability, however.

The first shortcoming of the response spectrum approach is that the time domain has been removed. Since maximum modal responses do not occur simultaneously, it is necessary to use a statistical combination of modal responses

such as root mean square in order to obtain realistic design loads. The actual combination of modal response depends on several factors related to the type of structure and the nature of the actual ground motion. Therefore, the use of a statistical approach to replace the effects of the removed time domain may not yield realistic results in certain cases.

Another deficiency in the response spectrum is that the duration of shaking is not accounted for by the spectrum. The major effect of duration will be on stiffness degradation and strength loss once the member begins yielding.

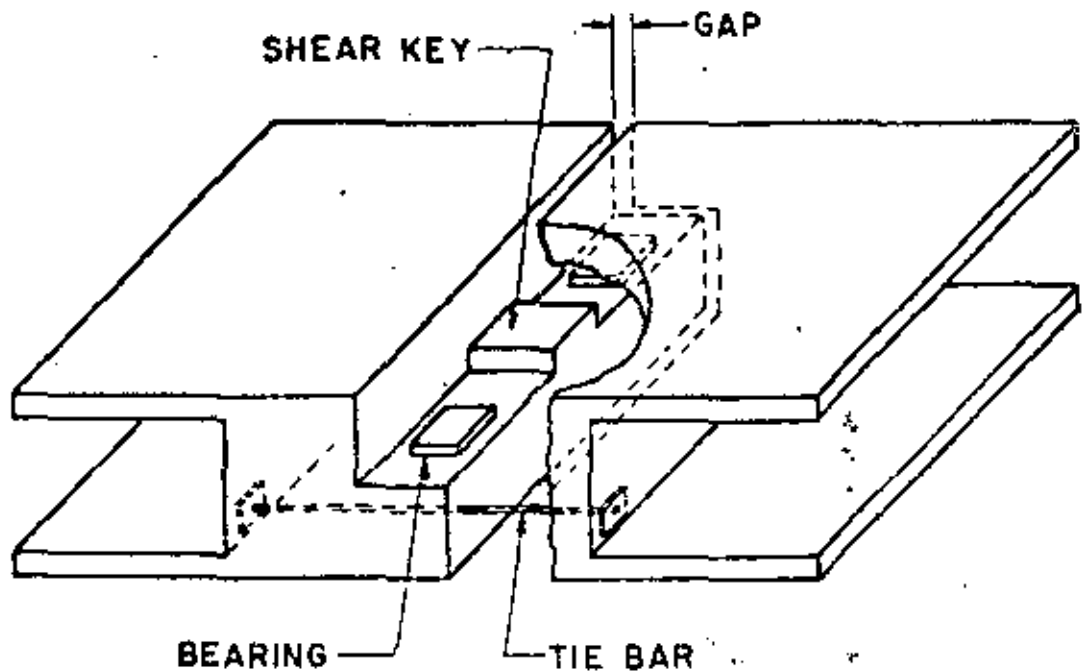
Since postelastic behavior is not specifically accounted for in the overall response analysis, a ductility factor or reduction factor is applied to reduce the forces obtained from a linear response spectrum analysis. This factor is applied either directly to the response spectrum or to the forces obtained from an unreduced spectrum. Because little is known about ductile behavior of bridges, the ductility factors used to determine the magnitude of reduction in bridge design have been extrapolated from research on building structures. Furthermore, the linear analysis does not account accurately for nonlinear behavior at expansion joint hinges, nor does it provide a means for assessing the redistribution of stress as yielding occurs in the ductile members. The analytical capabilities which evolved through the various phase of the University of California research project made it possible to evaluate the nonlinear behavior in the columns and expansion joint hinges. Recognizing both the limitations inherent in using elastic analysis techniques and the availability of improved analytical capabilities developed and refined during this research effort, case studies were conducted on three bridges to evaluate the analytical approaches currently used for seismic design of highway bridges.

The purpose of these case studies were to compare the results of a time history analysis that considers nonlinear behavior with results from both a linear time history and response spectrum analysis. Based on this comparison, the effectiveness of the current response spectrum approach as shown in Figure 1 can be evaluated.

#### Properties of the Bridges

Three bridges which were designed by the California Department of Transportation were selected for this study. All three structures consist of curved concrete box girder decks cast monolithically with single column bents. Because of the length of the bridges, each structure has one or more intermediate expansion joints to accommodate temperature movement.

This type of structure is common in California and is typically used in freeway interchanges. During the San Fernando earthquake of 1971, some of the most spectacular failures involved this type of bridge [2,11]. One of the primary cause of failure appeared to be the separation of expansion joint hinges. As a result, all structures of this type designed since the earthquake, including the three used in this study, have been fitted with restrainers designed to prevent separation. These restrainers must be gapped to allow freedom of movement for temperature, etc. A typical expansion joint hinge of this type is shown in Figure 8.



Typical Bridge Expansion Joint  
Figure 8

In order to obtain a better understanding of the behavior of this type of bridge, each of the structures selected had a different fundamental period of vibration. A summary of some of the important properties of these bridges is shown in Table 1. These bridges are shown in Figure 9, 10, and 11.

Bridge No.	Spans		Curve Radius (ft)	Column Lengths (ft)		Hinges		Periods of the First 20 Modes (Sec)	
	Length (ft)	No.		Min.	Max.	No.	Span Location	Max.	Min.
1	694	6	600	24.3	26.3	1	3	.40	.07
2	1138	8	1075	25.1	49.4	1	5	1.11	.15
3	1410	9	1050	60.7	85.6	2	3,7	1.94	.21

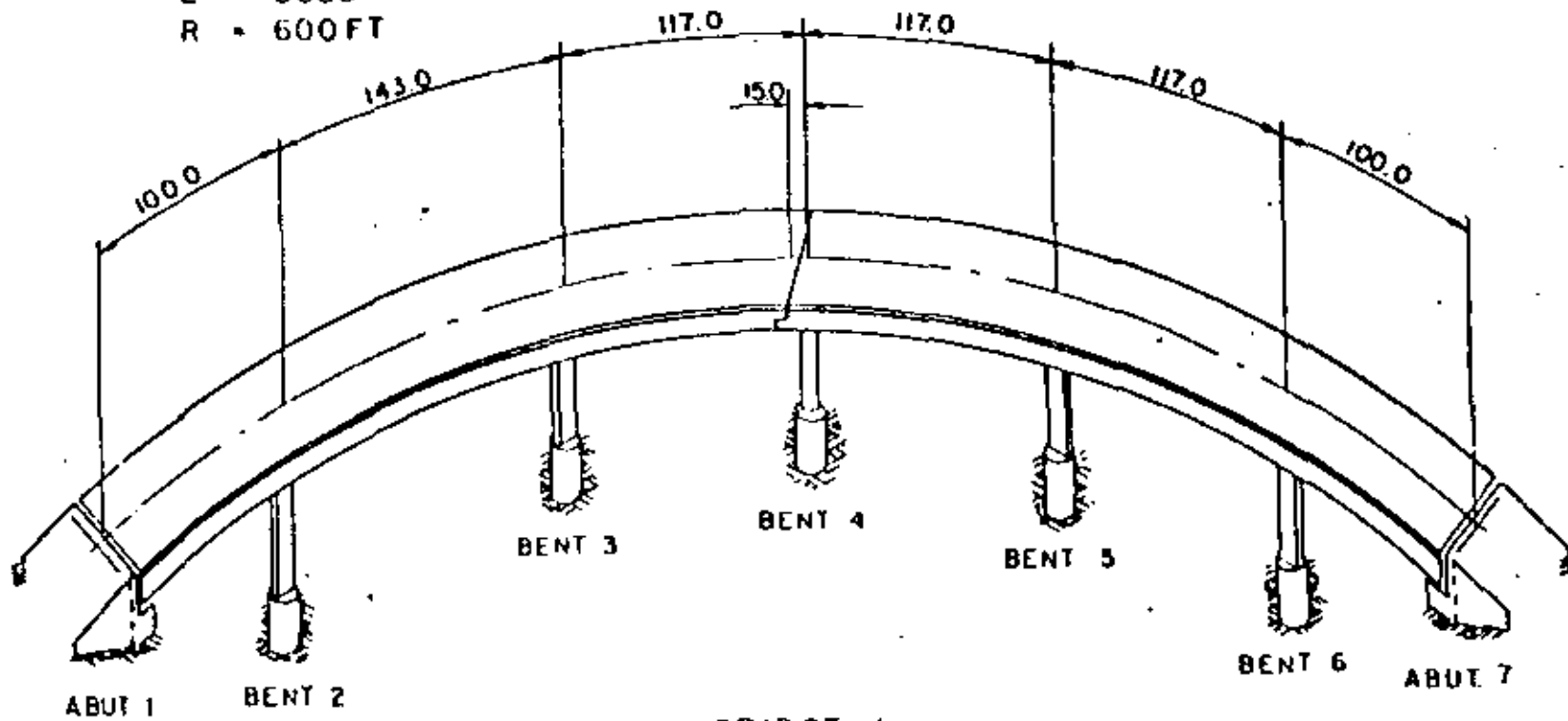
Basic Characteristics of Bridges Selected  
for Case Studies  
Table 1

Methods of Analysis

The following three types of analyses were performed on each of the three bridges selected.

SUPERSTRUCTURE PROPERTIES

- L = 694.0 FT
- A = 83.7 FT<sup>2</sup>
- I<sub>x</sub> = 814.1 FT<sup>4</sup>
- I<sub>y</sub> = 353.7 FT<sup>4</sup>
- I<sub>z</sub> = 12868.8 FT<sup>4</sup>
- DL = 12.56 K/FT
- E = 3000 KSI
- R = 600 FT



BRIDGE 1

ROUTE 80 ON-RAMP OVERCROSSING

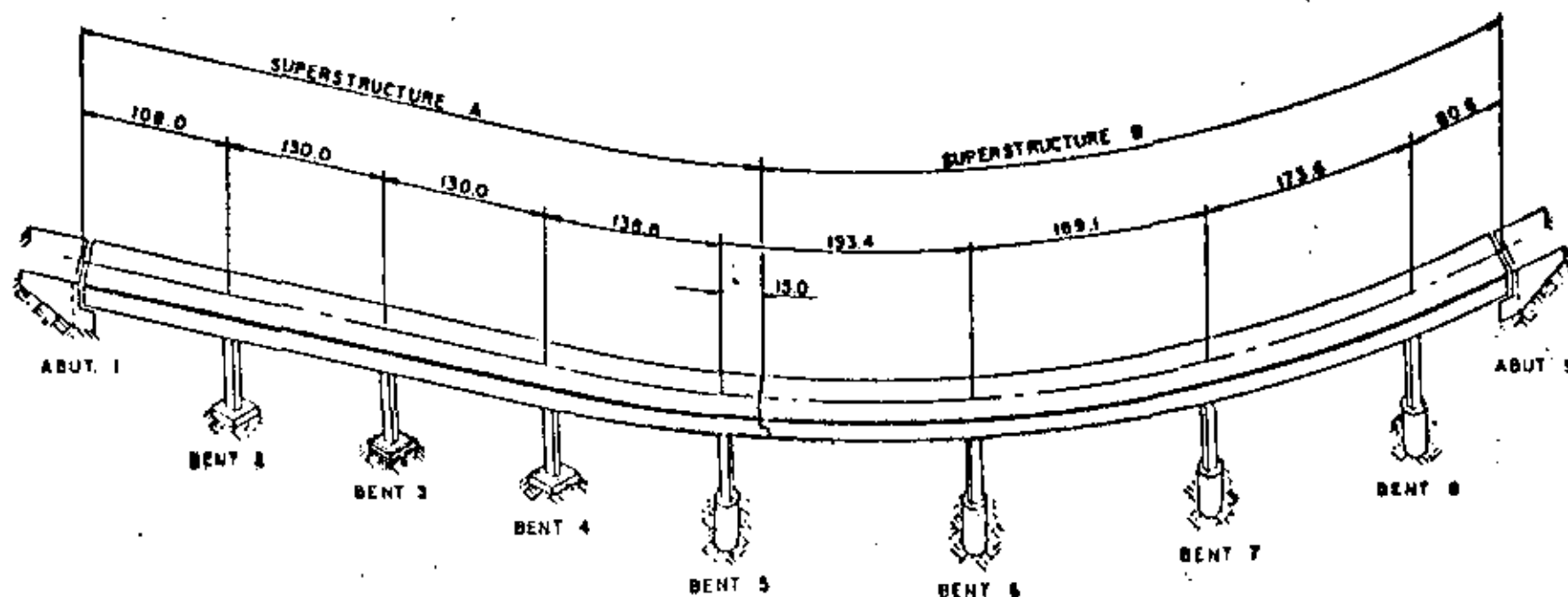
**SUPERSTRUCTURE A**

L = 521.8 FT  
 A = 48.0 FT<sup>2</sup>  
 $I_x = 850.0 \text{ FT}^2$   
 $I_y = 3130.5 \text{ FT}^4$   
 $I_z = 381.4 \text{ FT}^4$   
 DL = 7.2 K/FT  
 E = 3000 KSI

**SUPERSTRUCTURE B**

L = 621.7 FT  
 A = 54.5 FT<sup>2</sup>  
 $I_x = 850.0 \text{ FT}^2$   
 $I_y = 3528.3 \text{ FT}^4$   
 $I_z = 406.5 \text{ FT}^4$   
 DL = 8.175 K/FT  
 E = 3000 KSI  
 R = 1083 FT

-15-



20

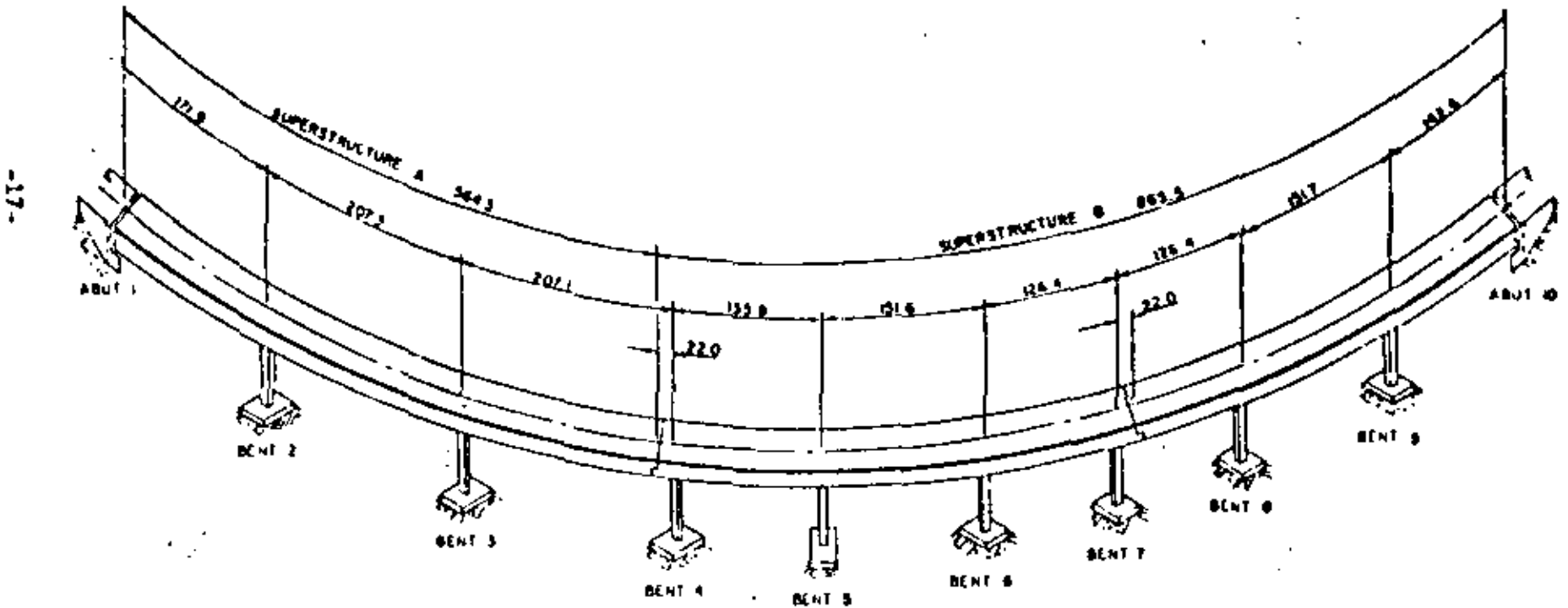
BRIDGE 2  
 NORTHEAST CONNECTOR OVERCROSSING

**SUPERSTRUCTURE A**

A = 813 FT<sup>2</sup>  
 $I_x = 1000 \text{ FT}^4$   
 $I_y = 9713.5 \text{ FT}^4$   
 $I_z = .6646 \text{ FT}^4$   
 $DL = 12.195 \text{ K/FT}$   
 $E = 3000 \text{ KSI}$   
 $R = 1062 \text{ FT}$

**SUPERSTRUCTURE B**

A = 755 FT<sup>2</sup>  
 $I_x = 980 \text{ FT}^4$   
 $I_y = 9152.9 \text{ FT}^4$   
 $I_z = 6400 \text{ FT}^4$   
 $DL = 11.325 \text{ K/FT}$   
 $E = 3000 \text{ KSI}$   
 $R = 1062 \text{ FT}$



**BRIDGE 3  
 SOUTHWEST CONNECTOR OVERCROSSING**

-17-

21

- (1) A response spectrum modal analysis, which is the approach that was used at CALTRANS, and appeared to be the most desirable for general use in bridge design.
- (2) A linear time history modal analysis, which includes consideration of the time domain but not the effects of nonlinear behavior.
- (3) A nonlinear dynamic analysis, which employed a step-by-step integration technique and included the effects of both expansion joint and column nonlinearity.

The linear analysis capabilities of STRUDL (STRuctural Design Language) were used to perform the response spectrum and linear time history analyses [12]. STRUDL is a well-known general purpose computer program for static and dynamic analysis of linear structural systems. The MCAUTO proprietary version was used [13].

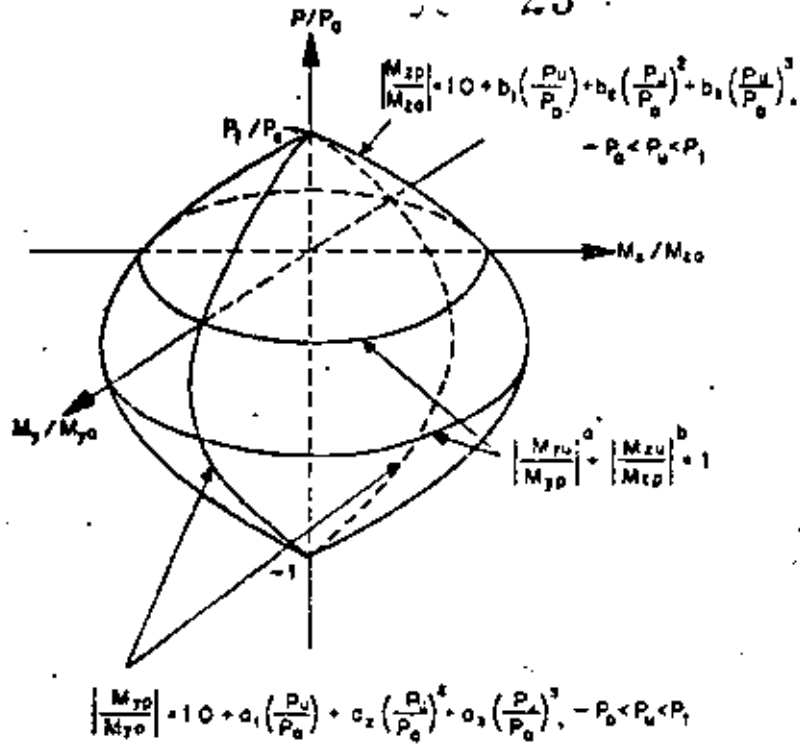
The nonlinear analysis was performed by the NEABS (Nonlinear Earthquake Analysis of Bridge Systems) program [3,7]. This computer program uses a step-by-step integration procedure which assumes piecewise linear behavior over each increment of time. The linear acceleration method was used for this study. Loading was input as rigid support accelerations. The program element library has the conventional linear elements plus the following nonlinear element types:

- (1) Elasto-plastic straight beam elements
- (2) Bi-linear boundary spring elements
- (3) Nonlinear expansion joint elements

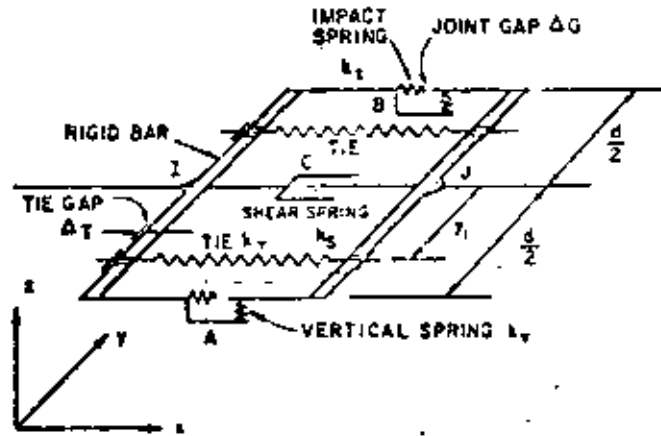
The two nonlinear parameters considered for this study were the yielding of the single column bents, and the nonlinearity of the expansion joint hinges.

The yielding of columns was limited to axial and flexural yielding along an interaction yield surface. The yield surface for a typical bridge column is shown in Figure 12. The ultimate capacity of the column in shear was considered to be infinite.

The nonlinear behavior of the expansion joint hinges were modeled using the expansion joint element shown in Figure 13. In this expansion joint hinge idealization, the restrainers were assumed inactive until movement at the joint was sufficient to take up the gaps which are normally placed in the restrainer anchorages to allow for normal movements of the joint. When the restrainers were active, they behaved in an ideally elasto-plastic manner. Relative movement at the hinge was limited by stiff impact springs which were activated upon closure of a seat gap. This represented banging of the two adjacent superstructure sections. The vertical and shear stiffnesses of the bearing pads were also included in the expansion joint element. Relative movement of the pads at the pad-concrete interface when the Coulomb friction force is overcome was also considered.



Yield Surface Description  
Figure 12



Expansion Joint Idealization  
Figure 13

Rigid support motion was used for all of the bridges. The SI 8+ time history ground motion developed by Seed and Idriss [14] for a simulated 8+ Richter magnitude earthquake was used. The response spectrum for this motion, shown in Figure 14, was generated for 5 percent damping. This ground motion was applied to the bridges in the two orthogonal directions. The longitudinal and transverse motions were directed parallel and perpendicular to a line between the abutments.

With three types of analysis for each of the three bridges studied and ground motion in two directions, the total number of cases examined amounted to 18.

The bridge decks and columns were modeled with space frame members. Masses in the deck were lumped at the quarter points. Column masses were lumped at the third points. For simplicity, the base of each column was assumed fixed at the footing. The abutments were assumed to be free to move in the longitudinal direction. A typical structure idealization showing the location of lumped masses is shown for each bridge in Figures 15, 16 and 17.

The hinge idealization for the elastic analyses was modeled by releasing main girder member axial forces, and superimposing transversely eccentric space frame members between both sections of the superstructure to account for the restrainers. This idealization assumes no gap and both tension and compression at the restrainers.

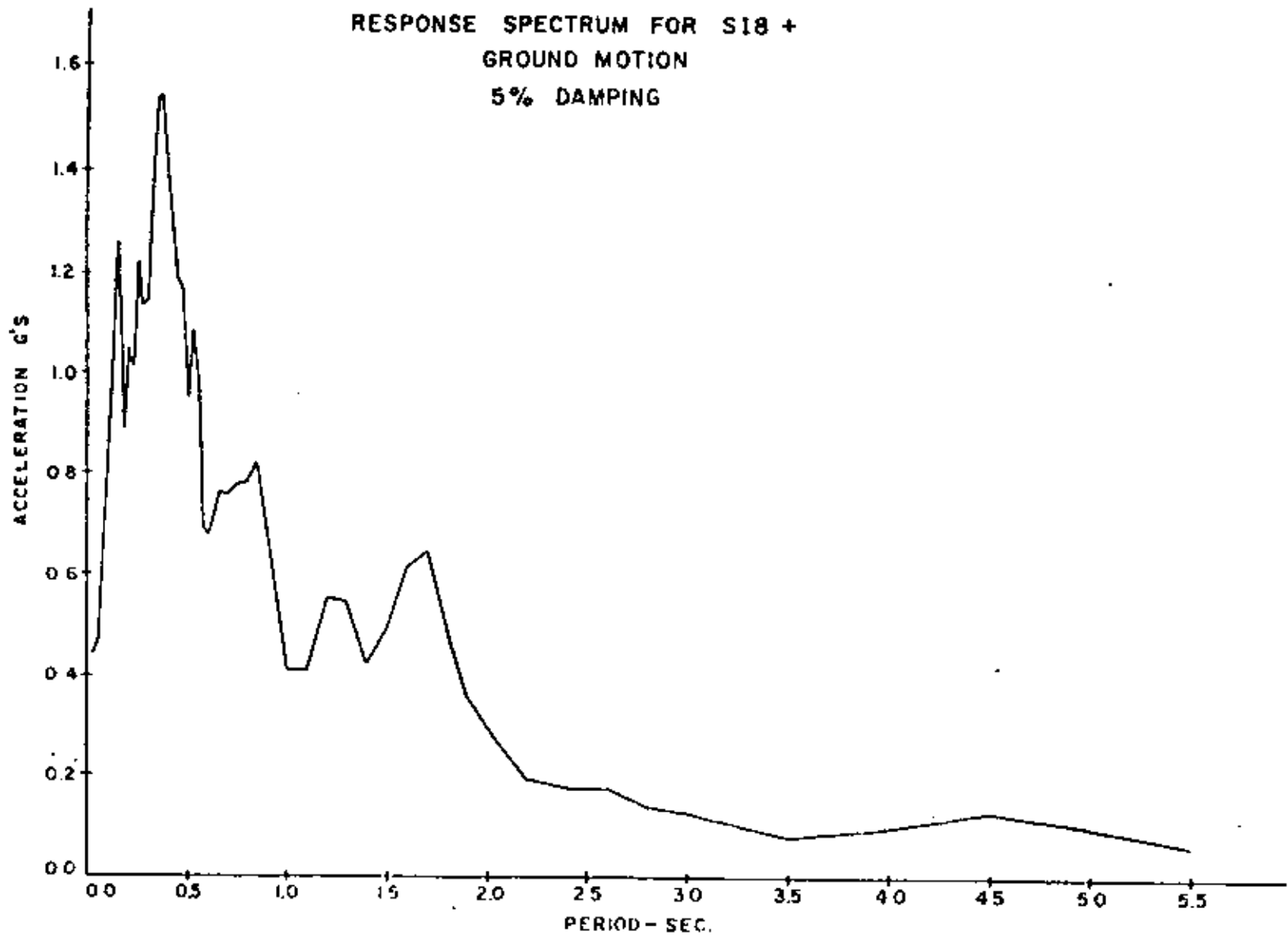
The expansion joint element used in the nonlinear analysis includes several parameters which more realistically describes the boundary conditions at the hinge. Design values shown on the plan drawings for tie and seat gaps were used. In actuality, these values will vary depending on such factors as temperature and shrinkage. Cable restrainer stiffnesses were calculated assuming an effective Young's modulus of 13,800 kips per square inch. The yield force in a typical 3/4 inch restrainer was taken as 30.6 kips. The shear stiffness of elastomeric bearing pads was calculated based on an assumed shear modulus of 135 psi. The coefficient of sliding friction for elastomeric pads on concrete was assumed to be 0.4. For lubricated sliding steel plates, the shear stiffness was assumed to be very high and the friction very low. For the purposes of modeling impacting of the superstructure, the impact spring was assumed to have the axial stiffness of the shortest adjacent section of superstructure.

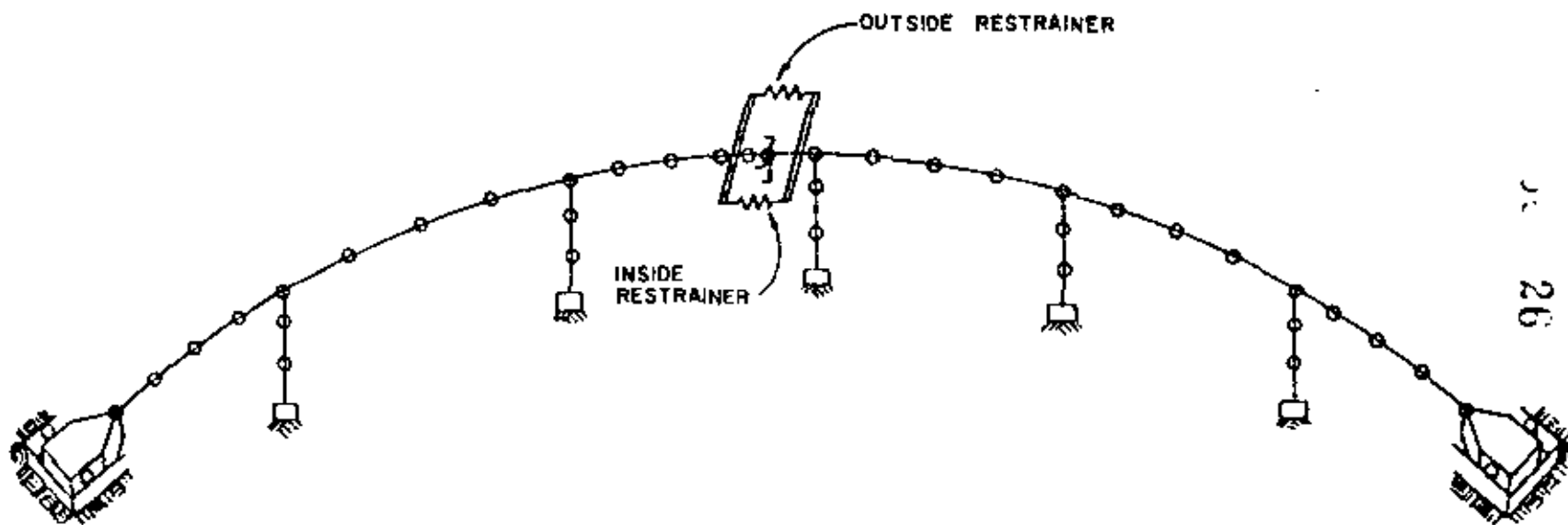
Nonlinear column elements were used at locations where column yielding might be expected. Nonlinear columns were modeled on NEABS by mathematically describing the yield surface as shown in Figure 12.

## Results

Modal participation factors indicated that all three structures had a tendency to respond in more than one mode. Also, because of the curved alignments, each of the bridges had some modes which included high participation in more than one global direction. This makes it likely that similar internal resisting forces will result due to seismic excitation in either global direction.

RESPONSE SPECTRUM FOR S18 +  
GROUND MOTION  
5% DAMPING

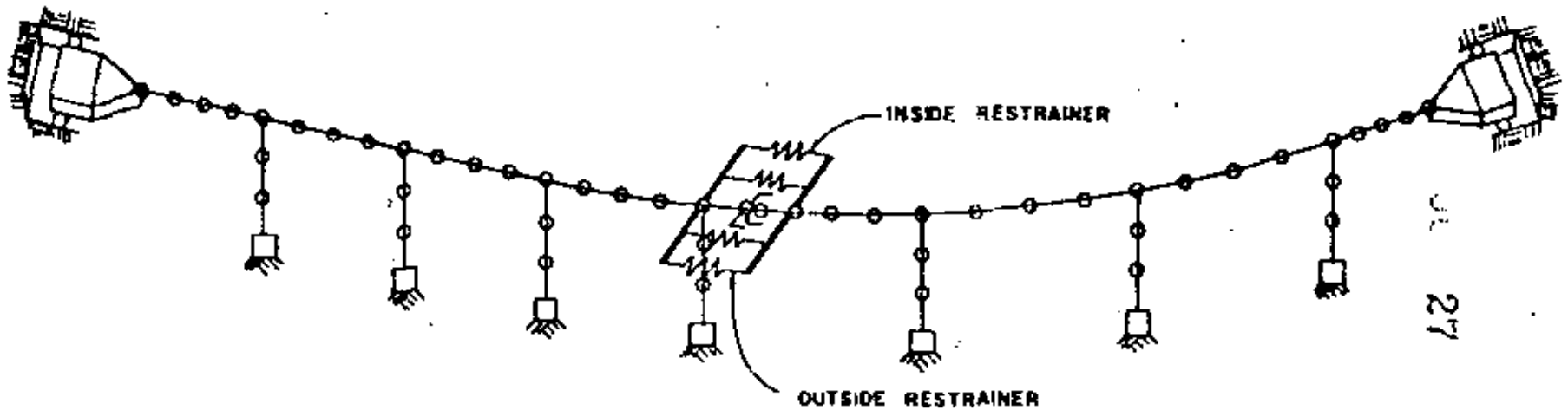




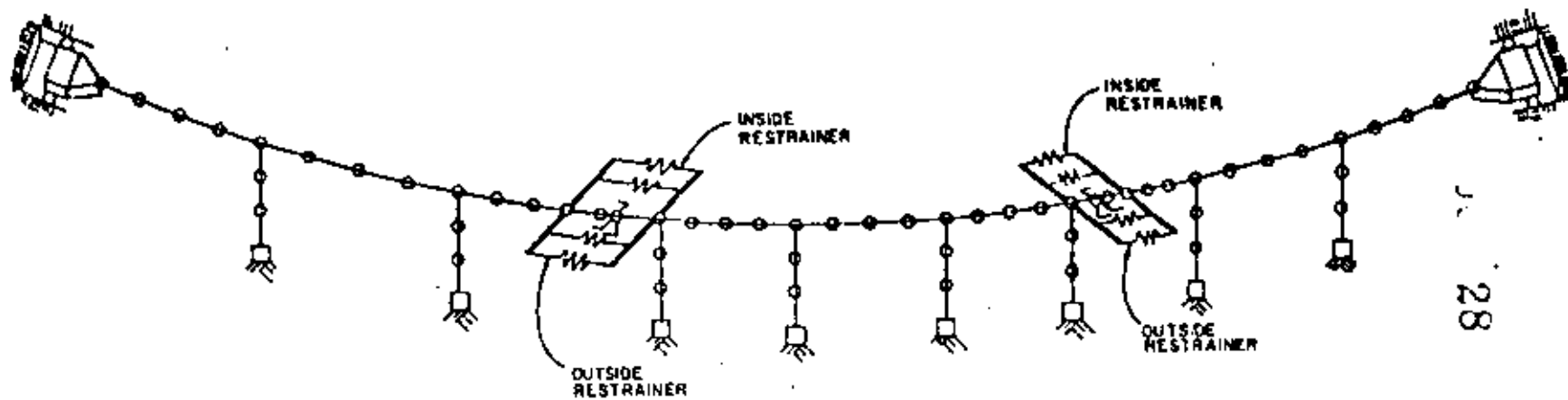
26

BRIDGE 1

ROUTE 80 ON-RAMP



BRIDGE 2  
NORTHEAST CONNECTOR OVERCROSSING



J. 28

BRIDGE 3  
SOUTHWEST CONNECTOR OVERCROSSING

Current bridge design practice is to consider seismic excitation in each of the global directions separately. However, because of the possibility of simultaneous excitation in more than one global direction, and the sensitivity of certain internal force components to excitation from different directions, it would appear that earthquake resistant design would be improved by considering some simultaneous contribution from seismic loading in each of the global directions.

In the case of Bridge 1, the modal periods of the first few modes were very close, and occurred near the peak on the response spectrum for the ground motion used. This resulted in the in-phase modal contributions in the direction of ground motion. In the horizontal direction perpendicular to the ground motion, however, the tendency was for the modes to respond almost exactly out of phase. This was accounted for in both the linear and nonlinear time history analysis. The response spectrum analysis, however, which was based on a root-mean-square combination of modal response, yielded results that did not agree well with the time histories. This was more pronounced as indicated by forces resulting in the direction perpendicular to the ground motion.

Because of the high response of several modes in each of the bridges studied, it was found that a combination of modes that included the peak response plus the RMS of the remaining responses yielded results more in agreement with the linear time history in most cases.

The nonlinear time history analysis results indicated that significant column yielding could be expected in Bridges 1 and 2 while Bridge 3 would have experienced very little yielding. Since these bridges were designed to resist different intensity loadings, this was not considered to be significant.

Bridge 1, because of its lower fundamental period, was subjected to a considerable number of stress reversals that resulted in substantial yielding of the columns. Intuitively, from observing the time history of yielding for these columns, it would appear that a great deal of column degradation would have occurred. Yet the ductility demands, which were based on the maximum nonlinear column deformations, were well below the values considered to be available based on monotonic loading experiments. This points up an interesting deficiency in the current method of designing bridge columns. Based on the above observation, it would appear that short period structures would have a reduced available ductility in the columns due to the increased column degradation that would occur during the larger number of excursions into the nonlinear range. Not only is this not considered in applying a ductility reduction factor to column forces derived from an elastic analysis, but it is common practice to further reduce the forces in short period structures by a risk factor of 2. It would appear that this is just opposite to what should be done.

The nonlinear results for Bridge 2 yielded the highest single maximum column ductility demand of all three structures. The ductility demands in the remaining columns were not as high. It was interesting to note that the elastic moments from this earthquake were approximately double the yield moments. Therefore, had the normal ductility reduction factor been used to design the column for this seismic loading, the ductility demands would have

been even higher. The reason for the high ductility demands in this single column, was the nonuniformity of column stiffness and yield moments which resulted in nonuniform yielding. The current practice of approximating nonlinear behavior by applying a constant ductility reduction factor to an elastic analysis cannot predict this type of behavior.

The effect of large deadload moments was demonstrated in the nonlinear results for Bridge 2. Column yielding was more pronounced in the direction of high deadload moments. This resulted in a biased response that resulted in a tendency to relieve the deadload moments due to yielding. Since this would effect the distribution of normal service load moments and shears following an earthquake, this should be considered during design.

In all the transverse loading cases where column yielding occurred, the nonlinear analysis yielded seismic shear forces at the abutments that were greater than the linear time history analysis results. This is because the columns were incapable of carrying all the shear forces determined in the elastic analysis, and the excess was transferred through the deck to the abutments. This same phenomenon was observed at the hinge in Bridge 2. This particular hinge was located near a stiff column that behaved similar to an abutment during an earthquake. In general, however, hinge shear key forces were slightly less in the nonlinear analysis.

The maximum deck displacements from the nonlinear analysis were almost always less than those from the elastic time history analysis. The exceptions to this were when localized maximum yielding occurred early in the earthquake, and when the deadload moments caused biased yielding as mentioned earlier. Classical methods of predicting nonlinear displacements based on equating strain energy from an elastic analysis to the sum of strain energy and energy dissipated in a yielded structure did not apply for these bridges.

It was obvious that because of reduced deck displacements and the normal gaps that are placed at the hinges to allow for free movement, that hinge restrainers were not stressed in the single hinge bridges. Stresses were developed in the restrainers in the two hinge bridge. The banging action that occurred between the adjacent sections of superstructure caused these forces to vary considerably from the elastic analysis, however. Currently, there appears to be no way of accurately predicting restrainer forces from an elastic analysis. The methods currently used seem to, at least for these bridges, yield conservative results.

#### CONCLUSIONS AND RECOMMENDATIONS

Based on the evaluation of the current methods for determining dynamic response to seismic loading, the following general recommendations can be made relative to the improvement of seismic design methodology for bridges:

- (1) The Uniform Load Method for applying the equivalent static force approach to seismic design of bridges is not totally satisfactory. An improved method using energy principles should be further developed and implemented into the bridge design process.

- (2) The response spectra currently used in the AASHTO specifications should be revised so as not to include the reduction for ductility. Ductility reductions should be made on an individual component basis.
- (3) Seismic design provisions should consider the simultaneous application of earthquake motion in the three component directions since there is in many types of bridges coupling between the component directions within each mode of vibration.
- (4) The PRMS (i.e., peak plus RMS of the remaining) combination of modal contributions resulting from a response spectrum analysis is an improvement for certain bridges analyzed by the response spectrum technique and may potentially be used for bridges having two modes of vibration with approximately equal periods.
- (5) Seismic design provisions should establish some threshold of yielding for moderate earthquakes expected to occur several times during the expected life of the bridge. The need for this aspect of seismic design becomes more prevalent when consideration is given to the unequal distribution of ductility demands in a structure having non-uniform column stiffnesses.
- (6) The number and levels of inelastic excursions which take place in reinforced concrete columns during a maximum credible earthquake should be such that stiffness and strength degradations are minimal. This control is accomplished by proper design and detailing of reinforcement.
- (7) The seismic design should provide for an increase of approximately 1.5 to 2 in the forces at the abutments derived from an elastic analysis if yielding in the columns is anticipated.
- (8) Design provision for combining girder moment due to dead and live-loads should include the effects of deadload moment redistribution due to possible relief of deadload moments at the location of a plastic hinge in the column during an earthquake.
- (9) The use of intermediate hinges should be avoided if possible in bridges located in areas of high seismicity.
- (10) Nonlinear computer capabilities should be made more user oriented for the practicing engineer and should be disseminated to the engineering profession so that they can be used to:
  - (a) Make parameter studies of the seismic nonlinear behavior of bridges
  - (b) Develop more realistic seismic design code provisions
  - (c) Apply nonlinear analysis as a design tool for complex bridges

The questions raised during the course of this evaluation indicate the need for future studies to perfect analytical capabilities for predicting seismic response. Some of the areas that need particular attention are as follows:

- (1) **Stiffness and Strength Degradation** - The possibility of occurrence and the effects of stiffness and strength degradations in reinforced concrete columns on nonlinear dynamic response should be considered.
- (2) **Energy Absorption** - The important role of inelastic energy absorption in the columns and expansion joint restrainers should be studied further. Special attention should be given to developing a clearer understanding of the concept of ductility and how it relates to bridge design so that elastic analysis techniques may be used with a greater degree of confidence by the bridge engineer.
- (3) **Restrainer Units** - Non-uniform yielding and ductility demands in columns result in larger forces at the restrainer units for bridges with more than one intermediate hinge. These effects should be studied further to investigate the current minimum specification in the code and to determine if elastic analysis techniques currently used can predict these restrainer forces.
- (4) **Response Spectrum Analysis** - Special studies to improve the results gained from a response spectrum analysis are needed. The determination of the most effective means of combining modal results for a particular bridge is especially needed.
- (5) **Equivalent Static Force** - Additional studies should be made to better define the degree of applicability of the generalized coordinate approach to the simplified equivalent static force method for the seismic analysis of bridges.

A computer capability such as NEABS represents a powerful research tool. It may be effectively used for studying special problems related to bridge design and analysis, and for analyzing bridge response due to past and future earthquakes. Because of its potential for advancing the state of knowledge, these computer capabilities should be made more user oriented to provide researchers and engineers with effective means for analytically studying bridge seismic behavior.

#### REFERENCES

1. Standard Specifications for Highway Bridges, Twelfth Edition, 1977, American Association of State Highway and Transportation Officials.
2. T. Iwasaki, J. Penzien, and R. W. Clough, "Literature Survey--Seismic Effects on Highway Bridges," Report No. EERC 71-11, Earthquake Engineering Research Center, University of California, Berkeley, November 1972.
3. W. S. Tseng and J. Penzien, "Analytical Investigations of the Seismic Response of Long Multiple-Span Highway Bridges," Report No. EERC 73-12, Earthquake Engineering Research Center, University of California, Berkeley, June 1973.

4. M. C. Chen and J. Penzien, "Analytical Investigations of Seismic Response of Short, Single or Multiple-Span Highway Bridges," Report No. EERC 75-4, Earthquake Engineering Research Center, University of California, Berkeley, January, 1975.
5. M. C. Chen and J. Penzien, "Nonlinear Soil-Structure Interaction of Skew Highway Bridges," Report No. UCB/EERC-77/24, Earthquake Engineering Research Center, University of California, Berkeley, August 1977.
6. D. Williams and W. G. Godden, "Experimental Model Studies on the Seismic Response of High Curved Overcrossings," Report No. EERC 76-18, Earthquake Engineering Research Center, University of California, Berkeley, June 1976.
7. K. Kawashima and J. Penzien, "Correlative Investigations on Theoretical and Experimental Dynamic Behavior of a Model Bridge Structure," Report No. EERC 76-26, Earthquake Engineering Research Center, University of California, Berkeley, July 1976.
8. R. Imbsen, R. V. Nutt, and J. Penzien, "Seismic Response of Bridges-Case Studies," Report No. UCB/EERC-78/14, Earthquake Engineering Research Center, University of California, Berkeley, June 1978.
9. W. G. Godden, R. A. Imbsen and J. Penzien, "A Summary Report on the Seismic Behavior of Reinforced Concrete Bridges," Report to the U.S. Department of Transportation, Federal Highway Administration, December 1978.
10. R. A. Imbsen, et al., "Applications of the 1973 California Earthquake Criteria," Report SM45, Division of Structures, Structure Mechanics, California Department of Transportation, Sacramento, California, September 1974.
11. G. Fung, R. LeBeau, E. Klein, J. Belvedere and A. Goldschmidt, "Field Investigation of Bridge Damage in the San Fernando Earthquake," State of California, Division of Highways, Bridge Department, 1971.
12. R. D. Logcher, B. B. Flachsart, E. J. Hall, C. M. Power, R. A. Wells, and A. J. Ferrante, "ICES STRUDL II The Structural Design Language, Engineering User's Manual, Volume 1, Frame Analysis," MIT Department of Civil Engineering Report R68-91, November 1968.
13. "STRUDL, STRUDL DYNAL and STRUDL Plots," by MCAUD and Multisystems, Inc.
14. H. B. Seed and I. M. Idress, "Rock Motion Accelerograms for High Magnitude Earthquakes," Report No. EERC 69-7, Earthquake Engineering Research Center, University of California, Berkeley, 1969.

# EARTHQUAKE-RESISTANT DESIGN OF BRIDGES

## CONTENTS

1. INTRODUCTION.
2. PROVISIONS FOR EARTHQUAKE-RESISTANT DESIGN OF BRIDGES.
  - 2.1. System of Current Specifications.
  - 2.2. Seismic Coefficient Method.
  - 2.3. Modified Coefficient Method Considering Dynamic Structural Response.
  - 2.4. Design Ground Surface.
  - 2.5. Seismic Earth Pressure.
  - 2.6. Hydrodynamic Pressure During Earthquake.
  - 2.7. Allowable Stresses.
  - 2.8. General Provisions for Design of Structural Details.
  - 2.9. Inertia Forces of Super-Structures Acting to Sub-Structures.
  - 2.10. Safety Factors for Foundation Design.
  - 2.11. Design of Spread Footing Foundations.
  - 2.12. Design of Tilt Foundations.
  - 2.13. Design of Column Foundations.
  - 2.14. Specifications for Earthquake-Resistant Design of Hambo-Shitoku Bridges.
3. EXAMPLES OF EARTHQUAKE-RESISTANT DESIGN OF BRIDGES.
  - 3.1. Introduction.
  - 3.2. Examples of Designing Sub-structure and Super-structure.
  - 3.3. Examples of Analytic Design of Supports and Joints.

## EDITORIAL GROUP

Hironichi Higashihara, Long Span Bridge Consultants, Inc.

Manabu Ito : University of Tokyo

Tsunoo Katsuyama : University of Tokyo

Assistance by Mr. Masaru Nakamura (Hamabo Shitoku Bridge Authority) and Mr. Akioyo Shimizu (Japanese National Railways) is gratefully acknowledged.

BRIDGE AND STRUCTURAL COMMITTEE,  
JAPAN SOCIETY OF CIVIL ENGINEERS

001 34

## I. INTRODUCTION

This is an almost complete revised version of "Earthquake Engineering of Bridges" contained in the fourth edition of this book published in 1971. The purpose here is to briefly summarize the current earthquake provisions for the design of bridge structures in Japan and to show some of the typical examples of the earthquake-resistant design of Japanese bridges.

There have been a number of revisions made in earthquake provisions on the design of bridges, which can be clearly seen in the past four editions of this book (1961, 1964, 1968 and 1973). As the concept of the seismic design of bridges became more clear in recent years, there has been an effort to establish a unified earthquake-resistant code. The establishment of the "Specifications for the Earthquake-Resistant Design of Highway Bridges" in 1971 is one of the results of such efforts. The content of this edition is intended to be more concise and systematically presented as compared with those of the earlier editions which had to necessarily include different clauses from different codes belonging to a number of organizations. Also in this edition, considerable part of "examples" of earthquake-resistant design was replaced by more recent ones.

It may be worth noting here that a good earthquake-resistant design of a bridge is not that of super structure or sub structure alone. The most economical and rational seismic design as a whole bridge system is only achieved when due consideration is paid for topographical, geological and soil conditions of the site.

## 2. PROVISIONS FOR EARTHQUAKE-RESISTANT DESIGN OF BRIDGES

### 2.1 SYSTEM OF CURRENT SPECIFICATIONS

There used to be a number of different earthquake provisions specified by various concerned organizations such as the Japanese Highway Public Corporation and the Tokyo Expressway Public Corporation. However, since 1971 when the "Specifications for the Earthquake-Resistant Design of Highway Bridges" was issued by the Japan Road Association, this superseded the provisions previously found in different codes as far as the seismic design of highway bridges is concerned. This specification was established in order to give a common basis for the design methodology and, therefore, places emphasis on the method of evaluating seismic forces, the basic principles to be exercised for treating soil conditions at the site, and the general provisions to be observed for structural details in the earthquake-resistant design of highway bridges. It does not include clauses explicitly describing the design procedures for substructures of highway bridges, which are currently designed according to the "Specifications for the Design of Sub Structures of Highway Bridges" also issued by the Japan Road Association.

Parallel with the specifications for highway bridges mentioned above, the Japanese National Railways has its own system of design specifications for the structures under the jurisdiction of JNR. There also are cases in which special specifications are treated for the

earthquake-resistant design of structures in important, large-scale projects. The "Specifications for Earthquake-Resistant Design of Honshu-Nishiku Bridges" is a typical example, which was established primarily for the seismic design of long-span suspension bridges having large foundations under the sea.

Since the general philosophies behind different earthquake provisions are similar, the specifications for highway bridges will be referred to in some of the following sections (2.2, 2.3, 2.4, 2.4.1 and 2.5), and those for the JNR bridges in Sections 2.5, 2.6, 2.10, 2.11, 2.12, and 2.13.

The specifications which will be frequently mentioned in the following sections are listed below with their abbreviations.

- SEHB "Specifications for the Earthquake-Resistant Design of Highway Bridges (1971)", Japan Road Association.
- SHSD "Specifications for the Design of Sub-Structures of Highway Bridges", Japan Road Association.
  - Survey and Design in General (1966)
  - Design of Pier Foundations (1964)
  - Design of Spread Footing Foundations (1967)
  - Design of Piers and Abutments (1968)
  - Design of Caisson Foundations (1970)
- SRS "Specifications for the Design of Railway Structures", Japanese National Railways.
  - Foundation Structures and Structures Resisting Earth Pressure (1974)

### 2.2. SEISMIC COEFFICIENT METHOD

For the design of highway bridges, SEHB specifies the seismic coefficient method if a structure has the fundamental natural period shorter than 0.5 seconds. The horizontal design seismic coefficient  $A_h$  in this case is obtained by the following formula,

$$A_h = r_1 r_2 r_3 A_s \quad \dots \dots (1)$$

- where:  $A_h$ : Horizontal design seismic coefficient,
- $A_s$ : Standard horizontal design seismic coefficient (=0.2),
- $r_1$ : Seismic zone factor,
- $r_2$ : Ground reaction factor, and
- $r_3$ : Importance factor.

The factors  $r_1$ ,  $r_2$  and  $r_3$  are given in Fig. 1 and Tables 1, 2 and 3. The coefficient  $A_s$  is

Table 1. Seismic Zone Factor  $r_1$   
(refer to Fig. 1)

Zone	Value of $r_1$
A	1.0
B	0.75
C	0.5

000 35

Table 2. Ground Condition Factor  $\alpha$

Group	Description <sup>1)</sup>	Value of $\alpha$
1	(11) Ground of the Tertiary era or older (defined as follows described) (12) Quaternary layer <sup>2)</sup> with depth less than 10 meters above bedrock	0.8
2	(13) Quaternary layer <sup>2)</sup> with depth between 10 to 20 meters above bedrock (14) Alluvial layer <sup>2)</sup> with depth less than 10 meters above bedrock	1.0
3	Alluvial layer <sup>2)</sup> with depth less than 20 meters, which has soft layer <sup>3)</sup> with depth less than 5 meters	1.2
4	Other than the above	1.5

Notes: 1) Since these definitions are not very comprehensive, the description of ground condition shall be made with additional consideration of the bridge site.  
2) Depth of layer indicated here shall be determined from the actual ground surface.  
3) Loose alluvial layer such as drain sand, silt, gravel layer, or siltstone, etc. are notched under this category.  
4) Alluvial layer includes a new sedimentary layer made by landslide.  
5) Layers whose bearing capacity should be improved shall be described as Section 3.4.

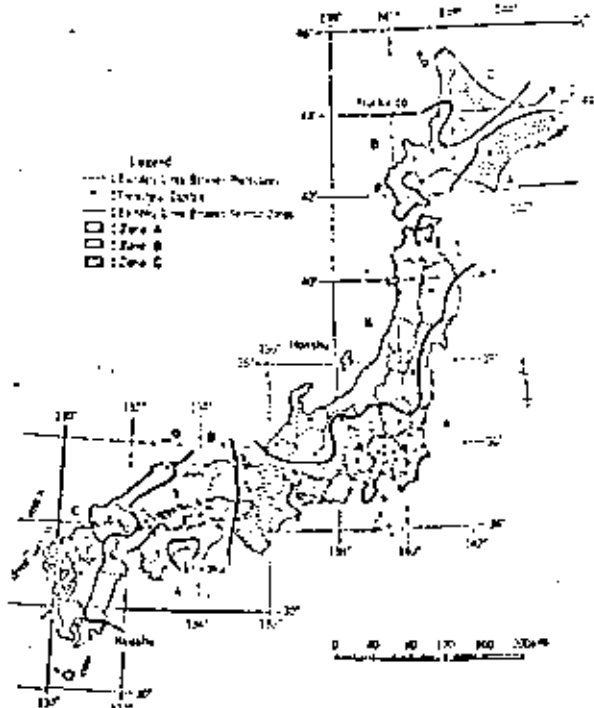


Fig. 1. Seismic Zoning Map.

Table 3. Importance Factor  $\gamma$

Group	Definition	Value of $\gamma$
1	Highways, expressways, arterial roads, highways, general national highways and principal arterials, and highways, important facilities on general arterial highways and national highways	1.0
2	Other than the above	0.8

Note: 1) The value of  $\gamma$  may be increased up to 1.20 for special cases in Group 1.

rounded to two decimals with the minimum value of 0.10. The maximum for coastal design seismic coefficient is 0.24 for most cases but may be increased to 0.30 as seen from the footnote of Table 3. The vertical seismic force is not considered in general except for design of bearing at the junction of super- and sub-structures. In the latter case, the vertical design seismic coefficient of  $k_v = 0.1$  is used.

For the structures under the jurisdiction of JNR, SCS specifies the basic horizontal seismic coefficient of 0.15 or 0.2 according to the zone classification, which is modified by considering the ground condition of the site and the importance of the structure. The minimum and the maximum value of the horizontal seismic coefficient are 0.11 and 0.27, respectively, and the vertical seismic coefficient of 0.10 should be taken into account.

### 2.3 MODIFIED SEISMIC COEFFICIENT METHOD CONSIDERING DYNAMIC STRUCTURAL RESPONSE.

When a bridge is supported on tall and flexible pier and its fundamental natural period is relatively large, the conventional seismic coefficient method usually becomes inadequate. For a highway bridge with the fundamental natural period of the super- and sub-structure system longer than 0.5 seconds, SEHB specifies that the seismic coefficient be modified by considering dynamic structural response:

$$k_{hd} = \beta k_s \tag{2}$$

where  $k_{hd}$  is the design horizontal seismic coefficient,  $k_s$  is the quantity as described in

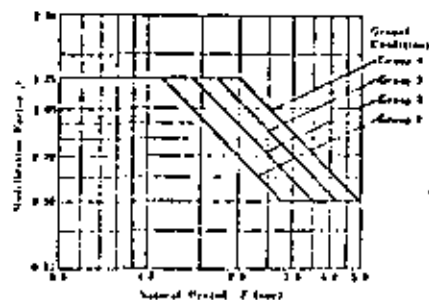


Fig. 2. Modification Factor  $\beta$  (refer to Table 4).

Section 2.2, and the modification factor  $\beta$  which depends on the fundamental natural period and the ground condition of the site as to be obtained from Fig. 2 and Table 4. The value of  $k_{sm}$  is also bounded to two decimals and the minimum value is 0.05. It should be noted that the natural period here is that of the whole bridge system consisting of super- and sub-structures and that the modified seismic coefficient  $k_{sm}$  should not be used for the design of the super-structures of suspension bridges, arch-type or cantilever-type bridges in which flexible super-structures result in long natural periods.

Table 6. Value of Mod. Seismic Factor  $\beta$ .

Group of Ground Conditions Given in Table 1	Value of $\beta$ for Fundamental Period $T$ (sec)		
	1	$\beta=1.0$ for $0.3 \leq T \leq 1.0$	$\beta=1.0/7$ for $1.0 < T \leq 2.0$
2	$\beta=1.0$ for $0.3 \leq T \leq 1.0$	$\beta=1.0/7$ for $1.0 < T \leq 2.0$	$\beta=0.8$ for $T > 2.0$
3	$\beta=1.0$ for $0.3 \leq T \leq 1.0$	$\beta=1.0/5$ for $1.0 < T \leq 2.0$	$\beta=0.8$ for $T > 2.0$
4	$\beta=1.0$ for $0.3 \leq T \leq 1.0$	$\beta=1.0/7$ for $1.0 < T \leq 2.0$	$\beta=0.8$ for $T > 2.0$

Table 8. Formulae for Fundamental Periods of Bridges Supported by Spread Foundations or Pile Foundations

Type of Structural System	Direction	Formulae for Fundamental Periods	
		Pier Material	
		Reinforced Concrete	Steel
Most of super-structures are of continuous type with fixed end-piers and fixed or free end-piers. For bridges with one or two piers, the pier height is measured from the top of the pier to the top of the deck. For bridges with two or more piers, the pier height is measured from the top of the pier to the top of the deck. For bridges with one or two piers, the pier height is measured from the top of the pier to the top of the deck. For bridges with two or more piers, the pier height is measured from the top of the pier to the top of the deck.	Transverse	$T = 2.0 \sqrt{\frac{W_p + W_{sp}}{k_p}}$ (A-1)	$T = 2.0 \sqrt{\frac{W_p + W_{sp}}{k_p}}$ (A-2)
		Longitudinal	$T = 1.0 \sqrt{\frac{W_p + W_{sp}}{k_p}}$ (A-3)
Other than the above and to include a bridge consisting of systems with both ends rigidly supported.	Longitudinal or Transverse	$T = 2.0 \sqrt{\frac{W_p + W_{sp}}{k_p}}$ (A-4)	

Note:  $T$  = Fundamental period in second of the system consisting of a sub-structure and the section of super-structure supported by it.

$W_p$  = Weight of the pier in k.

$W_{sp}$  = Weight of the section of super-structure fixed supported by the sub-structure under consideration.

$E$  = Young's modulus of the pier material in  $\text{ksi}^2$ .

$I$  = Moment of inertia of the pier in  $\text{in}^4$  in the direction considered (average value when cross-section varies with height).

$h$  = Height of the pier in ft. and

$g$  = Acceleration of gravity  $32.2 \text{ ft/sec}^2$ .

\* Eq. (A-2) shall be used when the ratio of the length between the supports,  $L$ , is both alternate to the width,  $B$ , between outside girders in the pier, approximately 30 (see Fig. 3).

substructure part of the bridge consisting of a pier and the super-structures supported by it. The ratio of the bridge is supported by piers with different heights, the modified design seismic coefficient differs for each pier. The fundamental natural period of the bridge supported by spread or pile foundations is obtained by the formulae given in Table 8 and that of the bridge supported by column foundation by the formulae in Table 6. Since the formulae in Table 8 are obtained by assuming that 1) the base of the footing is below the surface of the level supporting ground (the design ground surface described in Section 2.4) and 2) the elastic deformation of the pier above the footing has the primary effect on the overall deformation of the sub-structure, they should not be used if the base of the footing is above the design ground surface.

Table 8. Formulae for Fundamental Periods of Bridges Supported by Column Foundations

Type of Structural System	Direction	Formulae for Fundamental Periods	
		Transverse	Longitudinal
Type 1 in Table 5	Transverse	One of Eqs. (A-1) and (A-2) that gives the largest value of $T$ .	Eq. (A-3)
	Longitudinal	Eq. (A-3)	
Type 2 in Table 5	Transverse	One of Eqs. (A-1) and (A-2) that gives the largest value of $T$ .	
	Longitudinal	Eq. (A-3)	

Note: See also Table 6.

$$T = 2.0 \sqrt{\frac{W_p + W_{sp}}{k_p}} \quad (A-1)$$

Note:

1. Fundamental period is period of the system consisting of a sub-structure and the section of the super-structure supported by it.

2.  $W_p$  = Weight of one pier in k.

3.  $W_{sp}$  = Weight of the part of super-structure fixed supported by the sub-structure under consideration.

4.  $E$  = Young's modulus of the pier material in  $\text{ksi}^2$ .

5.  $I$  = Moment of inertia in  $\text{in}^4$ .

6.  $h$  = Height of pier in ft.

7.  $g$  = Acceleration of gravity in  $\text{ft/sec}^2$ .

8.  $L$  = Vertical distance between girders in ft. at the base of the column foundation.

9.  $B$  = Horizontal coefficient of subgrade reaction in  $\text{ksi/ft}^2$  at the base of the column foundation, and

10.  $L/B$  = Horizontal coefficient of subgrade reaction in  $\text{ft}^2$  at the base of the column foundation.



Fig. 3. An Example of Type I Structural System in Table 8.

## 2.4. DESIGN GROUND SURFACE.

SEIB specifies the soil layers whose bearing capacities are neglected in earthquake-resistant design. The design ground surface is defined as the level of the lower boundary of the neglected layer if it extends continuously below the actual ground surface. The neglected layer is assumed to have zero cohesion and a triangle of internal friction but its surcharge effect should be taken into account for the examination of the bearing capacity of the soil below the footing. It is not necessary to apply seismic forces to the structural parts, soils and water below the design ground surface nor to consider the seismic earth pressure to the substrate from the neglected layer.

The soil layers to be neglected in earthquake-resistant design are:

1) Sandy soil layers—Substrata—Saturated sandy soil layers within 10 m of the actual ground surface with a standard penetration test  $N$ -value less than 10, a coefficient of uniformity less than 6, and a  $D_{60}$  value of the grain size accumulation curve between 0.01 mm and 0.3 mm. If the  $D_{60}$  value is between 0.04 mm and 0.04 mm or between 0.5 mm and 1.2 mm, special consideration should be paid because of moderate liquefaction potential.

2) Extremely soft cohesive soil layers—Cohesive or silty soil layers within 5 m of the actual ground surface with a compressive strength  $q_u$  as determined by unconfined compression test or field test less than 0.2 kg/cm<sup>2</sup>.

## 2.5. SEISMIC EARTH PRESSURE.

For the design of structures to resist earth pressure, active earth pressure, passive earth pressure or earth pressure at rest is considered depending on the condition of the relative displacement between structure and soil. Design formulas are based on the Coulomb's earth pressure theory, from which the Moseley-Obolov's formulas for the calculation of seismic earth pressure are derived. Though there are some minor differences between the formulas specified in SEIB and SRS, they are basically the same. Table 7 summarizes the formulas used for the calculation of earth pressure specified in SRS, which is used for the design of structures under the jurisdiction of the Japanese National Railways.

## 2.6. HYDRODYNAMIC PRESSURE DURING EARTHQUAKES.

According to SRS, hydrodynamic pressure during an earthquake acting on a column-like structure is calculated by either of the following formulas:

(i) When  $h/H \leq 2$  and  $h/l \leq 3$ ,

$$p_w = a_h \gamma_w \left[ \frac{H}{L} \left( 1 - \frac{H}{4H} \right) \frac{z^2 \gamma^2}{H} \right] \quad \dots \dots (3)$$

(ii) When  $2 \leq h/H \leq 4$  and  $h/l \leq 3$

$$p_w = a_h \gamma_w \left[ \frac{H}{L} \left( 0.7 - \frac{H}{10H} \right) \frac{z^2 \gamma^2}{H} \right] \quad \dots \dots (4)$$

where

$p_w$  = Seismic hydrodynamic pressure per unit kg/cm<sup>2</sup> at depth  $z$  from the water surface,

Table 7. Summary of Formulas for Calculation

	Active Earth Pressure	
	Non-Cohesive Soils	Cohesive Soils
At Rest Earth Pressure	$P_w = \frac{1}{2} \gamma_w z \left[ \frac{1 + \sin \phi}{1 - \sin \phi} \right] \frac{z^2}{H}$	$P_w = \frac{1}{2} \gamma_w z \left[ \frac{1 + \sin \phi}{1 - \sin \phi} \right] \frac{z^2}{H}$
During Earthquake	$P_w = \frac{1}{2} \gamma_w z \left[ \frac{1 + \sin \phi}{1 - \sin \phi} \right] \frac{z^2}{H}$	$P_w = \frac{1}{2} \gamma_w z \left[ \frac{1 + \sin \phi}{1 - \sin \phi} \right] \frac{z^2}{H}$

Notes:  
 (1) Effect of hydrodynamic pressure should be considered in the case of active earth pressure and earth pressure at rest in deformable soils.  
 (2)  $a_h$ ,  $\gamma_w$  and  $z$  are shown in Fig. 8.

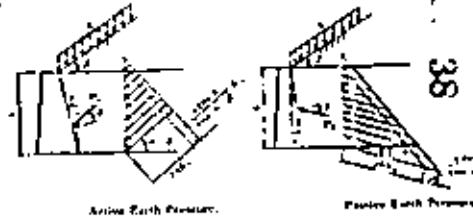


Fig. 8. Explanation of Some of the Symbols.  
 1.  $a_h$  - Active earth pressure.  
 2.  $P_w$  - Passive earth pressure.  
 3.  $P_w$  - Earth pressure at rest.  
 4.  $a_h$  - Active earth pressure during earthquake.

$k$  - Correction factor for different types of movements of a structure (usually = 1).  
 $L$  - Horizontal cross-sectional area of a structure (including hollows).  
 $L$  - Length of a structure parallel to the direction of ground shaking.  
 $B$  - Width of a structure perpendicular to the direction of ground shaking.

of Earth Pressure Specified in NR

Positive Earth Pressure		Earth Pressure Acting on Immovable Wall
Non-Cohesive Soils	Cohesive Soils	
$P_e = \frac{1}{2} \gamma H^2 K_a \cos^2 \beta$	$P_e = \frac{1}{2} \gamma H^2 K_a \cos^2 \beta + \frac{c \sin^2 \beta}{\cos \beta}$	Vertical wall $\beta = 90^\circ$ Inclined wall $\beta = \text{angle of wall}$ $\rho = \text{density of soil}$ $\rho = \text{density of water}$
$K_a = \frac{1 - \sin \phi}{1 + \sin \phi}$		
<p>Above groundwater table <math>\rho = \text{density of soil}</math></p>	<p>Pressure <math>\rho</math> in soil for water-saturated soils by <math>\frac{1}{2} \gamma_w H^2</math>, where <math>\gamma_w = \rho_w g</math> is the saturated unit weight.</p>	Vertical wall $\beta = 90^\circ$ Inclined wall $\beta = \text{angle of wall}$ Applied = $\rho_w g H^2$
<p>Below groundwater table Beginnings by <math>\frac{1}{2} \rho_w g H^2</math> for <math>\beta = 90^\circ</math>.</p>		
$K_a = \frac{1 - \sin \phi}{1 + \sin \phi}$		

- 1.  $P_e$  = Force of earth pressure during earthquake.
- 2.  $\beta$  = Angle of wall face to horizontal in direction of water during earthquake.
- 3.  $K_a$  = Active earth pressure coefficient.
- 4.  $\rho$  = Density of earth pressure coefficient.
- 5.  $\gamma$  = Unit weight of soil pressure at any depth for sand and medium to stiff clay with  $N_{60}$ .
- 6.  $\gamma_w$  = Unit weight of water pressure at any depth for sand and medium to stiff clay with  $N_{60}$ .
- 7.  $\rho$  = Density of earth pressure coefficient during earthquake.
- 8.  $\rho_w$  = Density of water pressure coefficient during earthquake.
- 9.  $\phi$  = Angle of internal friction.
- 10.  $\rho$  = Unit weight of soil.
- 11.  $\rho_w$  = Unit weight of water.
- 12.  $\rho_w$  = Unit weight of water.
- 13.  $\rho_w$  = Unit weight of water.
- 14.  $\rho_w$  = Unit weight of water.
- 15.  $\rho_w$  = Unit weight of water.
- 16.  $\rho_w$  = Unit weight of water.
- 17.  $\rho_w$  = Unit weight of water.
- 18.  $\rho_w$  = Unit weight of water.
- 19.  $\rho_w$  = Unit weight of water.
- 20.  $\rho_w$  = Unit weight of water.

$$K_a = \frac{1 - \sin \phi}{1 + \sin \phi}$$

- $K_a$  = Horizontal design seismic coefficient.
- $\gamma_w$  = Unit weight of water.
- $H$  = Total depth of water, and
- $y$  = Depth from the water surface.

However, since the hydrodynamic pressure is small for the plus of an ordinary cycle.

crossing bridge, its effect may generally be ignored.

SEER gives the following formulas for the total hydrodynamic force acting on the structure:

(1) Wall-type structure as shown in Fig. 4(a).

$$F = \frac{1}{12} \gamma_w H^3 \quad \dots \dots (1)$$

$$H_o = \frac{1}{2} H \quad \dots \dots (2)$$

(2) Column-type structure as shown in Fig. 4(b).

$$F = \frac{3}{4} \gamma_w H^3 \left(1 - \frac{H}{4H}\right) \quad \text{for } \frac{H}{H} \leq 2 \quad \dots \dots (3)$$

$$F = \frac{3}{8} \gamma_w H^3 \quad \text{for } \frac{H}{H} \geq 2 \quad \dots \dots (4)$$

$$H_o = \frac{1}{2} H \quad \dots \dots (5)$$

Eq. (3) is derived from the well-known Weisberg's formula, and the point of application of the hydrodynamic force is taken as a half of the depth of water for the purpose of simplicity and the increased safety margin. Eq. (7) is obtained from Eq. (3) by putting  $\alpha = 1$  and  $L = H$ , and by integrating over the distance  $y$  from zero to  $H$ . Eq. (8) shows that the hydrodynamic force for  $H/H \geq 2$  is assumed to be equal to that for  $H/H = 2$  since this force decreases with the increase in  $H/H$  as indicated by Eq. (3). The point of application of the force is again assumed to be  $0.5H$  from the bottom because of the same reasons described above.

For the seismic stability analysis of a wall-type structure as shown in Fig. 4(a), hydrostatic and hydrodynamic pressures and the inertia force of the structure are concurrently taken into account in the direction of the hydrostatic pressure, and only the inertia force and earth pressure are considered in the opposite direction. In the latter case, the effect of hydrostatic and hydrodynamic pressures is not considered for the purpose of increased safety margin. The hydrodynamic pressure in one direction alone is considered in the design of a column-like structure surrounded by water since hydrostatic pressure in this case is self-equilibrating.

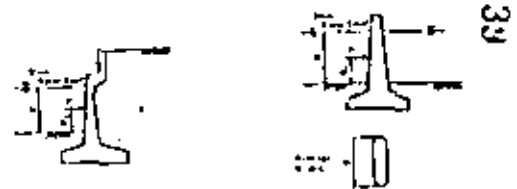


Fig. 4. Symbols Used in Eqs. (1)-(8).

## 2.7. ALLOWABLE STRESSES.

When earthquake forces are combined with primary loads (or dead load), allowable stresses are increased because the occurrence of such a combination is less frequent. Table 8 summarizes the factors used for increasing allowable stresses of steel and reinforced concrete members in bridge structures. Table 9 gives allowable tensile stresses of concrete and factors used for increasing allowable compressive stresses of prestressed concrete members. For the examination of the earthquake resistance of prestressed concrete bridges against failure, a factor of safety of not less than 1.5 should be observed for the most unfavorable combination of dead load and earthquake forces.

Table 8. Factors for Increasing Allowable Stresses for Combination of Earthquake Effect and Primary Loads.

	Specification	Combination	Factor for Increasing Allowable Stress
Steel	BS	$P+EQ+T$	1.30
	BSB	$D+EQ+T$	1.20
	BSIB	$P+EQ$	1.30
Reinforced Concrete	BS, BSIB and BSIB	$D+EQ$	1.30
		$D+T+EQ$	1.50

BSB = Specification for the Design of Highway Bridge.  
 BSIB = Specification for the Design of Reinforced Concrete Highway Bridges.  
 P = Double Live-Load + Gravitational Force.  
 T = Total Live-Load + Impact + Earth Pressure + Hydraulic Pressure + Wind.  
 EQ = Earthquake Force.  
 D = Effect of Temperature Variation.  
 T = Dead Load.  
 BS = Section of Design Standards.

Table 9. Allowable Stresses of Prestressed Concrete Members for Earthquake Effect.

	Allowable Tensile Stress as Traction Force of a Member (N/mm <sup>2</sup> )			Factor for Increasing Allowable Stress in Upper Part of a Member	Allowable Tensile Stress at Prestressing Bed of % $\sigma_{pc}$	Allowable Tensile Stress of Steel Wire
	Top	Mid	Bottom			
BS	0.5	0.5	0.5	100%	—	1.5 $\sigma_{pc}$ (without slip strand)
BSB	0.5	0.5	0.5	100%	1.5 $\sigma_{pc}$ (with strand)	1.5 $\sigma_{pc}$
BSIB	—	—	—	100%	As above	As above

\* Tensile stresses may be totally reduced by well laid and prestressing strands in a row leaving the strands

strength of concrete.

\*\* Allowable Tensile Stress of Top Part of a Member of a Member.

\*\*\* Specification for the Design of Reinforced Concrete Highway Bridges.

The earthquake-resistant design should provide sufficient stability against seismic distortions for a body as a whole and for its all component parts. It is essential for a bridge to maintain its structural integrity even in the event of a strong seismic motion. For this purpose, the importance of the design of structural details cannot be over-emphasized.

SEIBB states that special attention should be paid to the following aspects:

- 1) When abutments are constructed on soft ground, the possibility of failure of the surrounding soil should be examined.
- 2) When the substructures of a bridge are built on different types of ground, or of different structural types, or of different dimensions, the structural details should be designed by taking into account that the substructures may respond differently during an earthquake.
- 3) Joints between super- and substructures, connections between piers and foundations, or between bearings and piers in pier foundations are often vulnerable to seismic disturbances. Design of such structural details should be made by considering accuracy of evaluation of ground conditions, existence of construction joints, accuracy of construction, etc.

There are three possible methods applicable to the design of bridge supports with special reference to preventing spans from falling off their supports during earthquakes. They are 1) installation of adequate stoppers at expansion bearings to restrict excessive movement, 2) widening bridge seats, and 3) connecting adjacent girders or girders with pier or abutment. According to SEIBB, an expansion bearing should be provided with an adequate stopper, and in addition either 2) or 3) mentioned above should be incorporated. A stopper may be an integral part of a bearing or may be installed independently near the bearing. The horizontal design seismic coefficient used for the design of such stoppers is 1.5 times greater than that obtained by Eq. (1) or (2). SEIBB specifies that the length  $S$  (in cm) between the end of the bearing and the edge of the substructure (as shown in Fig. 5(a)) be not less than the following values:

$$20; 0.5L \quad \text{for } L < 100 \text{ m}$$

$$30; 0.4L \quad \text{for } L > 100 \text{ m}$$

in which  $L$  is the span length in meters. These values were determined from past experience and are considered sufficient to prevent collapse of girders and to prevent spalling of concrete in the peripheral region of the substructure's crest during strong earthquake disturbances. From similar considerations, the minimum length between the ends of girders at a suspended joint (as shown in Fig. 5(b)) is specified as 60 cm. For particularly important bridges constructed on soft ground (Group 4 ground in Table 2), it is desirable to have the length  $S$  greater than 35 cm and the length at a suspended joint greater than 70 cm.

Connections between super- and substructures should be so designed as to exhibit freedom of seismic inertia forces from the former to the latter. For this purpose, SEIBB specifies the following methods:

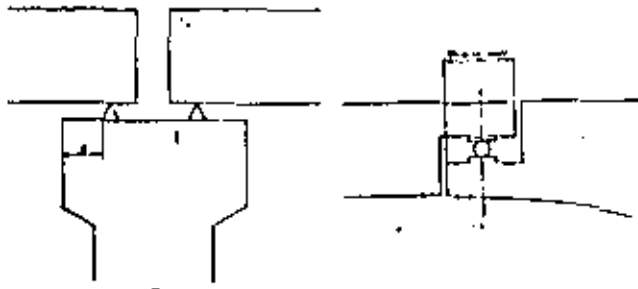


Fig. 5. Water Bridge Seats on Pier Top or at Suspended Joint.

1) For cast-in place reinforced concrete bridges, seismic forces should be transmitted by the bearing of the ribs on the underside of the shoe. The concrete near the shoe should be so reinforced as to resist seismic forces as an integrated part of the pier or the abutment. The transmission of seismic forces from the upper bearing assembly to the girder is made by the anchors fixed on the upper bearing assembly.

In case that the ribs of the shoe become unable to effectively transmit forces from the pier or the abutment, it is desirable to design the anchor bolts between the shoe and the sub-structure to transmit the total seismic force shoe.

This method is recommended not only for cast-in place reinforced concrete bridges but, if possible, for prefabricated concrete bridges and steel bridges.

2) When the bearing resistance of concrete is expressed, anchor bolts alone should be able to transmit the total seismic force. In this case, either of the following methods is to be used.

- (a) A steel plate is firmly tightened to the anchor bolts, which are buried in the sub-structure during its construction, and the shoe is welded to the steel plate after the erection of girders.
  - (b) A hole is prepared during the construction of sub-structure, the shoe with anchor bolts is placed on it and the hole is filled with efficient mortar. Or anchor bolts alone are first buried in cement mortar and the shoe is fixed to the bolts.
- 3) The diameter of anchor bolts should be not less than 25 mm, and the length within concrete not less than 10 times the diameter.

## 2.9. INERTIA FORCES OF SUPER-STRUCTURES ACTING TO SUB-STRUCTURES.

One of the most important loadings for the earthquake-resistant design of sub-structures is the inertia force of super-structures acting to the sub-structures through bearings. In SEIBS, these inertia forces are obtained as follows (refer to Fig. 6 for the symbols used):

- (i) Horizontal seismic force  $H_{L1}$  acting to left abutment;  
 $\text{Length of } k_1 W_1 \text{ and } (1/2) k_1 W_1 + R_{L1} f_{L1}$

- (ii) Horizontal seismic force  $H_{R1}$  acting to right abutment;  
 $k_2 W_2$ .

In the design of sub-structures, the inertia forces exerted from super-structures are assumed to act (i) at the level of the base of bearings in the longitudinal direction, and at the level of the center of gravity of the super-structures in the transverse direction.



- $H_1$  - Horizontal seismic force exerted by the pier or ab.
- $W_1$  - Dead load of super-structure A
- $W_2$  - Dead load of super-structure B
- $R_1$  - Reaction at left abutment due to  $W_1$
- $R_2$  - Reaction at pier due to  $W_1$
- $R_3$  - Reaction at pier due to  $W_2$
- $R_4$  - Reaction at right abutment due to  $W_2$
- $f_1$  - Coefficient of static friction at movable bearing on left abutment.
- $f_2$  - Coefficient of static friction at movable bearing on pier.

Fig. 6. Seismic Forces Acting to Sub-Structures from Super-Structures.

## 2.10. SAFETY FACTORS FOR FOUNDATION DESIGN.

As was mentioned in Section 2.4, the bearing capacities of the soils above the design ground surface are neglected in the earthquake-resistant design of foundation structures. This concept is also adopted in SNS, on which the contents of Sections 2.11, 2.12 and 2.13 are based.

For the evaluation of the vertical bearing capacity of the soil beneath the base of a spread footing foundation, it is useful to introduce the concept of the increased load, which is defined as:

$$\begin{aligned} & \text{(Increased Load)} = (\text{Vertical Load by Foundation}) \\ & \quad - (\text{Weight of Pre-existing Soil}) \\ & \quad = N - \gamma D_f A' \end{aligned} \quad \dots (10)$$

where  $\gamma$  is the unit weight of soil,  $D_f$  is the depth to the base of the footing, and  $A'$  is the effective bearing area of the footing. Then, by denoting the ultimate bearing capacity by  $Q$  and the factor of safety by  $F_s$ , the following condition must be satisfied for the foundation to be stable:

$$N - \gamma D_f A' \leq \frac{Q}{F_s} \quad \dots (11)$$

The factors of safety specified in SNS for foundation design are summarized in Table 10.

Table 10. Factors of Safety Specified in SIF for Stability of Foundation Structures.

Loading Condition	Factor of Safety
Primary Loads	3
Primary Loads + Temporary Loads	2
Earthquake Load	1.5 (1.7)

\* When live loads (sle loads) are considered

2.11. DESIGN OF SPREAD FOOTING FOUNDATIONS.

The stability of a spread footing foundation is examined for the vertical and horizontal bearing capacities of the surrounding soils and the overturning of the foundation.

The ultimate vertical bearing capacity for the increased load is calculated by

$$Q = A' [I_1 c_1 + I_2 \beta \gamma_1 H_1 + I_3 \gamma_2 D_f (N_6 - 1)] \dots (12)$$

and the allowable bearing capacity is obtained by

$$R_a = \frac{1}{F_s} Q + \gamma_2 D_f A' \dots (13)$$

in which the following notations are used (also refer to Fig. 7):

- $A' = B'L'$  = Effective area of footing.
- $B' = B - 2e_x$  = Effective width of footing.
- $L' = L - 2e_y$  = Effective length of footing.
- $e_x$  = Eccentricity of resultant in x-direction.
- $e_y$  = Eccentricity of resultant in y-direction.
- $B_1$  = Minimum of  $B'$  and  $L'$ .
- $I_1, I_2, I_3$  = Modification factors for inclined loads.
- $I_1 = I_2 = (1 - \delta/90)^2$
- $I_3 = (1 - \delta/\phi)^2$  where  $0 \leq 1 - \delta/\phi$ .
- $\delta = \tan^{-1}(H/N)$
- $H$  = Horizontal force acting on footing.
- $N$  = Effective vertical force at the base of footing.
- $\phi$  = Internal friction of the soil below footing.
- $\alpha, \beta$  = Shape factors of the base of footing (refer to Table 11).
- $c$  = Cohesion of the soil below footing.
- $\gamma_1$  = Effective unit weight of the soil below footing.
- $\gamma_2$  = Effective unit weight of the soil above the base of footing.
- $N_6, N_2, N_3$  = Bearing capacity factors of the soil below footing (refer to Table 12).
- $F_s$  = Factor of safety as given in Table 10.

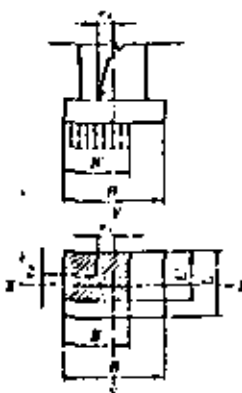


Fig. 7. Effective Width and Area of Rectangular Footing.

The ultimate horizontal bearing capacity at the base of footing is evaluated by

$$R_H = N \tan \delta + A' c' \dots (14)$$

and that due to earth pressures at the front face of footing is obtained by

$$R_p = \alpha I (\Sigma p_o Ah) = L (\Sigma p_o Ah) \dots (15)$$

Table 11. Shape Factors of Base of Footing.

Shape Factor	Shape of the Base of Footing			
	Long and Narrow Shape	Square	Rectangle	Circle
a	1.0	1.2	1 + 0.2 Min of B' & L' / Max of B' & L'	1.2
b	0.8	0.8	0.5 - 0.1 Min of B' & L' / Max of B' & L'	0.2

Table 12. Bearing Capacity Factors

$\phi$ (degree)	$N_2$	$N_3$	$N_6$
0	1.0	0	1.0
5	3.1	0	1.4
10	6.2	0	1.9
15	12.5	1.3	2.7
20	25.0	2.6	3.9
25	50.0	5.2	5.6
30	100.0	10.4	8.1
35	200.0	20.8	11.6
40	400.0	41.6	16.6
Equal or Greater than 45	95.7	10.0	11.2

or, for retaining walls, by

$$R_p = \alpha L (\Sigma p_o Ah) \dots (16)$$

By using the quantities calculated above, the allowable horizontal bearing capacities for the general case and for the design of retaining walls are evaluated by Eq. (17) and (18) shown below, respectively:

$$R_{oa} = \frac{1}{F_s} (R_H + R_p) \dots (17)$$

$$R_{oa}' = \frac{1}{F_s} R_H + R_p \dots (18)$$

In Eqs. (14) through (18), the following notations are used except for those already defined (also refer to Fig. 8):

$\delta$  = Angle of friction between the base of footing and the soil below.

Supporting Layer	When Footing Is Constructed In-Situ.	When Prefabricated Footing Is Placed.
Soil or Soft Rock	$\delta = \phi$	$\delta = 2/3 \phi$
Hard Rock	$\delta = 45^\circ$	$\delta = 30^\circ$

$$R_i = \frac{1}{F_s} Q_i + W_i \quad \dots \dots \dots (A)$$

- in which
- $R_i$  = Allowable pullout resistance at top of the pile, and
  - $Q_i$  = Ultimate pullout resistance of the pile.
- The stability against overturning during an earthquake is examined as follows:
- (i) The point of application of the resultant should be located inside of the center of the exterior pile in the pile group.
  - (ii) When the tensile load on some piles is found to exceed the allowable pullout resistance, the maximum compressive load recalculated by ignoring these tensile piles should be less than the allowable vertical carrying capacity.
  - (iii) When only the vertical carrying capacity is examined during design because of apparently favorable conditions, any pile in the pile group should not be subjected to tensile load.

Allowable displacements are not specified explicitly, but they are determined by considering the serviceability of the structure under consideration.

**2.13. DESIGN OF CAISSON FOUNDATIONS.**

Design of caisson foundations is performed by taking into account the vertical bearing capacities at the top and at the base of the caisson, the horizontal bearing capacity, the overturning moment and the displacements caused by the design loadings.

The allowable vertical bearing capacity for the increased load (cf. Section 2.10) at the base of a caisson is obtained by dividing the ultimate vertical bearing capacity calculated by an expression almost identical to Eq. (12) by an appropriate factor of safety given in Table 10. The vertical carrying capacity at the top of the caisson includes the effect of skin friction, and the allowable capacity is calculated by using a formula similar to Eq. (19). For the purpose of increased margin of safety, the effect of skin friction is usually neglected when examining the stability during earthquakes. The ultimate horizontal bearing capacity is obtained by using equations similar to Eqs. (14) and (15), and the allowable capacity is evaluated by Eq. (17). The allowable resisting moment is also obtained by dividing the ultimate resisting moment by an appropriate factor of safety. The methods adopted in SRS to evaluate various loads acting to the caisson and the ultimate resisting moment are too complicated to be included here.

**2.14. SPECIFICATIONS FOR EARTHQUAKE-RESISTANT DESIGN OF HONSHU-SHIKOKU BRIDGES.**

The Honshu-Shikoku Project now under way in Japan is a large-sized project to connect Honshu and Shikoku Islands by three independent routes of bridges over the Seto-Inland Sea. Though all of the project has not been finalized yet, there will be eleven suspension bridges and two cantilever-truss bridges with spans greater than 400 m to be constructed among other shorter-span bridges. Since the Japanese National Railways started to study the feasibility of constructing bridges connecting these two islands in 1955, investigations have been continued by the Ministry of Construction, the Japan

Highway Public Corporation and the Railway Construction Public Corporation. In 1970 the Honshu-Shikoku Bridge Authority was established by law to oversee the project.

The first report on the technical investigation was published by the Committee for Construction of Honshu-Shikoku Bridges established in the Japan Society of Civil Engineers in response to the request from both the Ministry of Construction and JNR. It contained design specifications on loads, materials and safety factors, and it also emphasized the necessity for further research into the earthquake-resistant problems. In order to further examine the results presented in the first report, a committee was organized in JSCE in 1970 and the Draft of the Specifications for Earthquake-Resistant Design of Honshu-Shikoku Bridges was issued in 1972. This draft was revised in 1974 and was finally adopted as the Specifications in 1976, which is currently used for the earthquake-resistant analysis of the proposed Honshu-Shikoku bridges.

This specifications is used for the design for bridges with span lengths greater than 200 m, and bridges with shorter span lengths are designed according to SEHB (Specifications for the Earthquake-Resistant Design of Highway Bridges (1971)).

The design horizontal acceleration is taken as 180 gal at the subsoil level where the foundation is supported. This value was obtained by assuming an M=8 class earthquake at about 150 km southeast of the construction sites. This design earthquake is expected to occur once or twice for every 100 years. The effect of smaller but near earthquakes on bridges was judged minor in comparison with that of the design earthquake.

Two design calculation methods are specified, as follows; 1) the preliminary earthquake-resistant design is performed by the modified seismic coefficient method, and the result is examined by the dynamic response analysis, and 2) when the preliminary design is obtained by the overriding factors other than seismic consideration, it is examined by means of the response spectrum technique. In the latter case, use of the dynamic response

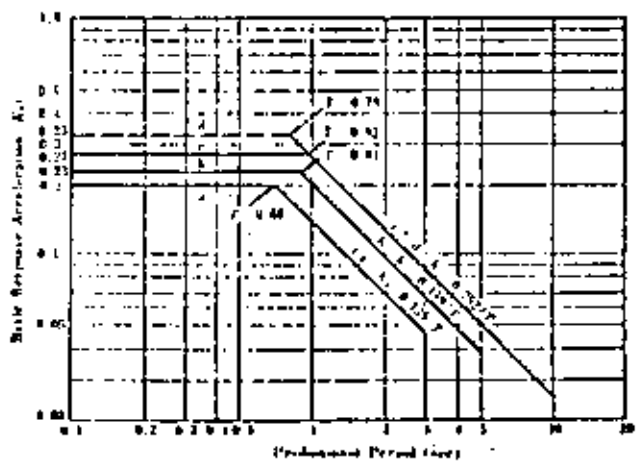


Fig. 12. Basic Response Acceleration Used for Modified Seismic Coefficient Method in Earthquake-Resistant Design of Honshu-Shikoku Bridges.

- $c$  = Cohesion between the base of footing and the soil below.
- $\alpha$  = Shape factor of the front face of footing as shown in Fig. 9 as a function of  $D_f/B$ ;  $\alpha = 1$  for retaining walls.
- $p_p = \gamma_s K_p + 2c \sqrt{K_p}$
- $p_a = \gamma_s K_a - 2c \sqrt{K_a}$
- $K_p$  = Passive earth pressure coefficient.
- $K_a$  = Active earth pressure coefficient.
- $\Delta h$  = Thickness of the layer whose horizontal resistance is taken into account.

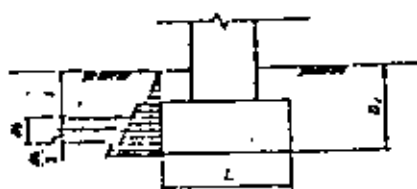


Fig. 8. Ultimate Horizontal Bearing Capacity at the Front Face of Footing.

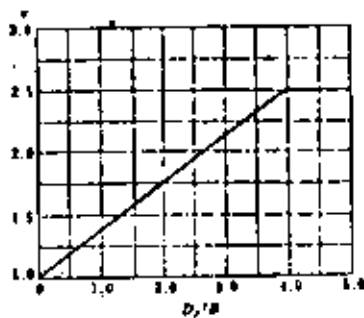


Fig. 9. Shape Factor ( $\alpha$ ) of the Front Face of Footing for the Evaluation of Eq. (15).

The stability of a spread footing against overturning is examined by the amount of eccentricity of the point of application of the load resultant acting to the base of the foundation. According to SRS, the eccentricity should not exceed the values shown below (also refer to Fig. 10):

- (i) For primary loads,  $e_o$  (but, if consolidation settlement is expected,  $e_o/2$ ).
- (ii) For primary plus temporary loads,  $e_o + \Delta s/4$ .
- (iii) For earthquake load,  $e_o + \Delta s/2$ .

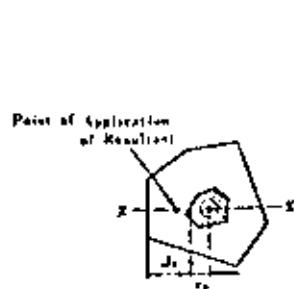


Fig. 10. Explanations of  $e_o$  and  $\Delta s$ .

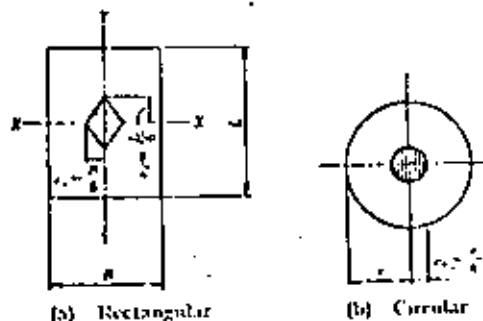


Fig. 11. Examples of  $e_o$ .

In the above expressions and in Fig. 10,

- $X-X'$ : The line connecting the center of resistance of foundation base and the point of application of the resultant.
- $e_o$ : The eccentricity that makes the minimum vertical subgrade reaction zero.
- $\Delta s$ : The distance in  $X-X'$  direction between the perimeter of the footing base and the point with  $e_o$ .

Fig. 11 and Table 13 illustrate two specific cases in which the shape of the footing base is rectangular or circular.

Table 13. Examples of Maximum Allowable Eccentricities.

Loading Condition	Maximum Allowable Eccentricity	
	Rectangular Footing	Circular Footing
Primary Loads	$\Delta s/4$	$e_o/2$
Primary Loads + Temporary Loads	$\Delta s/4$	$2e_o/3$
Earthquake Load	$\Delta s/2$	$2e_o/3$

\* Eccentricity only in the  $X-X'$  direction.

## 2.12. DESIGN OF PILE FOUNDATIONS.

In the design of pile foundations, considerations should be paid for 1) the vertical carrying capacity of the pile, 2) the overturning of the pile-supported structure, and 3) the displacement of the structure under the action of design loadings. Displacement here includes settlement, rotation and horizontal displacement.

The compressive load on a pile should not exceed the allowable vertical carrying capacity of the pile as obtained from the following formula:

$$R_a = \frac{1}{F_s} (Q_u + Q_f - (R_n)) - W_p + (W_s) + \gamma D_f A \quad (19)$$

in which

- $R_a$  = Allowable carrying capacity at the top of the pile,
- $F_s$  = Factor of safety given in Table 10,
- $Q_u$  = Ultimate resistance of the base of the pile,
- $Q_f$  = Ultimate skin friction over the embedded shaft length of the pile,
- $R_n$  = Negative skin friction (to be considered when necessary),
- $W_p$  = Dead weight of the pile,
- $W_s$  = Weight of the soil displaced by the pile (not considered when the ultimate carrying capacity is determined from loading tests),
- $\gamma$  = Average unit weight of the soil,
- $D_f$  = Depth from the ground surface to the base of the footing, and
- $A$  = Cross-sectional area of the pile (Effective area in the case of pile group).

The tensile load on a pile should not exceed the allowable pullout resistance calculated by

analysis by the numerical integration method is required for the result obtained by the spectrum technique.

In the seismic coefficient method, a structure is idealized as a one-degree-of-freedom system, in which the predominant period is defined as that period which produces the most unfavorable stress or deformation in the members of the main structural system under consideration. The basic response acceleration in terms of  $g$  (as acceleration of gravity) is obtained from Fig. 12. One of the curves (a)–(d) is selected from Fig. 12 according to the type of structure, namely

- Curve (a) : For foundation structures having large cross-sectional areas with sufficient embedded length, in which dissipation damping is expected to be more pronounced than structural damping.
- Curve (b) : For foundation structures which do not correspond to either Curve (a) or (c).
- Curve (c) : For foundation (or sub-) structures, mostly of steel members, with relatively long protruded length above the ground surface, in which most damping is due to structural damping.
- Curve (d) : For main towers, suspended structures and main cables of suspension bridges.

For the spectrum response technique, a sufficient number of modes should be taken into account so that maximum responses of various parts of the structure can be determined with the required accuracy. The total response acceleration spectra are represented by Curve (a) in Fig. 12 for a damping factor of 10%, Curve (b) for a damping factor of 5%, and Curve (d) for a damping factor of 2%.

In the dynamic response analysis, time histories of various responses of a structure, generally idealized as a multi-degree-of-freedom system, are calculated from the equations of motion by using recorded earthquake motions as input. The earthquake motions to be used for analysis are 1) representative ground motions recorded near the construction site, and 2) the 1940 El Centro records. For both cases, the maximum acceleration is normalized to 180 gal. The latter was chosen because there are a number of results available from past analysis obtained by using the El Centro records.

### 3. EXAMPLES OF EARTHQUAKE RESISTANT DESIGN OF BRIDGES

#### 3.1. INTRODUCTION.

There are various ways to design sub-structures of a bridge to resist earthquakes. Some examples are shown here in which special devices have been developed.

#### 3.2. EXAMPLES OF DESIGNING SUB-STRUCTURE AND SUPER-STRUCTURE.

##### 3.2.1. An Abutment Carrying All the Horizontal Seismic Force in Longitudinal Direction.

When it is difficult to make the intermediate piers so rigid as to carry all the horizontal seismic force, special abutments which carry the horizontal force are needed.

For the continuous girders of the Wainosugawa Railway Bridge (shown in Fig. 1), flexible intermediate piers were used because of the deep gorge. A special fixed abutment was constructed at the right-hand side to support the horizontal force due to an earthquake.

The symbols M, F and H indicate movable shoe, fixed shoe and hinge, respectively. Simple girders placed between the continuous girders and the fixed abutment are connected to them by horizontal connecting rods shown in the figure in order to transmit the horizontal force caused by an earthquake to the fixed abutment.

In the case of the Nakagawa Railway Bridge also, the horizontal seismic force in longitudinal direction is expected to be carried by the abutment situated at the right-hand

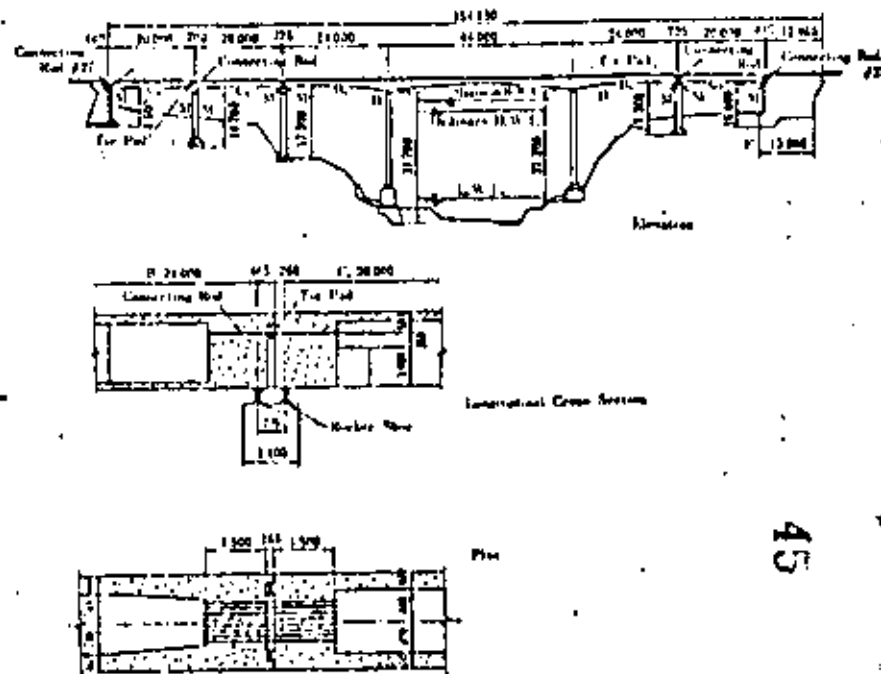


Fig. 1. Wainosugawa Railway Bridge.

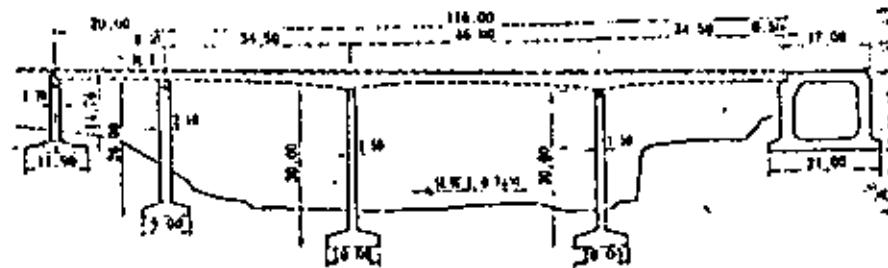


Fig. 2. Nakagawa Railway Bridge.

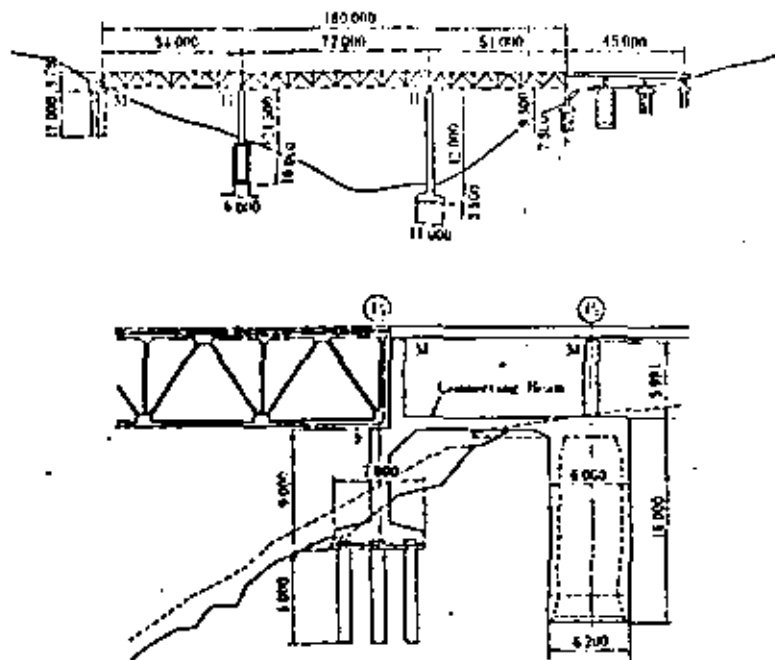


Fig. 3. Sakai-gawa Bridge.

side. Messenger Ribs with lead plates of 50 mm thickness are applied to the intermediate piers of the central 3-span continuous girder.

In the case of the Sakai-gawa Bridge<sup>21</sup> on the Chūō Expressway shown in Fig. 3, Piers 2 and 3 are connected by an underground tie beam as illustrated in the figure. They are designed to carry the longitudinal seismic force from the continuous truss. The tall intermediate piers are more affected by the transverse seismic force of the truss than by the longitudinal one. Analysis of the dynamic response of the bridge to earthquakes was carried out to investigate the influence of earthquake motions on the structural system as a whole.

### 3.2.2. Intermediate Piers Carrying All the Horizontal Seismic Force.

On the contrary, there are cases where the intermediate piers are employed which are so rigid to carry all the horizontal seismic force. Since the seismic displacement at the ends is assumed large in this case, special devices against the fall-down of the girder are required.

The Yoneyama Bridge<sup>22</sup> shown in Fig. 4 is a national highway bridge. It crosses over a deep valley with 3 span continuous curved steel girders. Steel box columns are used for the piers. Longitudinal seismic forces from the super-structure are transmitted by fixed shoes to piers 1 and 2 and carried by them. Evaluation of seismic effect was carried out by the conventional analysis and the design was examined by dynamic analysis. Movable shoes on pier 3 have stoppers to restrict an excessive displacement and the fall-down of the girders.

The girder of the Azumagawa Railway Bridge<sup>23</sup> is rigidly connected to the central pier so that the bending moment of the substructure due to seismic force is cut down, about 20 per cent. The design was examined by dynamic analysis.

### 3.2.3. Bridges on Soft Ground.

The Okakase Railway Bridge<sup>24</sup> shown in Fig. 5 is an elevated reinforced concrete bridge of multi-span continuous rigid-frame structure. The bridge was designed to carry the horizontal forces at abutments A, B and C built directly on the hard layer at the places where the soft layer was thin. Most of the transverse horizontal force is carried by the abutments at the both ends through the bending rigidity of the upper and lower slabs spanning 90 m between abutments A and B, and 80 m between abutments B and C.

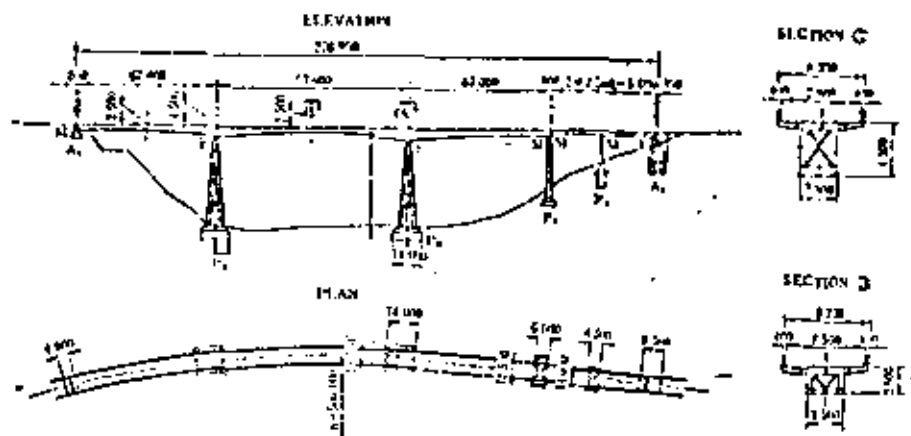


Fig. 4. Yoneyama Bridge

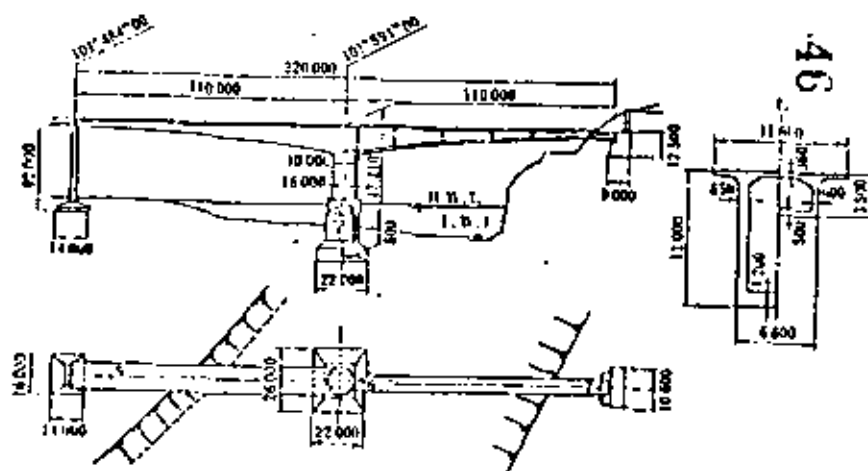


Fig. 5. Azumagawa Railway Bridge.

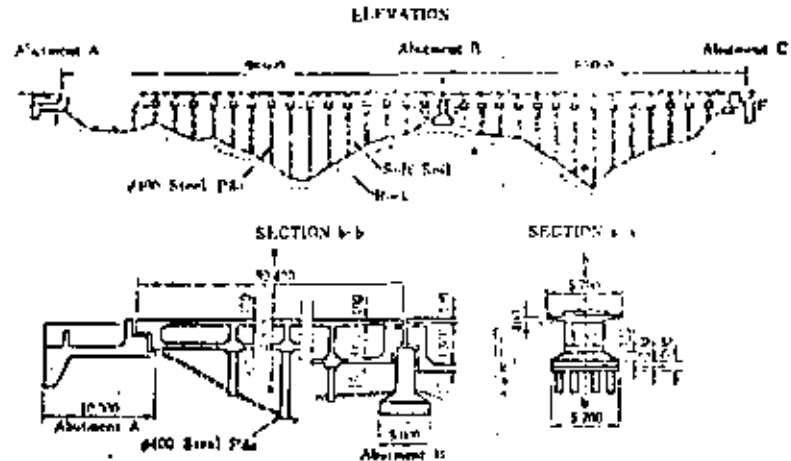


Fig. 6. Odakane Railway Bridge.

A similar idea is employed to the Olgawara Railway Bridge on the New Tohoku Line which is shown in Fig. 7. The piers are designed to follow the seismic motion of the ground of a large amplitude, where their shoes, carrying all the vertical forces, slide freely by the horizontal ones.

There are cases where the heads of the piles driven through soft soil layers to the bearing stratum and the girders are rigidly connected to make up a rigid frame structure to withstand the horizontal seismic force in the longitudinal and the transverse direction.

In the case of the Suzukinuma Railway Bridge<sup>21</sup> shown in Fig. 8 and in Photo. 1 & 2, the heads of steel pipe piles, 1 m in diameter, were rigidly connected to the concrete girders to form rigid frame structures. In the design calculations, the soft stratum was considered as liquid.

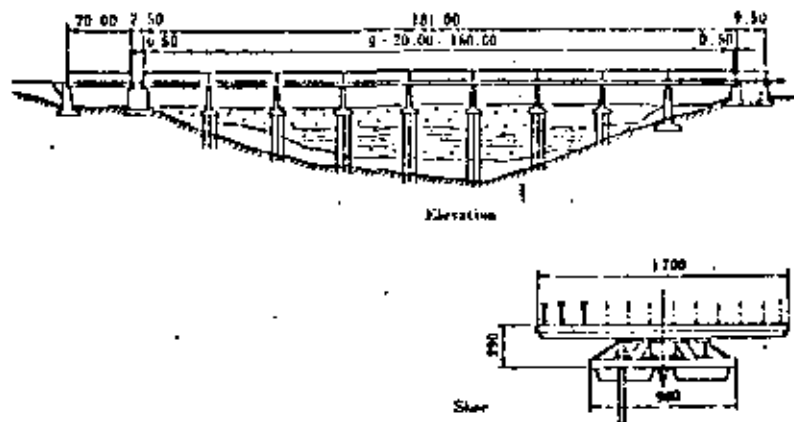


Fig. 7. Olgawara Railway Bridge.

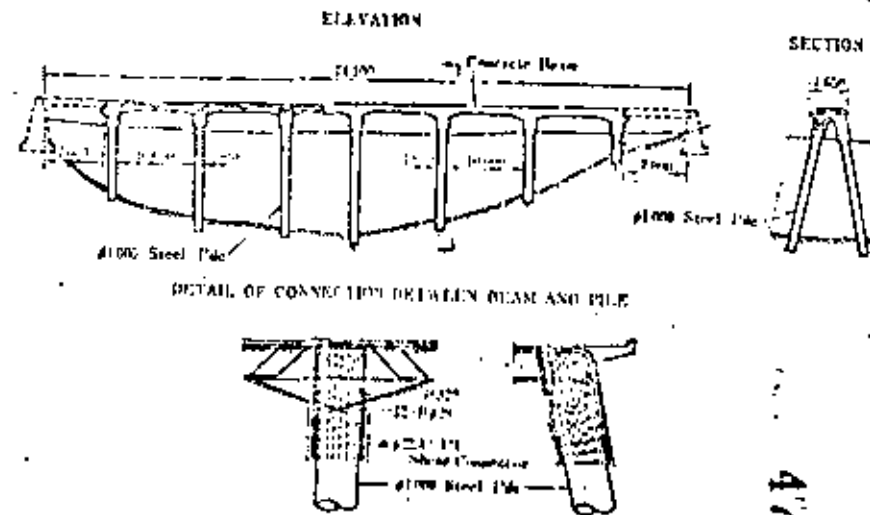


Fig. 8. Suzukinuma Railway Bridge.

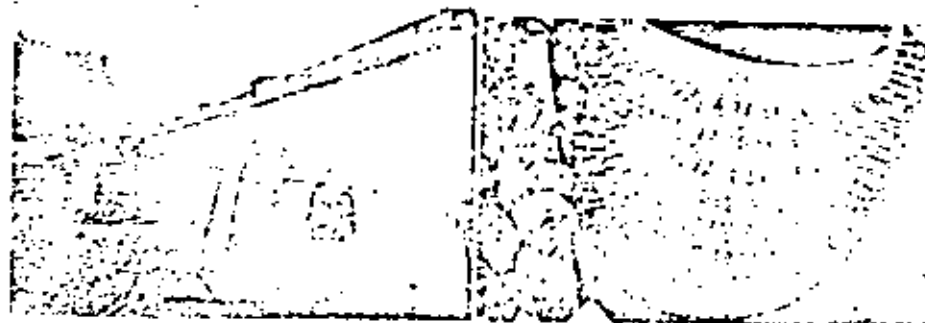


Photo. 1. Overall View

Photo. 2. Pile's Head

The intermediate piers of the Ushizugawa Railway Bridge on the Nagasaki Main Line shown in Fig. 9 are not designed to take the horizontal forces in the longitudinal direction but the abutments supported on reinforced concrete piles carry them. The connecting devices (see the details of joints A, B, and C) are designed to transmit the horizontal forces from the steel girders to the abutments.

In the case of the Hirai Bridge<sup>22</sup> shown in Fig. 10, a caisson is placed on the heads of the piles reaching to the bearing layer which are terminated in an intermediate layer of the soft ground. The horizontal force is mainly resisted by the passive earthpressure on the caisson. The vertical force is carried by the piles. The figure also shows the details of the connection between the piles and the caisson. To ascertain the combined action of the piles and the caisson, dynamic and static loading tests were conducted for a completed structure. Observations are being made by using seismometers, earthpressure gauges and accelerometers to investigate the vibration characteristics during an earthquake.

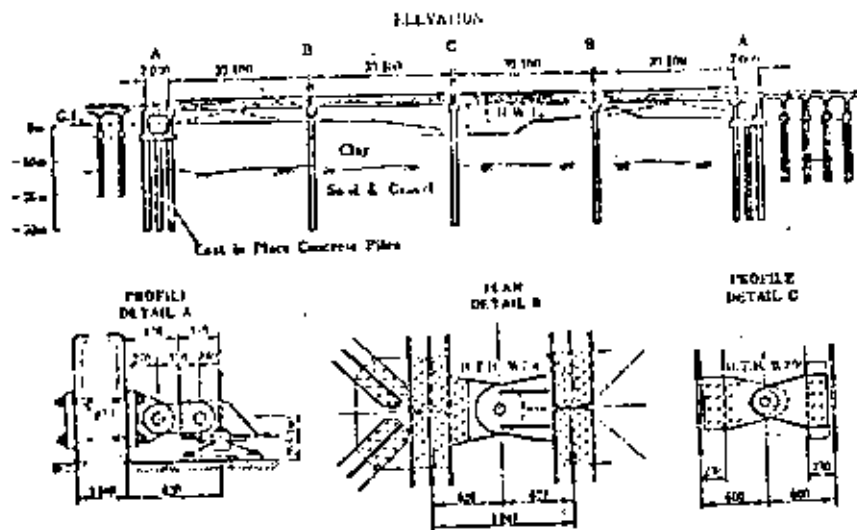


Fig. 9. Ushizugawa Railway Bridge.

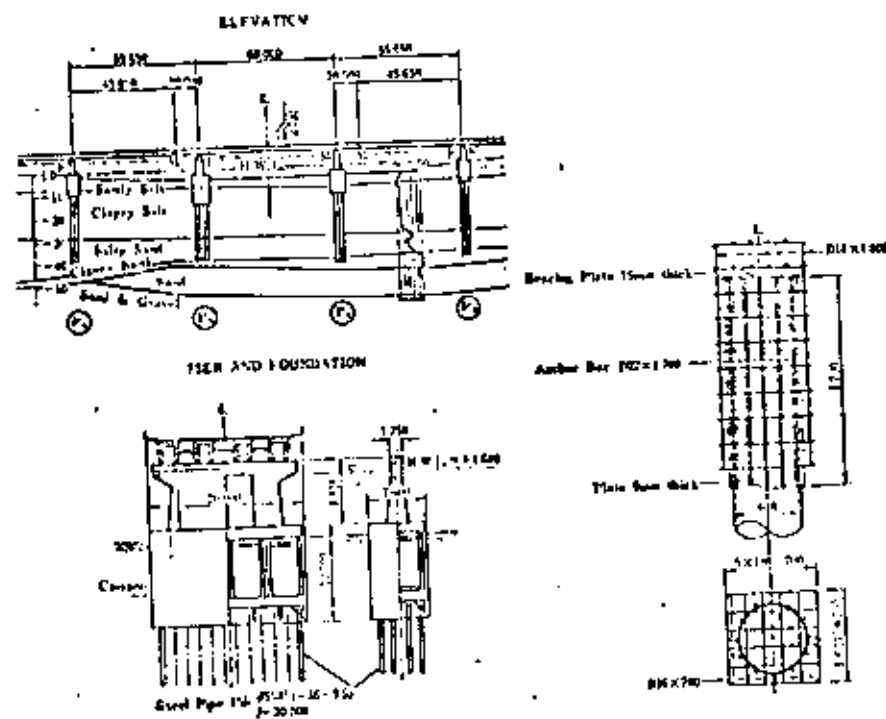


Fig. 10. Hirai Bridge.

### 3.2.4. Bridges on Bedrock.

In order to increase the stability of a bridge pier on the bedrock, there are cases where a footing is anchored to the bedrock with steel cables. When the cables are prestressed, the resistance of the footing against displacement can be increased.

Fig. 11 shows a pier foundation for the Yokohama-Haneda Expressway. The foundation is anchored by 12 Freyssinet cables of  $\phi 12.4$  mm.

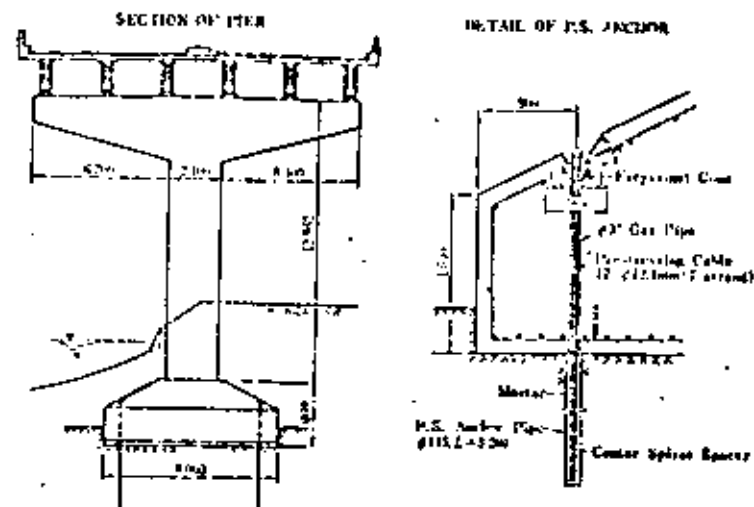


Fig. 11. Haneda Yokohama Expressway.

48

### 3.3. EXAMPLES OF SEISMIC DESIGN OF SUPPORTS AND JOINTS.

#### 3.3.1. Stoppers.

In an seismic design, it is important to prevent a girder from falling down. In order to achieve this, various devices have been invented and used for the supporting part and the girder ends.

In the case of a prestressed concrete railway bridge<sup>11</sup> over Arakawa River on the Tohoku Main Line, shown in Fig. 12, a stopper provided on the top of a pier fits in the holes cut in the slabs in order to prevent the girders from falling down. The girders are connected with one another by steel rods and clearances are given for the expansion and contraction of the girders due to temperature variation.

The same idea is adopted to the standard design of the New Tohoku Line as shown in Fig. 13.

In the case of the Tamagawa Railway Bridge on the Musashino Line, shown in Fig. 14, the movable bearing is so designed as to allow displacement caused by temperature variation, shrinkage and creep of concrete, but not to permit any excessive displacement due to an earthquake.

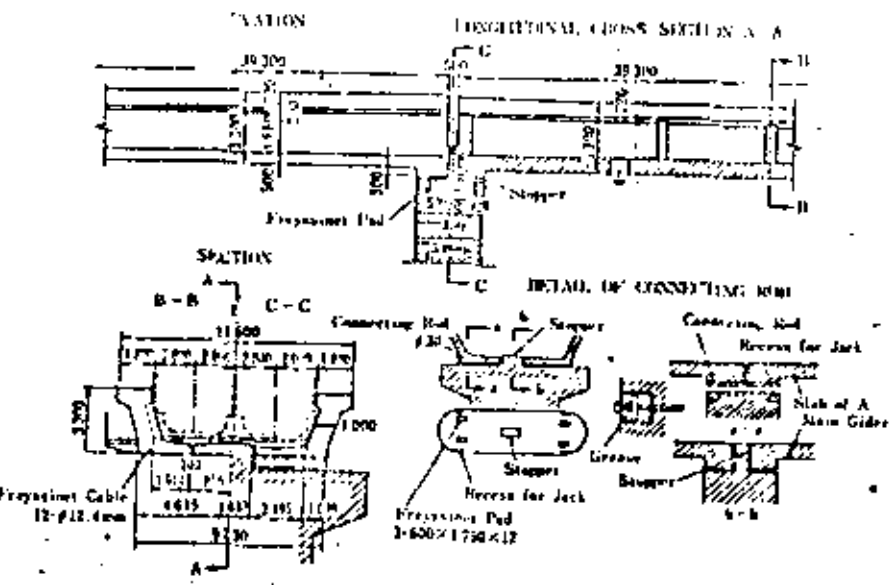


Fig. 12. Arakawa Railway Bridge.

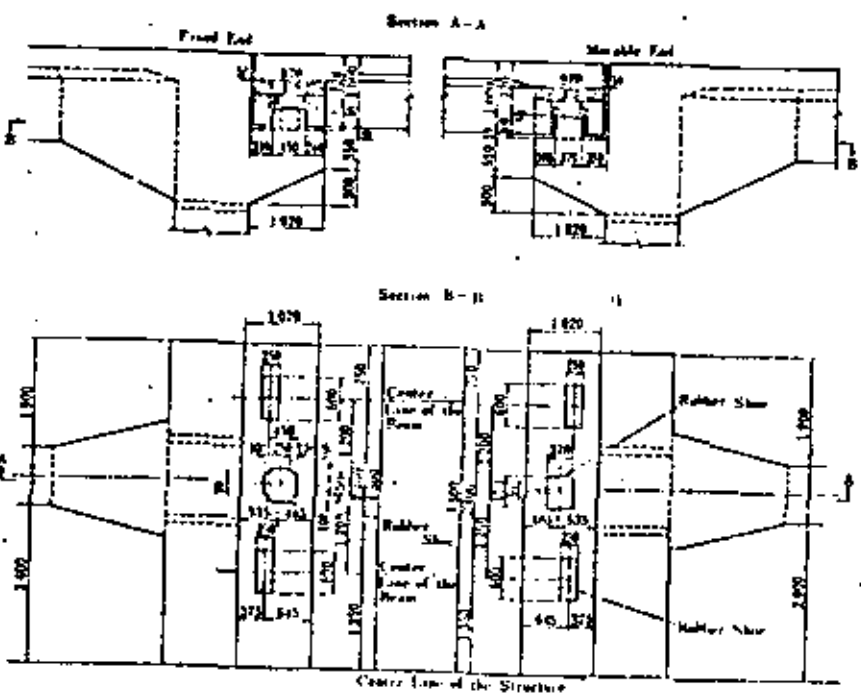


Fig. 13. Standard Design of the New Tohoku Line.

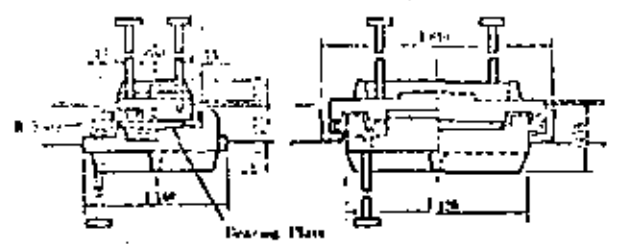


Fig. 14. Shoe of the Yamagawa Railway Bridge.

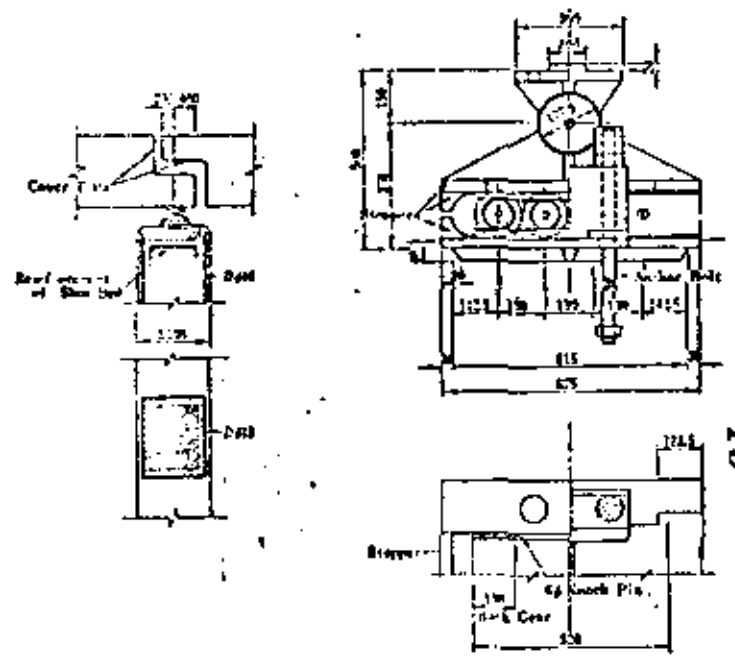


Fig. 15. Shoe of the Shin-Aoyagi Bridge.

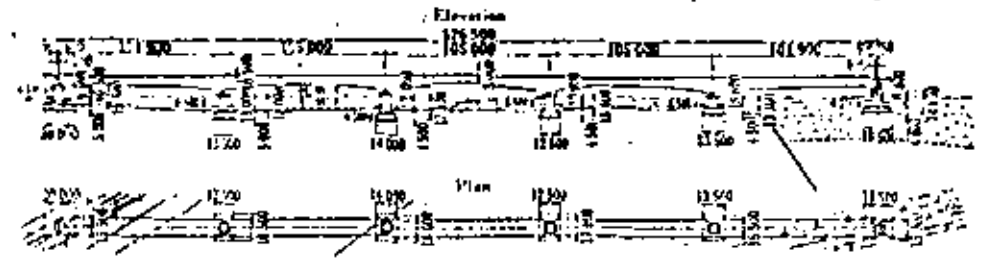


Fig. 16. Abukemagawa Railway Bridge.



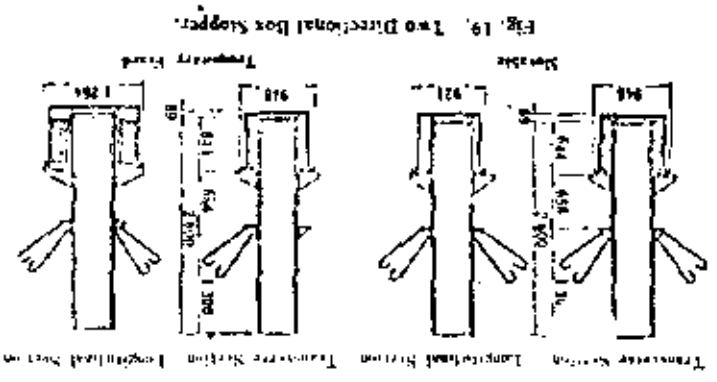


Fig. 19. Two Directional Box Stopper.

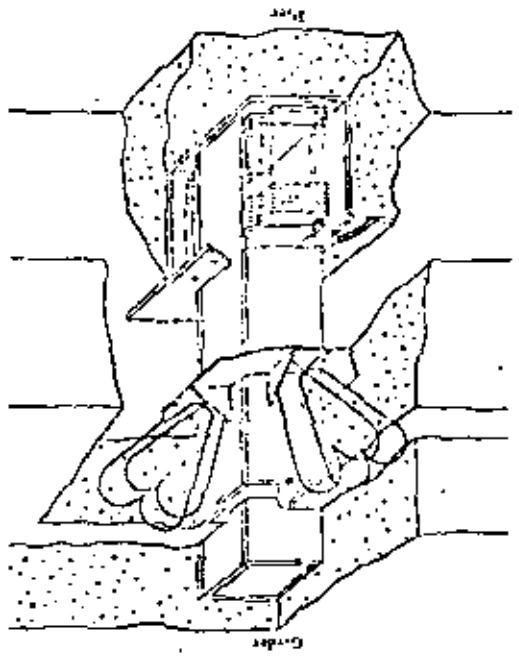


Fig. 20. Box Stopper of Shear Type.

The Tokyo Expressway Public Corporation adopted a method in which an oil "dangler" is installed on each support which may be assumed movable for the slow displacement due to temperature variation, while it acts as a fixed support providing a strong resistance to the abrupt displacement caused by an earthquake. (See Fig. 21, Photo 3).

3.3.3 Dangers.

Settle motions.

practical use. This stopper, called "Stopper of Slant Type", can react very quickly to the

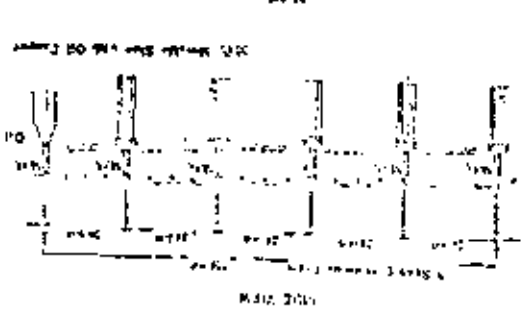


Fig. 21. Route No. 1 of the Tokyo Expressway.

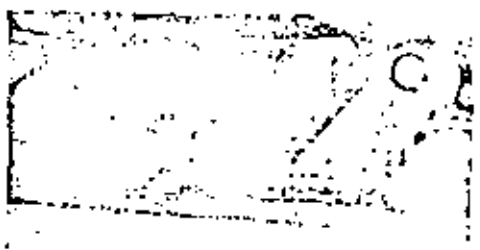


Photo 3. Oil Dangler.

to each part.

Another method applied to the same route of the Tokyo Expressway for the same purpose is shown in Fig. 22. Posts and girders are connected with prestressed wires which are called "St. Dangers" (See Photo 4). The wires have enough cross section and length to absorb the horizontal force due to temperature variation, shrinkage and creep of concrete girders and slabs. The total shrinkage force can be distributed almost uniformly

### 3.3.4. Connecting Devices.

In the case of the Shinkaturagawa Railway Bridge on the Chūo Main Line, shown in Fig. 23, composite girders consisting of steel girders and concrete slabs are placed on piers of about 40 m height, and the girder ends are connected with one another by steel plates to prevent them from falling down. A clearance is left for the relative displacement between girder ends. Moreover, H-shaped steel beams embedded at the top of a pier as

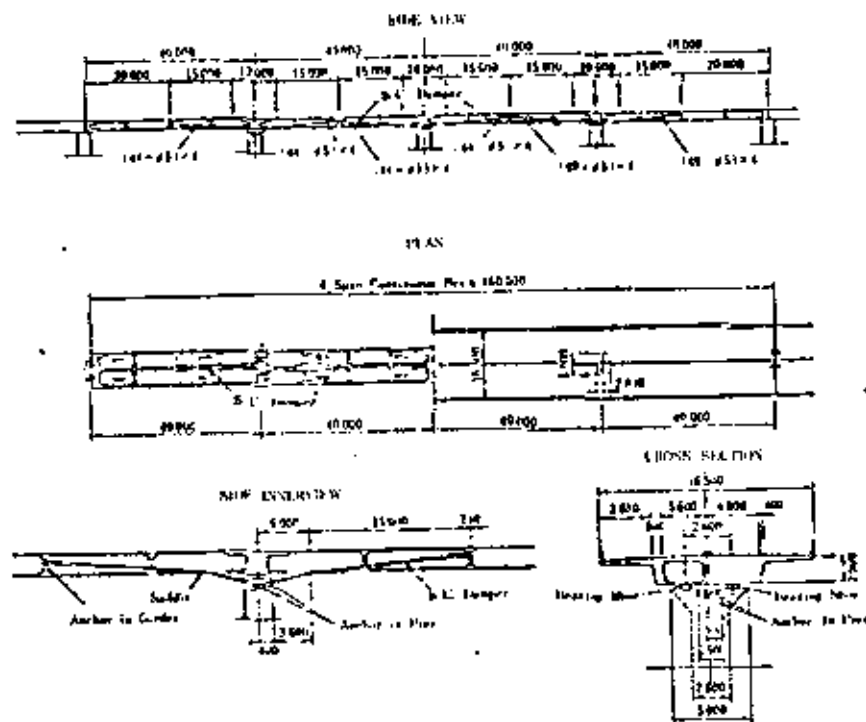


Fig. 22 Route No. 1 of the Tokyo Expressway.



Photo. 4. SU Damper.

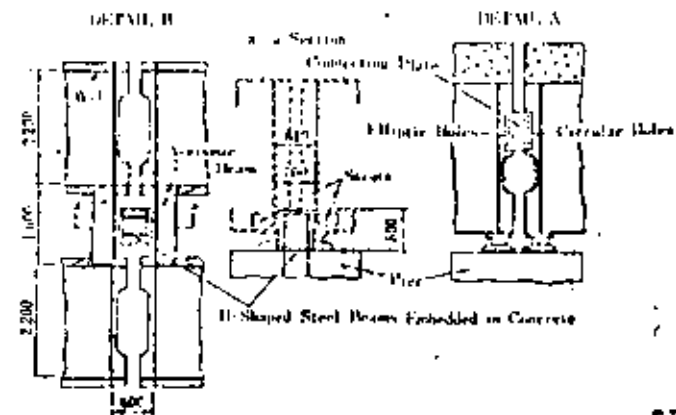
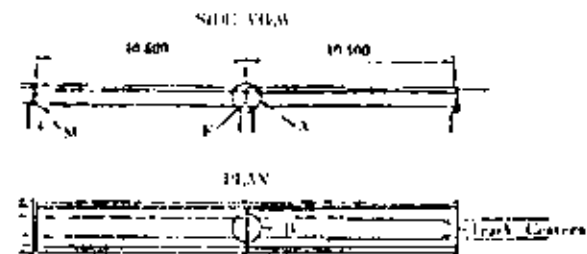


Fig. 23. Shinkaturagawa Railway Bridge.

52

shown in the figure are enclosed by the seismic beams installed at the girder ends to avoid the displacement of a girder beyond a certain limit.

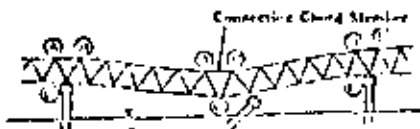
In the Shimoyutagawa Railway Bridge on the Tōkaidō Main Line, shown in Fig. 24, simple trusses of 64.2 m are connected with one another so that even when one breaks during an earthquake, the trusses would remain intact as cantilevers.

The method of connecting the ends of girders with connecting plates is adopted for bridges and elevated roads of the Tokyo Expressway Public Corporation.

There are cases where connecting installations are used to transmit the longitudinal horizontal force due to an earthquake.

In the case of the Idokawa Elevated Bridge<sup>100</sup> of prestressed concrete structure national highway, shown in Fig. 25, these installations are used to connect simple girders to make them act as continuous girders against the horizontal force in the longitudinal direction. Since a prestressed concrete girder shows a small angle of slope at ends, no expansion joint was provided between the girders and a continuous pier was made.

ELEVATION



PLAN

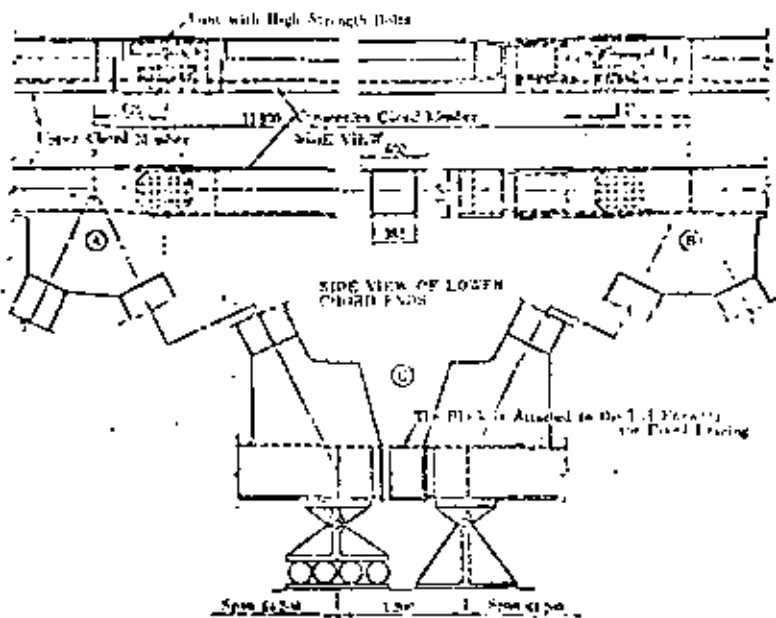


Fig. 24. Shimooyodogawa Railway Bridge.

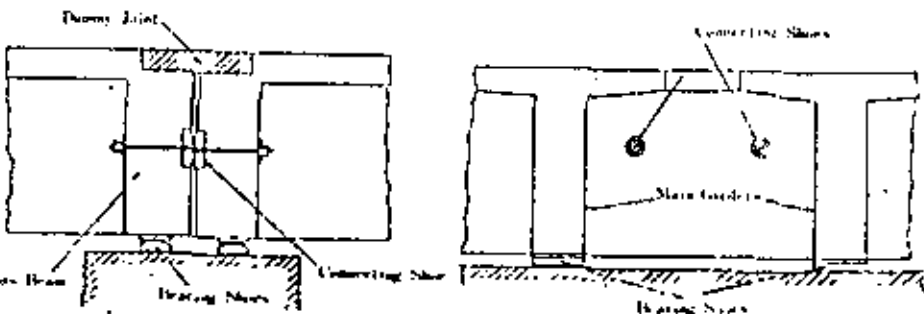


Fig. 25. Ichikawa Elevated Bridge.

REFERENCES

- 1) Report on Construction of the Washidomogawa Bridge, Feb., 1964, by Tozuka Construction Dept., Japanese National Railway, Prestressed Concrete, Vol. 4, No. 4, Aug. 1962.
- 2) A Study on Orders of High Bridge Pier, Feb., 1964, The Bridge Pier Panel, Highway Investigation Committee.
- 3) Tozokugijutu, Vol. 22, No. 3, March, 1967.
- 4) Ishibutsu Sekkei Shingyō, No. 45, March, 1971.
- 5) Tozokugijutu, Aug. - Sept., 1967, Tozoku Dabetsu, Feb., March, 1968.
- 6) Tozokugijutu, Vol. 23, No. 6.
- 7) Horizontal Resistance of Foundation Made Up with Caisson and Steel Piles, in the Collection of Works of the 8th Japan Road Congress.
- 8) Prestressed Concrete, Vol. 7, No. 6, Dec., 1965, Tozoku, Vol. 18, No. 5, Dec., 1967, No. 1, Tokyo Construction Division, Japanese National Railway.
- 9) The Proceedings of the Symposium (No. 9) on the New Ideas in Structural Design, 17th Oct. 1962, the Science Council of Japan, National Committee of Bridge and Structural Engineering.
- 10) Ishiyō to Issō, April, 1963.

JIC 53

## SEISMIC RESPONSE OF MULTI-SUPPORT STRUCTURES

L. Esteva<sup>I</sup>, S. E. Ruiz<sup>II</sup> and A. Reyes<sup>I</sup>

## SUMMARY

Probabilistic models are proposed for determination of design responses in structures sensitive to phase differences among ground motion histories at their supports. Selection of design values is based on approximate proportionalities between responses corresponding to given probabilities of exceedance and standard deviations of those responses at the end of a segment of random noise taken as equivalent to earthquake excitation. Detailed practical rules are proposed for mode and component superposition as well as for definition of internal-load combinations to be used when checking safety conditions at given critical sections.

## INTRODUCTION

Design values of internal forces produced by earthquakes are usually taken as those provided by an envelope to the values of those variables caused by the individual ground motion components, one at a time. When dealing with structures having small dimensions in plan, reasonable approximations to maximum response for the superposition of the various ground motion components can be obtained from a linear combination of maximum responses to each individual component at a given point of the ground-structure interface, provided modal responses can be taken as stochastically independent (1).

For structures extended in plan, such as long bridges, or founded on heterogeneous formations or irregular topography, such as dams, differences in ground motion among different supports or zones of the ground-structure interface may give place to quantitative and qualitative differences in internal actions as compared with those produced by in-phase motion of all supports. In addition, strong correlation may exist between pairs of parallel ground motion components at different points, and the correlation among the responses of a given mode to several (correlated) ground motion components can no longer be neglected.

The present paper explores several criteria for determining design responses, on the basis of the variance of the response to the various ground motion components, for a given assumption concerning the covariance structure of the generalized excitation<sup>III</sup>. Simplified rules for practical application are also discussed.

## DYNAMICS OF LINEAR SYSTEMS SUBJECTED TO OUT-OF-PHASE SUPPORT DISPLACEMENTS

Let the excitation acting on a multi-support system be described by vector  $X(t) = \{x_q\}$  of support displacements. Suppose the system is discretized and represented by the mass, stiffness and damping matrices  $M$ ,  $K$  and  $C$  respectively, where support displacements are not taken as degrees of freedom. The vector  $Y(t)$  of structural response components (displacements, stresses) can be obtained as follows (2,3).

$$Y(t) = \sum_q x_q(t) \tilde{Y}_q + U(t) \quad (1)$$

<sup>I</sup> Institute of Engineering, National University of Mexico

<sup>II</sup> Proyectos Marinos, S. C., Mexico City; formerly at Institute of Engineering, National University of Mexico

<sup>III</sup> More general assumptions are covered in Ref 2.

In this equation,  $\sum_q$  is taken to all the supports,  $\tilde{Y}_q$  is the vector of static response components produced by a unit displacement  $x_q$ , and  $U$  is the vector of dynamic response components, i.e. those measured at any given instant with respect to the superposition of the static configurations associated with support displacements  $x_q$  at the same instant.  $U$  can be expressed in terms of modal vectors  $Z_j = \{z_{ij}\}$

$$U(t) = \sum_q \int_0^t \ddot{x}_q(\tau) \sum_j a_{jq} Z_j h_j(t-\tau) d\tau \quad (2)$$

Here  $a_{jq}$  is the participation factor of mode  $j$  that corresponds to displacements of support  $q$ , and  $h_j(\tau)$  is the unit impulse response function for the mentioned mode. This factor can be determined from conditions  $Y = 0$ ,  $\dot{Y} = 0$ , at  $t = 0^+$ , immediately after application of a concentrated unit-area acceleration pulse  $\ddot{x}_q = \delta(t)$ . Thus (2,3),

$$a_{kq} = \frac{r_{qk}}{\omega_k^2 Z_k^T M Z_k} \quad (3)$$

where  $r_{qk}$  is the external reaction at support  $q$  when the system vibrates freely in its  $k$ 'th mode having shape  $Z_k$  and natural frequency  $\omega_k$ . From Eqs. 1 and 2, a given element  $Y_i$  of the response vector of the system can be expressed as follows

$$Y_i(t) = \sum_q x_q(t) \tilde{Y}_{iq} + \sum_q \sum_j a_{jq} Z_{ij} \int_0^t \ddot{x}_q(\tau) h_j(t-\tau) d\tau \quad (4)$$

In this equation,  $\tilde{Y}_{iq}$  and  $Z_{ij}$  denote the (time independent) values of  $Y_i$  associated with vectors  $\tilde{Y}_q$  and  $Z_j$ , respectively.

#### DYNAMIC RESPONSE ANALYSIS FOR STOCHASTIC GROUND MOTION

It will be assumed that  $x$  can be represented as the product of a Gaussian stationary process  $W_q(t)$  with spectral density  $G_q(\omega)$  by a deterministic envelope  $A_q(t)$ :

$$\ddot{x}_q(t) = A_q(t) W_q(t) \quad (5)$$

In order to determine the parameters that define  $Y_i(t)$  in probabilistic terms, it is advantageous to express that function independently of  $x_q(t)$ , by means of an integral expressed exclusively in terms of  $\ddot{x}_q(t)$  and of a response function  $g_{iq}(t)$  which takes into account both static and dynamic components. For an elementary accelerogram defined by a concentrated impulse  $\ddot{x}_q(t) = \delta(t)$ , one obtains  $\dot{x}_q(t) = H(t)$  and  $x_q(t) = tH(t)$ , where  $\delta(\cdot)$  and  $H(\cdot)$  are Dirac delta function and Heaviside step function, respectively.  $Y_i$  is then the unit impulse response function for acceleration of support  $q$ , and is given by the following equation, obtained from Eq. 4:

$$g_{iq}(t) = tH(t) \tilde{Y}_{iq} + \sum_j a_{jq} Z_{ij} h_j(t) \quad (6)$$

If the complete accelerogram at a given support is taken into account by integration of eq. 6 with respect to time, and if the contributions from all supports are added together, the following alternative to Eq. 4 is obtained:

$$Y_i(t) = \sum_q \int_0^t \ddot{x}_q(\tau) g_{iq}(t-\tau) d\tau \quad (7)$$

Taking into account Eq. 5, the last equation becomes

$$Y_i(t) = \sum_q \int_0^t A_q(z) W_q(z) g_{iq}(t-z) dz \quad (8)$$

Hence, the variance of  $Y_i(t)$  is

$$\text{var } Y_i(t) = \sum_q \sum_r \int_0^t \int_0^t A_q(z_1) A_r(z_2) R_{qr}(z_1, z_2) g_{iq}(t-z_1) g_{ir}(t-z_2) dz_1 dz_2 \quad (9)$$

where  $R_{qr}(z_1, z_2) = E[W_q(z_1) W_r(z_2)]$  is the cross-correlation function of  $W_q$  and  $W_r$ .

From Eqs. 5 and 8 and the approximate theory of Ref. 4 it is possible to determine the probability distribution of the maximum absolute value of  $Y_i(t)$  during an earthquake, but the amount of computations involved makes application of that theory impractical; adoption of simpler criteria is advantageous. Herein it is assumed that the values of responses which correspond to a given probability of exceedance during an earthquake of given intensity are proportional to the maximum values reached by the respective standard deviations while ground motion lasts. Thus, if  $\sigma_0^2$  is the maximum variance of ground acceleration during the earthquake and  $\ddot{x}_0(p)$  is the value of that acceleration which corresponds to probability  $p$  of being exceeded, and if  $\sigma_R$  and  $x_R(p)$  are the corresponding values associated with a response variable  $R$ , the assumption proposed implies that if the design criterion adopted is based on equal exceedance probabilities for all design responses, then the ratio of the design value of  $R$  to the specified peak ground acceleration should equal  $\sigma_R / \sigma_0$ .

Ref. 2 contains expressions for the variance of a response variable for several alternative assumptions concerning the covariance structure of the excitation. Only one particular case is discussed here: that where ground accelerations at the various supports are represented by segments of stationary white noise travelling undistorted along the ground surface:

$$\ddot{x}_q(t) = W_0(t - z_q), \quad q = 1, \dots, N \quad (10)$$

In this equation,  $W_0$  is white noise with spectral density  $G_0$ . The white-noise assumption is not restrictive, and the criterion derived from it can be applied to more general spectral shapes of excitation.

If the natural periods of the systems analyzed are short as compared with the duration of strong ground motion, maximum variances will be reached at the end of the excitation, i.e. for  $t=s$ :

$$\text{var } Y_i(s) = \sum_q \sum_r \tilde{Y}_{iq} \tilde{Y}_{ir} I_{qr}(s) + 2 \sum_q \sum_r \sum_k \tilde{Y}_{iq} \tilde{Y}_{kr} Z_{ik} I'_{kqr}(s) + \sum_q \sum_j \sum_k \sum_l \tilde{Y}_{iq} \tilde{Y}_{kr} Z_{ij} Z_{kl} I''_{jkqr}(s) \quad (11)$$

where, for the case defined by Eq. 10, making  $g(t) = tH(t)$ ,

$$I_{qr}(s) = \pi G_0 \int_0^s g(s-z_q-z) g(s-z_r-z) dz \quad (12a)$$

$$I'_{kqr}(s) = \pi G_0 \int_0^s g(s-z_q-z) h_k(s-z_r-z) dz \quad (12b)$$

$$I''_{jkqr}(s) = \pi G_0 \int_0^s h_j(s-z_q-z) h_k(s-z_r-z) dz \quad (12c)$$

Analytic expressions for these integrals are given in the Appendix.

#### SUPERPOSITION CRITERIA

The ground motion models given by Eq. 5 are reasonable representations of

earthquake accelerograms, in spite of the fact that they ignore frequency-content variations during a given event. These models lead to sufficiently accurate estimates of the variances of ground accelerations and of responses which are determined mainly by those accelerations; however, they do not lead to accurate estimates of variances of quantities sensitive to ground velocities or displacements (such as the dynamic response of structures possessing moderate or long natural periods, or the stresses produced by phase differences among support displacements), unless the spectral density of ground displacements (and not only of ground accelerations) is closely represented or base-line corrections are applied to accelerograms given by Eq. 5 so as to produce zero final ground velocities. As a consequence, the proportionality of design responses with square roots of variances described above cannot always be directly applied, particularly in those instances in which the proportionality refers simultaneously to quantities sensitive to ground accelerations, velocities and displacements. This difficulty can be overcome if the proportionality assumption is applied individually to each term in Eq. 11: although the displacement variances predicted on the basis of Eq. 5 may be excessive, the ratios of the variances of responses proportional to displacements predicted on the same basis will be good estimates of the ratios of the actual variances. Thus, the following equation results:

$$Q^2 = \sum_q \sum_r \left[ Q_q Q_r \alpha_{qr} D_{0q} D_{0r} + 2 \sum_k Q_k \alpha'_{kqr} Z_k \alpha''_{kqr} D_{0q} D_{0r} + \sum_j \sum_k \alpha_{jqkr} Z_j Z_k \alpha''_{jkqr} D_{jq} D_{kr} \right] \quad (13)$$

In this equation,  $Q$  is the design response,  $D_{0q}$  and  $D_{0r}$  are the peak ground displacements at supports  $q$  and  $r$ , respectively;  $D_{jq}$  and  $D_{kr}$  are the displacement spectral ordinates at the same supports for modes  $j$  and  $k$ ;  $Q_q$  is the static response to a unit displacement of support  $q$ , and  $\alpha_{qr}$ ,  $\alpha'_{kqr}$ ,  $\alpha''_{jkqr}$  are proportionality factors obtained as follows:

$$\alpha_{qr} = I_{qr}(s) / (J_{qq} J_{rr})^{1/2} \quad (14a)$$

$$\alpha'_{kqr} = I'_{kqr}(s) / (J_{qq} J_{kr})^{1/2} \quad (14b)$$

$$\alpha''_{jkqr} = I''_{jkqr}(s) / (J''_{jq} J''_{kr})^{1/2} \quad (14c)$$

$J_{qq}$  and  $J_{rr}$  are the values of  $I_{qq}(s)$  and  $I_{rr}(s)$  when time is measured from the instant when ground motion starts at supports  $q$  and  $r$ , respectively, and  $J''_{jk}$ ,  $J''_{kr}$  are the corresponding values of  $I''_{jq}$  and  $I''_{kr}$  for the same time origins. In other words, the contributions to design responses are expressed in terms of peak ground displacements at all supports as well as of the modal responses to each ground motion component taken as acting simultaneously at all supports.

Figs. 1-4 illustrate the variation of  $\alpha$ ,  $\alpha'$  and  $\alpha''$  (determined with Eqs. A1-A3) for several combinations of natural frequencies and time-lags. The latter are expressed as fractions of the duration  $s$  of the white noise segment used to represent the excitation. On firm ground,  $s$  can be taken as 20 sec.

#### DESIGN CRITERIA

It is assumed that design consists in determining probable combinations of internal forces at critical sections and verifying if those combinations lie within the specified safe regions. The criterion advocated herein for the determination of the mentioned combinations is based on the same concepts as that recommended in Ref. 1, but unlike the latter it takes into account the statistical correlation among support displacements. Both criteria assume that the joint probability distribution of the internal forces which determine the most unfavorable condition at a critical section is Gaussian multi-dimensional, and that a set of multidimensional ellipsoids can be built with centers at the expected values of the internal forces and principal axes in directions which are functions of the

correlation coefficients, so that to each ellipsoid corresponds a number of standard deviations of each internal force from its expected value and hence a given probability of containing the load combination of interest. A given design is adequate if the ellipsoid which corresponds to a specified probability lies within the safe region and is tangent to its boundary (1). Because constructing the mentioned ellipsoid would be excessively difficult for practical design, it is proposed to substitute the ellipsoid with a set of  $2^N$  points (combinations) where  $N$  is the number of cartesian components in each combination (IV). The design value of component  $Y_k$  in the  $j$ -th combination would equal  $\gamma_{kj}^* Y_k$ , where  $Y_k$  is the design value which would be assumed for  $Y_k$  if design were based exclusively on it,  $\gamma_{kj}^*$  equals  $\pm 1$  for  $k = j$  and  $\gamma_{kj}^* (\rho_{kj} \pm \alpha_3(1 - \rho_{kj}^2))$  for  $k \neq j$ , and  $\rho_{kj}$  is the correlation coefficient between  $Y_k(s)$  and  $Y_j(s)$ . An expression for  $\text{cov}(Y_k(s), Y_j(s))$  of the type of Eq. 13 can readily be derived starting from Eq. 4.

Take for instance the case illustrated in Fig. 5 for the cross section of a reinforced concrete column subjected to axial load  $P$  and bending moment  $M$  with respect to one of its principal axes of inertia. The cases when the correlation coefficient  $\rho_{MP}$  equals 0 and 0.5 will be considered. Assume also that the dotted line represents the section's interaction diagram, and that  $p$  and  $m$  are the design values of  $M$  and  $P$  should each of them be considered separately. For each value of  $\rho_{MP}$ ,  $N = 2$  and the number of internal-forces combinations to be considered equals  $2^2 = 4$ . For  $\rho_{MP} = 0$ ,  $\gamma_{MP}^* = \pm 0.3$ , and for  $\rho_{MP} = 0.5$ ,  $\gamma_{MP}^* = \pm (0.5 \pm 0.225)$ ; hence Figs. 5a, b.

#### APPLICATIONS

Fig 6 shows some results of applying Eq. 13 to define the design responses of a fixed-end arch when both supports move out of phase. Responses to vertical and horizontal ground displacements are analyzed separately. In each case, results are expressed in terms of both the ratio  $Z_g/s$  of the time-lag between support displacements to the duration of the white-noise segment and the apparent wave propagation velocity along the ground surface. Both qualitative and quantitative deviations with respect to the case of in-phase support motion are evident.

Another case of interest is shown in Fig. 7, which represents a bridge built of simply supported spans resting on columns with ends fixed on the ground surface. Variables studied include bending moments at column bases and tensions on tie-bars connecting beam spans. Again, the sensitivity of design responses to phase differences is obvious.

#### CONCLUSIONS

The seismic response of extended-in-plan structures can be very sensitive to phase differences among the motions of different points in the foundation. Under the assumption of linear behavior it is possible to formulate approximate criteria to obtain design values and response superposition models which account for all ground motion components. The resulting expressions are determined by the covariance structure of the ground motion histories at the different supports.

#### REFERENCES

1. Rosenblueth, E. and Contreras, H., "Approximate design for multicomponent earthquakes", *Proc. ASCE*, 102, EM5 (Oct. 1977)

(VI) The criterion proposed in Ref. 1 works with load vectors corresponding to each ground motion component.

2. Esteve, L., "Structural response to multicomponent earthquakes", *Advanced Seminar on Random Vibrations*, London (Organized by Computational Mechanics, Southampton, 1978)
3. Esteve, L., Rosenblueth, E., & Rascón, O.A., "Respuesta transitoria de estructuras elásticas a perturbaciones fuera de fase", *Boletín, Sociedad Mexicana de Ingeniería Sísmica*, 2 (Mar 1964)
4. Vanmarcke, E. H., "Structural response to earthquakes", Chap. 8 of *Seismic Risk and Engineering Decisions*, Edited by C. Lomnitz and E. Rosenblueth, Elsevier, Amsterdam (1976)

#### APPENDIX. VARIANCE INTEGRALS FOR SHIFTED IDENTICAL WHITE NOISE COMPONENTS

Analytical expressions for  $I_{qr}$ ,  $I'_{kqr}$ ,  $I''_{jkqr}$ , according to Eqs. 12a - c:

$$I_{qr}(t) = \frac{1}{3}(t^3 - t_1^3) = \frac{1}{2}(z_q + z_r)(t^2 - t_1^2) + z_q z_r (t - t_1) \quad (A1)$$

$$I'_{kqr}(t) = \frac{1}{2^2 \omega_k^2} \left\{ e^{-\gamma_k \omega_k (t - z_r)} \left[ (B_1 (1 + \gamma_k \omega_k t) - A_1 \omega_k t - \omega_k z_q D_1) \cos \omega_k (t - z_r) + (A_1 (1 + \gamma_k \omega_k t) + B_1 \omega_k t - \gamma_k \omega_k z_q D_1) \sin \omega_k (t - z_r) \right] - e^{-\gamma_k \omega_k (t_1 - z_r)} \left[ (B_1 (1 + \gamma_k \omega_k t_1) - A_1 \omega_k t_1 - \omega_k z_q D_1) \cos \omega_k (t_1 - z_r) + (A_1 (1 + \gamma_k \omega_k t_1) + B_1 \omega_k t_1 - \gamma_k \omega_k z_q D_1) \sin \omega_k (t_1 - z_r) \right] \right\} \quad (A2)$$

$$I''_{jkqr}(t) = \frac{e^{-\gamma t}}{2 \omega_j \omega_k} \left\{ e^{-At} \left[ \frac{A \cos(Z_1 - W_1 t) + W_1 \sin(Z_1 - W_1 t)}{A^2 + W_1^2} - \frac{A \cos(Z_2 - W_2 t) + W_2 \sin(Z_2 - W_2 t)}{A^2 + W_2^2} \right] - e^{-At_1} \left[ \frac{A \cos(Z_1 - W_1 t_1) + W_1 \sin(Z_1 - W_1 t_1)}{A^2 + W_1^2} - \frac{A \cos(Z_2 - W_2 t_1) + W_2 \sin(Z_2 - W_2 t_1)}{A^2 + W_2^2} \right] \right\} \quad (A3)$$

In these equations,

$$t_1 = \max(z_q, z_r)$$

$$A_1 = \gamma_k^2 \omega_k^2 - \omega_k'^2$$

$$B_1 = 2\gamma_k \omega_k \omega_k'$$

$$D_1 = \gamma_k^2 \omega_k^2 + \omega_k'^2$$

$$\gamma = \gamma_j \omega_j z_q + \gamma_k \omega_k z_r$$

$$A = \gamma_j \omega_j + \gamma_k \omega_k$$

$$Z_1 = \omega_j' z_q + \omega_k' z_r$$

$$Z_2 = \omega_j' z_q - \omega_k' z_r$$

$$W_1 = \omega_j' + \omega_k'$$

$$W_2 = \omega_j' - \omega_k'$$

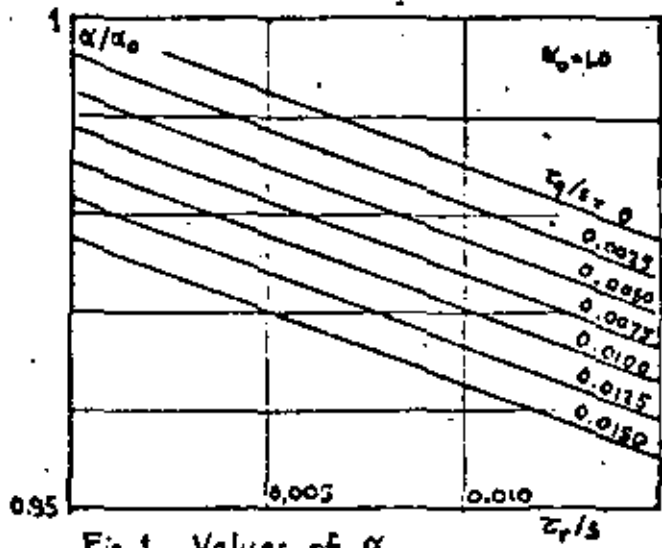


Fig. 1 Values of  $\alpha$

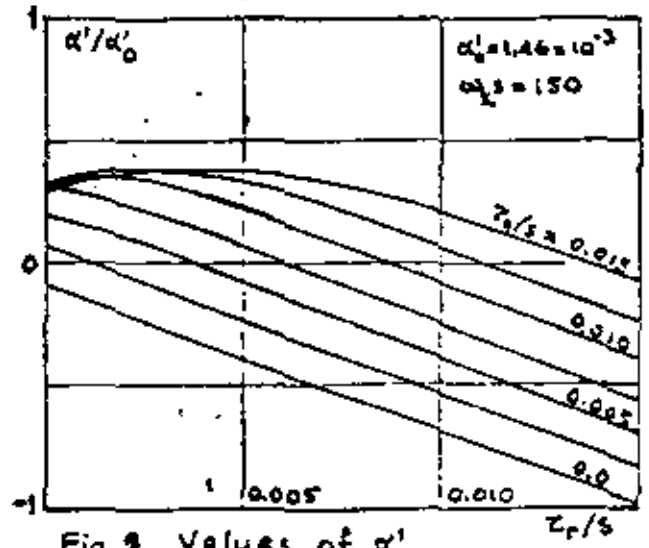


Fig. 2 Values of  $\alpha'$

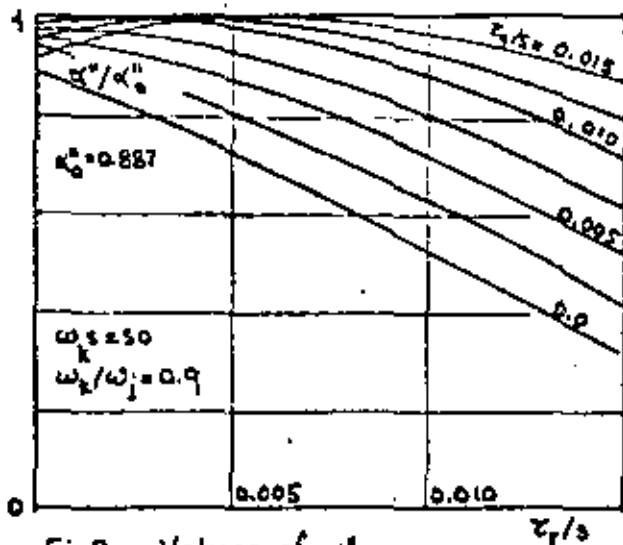


Fig. 3 Values of  $\alpha''$

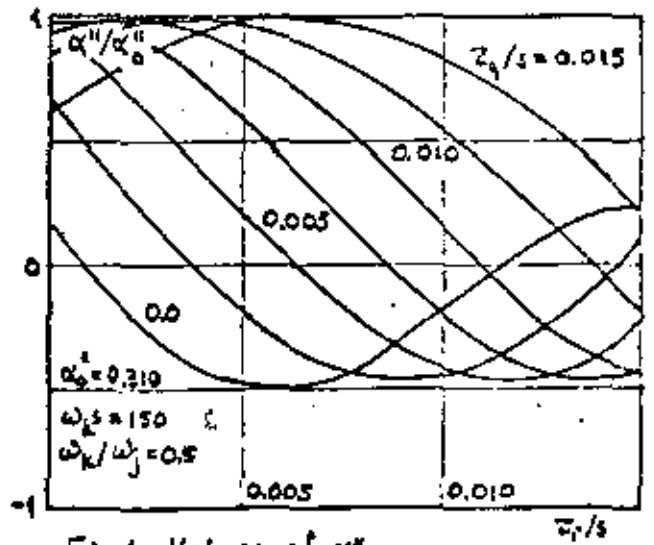


Fig. 4 Values of  $\alpha'''$

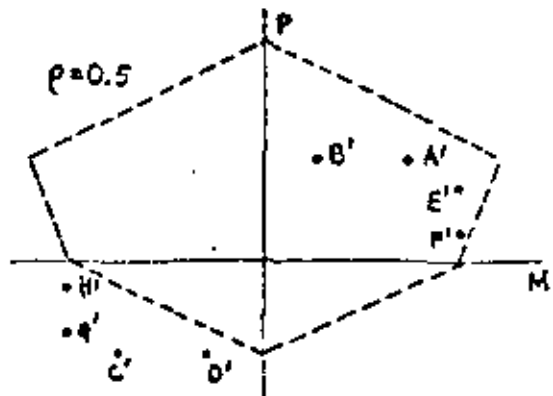
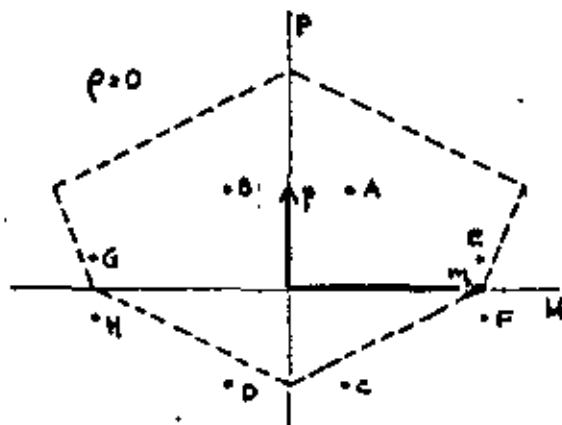
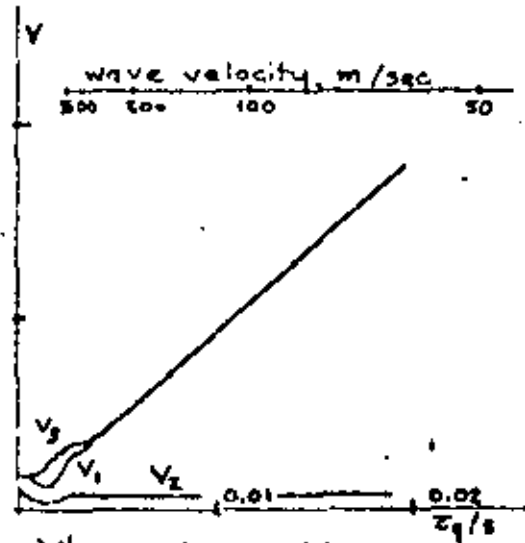
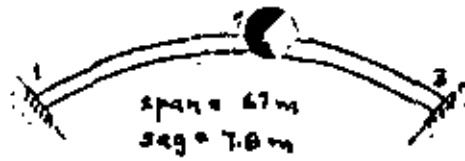
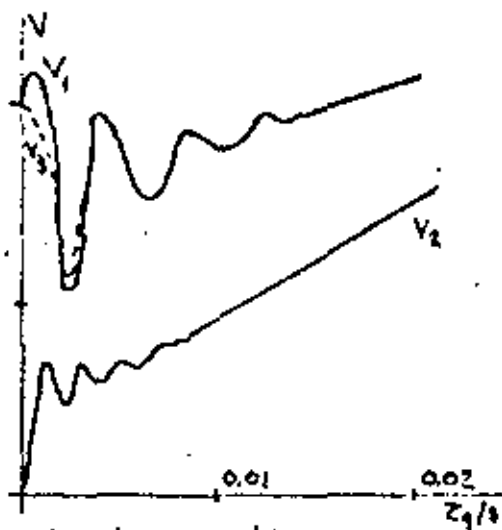


Fig. 5 Superposition of correlated responses

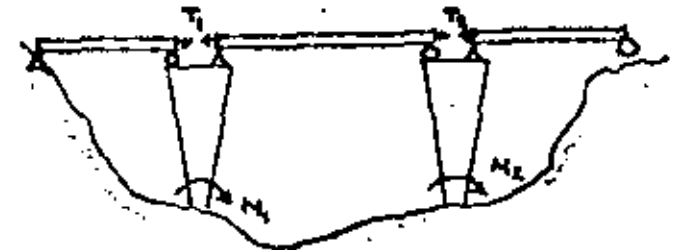
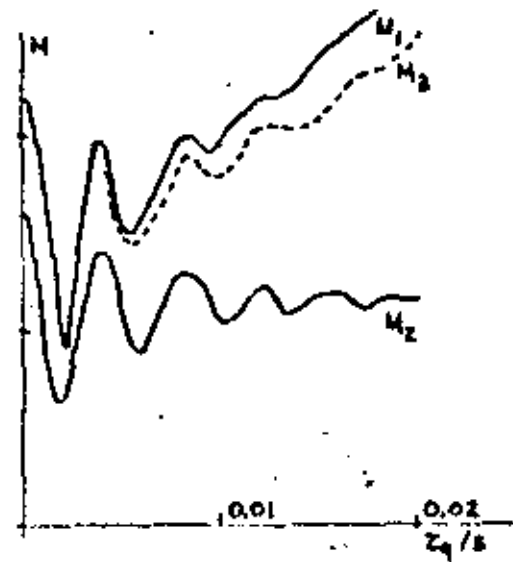
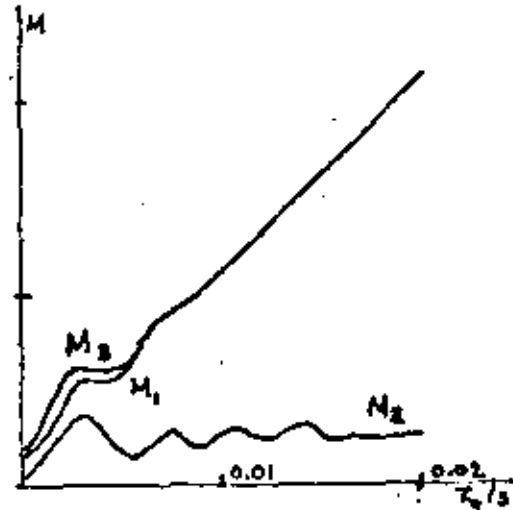
a) Structure studied.



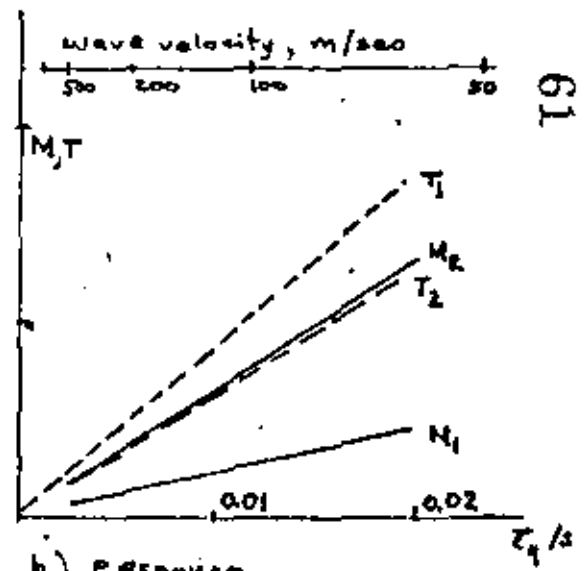
b) Horizontal motion



c) Vertical motion



a) Bridge with spans connected by ties



b) Response

Fig.6 Influence of phase differences in the seismic response of an arch

Fig.7 Bridge response

INFLUENCIA EN LA RESPUESTA SISMICA DEL PUENTE COATZACOALCOS II  
DE LAS DIFERENCIAS DE FASE EN LOS MOVIMIENTOS DE SUS APOYOS

Sonia E. Ruiz\*\*  
Luis Esteve\*\*  
David De León\*

Elaborado para

DIRECCION FEDERAL DE CARRETERAS FEDERALES  
SECRETARIA DE ASENTAMIENTOS HUMANOS Y  
OBRAS PUBLICAS

Proyecto 0754

Diciembre 1980

\*\* Investigador, Instituto de Ingeniería, UNAM  
\* Becario, Instituto de Ingeniería, UNAM

## INFLUENCIA EN LA RESPUESTA SISMICA DEL PUENTE COATZACOALCOS II DE LAS DIFERENCIAS DE FASE EN LOS MOVIMIENTOS DE SUS APOYOS

S. E. Ruiz, L. Esteva y D. De León\*

### INTRODUCCION

La Secretaría de Asentamientos Humanos y Obras Públicas proyecta construir un puente de 772 m de largo total sobre varios apoyos, sobre el río Coatzacoalcos, en la carretera Nuevo Teapa-Minatitlán en el Estado de Veracruz. Las características geométricas más importantes del puente se extrajeron del plano 4775 proporcionado por SAHOP modificando las longitudes del claro central a 288m, y de los dos adyacentes a 98.35m cada uno. Estos tres claros están suspendidos de las dos torres centrales mediante sendos sistemas de cables atirantados colocados en el plano longitudinal de simetría del puente. Los apoyos se desplantan sobre zapatas y pilas que atraviesan las formaciones sedimentarias del fondo del cauce, y que se apoyan a su vez sobre terreno firme a profundidades que fluctúan entre 6.6 y 30 m.

La configuración del puente y los valores de las distancias entre apoyos hacen pensar en la posibilidad de que las diferencias de fase entre los movimientos de dichos apoyos afecten en forma importante las respuestas sísmicas de diseño en algunas secciones críticas, en relación con las que se obtendrían bajo la hipótesis de que los movimientos de las bases ocurren en fase. La importancia del efecto se acentúa si se tiene en cuenta que en el sitio de interés el riesgo sísmico depende en gran parte de temblores de gran magnitud a distancias hipocentrales grandes, y que por tanto las ondas superficiales contribuirán de manera importante a la excitación sísmica. Además teniendo en cuenta que los elementos de apoyo de los claros centrales atraviesan formaciones sedimentarias, las velocidades de propagación de las ondas superficiales serán relativamente bajas, lo que habrá de traducirse en mayores diferencias de fase.

\* Instituto de Ingeniería, UNAM.

El criterio que en este estudio se adopta se basa en la ref 1; es de tipo probabilístico y supone que los movimientos de los distintos apoyos son iguales en forma, pero difieren en los tiempos de desfaseamiento; es decir, que se deben a un tren de ondas que viaja sin distorsionarse a lo largo de la superficie del terreno. Se adopta este modelo en ausencia de información experimental (registros de temblores reales) sobre las relaciones entre las características del movimientos del terreno en sitios cercanos.

#### SELECCION DE LA RESPUESTA DE DISEÑO

Según la ref 1 la selección de los valores de diseño de las respuestas se basa en la proporcionalidad aproximada entre las respuestas correspondientes a probabilidades dadas de excedencia y las desviaciones estándar de dichas respuestas al final de la excitación aleatoria que se emplea para representar al movimiento del terreno. A fin de obtener expresiones simples para las desviaciones estándar que se mencionan, en la ref 1 se introducen algunas hipótesis simplificadoras, entre las que destaca la que consiste en suponer que en cada apoyo el acelerograma es un segmento de ruido blanco con duración  $\Delta$  e intensidad  $S(\omega) = S_0$ ; la variación de  $s$  con  $\omega$  para fines de considerar adecuadamente la contribución de cada uno de los modos naturales de vibración a la variancia de la respuesta se toma en cuenta mediante la introducción de los factores de proporcionalidad  $\alpha$ ,  $\alpha'$  y  $\alpha''$  que se definen en las ecs 2a-c.

En resumen, las hipótesis citadas conducen, de acuerdo con la ref 1, a la siguiente expresión para determinar el valor de diseño de la respuesta  $Q$ :

$$Q^2 = \sum_q \sum_r \{ Q_q Q_r \alpha_{qr} D_{oq} D_{or} + 2 \sum_k Q_q a_{kr} Z_k \alpha'_{kqr} D_{oq} D_{kr} + \sum_j \sum_k a_{jq} a_{kr} Z_j Z_k \alpha''_{jkqr} D_{jq} D_{kr} \} \quad (1)$$

En esta ecuación,  $D_{oq}$  y  $D_{or}$  son los valores máximos (en este caso iguales) del desplazamiento del terreno en las bases de los apoyos  $q$  y  $r$ , respectivamente;  $D_{jq}$  y  $D_{kr}$  son las ordenadas del espectro de desplazamiento en dichos apoyos para los modos  $j$  y  $k$ ;  $Z_j$  y  $Z_k$  son los valores que toma la respuesta de interés para las configuraciones modales  $j$  y  $k$ ;  $a_{jq}$  y  $a_{kr}$  son los factores de

participación de los modos  $j$  y  $k$  para las configuraciones que resultan de aplicar gradualmente (en forma estática) desplazamientos unitarios a los apoyos  $q$  y  $r$ , respectivamente;  $Q_q$  y  $Q_r$  son las respuestas estáticas a dichos desplazamientos unitarios y  $\alpha_{qr}$ ,  $\alpha'_{kqr}$ ,  $\alpha''_{jkqr}$  son factores de proporcionalidad que se obtienen como sigue:

$$\alpha_{qr} = I_{qr}(s) / (J_{qq} J_{rr})^{1/2} \quad (2a)$$

$$\alpha'_{kqr} = I'_{kqr}(s) / (J_{qq} J''_{kr})^{1/2} \quad (2b)$$

$$\alpha''_{jkqr} = I''_{jkqr}(s) / (J''_{jq} J''_{kr})^{1/2} \quad (2c)$$

Aquí,  $I_{qr}(s)$ ,  $I'_{kqr}(s)$ ,  $I''_{jkqr}(s)$ , en donde  $s$  es la duración del segmento de ruido blando que representa a la excitación, resultan al formular expresiones para las variancias de las respuestas de interés incluyendo las componentes estáticas y dinámicas. Las funciones  $I$  se refieren a las covariancias entre las respuestas estáticas producidas por los desplazamientos de los diversos apoyos, las  $I''$  a las covariancias entre las respuestas dinámicas asociadas con los distintos apoyos y modos naturales de vibración y las  $I'$  a las covariancias entre las respuestas estáticas y las dinámicas.  $J_{qq}$  y  $J_{rr}$  son los valores de  $I_{qq}(s)$  e  $I_{rr}(s)$  cuando el tiempo se mide desde el instante en que el movimiento del terreno se inicia en los apoyos  $q$  y  $r$  respectivamente, y  $J''_{jq}$ ,  $J''_{kr}$  son los valores correspondientes de  $I''_{jjqq}$  e  $I''_{kkrr}$  para los mismos orígenes del tiempo. En otras palabras, las contribuciones a las respuestas de diseño se expresan en términos de los desplazamientos máximos del terreno en los distintos apoyos, así como de las respuestas modales a cada componente del movimiento del terreno como si actuara simultáneamente en todos los apoyos (1).

#### ESTRUCTURA ANALIZADA

Dada la complejidad del sistema estructural de interés y las aproximaciones y simplificaciones implícitas en el criterio de análisis propuesto, se consideró justificable llevar a cabo un estudio en un modelo simplificado de la

estructura, con un número reducido de grados de libertad, pero que preservara los rasgos importantes que podrían ser significativos en la influencia de las diferencias de fase sobre las respuestas de diseño. Así, en el presente trabajo se determinan, para el modelo simplificado que se describe más adelante, los valores de las fuerzas internas de diseño en las diversas secciones críticas, obtenidas respectivamente para las condiciones en que se incluyen y en que se ignoran las diferencias de fase. Comparando ambos grupos de resultados es fácil deducir los incrementos que deben aplicarse a los valores de las fuerzas de diseño obtenidas mediante un análisis dinámico convencional de un modelo detallado de la estructura sujeto a movimiento simultáneo de sus apoyos.

Como se mencionó antes, sólo se estudiaron las respuestas a las componentes longitudinales y verticales del movimiento del terreno. Los sistemas de cables de la estructura real se sustituyeron por cables únicos con rigideces lineales equivalentes; estos elementos pueden tomar incrementos positivos y negativos de carga axial. Los elementos de flexión se sustituyeron por unos cuantos elementos finitos, las masas distribuidas se sustituyeron por unas cuantas concentraciones, y la interacción dinámica entre la cimentación y la estructura en el desplante del apoyo 18 se tomó en cuenta mediante resortes y amortiguadores cuyas constantes se obtuvieron de la ref 2. En los demás apoyos la cimentación se consideró infinitamente rígida.

A fin de reducir aun más el número de grados de libertad y el número de apoyos que se mueven fuera de fase, el sistema simplificado se transformó en el de la fig 1, eliminando los claros y apoyos extremos, y representando sus rigideces en los nudos 1 y 22 de la fig 1 mediante resortes lineales y angulares cuyas constantes se obtuvieron a partir de los miembros iniciales mediante los criterios convencionales del análisis estructural lineal. Además, se supuso que los dos apoyos que quedaron en cada extremo de la nueva estructura simplificada de la fig 1 se movían en fase, como un solo apoyo, para fines de aplicar la ec 1 (fig 2).

La determinación de las respuestas estáticas  $Q_q$ ,  $Q_r$  y dinámicas modales  $Z_j$ ,

$Z_k$ , así como de los factores de participación  $a_{kr}$  se llevó a cabo empleando el programa SAP IV para calculadora digital (3). En las figs 3 a 7 se presentan las configuraciones de los primeros 5 modos naturales. El periodo fundamental resultó ser 1.97 seg, que se compara razonablemente bien con el de 2.56 seg, obtenido en la ref 2 empleando un modelo detallado de la estructura.

Para fines de calcular los coeficientes dados por las ecs 2a-c se supuso un coeficiente de amortiguamiento en cada modo igual a 0.2 del crítico. Este valor toma en cuenta la disipación de energía por comportamiento inelástico.

#### EXCITACION DE DISEÑO

Se adoptó para cada apoyo el espectro de diseño empleado en la ref 4. De las características de este espectro y las distancias a las fuentes sísmicas que más contribuyen al riesgo sísmico en el sitio de interés se concluyó que debería tomarse para el desplazamiento horizontal máximo del terreno un valor de 20 cm, y para el vertical de 14cm. Por otro lado, considerando la influencia de los sedimentos en las características de los temblores, se tomó  $s = 35$  seg, en vez de valores comprendidos entre 15 y 20 seg, que normalmente se recomiendan para la duración efectiva de segmentos de ruido blanco que se emplean en aplicaciones similares a la presente cuando se trata de temblores en terreno firme (5).

Se analizó la influencia de las diferencias de fase que provienen de suponer trenes de ondas superficiales que viajan en una dirección paralela a la longitudinal del puente. Las velocidades de propagación consideradas fueron  $\infty$  (movimiento en fase), 50, 100, 200, 300, 500, 1000, 2000 y 5000 m/seg. A fin de estimar la velocidad de las ondas superficiales aplicable al caso en estudio se analizaron varios modelos idealizados de la estratigrafía en el punto medio entre los dos apoyos centrales. El primer modelo consideró un estrato de 13 m de espesor con módulo dinámico de cortante igual a 1025 ton/m<sup>2</sup> y peso volumétrico de 1.7 ton/m<sup>3</sup>, de acuerdo con la ref 6; por debajo de dicho estrato se consideró un medio semi-infinito con un módulo de cortante

Igual a 5 veces el de arriba, lo que es congruente con las rigideces reportadas en los primeros metros de la formación en que se apoya la cimentación. Considerando que es probable que a pocos metros se encuentren formaciones bastante más rígidas, se analizó un segundo modelo que difiere del primero únicamente en que la formación inferior es 20 veces más rígida que el estrato superior. Para ondas de Rayleigh con periodo de un segundo las respectivas velocidades de propagación resultaron 120 y 230 m/seg.

## RESULTADOS

Las tablas 1 y 2 resumen los resultados de los estudios efectuados para movimiento horizontal y vertical respectivamente. La última columna corresponde al caso en que los apoyos se mueven en fase.

El número que precede a cada grupo de seis renglones es el de un miembro, de acuerdo con la numeración de la fig 1. Los seis renglones corresponden a fuerzas axiales, fuerzas cortantes y momentos flexionantes en los extremos izquierdo y derecho o superior e inferior, en unidades de ton y ton/m.

Los dos últimos renglones de cada tabla corresponden a las tensiones de los cables, elementos 7 y 8 de la fig 1.

En las tablas 1 y 2 se observa que en el caso vertical la mayor parte de los miembros las diferencias de fase pueden tener un efecto apreciable sobre las fuerzas internas de diseño, en ciertos casos incrementándolas y en otros reduciéndolas. El efecto citado es muy sensible a las velocidades efectivas\* de propagación de las ondas en la dirección paralela al puente. Las diferencias de fase en el movimiento horizontal no ocasionan amplificaciones importantes.

## DISCUSION Y RECOMENDACIONES

La información disponible sobre características del terreno en los sitios de

\* Se usa aquí este término para tener en cuenta que una onda que viaja con una velocidad nominal, en dirección oblicua al eje del puente, tiene una cierta velocidad efectiva en la dirección paralela a dicho eje.

Los apoyos cubren solo las capas de material blando y unos cuantos metros de material de rigidez moderada que yace debajo de ellas (en total, una profundidad de 35m); por ello no es posible estimar con precisión las velocidades de propagación de las ondas superficiales. Los cálculos de la sección anterior muestran que las velocidades en cuestión pueden encontrarse entre 120 y 230 m/seg, de acuerdo con las hipótesis que se hagan relativas a las características del terreno por debajo de los 35 m de profundidad.

A la incertidumbre sobre las velocidades nominales de propagación de ondas superficiales debe sumarse la asociada con el modelo adoptado y con la hipótesis conservadora que consiste en considerar que las ondas viajan precisamente en la dirección del puente. Si en vez de esto se considerara, por ejemplo, un ángulo de incidencia de  $45^\circ$  con respecto al plano longitudinal de simetría, la velocidad efectiva se obtendría multiplicando la nominal por la secante de  $45^\circ$ , es decir, por 1.41.

Los resultados que se presentan provienen de un análisis de respuesta dinámica lineal. De acuerdo con la práctica usual de diseño sísmico, pueden tomarse como valores de diseño si provienen de espectros reducidos que correspondan al nivel de ductilidad que la experiencia aconseja para el tipo de estructura en estudio.

Sin embargo, es razonable esperar que el comportamiento no lineal y la correspondiente redistribución de esfuerzos contribuyan a desenfaticar la influencia de las diferencias de fase. En la literatura técnica no se cuenta con información cuantitativa sobre este efecto.

En vista de las incertidumbres citadas, y tomando en cuenta consideraciones económicas, se propone tomar como respuestas de diseño las que muestran las tablas 1 y 2 para velocidades de propagación de ondas de 300 m/seg. Dichas respuestas en ningún caso deberán tomarse menores que las que corresponden a desplazamiento en fase en todos los apoyos, según el criterio convencional; por lo tanto, en este estudio sólo se tendrán incrementos en las respuestas ocasionadas por el defasamiento en el movimiento vertical.

REFERENCIAS

70

1. L. Esteva, S.E. Ruiz y A. Reyes, "Seismic response of multi-support structures", *Proc. 7WCEE*, Estambul, Turquía, 1980
2. Análisis dinámico de puente "Coatzacoalcos II" realizado por SOGELERG (Variante I), jul 1979
3. Bathe K, Wilson E. L. and Peterson F. E., "SAP IV, A Structural analysis program for static and dynamic response of linear systems", EERC 73-11, *Universidad de California*, Berkeley, Calif., 1973
4. Estudio de riesgo sísmico. Puente Coatzacoalcos II, realizado por COMEC, oct 1979
5. Newmark N M y Rosenblueth, E., "*Fundamentals of earthquake engineering*", Prentice Hall, Inc, 1971
6. Estudio de mecánica de suelos para el puente Coatzacoalcos II, realizado por GEOTEC, S.A., 1980

TABLA I  
MOVIMIENTO LONGITUDINAL



VEL. M/S	50	100	200	300	500	1000	2000	5000	EN PIES
AAI	15.52	11.37	15.89	15.31	14.96	20.47	23.07	23.94	24.11
AXL	15.52	11.39	15.89	15.31	14.96	20.47	23.07	23.94	24.11
COI	30.89	25.28	17.97	17.35	15.71	20.09	23.88	24.63	24.50
COJ	30.89	25.23	17.97	17.35	15.71	20.09	23.88	24.63	24.50
NOI	334.06	312.75	322.53	315.67	192.03	259.54	295.95	305.42	301.93
NOJ	1467.30	1203.64	853.93	925.63	746.90	994.49	1131.95	1170.67	1164.37
AAI	120.42	101.59	142.55	115.31	105.13	174.42	200.70	209.38	211.75
AXL	120.42	101.57	142.53	115.31	105.13	174.42	200.70	209.38	211.75
COI	275.42	197.17	212.50	203.60	192.79	244.01	304.95	319.64	322.98
COJ	275.42	197.17	212.50	203.60	192.79	244.01	304.95	319.64	322.98
NOI	4278.04	2632.56	3206.43	3027.37	2680.41	3291.35	4601.05	4823.58	4871.97
NOJ	4677.17	3310.73	3417.43	3310.24	3150.16	4250.53	4873.47	5127.77	5177.97
AAI	237.21	150.13	117.70	98.48	90.82	133.22	151.83	158.09	159.54
AXL	237.21	150.13	117.70	98.48	90.82	133.22	151.83	158.09	159.54
COI	149.36	77.69	130.77	117.16	109.29	173.31	179.94	209.99	211.55
COJ	149.36	97.84	140.57	117.16	109.29	173.31	179.94	209.99	211.55
NOI	3334.15	2112.26	2910.13	2576.22	2431.24	3424.32	4197.60	4237.67	4442.92
NOJ	1341.44	1243.19	1330.54	1047.73	917.62	1592.33	1825.54	1899.52	1899.52
AAI	170.91	126.45	173.55	141.90	128.29	196.46	227.31	239.59	241.03
AXL	170.91	126.45	173.55	141.90	128.29	196.46	227.01	239.59	241.03
COI	30.56	41.44	21.54	20.03	27.27	32.00	43.27	41.14	41.15
COJ	30.56	41.44	21.54	20.01	27.23	32.00	43.27	41.16	41.15
NOI	1341.44	1243.17	1330.54	1047.73	917.62	1592.33	1825.54	1899.52	1899.52
NOJ	1732.53	1911.74	1586.67	1656.02	1591.49	2005.10	2221.41	2304.62	2304.62
AAI	0.11	0.12	0.12	0.11	0.12	0.05	0.05	0.02	0.01
AXL	0.11	0.12	0.12	0.11	0.12	0.05	0.05	0.02	0.01
COI	26.17	23.27	25.97	28.22	23.72	32.00	39.17	41.34	42.20
COJ	25.87	23.27	25.97	28.22	23.72	33.80	39.17	41.34	42.20
NOI	0.00	0.00	0.00	0.00	0.00	0.00	0.00	0.00	0.00
NOJ	503.93	443.83	551.33	577.81	450.31	147.53	705.49	707.91	801.91

PAGE.

CONTINUACION TABLA 1

6	AXI	223.64	207.94	226.19	160.37	171.60	259.99	303.87	315.78	317.21
	AXJ	223.64	207.94	226.19	160.37	171.60	259.99	303.87	315.79	317.21
	LOI	157.90	157.34	141.20	113.51	120.90	105.40	216.41	226.93	220.64
	LOJ	157.90	157.34	141.20	144.51	135.99	105.40	215.41	226.93	220.64
	NOI	509.46	443.60	551.06	537.53	405.41	613.93	745.49	707.01	807.91
	NOJ	5175.21	3226.44	2734.99	2081.08	2632.51	3590.72	4150.68	4343.01	4243.05
7	AXI	224.32	207.32	227.09	141.20	132.52	241.69	305.09	317.92	319.40
	AXJ	224.32	207.32	227.09	141.20	132.52	241.69	305.09	317.92	319.40
	LOI	56.71	53.19	61.43	59.31	54.99	73.60	93.42	86.09	85.89
	LOJ	56.71	53.19	61.43	59.31	56.89	73.60	93.42	86.08	85.89
	NOI	3175.21	3226.44	2734.99	2851.08	2662.51	3590.72	4150.68	4346.01	4367.25
	NOJ	4771.35	4764.37	2859.31	3953.63	3746.39	4924.79	5733.53	5992.36	6006.49
8	AXI	239.44	219.40	240.28	173.81	139.77	291.76	330.78	344.25	346.00
	AXJ	239.44	219.40	240.28	173.81	139.77	291.76	330.78	344.25	346.00
	LOI	931.96	841.39	792.36	829.70	782.06	1043.43	1206.22	1262.68	1271.29
	LOJ	931.96	841.39	792.36	829.70	789.06	1043.43	1206.22	1262.68	1271.29
	NOI	5981.87	9276.06	7129.96	7445.51	6791.04	9467.03	11047.66	11527.92	11555.07
	NOJ	5977.54	7471.91	9119.22	8961.04	8713.61	11993.51	13421.35	14314.34	14495.09
9. PAGE.	AXI	243.29	217.71	244.62	179.05	142.34	290.01	310.68	354.76	356.71
	AXJ	243.29	217.71	244.62	179.05	142.34	290.01	310.68	354.76	356.71
	LOI	1913.06	920.30	887.11	921.73	875.03	1134.23	1349.27	1412.34	1422.39
	LOJ	1913.06	920.30	887.44	921.73	875.93	1144.23	1349.27	1412.34	1422.39
	NOI	9877.54	7471.92	9119.22	8961.04	8713.61	11993.51	13421.35	14344.34	14495.09
	NOJ	27324.44	23406.68	24250.91	24857.11	23975.57	31200.61	36722.61	39480.04	39799.09
10	AXI	903.84	785.70	400.20	598.60	563.05	743.40	883.22	886.85	890.47
	AXJ	903.84	785.70	400.20	598.60	563.05	743.40	883.22	886.85	890.47
	LOI	32.06	32.05	40.20	43.64	23.97	61.27	75.12	79.24	79.91
	LOJ	32.06	32.05	40.20	43.64	24.97	61.27	75.12	79.24	79.91
	NOI	2657.22	2669.57	2152.82	2024.10	1571.17	2760.61	3319.54	3402.47	3501.70
	NOJ	1913.02	1228.77	1519.16	1342.85	903.52	1891.16	2320.82	2427.55	2453.02
11	AXI	767.29	520.91	373.43	386.44	371.35	484.97	511.90	530.39	530.94
	AXJ	767.29	520.91	373.43	386.44	371.35	484.97	511.90	530.39	530.94
	LOI	21.50	17.98	22.68	21.60	11.73	23.44	30.00	31.03	32.32
	LOJ	21.50	17.98	22.68	21.60	11.73	23.44	30.00	31.03	32.32
	NOI	1515.02	1228.77	1519.16	1342.85	903.52	1871.16	2300.82	2427.55	2453.02
	NOJ	1736.73	1635.47	1426.33	1692.32	1011.52	1732.48	2123.71	2284.64	2320.63
	ONE	258.57	177.22	158.57	237.72	197.57	317.01	376.23	381.21	387.50
	TWO	251.12	266.30	233.29	171.51	151.72	209.59	205.73	317.58	319.24



72

PAGE.

TABLA 2  
MOVIMIENTO VERTICAL



VEL.M/S	50	100	200	300	500	1000	2000	5000	EN FA
1									
AAI	11.57	16.20	14.51	11.27	5.43	5.50	5.30	3.29	3.04
AAJ	11.57	16.20	14.51	11.27	5.43	5.50	5.30	3.29	3.04
COI	17.14	20.09	16.15	13.01	14.30	15.97	15.52	15.00	14.97
COJ	17.14	20.09	16.15	13.01	14.30	15.97	15.52	15.00	14.97
BOI	237.56	242.72	194.82	157.11	173.09	193.64	185.24	181.94	181.57
BOJ	237.56	242.72	194.82	157.11	173.09	193.64	185.24	181.94	181.57
2									
AAI	162.81	206.15	174.29	136.00	130.66	134.66	130.92	126.66	124.16
AAJ	162.81	206.15	174.29	136.00	130.66	134.66	130.92	126.66	124.16
COI	93.68	133.45	114.48	87.41	64.42	55.35	51.13	48.02	44.85
COJ	93.68	133.45	114.48	87.41	64.42	55.35	51.13	48.02	44.85
BOI	1340.79	2267.65	1947.24	1492.72	1160.53	1039.71	979.49	931.80	892.81
BOJ	1340.79	2267.65	1947.24	1492.72	1160.53	1039.71	979.49	931.80	892.81
3									
AAI	32.73	113.66	97.04	74.32	55.97	51.00	47.37	40.92	37.66
AAJ	32.73	113.66	97.04	74.32	55.97	51.00	47.37	40.92	37.66
COI	145.75	186.84	158.13	122.94	115.40	117.20	113.74	110.01	107.54
COJ	145.75	186.84	158.13	122.94	115.40	117.20	113.74	110.01	107.54
BOI	2324.67	3026.36	2623.90	2029.79	1502.60	1265.12	1204.92	1615.09	1594.10
BOJ	2324.67	3026.36	2623.90	2029.79	1502.60	1265.12	1204.92	1615.09	1594.10
4									
AAI	183.64	238.39	186.95	131.51	112.01	122.64	120.84	126.76	120.63
AAJ	183.64	238.39	186.95	131.51	112.01	122.64	120.84	126.76	120.63
COI	32.39	45.44	37.29	29.94	23.76	35.94	35.04	33.87	33.67
COJ	32.39	45.44	37.29	29.94	23.76	35.94	35.04	33.87	33.67
BOI	1816.95	2247.46	1888.23	1478.12	1451.03	1548.59	1527.29	1478.29	1474.93
BOJ	1816.95	2247.46	1888.23	1478.12	1451.03	1548.59	1527.29	1478.29	1474.93
5									
AAI	0.23	0.21	0.22	0.14	0.20	0.34	0.32	0.20	0.14
AAJ	0.23	0.21	0.22	0.14	0.20	0.34	0.32	0.20	0.14
COI	28.63	29.50	29.13	22.94	24.00	31.92	33.10	34.13	31.37
COJ	28.63	29.50	29.13	22.94	24.00	31.92	33.10	34.13	31.37
BOI	0.00	0.00	0.00	0.00	0.00	0.00	0.00	0.00	0.00
BOJ	534.65	543.25	556.81	475.57	512.15	431.21	470.54	450.12	454.49
6									
AAI	294.42	377.85	302.93	225.01	195.72	195.72	200.95	204.49	211.52
AAJ	294.42	377.85	302.93	225.01	195.72	195.72	200.95	204.49	211.52
COI	45.62	54.72	36.37	21.81	23.74	23.12	24.22	25.82	21.26
COJ	45.62	54.72	36.37	21.81	23.74	23.12	24.22	25.82	21.26
BOI	534.05	563.75	511.71	325.27	312.12	234.29	270.54	250.12	254.29
BOJ	1202.25	1453.08	926.74	632.57	606.40	619.05	612.28	607.74	630.10

PAGE.

73

PAGE.

11



CONTINUACION TABLA 2

7	AXI	292.09	370.69	293.01	310.42	189.75	195.18	200.85	206.62	211.49
	AXJ	292.09	370.69	293.01	310.42	189.75	195.18	200.85	206.62	211.49
	COI	51.38	62.30	42.46	73.90	75.19	77.34	78.29	79.35	40.27
	COJ	51.38	62.30	42.46	73.90	75.19	77.34	78.29	79.35	40.27
	NOI	1005.25	1458.08	905.74	842.53	890.49	949.05	917.28	907.76	930.18
	NOJ	2167.46	2637.71	1780.09	1474.30	1550.56	1611.37	1713.42	1641.72	1693.44
6	AXI	300.31	397.58	311.71	219.75	192.43	204.54	213.57	220.61	226.76
	AXJ	300.31	397.58	311.71	219.75	192.43	204.54	213.57	220.61	226.76
	COI	106.85	262.93	101.73	143.92	121.53	118.95	106.39	107.19	109.91
	COJ	106.85	262.93	101.73	143.92	121.53	118.95	106.39	107.19	109.91
	NOI	4950.55	5801.73	4149.09	3328.09	3473.93	3475.14	3427.57	3460.01	3517.59
	NOJ	5113.16	5801.14	4909.06	3485.05	2419.59	1971.33	1701.05	1554.10	1447.09
9. PAGE	AXI	310.58	401.75	316.53	222.04	191.52	203.71	212.52	219.53	225.69
	AXJ	310.58	401.75	316.53	222.04	191.52	203.71	212.52	219.53	225.69
	COI	197.71	279.07	197.61	175.94	171.65	171.54	112.49	104.89	110.92
	COJ	197.71	279.07	197.61	175.94	171.65	171.54	112.49	104.89	110.92
	NOI	4113.16	5801.14	4909.06	3485.05	2419.59	1971.33	1701.05	1554.10	1447.09
	NOJ	6057.77	9110.33	7461.52	5054.99	3403.00	2889.09	1611.55	779.81	534.21
10	AXI	353.43	438.05	294.31	236.61	243.10	251.73	262.38	273.16	283.44
	AXJ	353.43	438.05	294.31	236.61	243.10	251.73	262.38	273.16	283.44
	COI	45.04	40.66	49.00	55.76	24.32	22.30	22.25	22.89	23.63
	COJ	45.04	60.66	49.40	34.74	24.17	22.30	22.25	22.89	23.63
	NOI	1907.19	2440.95	1080.56	1400.09	1750.24	1143.36	1193.90	1219.02	1253.49
	NOJ	1450.60	1977.89	1699.06	1277.28	715.55	426.10	390.06	382.79	400.26
11	AXI	158.55	200.14	135.64	113.09	104.24	90.51	114.29	142.26	155.30
	AXJ	158.55	200.14	135.64	113.09	104.24	90.51	114.29	142.26	155.30
	COI	18.15	25.34	21.96	17.50	10.04	6.09	3.95	1.67	1.09
	COJ	18.15	25.34	21.96	17.50	10.04	6.09	3.95	1.67	1.09
	NOI	1450.60	1977.89	1699.06	1277.28	714.25	426.10	390.06	382.79	400.26
	NOJ	1496.59	2030.24	1699.07	1477.00	1030.34	751.40	447.44	585.72	550.05
	OR8	200.62	301.69	203.27	220.40	194.54	190.75	180.53	192.07	194.03
	OR9	220.55	335.69	220.45	197.42	189.20	200.04	220.62	271.10	239.26

74

PAGE.

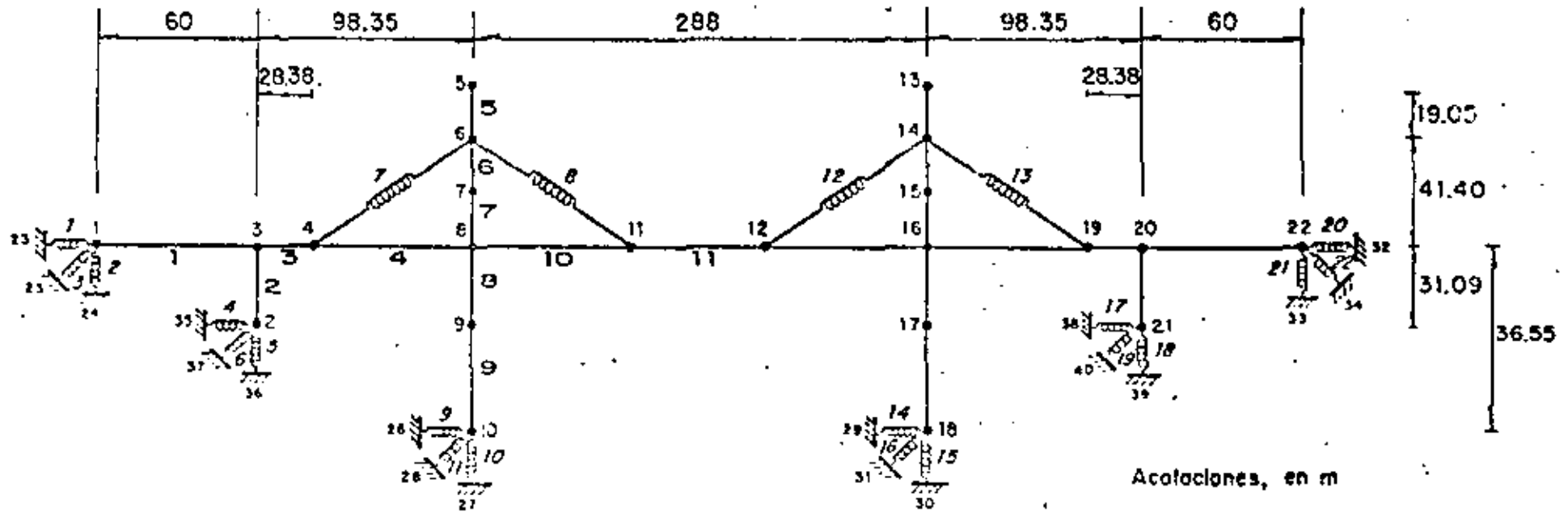


Fig 1. Modelo simplificado. Puente Coatzacoalcos II

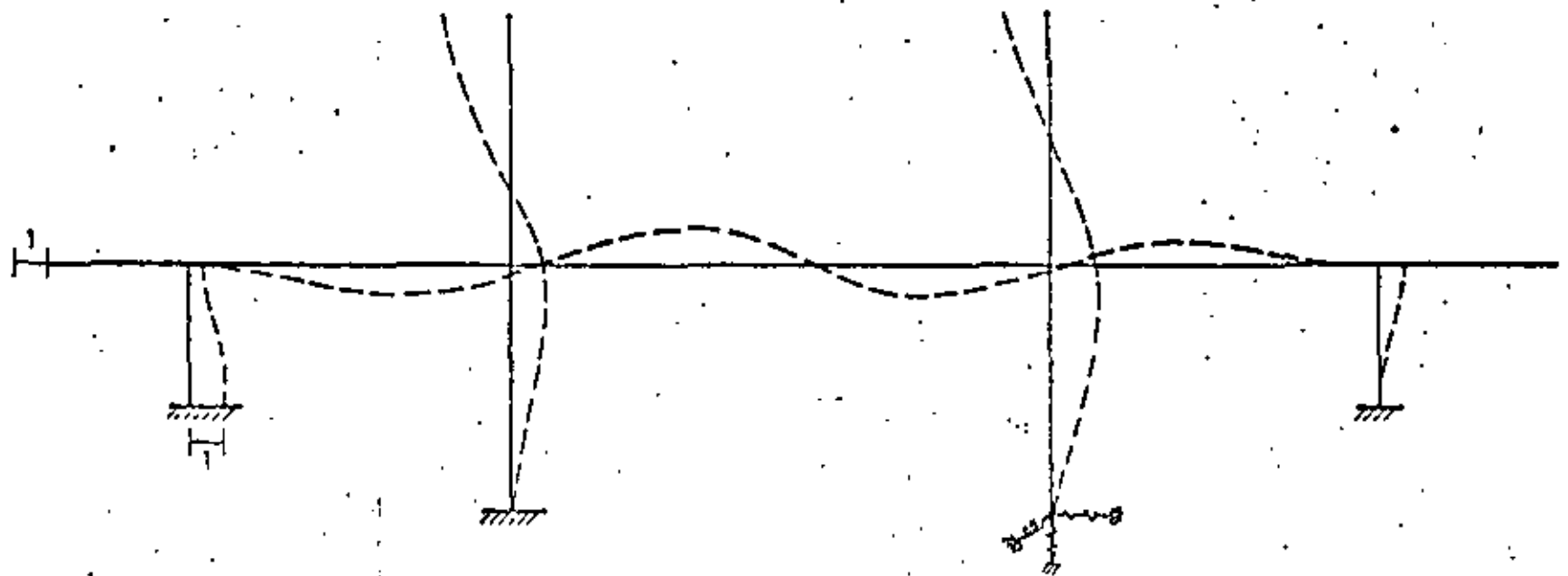


Fig 2. Configuración debida a desplazamiento horizontal unitario dado en los apoyos 1 y 2

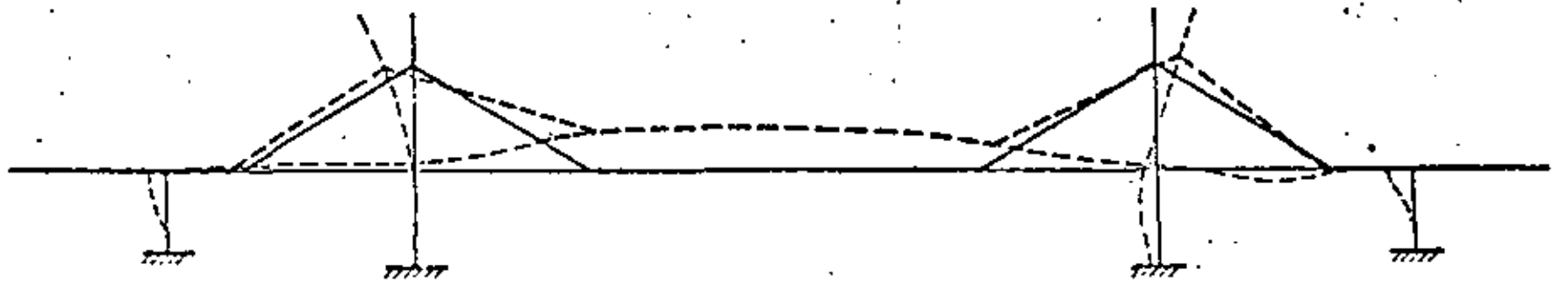


Fig 3. Configuración del modo 1



Fig 4. Configuración del modo 2

1.4

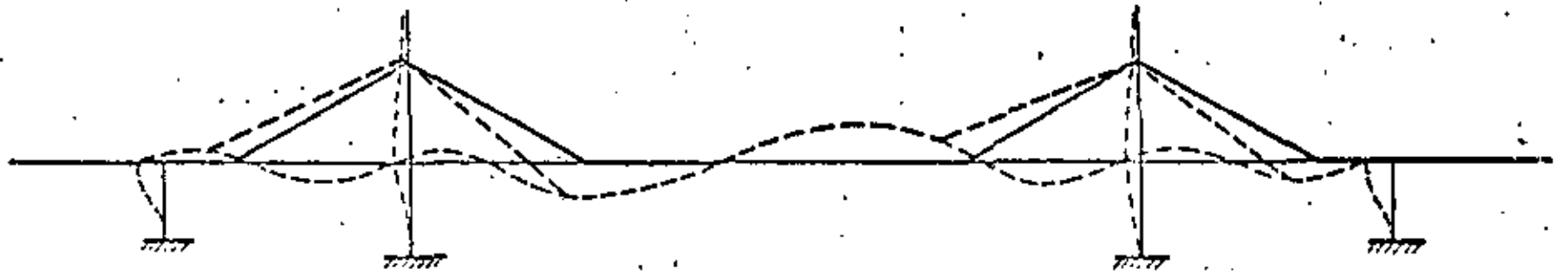


Fig 5. Configuración del modo 3

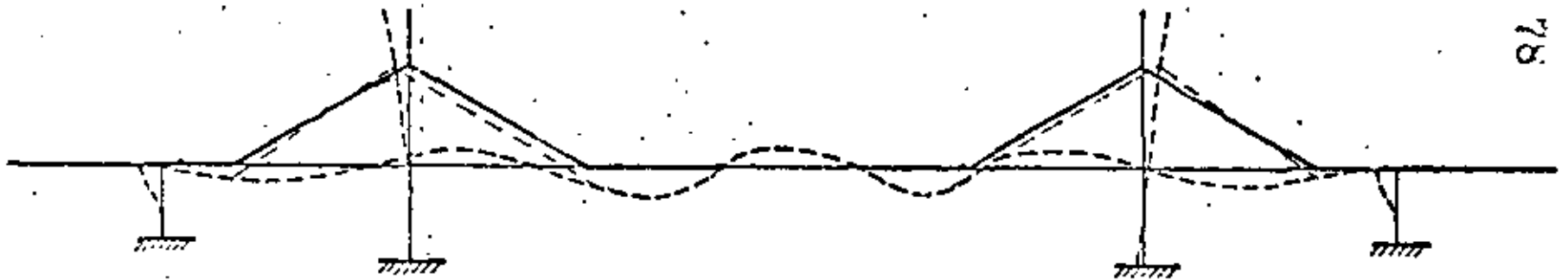


Fig 6. Configuración del modo 4

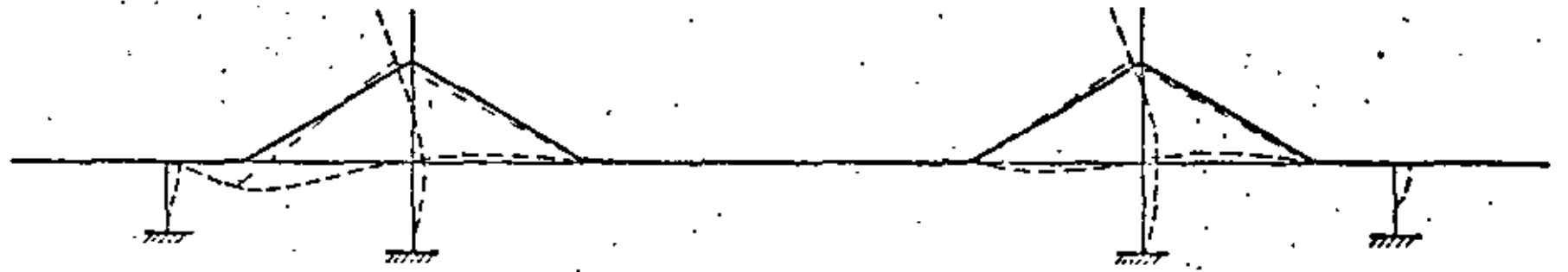


Fig 7. Configuración del modo 5

INFLUENCIA DE LA RESPUESTA SISMICA DEL  
PUENTE COATZACOALCOS II DE LAS DIFERENCIAS  
DE FASE EN LOS MOVIMIENTOS DE SUS APOYOS

SEGUNDA PARTE

INFLUENCIA DE LA RESPUESTA NO LINEAL

L. Esteva\*  
D. de León\*\*

Elaborado para  
DIRECCION FEDERAL DE CARRETERAS FEDERALES  
SECRETARIA DE ASENTAMIENTOS HUMANOS Y  
OBRAS PUBLICAS

Proy 0754

DICIEMBRE 1980

\* Investigador, Instituto de Ingeniería, UNAM  
\*\* Becario, Instituto de Ingeniería, UNAM

INFLUENCIA DE LA RESPUESTA SISMICA DEL PUENTE COATZACOALCOS II  
DE LAS DIFERENCIAS DE FASE EN LOS MOVIMIENTOS DE SUS APOYOS

SEGUNDA PARTE  
INFLUENCIA DE LA RESPUESTA NO LINEAL

L. Esteva y D. de León

Antecedentes

En diciembre de 1980 el Instituto de Ingeniería entregó a la Secretaría de Asentamientos Humanos y Obras Públicas el informe de un estudio que realizó por su encargo sobre la influencia en la respuesta sísmica del puente Coatzacoálcos II de las diferencias de fase en los movimientos de sus apoyos (1). Los resultados mostraron que para el caso en que se consideran diferencias de fase en la componente vertical del movimiento de los apoyos se encuentran amplificaciones excesivas del momento en el apoyo central izquierdo en relación con el valor de dicho momento para el caso en que los apoyos se ven sometidos a movimiento vertical en fase. En consecuencia, la Secretaría citada solicitó que se revisarían los cálculos y resultados del informe antes mencionado.

Después de una revisión muy detallada y rigurosa de los cálculos se concluyó que estaban correctos y que representaban adecuadamente la respuesta dinámica del puente sujeto a excitaciones fuera de fase en sus apoyos bajo la hipótesis de comportamiento lineal. Se concluyó que dadas las características del sistema y de la excitación era indispensable obtener las fuerzas de diseño a partir de un análisis que considerara abiertamente el comportamiento no lineal de la estructura. Aquí se presentan los resultados de un análisis aproximado que incluye este concepto.

Respuesta no lineal de sistemas sujetos a movimientos fuera de fase en sus apoyos.

El diseño sísmico de estructuras considera que ante temblores intensos dichas estructuras responderán haciendo uso de su capacidad de disipar energía mediante comportamiento inelástico. Esto permite reducir los espectros de diseño teniendo en cuenta los factores de ductilidad que se consideran aceptables para cada tipo de estructura. Si los apoyos no se mueven en fase, no basta con reducir los espectros de diseño: es necesario reducir las rigideces de los miembros estructurales a fin de estimar con la misma aproximación y bajo un criterio unificado la parte de la respuesta que se debe al movimiento de los apoyos como si actuaran en fase y la que se debe a las diferencias de fase. Para ello se propuso el criterio de análisis que se describe a continuación.

Del estudio de la respuesta dinámica de sistemas con curva carga-deformación elasto-plástica se ha deducido el criterio para reducir los espectros de diseño en términos de la ductilidad que se emplea para las estructuras convencionales: en el intervalo de periodos naturales moderados y largos se reducen las ordenadas del espectro elástico dividiéndolas entre el factor de ductilidad  $Q$ , y para periodos cortos se impone la condición de que para  $T = 0$  la ordenada del espectro de aceleraciones es igual a la aceleración máxima del terreno,  $a_0$ , independientemente del factor de ductilidad o del amortiguamiento. El espectro así obtenido es el que en la fig 1 se designa como espectro reducido por ductilidad: para emplearlo se entra con los periodos naturales de las estructuras calculados en función de las rigideces elásticas iniciales de todos sus miembros.

Para nuestros fines es necesario trabajar con un sistema equivalente con rigideces reducidas en forma inversamente proporcional a la rigidez tolerable (2). Los resultados de este análisis son congruentes con el criterio convencional del espectro elasto-plástico si se desarrolla un nuevo espectro, que en la fig se designa como espectro para sistema equivalente y que es igual al espectro reducido por ductilidad excepto porque la escala horizontal está transformada de manera que los periodos están multiplicados por  $\sqrt{Q}$ . A este espectro se entra con los periodos naturales equivalentes del sistema no lineal, que se obtienen tomando en cuenta las rigideces del sistema equivalente, es decir, las elásticas iniciales divididas entre el factor de ductilidad.

#### Resultados y conclusiones

Los resultados de analizar el sistema equivalente para  $Q = 4$  con los criterios descritos en el informe de diciembre de 1980 se muestran en la fig 2. En ella se observa que los factores de amplificación de la respuesta para excitación fuera de fase con respecto a la que se tiene en fase no exceden de 2 en las secciones de esfuerzos más elevados, aunque se encuentran valores mayores en zonas de esfuerzos pequeños o casi nulos. Los factores de amplificación de esta figura se consideran adecuados para diseño sísmico del puente bajo la hipótesis que es aceptable una ductilidad de 4.

## REFERENCIAS

1. Rufz, S.E., Esteva, L. y de León D. "Influencia de la respuesta sísmica del puente Coatzacoalcos II de las diferencias de fase en los movimientos de sus apoyos", Informe a SAHOP, Instituto de Ingeniería (diciembre, 1980).
2. Shibata, A., y Sozen, M.A., "The substitute structure method for seismic design in reinforced concrete", Journal ASCE, Vol. 102, No ST1 (enero, 1976).

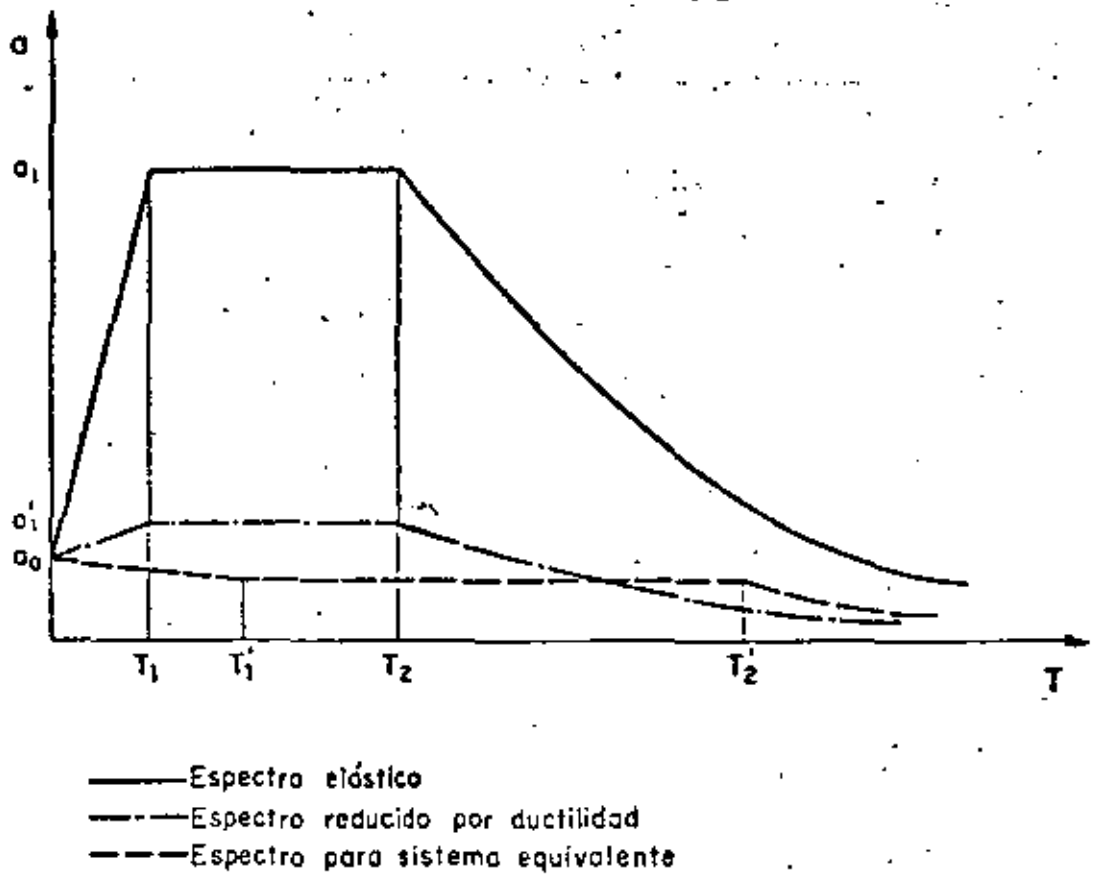
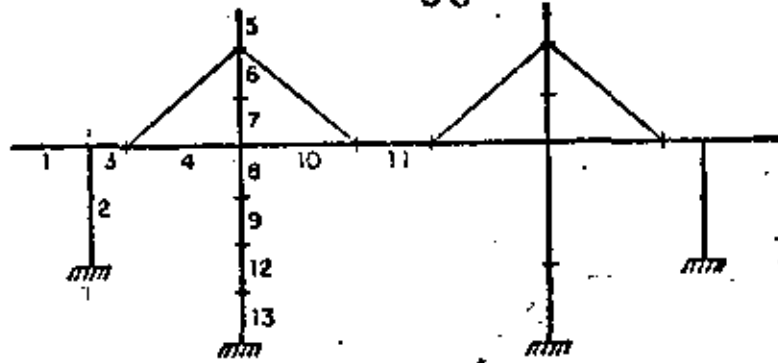


Fig 1. Espectros para diseño de estructuras inelásticas



$$1 \begin{cases} 3.49 & 1.06 \\ 24.19 & 1.25 \\ 419.00 & 1.25 \\ 1032.00 & 1.25 \end{cases}$$

$$2 \begin{cases} 166.7 & 1.35 \\ 52.2 & 1.70 \\ 1077.0 & 1.58 \\ 546.0 & 1.95 \end{cases}$$

$$3 \begin{cases} 58.46 & 1.27 \\ 142.20 & 1.37 \\ 2108.90 & 1.41 \\ 1927.20 & 1.32 \end{cases}$$

$$4 \begin{cases} 294.7 & 0.91 \\ 45.5 & 1.28 \\ 1927.0 & 1.32 \\ 1257.0 & 1.23 \end{cases}$$

$$5 \begin{cases} 1.12 & 0.78 \\ 54.20 & 0.89 \\ 0 & 0 \\ 1032.00 & 0.89 \end{cases}$$

$$6 \begin{cases} 396.0 & 0.90 \\ 35.7 & 0.80 \\ 1032.0 & 0.89 \\ 703.0 & 1.11 \end{cases}$$

$$7 \begin{cases} 398.0 & 0.90 \\ 39.8 & 0.99 \\ 703.0 & 1.11 \\ 1170.0 & 1.15 \end{cases}$$

$$8 \begin{cases} 405.0 & 0.85 \\ 101.0 & 4.70 \\ 2858.0 & 1.26 \\ 2244.0 & 1.31 \end{cases}$$

$$9 \begin{cases} 416.0 & 0.86 \\ 85.0 & 4.19 \\ 2244.0 & 1.31 \\ 1407.0 & 2.19 \end{cases}$$

$$10 \begin{cases} 399.0 & 0.93 \\ 13.0 & 1.62 \\ 683.0 & 1.30 \\ 246.0 & 2.57 \end{cases}$$

$$11 \begin{cases} 109.00 & 1.04 \\ 0.38 & 23.50 \\ 246.00 & 2.57 \\ 301.00 & 2.80 \end{cases}$$

$$12 \begin{cases} 407.0 & 0.85 \\ 103.0 & 1.10 \\ 1293.0 & 1.37 \\ 260.0 & 4.07 \end{cases}$$

$$13 \begin{cases} 392.0 & 0.85 \\ 331.0 & 1.55 \\ 990.0 & 1.12 \\ 2500.0 & 1.58 \end{cases}$$

Fig. 2. Fuerzas internas y factores de amplificación



**DIVISION DE EDUCACION CONTINUA  
FACULTAD DE INGENIERIA U.N.A.M.**

VII CURSO INTERNACIONAL DE INGENIERIA SISMICA

DISEÑO SISMICO DE ESTRUCTURAS ESPECIALES

ESTRUCTURAS DE CONCRETO PRESFORZADO

Profesor: Ing José Luis Camba Castañeda

Julio, 1981

## DISEÑO SISMICO DE EDIFICIOS DE CONCRETO PREFORZADO.

- 1.- Comportamiento de trabes en flexión.
- 2.- Ductilidad de miembros de concreto presforzado.
- 3.- Conexiones tipo en concreto presforzado.
- 4.- Reglamentos.
- 5.- Ejemplos.

José Luis Camba Castañeda.

## INTRODUCCION.

La aplicación del presfuerzo en estructuras de concreto - ha tenido un incremento importante en los últimos años, debido a las ventajas que presenta sobre el concreto reforzado - principalmente en lo referente a escuadrías, a un mejor control de las deformaciones y el agrietamiento en el estado límite de servicio, bajo el efecto de cargas gravitacionales.

Sin embargo, la utilización del concreto presforzado para resistir efectos sísmicos es menos aceptada. Esto se debe principalmente a que se tiene poca información al respecto y a que comparativamente, con estructuras de concreto reforzado se observa cierto temor debido a que el primero tiene menor capacidad para disipar energía y por tratarse de un material - menos dúctil que el concreto reforzado. En las presentes notas se comentan algunos detalles del comportamiento de miembros - presforzados bajo cargas monotónicas y dinámicas, así como el detalle de conexiones y algunos lineamientos de reglamentos de construcción referentes al concreto presforzado.

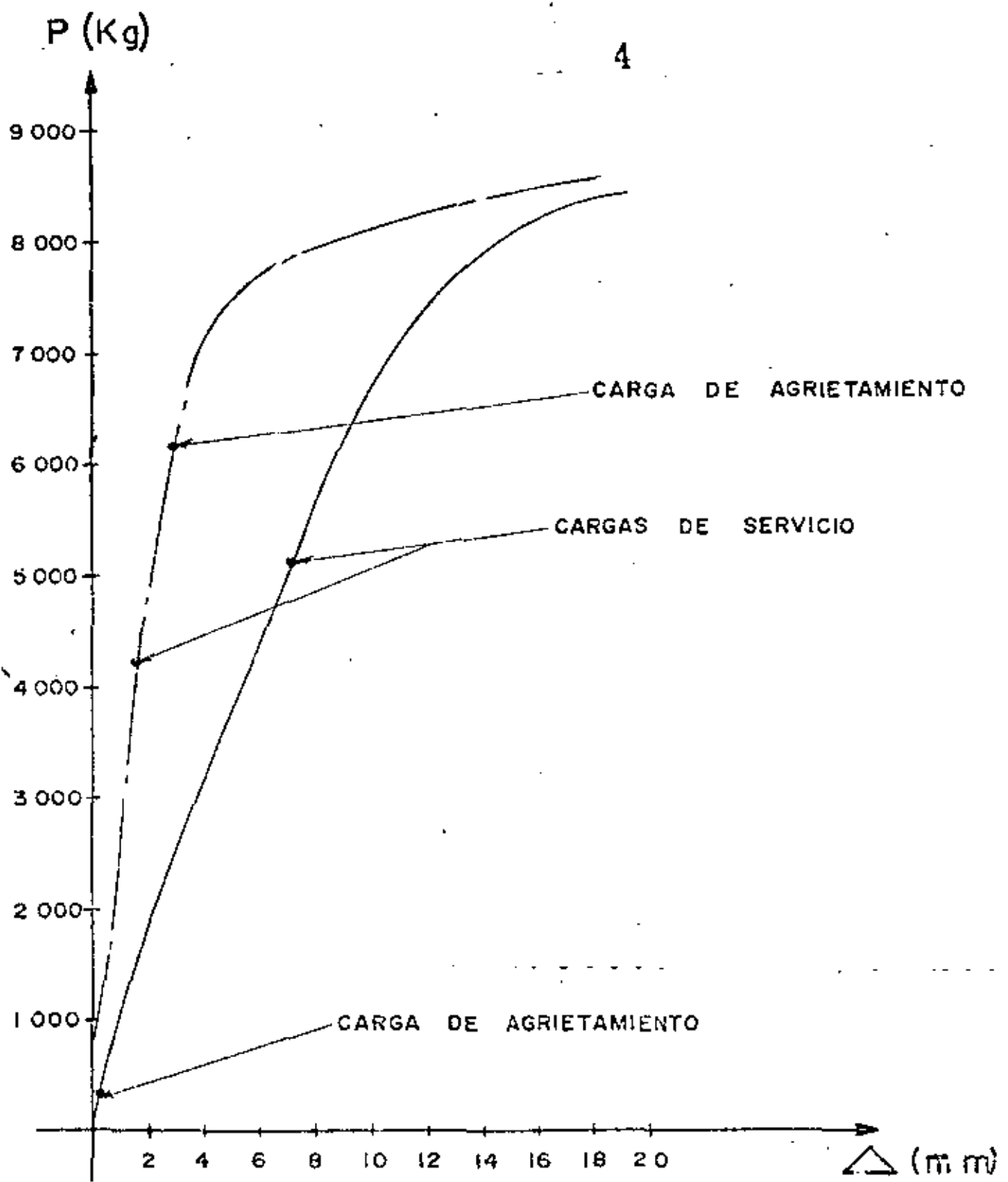
## 1.- COMPORTAMIENTO DE TRABES PREESFORZAS EN FLEXION.

1.1 Concepto acción respuesta.

1.2 Diagramas carga-deflexión.

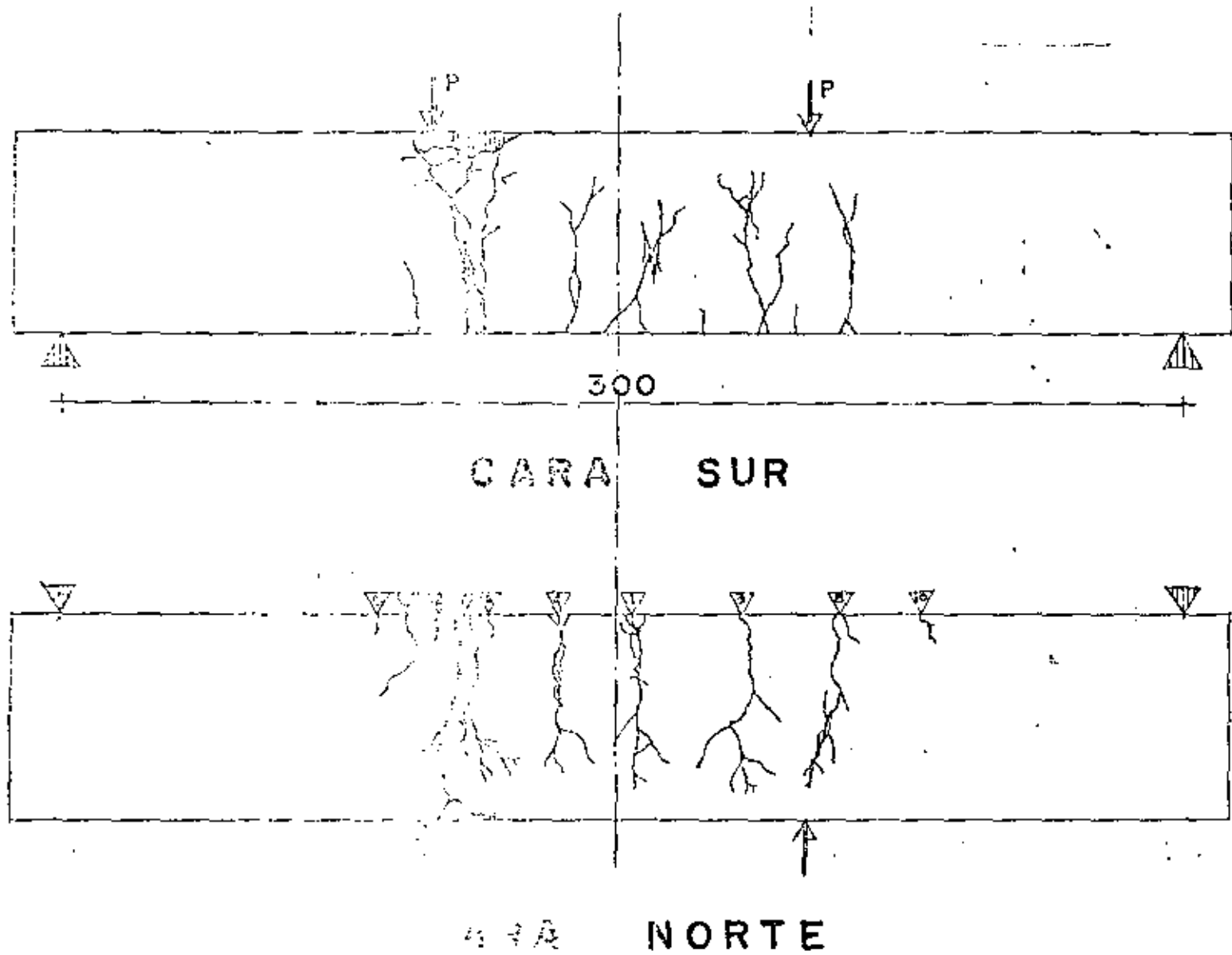
1.3 Variables que intervienen en el comportamiento de trabes-presforzadas.

1.4 Estado límite de Palla.

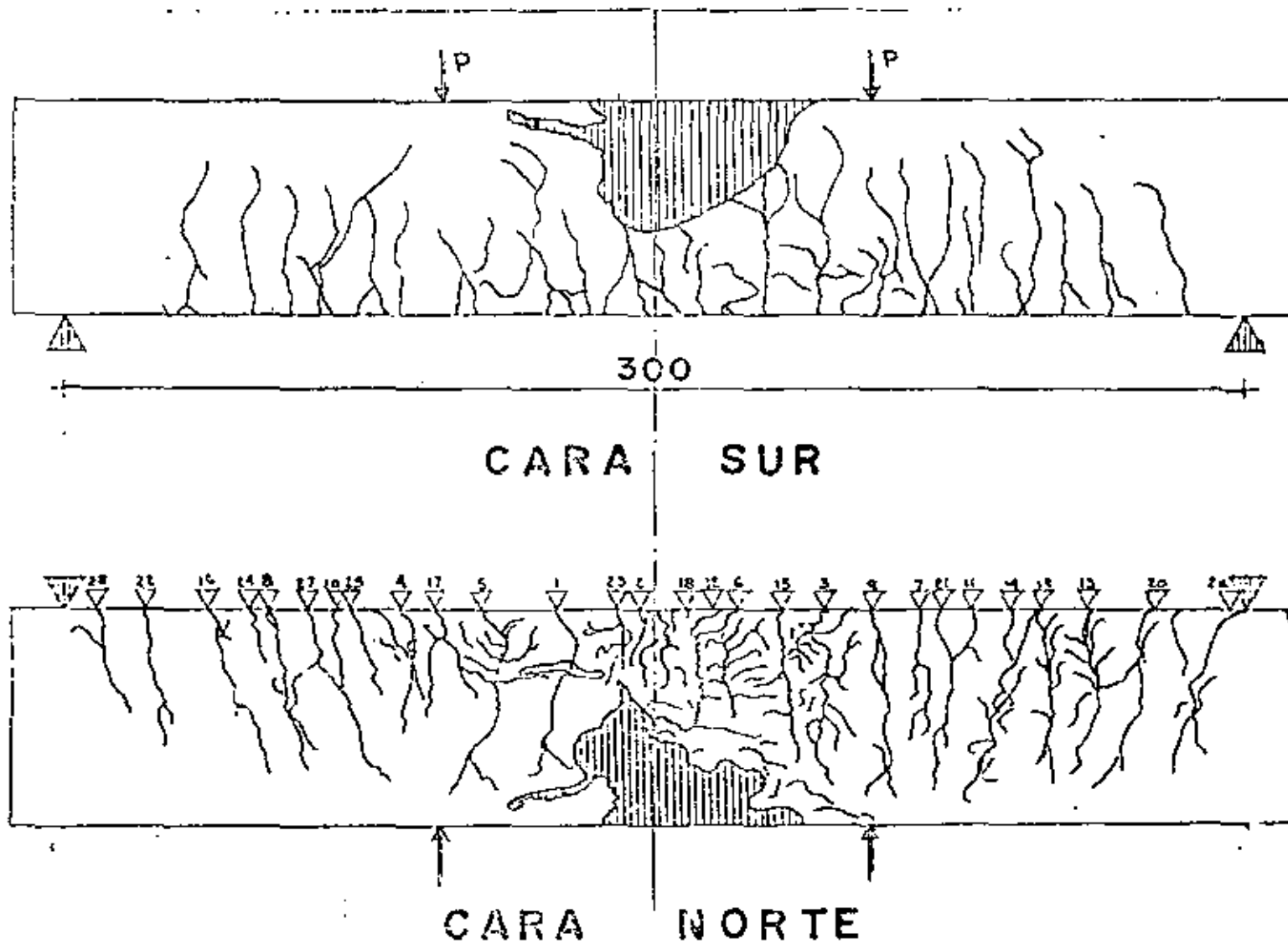


————— TRABE DE CONCRETO REFORZADO  
- - - - - TRABE DE CONCRETO PRESFORZADO

# AGRIETAMIENTO TRABE DE CONCRETO PRESFORZADO



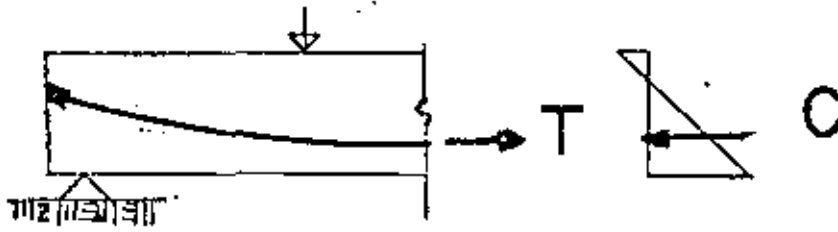
# AGRIETAMIENTO TRABE DE CONCRETO REFORZADO



# ESTADO LIMITE DE FALLA

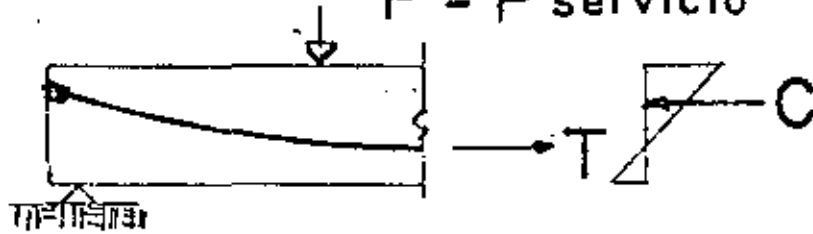
b).- Presfuerzo  
elemente

$$P = 0$$



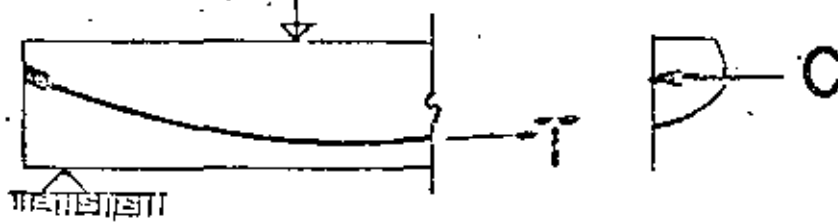
c).- En servicio

$$P = P_{\text{servicio}}$$



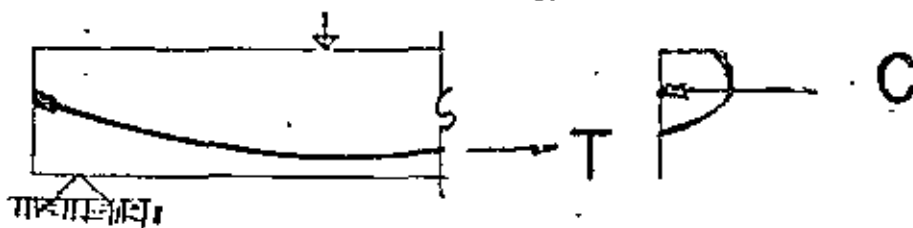
d).- Al presentarse el agrietamiento

$$P > P_{\text{servicio}}$$

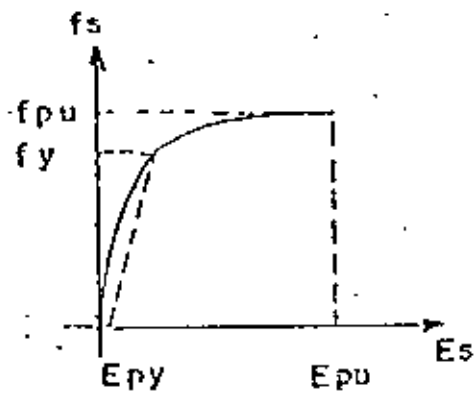


e).- En la falla

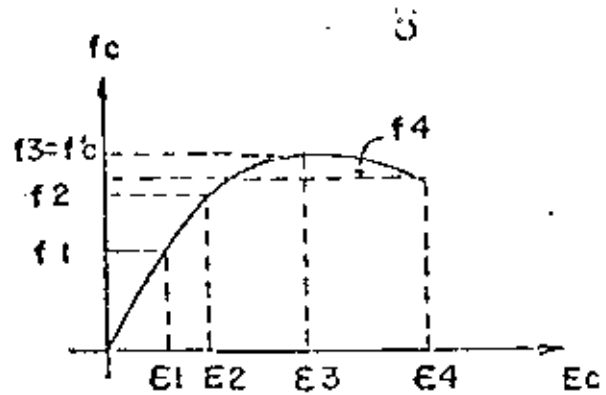
$$P = P_u$$



# ESTADO LIMITE DE FALLA

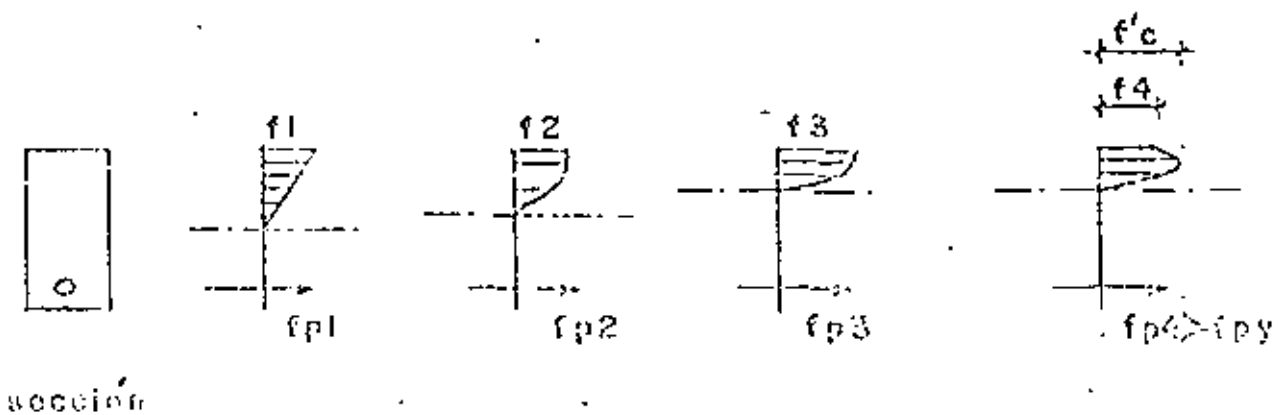


Acero de pretensado

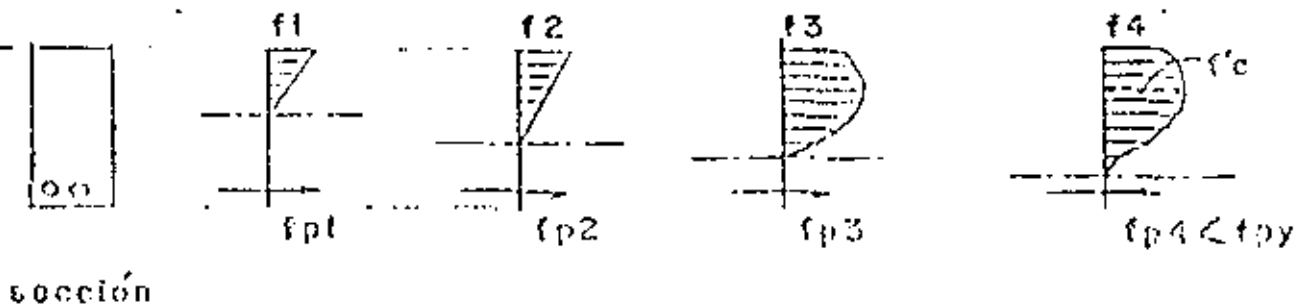


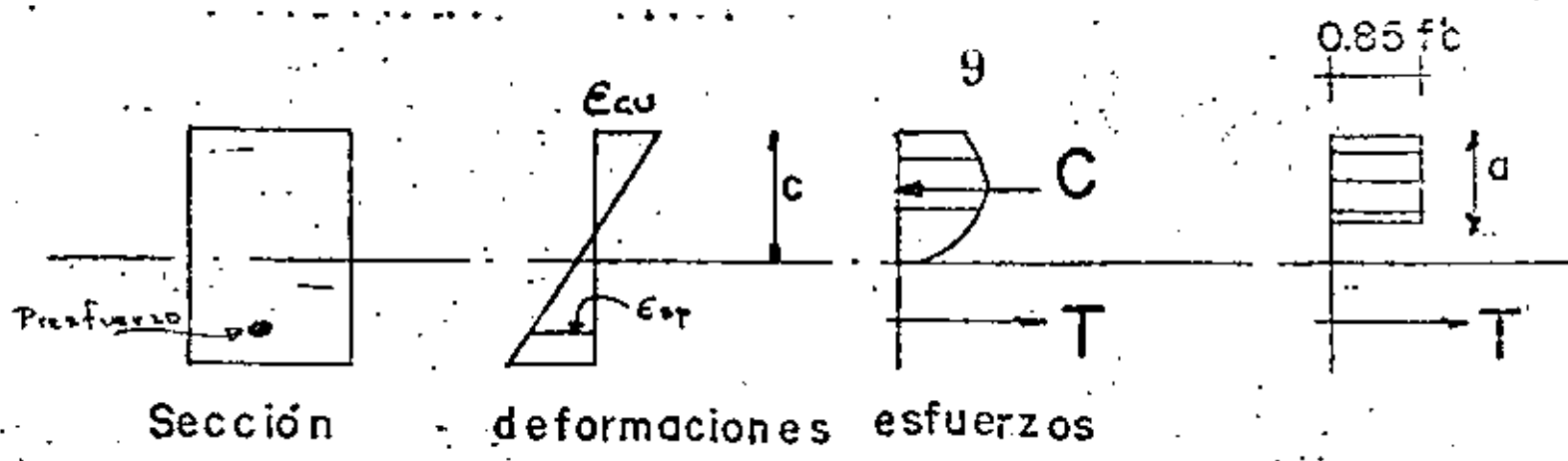
Concreto

## a) Trabe subreforzada



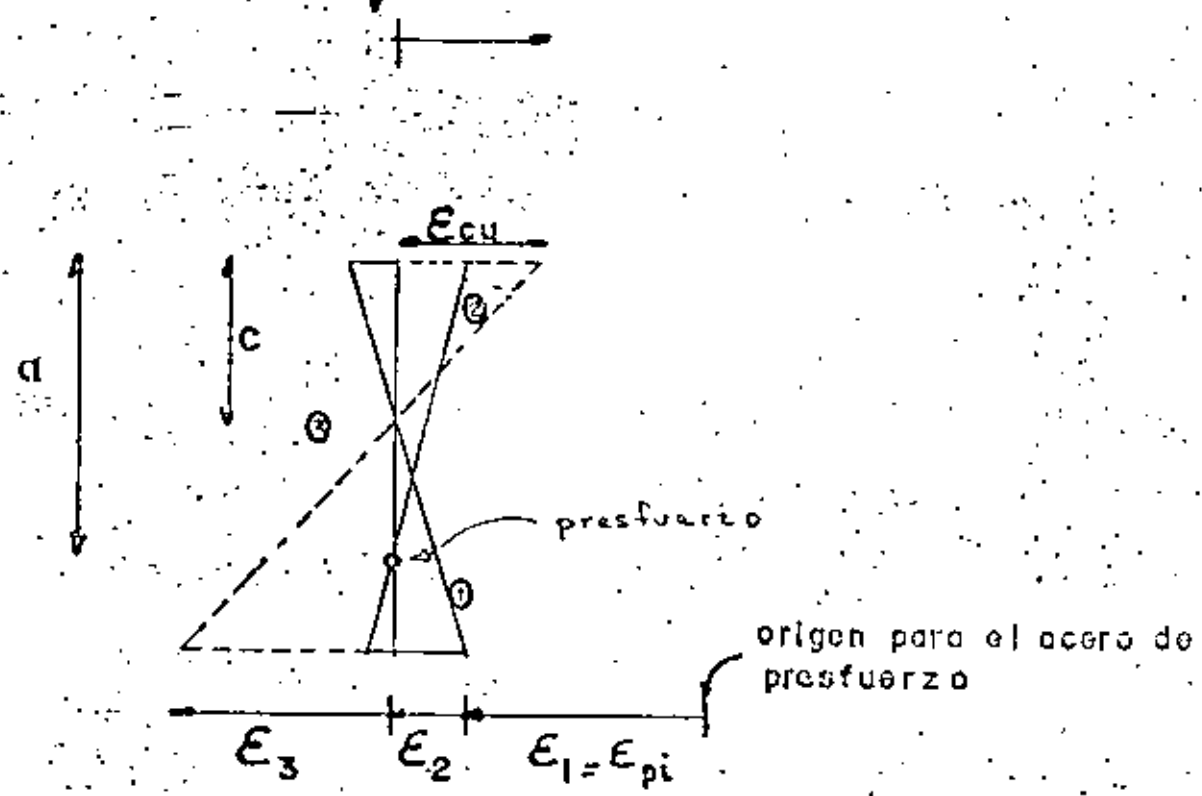
## b) Trabe sobrerreforzada





a).- Hipótesis

origen para el concreto



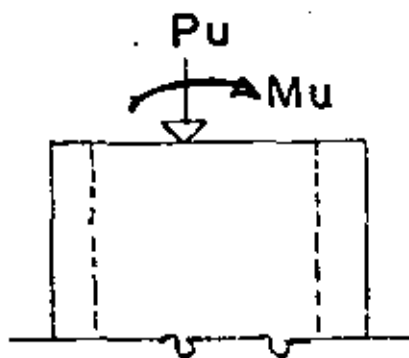
b).- Diagrama de deformaciones

# COLUMNAS PRESTFORZADAS

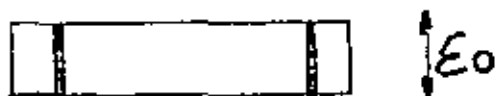
a).- Sección



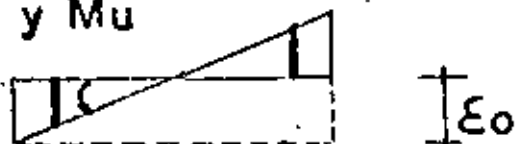
b).- Elevación.



c).- Deformaciones bajo carga axial uniforme



d).- Deformaciones bajo Pu y Mu



e).- Deformaciones debidas a momento únicamente

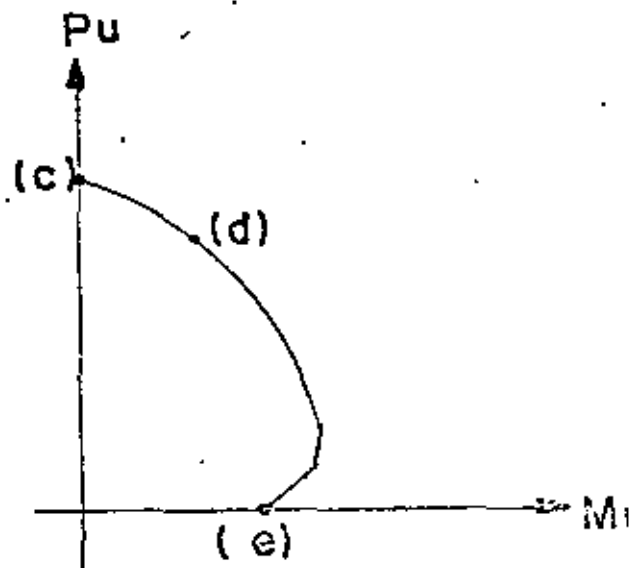
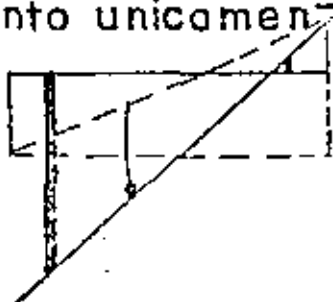


Diagrama típico de interacción

## 2.- DUCTILIDAD DE MIEMBROS DE CONCRETO PRESFORZADO.

2.1 Resumen histórico.

2.2 Análisis de miembros presforzados en flexión.

2.3 Amortiguamiento.

## DUCTILIDAD DE MIEMBROS DE CONCRETO PREFORZADO.

Resumen histórico de estudios realizados. Es conocido que un análisis dinámico de la respuesta elástica de estructuras usando aceleraciones sísmicas, ponen de manifiesto que una estructura puede estar sujeta a cargas mayores que las especificadas por reglamentos, lo cual implica que una estructura debe ser capaz de desarrollar grandes deformaciones antes de llegar a la falla en caso de sismos severos. Por tanto, es importante conocer la ductilidad que puede obtenerse en miembros de concreto preforzado.

La relación momento-curvatura para concreto preforzado bajo cargas monotónicas y cíclicas, permite comprender la ductilidad y la energía de disipación.

T.Y. Lin (1) presentó algunos aspectos importantes para el diseño sísmico de estructuras preforzadas, referentes a los factores de carga y esfuerzos permisibles así como algunos ensayos estudiando la capacidad de absorber energía, concluyendo Lin en su artículo en que los diagramas Momento-Curvatura en vigas de concreto preforzado en flexión se presentaban áreas importantes

que mostraban alta capacidad para absorber energía.

Rosenblueth (2) comentando el artículo de Lin, enfatizaba el inconveniente de establecer conclusiones basadas en la curva de primera carga, indicando la importancia de las curvas idealizadas carga-deformación en la descarga Fig.1, para miembros de concreto presforzado y miembros de concreto reforzado presentaban que para masas y rigideces comparables una estructura de concreto presforzado tendría probablemente mayores deformaciones debido a su baja capacidad de amortiguamiento que una de concreto reforzado y que así mismo sería más flexible la primera, lo cual contrarrestaría en parte el efecto de su baja capacidad para absorber energía.

Despeyroux (3) concluye que las áreas bajo el diagrama Momento-Curvatura en concreto presforzado y reforzado son comparables y no necesariamente menores las de concreto presforzado, pero que un factor importante que afecta la respuesta sísmica de estructura es su capacidad para disipar energía, En su artículo, de acuerdo con la Fig.2 concluye que la energía absorbida es efectivamente comparable en miembros de concreto presforzado y reforzado pero que la energía disipada es bastante menor en los miembros de concreto presforzado, lo cual representará que la respuesta en estos últimos bajo el sismo será mayor.

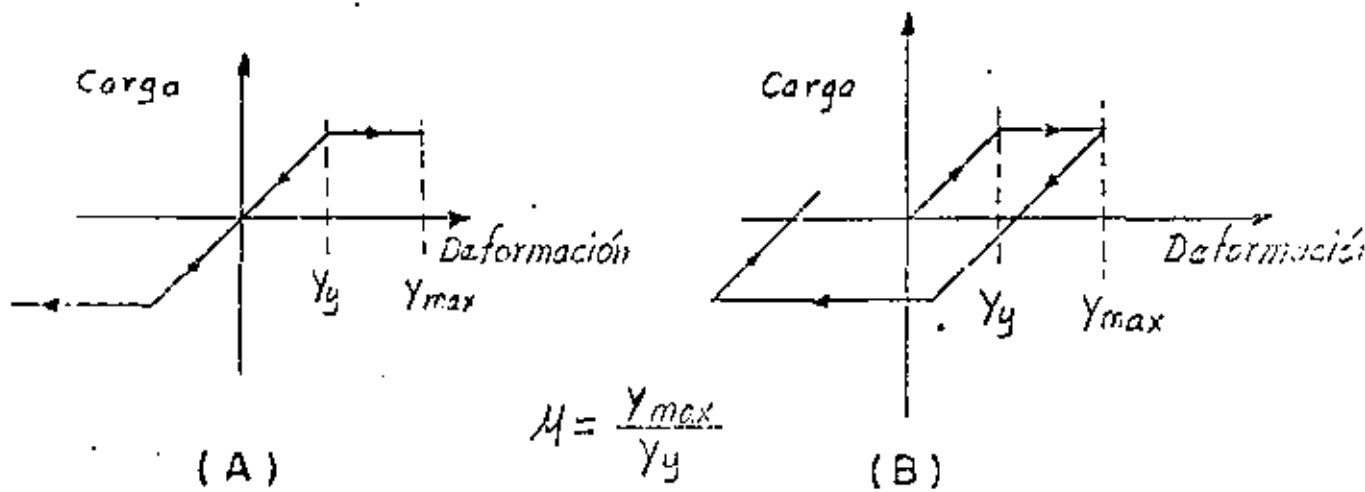


Fig. 1 Idealización de curvas típicas carga-deformación

A) concreto presforzado

B) concreto reforzado

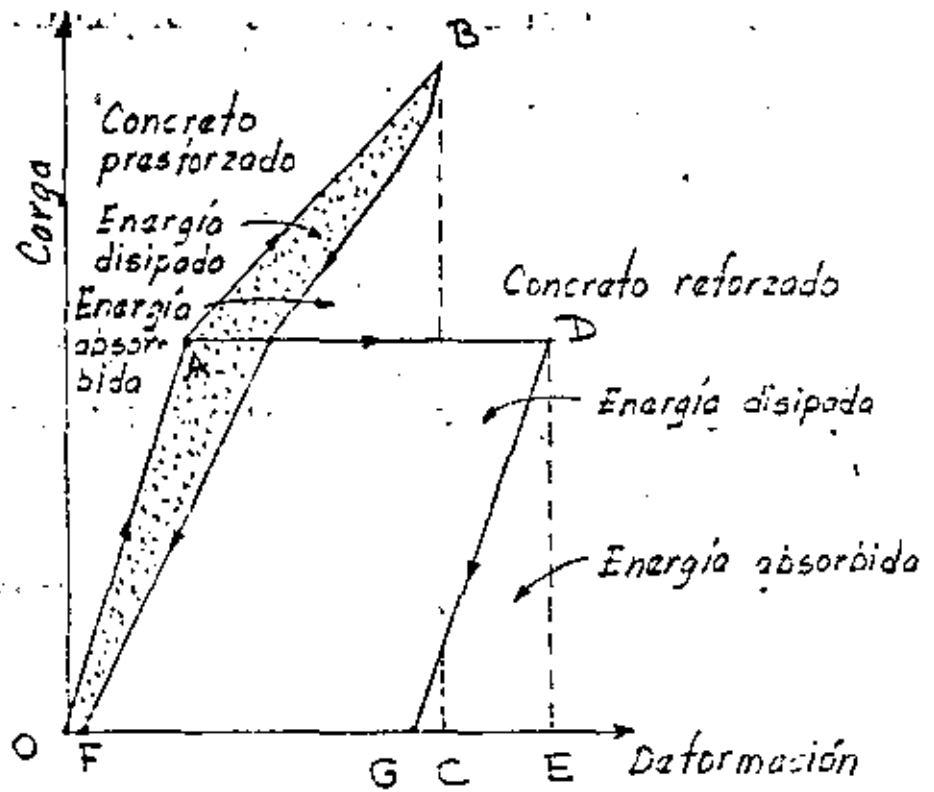


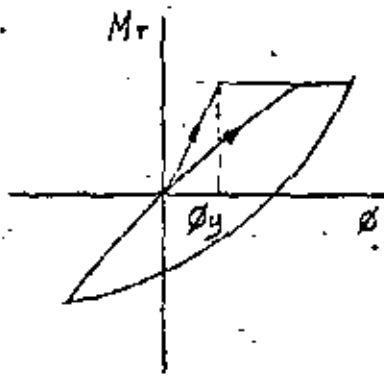
Fig. 2 Idealización de curvas típicas de disipación de energía.

Un estudio reciente realizado por Blakeley (4) sobre la respuesta dinámica no lineal de sistemas de concreto presforzado - concluyó que el desplazamiento máximo obtenido es del orden de - 40% mayor que el de un sistema de concreto reforzado con misma - resistencia, rigidez inicial y mismo porcentaje de amortiguamiento viscoso.

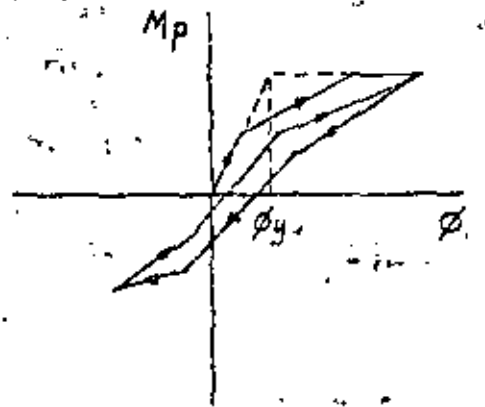
Thompson (5) hizo un estudio comparando las respuestas de - miembros presforzados, parcialmente presforzados y reforzados - bajo diversos movimientos sísmicos, idealizando los diagramas - Momento-Curvatura como lo indica la Fig. 3 y tomando los registros del sismo de El Centro 1940, N-3.

El factor de ductilidad se define como la relación que existe entre el desplazamiento en la falla y el desplazamiento correspondiente a la primera fluencia. Thompson encontró que para pequeños períodos el factor de ductilidad era mayor y que la tendencia a disminuir el desplazamiento se debía a un incremento en el acero de presfuerzo.

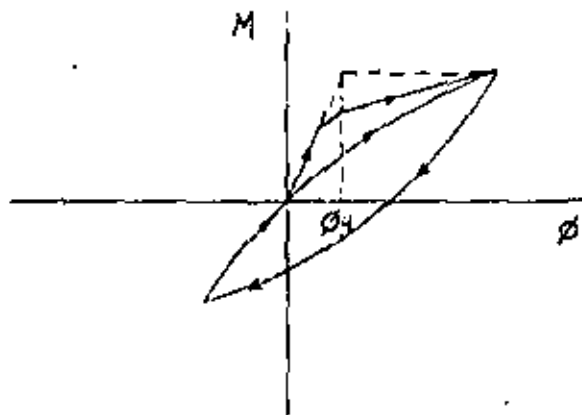
Análisis de miembros presforzados en flexión. Los estudios realizados por Blakeley (4) para determinar las relaciones Momento-Curvatura bajo carga monotónica, demostraron que la curva ob-



a) *Concreto reforzado*



b) *Concreto pretorzado*



c) *Concreto parcialmente pretorzado*

Fig. 3 Diagramas idealizados de Momento Curvatura

tenida para este tipo de carga es colineal con la curva envolvente de cargas cíclicas en miembros de concreto presforzado y que por lo tanto este análisis puede efectuarse para el estudio de la ductilidad bajo cargas sísmicas.

Se realizaron ensayos para obtener diagramas Momento-Curvatura en trabes haciendo variar el valor de la fuerza de presfuerzo, las posiciones del mismo en la sección y la cantidad de refuerzo transversal.

Asimismo, Thompson (5) realizó ensayos en uniones presforzadas viga-columna, reforzando el núcleo de acuerdo con las especificaciones de cortante del ACI 318-71. Las columnas se diseñaron de tal forma que tuvieran una mayor resistencia que las vigas y los ensayos se hicieron con carga cíclica estática simulando la carga sísmica.

Los resultados obtenidos por los estudios mencionados (4) y (5) se resumen a continuación:

a) Porcentaje del acero de presfuerzo.

El efecto de la variación de la relación área presfuerzo a concreto,  $p = A_s/bh$ , se muestra en la Fig. 4. La forma de las curvas indican claramente que a un incremento de capacidad de momento corresponde una disminución de ductilidad. El --

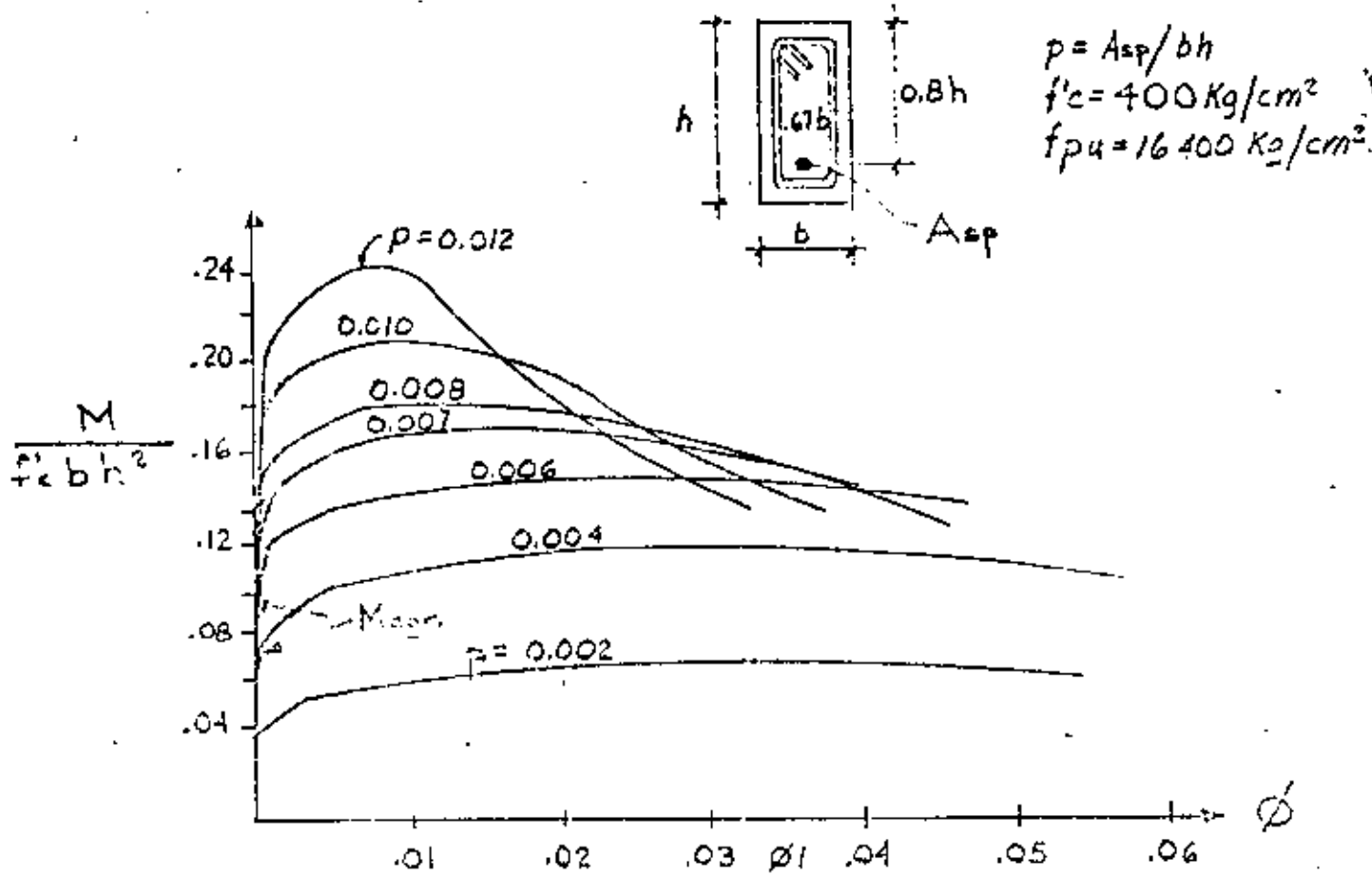


Fig. 4 Relaciones momento-curvatura para una sección con diferentes cantidades de presfuerzo excéntrico

ACI 318-71, especifica que la máxima cantidad de acero de presfuerzo que debe tener una trabe para prevenir una falla frágil es:

$$\frac{f_s A_s}{b d f'_c} \leq 0.3 \quad (1)$$

Este límite corresponde a  $p = 0.0069$ . El estudio de las curvas de la Fig. 4 indica que para asegurar una ductilidad razonable en diseño sísmico, Blakeley y Thompson recomiendan disminuir la expresión anterior a 0.2, lo cual conduciría a  $p = 0.0043$ . La ecuación (1) significa que la máxima fuerza de tensión es  $0.21 f'_c b d$ , lo cual implica que en el bloque de esfuerzos en una sección rectangular se tendrá:

$$a = \frac{0.2 f'_c b d}{0.85 f'_c b} = 0.235 d$$

y si  $d = 0.85t$ , la condición queda como:

$$a \leq 0.20t$$

## b) Distribución del acero de presfuerzo.

En una sección transversal de una trabe se hizo variar el número y la posición en los cables de presfuerzo, permaneciendo constante la fuerza total de presfuerzo,  $p = 0.0069$  -

Así mismo, se observó que si se aumenta el acero de presfuerzo en la zona de compresión, la curvatura no disminuye, debido a que el cable de presfuerzo actúa como acero de compresión en curvaturas grandes. Cuando el acero de presfuerzo se concentra en un solo cable centrado hay una pérdida considerable de capacidad de momento para grandes curvaturas. En cambio solo existe una pequeña diferencia entre dos o más cables. Por tanto, se recomienda que el acero de presfuerzo se distribuya en dos o más posiciones por efecto de ductilidad.

## c) Efecto del refuerzo transversal.

En los ensayos realizados, la cantidad de refuerzo transversal tuvo poco efecto en la ductilidad de trabes, ya que triplicando el número de estribos normalmente especificado se logró un incremento relativamente pequeño en la capacidad de momento.

## d) Ductilidad en columnas de concreto presforzado.

En los ensayos de columnas bajo cargas cíclicas, las curvas experimentales se trazaron para una articulación plástica

directamente sobre la trabe, provocándose así el mecanismo en un marco de un nivel. El diagrama Momento-Curvatura en la columna de concreto presforzado se reduce con un nivel de carga axial y se requiere un refuerzo transversal especial cuando la carga alcanza valores de  $0.1 P_o$ , siendo  $P_o$  la resistencia de la columna con carga axial concéntrica únicamente. Hay poco conocimiento del comportamiento de acero presforzado de miembros a compresión, sin embargo de los estudios realizados se pudo concluir que en las curvas de Momento-Curvaturas, la correspondiente a  $p/f'cbd = 0.12$ , corresponde a la máxima curvatura obtenida en los ensayos.

Amortiguamiento de miembros de concreto presforzado. En la referencia (2), se menciona la relativamente baja capacidad de amortiguamiento en estructuras presforzadas.

Depeyroux (3) hace notar que el amortiguamiento del concreto presforzado es comparable al de las estructuras metálicas, es decir del orden del 3% del crítico. En cambio en concreto reforzado es del orden 10% del crítico. Nakano (5) encontró valores mayores del 7% del crítico para estructuras presforzadas.

Esto significaría que deberán tomarse coeficientes sísmicos mayores para estructuras de concreto presforzado, parti-

ejemplo del orden de 20% mayores que los aplicados al concreto reforzado.

Una investigación reciente de Penzien (7) sobre el amortiguamiento en trabes de concreto presforzado, mostraron que el presfuerzo y la resistencia del concreto tienen efecto sobre el amortiguamiento solo cuando se aproximaba al momento del colapso.

Sin embargo el efecto desfavorable del concreto presforzado referente a su baja capacidad de amortiguamiento que se traduce en desplazamientos mayores, se contrarresta en parte por el hecho de que las estructuras de concreto presforzado debido a sus menores escuadrías que en el concreto reforzado, requieren una reducción en la demanda de ductilidad (8).

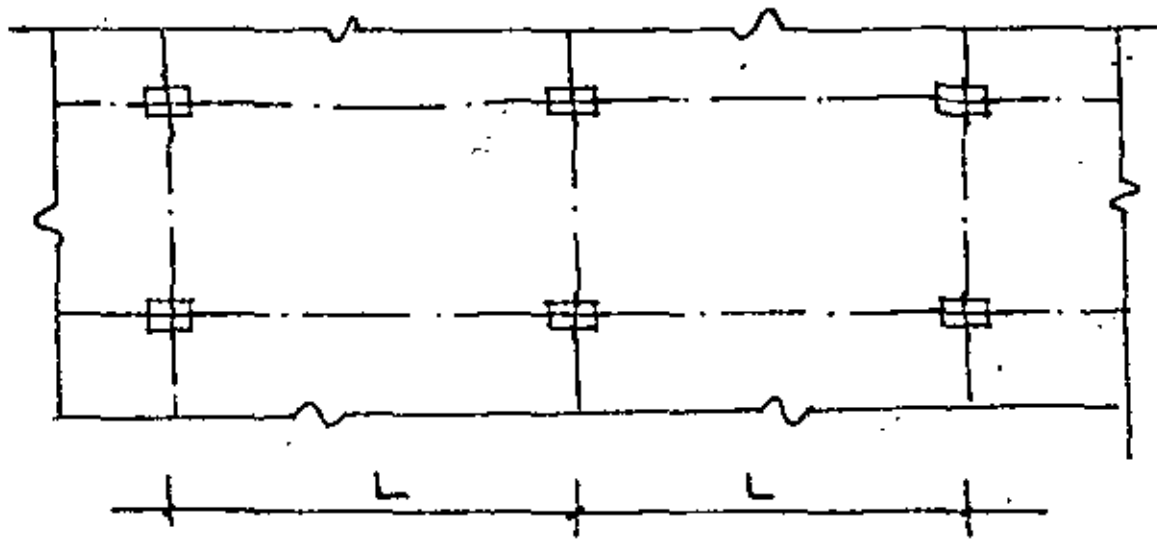
## REFERENCIAS.

1. Lin, T.Y. "Desing of Prestressed Concrete Buildings for - Earthquake Resistance", Journal of the PCI, Vol. 9, No. 6, Dic. 1964, pp. 15-31.
2. Rosembluet, E. Discusión del artículo de T.Y. Lin "Desingn of Prestressed Concrte Building for Earthquake Resistance", Journal of the Structural Division, American Society of - Civil Engineers, Vol. 92 Feb. 1966.
3. Despeyroux, J. "L'utilization du béton précontraint dans - la construction parasismique "Travaux", No. 375, 1966.
4. Blakeley, R.W.G. "Ductility of Prestressed Concrete Fra - mes Under Seismic Loading", University de Canterbury, Nue - va Zelandia, 1978.
5. Thompson, K. J. "Ductility of Prestressed Concrete Frames Under Seismic Loading". Ph. D. Thesis University of Canter - bury, Nueva Zelandia, 1971.
6. Nakano "Experiment on behavior under lateral force of pres - tressed concrete frames". Reporte del Instituto de la Cons - trucción, Tokyo, julio 1967.
7. Penzien, J. "Damping Characteristics of Prestressed Concre - te", ACI Journal, Vol. 61, No. 9.
8. Camba, J. "Edificios altos prefabricados parcialmente pres - forzados", Conferencia Regional de Edificios Altos, México, D.F., abril 1973.
9. Dowrick, D.J. "Earthquake resistant Desing" John Wiley and Sons, New York, 1977.

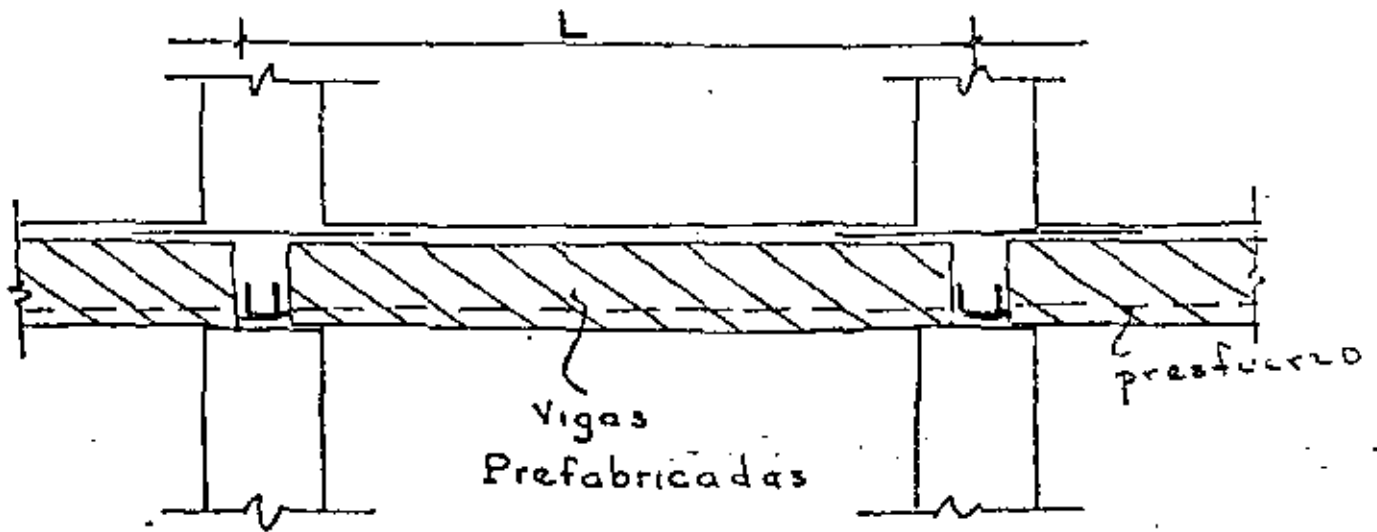
3.- CONEXIONES TIPO DE MIEMBROS PRENSFORZADOS.

3-1.- Estructuraciones préforzadas.

3.2 Estructuraciones postensadas.

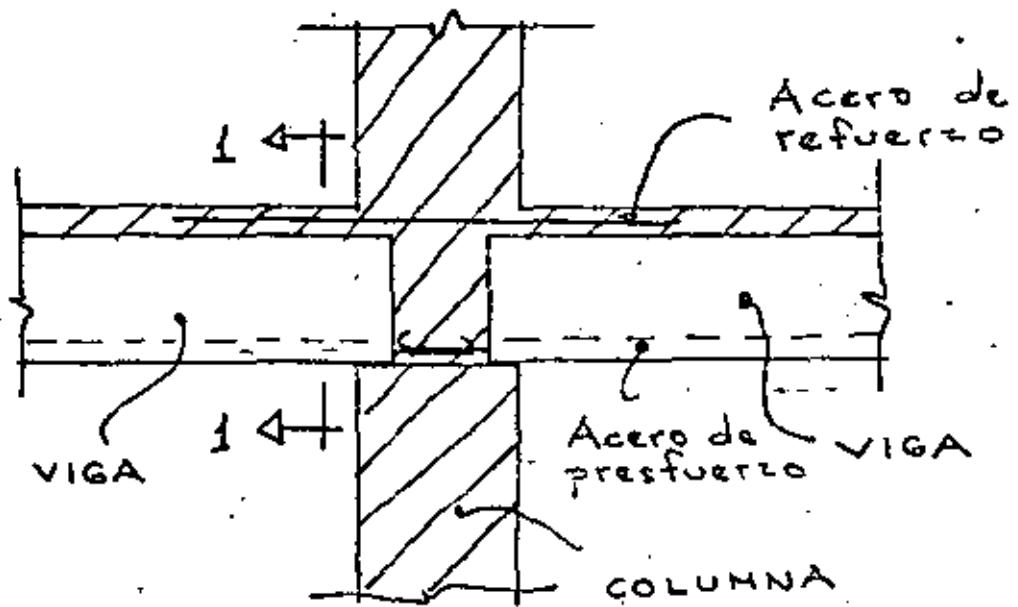


PLANTA

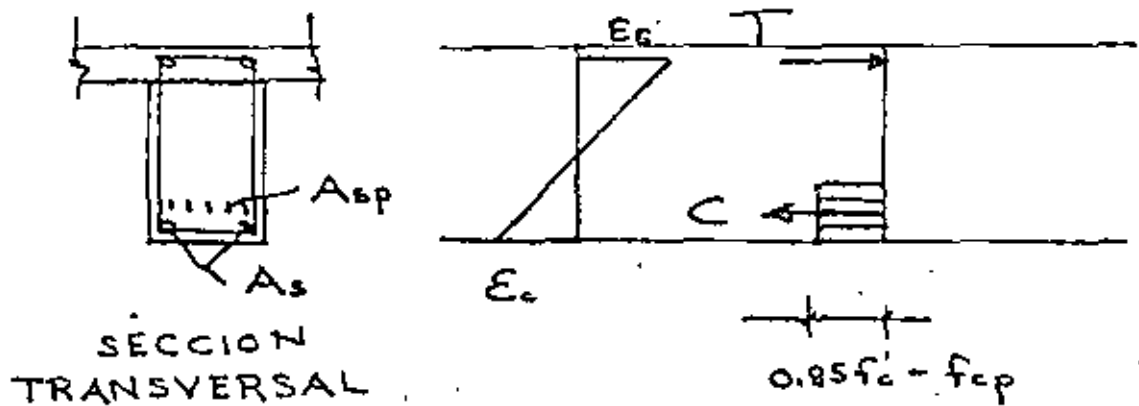


ELEVACION

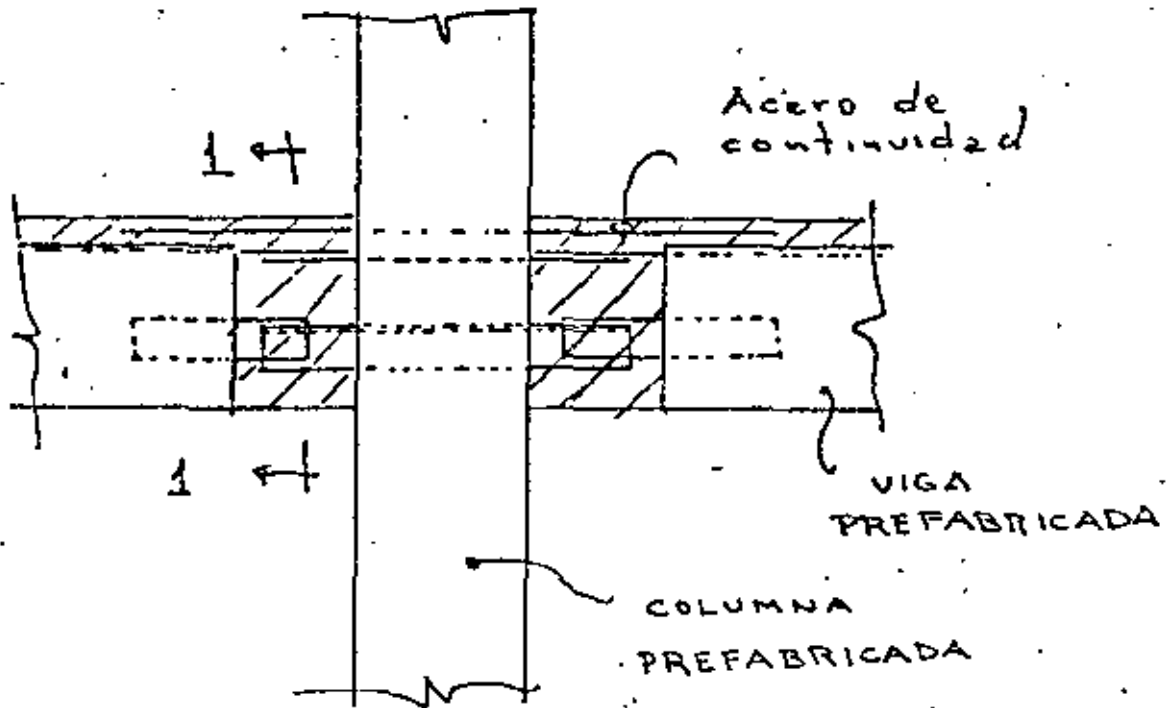
ESTRUCTURACION PRETENSADA



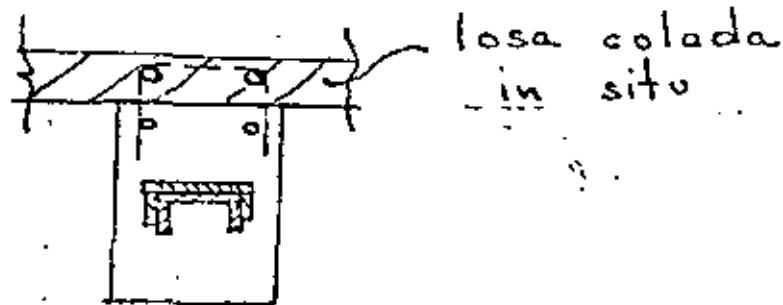
## ELEVACION



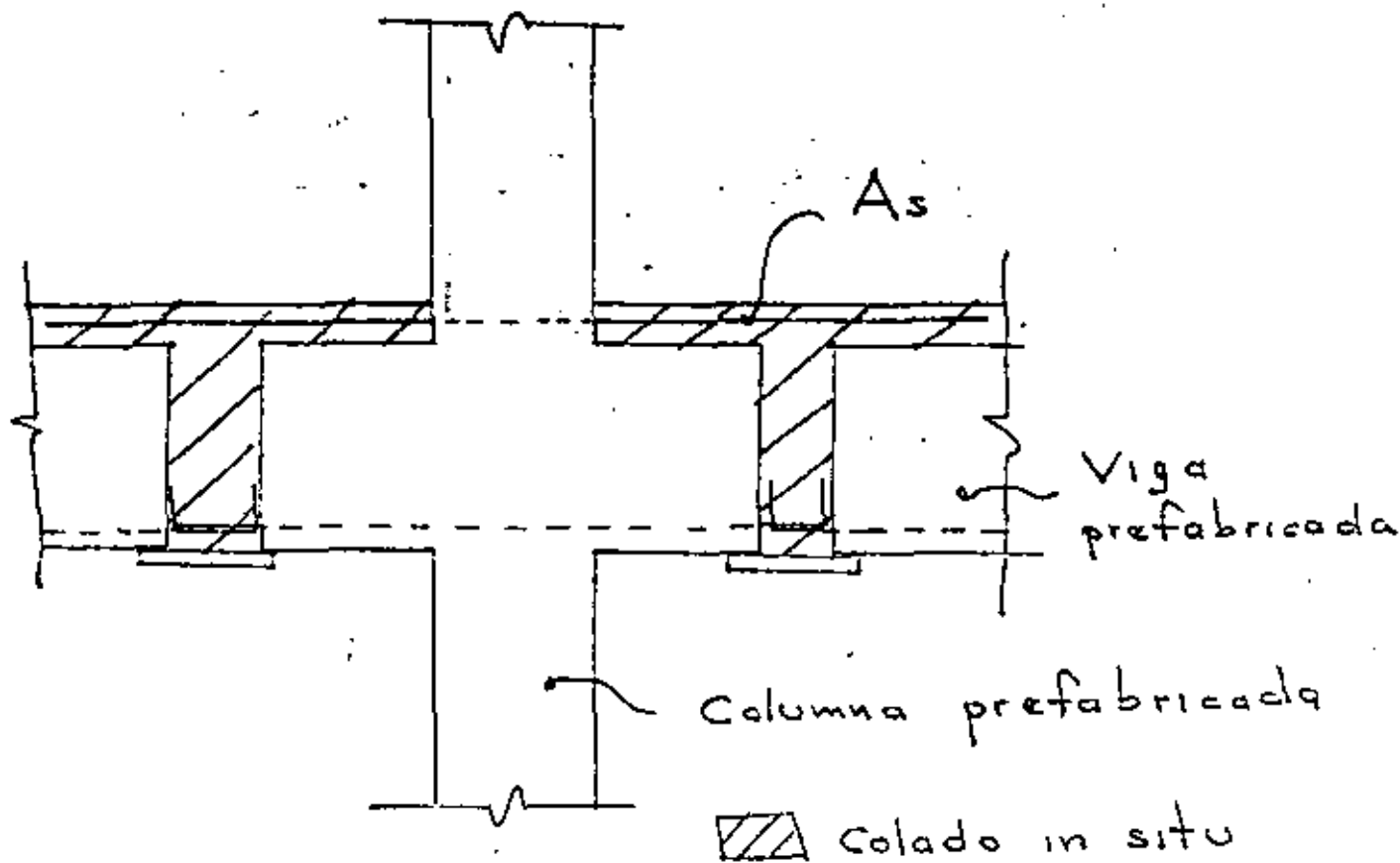
## CORTE 1-1



ELEVACION



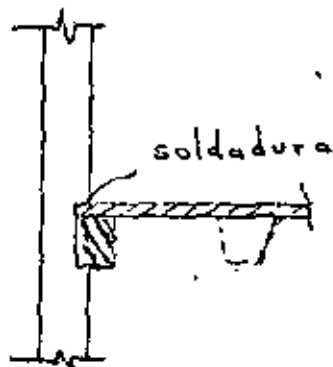
CORTE 1-1



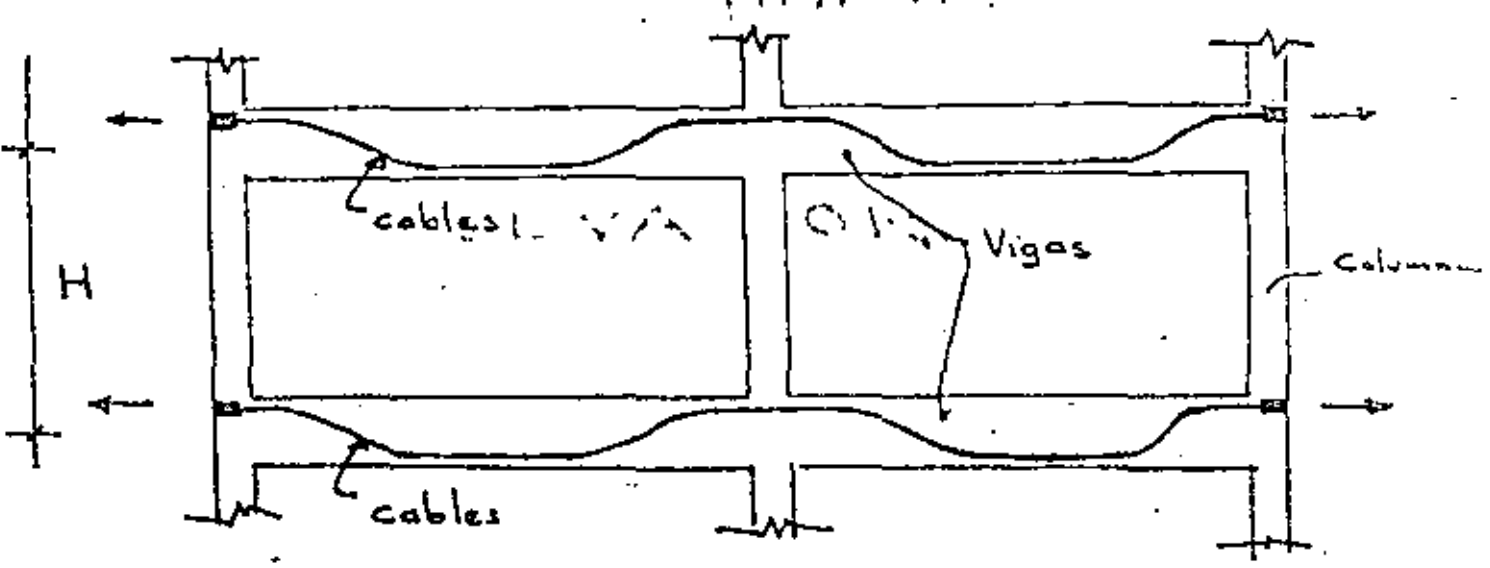
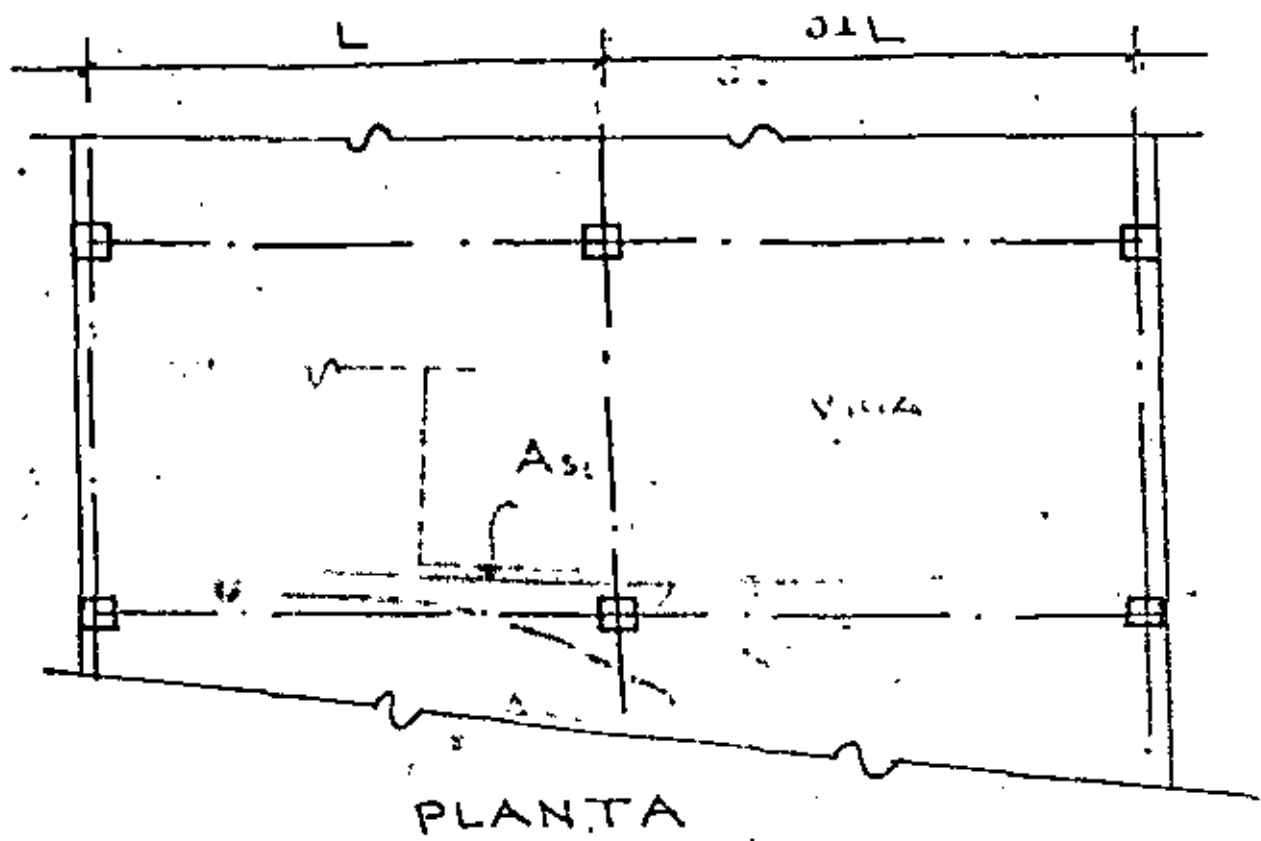
CONEXION PREFABRICADA  
FUERA DEL NUDO



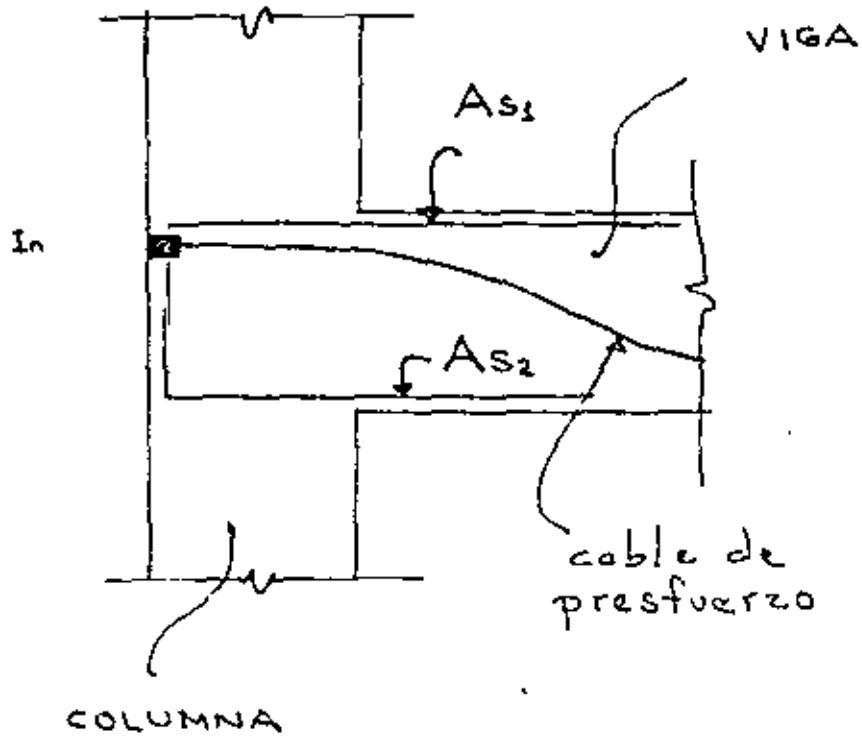
DIAFRAGMAS SOBRE  
ELEMENTOS PRETENSADOS



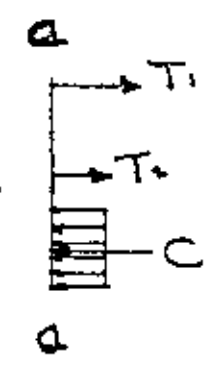
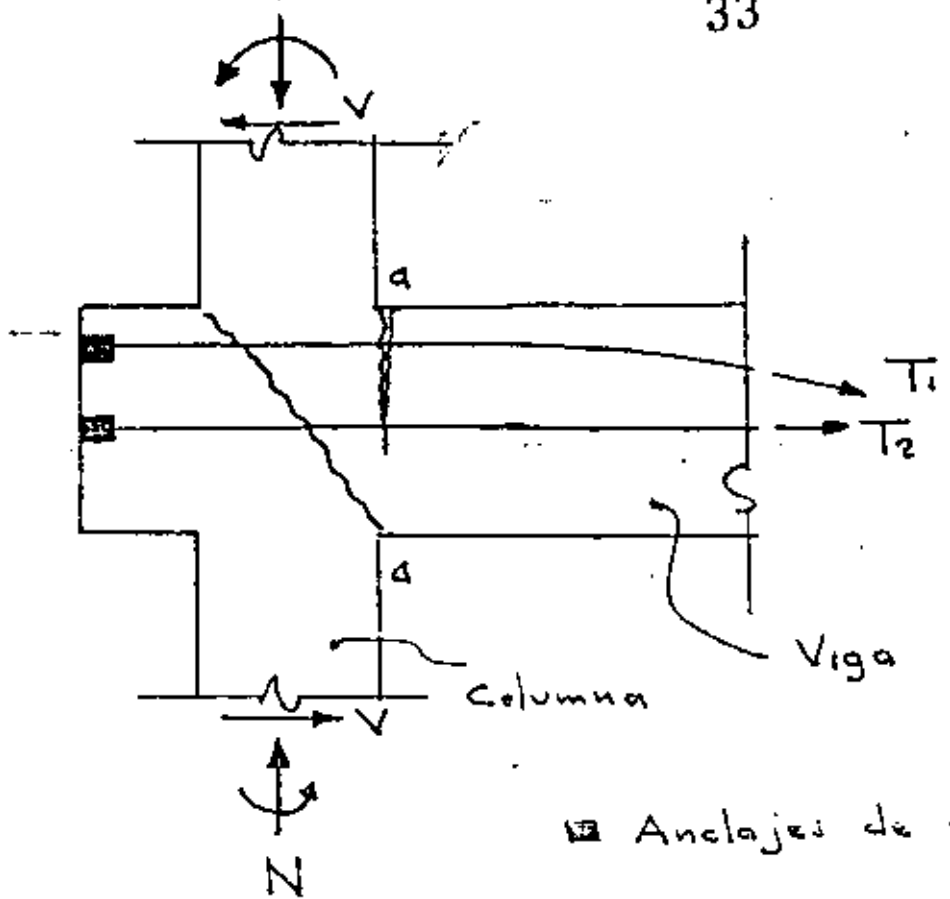
UNION DE DIAFRAGMA  
CON MUROS DE CORTANTE



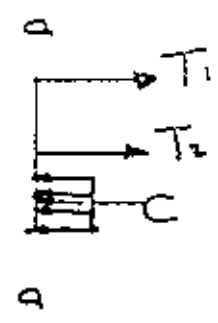
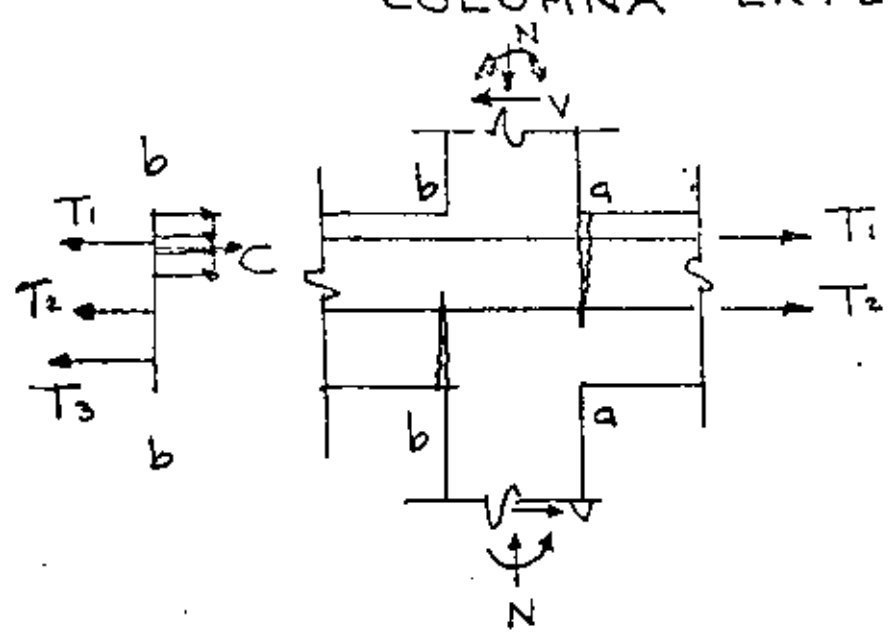
ESTRUCTURACION POSTENSADA



ELEVACION



COLUMNA EXTERIOR



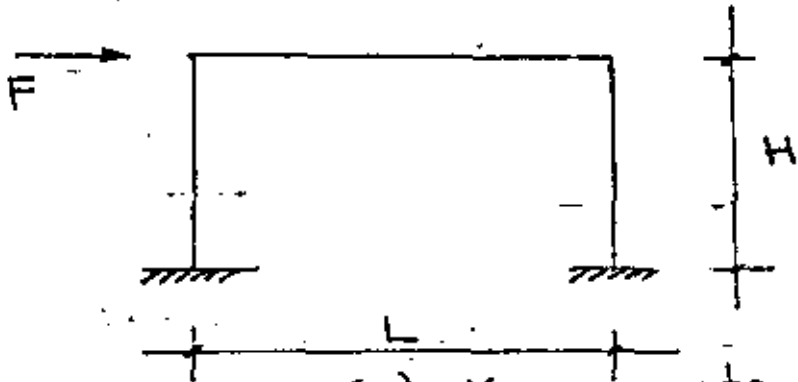
COLUMNA INTERIOR

#### 4.- REGLAMENTOS.

4.1 Reglamento del Distrito Federal.

4.2 Reglamento ACI 318-71.

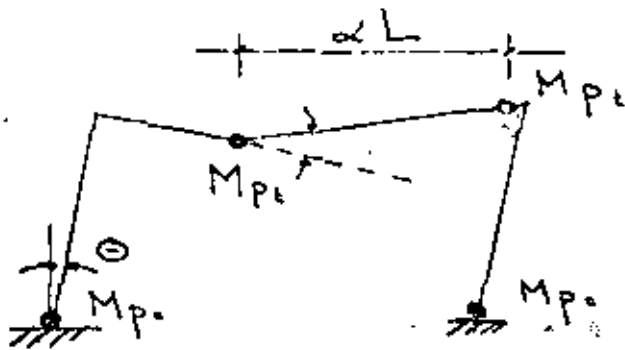
4.3 Recomendaciones C.F.B.- FIP.



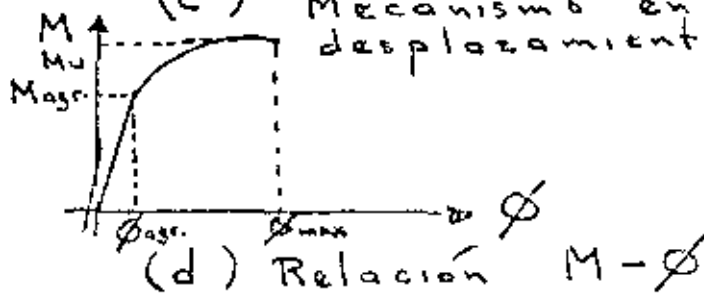
(a) Marco sujeto a fuerza sísmica



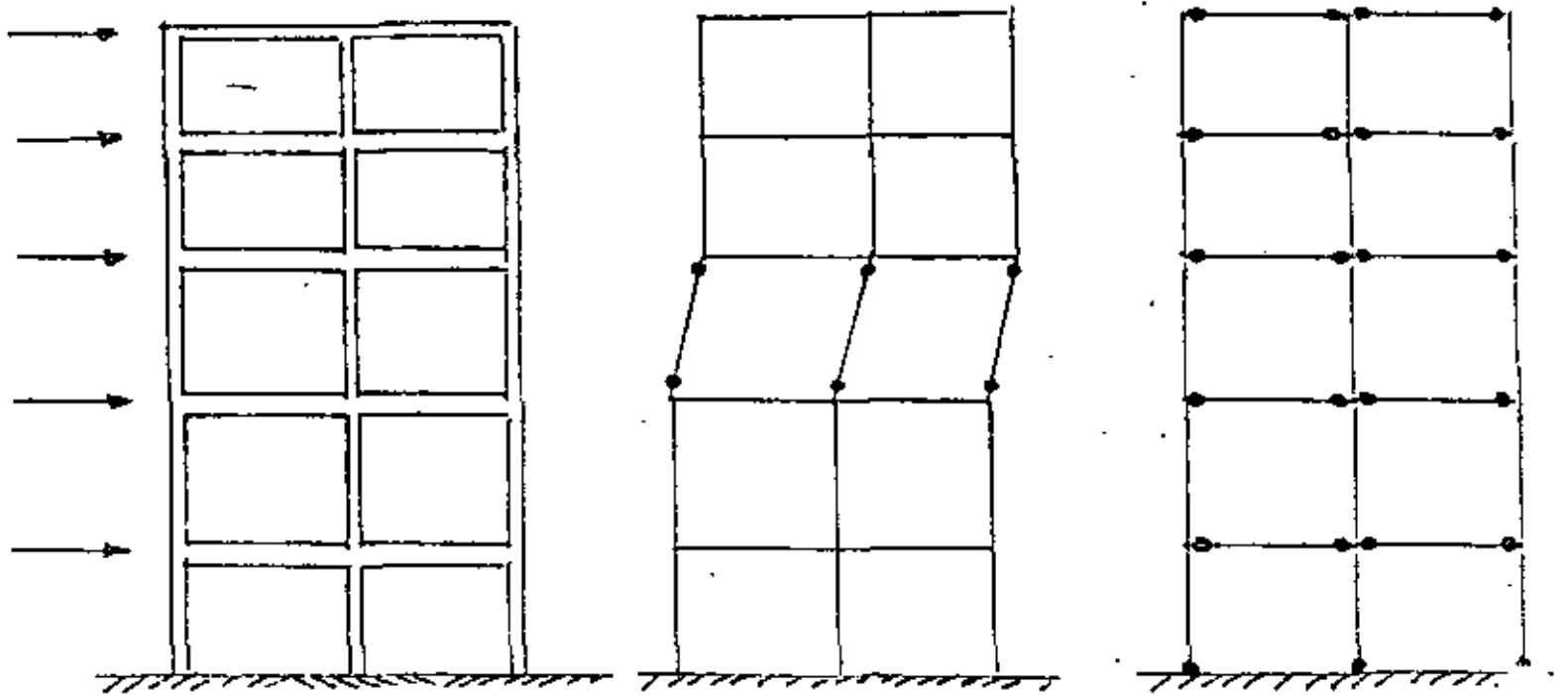
(b) Mecanismo de columnas



(c) Mecanismo en traves con desplazamiento



(d) Relación  $M-\phi$



(a)

Marco  
Rígidos

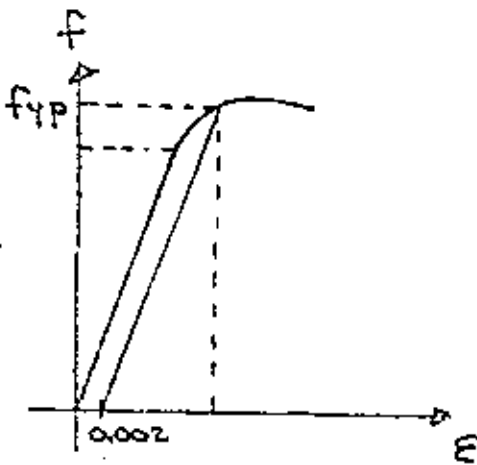
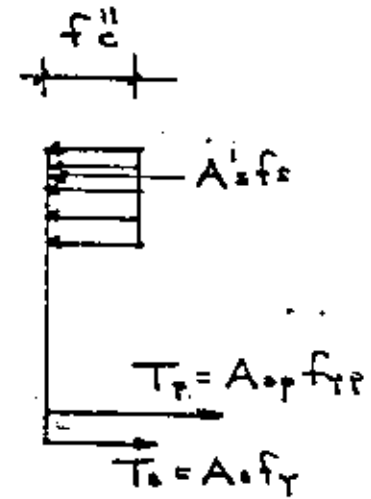
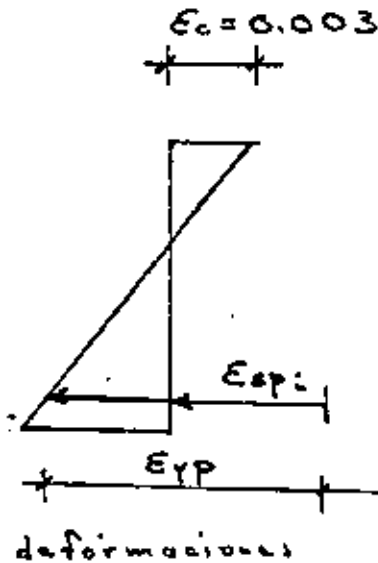
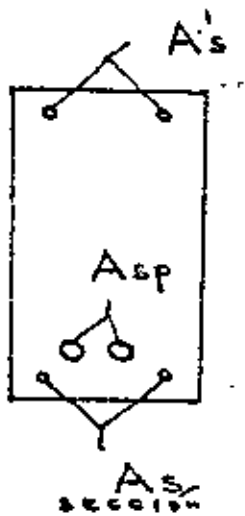
(b)

Mecanismo de  
columnas

(c)

Mecanismo  
de trabes

MECANISMOS DE COLAPSO BAJO  
FUERZAS SISMICAS



Gráfica  $f$ - $\epsilon$  del acero de pretuerzo

Refuerzo máximo en miembros a flexión:

$$T_{\max} = A_s f_s + A_{sp} f_{sp} \leq 0.75 T_{bol.}$$

en la cual:

$A_s$  = área de acero ordinario en tensión  
 $A_{sp}$  = " " " de pretuerzo " "

$f_s$  = esfuerzo en el acero ordinario de tensión al alcanzar la resistencia.

$f_{sp}$  = esfuerzo en el acero de pretuerzo cuando se alcanza la resistencia.

Falla balanceada en una sección pretorzada

REGLAMENTO D.F.

Refuerzo prestrozado unicamente:

$$(1) \quad \rho_r = P \frac{f_{rp}}{f'_c} \leq 0.3 \quad ; \quad P = \frac{A_{sp}}{bd}$$

Refuerzo prestrozado y refuerzo normal:

$$\rho_r + \rho - \rho' \leq 0.3 \quad ; \quad \rho = \frac{A_s}{bd}$$

$$\rho' = \frac{A'_s}{bd}$$

A) Porcentajes máximos de refuerzo

$$\% \text{ máx} = 20 \left( 1 - \frac{\rho_r + \rho - \rho'}{0.30} \right)$$

B) Redistribución de momentos negativos

REGLAMENTO ACI 318-71

RECOMENDACIONES DE LA FIP PARA EL DISEÑO SISMICO DE ESTRUCTURAS. (LONDRES 1978).

Se presentan a continuación un resumen de las principales recomendaciones.

1) Se considerarán dos estados límite de sismo: moderado y severo. En sismos severos la estructura no debe fallar, debiendo formarse un número significativo de articulaciones plásticas capaces de disipar energía.

2) Son válidos los análisis estático o dinámico para determinar las fuerzas sísmicas y las estructuras deberán analizarse en dos direcciones principales.

3) La ductilidad por flexión debe asegurarse mediante la posición de articulaciones plásticas bajo sismos severos. En esas articulaciones el eje neutro debe estar a  $0.25h$  en puntos donde ocurran inversión de momentos y el momento último deberá ser como mínimo 1.3 el momento de ruptura.

4) En las articulaciones plásticas, todo el cortante deberá ser tomado con estribos.

5) De preferencia los cables deberán lechudarse.

6) Los anclajes de presfuerzo deberán colocarse en zonas - alejadas a las de máximos esfuerzos como lo son las articulaciones plásticas.

7) Las uniones trabe-columna deberán diseñarse en tal forma que aseguren que la falla por cortante no ocurre en el núcleo de la unión.

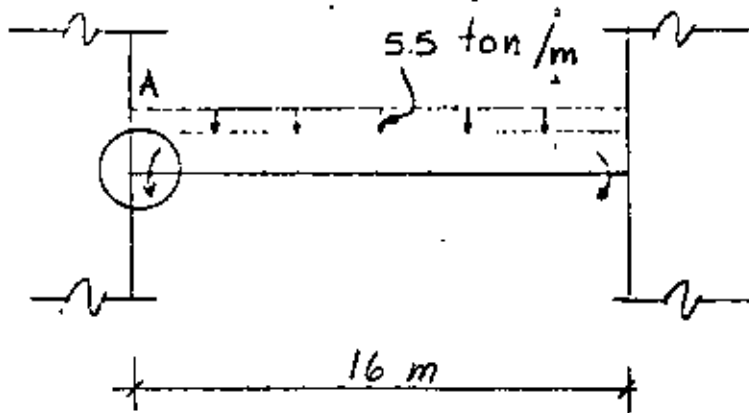
Una consideración importante en las Recomendaciones de Nueva Zelanda para estructuras presforzadas en zonas sísmicas es - la de tomar un coeficiente de 20% mayor que las de concreto reforzado. Como un intento que permita incrementar la respuesta en estructuras presforzadas (5).

5.- EJEMPLOS.

5.1.- Trabe postensada.

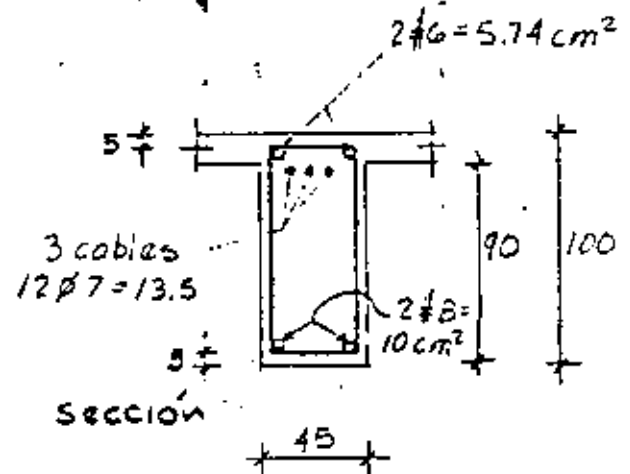
5.2 Trabe pretensada.

EJEMPLO 1.- Verificar si la sección propuesta en concreto pretensado cumple los requisitos del reglamento del D.F. Los elementos mecánicos son los de servicio.



$$M_{c.v.} = -75 \text{ tm}$$

$$M_{sismo} = -50 \text{ tm}$$



Características de materiales:

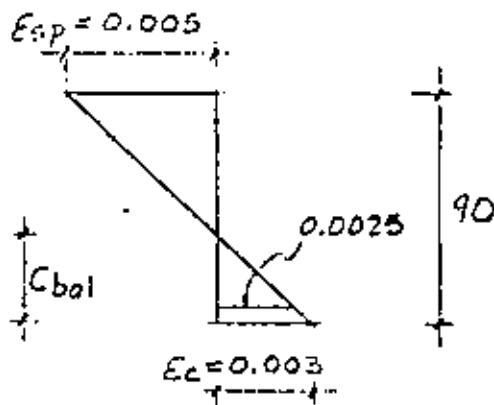
$$f'_c = 300 \text{ Kg/cm}^2$$

$$f_{sp} = 13,000 \text{ Kg/cm}^2$$

$$f_y = 4,000 \text{ Kg/cm}^2$$

SOLUCION :-

a) Verificación de limitación de acero



$$C_{bal} = \frac{90 \times 0.003}{0.008} = 33.7 \text{ cm}$$

$$\therefore a_{bal} = 0.8 \times 33.7 = 27 \text{ cm}$$

Calculo de resistencias reducidas:

$$f^*_c = 0.8 \times 300 = 240 \text{ Kg/cm}^2$$

$$f''_c = 0.8 f^*_c = 192 \text{ Kg/cm}^2$$

La fuerza de compresión valdrá:

$$C_{bal} = 45 \times 27 \times 192 + 10 \times 4000$$

$$= 233\ 280 + 40\ 000 = 273\ 280 \text{ Kg}$$

$$\therefore T_{bal} = 273.3 \text{ ton}$$

De acuerdo con el reglamento del D.F.

$$T_{m\acute{a}x.} = 0.75 T_{bal} = 0.75 \times 273.3 = 204 \text{ ton}$$

En la sección propuesta, suponiendo la fluencia del acero de prestuerzo.

$$T = A_{sp} f_{yp} + A_s f_y$$

$$= 13.5 \times 13\ 000 + 5.74 \times 4\ 000$$

$$= 175\ 500 + 22\ 960 = 198.4 \text{ ton}$$

$$\therefore T \leq T_{m\acute{a}x.} \quad \text{o.k.}$$

Suponiendo la fluencia del acero de prestuerzo:

Por equilibrio de fuerzas:

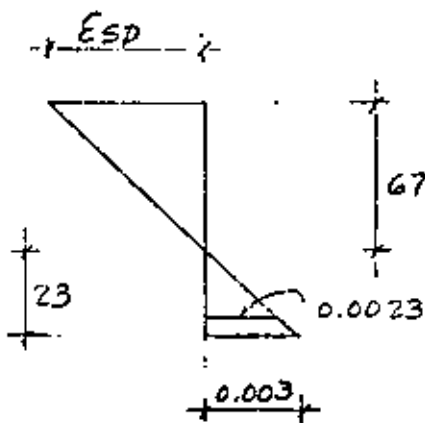
$$C = 45 \times 192 \times a + 10 \times 4000$$

$$T = 175.5 + 22.9 = 198.4$$

$$a = \frac{158,400}{8640} = 18.3 \text{ cm}$$

$$c = \frac{18.3}{0.8} = 23 \text{ cm}$$

Verificando el tipo de falla



$$E_{sp} = \frac{6.7}{23} \times 0.003 = 0.0087$$

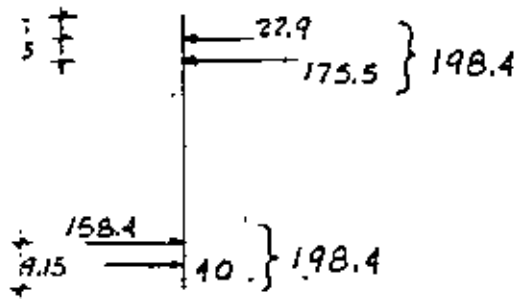
$$E_{sp \text{ total}} = 0.005 + 0.0087 = 0.0137$$

$$E_{sp} > \epsilon_y$$

∴ El acero de prestuerzo fluye y la suposición es correcta.

El momento resistente valdrá:

45



$$z = 100 - 8.31 - 9.42 = 82.2 \text{ cm}$$

$$M_{\text{resist.}} = \phi C_z = \phi T_z$$

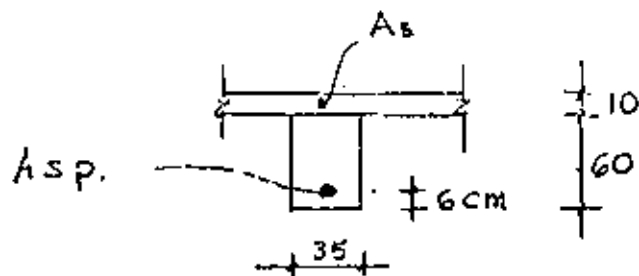
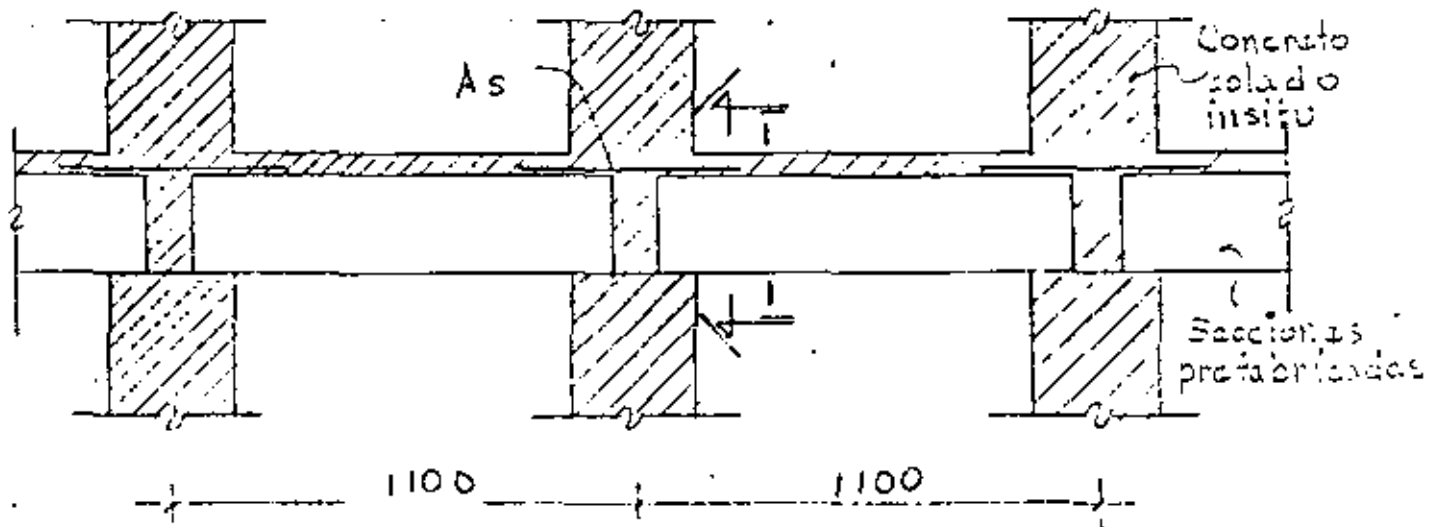
$$\begin{aligned} M_{\text{resist.}} &= 0.9 \times 198.4 \times 0.82 \\ &= 146.4 \text{ t m} \end{aligned}$$

$$M_{\text{actuante}} = (75 + 50) 1.1 = 137 \text{ t m}$$

$$M_{\text{resist}} > M_{\text{actuante}}$$

∴ La sección y armado propuestos sí cumplen los requisitos del reglamento del D. F. en flexión.

EJEMPLO 2.- Calcular el área de acero de refuerzo en la viga pretensada de la figura para momento negativo debido a carga viva y sismo.



CORTE I - I

$$M_{c.v.} = -10 \text{ tm}$$

$$M_{\text{sismo}} = -15 \text{ tm}$$

$$f'_c = 350 \text{ Kg/cm}^2$$

$$f_y = 4000 \text{ Kg/cm}^2$$

$$f_{sp} = 15,000 \text{ Kg/cm}^2$$

$$A_{sp} = 6 \text{ torones } 1/2''$$

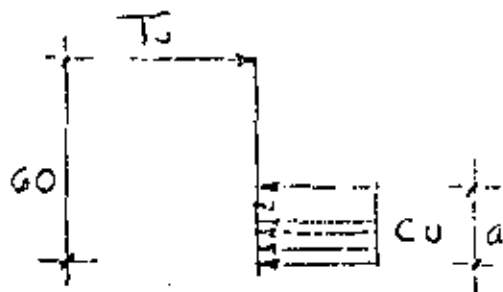
1) Cálculo del área acero para momento negativo.

$$M_u (-) = (10 + 16) \cdot 1.1 = 28.6 \text{ t m}$$

$$A_s \approx \frac{M_u}{0.9 \times 0.85 d \times f_y} = \frac{28.6 \times 10^5}{0.9 \times 0.85 \times 35 \times 4000} = 14.5 \text{ cm}^2$$

se colocarán 2#8 + 2#6  $\rightarrow A_s 15.7 \text{ cm}^2$ .

Estableciendo el equilibrio en el apoyo:



$$C_u = T_u$$

$$C_u = (224 - f_{cp}) A_s'$$

$$T_u = 15.7 \times 4000$$

$$T_u = 62,800 \text{ Kg.}$$

$$f_c'' - f_{cp}$$

compresión  
debida al pretuerzo

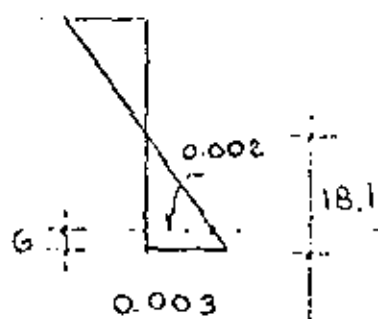
Suponiendo una compresión debida al pretuerzo de  $100 \text{ Kg/cm}^2$ .

$$a = \frac{62.300}{124 \times 0.85} = 14.5 \text{ cm}$$

$\therefore c = \frac{14.5}{0.8} = 18.1 \text{ cm}$  ; verificando la falla se confirma la fluencia del acero  $A_s$

Si verificamos ahora la compresión supuesta en el concreto:

Del diagrama de deformaciones obtenido:



$$E_{sp} = 0.002$$

La deformación del acero al tensarse se supone de 0.005

$$E_{sp} = 0.005 - 0.002 = 0.003$$

$$f_{sp} = E_{sp} \times E_s = 0.003 \times 21000$$

$$= 6,300 \text{ Kg/cm}^2$$

La fuerza de prestuerzo valdrá: 40

$$F = 6000 \times 0.93 \times 6 = 33480 \text{ Kg}$$

y la compresión en el concreto debida al prestuerzo será:

$$f_{cp} = \frac{33480}{35 \times 14.1} = 67 \text{ Kg/cm}^2$$

$$67 \neq 100 \text{ Kg/cm}^2 \text{ supuestos}$$

Haciendo un segundo tanteo con el promedio de los dos:  $80 \text{ Kg/cm}^2$  y repitiendo el proceso anterior, se tendrá:

$$a = \frac{62800}{144 \times 35} = 12.5 \text{ cm}$$

$$c = 15.6 \text{ cm}$$

$$E_{sp} = 0.0018$$

$$\therefore E_{sp} \text{ final} = \underbrace{0.005}_{\text{al tensar}} - 0.0018 = 0.0032$$

$$E_{cp} = 0.0032 \times 2 \times 10^6 = 6400 \text{ Kg/cm}^2$$

$$F = 6400 \times 0.93 \times 6 = 35712 \text{ Kg}$$

$$f_{cp} = \frac{35712}{35 \times 12.5} = 81 \text{ Kg/cm}^2$$

$$80 \approx 81 \text{ Kg/cm}^2 \quad \text{O.K.}$$

El momento resistente valdrá: 50

$$M_{resist} = \phi T_v z$$

$$= 0.9 \times 62\,800 \left(60 - \frac{12.5}{2}\right)$$

$$= 30.4 \text{ tm} > 28.6 \text{ tm}$$

Nota.- La condición de  $T < T_{bal}$  se cumple con amplio margen, ya que el valor de  $T_{bal}$  es de 108.86 ton.



**DIVISION DE EDUCACION CONTINUA  
FACULTAD DE INGENIERIA U.N.A.M.**

VII CURSO INTERNACIONAL DE INGENIERIA SISMICA

DISEÑO SISMICO DE ESTRUCTURAS ESPECIALES

INSTALACIONES ESPECIALES

Profesor: M en C Jorge Prince Alfaro

Julio, 1981

## INSTALACIONES ESPECIALES

- \* Earthquake design of structures with brittle members and heavy artificial damping by the method of direct integration
- \*\* Seismic qualification tests of electric equipment for cuorso nuclear plant: comments on adopted test procedure and results
- \*\*\* Las especificaciones sísmicas de la ENDESA para el equipo de alta tensión  
Especificaciones sísmicas para el equipo de alta tensión ( 220 kv)
- \*\*\*\* Countermeasures for earthquakes in the electric utility industry of japan
- \*\*\*\*\* Electrical power and communication lifelines  
Protecting a power lifeline against earthquakes  
Advances in mitigating seismic effects on power systems  
Aseismic design of 500kv air circuit breaker with friction dampers

julio, 1981

# EARTHQUAKE DESIGN OF STRUCTURES WITH BRITTLE MEMBERS AND HEAVY ARTIFICIAL DAMPING BY THE METHOD OF DIRECT INTEGRATION

D. A. Winthrop and H. C. Hitchcock\*

## Introduction

This paper outlines an investigation by the New Zealand Electricity Department into possible methods of increasing the seismic strength of 220kV airblast circuit breakers. The circuit breaker was idealised as a two mass vibrating system whose behaviour in different earthquakes was examined by the method of direct integration of the equations of motion.

## History

The circuit breakers had been purchased under a specification requiring a seismic design factor of 0.25g. However earthquake damage to similar breakers in a number of countries together with a more detailed understanding of the response of structures to earthquakes lead to the adoption by the New Zealand Electricity Department of standard design spectrum curves based on a set of single mass response spectra compiled by Skinner<sup>(1)</sup>.

These spectra were produced from the eight components of four well known earthquakes, El Centro 1940 and 1934, Olympia 1949 and Taft 1952. The records were scaled to the 1940 El Centro A-S size then their spectra were averaged and smoothed. The present N.Z.E.D. specification for equipment with brittle components requires them to withstand earthquake forces obtained from the appropriate design spectra curve with a factor of safety of at least two.

The La Ligua earthquake of 1905 (Chile), magnitude 7-7.5 on the Richter scale had its epicentre 80 miles from San Pedro substation where 8 airblast circuit breakers of a type in common use in New Zealand were extensively damaged. Out of a total of forty-eight 110kV support columns, thirty-eight were fractured at their base. Although the ground acceleration did not exceed an estimated 0.16g, the maximum response of the airblast heads was considered to be in the region 1.5-2.5g (ref.2). The New Zealand Electricity Department has over eighty of this type of breaker installed throughout the country, rated from 60kV to 245 kV. The maximum acceleration the 220kV circuit breaker porcelain columns can withstand is approximately 0.6g. The need for some form of strengthening of the columns became apparent after the San Pedro and similar incidents.

The manufacturer offered to supply vibrators, damping devices for fitting at the insulator column bases but because of the type of construction, the existing porcelain columns

\* Engineer, New Zealand Electricity Department, Wellington.

\*\* Senior Research Engineer, New Zealand Electricity Department, Wellington.

would also require replacing. The total cost of modifying each circuit breaker was such that alternative means of increasing the circuit breaker seismic resistance was sought.

One such proposal was to provide the circuit breaker base with a more flexible mounting together with heavy viscous damping. An elementary treatment of this arrangement was described in reference 3 and this suggests that large values of viscous damping in the support structure could to an appreciable extent make up for the lack of damping in the porcelain columns. When computer facilities became available the present more detailed study representing the circuit breaker as a two mass system was undertaken.

## Method of Analysis of Circuit Breaker Response

Since the flexibility of the porcelain columns was not negligible and since their strength was limited, it was desired to obtain more definite information on the deflection and stressing of the porcelain by representing each pole of the breaker as a two mass system. The upper mass represents the three sets of airblast heads which are mechanically coupled so that they move virtually as one body and the lower mass represents the compressed air tank which forms the base of the circuit breaker.

It is difficult to determine the earthquake response of a two mass system with widely varying damping by modal analysis. Instead we studied the response of the two mass system to four of the earthquake records used by Skinner in obtaining his original response design curves.

The Department has available a package computer program known as Continuous System Modelling Program, or C.S.M.P. This is designed to simulate any continuous systems represented by one or more linear differential equations. C.S.M.P. has facilities for both linear and quadratic interpolation of ground acceleration from the digitised earthquake records. The first method was used by us primarily to limit computer operating time. The machine used for the operation was an IBM360/40 shared jointly by the New Zealand Electricity Department and the Ministry of Works.

## Scaling of Accelerograms

Several methods of measuring the 'size' of an earthquake have been used.

- (a) according to maximum ground acceleration
- (b) according to the mean value of the velocity response spectrum between 0.1 and 2.5 seconds natural period for a value of damp-

ing, appropriate to the structure being considered (Housner).

2

- (c) according to the mean value of acceleration response spectrum between 0.1 and 2.5 seconds for 2 percent critical damping (Skinner).
- (d) according to the r.m.s. value of the strong motion portion of the accelogram (Jennings).
- (e) according to the mean value of the velocity spectrum for 20% damping between 0.3 and 3 cycles per second plotted logarithmically (Plichon ref. 4).

The scaling factors indicated by the different methods are shown in Table 1. For our study we used the scaling factors generally as derived by Skinner but calculated from the period range applicable to our structure, namely 0.1 to 1.2 seconds. Table 1 shows that the difference between Skinners and the authors figures are small.

Application of Accelerograms

The two body arrangement representing the circuit breaker is shown in Fig. I. The equations of motion governing the systems are:

$$\ddot{x}_1 = -\ddot{Z} - \frac{x_1(K_1 + K_2)}{M_1} - \frac{\dot{x}_1(C_1 + C_2)}{M_1} + x_2 \left( \frac{K_2}{M_1} \right) + \dot{x}_2 \left( \frac{C_2}{M_1} \right)$$

$$\ddot{x}_2 = -\ddot{Z} + x_2 \left( \frac{K_2}{M_2} \right) + \dot{x}_2 \left( \frac{C_2}{M_2} \right) - x_1 \left( \frac{K_2}{M_2} \right) - \dot{x}_1 \left( \frac{C_2}{M_2} \right)$$

The maximum stress to which the columns is subjected are proportional to the maximum displacement of the circuit breaker head relative to the tank.

The structure was first subjected to the 1940 El Centro A-S acceleration record and the response of the airblast heads is shown on Fig III for different values of support structure stiffness and damping.

Scaled up versions of the other three earthquakes were then applied to the structure for the values of support structure stiffness most likely to be of interest. The circuit breaker head response is shown on Fig. IV.

Conclusions

- (1) Fig II compares Skinners response spectrum for 2% damping with the response spectra recalculated by us for four of the eight individual earthquakes which were scaled up by Skinner when deriving the standard. It suggests that the use of these accelerograms in direct integration methods is reasonably equivalent to the use of the design spectrum but is perhaps slightly on the optimistic side.
- (2) Fig III shows that the greatest reduction in loading on the porcelain columns was given by high flexibility and damping. Damping even as high as 0.6 of critical gives an improvement. The curves showing the response of airblast heads to four earthquakes in Fig IV indicate:
  - (a) that the scatter of response for the four earthquakes decreases for heavy damping and low spring stiffness.

(b) that with 12000 lb/foot stiffness in the support and damping between 0.4 and 0.6 of critical, the response of the circuit breaker top to an El Centro sized earthquake is likely to be below 0.4g.

(c) That with 24,000 lb/foot stiffness and damping which represents the recommendation the earlier elementary study (3) based on the treatment of the circuit breakers as a single mass system, the response to two of the first earthquakes is as predicted by that study and to the other two is about 30% larger.

To limit the deflection of the circuit breaker due to wind forces, to about 1 inch at 90-100 m.p.h. it would be necessary to limit the stiffness of the supports to not less than 12000 lb/foot.

The results of this investigation confirm that by choosing supports of low stiffness and heavy viscous damping, a substantial improvement in circuit breaker seismic strength is possible. Preliminary investigations of the mechanical design indicate that the provision of these features is both practical and economic.

References:

- (1) Skinner R. I. "Earthquake-Generated Forces and Movements in Tall Buildings". Bulletin 66, New Zealand Department of Scientific and Industrial Research.
- (2) Novoa F. "Earthquakes and the Substation Equipment Arrangement and Specification," 1970 CIGRE conference.
- (3) Hitchcock H.C. "Electrical Equipment at Earthquakes" Jan. 1969 New Zealand Engineering.
- (4) Plichon C. E. "Dynamic Analysis of Nuclear Power Plant Behaviour to Seismic Excitation", 'Nuclear Engineering and Design' 1970 Vol.12.

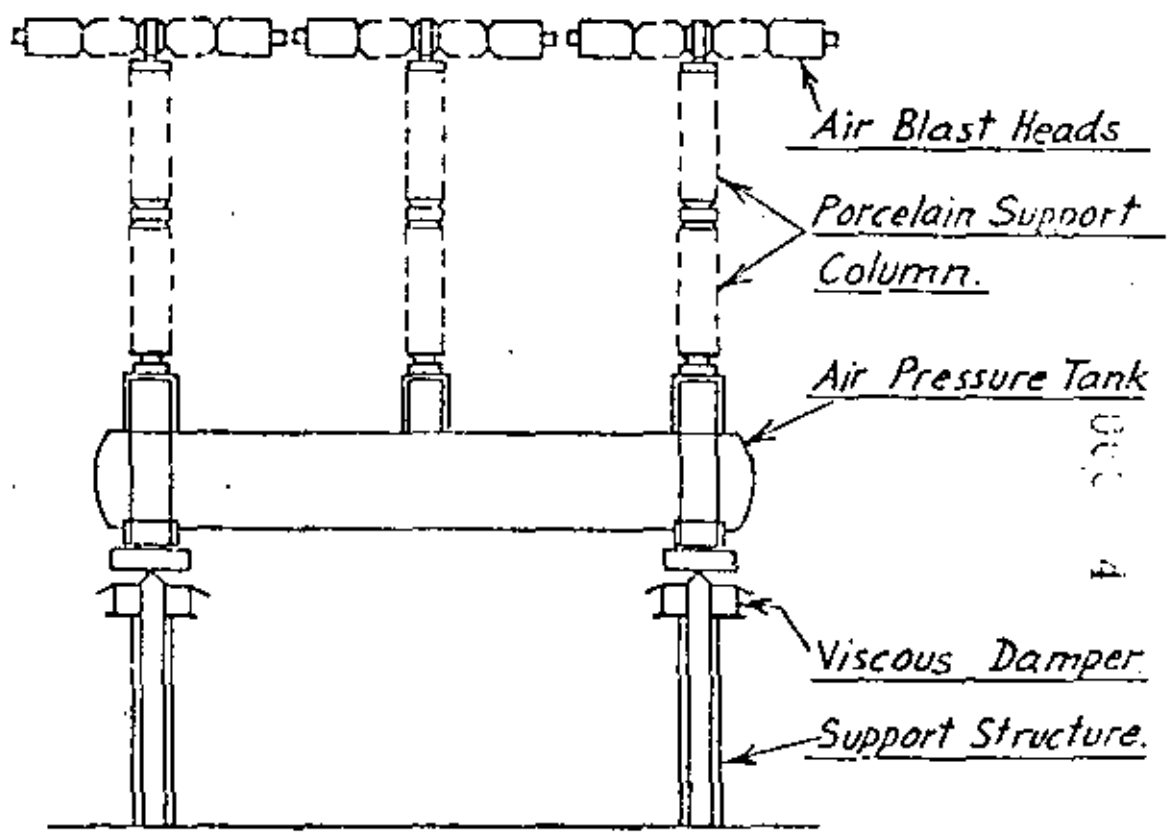
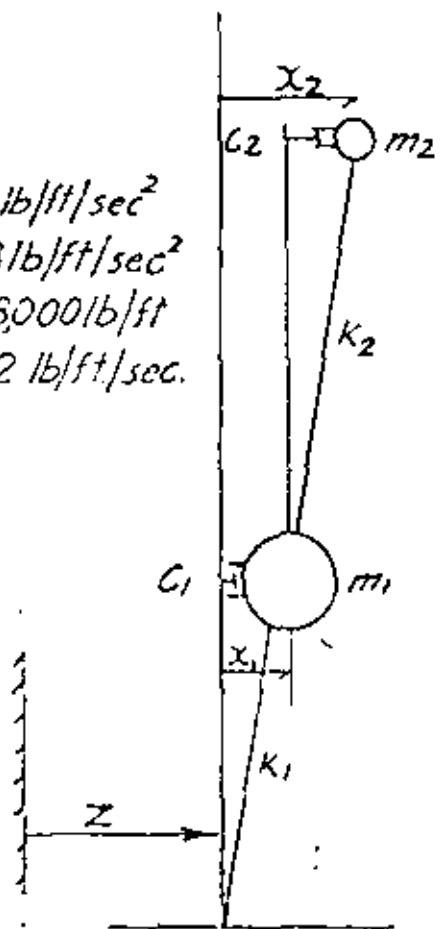


TABLE 1

	EL CENTRO 1940 N.S.	OLYMPIA 1949 N10W	OLYMPIA 1949 NE0E	TAFT 1952 S21W
Max Ground acceln FACTOR	0.33 1.00	0.17 1.94	0.32 1.03	0.18 1.84
Spectral Intensity (Housner) Zero damping, 0.1-2.5 secs FACTOR	6.94 1.0	5.59 1.6	6.05 1.58	4.53 1.97
Mean accel. response (Skinner) 2% damping 0.1-2.5 secs FACTOR	1.3 1.00	0.74 1.75	0.91 1.42	0.59 2.19
Mean accel. response (Authors) 2% damping 0.1-1.2 secs FACTOR	0.809 1.00	0.446 1.82	0.612 1.32	0.186 2.10
R.M.S. Accel. (Jennings) FACTOR	2.20 1.00	1.57 1.4	1.95 1.13	1.42 1.55

300  
3

$m_1 = 59 \text{ lb/ft/sec}^2$   
 $m_2 = 78 \text{ lb/ft/sec}^2$   
 $k_2 = 68,000 \text{ lb/ft}$   
 $c_2 = 92 \text{ lb/ft/sec}$



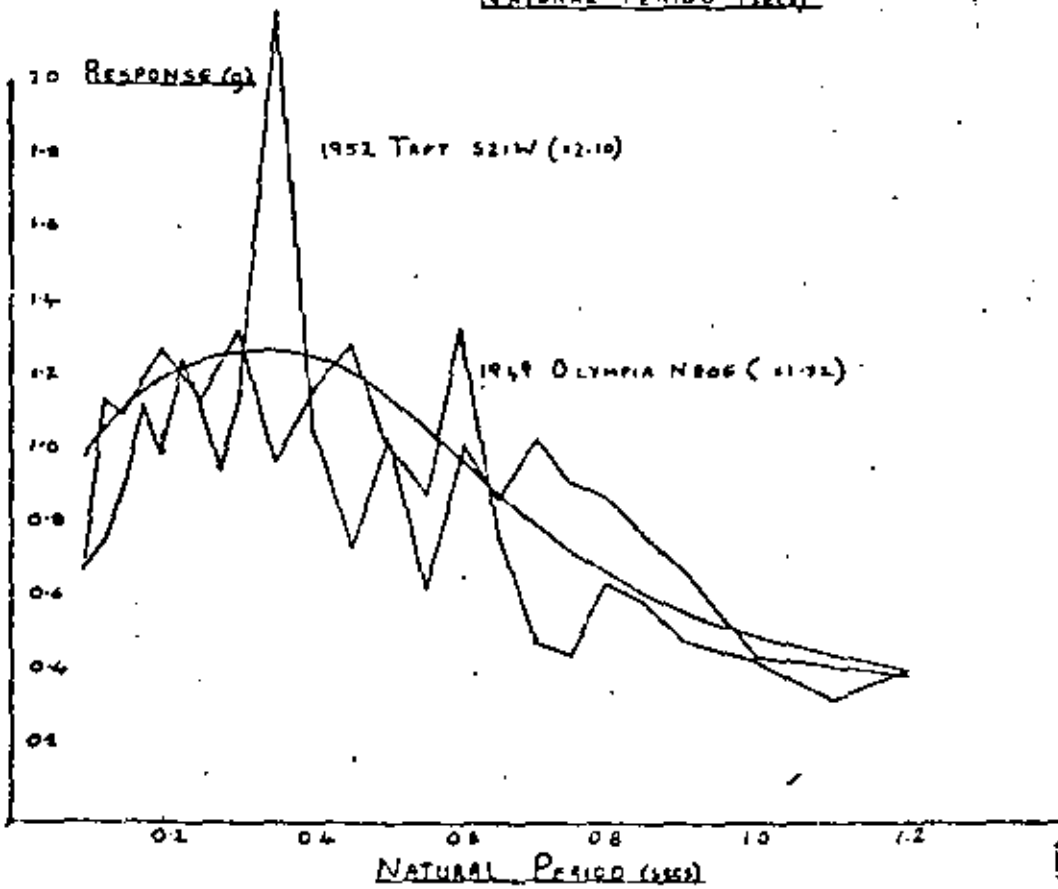
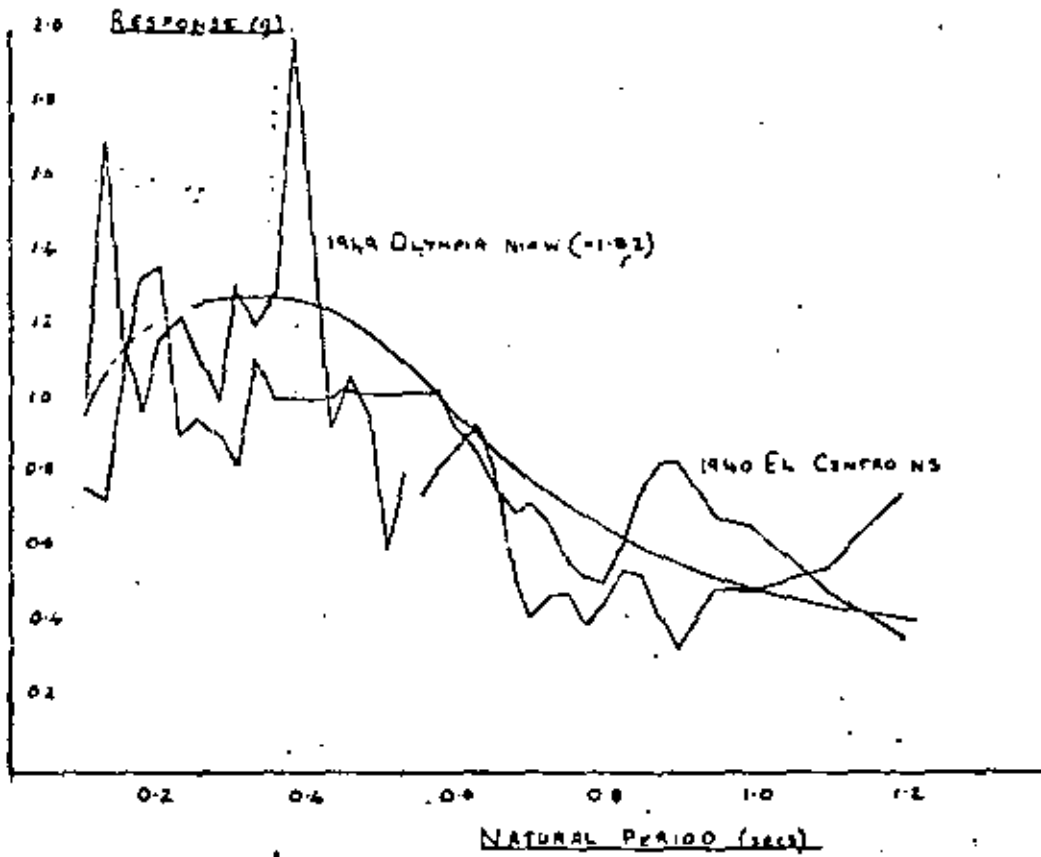
Single Pole of Circuit Breaker

$m_1, m_2$  mass constants  
 $k_1, k_2$  stiffness constants  
 $c_1, c_2$  damping constants,  
 where  $c = 2N\sqrt{m \cdot k}$ .  
 $N$  is fraction of critical damping  
 $x_1, x_2$  displacements of  $m_1$  and  $m_2$ .  
 $z$  " " of ground.

220kV. AIR BLAST CIRCUIT BREAKER

FIG. I

RESPONSE SPECTRA (0.02 DAMPING FACTOR)



RESPONSE OF AIRBLAST HEADS TO  
1840 Ft. CENTRE CONDITIONS (N-3)

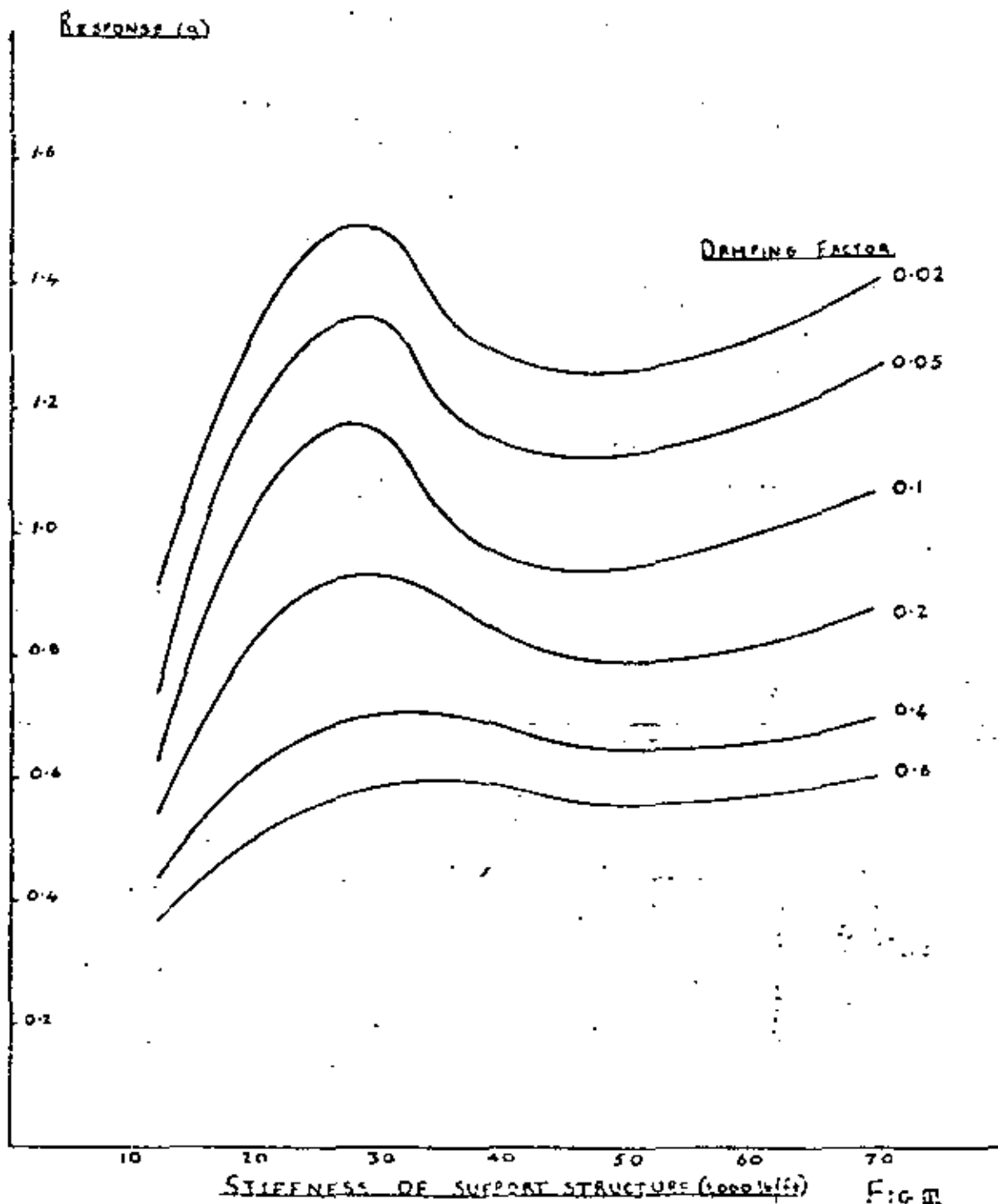
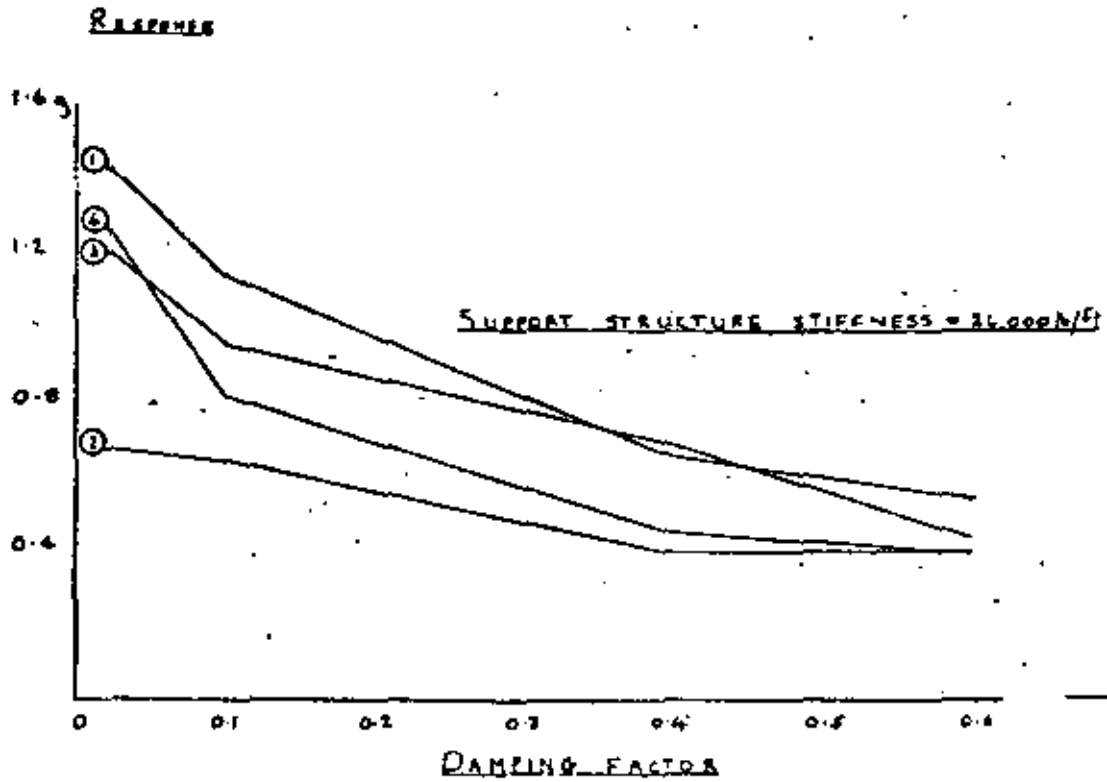
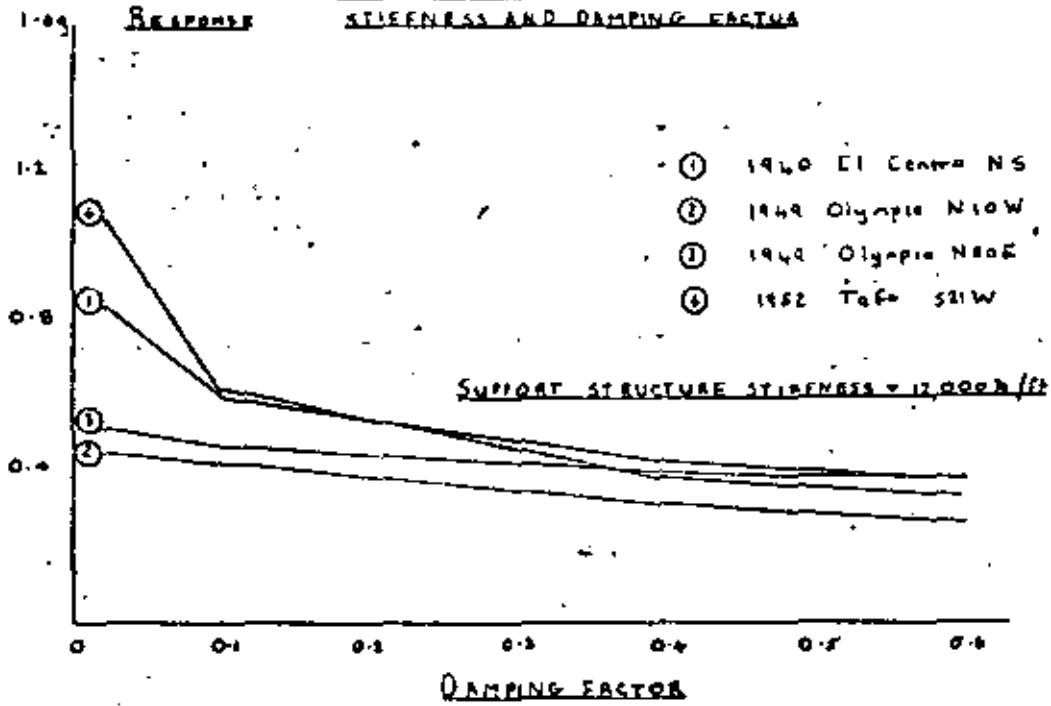


FIG. III

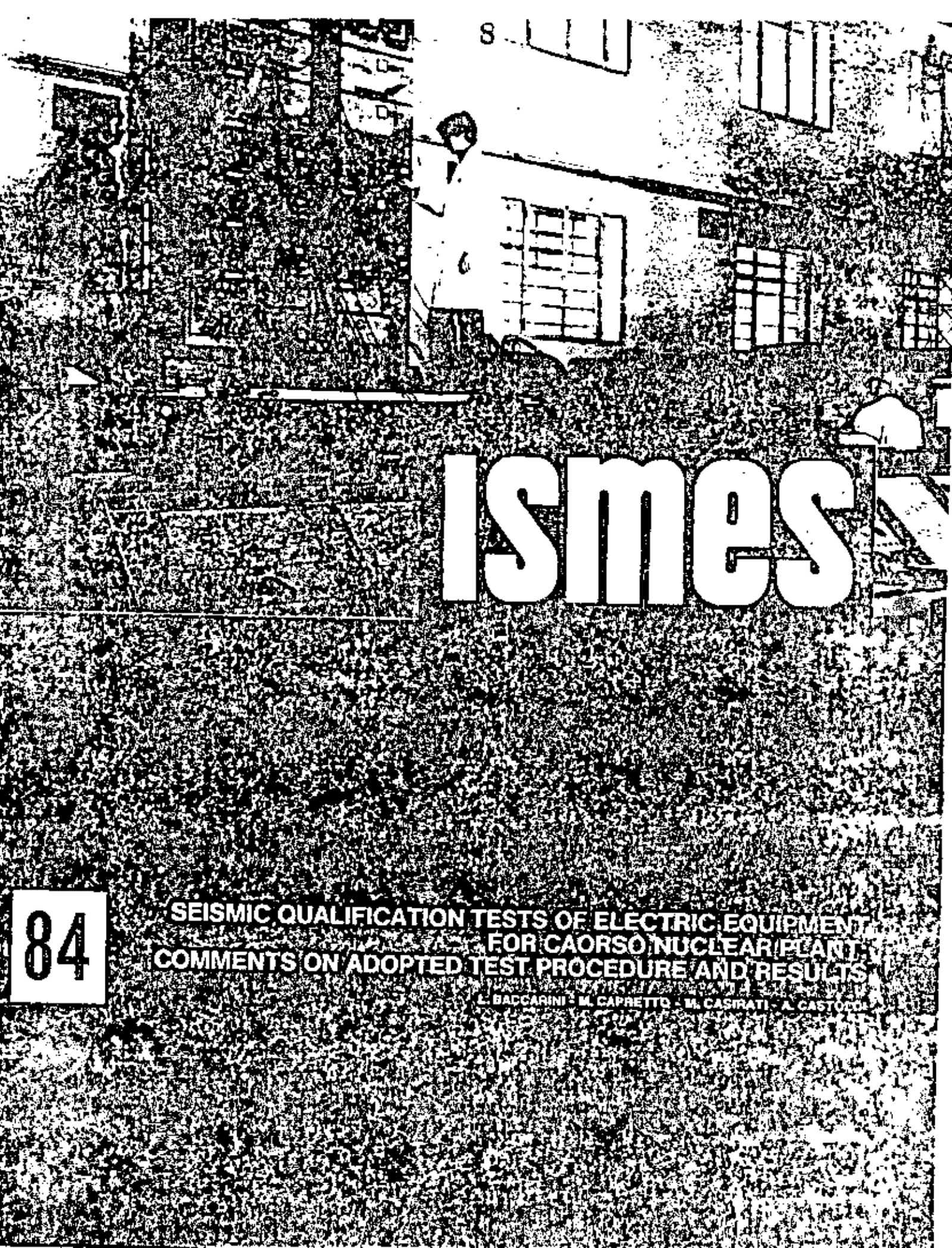
000 7

MAXIMUM RESPONSE OF AIRBLAST HEADS  
FOR VARIATIONS IN SUPPORT STRUCTURE  
STIFFNESS AND DAMPING FACTOR



10/11/52  
 10/11/52  
 10/11/52

FIGURE



# ISMES

**84** SEISMIC QUALIFICATION TESTS OF ELECTRIC EQUIPMENT  
FOR CAORSO NUCLEAR PLANT  
COMMENTS ON ADOPTED TEST PROCEDURE AND RESULTS

L. BACCARINI - M. CAPRETTO - M. CASIRATI - A. CASTOLDI

# ISMES

**Seismic qualification tests of electric  
equipment for caorso nuclear plant:  
comments on adopted  
test procedure and results**

**84**

# SEISMIC QUALIFICATION TESTS OF ELECTRIC EQUIPMENT FOR CAORSO NUCLEAR PLANT: COMMENTS ON ADOPTED TEST PROCEDURE AND RESULTS

L. BACCARINI, M. CAPRETTO

*Pan-Electric, I-28100 Novara, Italy.*

M. CASIRATI, A. CASTOLDI

*ISMES, Istituto Sperimentale Modelli e Strutture, I-24100 Bergamo, Italy*

## SUMMARY

The seismic tests on Class I electric equipment for the nuclear power plant of ENEL at Caorso have been carried out at ISMES in the last two years. The testing procedure, supplied by the customers, is mainly based on the "IEEE Guide" Std. 344-1971, and is summarized as follows:

- complete panels (fully equipped with operated and non operated devices): resonance search at low acceleration level; determination of amplification and damping at the found resonances; vibration tests at the resonance frequencies (continuous sine) with acceleration to be related to the floor response spectrum (f.r.s.) on the basis of the results of the previous tests;
- devices (operated and monitored): resonance search as above; vibration tests at the resonance frequencies, or at 33 cps if resonances are not found, with increasing acceleration until the device ceases to perform.

Without going into details as to the reliability of the f.r.s. a proper correlation between the results of the resonance search tests and the f.r.s. is easily made could the panel be considered a single degree of freedom, linear and viscously damped system. Actually, almost all the panels show a very complex behaviour with numerous resonances, which, in turn, is highly non-linear. To determine the damping value is then an almost unsolvable problem, and the correlation between the test acceleration and the f.r.s. is very difficult. As regards the responses recorded in points of the panel, high accelerations are due to local resonances of small non-structural parts, so that the choice of the gage points should be done very carefully when the overall behaviour is to be determined. As to the meaning of the "structural integrity" as a criterion of seismic adequacy, the question is debatable. Structural damage occurs very seldom, and affects small parts of scarce importance unless fatigue effects, unlikely to play a noticeable role during an earthquake, are introduced. On the other hand, structural damage may not affect the performance of the devices placed in the panel, where their bad performance may occur without structural damage to the panel itself. Moreover, the influence of the mounting (weldings, boltings, connections) greatly affects the dynamic behaviour of the panels, especially when the first resonance frequency is concerned.

On the basis of these considerations, a more reliable testing procedure should be: a continuous frequency sweep at low acceleration (sinusoidal), to record the behaviour of the most significant points; a random excitation whose spectrum matches with the given f.r.s., or—for a more general test procedure—, envelops a number of expected earthquake spectra; to repeat the frequency sweep to make evident possible differences in the panel behaviour due to important structural failures.

Criteria for a correct choice of a specimen panel to be tested are discussed in detail.

As regards the devices, the determination of the resonances frequencies is sometimes difficult (due to the small dimensions of the device its behaviour might be modified by the presence of the pick-up mass), and in most cases, it has no meaning. In effect, a bad performance of the device is mainly due to local resonances (of springs, contacts, connections) which can be discovered only by monitoring.

The tests at 33 cps when resonances are not found have little meaning, because, mainly due to the non-linear behaviour of contacts and other moving parts of the devices (switch on—switch off positions), bad performance may occur suddenly at any frequency for lower acceleration levels.

A better testing technique seems then to be to test the device, its performance being monitored, with continuous sweeps in the frequency range of interest and increasing the acceleration, until it ceases to perform correctly.

## 1. FOREWORD

Due to the large forces in play, and to the fact it affects the whole structure, a strong earthquake is indeed one of the most important and dangerous accidents which may occur to a nuclear power plant. Of great importance as regards the seismic safety of the plant is the good performance of all the electric and electronic equipment installed. Its continuous performance must be always guaranteed: for the most dangerous condition in order to control and, if necessary, to shut down the plant; during emergency in order to avoid the activity of the plant itself being interrupted. Despite its importance, the seismic verification of this equipment is based on a testing procedure still unsatisfactory.

The problem has two distinct aspects. The first is related to the knowledge of the characteristics of the motion generated by the earthquake at the point of the structure at which the equipment is connected. In normal practice, this information is supplied by the so called "floor response spectrum" (f.r.s.). The second is to find out a suitable and reliable testing method, whatever the technique used in order to obtain the f.r.s., and however reliable it is.

This paper is an analysis of the problems arisen: a) from the choice of the testing technique adopted for the seismic check, carried out by means of the testing facilities of ISMES, of panels and electrical components to be installed, by Pan Electric and others, at the ENEL IV power plant; b) for the interpretation of the results obtained from the tests.

## 2. SEISMIC TESTING PROCEDURE ADOPTED FOR ENEL IV NUCLEAR PLANT

The seismic qualification of the electric equipment for ENEL IV nuclear plant has been carried out according to the following two steps:

- a) qualification tests of modular panels, monitoring acceleration levels at component installation points;
- b) qualification tests of components.

According to the adopted procedure, panels which may be different from the one tested (due to possible slight changes in number and type of the installed components) are considered to be qualified by just testing the new components without requalifying the entire electrical board. Among the different testing methods (sinusoidal, sine beat, multifrequency motion) suggested by some standards - as, for example, the IEEE Guides - a sinusoidal excitation has been chosen to carry out the tests. In particular, the following procedure has been used:

- a) as regards the panels, they were tested fully equipped with non operated devices, or dummy loads, and were mounted on a vibrating table in the same way as they will be mounted in the plant. Motion was applied in the three orthogonal directions separately.

A first test consisted of a resonance search carried out with a sinusoidal vibration at low acceleration level ( $0.05 + 0.10$  g) and with variable frequency between 2 and 33 cps approximately. In many points of the structure, selected on the basis of the probable behaviour of the panel and near the mounting points of the components, accelerometers were placed, and the relevant response curves were recorded. When these curves showed a clearly delineated first mode, that is, when the amplification factor had a pattern as shown in fig. 1 a), on their basis a "representative point" of the panel was chosen, in most cases located near the center of gravity of the panel. Besides the value  $A_{max}$  of the amplification, the natural period  $T_0 = 1/f_0$  and damping factor of the structure under test were determined from the amplification curve. These values enabled to obtain, on the f. r. a. curve (fig. 1 b) the value  $a_g$  of the acceleration that the representative point has to reach during the qualification test. This test was then carried out at a frequency slightly varying around  $f_0$ , and with a base acceleration slowly increasing until reaching, at the representative point of the structure, the value  $a_g$  previously determined. During this test the acceleration levels at the component mounting points were monitored in order to compare them with the level each component can withstand without damage. The Pan Electric panels were tested according to this procedure.

When the response curves showed more than one important resonance, the same procedure was applied at each of these frequencies. In turn, when clear resonances could not be found, the maximum acceleration value at floor level was adopted as test input.

b) As regards the components, tests were quite similar and also consisted of two steps. The component was first fixed on the shaking table either directly or by means of a stiff supporting structure. The mounting of the component was carried out in the same way as when in operating conditions on the electric panel. A continuous sweep was performed over the entire frequency range in order to determine, separately for the three principal axes, the resonance frequencies of the component. At the resonance frequencies or, if they are not found, at 33 cps, a vibration test was carried out with input acceleration slowly increasing until the level is reached at which the component no longer operates correctly. During this test the performance of the component under normal operating conditions was monitored.

As regards the quality control tests, a certain percentage of the total amount of a given component has been tested at the same frequencies as before (resonance frequencies or 33 cps) with lower acceleration levels.

### 3. COMMENTS ON THE TESTING PROCEDURE

In the course of the tests, and depending on the results obtained from time to time, a number of problems arose about the correct application to the single cases of the recom-

mented test procedure. The three main points under discussion are:

- a) the correlation between the adopted test excitation and the given f. r. s.;
- b) the criteria used for the analysis of the test results and the consequent assessment as to the seismic adequacy of the panels and components;
- c) the generalization of the test results, that is the capability of the "specimen" tested to represent the standard behaviour.

3.1. From a theoretical point of view, the correlation between the f. r. s. (which is a description of a random motion), and the sinusoidal vibration (which excites only a single frequency at a time) is never possible, unless only one vibration mode is considered to be of importance for the dynamic response of the panel. In this case, the correct correlation is given, in resonance conditions, by the simple relationship:

$$a_{r_i} = C \cdot \beta_i \cdot \frac{1}{2\zeta} \cdot a_b$$

where:

$a_{r_i}$  is the amplitude of the response at point  $i$  of the structure

$a_b$  is the amplitude of the base motion

$C$  is the coefficient of participation of the mode considered

$\beta_i$  is the "amplitude" of the normalized mode shape at point  $i$

$\zeta$  is the percentage of critical damping.

The "representative point" of the structure under test has to be determined through the knowledge of the mode shape and the relevant coefficient of participation, as the point at which  $C \cdot \beta = 1$ . In fact, at this point, the amplification factor of the panel equals that of a single degree of freedom system. Generally, this point is higher than the center of gravity; it follows that to adopt the center of gravity as the representative point means to increase the base acceleration and the test becomes more conservative. Anyway, as the results of the resonance search supply all the necessary data to evaluate the response, the testing method could be, in this case, fully satisfactory.

However, many tests carried out on a number of different panels show that their actual behaviour does not meet the above stated assumptions, as the panels cannot be considered linear single degree of freedom systems. In fact, a panel is generally a framed structure made of steel bended sheets, connected by bolts or weldings in a vertical arrangement. It supports steel doors and walls, in and on which are mounted many electrical components of various types, such as relays, switches, transformers, etc. It is then a rather complex system of parts with different masses and stiffnesses (figs. 2 - 3) and its dynamic behaviour is usually involved. From the tests, in many cases response curves are obtained which show a large number of resonances even in narrow frequency intervals. Too many

tests would then be required, and the use of an impractical and expensive quantity of gauge points, in order to determine the value of the participation coefficient. On the other hand, as to the influence on the components more than the first mode (which is usually related to the overall structural behaviour of the panel) higher modes are of importance, which depend on local vibrations of nonstructural parts (fig. 5).

The dynamic response of the panels is made more involved by their strongly non-linear behaviour, as clearly shown in fig. 6. Increasing input acceleration levels generally cause decreasing values of the peak frequencies and of the amplification, and produce deep modification in the response. The values obtained for resonance frequencies, damping and amplification factors during the frequency sweep at low acceleration are no more the ones in play during the qualification tests, carried out with higher acceleration levels. This is the main reason for the attempts which have been made during the qualification tests, in order to adjust the value  $a_D$  of the input acceleration to the value  $a_S$  required by the f. r. s., instead of using directly the simple ratio  $a_D = a_S / A_{max}$ .

3.2. As regards the interpretation of the test results, it is necessary to take into account that the eventual task of the panel is to allow the performance of the components. Its seismic adequacy has then to be judged on the basis of the operative integrity of the devices it must assure. Of course, the integrity of the component depends on the amplification of the panel at the mounting point, which is in turn dependent on possible structural degrading of the panel, due to fatigue effects. This occurred on some occasions during the course of the tests, owing to the uncertainties about the correlation between input acceleration and f. r. s. In fact, in many cases - as mentioned above - the qualification value was reached after a number of tentative tests, and, in other cases, a very high input value was adopted. Despite this, the tests might have not been conservative, as the determined amplification may be less than that occurring on an intact panel.

The structural integrity of the electric panel during and after the seismic test is not a decisive criterion for judging its seismic adequacy. Structural damage may not affect the performance of the devices, whereas their malfunction may occur without any structural fault of the panel. Nevertheless, an essential requirement for the seismic qualification of the panel should be that its overall behaviour before and after the test remains unchanged.

Another important point for the evaluation of the results, is that, even for input motion in a single direction, a point on the panel may have a response along three axes. The choice of the gauge points has then to be made with care, and, at least for the most important devices, should give a complete picture of the response.

As regards the results of component tests, the following considerations can be drawn. The resonance search is sometimes practically difficult, due to the reduced size of the devices under test; when possible, it usually puts in evidence the resonances of the

frame or of the box into which the device is placed. However, generally these resonances have small influence, if any, on the malfunction of the component. Its performance depends in fact on the possible vibrations of the springs, contacts, and connections the component contains; the resonances of these parts can be discovered only by means of electrical monitoring. However, should the input excitation give rise to a motion lower than the stroke of the contacts, which have a discontinuous behaviour (switch on - switch off positions), even the electric monitoring may not show resonances which actually are present. Of course, the malfunction search at resonance frequencies or at 33 cps, even at very high acceleration levels, does not ensure that malfunction may not occur suddenly for lower acceleration at any other frequency.

3.3. The necessity of selecting a single specimen to be tested among the numerous panels of a set, caused the problem of the choice of a panel representing the "average" behaviour, taking into account the possible differences. Among these should be mentioned:

- differences due to manufacturing, such as welding, bolting, other connecting operations, whose uniformity should be guaranteed. Weldings having the same external appearance should have also the same strength; bolts or screw connections should be tightened in the same way and have uniform mechanical properties, to ensure the same performance;
- differences in number, type, weight and arrangement of components which panels of the same structure hold. Considerable changes in weight and position may be of noticeable importance, as they may give rise to new vibration modes, such as torsional resonances, which may modify the response amplitude in a way difficult to forecast, unless the weight and arrangement are not very different from those of the tested panel. Similar panels can be considered qualified on the basis of the test results of the specimen only when the amount and distribution of the masses are "more or less" the same even with different components, and new devices are mounted on rigid supports, without modifying the main structures of the panel;
- differences of mounting conditions of the panels. Sometimes many similar panels are joined together to obtain a single electrical board of large size; in other cases a board already tested has to be completed with an additional panel for another installation plant. Then the problem of extrapolating the behaviour of the complete board on the basis of the results of a partial test arises. In particular, the minimum number of panels to be tested together and their arrangement is a debatable question. It is difficult to provide a general answer to these problems, and, owing to lack of regulations, at the present level of knowledge, they should be examined one at a time.

As to the components, the tests are generally made on a specimen which is considered representative of the set of equipment to be tested. Modularity problems arise also

in this case: they may sometimes be solved by means of a previous detailed examination of the modifications introduced into the mechanical structure of the component by the variation of some characteristics, as its nominal current and voltage, number of auxiliary contacts, etc. The quality control tests (carried out - as mentioned above - in a statistical way on a percentage of the total amount of the equipment set) may simply require, especially when mass-produced components are concerned, the control of the main characteristics of the device during vibration.

#### 4. CONCLUSIONS

4.1. On the basis of the considerations laid out in chapter 3, which rise from the experience presently available, it is possible to infer that the problem of seismic qualification of electric equipment for nuclear plants has not yet received a satisfactory definition.

Besides the important problems related to the choice of a reliable f. r. s. and of a suitable testing equipment, which are beyond the scope of this paper, it should be underlined that the use of a sinusoidal excitation makes impossible a theoretically correct correlation with the f. r. s. From a practical point of view the problem has been overtaken adopting, in a number of cases, undue input acceleration values.

The use of a single frequency excitation at the resonant frequencies to check seismic adequacy has generally as its consequence the overtesting of the panels with respect both to the amplitude of the input motion, and to the test duration, as tests have to be repeated at the main resonances, or in order to adjust the input to the required f. r. s. acceleration. Fatigue effects may then arise and sometimes damage the panel.

The use of a sine beat motion of given characteristics, as suggested by some standards, does not overcome these problems. The resonance search has to be made also in this case and qualification tests should be repeated for each found resonance. As regards the correlation with the f. r. s., the same consideration for the sinusoidal input can be made. The slight advantage of a less marked influence of an incorrect damping determination is balanced by the more involved testing equipment necessary to generate the sine beat.

For qualification tests, a more convenient procedure, which is in turn more correct from a theoretical point of view, and supplies at the same time more reliable results should be, in our opinion, the application to the panel of a random excitation whose spectrum matches with the given f. r. s. This method requires the use of a rather sophisticated testing equipment; on the other hand it does not depend on parameters of uncertain, if not impossible, determination and makes immaterial the previous knowledge of the characteristics of the structure. Tests become simpler, as it is enough to measure the acceleration levels reached at component mounting points, thus reducing test duration and avoiding possible overtesting.

The sinusoidal input should be used better as a research step during the design stage of the prototype panel, the correct determination of the structural behaviour of which can in this case be justified.

The problem of finding one or more time histories having a given f. r. s. is still open; from a practical point of view, however, a too detailed matching of the f. r. s. is not strictly necessary. In fact, a completely reliable f. r. s. can never be obtained as the methods used in order to determine it involve generally a number of assumptions regarding a proper definition of the earthquake, a suitable structural schematization of the plant building, an estimate of the values of the parameters in play (soil characteristics, damping etc.). In turn, the problem becomes easier if it is considered that the correlation between time history and f. r. s. should be achieved for a narrow band of damping values, and, eventually, that the equipment manufacturers - for economical reasons - aim to qualify their products for more than a single plant. In this case, time histories should be used whose spectra envelop a number of possible f. r. s., and consequently show smooth shapes.

4.2. As far as the components are concerned, taking into account their different operating conditions, as they are mounted on panels having very different behaviour, the simplest and most reliable procedure seems to be to adopt a sinusoidal sweep over the entire frequency range, disregarding the resonance search and the vibration test at resonance or at 33 cps. As fatigue effects are unlikely to occur, each sweep should be repeated with increased acceleration levels, until malfunction occurs, which has to be shown by means of a continuous electric monitoring.

4.3. The effect of an excitation in three directions simultaneously is at present a problem far from being theoretically solved, due to the complexity and nonlinearity of the panels, even on the basis of the knowledge of the single direction behaviour; from an experimental point of view it should require the use of very sophisticated and expensive testing facilities, which in reality is not justifiable.

4.4. As mentioned above, also the problems which arise as to the representative nature of the specimen under test, can not be completely solved at the present stage of available experience. Whereas a statistic test for the components seems to be suitable in order to assure their quality (different devices may require, however, different percentages of the total amount to be tested), the problem is more involved as regards the panel tests. The standards should establish proper criteria in order to judge when the differences arising from different number and arrangement of the devices, addition or connection of modular panels in the electric boards, modify the behaviour with respect to the specimen panel in such a way as to make necessary supplementary tests.

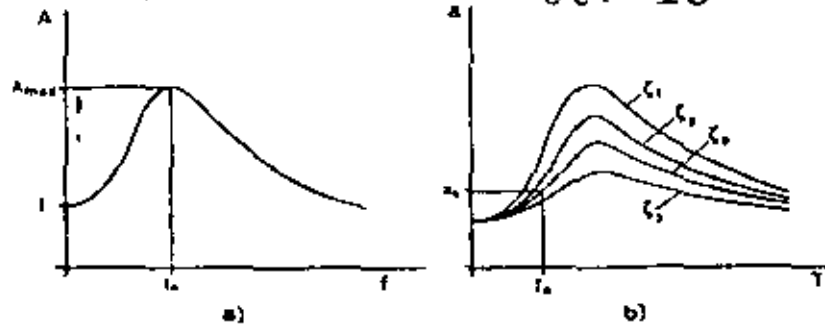


Fig. 1 a) Schematization of the amplification curve.

b) Schematization of the floor response spectrum curves  
( $\zeta$  = percentage of critical damping).

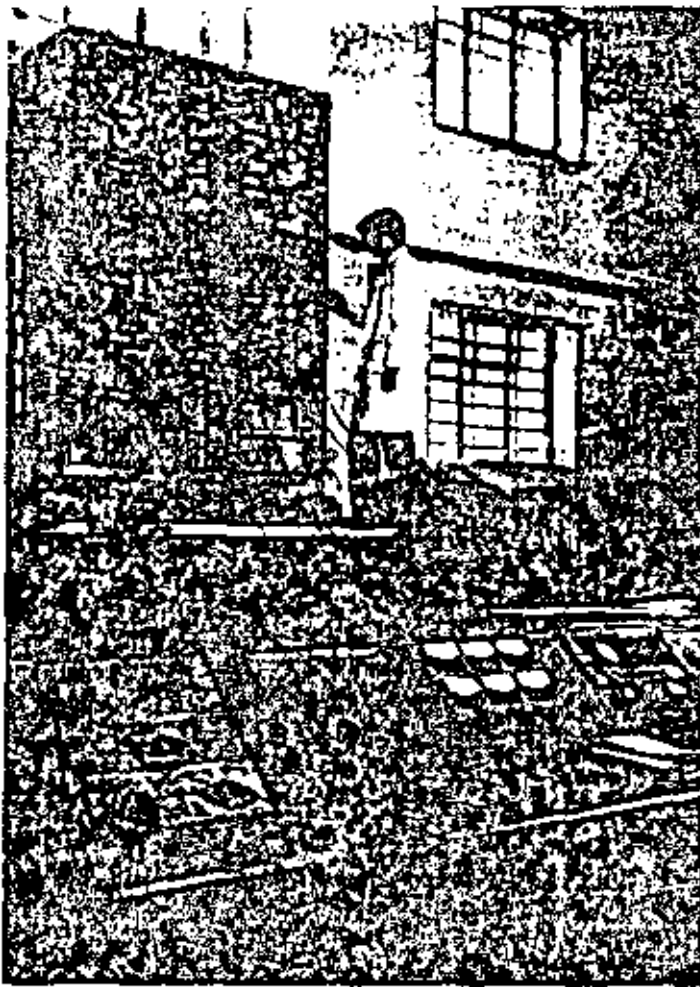


Fig. 2 Pan Electric motor control center, DECABLOC type, during the seismic tests.

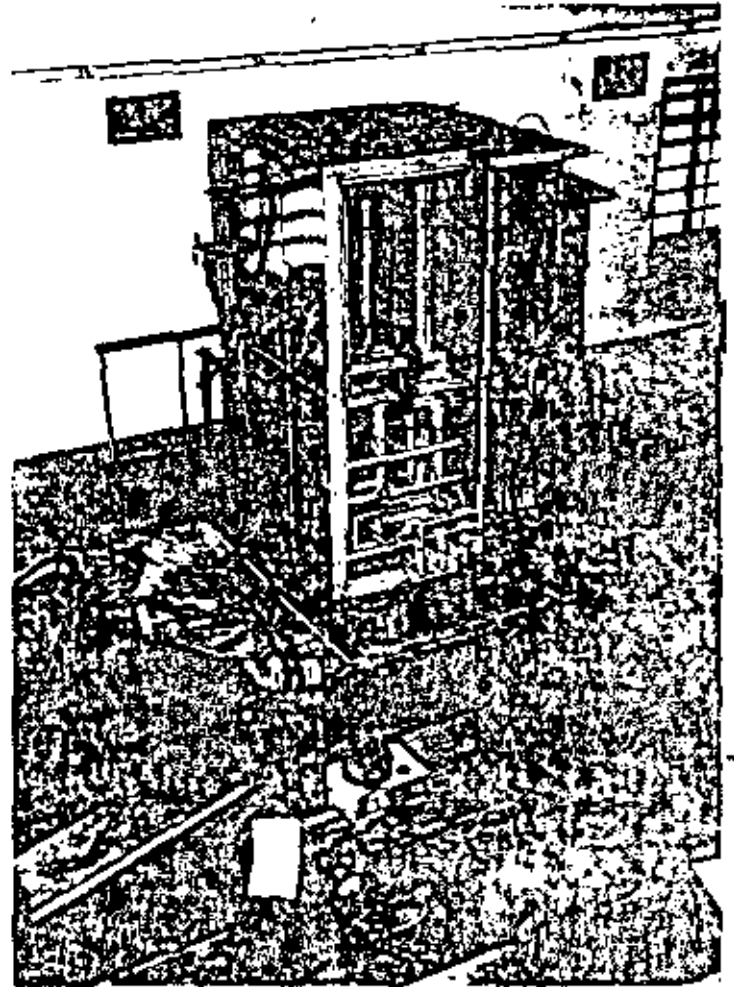


Fig. 3 Pan Electric power center on the ISMES shaking table.

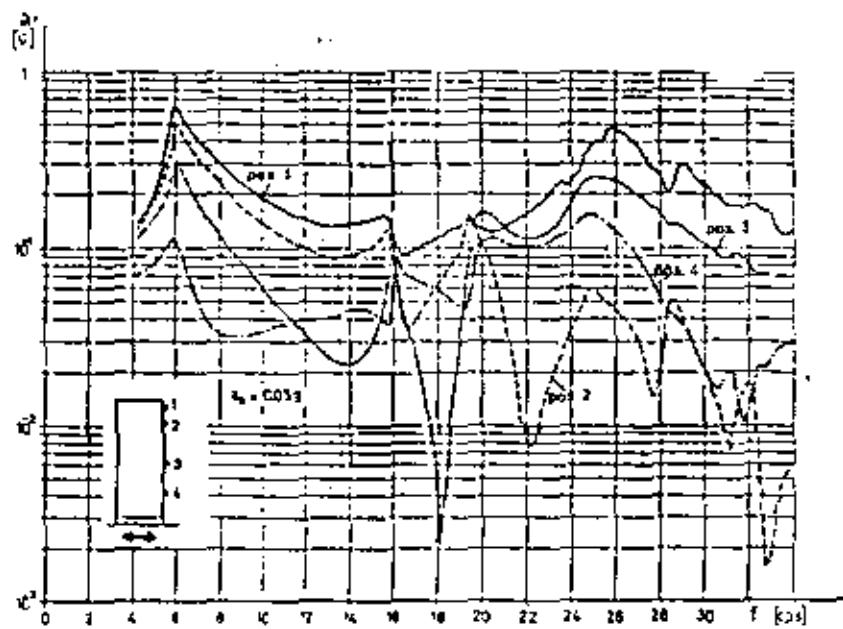


Fig. 4 Response curves recorded in different points of a power center.

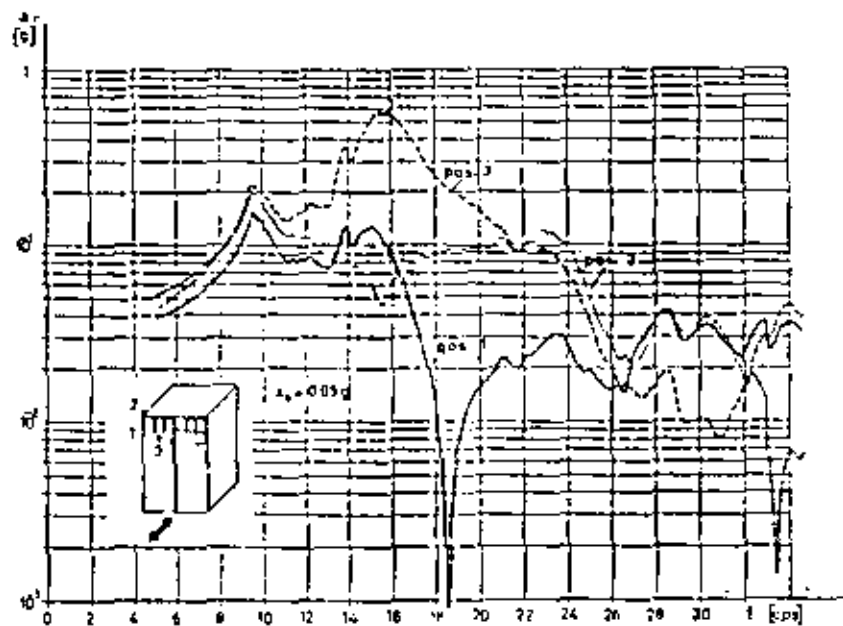


Fig. 5 Response curves of a medium voltage switchgear board, recorded  
 - on the structural frame (pos. 1 - 2)  
 - near the mounting point of a relay (pos. 3).

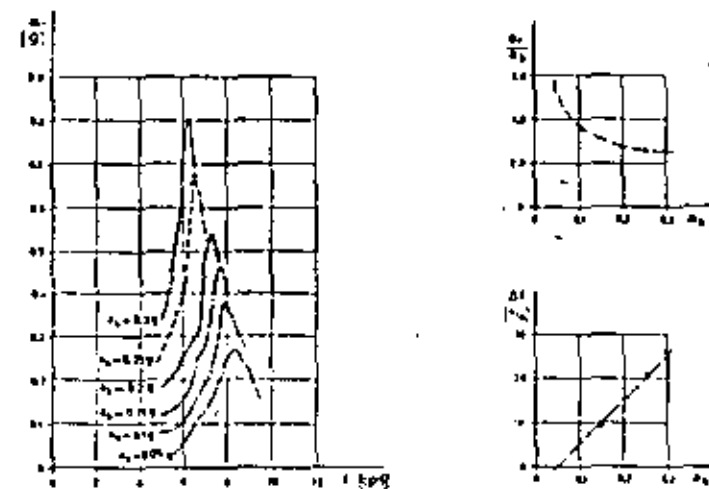


Fig. 6 Non-linear behaviour of an electric panel.

## ISMES PUBLICATIONS

- 1 - ISMES Organizzazione - Impianti - Attività - Settembre 1953.
- 2 - Sulla valutazione del coefficiente globale di sicurezza di una struttura mediante esperienze su modelli (G. Oberti) - Giugno 1954.
- 3 - Cenni illustrativi sulle esperienze eseguite nel primo quadriennio (1951-55) - Ottobre 1955.
- 4 - Contributi al 5° Congresso «Des Grands Barrages» (G. Oberti - E. Fumagalli - E. Lauletta) - Parigi 1955 - Aprile 1956.
- 5 - Ausilio dei modelli nello studio del comportamento statico e dinamico delle costruzioni (G. Oberti) - Luglio 1956.
- 6 - Development of seismic design and construction in Italy by means of research on large models (G. Oberti) - June 1957.
- 7 - Essais sur modèles des barrages (G. Oberti) - Juillet 1957.
- 8 - ISMES. From the «Cement and Concrete Association - Technical Reports» (R. E. Rowe) - March 1957.
- 9 - Arch dams: development of model researches in Italy (G. Oberti) - December 1957.
- 10 - Contributi al 6° Congresso «Des Grands Barrages» (G. Oberti - E. Fumagalli - E. Lauletta) - New York - 1958.
- 11 - Memoria presentata al X Congresso Nazionale degli Ingegneri Italiani (G. Oberti - E. Fumagalli) - Novembre 1957.
- 12 - Large scale model testing of structures outside the elastic limit (G. Oberti) - April 1959.
- 13 - Matériaux pour modèles réduits et installations de charge (E. Fumagalli) - Avril 1959.
- 14 - Italian arch dam design and model confirmation (G. Oberti) - March 1960.
- 15 - Experimentelle Untersuchungen über die Charakteristika der Verformbarkeit der Felsen (G. Oberti) - April 1960.
- 16 - Calcestruzzi da «termaggio biologico per reattori di potenza (E. Fumagalli) - Novembre 1960.
- 17 - Tecnica e materiali per la modellazione delle rocce di fondazione di sbarramenti idraulici (E. Fumagalli) - Maggio 1962.
- 18 - Il regime degli sforzi in un tubo cilindrico cavo in calcestruzzo di lunghezza finita per effetto di un campo stazionario di temperatura con sorgente di calore lineare disposta sull'asse del tubo stesso (L. Goffi). Esperienze termiche su modelli e materiali (E. Fumagalli) - Giugno 1962.
- 19 - Dynamic tests on models of structures (G. Oberti - E. Lauletta) - Luglio 1962.
- 20 - Fenomeni termici nelle dighe ad arco. Valutazione delle sollecitazioni (R. Sammartino) - Settembre 1962.
- 21 - L'Institut expérimental d'essais sur modèles réduits de Bergame (Italie) - Avril 1963. - Rapport publié sur le «Génie Civil» - Paris, 15 Décembre 1962.
- 22 - La ricerca sperimentale su modelli strutturali e la ISMES - Gennaio 1964. - Estratto da «L'Industria Italiana del Cemento» - Anno XXXIII - n. 5 (G. Oberti) - Maggio 1963.
- 23 - Propriétés physico-mécaniques des roches d'appui aux grands barrages et leur influence statique documentée par les modèles (G. Oberti - E. Fumagalli) - Bergame - Août 1964.
- 24 - Dynamic features of a recent Italian arch dam (E. Lauletta) - October 1964.
- 25 - Evaluation criteria for factors of safety. Model test results (G. Oberti - E. Lauletta) - October 1964.
- 26 - Modèles géomécaniques des réservoirs artificiels: matériaux, technique d'essais, exemples de reproduction sur modèles (E. Fumagalli). Results obtained in geomechanical model studies (G. Oberti - E. Fumagalli) - October 1964.
- 27 - Thermoelastic tests on arch dam models (E. Lauletta) - October 1964.
- 28 - Theoretical considerations and experimental research on the behavior of tall buildings during earthquakes (E. Lauletta) - January 1965.
- 29 - Results and interpretation of measurements made on large dams of all types, including earthquake observations (G. Oberti) - January 1965.
- 30 - Caratteristiche di resistenza dei conglomerati cementizi per stati di compressione pluriaassiali (E. Fumagalli) - Ottobre 1965.
- 31 - Equilibrio geomeccanico del banco di sottofondazione alla diga del «Pertusillo» (E. Fumagalli) - Febbraio 1966.
- 32 - Stability of arch dam rock abutments (E. Fumagalli) - Maggio 1967.
- 33 - Structural models for the study of dam earthquake resistance (G. Oberti - E. Lauletta) - Agosto 1967.
- 34 - Un tavolo vibrante per prove «random» (E. Lauletta - A. Castoldi) - Settembre 1967.
- 35 - Osservazioni sulla statica delle volte sottili a paraboloide iperbolico (E. Lauletta) - Novembre 1967.
- 36 - Bedrock stability behavior with time at the Place Moulin arch-gravity dam (G. Oberti - A. Rebaudi) - November 1967.
- 37 - Modelos de presas de concreto y túneles (G. Oberti) - Diciembre 1967.
- 38 - Model simulation of rock mechanics problems (E. Fumagalli) - October 1968.
- 39 - A photogrammetric method for assessing the displacements under stress of large structure models. - Experimental applications (F. Bernini - M. Cunietti - R. Galetto) - March 1969.
- 40 - Tests on cohesionless materials for rockfill dams (E. Fumagalli) - September 1969.
- 41 - Model analysis for structural safety and optimization (G. Oberti) - February 1970.
- 42 - Compression properties of incoherent rock materials for large embankments (E. Fumagalli) - Laboratory tests on materials and static models for rockfill dams (E. Fumagalli - B. Mosconi - P.P. Rossi) - June 1970.
- 43 - Techniques for rupture testing of prestressed concrete vessel models (F. Scotta) - July 1970.
- 44 - Improvements in Geophysical Methods for Measuring Elastic Properties of Foundation Rocks (E. Carabelli) - August 1970.
- 45 - Comportement statique des massifs rocheux (calcaires) dans la réalisation de grands ouvrages souterrains (G. Oberti - A. Rebaudi - L. Goffi) - Septembre 1970.

- 46 - Influence des fondations sur la mécanique de rupture des barrages voûte (E. Fumagalli) - Octobre 1970.
- 47 - Sul funzionamento statico della diga di «Susquea» dall'analisi dei risultati sperimentali su modello (G. Oberti - E. Fumagalli) - Novembre 1970.
- 48 - Earthquake simulation by a shake table (E. Lauletta - A. Castoldi) - December 1970.
- 49 - Static tests on a model of a prestressed concrete pressure vessel for a THTR nuclear reactor (E. Fumagalli - G. Verdelli) - December 1970.
- 50 - Contribution to experimental solution of the effect of heavy vibrations on an elasto-plastic oscillator (Ondrej Fischer) - May 1972.
- 51 - Il comportamento dinamico di dighe in materiale sciolto studiato per mezzo di modelli elastici (G. Oberti - A. Castoldi - M. Casirati) - Ottobre 1972.
- 52 - Il comportamento dinamico dei ponti sospesi studiato a mezzo di modelli (E. Lauletta - A. Castoldi) - Ottobre 1972.
- 53 - New trends in model research on large structures (G. Oberti - A. Castoldi) - January 1973.
- 54 - Stato e prospettive delle applicazioni industriali delle radiazioni nucleari (E. Fumagalli) - Marzo 1973.
- 55 - Verification par modèles des revêtements des tunnels (E. Fumagalli) - Mai 1973.
- 56 - New techniques of model investigation of the seismic behavior of large structure.
- 57 - Interpretazione delle misure di spostamento durante l'escavazione di una grande centrale in caverna (R. Riccioni) - Aprile 1973.
- 58 - Calcoli svolti per l'interpretazione delle misure di spostamento durante l'escavazione della centrale in caverna del lago Osljo (M. Fanelli - R. Riccioni) - Maggio 1973.
- 59 - L'impiego di elementi finiti di alto ordine nella meccanica dei terreni e delle rocce (S. Martinetti - G. Montani - R. Ribacchi - R. Riccioni) - Giugno 1973.
- 60 - Caméras de prises de vues pour le mesurage des déformations d'objets rapprochés (F. Bernini - M. Cuniatti) - Août 1973.
- 61 - Indagine sul comportamento di lastre in cemento armato sollecitate a flessione biassiale pura (L. Goffi - G. Simonetti) - Novembre 1973.
- 62 - Introduzione ai metodi di calcolo per elementi finiti (R. Riccioni) - Marzo 1974.
- 63 - Observations extensométriques sur des oeuvres en béton de grande épaisseur (barrage de Place Moulin) (L. Goffi) - Novembre 1974.
- 64 - Finite Element Analysis of Prestressed Concrete Pressure Vessel (M. Fanelli - R. Riccioni - G. Robutti) - November 1974.
- 65 - Triaxial State of Stress «Tiny Walled» PCPV for HTGR. Comparison with a Conventional «Thick Solution» (F. L. Scotto) - November 1974.
- 66 - Small Scale Models of PCPV for High Temperature Gas Reactors. Modelling Criteria and Typical Results (E. Fumagalli - G. Verdelli) - November 1974.
- 67 - Philosophie sur la technique des modèles statiques adoptée à l'ISMES pour les structures massives (E. Fumagalli) - Novembre 1974.
- 68 - Détermination des contraintes dans la console et les arcs du barrage de frère moyennant témoins sonores placés dans des cubes de béton préalablement soumis à étalonnage triaxial (L. Carati) - Novembre 1974.
- 69 - Observations on the Procedures and on the Interpretation of the Plate Bearing Test (G. Manfredini - S. Martinetti - P.P. Rossi - A. Sampaolo) - June 1975.
- 70 - Ultimate Load Capacity of Circular Strongly Reinforced Concrete Columns (G. Oberti) - June 1975.
- 71 - Nota su alcune esperienze di modellazione di frane di roccia eseguite all'ISMES (E. Fumagalli - G. F. Campanovo) - Agosto 1975.
- 72 - Contenitori in cemento armato precompresso per reattori a gas «HTGR» ed acqua bollente «BWR» indagini sperimentali su modelli in scala ridotta (E. Fumagalli - G. Verdelli) - Dicembre 1975.
- 73 - Examples of advanced geomechanical modelling (E. Fumagalli) - Febbraio 1976.
- 74 - Experimental techniques for the dynamic analysis of complex structures (A. Castoldi - M. Casirati) - Febbraio 1976.
- 75 - Concrete dam problems: An outline of the role, potential and limitations of numerical analysis (P. Bonaldi - A. Di Monaco - M. Fanelli - G. Giunnetti - R. Riccioni) - Giugno 1976.
- 76 - Contributo alla sperimentazione nelle tecniche di prefabbricazione (E. Fumagalli - L. Goffi) - Settembre 1976.
- 77 - The significance of model testing in problems of foundations and slopes (Prof. Dr. Ing. E. Fumagalli) - Settembre 1976.
- 78 - Contribution des modèles à l'évolution des barrages-voûte (E. Fumagalli) - Settembre 1976.
- 79 - Analisi tensionali ad elementi finiti di due soluzioni avanzate di contenitori in «C.A.P.» per reattori nucleari ad acqua ed a gas (M. Fanelli - R. Riccioni - G. Robutti) - Settembre 1976.
- 80 - Modelli matematici ad elementi finiti per lo studio della diffusione di inquinanti in correnti idriche naturali (P. Bonaldi - A. Di Monaco - M. Fanelli) - Settembre 1976.
- 81 - Finite element structural analysis of a P.C.P.V. for a B.W.R. (R. Riccioni - G. Robutti - F. L. Scotto) September 1976.
- 82 - Analysis of large underground openings in rock with finite element linear and non linear mathematical models (A. Di Monaco - M. Fanelli - R. Riccioni) - September 1976.
- 83 - Numerical analysis compared to model analysis for a dam subject to earthquakes (A. Castellani - A. Castoldi - M. Ionati) - September 1976.

## LAS ESPECIFICACIONES SISMICAS DE LA ENDESA PARA EL EQUIPO DE ALTA TENSION (1)

---

En los últimos 25 años, el diseño del equipo eléctrico de alta y muy alta tensión ha ido afirmando una tendencia hacia el empleo de elementos normalizados, de volumen relativamente reducido y que, con características eléctricas funcionalmente bien definidas, puedan ser combinados en aparatos de diferentes voltajes y capacidades. Una tendencia en este sentido puede detectarse, en mayor o menor grado, en el desarrollo de equipos tan diferentes como son los interruptores de potencia, los transformadores de medida, los desconectores, los pararrayos, etc.; es decir, todos aquellos aparatos que pueden ser englobados bajo el nombre de equipo primario de maniobra y de protección.

Esta tendencia hacia la composición de aparatos a partir de unidades normales se ha unido a la de racionalización de los elementos aisladores, para reducir en lo posible sus dimensiones y disminuir el número de piezas diferentes de porcelana.

Ambas tendencias pueden decirse que han provocado una convergencia, en los diseños de equipos de alta y de muy alta tensión, hacia disposiciones estructurales esbeltas y flexibles, con sus elementos dispuestos de manera que resulta, en general, propensa a la formación de respuestas elevadas a las oscilaciones de un temblor.

Los primeros equipos de hasta 154 kV con esta disposición, comenzaron a ser instalados por la ENDESA hacia 1950. Por entonces creíamos suficiente especificar, como condiciones sísmicas para estos equipos, que fueran capaces de resistir "una aceleración sísmica horizontal de 0,3g, y una vertical de 0,1g", en que "g" es la aceleración de gravedad, combinadas en la dirección más desfa-

(1) Versión revisada de un artículo presentado por F. Novoa al Congreso Panamericano de Ingeniería Mecánica, Eléctrica y Ramas Afines, 4a. reunión efectuada en Lima (Perú), del 7 al 13 de noviembre de 1971.

favorable. Es decir, elegíamos simplemente un factor sísmico relativamente menor entre los usuales de los códigos de entonces para la asismicidad de los edificios.

Los equipos, los seleccionábamos entre los que tuvieran una estructura favorable, en relación con las masas soportadas y adoptábamos, en general, disposiciones de instalación que evitaran la transmisión de esfuerzos durante un temblor, a través de las conexiones, introduciendo uniones flexibles o deslizantes, en las de tubos IPS, y dejando una huelga en las de cable.

Disponíamos el equipo con sus partes de alta tensión en un plano horizontal, soportado en estructuras reticulares de perfiles livianos de acero, relativamente rígidas. Intuitivamente, tendíamos a disponer una estructura separada para cada elemento importante, como ser, cada interruptor de 66 kV, cada polo de interruptor de 110 o de 154 kV y cada transformador de medida. Los desconectores, y algunos pararrayos, en razón de su peso más reducido, los disponíamos en una estructura común para los tres polos.

Hasta 1960, la experiencia acumulada a través de diversos sismos menores había confirmado que, en general, dichas medidas parecían acertadas, pero que, en determinados casos, era necesario considerar el efecto dinámico de las oscilaciones del temblor ya que, típicamente, por ejemplo, los relés sistema Buchholz de los transformadores, operaban incorrectamente debido únicamente a las sacudidas del mercurio de los contactos utilizados en ellos. Para tomar en cuenta estos efectos, y otros que podrían temerse en los mecanismos de operación de los interruptores, por ejemplo, agregamos en nuestras especificaciones la frase: "el equipo deberá operar correctamente bajo la acción de oscilaciones de frecuencia entre 1 y 10 Hz y amplitud no mayor que 10 mm".

Los terremotos de mayo de 1960 en la zona central - sur del país, cuatro de los cuales alcanzaron magnitudes Richter entre 7,5 y 8,5, causaron ciertos daños en nuestras instalaciones, siendo los principales, la destrucción de un banco de condensadores con unidades dispuestas en columnas, y la saltadura de sus vías de dos transformadores, con riesgo evidente de volcamiento. El análisis de éstos y su

comparación con desperfectos constatados en instalaciones bien proyectadas, como las de la acerería de Huachipato, nos hizo agregar a nuestras prácticas :

1) Aumento de los factores sísmicos de especificación a 0,5 g en horizontal y a 0,2 g en vertical, para tener en cuenta la disposición del equipo sobre estructuras algo flexibles y poco amortiguadas.

2) Exclusión efectiva de toda transmisión de esfuerzos entre partes sujetas a oscilaciones diferentes, por mejora de las conexiones flexibles y holgadas entre los equipos, y destierro definitivo de las conexiones en tubos IPS.

3) Consideración más cuidadosa de las disposiciones en columna, para evitar las de resistencia horizontal insuficiente.

4) Montaje de los transformadores de potencia sobre bases planas de concreto a ras del suelo, con anclajes dimensionados según 1).

En marzo de 1965, sin embargo, un temblor de magnitud Richter entre 7 y 7,5 en la zona central, produjo daños extensos en las instalaciones existentes en San Pedro, cerca de Quillota, y alcanzó a producir algunos daños en Cerro Navia y otras subestaciones en Santiago, en donde se midió una aceleración máxima horizontal en terreno de fundación, de 0,16 g.

En San Pedro, 35 columnas sobre 48 de los interruptores de aire comprimido de la compañía concesionaria de la distribución, se quebraron en la base. Estos interruptores se encontraban, cada 3 polos y 3 transformadores de corriente, sobre una estructura de entramado liviano, aparentemente rígida, proyectada por el fabricante. De la ENDESA, se derrumbaron dos polos de un interruptor de pequeño volumen de aceite, de disposición vertical muy elevada, arrastrando consigo dos transformadores de corriente, y se quebraron en la base 3 transformadores de potencial con aisladores muy débiles.

En Cerro Navia y otra subestación de la empresa distribuidora en Santiago, 3 columnas de interruptores como los de San Pedro, en estructuras similares, se quebraron en la base. Sin embargo, 6 columnas idénticas de la ENDESA a no más de 50 metros, y 30 columnas más desfavorables de 154 kV a no más de 150 metros de distancia, no sufrieron daños, estando sus polos correspondientes sobre estructuras separadas.

Concluimos, por lo tanto :

1) Que los factores sísmicos especificados para el equipo destruido habían resultado absolutamente inadecuados para representar el efecto dinámico del temblor.

2) Que, en Santiago, era evidente una influencia del tipo de estructura, que era favorable al sistema empleado por la ENDESA.

Esta, tenía colocada una orden importante por interruptores hasta 220 kV del mismo tipo que los afectados en San Pedro. Requerimos, por lo tanto, de los fabricantes, que investigaran en una mesa vibratoria, cuál era la acción dinámica de la mesa capaz de reproducir las rupturas constatadas, y determinar los medios necesarios para impedirias, bajo esa misma acción. Mientras tanto, estudiaríamos especificaciones que estábamos dispuestos a discutir con ellos, para determinar el grado final de seguridad que se alcanzaría contra los terremotos reales.

Una discusión más completa de los factores involucrados puede encontrarse en otro lugar (1); baste indicar aquí, que la solución sólo pudo ser encontrada a través de la disminución de la respuesta sísmica de las columnas, mediante el agregado de amortiguadores en la base de cada una de ellas. Como dichos amortiguadores involucraban una considerable elasticidad, debió suprimirse todo elemento de restricción lateral de las columnas, y establecer solamente conexiones flexibles entre ellas.

(1) CIGRE, Sesión de 1970, informe N° 23-02.

Para representar la acción dinámica de los temblores, adoptamos un "espectro de respuesta" de aceleración. Esta curva representa, con sus coordenadas, la máxima aceleración instantánea que llegará a tomar un oscilador lineal de un grado de libertad, de la frecuencia propia dada por la abscisa, cuando es sometido a una determinada curva de aceleraciones en función del tiempo. Se obtiene, descomponiendo la curva de aceleraciones en una sucesión de impulsos "a; Δ t", cada uno de los cuales, aislado, produciría una oscilación transiente amortiguada del oscilador. La oscilación resultante de éste, será la suma de dichas respuestas transientes que, en términos del cálculo operacional, está dada por la integral de convolución de la función de aceleraciones sobre la función de respuesta del oscilador, cuyo valor máximo dependerá fundamentalmente de la frecuencia propia y de la amortiguación de éste, y puede ser determinado por computador.

Comparando los espectros de respuestas calculados para marzo de 1965 en Santiago, los de otros dos temblores en Chile central y los efectos de los sismos en Huachipato en 1960, se resolvió adoptar la curva empírica:

$$a_{10\%} = 0.4 \sqrt{T} \leq 0.8 g$$

equivalente, grosso modo, al doble del espectro medio calculado por Housner para amortiguación 10 %, para el sismo de El Centro, en 1940, como representativa para comparar con la resistencia a la ruptura de las columnas.

Se pidió determinar la frecuencia propia y la amortiguación de las columnas mediante una prueba de oscilación libre, y aplicar luego en mesa vibratoria al equipo, la excitación sinusoidal que fuese capaz de producir en ellas la respuesta que les correspondería según la curva. Previamente, se habría verificado en la misma mesa, la frecuencia dinámica de resonancia de las columnas, mediante una prueba de excitación reducida, a frecuencia variable entre 0,5 y 20 Hz.

Los interruptores adicionales de los amortiguadores en la base de las columnas resultaron dotados de un factor de seguridad superior a 2, con respecto a la curva de respuesta mencionada. Sometidos a prueba los desconectadores y los transformadores de medida, se pudo ver que, en los primeros, la respuesta crítica de un buen diseño tendía a ser la de desplazamiento de los contactos, y no la de aceleración horizontal; y en los segundos, la frecuencia y amortiguación

relativamente altas de los buenos diseños, no los hacían peligrar, en general.

Mientras se realizaban estudios más completos y se obtenían los resultados de las pruebas, debieron emplearse, para los equipos del sistema El Toro, ordenados entre 1967 y principios de 1969 especificaciones parecidas.

Los estudios fueron demostrando, sin embargo, que la especificación de la respuesta de 1966, adolecía de defectos serios:

1) La respuesta constante supuesta para períodos inferiores a 0,5 s, no permitía coordinación lógica con el hecho evidente de que un elemento suficientemente rígido, tendría una respuesta no mayor que la del suelo.

2) La respuesta límite adoptada para dichos períodos, que abarcaron prácticamente toda la gama de diseños usuales de interruptores, desconectores y otros, junto con la fórmula de extrapolación para amortiguaciones inferiores a 10% (1), no explicaba satisfactoriamente la ruptura en masa de las columnas en San Pedro.

Estas contradicciones pudimos notar que tendían a desaparecer, si se adoptaba el método propuesto por Newmark y Hall en 1969 (2) para fijar respuestas máximas de diseño.

En dicho procedimiento, se hace uso del resultado del estudio comparativo de muchos espectros de respuesta de terremotos registrados en lugares cercanos al epicentro. Cuando dichos espectros de respuesta son representados en un gráfico logarítmico triaxial, cuyas ordenadas de máxima aceleración A, velocidad V y desplazamiento D hayan sido trazadas en función de la frecuencia propia f de manera de que satisfagan la condición del movimiento armónico simple de un oscilador:

$$A : g = 2\pi f \cdot V = 4\pi^2 f^2 \cdot D \quad (g = 980.665 \text{ cm/s}^2)$$

puede observarse en dicho gráfico que los espectros de máxima respuesta tienden a quedar representados por una máxima aceleración constante,

(1)  $a_n g_0 = a_{10} g_0 (10/n)^{1,4}$

(2) "Seismic Design Criteria for Nuclear Reactor Facilities, IV th World Conf. Earthq. Eng., Santiago, 1969, B-4, pp 37 - 50.

para las frecuencias elevadas, por una máxima velocidad constante para las frecuencias medias y por un máximo desplazamiento constante o decreciente, para las frecuencias bajas del oscilador.

Estudios como los de Kanai y otros muestran la relación que existe entre las máximas respuestas de aceleración, de velocidad y de desplazamiento en el terreno y la magnitud absoluta (magnitud Richter) y distancia al epicentro del temblor que se considere posible. Es posible, entonces, elegir, para las condiciones de sismicidad que se requieran, un juego de valores de respuestas máximas de aceleración, de velocidad y de desplazamiento en el terreno de fundación, del cual podrán ser obtenidos, mediante factores de multiplicación adecuados, según el método propuesto en el artículo citado, los espectros respuestas máximas para osciladores con diferentes factores de amortiguación.

De acuerdo con nuestra experiencia anterior y considerando las condiciones sísmicas en Chile, hemos llegado a que es aconsejable adoptar, como valores de máxima respuesta en el terreno de fundación, los de 0,5 g para la aceleración, de 60 cm/s para la velocidad y de 46 cm para el desplazamiento. Estos valores han sido considerados por los autores del artículo citado como recomendables en países sísmicos con registros insuficientes de terremotos destructivos, como sería el caso de Chile. Los valores coordinan, además, con los factores sísmicos utilizados hasta ahora por la ENDESA para elementos rígidos, que se seguirán utilizando.

En cuanto a la influencia posible de las estructuras soporte, nuestro estudio procuró abordarla a través del acoplamiento entre el oscilador que representa una columna del equipo y el oscilador que representa la estructura, soportando las masas de la base (CIGRE, ref. cit.). Aplicando los conceptos desarrollados por la teoría de las comunicaciones para el estudio de la propagación de señales aleatorias a través de circuitos oscilantes dados, puede llegarse, como se muestra en un estudio académico del autor, en preparación, a la valoración cuantitativa del efecto que tiene, sobre la respuesta del oscilador superior, la razón entre las frecuencias propias de dicho oscilador solo y del oscilador inferior solo, y la razón entre las masas de ambos.

Para una razón de frecuencias propias en las vecindades de 1, el factor de amplificación que representa para la respuesta del oscilador superior (la columna), su acoplamiento con el oscilador inferior (las masas de la base y la estructura), alcanza valores numéricos principalmente limitados por el valor de la razón entre las masas. Cuando dicha relación es, por ejemplo, de 1/6, el factor de multiplicación de la respuesta del oscilador superior puede alcanzar valores entre 4 y 5, para amortiguaciones como las que se presentan en las columnas o en las estructuras. Se creyó, por lo tanto, que circunstancias como éstas podrían dar la explicación de las rupturas de los interruptores de San Pedro, en 1965, en atención a que la masa del oscilador inferior, representante de la estructura, podría ser elevada, en razón del agrupamiento de 3 polos y de 3 transformadores de corriente sobre la misma estructura.

Estas ideas teóricas encontraron inesperada y dramática verificación en 1971.

Después del sismo de marzo de 1965, los interruptores de aire comprimido en San Pedro fueron mantenidos, por razones económicas, en las condiciones en que se encontraban antes del sismo. Aparte del reemplazo de las columnas destruidas por otras del mismo tipo, no sufrieron modificaciones en su disposición. En Cerro Navia, en cambio, 4 de los interruptores más importantes desde el punto de vista del servicio, fueron desmontados, para reemplazar sus estructuras soporte por otras rígidas, individuales para cada polo y para cada transformador de corriente.

El 8 de Julio de 1971, un nuevo terremoto afectó las provincias centrales del país. La intensidad en Santiago, fué ligeramente inferior a la de marzo de 1965; en San Pedro, fué igual que la de entonces. Los interruptores de San Pedro volvieron a sufrir prácticamente los mismos daños que en 1965 (1) y, en Santiago, en Cerro Navia, dos columnas de los interruptores cuyas estructuras no tuvieron modificaciones, se rompieron.

Nuevamente, sin embargo, no se constataron daños en los interruptores de 110 y de 154 kV de la ENDESA, a corta distancia. La nueva subestación de 220 kV de esta empresa en el mismo lugar, con interruptores de columnas amortiguadas, no sufrió tampoco

---

(1) De un total de 54 columnas, 46 resultaron quebradas en la base.

el más ligero daño o perturbación. Una subestación más pequeña de la ENDESA en la zona epicéntrica de este temblor, tampoco sufrió daños.

La investigación que se iniciara por este motivo, ha demostrado lo siguiente :

Los 3 polos de los interruptores afectados en San Pedro y Cerro Navia, van apoyados sobre dos vigas que corren a lo ancho de la estructura soporte. Dichas vigas trabajan libremente a la flexión, de modo que cuando se excita la oscilación de un polo lateral, oscilan con la misma amplitud, en dirección contraria al polo del centro, y en la misma dirección, el polo opuesto. Los tres polos forman por lo tanto un oscilador, con las vigas trabajando a flexión como elemento elástico. La frecuencia propia de este oscilador es muy similar a la de oscilación de las columnas sobre la base del polo. Se cumplen, por lo tanto, todas las condiciones para que exista un factor de amplificación del orden de 3,5 de la respuesta de las columnas.

Aceptando que, en Santiago, la máxima aceleración en el suelo, fué del orden de 0,15 g, la respuesta de una columna de estos interruptores, debido a su período propio y a su amortiguación, sería unas 4 veces superior, es decir, de 0,6 g. El factor de amplificación de la respuesta, por el apoyo flexible de los polos sobre las vigas mencionadas, llevaría sin embargo la respuesta total a  $3,5 \times 0,6 = 2,1$  g. Esta aceleración es justamente igual a la mínima de ruptura de las columnas, lo que explicaría las dos columnas rotas en Cerro Navia en esta ocasión.

En San Pedro, bastaría suponer una aceleración máxima del suelo de 0,25 g, para llegar a 3,5 g de respuesta total en las columnas, suficiente para explicar la ruptura en masa de ellas.

Este factor de amplificación por acoplamiento entre osciladores, resulta también de fundamental importancia para verificar el equipo solo. Esto es lo que se hace, cuando está asegurado que toda oscilación de la estructura de soporte se efectúe con frecuencia propia de 15 Hz o más, ya que entonces, la respuesta máxima de tal oscilador no podrá ser mayor que la respuesta en el terreno. Pero, aún en este caso, si se presenta una base de un grupo de columnas que no pueda ser considerada rígida en comparación con ellas, o un elemento

flexible liviano con su base fija sobre otro elemento flexible o, aún, una parte superior de columna considerablemente más liviana que una inferior y flexible, pueden presentarse, dentro del equipo mismo, condiciones suficientes para la aparición de un factor de amplificación considerable en las respuestas.

Es necesario concluir, por lo tanto, que los factores de verdadera importancia para la verificación de la asismicidad del equipo eléctrico de alta tensión serían:

1) Amplificación de las sollicitaciones sísmicas por la respuesta de un elemento flexible que quede dentro del rango de frecuencias típicas de este equipo.

2) Amplificación de las respuestas sísmicas por acoplamiento mutuo entre elementos flexibles de frecuencias propias similares combinados estructuralmente.

3) Transmisión indebida de esfuerzos entre elementos flexibles separados, por exceso de desplazamiento relativo entre los extremos de uniones eventuales entre ellos.

Las especificaciones sísmicas que hemos preparado, junto con tomar en cuenta nuestra experiencia descrita más arriba, dan la debida prominencia a dichos tres factores, en un procedimiento aproximado de verificación. El margen de duda y de variación que permite dicha aproximación, hacen necesario considerar, en la mayoría de los casos, pruebas tipo de vibración del equipo. Las pruebas exigibles, así como sus condiciones mínimas de ejecución han sido también consideradas en estas especificaciones.

FIM/LMBA

ESPECIFICACIONES SISMICAS PARA EL  
EQUIPO ELECTRICO DE ALTA TENSION ( $\leq 220$  kV)

0.- ALCANCE.

- 0.1.- Esta especificación se aplica al equipo eléctrico de tensión igual o inferior a 220 kV, en especial, al de disposición estructural relativamente esbelta, en columnas aislantes, como interruptores, transformadores de medida, desconectores y todos aquellos equipos o partes de alta tensión cuyas condiciones estructurales puedan considerarse asimilables a éstas.
- 0.2.- Otras especificaciones sísmicas que, en la presente, se consideran específicamente excluidas, son :
- a) Especificaciones sísmicas para el equipo eléctrico de muy alta tensión (mayor que 220 kV) ;
  - b) Especificaciones sísmicas para transformadores de poder;
  - c) Especificaciones sísmicas para instalaciones eléctricas primarias en Centrales y Subestaciones ;
  - d) Especificaciones sísmicas para instalaciones eléctricas auxiliares y de control, en Centrales y Subestaciones.

1.- GENERAL.

- 1.1.- El equipo eléctrico de alta tensión deberá estar diseñado de manera que sea capaz de resistir, sin daños ni perturbaciones de servicio, los efectos de movimientos sísmicos de las siguientes amplitudes máximas de oscilación horizontal, correspondientes al terreno de fundación (1) :

---

(1) Se supone un terreno firme de fundación. Si las condiciones de la obra obligan a fundar en terreno suelto o de relleno, estas características deberán ser revisadas.

Aceleración, menor o igual que 0,5 g.

Velocidad, menor o igual que 60 cm/s.

Desplazamiento, menor o igual que 46 cm.

en que "g" designa la aceleración de gravedad ( $980 \text{ cm/s}^2$ ).

En los casos en que se señale expresamente, se considerará también un movimiento oscilatorio vertical de aceleración máxima 0,2 g.

- 1.2.- Se aceptará que las respuestas horizontales máximas más desfavorables en cuanto a aceleración, velocidad o desplazamiento, de un oscilador simple sometido a movimientos sísmicos de duración media y con las características máximas indicadas en el artículo 1.1, quedan dadas por los espectros de respuesta de la fig. 1, en función de la frecuencia propia y de la amortiguación de dicho oscilador.

## 2.- DISPOSICION GENERAL Y MONTAJE DEL EQUIPO.

- 2.1.- El equipo puede ser clasificado en dos tipos de disposición estructural :

Tipo I, los equipos que, por tener sus partes principales de alta tensión encerradas en una envoltura metálica al potencial de tierra, presentan una disposición estructural cuya rigidez y características elásticas no están generalmente limitadas por razones de diseño.

Tipo II, los equipos que, por tener sus partes principales de alta tensión soportadas en aisladores, o por consistir esencialmente su estructura en un aislador, tienen una disposición estructural básicamente limitada por razones de diseño.

- 2.2.- Los equipos del tipo I deberán estar contruidos de manera que, al ser fijados sobre una base rígida con los medios previstos al efecto en su diseño, y bajo una fuerza horizontal igual al 50 % de su peso, aplicada en su centro de gravedad, el desplazamiento de éste con respecto a la base, por efecto de las deformaciones elásticas en la estructura, no sea superior a 0,5 mm.

- 2.3.- Los equipos del tipo II deberán estar, preferentemente, contruidos de manera que sus elementos de alta tensión consistan en simples columnas, estructuralmente aisladas y soportadas solamente en la base, con el objeto de facilitar su oscilación libre durante el temblor.
- 2.4.- El equipo estará, en general, destinado a ser montado apoyado sobre estructuras relativamente rígidas, que aseguren una frecuencia propia de oscilación, del centro de gravedad del equipo o de cada grupo de columnas soportadas en una base común, igual o mayor que 15 Hz.
- 2.5.- Los equipos del tipo II que consten de una sola columna, sobre una base de dimensiones pequeñas en relación con las de aquella, deberán poder ser montados sobre estructuras de rigidez inferior a la indicada en el artículo anterior, capaces solamente de asegurar una frecuencia entre 7,5 y 12 Hz en el centro de gravedad del equipo.

### 3.- ESTRUCTURAS DE SOPORTE.

- 3.1.- Cuando el diseño del equipo incluya estructuras de soporte destinadas a ser ancladas directamente a la fundación, o cuando la orden de compra incluya las estructuras de soporte, se interpretará que éstas cumplen con la condición del artículo 2.4, si se verifica que :

El desplazamiento horizontal del centro de gravedad del equipo, por efecto de desplazamiento horizontal de la estructura en los puntos de fijación del equipo y por efecto de la inclinación del plano de sujeción del equipo con respecto a la horizontal, cuando actúan sobre el equipo y la estructura fuerzas horizontales iguales al 50 % de los pesos en los centros respectivos de gravedad, sea igual o menor que 0,5 cm.

- 3.2.- La verificación indicada en el artículo 3.1 se hará tomando en cuenta solamente las deformaciones elásticas de la estructura soporte, sin incluir desplazamientos de pernos en los nudos o asentamientos en la fundación. Naturalmente, la ejecución de los nudos deberá ser adecuada para prácticamente eliminar la posibilidad de dichos desplazamientos, durante el período de formación de la respuesta máxima de la estructura al movimiento oscilatorio del temblor.

- 3.3.- En el caso de que una misma estructura sirva para soportar varios grupos de columnas, cada grupo en una base separada, la verificación indicada en el artículo 3.1 deberá considerar la fuerza horizontal actuando en cada grupo, en el sentido más desfavorable al desplazamiento del centro de gravedad de cualquiera de ellos.
- 3.4.- La resistencia de las estructuras soporte que cumplan con el artículo 3.1 deberá ser verificada agregando a las cargas usuales en este tipo de estructuras, un esfuerzo sísmico horizontal igual al 50 % de los pesos de las estructuras y del equipo, actuando en los respectivos centros de gravedad, y en la dirección más desfavorable. La resistencia de los puntos de anclaje a la fundación deberá verificarse agregando, además un esfuerzo sísmico vertical igual al 20 % de los pesos, en la dirección más desfavorable al volcamiento de la estructura.

#### 4.- VERIFICACION DEL EQUIPO.

- 4.1.- El equipo del tipo I que cumpla con el artículo 2.2, deberá verificarse como sigue :
- 4.1.1.- Todo elemento o grupo de elementos, cuya frecuencia propia de oscilación, determinada según el capítulo 7, sea igual o superior a 15 Hz, deberá resistir una aceleración horizontal igual a 0,5 g y una vertical igual a 0,2 g combinadas en la dirección más desfavorable, sin daños para el elemento o grupo de elementos ni perturbaciones para el servicio.
- 4.1.2.- Si algún elemento o grupo de elementos tiene una frecuencia propia de oscilación inferior a 15 Hz, dicho elemento o grupo de elementos deberá ser sometido a las mismas verificaciones que se especifican para elementos del equipo del tipo II, según las disposiciones del artículo 4.2.
- 4.2.- Los equipos del tipo II que cumplan con las condiciones de los artículos 2.3 y 2.4, serán verificados como sigue :
- 4.2.1.- Cada elemento, o porción de elemento, cuya columna sea de sección transversal uniforme o asimilable a ella, podrá ser considerado como un oscilador simple, con la masa total que soporta concentrada en su centro de gravedad, y con la frecuencia propia de oscilación y el factor de amortiguación que se deducen de su prueba según el capítulo 7.

4.2.2.- Para cada elemento definido como en 4.2.1, supuesto soportando el conjunto más desfavorable de masas a que está destinado, deberá verificarse :

- a) que resiste, en las condiciones que se fijan en 4.4, una aceleración horizontal en la dirección más desfavorable, de valor igual al que se deduce para la frecuencia propia del elemento, en la curva de respuesta que corresponde a su factor de amortiguación, en el gráfico de fig. 1;
- b) que es capaz de tomar, en la dirección más desfavorable, sin que ninguna de sus partes sobrepase las condiciones 4.4 ni altere las condiciones de trabajo previstas en el diseño, un movimiento oscilatorio de la amplitud que se deduce, para su centro de gravedad, según su frecuencia propia, en la curva mencionada.
- c) que no dará lugar a perturbaciones en el servicio cuando sus respuestas de aceleración y de desplazamiento sean las determinadas según a) y b).

4.2.3.- Toda unión entre elementos diferentes del equipo deberá permitir, sin que aparezca un esfuerzo apreciable de reacción sobre ellos, un desplazamiento relativo entre sus extremos, igual a la combinación más desfavorable de movimientos determinados según 4.2.2.b) para los respectivos elementos. Si un elemento puede asimilarse a una columna con masa repartida uniformemente, deberá tomarse en cuenta, para este objeto, que el desplazamiento de su parte superior puede alcanzar a 3 veces el valor del desplazamiento en el centro de gravedad.

4.2.4.- Cuando un elemento de frecuencia propia de oscilación inferior a 15 Hz, tenga su base de oscilación fija sobre otro elemento de frecuencia propia inferior a 15 Hz, el elemento soportado deberá verificarse como en 4.2.2 y 4.2.3, pero con sus respuestas de aceleración y de desplazamiento amplificadas por el siguiente factor :

$$k = (m_2/m_1) \quad 1,8(f_1/f_2 - 0,5) \quad \text{para } 0,5 \leq f_1/f_2 \leq 1$$

$$k = (m_2/m_1) \quad 1,2(f_2/f_1 - 0,25) \quad \text{para } 1 \leq f_1/f_2 \leq 1$$

siendo "k" un factor de multiplicación, "m<sub>1</sub>" la masa oscilante del elemento soportado y "m<sub>2</sub>" la masa oscilante que corresponde al elemento soportante, "f<sub>1</sub>" la frecuencia propia del elemento soportado y "f<sub>2</sub>" la frecuencia propia que corresponde al elemento soportante. Cuando este último está representado por la base del elemento soportado, sujeta a una oscilación angular de su plano de fijación, la razón de masas deberá reemplazarse por la razón de momentos de inercia en torno al eje respectivo.

Es importante, en la determinación del factor de multiplicación "k", que en el valor de la masa "m<sub>2</sub>" se considere el efecto de todas las masas (o momentos de inercia) que contribuyan simultáneamente al modo de oscilación de que forma parte el elemento soportante.

Para  $f_1/f_2 < 0,5$  o para  $f_1/f_2 > 4$ , el factor de multiplicación podrá considerarse igual a 1, cualquiera que sea el valor de la razón "m<sub>2</sub>/m<sub>1</sub>".

- 4.3.- Los equipos del tipo II que se encuentran en las condiciones del artículo 2.5, deberán ser verificados como en el artículo 4.2, tomando en cuenta que la estructura soporte representa un elemento oscilante, que introducirá un factor de amplificación de las respuestas, como se indica en 4.2.4. Se supondrá como mínimo, en estos casos, un factor k = 1,5.
- 4.4.- La resistencia de los elementos de los equipos considerados en los artículos 4.1 a 4.3 será considerada aceptable, cuando las tensiones elásticas máximas que resulten en cada una de las piezas, para las condiciones más desfavorables de las aceleraciones de verificación, sean inferiores a la carga unitaria mínima de ruptura dinámica de los materiales frágiles o al límite inferior de fluencia de los materiales dúctiles que las componen, para el tipo de trabajo que corresponda a la respuesta, teniendo en cuenta todas las concentraciones de forma que pueden provenir de la disposición final de montaje de la pieza. El trabajo de las piezas, en las condiciones de carga señaladas, no podrá implicar la alteración de ninguna de las condiciones adecuadas para el servicio en otras piezas.
- 4.5.- Las verificaciones detalladas previstas en los artículos 4.1 a 4.3 podrán ser dispensadas en aquellos elementos cuya resistencia mínima al tipo de trabajo proveniente de la respuesta

(\*)...verificación sumada de las aceleraciones específicas de servicio, con inferioridad.....

al temblor, en las condiciones prescritas en 4.4, sea igual o superior a 4  $\sigma$ , verificada según el capítulo 6.

- 4.6.- Los equipos del tipo II cuya disposición estructural no cumpla con las disposiciones del artículo 2.3, por presentar restricciones hiperestáticas en la estructura de sus elementos, no podrán ser sometidos a verificación bajo los métodos aproximados del presente capítulo. Sólo podrán ser verificados representando su estructura por un número suficiente de masas concentradas para poder acudir sus diferentes modos de oscilación, sometiénolos a prueba como se indica en el artículo 7.14 para determinar las características oscilatorias de dichos modos, y calculando luego las solicitaciones más desfavorables de sus elementos, por la combinación de las respuestas de los diferentes modos, calculada según los espectros de la fig. 1. Dichas solicitaciones más desfavorables deberán cumplir con el artículo 4.4.

#### 5.- ADAPTACION DEL EQUIPO A LAS CONDICIONES SISMICAS.

- 5.1.- En el caso de que algún elemento del equipo no satisfaga las condiciones que se indican en el capítulo 4, podrán aceptarse modificaciones en el diseño bajo las siguientes condiciones :
- a) Antes de recurrirse al aumento de la resistencia de las piezas afectadas, deberán haberse agotado las posibilidades de reducir cualquier factor eventual de amplificación de la respuesta del elemento por motivos como los señalados en 4.2.4, y las de reducir las respuestas propias del elemento a través del aumento de su factor de amortiguación o de la modificación de su frecuencia propia de oscilación.
  - b) Todo efecto de amortiguación deberá introducirse, en lo posible, en el lugar y del modo en que incida más directamente en la reducción de la respuesta del elemento afectado.
  - c) La modificación deberá hacerse de manera que no se produzca una pérdida apreciable de ninguna de las cualidades de servicio o de mantención ya logradas para el equipo en su diseño normal.
  - d) La modificación, tanto en su diseño como en sus materiales, deberá estar sancionada por una clara experiencia anterior del fabricante en dispositivos similares, sometidos a condiciones de servicio comparables con las que deberá satisfacer en el equipo modificado.

5.2.- En igualdad de condiciones, se dará preferencia :

- a) Al equipo que con su diseño normal, satisfaga las condiciones sísmicas de las presentes especificaciones, frente al equipo que requiera de modificaciones.
- b) Al equipo cuyas modificaciones consistan sólo en el reemplazo de partes del diseño normal, por partes adecuadas de diseños normales para otras condiciones de servicio.
- c) Al equipo que presente un factor de seguridad más adecuado en el cumplimiento de las presentes especificaciones.
- d) Al equipo cuyas características de respuesta puedan adaptarse más favorablemente a posibles variaciones individuales en el acelerograma de un determinado movimiento sísmico, y a posibles variantes en la combinación más desfavorable de sollicitaciones dentro de los máximos señalados en el artículo 1.1.

5.3.- Sólo podrán aceptarse disposiciones que alteren el montaje del equipo, con respecto a lo especificado en el artículo 2.4, cuando se demuestre :

- a) que la solución recomendada satisface las condiciones del artículo 5.1 y representa ventajas en el sentido del artículo 5.2;
- b) que se pueda realizar una prueba efectiva para las condiciones de respuesta más desfavorables a movimientos sísmicos de las características señaladas en el capítulo 1;
- c) que existe una ventaja económica capaz de compensar los mayores costos que pueda representar el nuevo sistema de montaje;
- d) que el sistema de montaje no interfiera con la disposición general del resto del equipo en la subestación.

#### 6.- VERIFICACIONES Y PRUEBAS EXIGIBLES.

- 6.1.- El fabricante de cualquier equipo de alta tensión deberá proporcionar, junto con la propuesta, la frecuencia de oscilación de cualquier elemento o grupo de elementos susceptible de ser excitado en vibración por las oscilaciones de un temblor.

- 6.2.- Para aquellos elementos o grupos de elementos cuya frecuencia propia quede por debajo de 15 Hz, deberá proporcionarse además el factor de amortiguación de las oscilaciones, expresado en por ciento de la amortiguación crítica.
- 6.3.- En el equipo del tipo I, vale decir, interruptores, transformadores de medida o especiales en estanque a tierra y con aisladores de paso, equipos blindados con carcasa a tierra y similares, la estructura del equipo y sus soportes deberán ser verificados de acuerdo con lo dispuesto en el artículo 2.2 y el capítulo 3. Todo elemento o grupo de elementos susceptible de ser excitado en vibración deberá ser sometido a las verificaciones que correspondan según el capítulo 4, previa determinación de su frecuencia propia de oscilación y de su factor de amortiguación en conformidad con los artículos 7.1 a 7.3.
- 6.4.- Si en un equipo del tipo I pueden existir dudas respecto de la capacidad efectiva, del conjunto o de cualquiera de sus elementos, para cumplir sin reparo las condiciones del capítulo 4, dicho equipo deberá ser sometido a una prueba de respuesta máxima en mesa vibratoria, como se indica en el capítulo 7. Si la duda se restringe a la resistencia estructural de un elemento o grupo de elementos dados, la prueba podrá restringirse a una de resistencia mínima a la ruptura, según el artículo 7.4.
- 6.5.- El equipo del tipo II, es decir, interruptores de aire comprimido o pequeño volumen de aceite, con sus cámaras de ruptura sobre columnas aislantes, desconectores, transformadores de medida de columna, pararrayos y otros elementos de alta tensión similares, en columnas flexibles aislantes, deberá cumplir con los artículos 2.3 a 2.5 y el capítulo 3 cuando corresponda, y cada uno de sus elementos deberá ser verificado de acuerdo con el capítulo 4. Para esto, deberán determinarse la frecuencia propia y la amortiguación de ellos, de acuerdo con los artículos 7.1 a 7.3.
- 6.6.- El equipo del tipo II que consista en grupos de columnas con relación funcional entre ellas, o que contenga en sus columnas otros elementos susceptibles por sus respuestas de aceleración o de desplazamiento, como son los interruptores de potencia, desconectores, algunos transformadores de medida, pararrayos y otros, deberá ser sometido a pruebas tipo de aceptación en mesa vibratoria, como se indica en 7.5 y siguientes. Estas pruebas se harán además de las verificaciones 6.5, que necesariamente deberán incluir la de todo elemento susceptible interior. Como quiera que alguno de dichos elementos resulte crítico en el sentido de las condiciones del capítulo 4, deberá ser expresamente tomado en cuenta durante la prueba, considerando, en caso necesario, las disposiciones del artículo 7.12.

6.7.- Los equipos o elementos del tipo II que consistan en simples columnas y que no presenten partes que resulten tan críticas en sus respuestas como la misma columna, como es el caso de diversos transformadores de medida y pararrayos, y de los aisladores soportes y de paso, terminales para cable y similares en general, en lugar de la prueba especificada en 6.6, podrán ser sometidos a una prueba de mínima resistencia dinámica horizontal, como se indica en 7.4, para la respuesta de aceleración que les corresponda según el capítulo 4.

La determinación de la respuesta, con determinación previa de la frecuencia propia y del factor de amortiguación, podrá además ser evitada en aquellos elementos de disposición estructural homogénea, como aisladores soportes y de paso, terminales para cable, etc., siempre que el elemento sea capaz de resistir en esa prueba, según 7.4, una respuesta de valor igual o superior a 4 g.

#### 7.- CONDICIONES MÍNIMAS PARA LAS PRUEBAS.

- 7.1.- Para la determinación de la frecuencia propia de los elementos, según se pide en los artículos 6.3 y 6.5, el equipo, en condiciones reales de servicio, será fijado, por los medios previstos al efecto en su diseño, sobre una base rígida. Sobre el centro de gravedad de cada uno de los elementos cuya frecuencia se requiere determinar se aplicará una tracción, en la dirección de la máxima amplitud de las oscilaciones, de valor no inferior a  $1/3$  del peso del elemento oscilante, y se registrarán las oscilaciones que el elemento efectúe por segundo, cuando se interrumpa bruscamente la tracción aplicada.
- 7.2.- Para la determinación del factor de amortiguación, se aplicará el mismo procedimiento que en el artículo anterior, pero en este caso, el registro de las oscilaciones deberá realizarse por medios que proporcionen sensibilidad y precisión suficientes para determinar el decremento de las oscilaciones en función del tiempo transcurrido desde la interrupción de la tracción. El factor de amortiguación equivalente se determinará de acuerdo con el gráfico de la figura 2, a través de la sucesión de máximos de las ondas en la zona del registro en que el decremento aparece con claridad y precisión suficientes.
- 7.3.- Cuando el equipo contenga diversos elementos susceptibles de vibración, las pruebas de los artículos 7.1 y 7.2 se efectuarán aplicando tracciones en los centros de gravedad de las diversas masas sujetas a oscilación, y registrando simultáneamente las oscilaciones de los puntos correspondientes a las mayores amplitudes, para tratar de detectar todos los modos de oscilación de la

disposición. En estos casos, es posible que el decrecimiento de las oscilaciones de un elemento se vea interferido por batimientos con las oscilaciones de otro elemento de frecuencia parecida, en cuyo caso deberá procederse como se indica en la fig. 2.

7.4.- La prueba de resistencia dinámica mínima a la ruptura horizontal prevista en el artículo 6.7, será efectuada en forma similar a la del artículo 7.1 pero aplicando una tracción igual a unas ~~tres~~ <sup>1,3</sup> veces la respuesta de aceleración que corresponde al elemento según el capítulo 4.; La prueba deberá efectuarse sucesivamente a cada elemento definido según el artículo 4.2.1, y será necesario registrar las aceleraciones instantáneas en el centro de gravedad del elemento, en función del tiempo transcurrido desde que se interrumpe bruscamente la tracción. El valor cuadrático medio de las dos primeras semiondas, deberá alcanzar para cada elemento, un valor igual o mayor que  $a/\sqrt{2}$  (siendo "a" la respuesta de aceleración). El equipo sometido a la prueba no deberá presentar, después de ésta, ningún daño, deformación o filtración y deberá estar plenamente apto para resistir cualquiera de las pruebas especificadas de recepción.

7.5.- Las pruebas en mesa vibratoria que se prescriben en el artículo 6.6 deberán ser realizadas en un laboratorio autorizado que cuente con el equipo y la experiencia necesarios para la prueba.

Las pruebas consistirán en la aplicación, en régimen forzado, de oscilaciones sinusoidales horizontales, a la base del equipo en condiciones reales de servicio para :

- a) Verificar las frecuencias de resonancia de sus distintos modos o elementos (artículos 7.9 y 7.10) ;
- b) Reproducir en los distintos elementos las respuestas máximas que les correspondan según las especificaciones del capítulo 4, para comprobar si se cumplen las principales condiciones establecidas para ellas (artículo 7.11).

Se reemplaza artículo 7.5 b. Ver página 1.

7.6.- La prueba deberá efectuarse sobre un conjunto completo del equipo en condiciones de servicio. Este conjunto deberá comprender todos aquellos elementos montados en columnas sobre una base común, la que deberá ser fijada por los medios previstos en su diseño, y teniendo especial cuidado de no alterar sus condiciones naturales de rigidez, a una mesa vibratoria de capacidad suficiente para la masa y dimensiones del conjunto, según las disposiciones del artículo 7.13.

- 7.7.- En el caso de conjuntos con diferentes planos verticales de simetría, la prueba deberá efectuarse aplicando oscilaciones en la dirección de cada uno de estos planos. Si el conjunto puede alterar sus condiciones estructurales cuando se encuentra en distintas condiciones de servicio, como sería el caso de un polo de desconector en posiciones "abierto" o "cerrado", la prueba deberá efectuarse en cada una de dichas condiciones de servicio.
- 7.8.- Durante la prueba deberán registrarse las variaciones instantáneas en función del tiempo de los siguientes valores cuando menos :
- a) respuesta de aceleración horizontal en el centro de gravedad de cada uno de los elementos sujetos a verificación;
  - b) tensiones elásticas máximas en no menos de dos puntos de la pieza más solicitada por la respuesta de cada elemento;
  - c) desplazamiento relativo entre aquellas piezas cuya respuesta de desplazamiento pueda ser de importancia para el resultado de la prueba (contactos de un desconector por ej.);
  - d) desplazamientos de la base del conjunto con respecto a la mesa vibratoria, en un número suficiente de puntos como para caracterizar los modos de oscilación propios de dicha base;
  - e) aceleración o desplazamiento de la mesa vibratoria.

El registro de las respuestas de aceleración indicado en a) deberá indicar valores medios cuadráticos. Las lecturas de los detectores de tensiones del punto b) deberán ser calibradas aplicando en cada elemento una fuerza horizontal variable entre 0 y 50 % de su peso oscilante, para registrar las lecturas correspondientes.

- 7.9.- Para una amplitud constante de oscilación de la mesa, tal que la respuesta de ninguno de los elementos sobrepase un 80 % de la máxima respuesta sísmica que le corresponde según el capítulo 4, se efectuará una prueba de frecuencia variable, haciendo variar la frecuencia por escalones, y manteniéndola constante en cada escalón durante un tiempo suficiente para que se establezca la máxima respuesta de los elementos a esa frecuencia de excitación. La prueba se repetirá para distintas amplitudes de la mesa, hasta lograr registros de respuestas máximas en los distintos elementos del equipo con lecturas no inferiores a 10 veces la mínima sensibilidad de la medida, para frecuencias de excitación entre 0,5 y 20 Hz.

- 7.10.- Los resultados de la prueba 7.9 serán representados en curvas de respuesta de cada elemento en función de la frecuencia de excitación, para diferentes amplitudes constantes de excitación. En estas curvas aparecerán máximos correspondientes a diferentes resonancias secundarias, que podrán ser identificados por interpretación de los registros en 7.8. En el caso de efectos no lineales o semiplásticos de amortiguación, la frecuencia de resonancia de cada elemento variará apreciablemente en función de la amplitud de excitación, por lo que deberá ser estimada por extrapolación de dicha variación.
- 7.11.- A cada una de las frecuencias correspondientes a una resonancia en las curvas indicadas en 7.10, se efectuará una prueba de excitación a frecuencia constante, con una amplitud tal que la respuesta media cuadrática del elemento o modo correspondiente sea igual a la máxima que le corresponde según el capítulo 4. La amplitud de excitación necesaria en la mesa, se determinará aproximadamente de la razón respuesta-excitación obtenida para esa frecuencia durante la prueba 7.9.
- 7.12.- En caso de que la excitación de un elemento a la respuesta que le corresponde según capítulo 4, no sea posible por el procedimiento establecido en el artículo 7.11, debido a que se sobrepase la respuesta correspondiente a un elemento de apoyo del elemento en cuestión, o cuando el elemento no sea accesible para medir su respuesta, deberá realizarse una prueba separada sobre dicho elemento, montado sobre una base rígida, fijándolo por medios idénticos a aquellos por los que va montado en el equipo en condiciones reales.
- 7.13.- Las pruebas que se especifican en el artículo 7.5 deberán ser realizadas en una instalación de las siguientes características mínimas :
- a) La mesa vibratoria deberá ser de dimensiones y masa suficientes para que se pueda lograr una oscilación predominantemente sinusoidal con el equipo montado sobre ella en condiciones de prueba. Se interpretará cumplida esta condición cuando la amplitud de la suma de las armónicas en la onda de desplazamiento de la mesa no sobrepase un 15 % de la amplitud de la fundamental.
  - b) La frecuencia de la mesa deberá ser ajustable entre 0,5 y 20 Hz con una precisión mejor que el 1 % del valor de la frecuencia ajustada, con el objeto de lograr estabilidad de excitación en los puntos de resonancia.

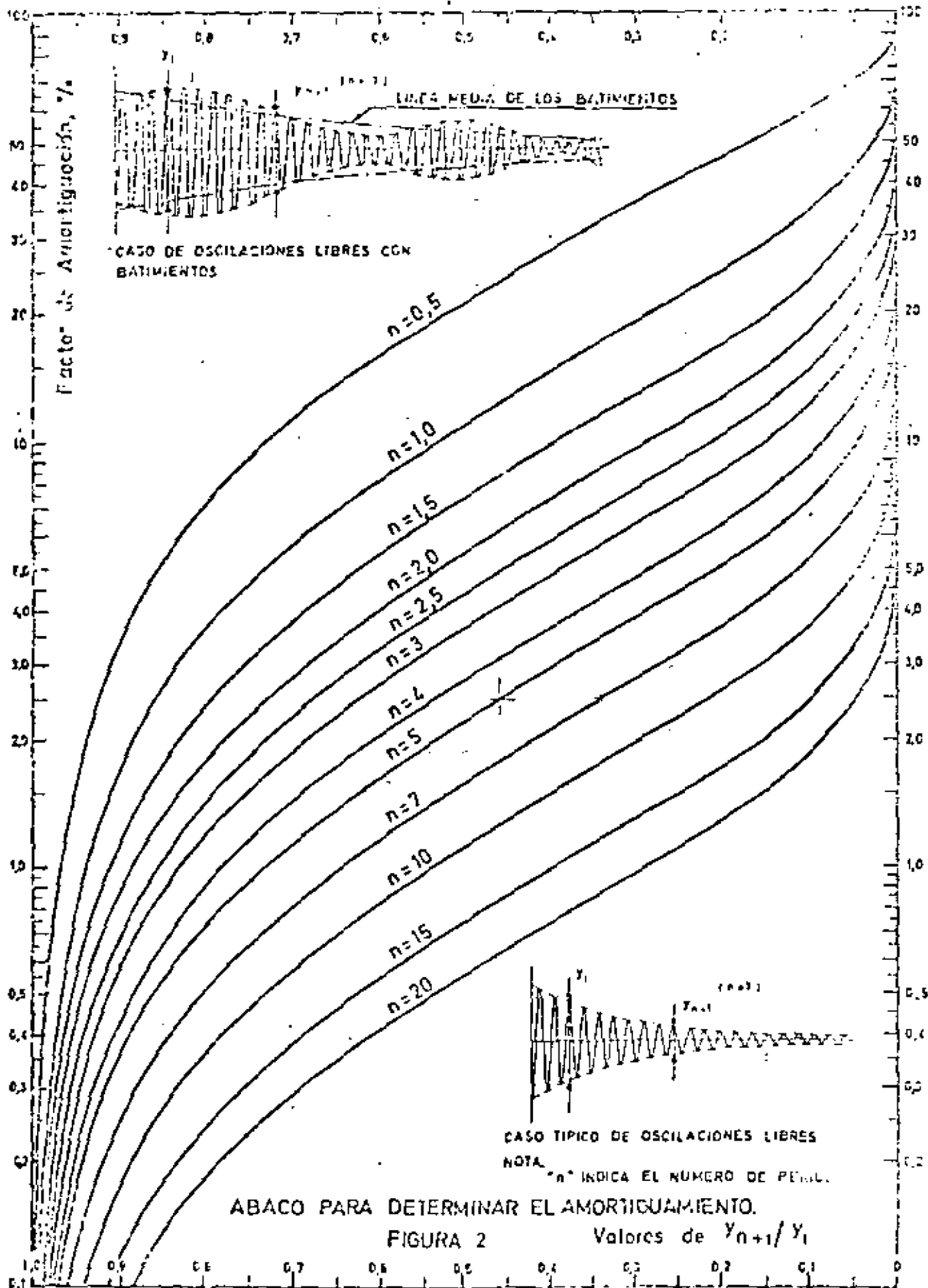
7.14.- Los equipos del tipo II, cuya disposición estructural no queda dentro de las disposiciones del artículo 2.3, deberán ser sometidos a una investigación detallada de sus modos de oscilación, aplicando en lo posible métodos similares a los de los artículos 7.1 a 7.3. No se puede asegurar que las respuestas máximas de sus elementos sean posibles de obtener durante una prueba como la del artículo 7.12, por lo que será necesario verificarla, en todo caso, de la combinación por cálculo de las respuestas de sus distintos modos de oscilación, como se indicó en el artículo 4.6.

#### 8.- APLICABILIDAD DE LAS PRESENTES ESPECIFICACIONES.

8.1.- Dado que las disposiciones de las presentes especificaciones se basan en muchos casos en una representación aproximada de las condiciones reales, los casos de dudas solo podrán ser resueltos mediante la discusión teórica de un modelo más detallado de la estructura del equipo, en forma similar a la indicada en los artículos 4.6 y 7.14.

#### Modificación del artículo 7.5.

b) Reproducir en los distintos elementos las respuestas máximas que le correspondan según las especificaciones del capítulo 4 (véase 7.11). Las tensiones elásticas máximas durante esta prueba, combinadas con las que se calculen para los esfuerzos de servicio especificados, deberán quedar dentro de los límites del artículo 4.4. El equipo no deberá presentar, después de la prueba, ningún daño, desplazamiento ni alteración de sus elementos, y deberá encontrarse plenamente apto para pasar cualquiera de las otras pruebas de recepción especificadas.



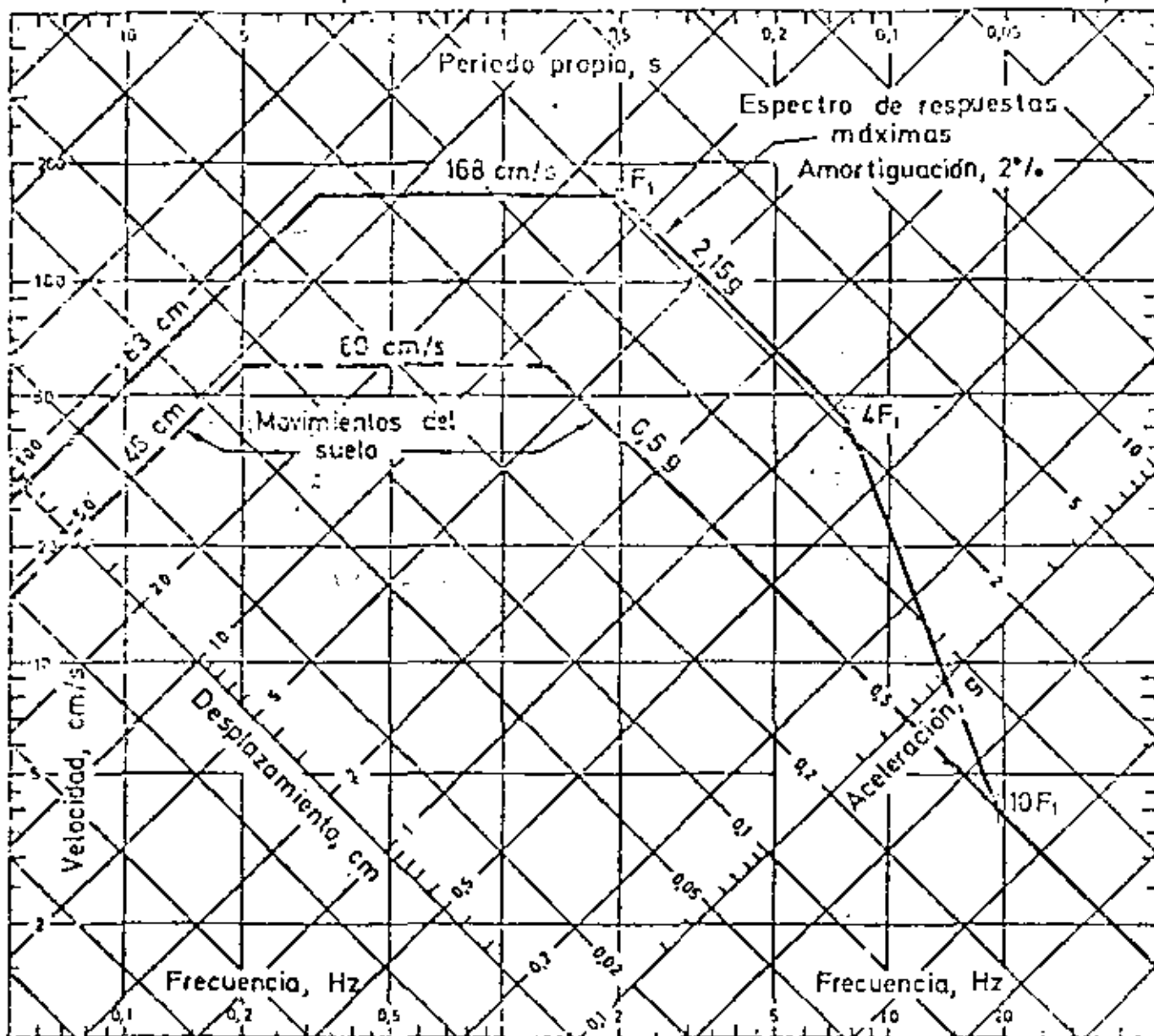


FIGURA 1

FACTOR DE AMORTIGUACION, %	0	0,5	1	2	5	7	10	20
AMPLIFICACION DE LA ACELERACION	6,4	5,8	5,2	4,5	2,6	1,9	1,5	1,2
AMPLIFICACION DE LA VELOCIDAD	4,0	3,6	3,2	2,8	1,9	1,5	1,3	1,1
AMPLIFICACION DEL DESPLAZAMIENTO	2,5	2,2	2,0	1,8	1,4	1,2	1,1	1,0

NOTA:

PARA OBTENER EL ESPECTRO DE RESPUESTAS MAXIMAS CORRESPONDIENTE A UN FACTOR DE AMORTIGUACION DADO, SE AMPLIFICARAN LAS RESPUESTAS CORRESPONDIENTES A "MOVIMIENTOS DEL SUELO" POR LOS VALORES INDICADOS EN LA TABLA, INTERPOLANDO LINEALMENTE PARA FACTORES DE AMORTIGUACION INTERMEDIOS. DONDE SE CORTAN LA LINEA DE RESPUESTA MAXIMA DE VELOCIDAD CON LA DE RESPUESTA MAXIMA DE ACELERACION, SE OBTIENE LA FRECUENCIA  $F_1$ , DE LA CUAL SE DEDUCE LA FORMA DEL ESPECTRO, A TRAVES DE LOS PUNTOS  $4F_1$  Y  $10F_1$ , COMO SE INDICA EN EL GRAFICO ESTE PROCEDIMIENTO ES EL PROPUESTO POR NEWMARK Y HALL (4TH WORLD CONF. EARTHQ. ENG., 1969)

"COUNTERMEASURES FOR EARTHQUAKES

IN

THE ELECTRIC UTILITY INDUSTRY OF JAPAN"

by

K. Anjo

and the

Japan IERE Council

Presented at 11th Annual Meeting

INTERNATIONAL ELECTRIC RESEARCH EXCHANGE

Tokyo, Japan

October 13-15, 1980

- President Hiroshi NARITA
- Chairman Naohel YAMADA
- Vice Chairman Ichiro HORI
- Executive Secretary Kentichi MASUI

- 1. Introduction ..... 1
- 2. The Earthquake Hazard ..... 1
- 3. Experiences and Lessons Derived from the Miyagiken-oki Earthquake ..... 2
  - 3.1 Damage to Substations ..... 3
  - 3.2 Damage to Transmission and Distribution Facilities ..... 4
- 4. Countermeasures for Earthquakes by the Electric Utilities ..... 4
  - 4.1 Substation Facilities ..... 4
  - 4.2 Nuclear Power Facilities ..... 6
  - 4.3 Hydro-power Dam Installation ..... 6
  - 4.4 Thermal Power Generating Facilities ..... 6
  - 4.5 Transmission Facilities ..... 6
  - 4.6 Distribution Facilities ..... 7
  - 4.7 Telecommunication Equipment and Computers ..... 7
  - 4.8 Service Restoration Policies ..... 7
  - 4.9 Research Needs ..... 8
- 5. Conclusion ..... 8
  - Tables 1 to 11 ..... 9 to 16
  - Figures 1 to 10 ..... 17 to 21

48

Address: Central Research Institute of Electric Power Industry (CRIEPI)  
 Otemachi Bldg., 1-6-1 Otemachi  
 Chiyoda-ku, Tokyo 100, Japan

48

## 1. Introduction

Japan is well known for the most frequent occurrence of earthquakes in the world.

It is absolutely necessary for the electric utility companies to make complete provisions for the safety and efficient restoration of electric facilities after an earthquake because the utility has a responsibility for the continuous supply of electricity to the community.

We wish to explain here the many examples of seismic damage to electric utilities which have occurred in Japan in the past and the measures which the electric utilities have adopted to counteract seismic effects.

## 2. The Earthquake Hazard

Magnitude 8 earthquakes have occurred about once every 10 years; and M7 or less occur almost yearly. Following is a brief description of the damage caused by major seisms in modern times.

- a. The Kanto Earthquake, M7.9 (1923) extensively damaged electrical facilities in the vicinity of Tokyo and Yokohama. Service restoration took several months. In later earthquakes the electrical system was more resistant, damage was considerably less severe and service outages lasted only a day or two.
- b. The Fukui Earthquake, M7.3 (1948) led to adoption of an earthquake strength provision in the Japanese Building Law.
- c. The Niigata Earthquake, M7.5 (1964) was the first occasion on which the infrastructure of a modern Japanese city was subjected to a damaging seism. Many buildings and industrial structures were damaged by soil failures. The utilities (water, gas and electricity) were all simultaneously disrupted, so the city's functions were virtually paralyzed.
- d. The Matsushiro earthquake swarms (1965 to 1968) were only moderately damaging, but provided valuable opportunities for observation of seismic response of full-scale structures and to develop seismic prediction techniques.
- e. The Tokachi-offshore Earthquake, M7.5 (1968) disrupted various telecommunication facilities. In its aftermath, the Seismological Prediction Liaison Council was established.
- f. The Miyagi-ken-oki Earthquake M7.4 (1978) caused much damage to the utility systems of Sendai City.

In all of these earthquakes, we have never seen any major damage to generating equipment, due to seismic shaking, either in thermal or nuclear power plants. In each of the Niigata, Tokachi, and Miyagi earthquakes, apparently due to ground liquefaction or subsidence, there was typically one instance of minor damage to a thermal power plant, affecting the fuel-feed system or the buried distribution piping.

Table 1 shows the number of cases of seismic damage in overhead transmission and distribution facilities in the various earthquakes. There was no damage due to ground shaking, but we perceived secondary damage due to ground settlement or ground cracking and liquefaction.

There was no damage to structures on firm ground. Some damage occurred to pole-transformers due to support failure but there were very few cases in which the transformers actually dropped off the poles.

We did not perceive any damage to underground facilities due to ground shaking. Secondary damage, owing to soil liquefaction, was slight in tunnels and direct burial lines, but comparatively great in duct lines. (See Table 2).

Table 3 shows many examples of damage to substation transformers, circuit breakers, and lightning arresters, disconnecting switches and potential transformers.

## 3. Experiences and Lessons Derived From the Miyagi-ken-oki Earthquake

On 12 June, 1978, the Miyagi-ken-oki earthquake, M7.4, shook the Tohoku district. Damage was especially great, with 27 persons dead, more than 10,000 persons injured, and at least 172,000 houses collapsed. Public utilities were severely damaged.

Electric generating capacity of 1130 MW went out of service and about 680,000 houses (20% of all the customers in the district) suffered power failure.

Both the Sendai and Miyagi 275 KV substations, as well as 7 units of one 154 KV station, and 9 units of one 66 KV station, were heavily damaged, mostly in bushings, disconnecting switches, arresters, and circuit breakers. (See Figure 1).

Four thermal electric generating units tripped out of service. There were no outages resulting from damage to a boiler, turbine or generator. We did find some damage to auxiliary machines and, in one case, in the piping system.

There was no damage which caused malfunction of transmission lines. On the other hand, in the distribution lines there was breaking and

tilting of supports. Also, we found damage by tilting of transformers situated in poor soil areas.

Most of the damage to power equipment comprised breakage of large porcelain tubes at high voltage substations.

### 3.1 Damage to Substations

In the aftermath of the earthquake, soil conditions were investigated at the 275 KV Sendai Substation, which had experienced the most extreme damage among all of the substations in the area. Reasons for the unusually severe damage are described below.

It is clear that there were significant differences of ground acceleration and predominant vibration frequency on different types of soil.

Ground acceleration was increasingly amplified in moving from cut ground to native ground to filled ground, as shown in Table 4. (However, damage to transformers and porcelain type equipment was almost the same for those installed on filled ground and on native ground.)

At the site of damaged 275 KV equipment, we conducted vibration tests and a response analysis. Almost all of the devices lacked strength under dynamic design conditions (resonant frequency, sinusoidal 3-wave with 0.3G). As a consequence, three principal causes of damage appeared, as shown in Table 5.

Judging from observed damage of equipment like condensers and arresters, it appears that these devices interact with each other by way of the conductors which connect them.

Seismic strength of current transformers is considerable. Their vulnerability lies in their susceptibility to porcelain tube flange-cracks. Also, equipment adjacent to these is apt to break due to interaction with these very rigid devices.

Table 6 lists bushing damage of the 275 KV transformers at Sendai Substation. The damage initiated with breakage at the lower inside parts of the porcelain tubes. See Figure 3.

In order to verify this, we have done field vibration tests and also a response analysis of the combined system of foundation and ground. The results are shown in Figs. 4 and 5. From the results of these tests, we could confirm that when the natural frequency of the transformer bushing, natural frequency of the foundation-and-ground system, and predominant frequency of ground motion are all approximately equal, the bushing response becomes several times larger than the ground acceleration.

This is because the use of rubber pads for noise suppression results in strong rocking of transformer and this induces resonant amplification of the seismic input to the bushings.

### 3.2 Damage to Transmission and Distribution Facilities

As regards transmission facilities, there occurred a ground crack around the base of a steel tower, and partial wall breakage. Also, there were a few minor damages such as tilting of poles and loosening of guy wires in poor ground.

The underground duct-lines, due to lessons derived from the Niigata earthquake, were in steel pipes; also, location of the lines was carefully selected. Therefore, there was no damage to duct-lines due to soil movements.

The most notable feature in the distribution facilities was extensive breakage or tilting of poles and supports in Sendai City and its environs, especially on poor ground. The lessons derived from the Niigata and Tokachi seisms had been adopted to prevent seismic damage; so, in this earthquake there was no falling down of transformers, and also no damage to substation bus-bars.

Damage to the supports and wires caused by ground shaking was, in reality, very slight in distribution systems. By far the greatest part of the damage occurred for secondary reasons, such as ground shifting and liquefaction.

In the telecommunication system there occurred breakage of wave guides at micro-wave stations, but this did not interfere with their operation.

## 4. Countermeasures for Earthquakes by the Electric Utilities

Based on review of the damage caused by the Niigata-oki earthquake seismic design concepts for power equipment have been developed.

### 4.1 Substation Facilities

In case of substation facilities, especially large equipment such as transformers and circuit breakers formerly were designed with seismic coefficient of 0.5.

However, the damage experienced in recent seisms has demonstrated that, if the predominant frequency of the ground and a natural frequency of the device match each other, a resonance phenomenon occurs and this results in a larger stress than that to a 0.5g static equivalent load.

Therefore, a dynamic design standard input (resonance, sinusoidal 3-wave with 0.3g maximum) has been adopted for the large, critical equipment, especially at 500 KV substations. (See Table 7).

The substation facilities consist of the foundation (including the ground), the supports and the devices. Strength is decided by dynamic design rather than from a static equivalent.

Taking into consideration future seismic and also occurrence of large earthquakes over the last 50 years in Japan, peak ground acceleration of 0.3g has been adopted as a standard seismic loading.

As shown in Fig. 6, natural frequencies of the 275 KV and 500 KV class equipment exist over a wide frequency range, in general. Therefore, the possibility is high to develop resonance under seismic loading.

As a conservative dynamic loading, it is necessary to consider sinusoidal wave input which has a natural-frequency equal to that of the equipment.

Fig. 7 shows that when the equipment, idealized as a one-dimensional lumped-mass system, has resonance against a ground motion input, response amplification will occur. This amplification of acceleration is compared with those of resonant sinusoidal 2-wave & 3-wave inputs.

Here, the amplification due to resonant sinusoidal 2-wave input covers almost the full range of acceleration response magnification due to an actual seismic wave, and no earthquake response exceeds that induced by the resonant sinusoidal 3-wave. Accordingly, we have adopted the resonant sinusoidal 2-wave as the input waveform for designing substation facilities. Tables 8, 9 and 10 show seismic design criteria for substation facilities.

Improvement of dynamic performance of transformer bushings may be achieved by eliminating rubber pads between transformer and foundation inasmuch as sound isolation devices can cause adverse reaction to seismic inputs. Figures 4 and 5 indicate how ground accelerations at Sendai Substation were amplified from foundation to tank to bushings.

Usually, special investigation of soil conditions is performed only if fill is to be placed. If the existing ground is known to be weak, improvements can be made, e.g., densification or consolidation, pile placing, or bearing pressure can be reduced by using larger foundations.

See Figures 9 and 10 for suggestions for improvements of seismic strength of porcelain type equipment.

#### 4.2 Nuclear Power Facilities

We have never yet experienced damage to a nuclear power plant due to an earthquake. However, to guarantee that no release of radioactivity could result from a seismic, we practice stricter seismic-proof measures for nuclear equipment than for other power equipment.

At nuclear power facilities, the building, structure, equipment and piping systems are all classified, by seismic categories related to the safety of the facilities, and their seismic designs are conducted in accordance with their classification.

Two kinds of seismic motions (on the basis of the strongest seismic and the marginal seismic) are stipulated based on the seismic history, active faults, and seismic geological structure at the generating power sites; and seismic design incorporates dynamic analytical methods.

Building foundations are usually installed directly on bedrock. The piping systems are designed to prevent resonance with the building, by being made as stiff as possible.

In order to obtain maximum safety, a seismic detecting device is installed to initiate shut-down of the reactor in case of an earthquake greater than anticipated.

When a reactor suddenly is "scrammed" during its operation owing to earthquake shocks, thorough inspection of the nuclear power facility must be carried out immediately to determine if the plant has been damaged.

#### 4.3 Hydro-power Dam Installation

Seismic design is required, based on a pseudodynamic process. However, for especially important structures, dynamic response analysis is included in the design process. Also, for principal hydraulic dams, continuous seismic monitoring instrumentation has been set up; thereby, the actual dynamic properties of the major dams have been determined.

#### 4.4 Thermal Power Generating Facilities

For thermal power facilities Table 11 shows seismic design criteria for each equipment.

#### 4.5 Transmission Facilities

In the design of overhead transmission lines, the stress due to wind loads is always greater than seismic.

In the case of transmission route selection, we avoid bad ground as much as possible.

50. 51

Although underground transmission cables are not directly affected by the ground shaking itself, the following design precautions are necessary:

- (a) When the routes are selected, liquefiable sand subgrades or filled ground are studiously avoided.
- (b) We use flexible joints in buried lines, so that the ground strains do not transfer to the buried conduits.
- (c) Potheads and oil supply devices are designed for shaking loads.

#### 4.6 Distribution Facilities

Distribution facilities have usually exhibited substantial resistance to earthquakes. By selecting the routes and duplexing the circuits, sufficient seismic protection is obtained, as long as we avoid poor ground.

#### 4.7 Telecommunication Equipment and Computers

Seismic design for telecommunication equipment and strengthened techniques of installation of flexible micro-wave guides have all been carried out. The important facilities are provided with permanent emergency power sources. Therefore, by the use of duplex circuits, the telecommunication functions will be maintained.

Computer systems have been provided with sufficient protective devices to insure that operations will not be interrupted by seismic.

#### 4.8 Service Restoration Policies

All electric power companies in Japan have established their own emergency damage recovery systems.

At a time of unexpected accidents power is sent to another company if a power supply shortage occurs. This is done under a mutual aid agreement. If necessary, personnel and materials will also be dispatched to assist in emergency recovery.

First priority for restoration of power is assigned to those facilities vital for prevention of further damage and for speedy recovery of community functions. This includes hospitals and subway shopping streets, which are important places for sheltering and conserving lives. Also, recovery facilities such as damage-relief headquarters, governmental agencies and gas, water, and traffic systems are assigned high priority.

Also, high priority is assigned to news media as they are essential to allay anxiety in the community.

#### 4.9 Research Needs

- a. It is desirable for us to conduct a seismic study, with an evaluation of center-clamp-type bushing failure mechanisms, by examining transformer behavior in actual seismic.
- b. We wish to evaluate the effect of ground improvement, by conducting tests on various improving methods, such as using soil-cement.
- c. At the Nuclear Industrial Center, a large seismic shaking table is under construction. This apparatus has a 15m x 15m vibrating platform weighing 1,000 tons. It is a biaxial machine, which will be able to develop maximum inertia force of 3000 tons. We plan to conduct full-scale seismic reliability tests on large nuclear power components to determine seismic design margins.

#### 5. Conclusion

We have described in this paper the seismic resistance measures adopted by the Japanese electric utility industry.

Early restoration of power facilities at the time of seismic disaster will contribute greatly to the recovery of both civic function and industrial-economic activity and will be reassuring to the public.

We of the electric utility industry recognize that we must take all reasonable countermeasures to protect against effects of earthquakes in Japan.

Table 3. Damage to substation equipment

Table 1. Damage to overhead facilities

(1) Transmission

Installation	Unit	Tohoku	Hokkaido	Honshu	Shikoku	Kyushu	Others
insulation	unit	56	83	1	0	0	13
support (tower)	unit	537	87	0	0	0	14
support (wood)	unit	36	24	0	0	0	0
electric wire	unit	3	7	0	0	0	0
underground	unit	0	0	0	0	0	0

(2) Distribution

Installation	Unit	Tohoku	Hokkaido	Honshu	Shikoku	Kyushu	Others
support	unit	7,355	7,060	550	0	0	2,317
high voltage electric wire	unit	5,074	4,551	211	0	0	944
transformer	unit	3,419	5,193	21	0	0	4,082

Source: Nov. 1970

Table 2. Damage to underground transmission facilities

Name of place	Type			Cause of failure				Transmission faults (circuits)	Remarks
	Break	Non-connection	Others	Bad insulation, all leads	Joint slip-off	Joint failure	Other		
Hiroshima	1	2	11	15	2	3	2	7	6 circuits to Hiroshima City (underground transmission lines)
Tohoku	-	-	9	2	-	-	-	-	Label errors at insulating joints, and oil leaks of oil glands
Hiroshi	-	-	2	-	-	-	-	-	Slight, 100 m <sup>2</sup> tunnel cracks

Source: Dec. 1970

Area	Date occurred	Equipment	No. of units	Voltage (kV)	No. of circuits	Damaged substation facilities			Remarks
						Kir-blank breaker	Transformer	Others	
HN	1950.1.21	Tohoku	4	6.6	10			1/2 x 1 (blowing)	
	1961.10.13	South of Niigata-Kan	4	6.6	20			1/2 x 1 (transformer off)	
HO	1948.5.16	Tohoku Off-shore	0	7.0	20	100%		1/2 x 1 (transformer off) 1/2 x 1 (transformer off)	Tohoku
	1970.1.22	Nishi-Kan	5	6.6	20	100%		1/2 x 1 (blow pressure plate)	
HO	1971.6.17	South of Niigata-Kan	0	1.0	-	100%		1/2 x 1 (base)	
	1972.9.24	Central	0	7.5	20	100%			
HN	1949.10.19	Central	0	6.6	10-20	100%		1/2 x 1 (transformer), 1/2 x 1 (transformer)	
	1967.8.20	South of Niigata-Kan	0	6.6	0			DC support insulator on 10 base	East
HO	1964.6.18	Hiroshima City	0	7.0	20			1/2 x 1 (transformer), 1/2 x 1 (transformer)	Hiroshima
	1971.7.26	South of Niigata-Kan	4	1.0	0	100%			
HO	1970.8.11	Niigata-Kan	0	7.4	20	75	250%	1/2 x 1 (transformer) 1/2 x 1 (transformer)	Niigata-Kan
	1965.5.8	South of Niigata-Kan	4	6.6	20	5		1/2 x 1	
HO	1968.4.2	Central-Kan	4	1.0	20	5			
	1969.7.3	Honshu-Kan	0	6.6	20	1			
HO	1973.1.21	East of Niigata-Kan	1	4.0	20	1			
	1974.9.4	East of Niigata-Kan	0	6.6	20	1			
HN	1961.9.20	Hiroshima City	0	6.6	20	0	100%	1/2 x 1 (transformer) 1/2 x 1 (transformer)	Hiroshima
	1966.1.20	Central-Kan	5	6.6	-	2			
HO	1966.8.29	Central	0	6.6	-			1/2 x 1 (transformer)	
	1969.9.7	Central-Kan	0	6.6	0	100%		1/2 x 1 (transformer), 1/2 x 1 (transformer)	
HO	1972.1.5	Central-Kan	4	6.6	20		100%		
	1974.5.4	East of Niigata-Kan	4	6.6	10				
HO	1971.7.18	South of Niigata-Kan	1	6.6	20		100%	1/2 x 1 (transformer)	
	1975.8.18	East of Niigata-Kan	4	6.6	20			1/2 x 1 (transformer off)	
HO	1966.6.20	South of Niigata-Kan	0	6.6	20		12	1/2 x 1 (transformer) 1/2 x 1 (transformer)	Tohoku
	1972.7.14	South of Niigata-Kan	4	6.6	20			1/2 x 1 (transformer)	
HO	1965.7.21	South of Niigata-Kan	0	6.6	0			1/2 x 1 (transformer) 1/2 x 1 (transformer)	
	1970.1.1	Central-Kan	0	6.6	0		14	1/2 x 1 (transformer) 1/2 x 1 (transformer)	

Source: Agency for Rebuilding, 1971, 74, 75, 76, 77

Table 4. Ground surface acceleration on various types of soil

Soil type	Maximum ground acceleration (gal), calculated*	Dominant frequency (Hz), calculated*
F111	290 to 550	1.9 to 8
Undisturbed	270 to 380	2.5 to 8
Cut	210 to 230	4 to 10

\*Based on multiple reflection theory, assuming 200 gal in firm ground.

Table 5. Damage to porcelain type equipment (275 KV)

Classification	Study Design	Safety factor*	Number installed	Number damaged	Type of damage		
					Lack of strength	Mutual inter-failure by leads between devices	Secondary damage by other device breakage
275 KV ABB Breaker (air)	Static	0.6	3 units	3 units	3		
275 KV GEB Breaker (gas)	Dynamic	0.9 (double load)	6 "	4 " (1 unit under construction)	4		
275 KV LA Reactor	Static	0.7	12 " (part)	11 " (part)	1		
"	"	1.2	4 " ( " )	4 " ( " )		1	
275 KV CI Condenser	"	1.5	12 " ( " )	6 " ( " )			1
"	"	2.0	3 " ( " )	1 " ( " )			1
"	"	2.0	1 " ( " )	3 " ( " )			1
275 KV LS	"	0.9	24 "	3 " (one under construction)	1		
275 KV LPD	"	1.3	6 "	3 "		1 (1 unit)	1 (2 units)
" CC	"	1.3	12 "	10 "		2 (2 units)	1 (4 units)

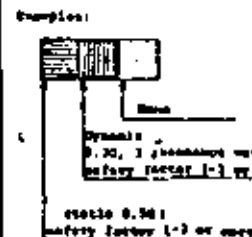
\*Safety factor determined from input of 0.7g, at resonance, sinusoidal 3 waves, at the base of the equipment's support.

Table 6. Damage to transformer bushings

Capacity	Extent of damage
275/154 KV 250 MVA	No. 1 Transformer 275 KV, No. 2 bushing A, B phases: Breakage of upper porcelain tube, C phase: Breakage of upper porcelain tube
	No. 2 Transformer 275 KV, No. 2 bushing (under installation); oil leakage B, C phases: Breakage of upper porcelain tube tip-out; oil leakage B phase: Breakage of upper porcelain tube cracks; oil leakage
	No. 3 Transformer 275 KV, No. 2 bushing 1 phase (all the same) upper porcelain tube tilting, oil leakage. (No pressure cut-off in O ring)

Table 7. Seismic design condition, classified by the voltage and the type of device

Voltage (KV) Design condition	000		101-175		100-104		00-77	
	Static	Dynamic	Static	Dynamic	Static	Dynamic	Static	Dynamic
Transformer	Shaded	Shaded						
Shunt reactor								
Circuit breaker								
Disconnecting switch								
Potential transformer								
Reactor								
Neutral point isolator								
Power transformer								
Aluminum pipe bus bar								
Bushing								



Note: In the aftermath of the damage caused by the Niigata-oki earthquake, the dynamic design method has been extended to the transformer, also.

Table 8. General seismic design criteria for substation facilities

Items	Porcelain-type devices	Transformer bushing
Seismic design force, which is the basic input into ground surface: A	Indicial application of resonance sine 2-wave with 0.3G maximum	Same as at left
Amplification factor, due to the foundation: B	1.2	2.0 (inclusive of amplification of transformer proper)
Uncertainty factor, based on vertical acceleration, effect of connecting conductors, etc.: C	1.1	1.1
Correction factor (B x C): D	$1.2 \times 1.1 = 1.3$	$2.0 \times 1.1 = 2.2$
Seismic design force calculations.	A x D = resonance sine 2-wave with a 0.39G; but, in terms of traditional usage: 3-wave acceleration $= 0.39G \times \frac{1}{1.3} = 0.3G$ (See Note)	A x D = resonance sine 2-wave with a 0.66G; but, in terms of traditional usage: 3-wave acceleration $= 0.66G \times \frac{1}{1.3} = 0.5G$ (See Note)
Seismic force to be used in design of devices	Resonance sine 3-wave with 0.3G maximum applied at the lowest parts of the device	Resonance sine 3-wave with 0.5G maximum, applied at the lowest part of bushing pocket

Table 9. Seismic design of porcelain devices

1. Ground	The equipment should be built on ground which has more than 150 m/s speed of S-wave, or Standard Penetration Test value, $N \geq 5$ .
2. Design approach	Quasi-resonance method.
3. Seismic design input	Resonant sine 3-wave with 0.3G maximum (indicial application)
4. Dynamic load point	The lowest parts of the device.
5. Judgement criteria	The stress which is generated in the porcelain tube is not to overrun the destructive stress value.
6. Range of Frequency	As for the device whose natural-frequency is in the range of 0.5 - 10 Hz, use the natural frequency; as to those which are under or above this band: in case of less than 0.5 Hz, assume 0.5 Hz is its natural frequency; in case of 10 Hz or more, assume 10 Hz is its natural frequency.

Note: This is a conversion of the desired (newer) 2-wave input to the equivalent "traditional" 3-wave input. Amplification is greater for 3-wave input, as shown in Fig. 7.

Table 10. Seismic design criteria for transformer buildings

Ground	Design Approach	Seismic Input	Dynamic Load Point	Critical Judgment	B. Frequency Range
1. Ground The standard is to put 5% on ground of more than 150 m/s speed of S-wave (for N + 5) amplification of ground motion by combination of soil foundation and-trans-former should be less than 2.	2. Design Approach Flange system: Center clamp system Quest-resonance	Seismic design input Indicial application of resonant sine wave with 0.5g maximum (from Table B)	Dynamic Load Point The lowest parts of Bushing pocket at the lowest part of Bushing point is obtained from calculation and experiment.	Critical Judgment Flange system, The same as porcelain devices. The weight should not open. Even if it is judged "no good", it is acceptable if passed with a second. Any check.	B. Frequency Range If natural-frequency is in the 0.5-10 Hz range in Bushing pocket, use the natural-frequency level. In those beyond this range: 0.5 Hz or less, assume 0.5 Hz; 10 Hz or more, assume 10 Hz as natural-frequency.
Secondary check	Primary check				Same as at left.

Table 11. Seismic design criteria for thermal power facilities

Equipment	Boiler	Boiler Structure	Pipings	Turbine generator	Main auxiliary machines	Phase Bar-bars	Protective relays	Fuel oil tanks	LMS tank
Seismic coefficient	0.20	0.25	0.25	(0.2 to 0.30)	(0.2 to 0.30)	0.35	0.225	0.30	0.30
Remarks	Based on Code	Based on Code and Steel Structure Criteria of Academy of Architecture, for seismic design, piping are full of water.	Pipe supports are designed for seismic load. Allocation of piping is governed by using submers. Principal piping gets dynamic analysis.	Seismic loads do not govern the design. Actual seismic resistance capacity is about 0.5g.	Seismic loads do not govern the design. Based on experience, there is a seismic resistance capacity of more than 0.20. Static strength of the casings are checked for lateral forces.	Mind load (kg/m <sup>2</sup> ) may govern.	This design is based on JEC 174, for components of low seismic resistivity, phase tests are conducted.	Based on Fire Ingress Law, Flexible joints are used. Flashing requirements determine free-board height.	Based on Electric Industrial Law, and Seismic Intensity Code. In some cases, a dynamic analysis is conducted.

Code = "BUILDING Standard Law"

(JRM, June 1978)

→ To be applied if (a) bushing falls to satisfy the "primary" check, or (b) ground motion amplification by combined transformer-foundation ant-soil is greater than 2.

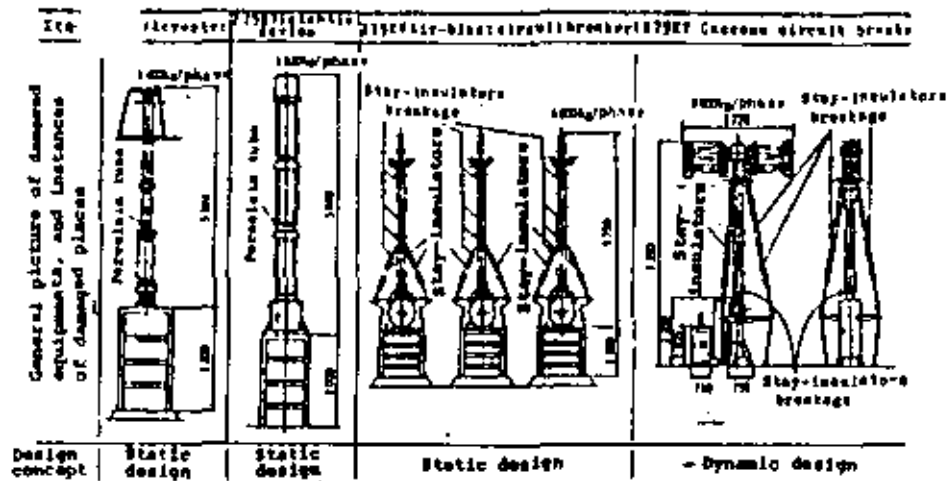


Fig. 1. Damage to the equipment

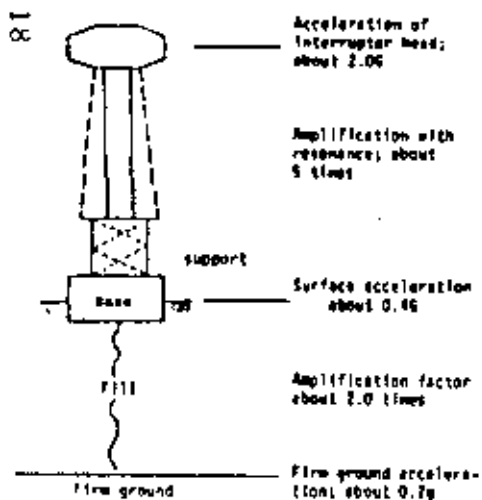


Fig. 7. Response of damaged circuit breakers on filled ground at Sendai Substation

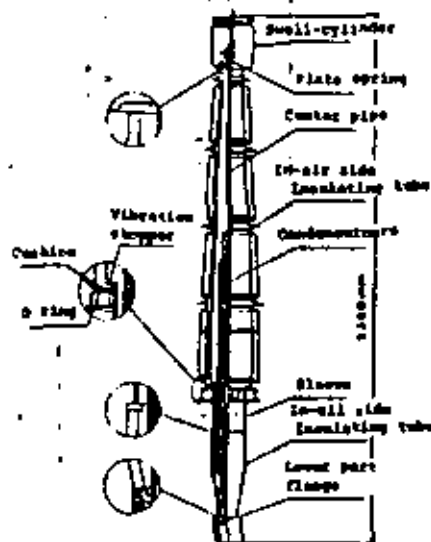
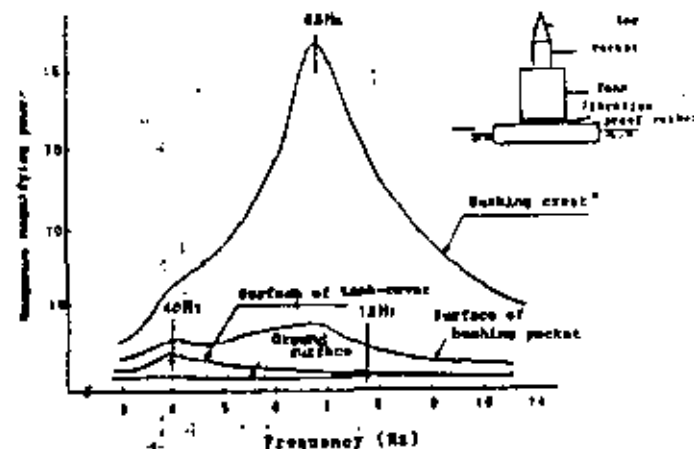


Fig. 3. Structure of bushing



\*This value is that of center-clamp-type bushing when its mouth does not open. In reality, the mouth opens and the value becomes less.

Fig. 4. 275 KV transformer's frequency characteristic at Sendai Substation (sine wave acceleration time's calculation)

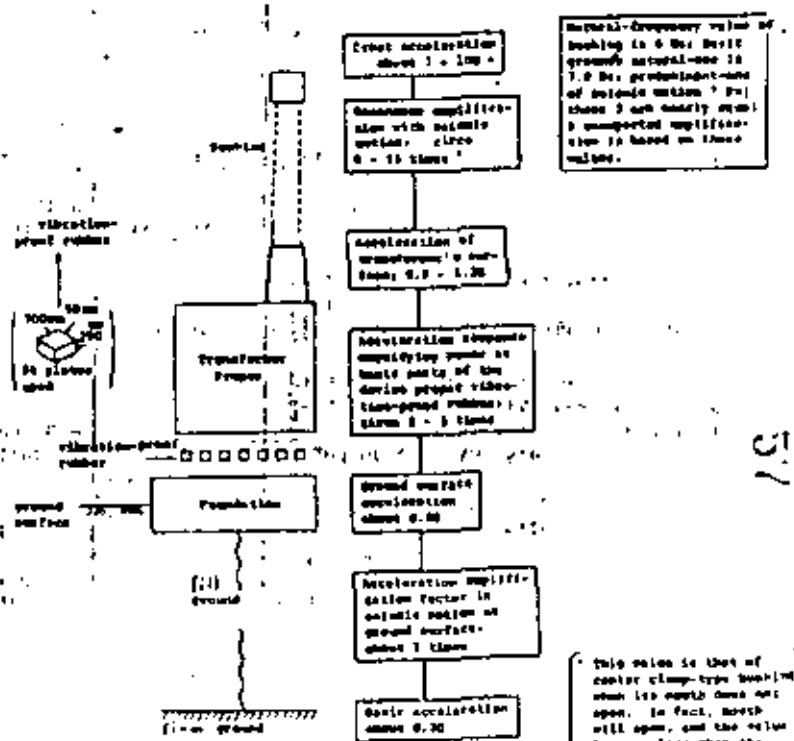
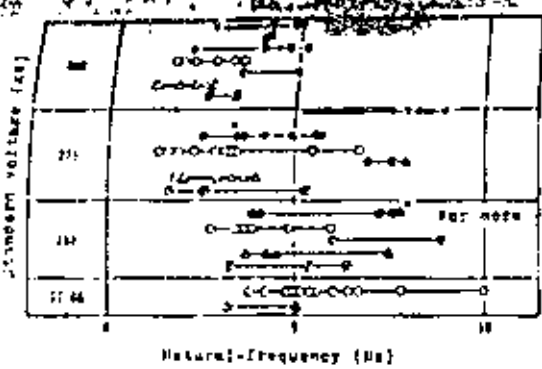
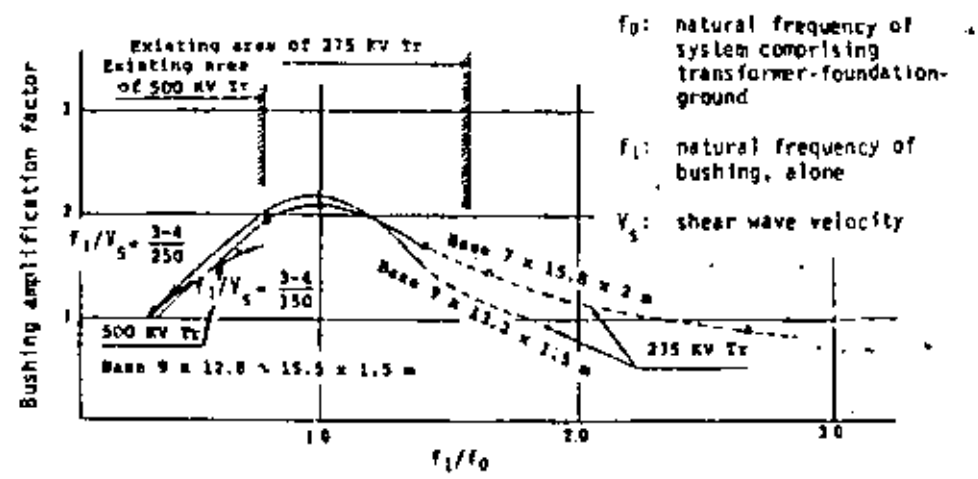


Fig. 5. Chart of response features of transformers damaged at Sendai Substation.



- bushing for transformer
- instrument transformer
- current transformer
- insulator-type circuit breaker
- tank-type circuit breaker
- arrester
- disconnecting switch

Fig. 6. Range of natural-frequency of substation equipment



Note: Bushing, mounted without rubber blocks, was subjected to 3-wave sinusoidal input at different values of  $f_0$ .

Fig. 8. Bushing response as influenced by dynamic characteristics of transformer-foundation-ground.

61

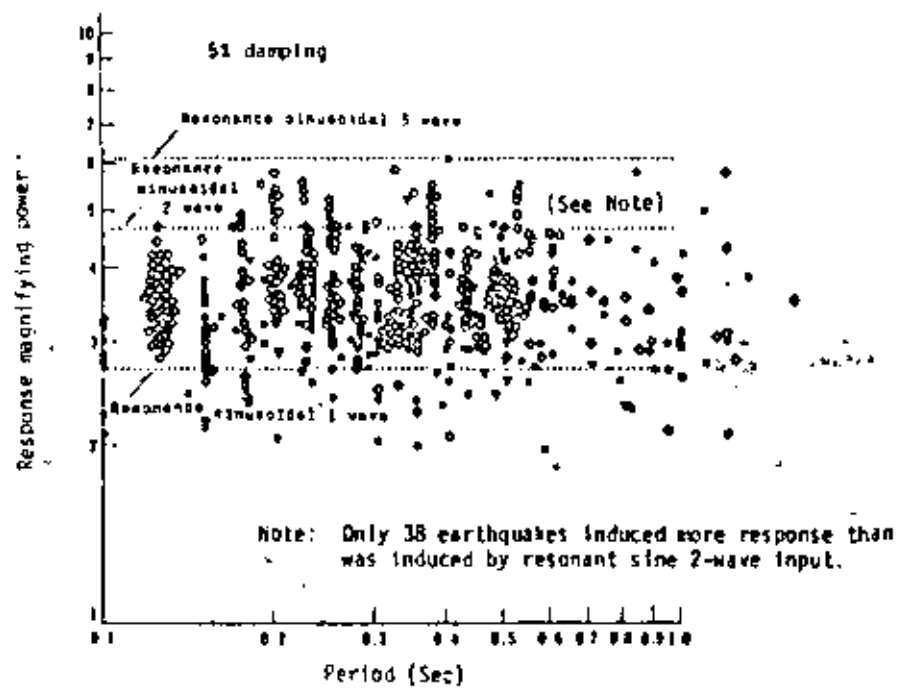


Fig. 7. Response to resonant sinusoidal input compared to response to actual seismic accelerograms.

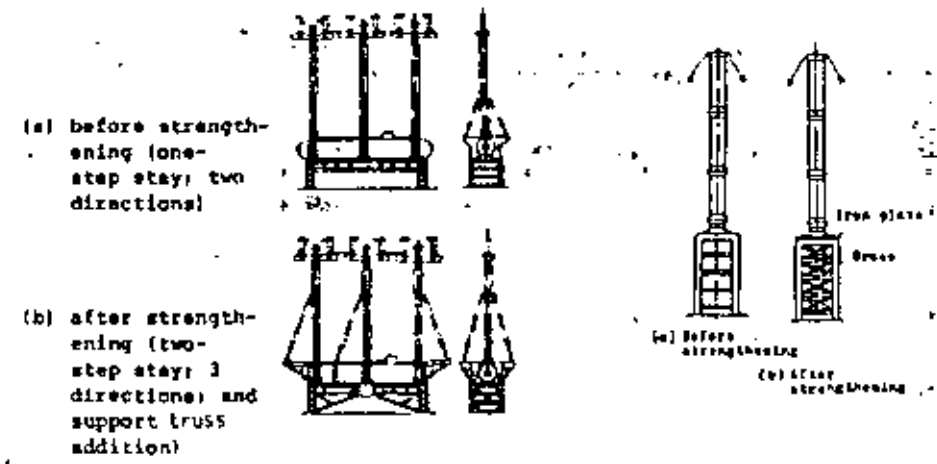


Fig. 9 Asismic strengthening of 275 KV air-blast circuit breaker

Fig. 10 Asismic strengthening of 275 KV lightning arrester

55

- (9) McGuire, K. P., "Methodology for Incorporating Parameter Uncertainties into Seismic Hazard Analysis for Low Risk Design Intensities", Proceedings of the International Symposium on Earthquake Structural Engineering, St. Louis, Missouri, August 1976, pp. 1007-1021.
- (10) Gupta, V. M. and Nuttli, W. O., "Spatial Alternation of Intensities for Central United States Earthquakes", Bulletin of Seismological Society of America, Volume 66, No. 3, June 1976, pp. 746-751.
- (11) Oppenheim, T. J., "Vulnerability of Transportation and Water Systems to Seismic Hazard Methodology for Hazard Cost Evaluation", A Paper submitted to TCLE Specialty Conference in Los Angeles, California, September 1977.
- (12) "Seismic Analysis: Beaver Valley Power Station of the Duquesne Light Company, Shippingport, Pennsylvania", by Weston Geophysical Research, Inc., Weston, Massachusetts, Westinghouse Electric Corporation, "Draft of WBR Safety Analysis Report", Material Document No. WAPD-LD(TS)8, 1974.
- (13) Buchanan, G. G. et al., "Facing the Cost of Water Quality", Journal AWWA, Volume 69, No. 4, January 1977, pp. 46-51.

TABLE 1. - Distribution System Damage  
Number of Failures per Pipe Group

Average Pipe Group Size in Inches	Percent of Total Length	Modified Mercalli Intensity*					
		5.8	7.2	7.5	8.3	8.7	9.0
4	2.9	0	2	6	154	1,105	4,221
6	51.5	4	25	97	2,678	19,470	74,339
8	19.0	2	9	35	961	6,989	26,686
10-12	10.8	1	5	19	525	3,815	14,568
14-16	9.2	0	2	7	192	1,331	5,310
18-20	3.6	0	1	6	157	1,141	4,357
24-30	4.3	0	1	6	157	1,141	4,357
36	1.6	0	1	2	54	392	1,498
42	0.5	0	0	0	10	71	272
48-50	0.7	0	0	1	15	107	408
50-60	0.7	0	0	0	5	36	136
TOTAL BREAKS		7	46	179	4,907	35,658	136,142

\*M41 corresponding to a given ground acceleration based on Trifunac and Brady (5) correlation.

ELECTRICAL POWER AND COMMUNICATION LIFELINES

Publication:  
The current state of knowledge  
of LIFELINE EARTHQUAKE  
ENGINEERING

ASCE, 1977

## COMMUNICATIONS LIFELINES IN EARTHQUAKES

By J. W. Foss,<sup>1</sup> M. ASCE

**ABSTRACT:** State-of-the-art information is presented on protection of communications lifelines against earthquake damage. Seismic effects, design objectives, and strengthening techniques are discussed for cable and radio systems and for equipment in buildings.

### INTRODUCTION

Communications lifelines, always necessary, become immensely vital in the period following an earthquake. Radio, television, telephone, telegraph, and other communications media must close the information gaps in normal life that are caused by earthquake damage. Obviously, communications are needed to summon emergency aid, to coordinate possible rescue and medical efforts, to collect damage data on utilities and other facilities, to aid speedy and safe reconstruction efforts, and to keep people informed. And, when there is danger of aftershock damage--for example, a weakened dam about to fail--communications can save thousands of lives by providing ample warning time for evacuation to take place.

Although there are many communications avenues, the strain during any reconstruction period will necessarily fall on those facilities which are still usable. This is where overloads or malfunctions can occur if system checks or controls are not incorporated into designs and engineering plans. For example, the telephone switching machines in the Los Angeles area were able to operate successfully after the 1971 San Fernando earthquake because the bulk of nonemergency incoming calls were selectively blocked. This prevented overloading the network and allowed the more important outgoing and local calls to be processed.

Perhaps the single most important deterrent to complete breakdown of communications is the redundancy in the many systems available. These systems are spread in a web-like matrix over regions significantly larger than destroyed

areas. Path rerouting will divert major communications around the destroyed area while communications within that area will be partially restored with available mobile or transportable facilities prior to repair or replacement of the initial system. However, the enormous need for post-earthquake communications demands that measures be taken before an earthquake occurs to assure survival of as much of the total lifeline plant as is economically feasible.

### NETWORK STRUCTURE

The lifeline referred to consists of communications networks made up of a series of nodes or end points interconnected by distribution systems as shown in Figure 1. Communications main centers or nodes most often consist of buildings, or structures housing equipment. The distribution system is generally configured of pole lines or buried cable as well as radio links that interconnect each node point. In most instances, the high diversity in these systems allows for loss or failure of certain elements without complete loss of communication in the specific areas where failures occur. The effects of system redundancy vary from one region to another. This makes it logical to consider seismic requirements on a local basis rather than codifying criteria independent of regional considerations. Using this approach is a sensible way to assure optimum and balanced seismic resistance of lifelines.

Working with the knowledge of likely earthquake epicenters and motion-distance effects for a particular region, one can perform a network analysis to find the desirable balance design level of seismic resistance. The distribution paths in the network form very complex circuits. From the standpoint of survivability studies, these may be simpler to analyze by using decomposition techniques to reduce them to a number of series or parallel systems rather than by studying the circuits themselves. An analyst requires not only the network and seismic data but also information on the fragility level of each network element. Generally, equipment in structures at the nodes will be significantly more vulnerable to ground excitations than the cable or radio distribution plant. And, because earthquake-induced motion will spread over large areas, much emphasis must be placed upon improving the fragility levels of equipment. This will be discussed in subsequent sections.

### SEISMIC EFFECTS ON COMMUNICATIONS LIFELINES

Earthquake effects on communications will vary in magnitude and frequency of occurrence throughout the country as dictated by the complex action of global tectonics. Zoning maps portraying information on local seismic risk are being developed to aid system designers in choosing design levels appropriate to achieve optimum performance. Through the years, the sophistication used in developing these maps has

<sup>1</sup> J. W. Foss, Chmn, Power & Communications Committee, ASCE-TLSP; Supervisor, Building and Equipment Engineering Department, Bell Telephone Laboratories, Whippany, N. J.

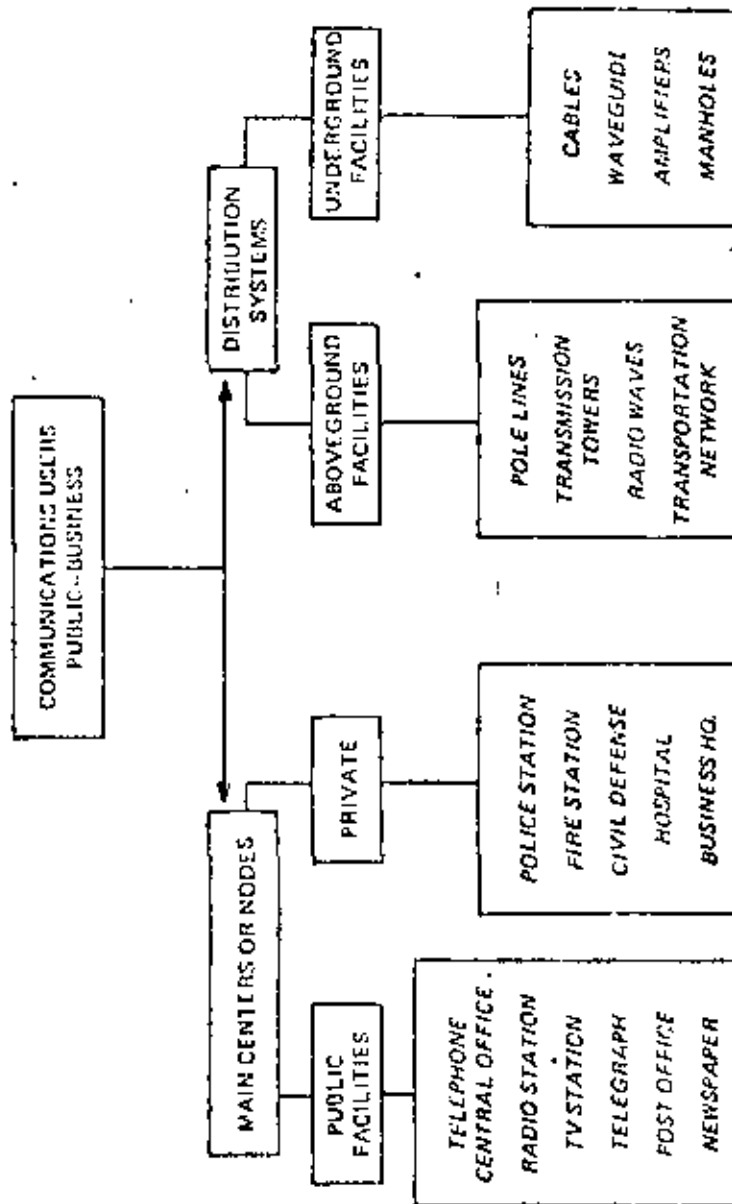


FIG. 1.-Communication network elements

seen increasing, with later versions based upon microzonation techniques. Such techniques combine historical earthquake data and seismological and geological information with statistical models to predict likely earthquake occurrence and local effects.

The most complete recent report on earthquake effects and zoning appears in Reference 1, "Recommended Comprehensive Seismic Design Provision for Buildings," prepared by the Applied Technology Council, January 1977, and soon to be released. This reference contains ground motion regionalization maps of the United States showing effective peak acceleration and velocity levels not likely to be exceeded over a 50-year period. It also goes into considerable detail in defining how to obtain the recommended design levels for buildings and appurtenances. Reference 2 gives the building floor accelerations shown in Table I for the different seismic zones mapped in Figure 2. These criteria have been prepared for use in the design of new installations of central office equipment in Bell System communications facilities.

Table I

Floor Accelerations for Different Seismic Zones and Locations in Buildings

Location	Floor Accelerations (g) in Seismic Zones			
	1	2	3	4
Ground Level	0.05 - 0.1	0.1 - 0.2	0.2 - 0.4	0.4 - 0.8
1st Floor				
Upper Floors	0.2 - 0.3	0.3 - 0.4	0.4 - 0.6	0.4 - 1.0

The sensitivity to earthquake effects of communications buildings and structure-housed equipment is different than cable or radio distribution systems. The former are very sensitive to ground accelerations or repetitive shock-type loadings, while the latter are more sensitive to relative ground displacements and generally less sensitive to ground acceleration effects. Relative ground displacements include those occurring at the fault slip plane and areas of overthrusting and fissuring as well as the oscillations caused by compressional and shear waves propagating from the earthquake source.

While considerable work has been done to develop criteria on earthquake acceleration effects, only limited research has been done on the development of criteria covering ground displacements and relative motion. Displacement studies

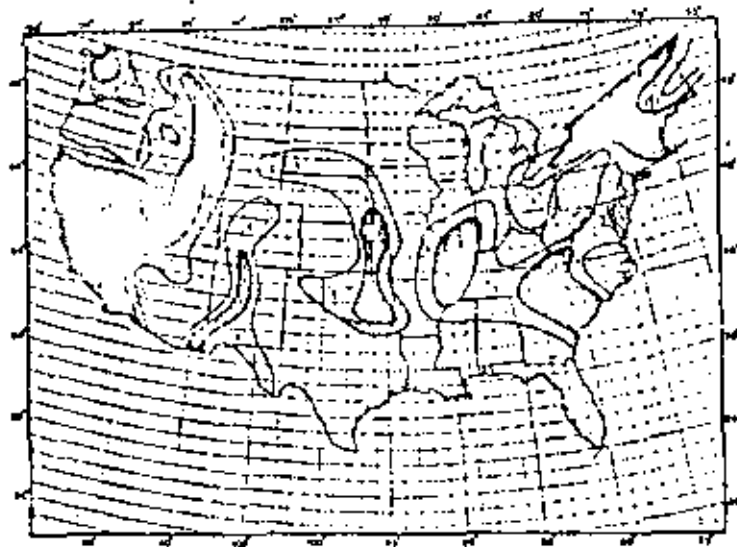


FIG. 2. - Earthquake zoning map  
(Reference 2)

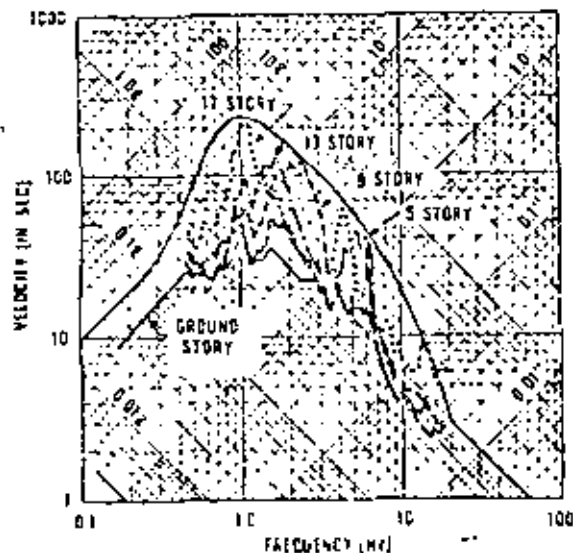


FIG. 3. - Typical Zone 4 multi-story building  
upper floor response spectra (Reference 2)

have been made for use in the design of the Alaskan pipeline (Ref. 3). Reference 4 presents a brief review of some formulas used to estimate relative ground motions. Much additional work is required to develop usable criteria for different regions of the country, different soil site conditions and for different types of seismic excitations.

#### DISTRIBUTION NETWORK PROTECTION

##### \* Cable in the Ground

Earthquakes may damage cables buried in shallow trenches where such cables cross the region of fault slipping, rupturing or fissuring and where relative motions induced by seismic waves in the ground "pulse" the cable along its length. Compression of the cable by local hard objects such as stones or pavement can also cause damage--especially to the coaxial variety. Most cable has a great deal of flexibility and can be significantly bent and twisted with minimal effects upon transmission. Also, the shock resistance, or the ability of the cable to withstand ground velocity changes, is sufficiently great that this type of loading is of little concern during earthquakes.

Axial elongations of the cable pose the greatest threat to its ability to carry signals. Elongations can occur on cables crossing faults as the ground ruptures and shears at these locations. They can also occur as seismic compression waves move through the ground along the cable length. Possible effects include: (1) a failure in tension by necking down at a particular location, (2) a capacitance change sufficient to cause signal impairment, or (3) the separation of connections at manhole and building splices.

A variety of strengthening procedures are used to improve the resistance of important cables which cross known active faults. One such procedure designed to protect major high-capacity telephone trunk lines crossing the San Andreas fault in California involves using steel double-armored cable laid in "S" loops along a 1,000 foot trench that straddles the fault. The trench is 4 foot deep and 10 foot wide at the top with 45-degree angle side slopes. Noncohesive gravel backfill is used in the trench to allow the cable to undergo large motions without damage. Further, the cable trench is placed at an angle to the fault crossing so that fault shifting in the expected direction tends to normalize the cable position and minimize stress.

Protection of buried cable from elongation failures caused by seismic stress waves traversing the ground may best be accomplished by designing displacement tolerances into the cable run. This may be done by laying cable loosely in trenches; by providing loose, porous, noncohesive backfill; and most important, either by leaving some slack or by

providing full cable strength at connections in manholes, at splice points, and at the building attachment.

Also at the building attachment, the cable must be protected against shearing. Shearing is caused by (a) seismic-induced settling of backfill soil around the building causing cable motion relative to the building, or (b) seismic-induced building settling causing cable motion relative to the soil. At locations where soil conditions are poor or settling is likely, the cable may be protected by placing it in a length of steel pipe anchored at one end to the building foundation.

#### • Cable on Pole Lines

Cable supported by poles extending from the ground will be exposed to earthquake effects similar to those described for buried cable. In addition, a whipping motion of the cable-pole system may cause further damage. Heavy splice cases and amplifier equipment on suspended cable spans are likely to experience severe cable oscillations during major earthquakes. Such oscillations are caused by response of the pole-line system to motions normal to the run as well as to seismic "pulse" motions in the ground in a direction along the run. In the latter case, one concern is with motions caused by a slack cable with a heavy mass attached suddenly becoming taut. The principal strength member of most aerial cable is a continuous steel strand to which the cable is attached. The strand will carry all major stresses along the line and prevent axial loadings from straining splices or other line-supported apparatus. Methods of protecting pole-line systems against earthquake effects include securely attaching the cable and other supported apparatus to the steel strand and the strand to the supporting poles. Pole-mounted equipment, such as amplifier cases, must be securely attached to prevent separation which can cause line failure and produce dangerous falling objects.

#### • Radio and Television Towers

Radio and television towers may be structured as free-standing cantilevers on the ground; guyed to the ground; or free-standing and/or guyed on top of other structures such as buildings. Most towers are of relatively light metal lattice or pole-type construction. Because of the relatively light weight of the tower structure, wind loadings generally dictate the design strength even in areas where earthquake codes stipulate seismic loadings.

There may be, however, seismic considerations important in the design of certain types of towers that have not in the past been accounted for.

1. Towers supported upon multistory buildings will experience earthquake motions that may be amplified by the

supporting building structure. Multistory buildings may whip the tower horizontally and also propagate amplified vertical motions to the tower. When vibrational frequency-matching is right, these combined horizontal and vertical motions induced by the earthquake may produce tower stresses significantly higher than those caused by wind loadings. Computer solutions considering the dynamic response to seismic forces are generally required to analyze the building-tower entity. The point of maximum stress, like that which occurs on flagpoles similarly supported and exposed to vibration inputs, is likely to occur between the tower base and mid-tower height.

2. Tall radio and television towers that are guyed and supported on the ground are often constructed with a substantial distance between the concrete blocks which provide anchorage to the guy cables. Thus, in some cases, earthquake dilatational waves in the ground may possess half wavelengths that are as short or shorter than the distance between the anchor blocks. Under such conditions, the seismic motions may slacken or tense the guy cables unequally and thus induce damaging relative motions between guy point anchorages. Vertical motions acting at the same time may further lead to excessive stresses in the guy system or tower mast.
3. Certainly, communications equipment attached to towers must be well supported to be capable of sustaining the seismic vibration response of the mast. Antennas, feedhorns, waveguides, couplers, etc., should be rigidly attached to prevent resonance from occurring with the tower structural system. However, sufficient flexibility should be allowed in waveguide runs between towers and equipment buildings to avoid displacement-induced damage to the waveguide. Elements such as waveguides that might be damaged by falling objects should be protected with overhead metal plates.

#### NODE POINT PROTECTION

Communications facilities at node or terminal points include building/structure-equipment assemblies used to produce, disseminate, amplify, or switch voice or data signals. Seismic analysis and design techniques for buildings are now reasonably well understood and documented after several decades of research and test work conducted by universities, research organizations, architect engineering firms and industry. Reference 1 presents the latest and most comprehensive information on this subject.

Broad scale progress on equipment protection research and development has lagged behind that applied to buildings and structures. Data gathered from the great Alaskan

earthquake of 1964, the San Fernando earthquake of 1971, and Japanese and other recent earthquakes throughout the world have shown that equipment failures form a large part of the destruction loss. Further, equipment failures have greatly delayed efforts to restore an area after an earthquake.

In communications facilities, the net worth of the equipment is often many times that of the building or structure in which it is housed. Most buildings, even if not specially designed and constructed to withstand earthquake effects, possess a measure of resistance by the very way they are constructed to withstand other loadings, such as wind. Except for special earthquake-resistant designs, equipment is generally designed only for gravity and handling loadings and in many cases is not capable of withstanding lateral seismic forces of any significance. A result of this may be collapse of equipment situated in buildings which themselves sustain only minimum seismic damage.

Preventing equipment damage during an earthquake is mainly a job of holding it in place during the shaking to keep it from sliding, overturning, or bouncing around and striking other equipment or building elements. When equipment frameworks are properly secured or restrained, the components within are in most cases capable of withstanding low-frequency seismic vibrations. There are, however, some exceptions, e.g., the air-supported disc memories used in electronic data processing systems.

Equipment situated on upper stories of multistory buildings will usually experience a more severe shaking than that situated on the ground floor. This is due to building amplifications that occur because the natural frequencies of tall buildings lie close to those of ground excitations (0.5 to 10 Hz), and resonant buildup occurs. Further resonant buildup may occur when the fundamental frequencies of the equipment also lie in this band. Table 1 indicates the difference between the ground and upper floor acceleration levels for the different seismic zones shown in the map in Figure 2. Notice that the amplification decreases as the zone earthquake level increases. This is because of the increased elastoplasticity and damping action of the building in severe environments.

Figure 3 shows floor response spectra prepared for use as design criteria for new Bell System central office communications facilities (Refs 2 and 5). The particular envelope spectrum shown in Figure 3 is used in designing lightly damped equipment situated on upper floors of buildings in Zone 4 and includes all necessary safety factors. Notice that the maximum 5g acceleration response limit indicated in Figure 3 will be experienced by equipment with fundamental frequencies between approximately 1 and 7 Hz.

### • Design Objectives

Design objectives to improve the mechanical resistance of communications equipment are noted below:

1. Strengthening at Building Connections. Many equipment failures that occur during actual earthquakes as well as those simulated in the laboratory are caused by inadequate strength of the connection used to attach the equipment to the building. Weldments, bolts, and inserts to concrete fail most frequently because of inadequate strength. Equipment supported by vibration isolators may shake loose and topple if snubbers or limit stops are not strong enough to resist the motions amplified through resonance with the isolator.
2. Lowering Center of Gravity. Lowering the center of gravity by placing heavy components closer to the bottom (or to the support points) reduces the bending moment induced by inertial response to the seismic motion.
3. Increasing Frequency. Increasing the natural frequency of the equipment by stiffening it or reducing weight generally decreases displacement and acceleration response through decoupling from a near-resonance condition with building and earthquake motions. Where possible, the resonant frequency of equipment components should exceed 10 to 20 Hz to avoid amplifications due to resonance. This is often difficult to achieve for tall, slender equipment bays (frameworks) used in communications systems because of size, weight, and space constraints. However, it is desirable to keep the fundamental frequencies of frameworks above 3 Hz to hold displacements to reasonable limits. In this respect, equipment design differs from building design. Designers of tall, slender buildings achieve a beneficial effect by designing for structural frequencies below those of earthquakes. Doing so minimizes acceleration forces which may act upon structures because they will behave as low-pass filters. For equipment, in contrast, the displacements associated with low-frequency design become intolerable. For example, a 1-foot relative displacement at the top of a 300-foot building may be acceptable, but similar motions at the top of a 7-foot equipment frame with a comparable natural frequency would be destructive.
4. Increasing Damping. Even small increases in damping diminish the amplification of motions caused by closely coupled equipment-building systems. An increase in damping from 2 to 5 percent may reduce equipment response by 30 percent in the critical resonance band between 1 and 7 Hz.

5. Reserve Ductility. One of the most desirable characteristics in any seismic-resistant component is its capability of absorbing energy after being stressed to the design limit. To yield and still carry load rather than suddenly fail through buckling or fracture provides a significant safety factor, allowing conservative and less costly designs.
6. Vertical Strength. Because equipment is designed to withstand gravity and handling forces in the vertical direction, it usually can also withstand seismic forces under  $1g$  in this direction without exceeding the safety factor for conventional design. However, when equipment is braced between the floor and ceiling, vertical motions must be considered to accommodate the relative displacements resulting from out-of-phase response of the building floors. Also, when designing against horizontal motions, one cannot count on the stabilizing effect of gravity loads of the equipment because of unweighting due to vertical seismic forces. Likewise, added stresses caused by vertical earthquake motions combining with gravity-induced stresses must be considered because these stresses may act vertically upon horizontally deflected equipment (P -  $\Delta$  effect).
7. Achieving Symmetry and Rigidity. Components with eccentrically loaded or irregularly framed structures experience unnecessary and sometimes excessive seismic stress caused by torsion or unevenly distributed response load. Symmetrical structures well balanced around the mass provide better support and may be less costly in the long run. Slender tube or channel-type structural elements such as those used on framework uprights may roll and buckle if not stabilized properly. Increased material thickness, stiffeners, and rigid end constraints minimize this problem.

#### Equipment Strengthening

Equipment strengthening to meet the above design objectives will be achieved through careful attention to even the smallest detail. Below are some typical protection concepts for communications hardware:

1. Batteries. Batteries for equipment operation or for standby power generally constitute the heaviest loading to be considered in communications centers. Batteries situated on metal frames or on shelves in metal cabinets must be secured to prevent them from pounding together or sliding and falling to the floor. The frames or cabinets must be securely braced and firmly attached to the building to prevent collapse of the entire assembly.

2. Cabinets. Equipment such as computers, rectifiers, and radio gear is packaged in cabinets constructed of sheetmetal sides with top and bottom held together by structural angle corner pieces. Much commercial cabinetry of this type does not incorporate diagonal braces to carry earthquake-induced shear loadings from the upper parts to the floor supports. When diagonal members are not present, the shearing forces must be carried by the metal skin of the cabinet, which in this case behaves as a diaphragm. This arrangement requires a good structural connection between the skin and the angle corner members. Some commercial cabinetry incorporates little or no connection of this type and, for this reason, should not be used in earthquake-prone areas unless specifically strengthened. Metal cabinets equipped with large swing open doors in one or more sides must have the remaining sides and top constructed to carry out not only shear but the resulting torsion and bending moments as well. The bottom of the cabinet must be sufficiently strong to transfer the shears and moments to the anchor bolts in the building floor.
3. Frame-Mounted Components. Equipment frames subject to the most severe earthquake excitations may respond with accelerations of up to about 5 g's with single-amplitude displacements of 6 inches or more at the frame top relative to the floor. The absolute displacement of the frame is usually much higher when the motion of the floor is added. Absolute horizontal single-amplitude motion may total 2 feet or more in major earthquakes depending upon the construction of the building. Further, vertical motions up to  $1\frac{3}{4}g$  above gravity may act at the same time as the horizontal motions. Components supported by the equipment frames must resist such motions unless separations or other types of malfunctions are considered acceptable in that they may be repaired after the quake.

Care should be taken to provide solid support for heavy items such as transformers. Eccentricity in the connections should be minimized to prevent overstress of materials or fatigue failure of the fastener. Wire wraps, where used, should be secure. In the maximum seismic risk areas, heavy circuit packs should be equipped with restraining latches to prevent them from being dislodged from their connectors and ejected from the framework. Tests have shown that the static withdrawal force of typical current circuit packs ranges from about 2 to 15 pounds depending upon the type of connector and the lubricant used on the contacts. An average value of about 8 pounds is typical. The withdrawal forces under dynamic conditions are very close to the static withdrawal forces in the frequency response band of most frameworks. Therefore, without

latches, a frame acceleration of 1 g's may dislodge circuit packs weighing more than 2 pounds if the static withdrawal force is 8 pounds.

4. Attachment Hardware Details. Strength designed into equipment is of no avail unless all of the critical components conform as intended to the earthquake loading standards. For example, a strong well-designed framework will not survive in an earthquake if the anchor bolts supporting it easily withdraw from the building. Bolts to the floor or other parts of a building require meticulous control in design and in installation. Frequently, expansion-type anchors are used to secure the bolts to the building masonry. Care must be taken in drilling holes for such devices to keep the holes from being oversized. Oversize holes result from using worn masonry drill bits and greatly reduce the carrying capacities of the anchor. Self-drilling anchor systems are usually more reliable in concrete because each device is equipped with an integral drill bit. Anchors placed in the building concrete during construction should be made from a material of toughness and some ductility--not cast iron, which may easily be snapped.

Since building floors may not be perfectly level, leveling shims are sometimes used under the metal frameworks or cabinets. Shims must extend fully to the vertical or side face of the equipment frame. When they do not, the motion may force the frame or cabinet base to bend around the shim, giving rise to a large sideways response and gross reductions in frame stiffness and response frequency.

Raised floors supporting equipment should be provided with sufficient lateral support and removable floor panels should be secured to the understructure when attached equipment loadings may be large enough to cause tipping.

Attaching equipment to steel bracing elements of the building is sometimes accomplished by using forgings or cold-bent steel fasteners such as J bolts. It is important that material for these devices be ductile, for example, mild steel, so that brittle failures are avoided during an earthquake.

#### Seismic Testing

Determining the true earthquake resistance of equipment through calculation alone frequently is relatively difficult because of the mechanical complexity, as well as because of the nonlinear and inelastic response of some individual components. On the other hand, testing on a hydraulic shaker

programmed to match the seismic motions at the equipment support points evaluates the design and allows modifications before field use.

A qualification test should be used to prove-in equipment. Synthesized time history waveforms can be prepared that closely resemble actual earthquake motions in a building and match the response spectrum of the various earthquake zones. Figure 4 shows a waveform (Ref 6) used to match the response spectrum of Figure 3. The amplitude of the waveform is scaled downward to match the floor accelerations shown in Table 1 for use in testing gear for installations in less severe seismic zones. Sine sweep vibration tests may also be used but should be limited to equipment that does not respond in a nonlinear or heavily damped manner.

When testing is performed it is preferable that the equipment or component and its supporting medium simulate as closely as possible that actually used in practice.

#### COST ASPECTS

Protecting communications networks from earthquake damage is desirable to minimize the loss of vital services and expensive plant. The costs incurred to implement the protective features may be estimated and related to costs associated with the potential loss of service and plant.

Earthquake protection is cost-effective when the total amount spent in protecting all installations is less than the dollar value of the singular or discrete service and plant losses. Figure 5 illustrates this. Shown are discrete losses incurred during each earthquake damage event related to the communications system. The amount of each discrete loss will increase with time because of inflation and because of greater plant exposure as a result of growth of the system. Likewise, the time spacing of discrete losses diminishes with time because there is a greater probability of damage by a given earthquake in a system with many elements than there is in one with fewer components.

The discrete losses may be averaged over time as shown in the figure and compared with the average cost of earthquake protection plus the reduced average losses of the protected system. The net cost advantage of the protected system is, of course, the difference between the loss and cost curves summed over the period of interest.

Earthquake protection in areas of significant earthquake occurrence is generally cost-effective in new construction since the price of such protection amounts to only a very small percentage of the value of the installation. However, retrofit strengthening of existing installations is very costly. Also, installations in marginal earthquake areas

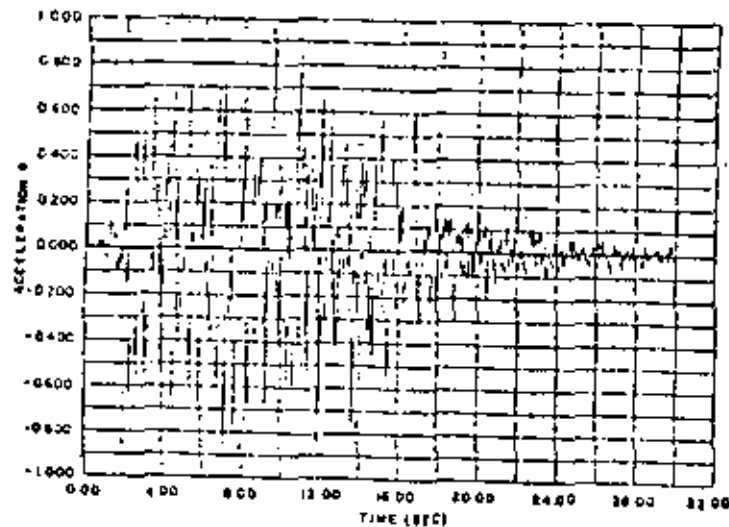


FIG. 4.-Analytically Developed Accelerogram

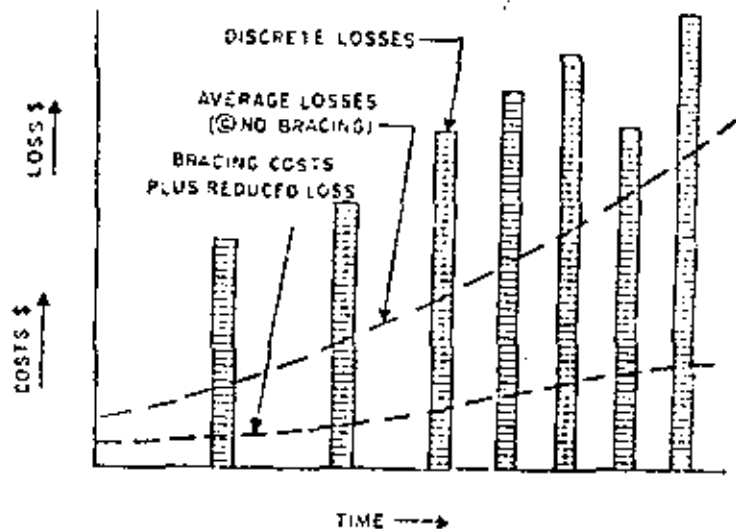


FIG. 5.-Bracing Cost and Loss Relationship

need to be evaluated from the cost standpoint, to determine the degree to which such strengthening should be employed. In the latter case, the importance of the installation relative to that of the entire spectrum of communications must be considered.

#### SUMMARY

Communications distribution systems such as buried cable and pole lines are most sensitive to axial elongations caused by the ground motions of an earthquake. Proper siting and control of backfill together with sufficient cable slack and strength at splices, manholes, and buildings will help minimize damage. Survivability is further improved through avoidance of other structures or utilities which may fail and damage communications, for example, a gas line exploding in an adjacent trench or a bridge collapsing and destroying any cables it carries.

Building-housed equipment, if not properly braced during an earthquake, forms one of the most vulnerable segments of a communications system. The building floors that support equipment will undergo seismic motions with accelerations up to 1g in major earthquake zones. Responding to these motions, equipment whose vibration frequencies lie below 10 Hz may sustain accelerations up to about 5g's. Thus, the strength of the equipment and that of its fastening or bracing to the building must be equal to the forces induced by such accelerations.

Resistance of equipment to seismic shaking is enhanced by designing for high stiffness, frequency, damping, and ductility, and low center of gravity in a symmetric, torsion-resistant structural framework. Subcomponents must be securely attached or latched into place to prevent being dislodged from their supports. Damage to cabling, ducts, or piping caused by unequal or out-of-phase motions between adjacent pieces of equipment is prevented by minimizing or eliminating the relative response--as for example, through the use of tie-struts.

Earthquake protection of communications equipment is generally cost effective in major seismic risk areas. The feasibility of similar protection in low-risk or marginal earthquake areas may be determined from cost/loss analyses which consider the importance of the facility as well as plant expenditures. Applique bracing that is graded in strength to match the zonal and/or importance classifications may provide a low-cost option for such areas.

## Appendix 1 -- REFERENCES

1. Applied Technology Council, "Recommended Comprehensive Seismic Design Provisions For Buildings." Final Review Draft, Jan. 1977.
2. Foss, J. W., "Protecting Communications Equipment Against Earthquakes," Proceedings--U. S.-Japan Seminar on Earthquakes and Lifeline Systems, Tokyo, Japan, Nov. 1976.
3. Page, R., Bocre, D. M., et al, "Ground Motion Values for Use in the Design of the Trans-Alaska Pipeline System," Geological Survey Circular 672, Washington, 1972.
4. Christian, J. T., "Relative Motion of Two Points During an Earthquake," ASCE Journal of the Geotechnical Engineering Division, Nov. 1976, Technical Notes, pp 1191-1194.
5. Liu, S. C., Fagel, L. W., and Dougherty, M. R., "Earthquake-Induced In-Building Motion Criteria," ASCE Journal of the Structural Division, Jan. 1977. pp 133-162.
6. De Capua, N. J., Hetman, M. G., and Liu, S. C., "Earthquake Test Environment-Simulation Procedure for Communications Equipment," Shock and Vibration Bulletin, Aug. 1976.

PROTECTING A POWER LIFELINE AGAINST EARTHQUAKES<sup>1</sup>

by

Otto W. Steinhardt<sup>2</sup>, M.ASCE

## ABSTRACT

An electric power system is described, its relevance to the life of the community is examined, and its seismic withstand capability is evaluated. Recommendations are made to assure that this lifeline will be able to keep the vital functions of the community going in the face of seismic disaster.

## INTRODUCTION

An electric power system consists of many diverse elements and covers much area. To evaluate its ability to withstand an earthquake requires that the system be analyzed as a whole. Failure of one element may constitute failure of the system, but perhaps the system can function well enough, at least temporarily, even if some of its parts have been knocked out of service.

When an earthquake strikes, the lights may dim, but in most parts of the city they won't go out -- at least not in a city where the power company has built and maintained its system with a reasonable standard of seismic resistance.

What is a "reasonable" standard? To answer that question, we first need to consider why electric power is important to a community in the aftermath of an earthquake, what a power system is made up of and which parts are necessary for providing uninterrupted power. Also we need to ask what earthquakes actually have done to power systems, what is the earthquake withstandability of a large power system, what additional capability can be provided in the future through replacements and new construction, and what recommendations should be implemented so that the response to the great earthquake when it happens will be all that anyone could reasonably hope for.

<sup>1</sup>Prepared for presentation at ASCE TCLEE Specialty Conference, Los Angeles, California, August 30-31, 1977

<sup>2</sup>Senior Civil Engineer, Pacific Gas and Electric Company  
San Francisco, California

## LIFELINE FUNCTIONS

Hospitals, pumping stations, telephone exchanges and certain other important facilities are equipped with emergency power generators, but these generators may not start when most needed. Also, there are many important facilities which are not so equipped. In some cases a system may be so spread out that it would not be practical to provide emergency power at every place where power would be needed. Cold-storage warehouses, walk-in refrigerators in supermarkets, gasoline pumps, and transit systems are just a few of the power-dependent facilities which are quickly felt by their absence when they stop functioning. Television and radio stations and newspaper printing plants are needed in disaster-stricken communities to keep up morale and help counteract the panic-inducing rumors which quickly start circulating. Home freezers contain much food which should be saved from spoiling if possible. Even in places which have emergency generators, the need for power is usually much greater than can be provided by the standby units in order for the facilities to function at anywhere near full capability. Clearly, it is important to the community that there should be no widespread power outage resulting from an earthquake.

## DESCRIPTION OF POWER SYSTEM

An electric power system consists of generating stations, transmission lines and distribution lines. Besides these strictly electrical components, there are the backup systems: communications and power control, repair and maintenance service, warehouses, shops and fuel-handling facilities.

The generators are driven by turbines which are, in turn, driven by water, steam or hot gases. The steam may originate in a boiler heated by fossil fuels or in a nuclear reactor, or may come from a geothermal well. Gas turbines, which are actually modified jet aircraft engines, are used to drive generators, also.

Because bulk power is most efficiently transmitted at voltages much higher than practical levels at which it can be generated step-up transformers are provided at all generating stations. Then, when the power enters the distribution system, it must be stepped-down to levels which are efficiently usable by the customers. To maintain the predetermined voltage, autotransformers and voltage regulators are used. Capacitors are used to improve the power factor by keeping the three phases of a transmission circuit in good relationship to each other. To protect transformers against power surges resulting from short circuits, circuit breakers of various types are provided, and, for long term interruption of a circuit, isolating switches are used. To protect the system against voltage spikes resulting from lightning, lightning arresters are used; they resist the passage of current at normal voltages but allow transient peaks of overvoltage to go into the ground. Wave traps are used to enable transmission of supervisory signals through the power lines. Buses provide low-loss transmission linkage of the many and varied components within a switchyard or substation.

The minimal essentials to keep power flowing are the generating stations (although sometimes bulk power is available from outside sources), transmission lines, transformers, circuit breakers, and switches (although bypasses can sometimes be rigged). Bus structures must not collapse. The communications system is vital for controlling the flow of power and enabling quick restoration of service. The many other components of the system, valuable as they are in daily service, can be dispensed with, bypassed, or substituted for in an emergency. Efficiency will suffer and system capacity will be lowered, but power still will flow to those customers able to use it. Of course, in a great earthquake a large number of customers will be knocked out and so, temporarily at least, the demand for power will be down. It is hoped that the repair rate will exceed the rate of recovery of the demand for power.

## EFFECTS OF PAST EARTHQUAKES

Subjecting a system to an earthquake is a good way to test its ability to withstand other earthquakes. So, let us take a look at what earthquakes have done to power systems.

1. When the great earthquake occurred in San Francisco and along the coastal zone north and south of there in 1906 ( $M=8.3$ ), there wasn't a great deal of damage to electric systems because not much of a system existed. Power system damage came from a falling roof, falling chunks of brickwork and a broken smoke stack. Pole lines and underground ducts were not heavily damaged, except in locations where the soil failed. (1)
2. In the great Kanto (Japan) earthquake of 1923 ( $M=8.2$ ), 23 out of 91 hydroelectric plants and all 11 steam-electric stations in and near Tokyo were damaged. There was much destruction of wood pole transmission lines and substations, mostly owing to the fire which followed the quake. Unreinforced masonry failures were responsible for damage of reservoirs, canals and penstock intakes. This, in turn, led to washouts and landsliding which damaged the penstocks and powerhouses. Except where the foundations settled, ground shaking caused no damage to generators. Transformers survived where they had been anchored. Circuit breakers were undamaged if they had flexible connections to the buses. Bus structures survived if the buildings to which they were attached did not collapse. Of 2400 transmission towers about 10% were damaged. Wherever a tower was a complete failure the cause was landsliding. Some were damaged because of foundation failure; the few structural failures which occurred were in lines which were "at right angles to the seismic waves." (2)
3. In Long Beach, California, in 1933 ( $M=6.3$ ), transformers shifted, bushings broke, oil spilled from transformers and switches. Transmission towers were undamaged. All circuits were back in service in 5 minutes. In Compton, the substation was back in service in 47 minutes; however, several

- distribution lines were down so full restoration of service took longer. (3)
4. The strongest earthquake to strike California since 1906 was the 1952 Kern County (Arvin-Techachapi) earthquake (M=7.7). It did enough damage to electrical equipment to cause the California electric power companies to take notice. Substation transformers rolled off their foundation rails unless they were strongly anchored. Pole transformers fell off of platforms except where they were bolted in place or otherwise securely fastened. Standard procedures for installing transformers were changed as a result of the type of damage observed in this earthquake. There were other kinds of damage: fan blades bent, pump bearings burned out, oil sloshed over the top of storage tank walls and in some cases wrecked the roof. Some transmission towers were disabled because of landslides or foundation failures. In many spans of transmission and distribution lines the conductors slapped against each other because of swinging, and some burned down as a consequence. A hydroelectric plant in Kern Canyon was damaged by falling rocks and dirt, but it continued operating at reduced capacity. (4), (5)
  5. In 1964, Niigata, Japan, was hit by a strong (M=7.5) earthquake. Seven out of 8 substations were heavily damaged. A steam power station suffered damage to the condenser and cooling lines. Eleven hydroelectric stations out of 230 in the district were put out of service; 47% of the city's power was out for nearly five days. Portable transformers were helpful in getting service restored. Underground lines were damaged, probably because of soil liquefaction.
  6. Alaska was struck by an even greater earthquake (M=8.4) in that same year (1964). At the Eklutna hydroelectric project near Anchorage, the operator on duty thought an atom bomb had exploded and had triggered a huge landslide. The plant was able to go back on line within 20 minutes, but the power had no place to go until temporary jumpers could be installed around wrecked circuit breakers. Intermittent rock and snow slides and reservoir cave-ins made operation of the plant a touch-and-go matter for the next six weeks. In Anchorage, an oil storage tank ruptured and gasoline supply lines broke, so the city's gas turbines and diesel generators couldn't operate. Heroic efforts by all hands, made possible a 90% restoration of power within 3 days. (7), (8)
  7. In Chile in 1960 (M=8.5) and again in 1965 (M=6.4) circuit breakers, transformers, and capacitor banks were damaged in considerable numbers. This was the first time that high voltage substation equipment, other than unanchored transformers, had been seriously damaged in an earthquake. Until that time it seemed that there was no particular need to provide seismic resistance when designing such equipment. (9)

8. The San Fernando Valley earthquake of 1971 (M=6.6) dramatically demonstrated that seismic design of major equipment needed more attention than it had been given in the past. The quake tripped out 4 major steam units, although they were not damaged. A landslide wrecked a small, 50-year old hydroelectric plant. Ground shaking seriously damaged two switching stations, resulting in electrical isolation of 10 bulk power substations and many outages on the distribution system. Most customers who could receive power were reenergized within a few hours and nearly all within 5 days. Nevertheless, some severe damage occurred at locations near the epicenter of this "moderate" earthquake. At Sylmar Switching Station, all of the 230 KV air-blast circuit breakers were damaged badly; all 26 disconnect switches were damaged, especially in the bearings of the rotating columns; most of the 12 potential transformers were damaged; all of the wave traps broke off of their columns; several lightning arresters fell; some of the 230 KV rigid bus broke loose from supports; some transformer anchor welds broke.
- Olive Switching Station also was heavily damaged, and the Sylmar high voltage DC Converter Station was 40% destroyed and required over 18 months to be restored to service. There was significant damage at several receiving stations (transmission terminal substations) and at five distribution substations, and less damage at about two dozen distribution substations and three receiving stations. About a mile of 34.5 KV underground cable, and a half mile of 5 KV, had to be replaced, along with six manholes and some potheads and trifurcators. (10), (11)
9. In the December 1972 Managua, Nicaragua, earthquake (M=6.5), the Managua Power Plant, 70MW, was less than a mile from one of the major fault traces. This plant was designed for 0:1g by static equivalent load method; it had to shut down for repair. Switchgear and batteries were damaged. A 40 MW and two 15 MW turbine-generator units were damaged because of hammering of turbine pedestals against the surrounding concrete floor. The smaller machines were repaired within 4 weeks but the 40 MW unit required replacement parts and technicians from Europe so repairs took about 4 months.
- The plant had two 16,000 barrel oil tanks. The floor plate of one tank ruptured where a roof support column was welded to the floor. The other tank was undamaged. In the plant switchyard, rail-mounted transformers derailed and some bushings broke. Substations suffered transformer and insulator damage. Wood pole distribution lines were not damaged by ground shaking. By December 29, six days after the earthquake, electric service was almost fully restored to Managua. (12), (13)
10. Guatemala was struck by an earthquake, M=7.5, in February 1976. An electric power plant, 42.5MW, in Guatemala City,

was designed and built in 1958 by EBASCO, a US firm. There are 4 gas turbines and one oil-fired boiler unit. The plant was probably designed according to typical US design practice for seismic areas like California, i.e., using 0.2W (or less) static equivalent force. The power plant is 100 miles from the epicenter, but only 25 miles from the nearest part of the fault trace. The plant was tripped out by the earthquake and was out of service for 40 minutes but suffered no damage. The oil tanks apparently were undamaged as they are not mentioned in the report. (14)

#### ABILITY TO WITHSTAND EARTHQUAKES

Now that we know something about what earthquakes have done to power systems, what guesses can we make about what a future earthquake will do to a particular power system?

The particular system I have in mind is the Pacific Gas and Electric Company which serves 47 counties in northern and central California (Figure 1). It can generate over 14,000 megawatts (MW), of which 60% is in steam plants and 40% is hydroelectric capacity.

Because PG&E is in California, the threat posed by earthquake is accepted as a fact of life. There have been at least 10 strong earthquakes (Richter Magnitude over 6.0) in the service area in the last 60 years, and there have been at least three great earthquakes (RM over 8.0) in the last 200 years (San Francisco 1838 and 1906; Fort Tejon 1857). There are about a dozen active faults (Figure 2), of which the most threatening are the San Andreas, the Hayward, and the Calaveras faults.

By far the greatest part of the PG&E system is of modern vintage. The four largest steam plants, with combined capacity equal to 45% of that of the total system are at Pittsburg, Contra Costa, Moss Landing and Morro Bay. Two-thirds of their capacity is in units of 300 MW or larger, housed in braced steel frameworks designed for 0.2W static equivalent lateral load. In their design close attention has been given to the details which often make the difference between what survives an earthquake and what doesn't.

Hydroelectric development on the McCloud, Pit, Kings, and Feather rivers, added 10% of system capacity, between 1952 and 1965. Also, nearly 4% of system capacity has been installed in the Geysers geothermal steam field since 1959, and a 63 MW nuclear unit was built at Humboldt Bay only 15 years ago.

In the next few years the system will be further enlarged by the addition of a large pumped storage hydroelectric plant and by the two large nuclear units at Diablo Canyon which will add 16% to system capacity. The Diablo Canyon plant is nearly complete but is not yet licensed to operate. Another nuclear plant, a coal-burning plant, and several gas-turbine units are planned for the future.

The transmission lines, mostly of modern construction, are widely

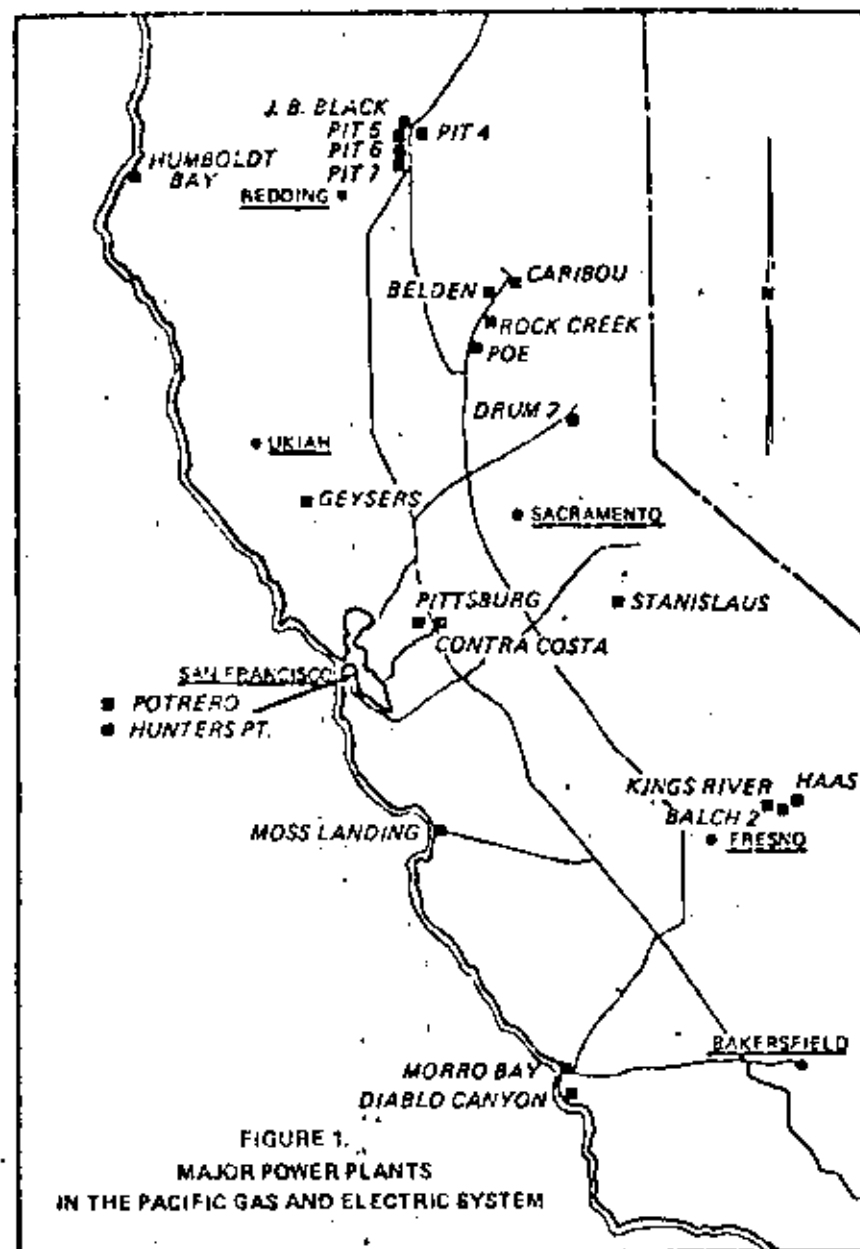


FIGURE 1.  
MAJOR POWER PLANTS  
IN THE PACIFIC GAS AND ELECTRIC SYSTEM

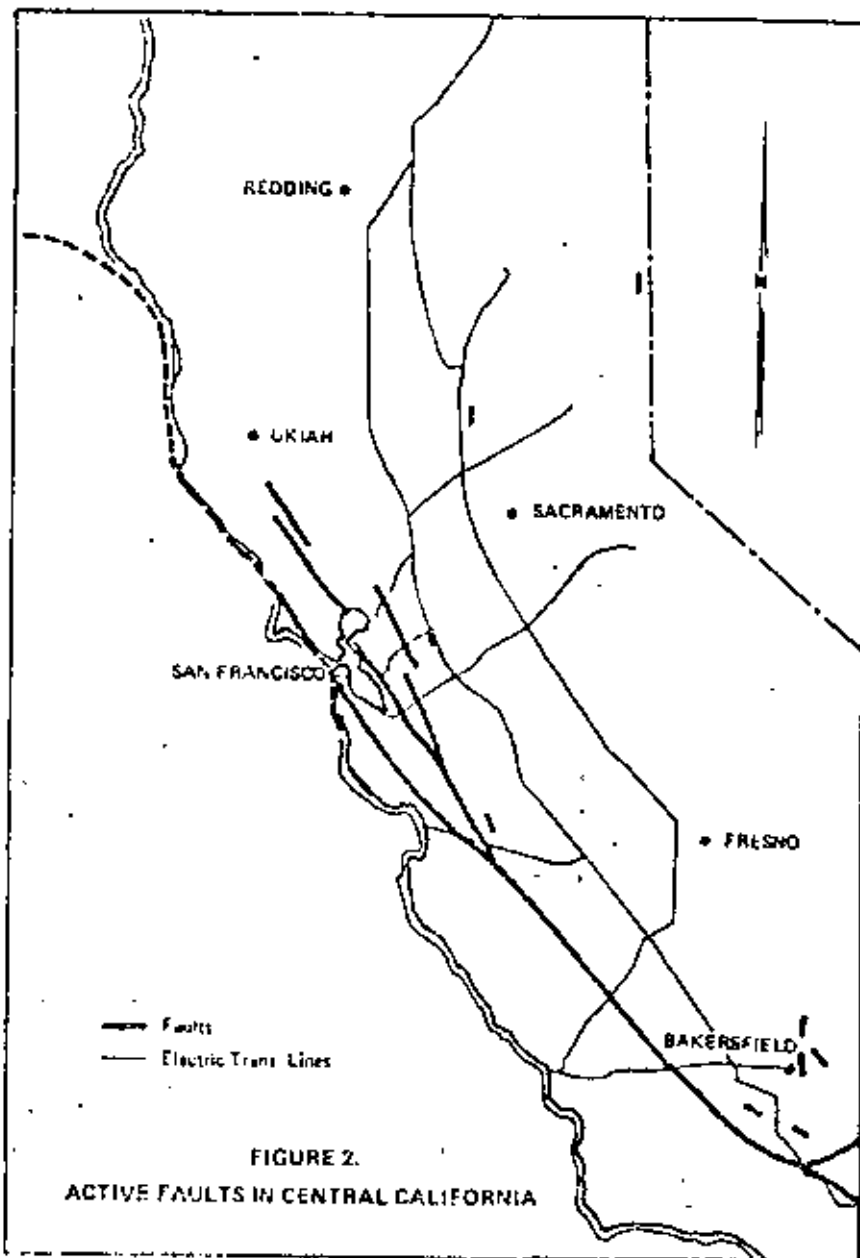


FIGURE 2.  
ACTIVE FAULTS IN CENTRAL CALIFORNIA

dispersed. This factor lessens the danger of earthquake damage. Also, transmission lines have never suffered much from seismic shaking, because the towers are designed to survive heavy loads resulting from ice, wind and broken wires, so the seismic load doesn't have much influence on the design. However, a tower may be damaged by landslides, rolling boulders, or liquefaction of the supporting soil. Also, power lines sometimes swing so wildly when shaken that they slap against each other and burn down, or at least trip out the circuit. The hazards of landslides, etc., can be minimized by careful site selection and good foundation design. As for the problem of conductor slapping, wider spacing of conductors would be of some benefit but considerably more expensive. Inasmuch as this hazard seldom occurs, it's not justifiable to spend money to prevent it from happening.

Some transmission lines are underground. Fault slippage is not likely to damage such underground lines because of their thick-wall welded steel pipe jacket. Shaking has never been a source of damage to such lines except where it has led to failure of the earth masses in which the line is buried. Displacement of manholes from the conduits in which the cables are laid sometimes can cause the line to fail. In case an underground line is knocked out, repair usually takes a long time and an overhead line would probably be rigged as a temporary bypass.

Substations and switchyards are vulnerable to earthquake damage. Substation equipment installed before the San Fernando Valley earthquake (1971) was purchased under specifications which required that the equipment be able to withstand 0.2 W lateral load applied statically. After 1971, specifications changed to a higher level to meet the demonstrated need. Now, substation equipment which is necessary for continuity of power supply (the minimum essential system) is required to withstand maximum horizontal ground acceleration of at least 0.4g horizontal acceleration and 2/3 as much vertical using designated response spectra. Equipment which is not part of the minimum essential system is required to withstand at least 0.2 W lateral load, as before.

If critical equipment is to be supported on a structure, dynamic modeling of equipment and structure is included in the design. In case the equipment is unable to take the seismic loads under these conditions, modifications are made.

Many types of substation equipment have been dynamically evaluated in the last 5 or 6 years, either in-house or by the manufacturers. Some modifications of design have resulted, and in a few cases installed equipment has been back-fitted or replaced. In many cases the analysis has shown that all that's needed is to provide sufficient anchorage to the supports.

Seismic design criteria for distribution nets are not as conservative as for transmission facilities. It is expected that after a seismic event line repair crews, reinforced by electrical contractors, using on-hand materials from Company and other warehouses, will be able to restore service to damaged areas at least as quickly as the customers' demand for power recovers from the disruptive effects of

the cause.

In San Francisco, an energy control center is housed in a low-rise building which was designed to withstand the effects of debris falling from the nearby high-rise buildings. The nonstructural partitions, the suspended ceiling, the operational map boards and other installed equipment have been subjected to a post-construction review to identify seismic vulnerability and a modification program is currently underway to correct the deficiencies which were found.

Besides keeping generating stations and transmission facilities from being knocked out we need to be sure that the fuel supply won't be disrupted.

The fossil fuel steam plants burn oil or natural gas. A two month supply of oil is stored at each such plant. In the last six years, twenty-four oil storage tanks, mostly the half million barrel size, have been installed. They were designed for 0.2 W lateral load and have been checked by dynamic analysis and found capable of sustaining 0.67g maximum ground acceleration without buckling or overtopping by sloshing.

The supply of natural gas comes from California (17%), from Texas (30%), and from Alberta (45%). The 78 billion cubic foot reserve is stored in what was a nearly-depleted gas field in central California.

The oil and gas pipelines cross active faults at several locations. These crossings have been plotted on maps of the system so that if a fault breaks the lines crossing it, the damaged places can quickly be found and inspected. In many instances there is little to worry about because the amount of fault slippage would probably be only a few inches. A welded steel pipeline properly installed in a sand filled trench can take many inches of fault offset. This was dramatically demonstrated after the Kern County earthquake (1952) when a 34-inch diameter high-pressure gas main was offset more than two feet with no significant damage. The pipe was later cut to relieve the locked-in stresses and the cut ends sprang out of alignment by about four inches.

The hydroelectric system depends on dams and penstocks for its "fuel." There are over 150 dams of various types and sizes in the PG&E system. Some are at least 100 years old, having been built by other groups for other purposes, like gold-mining. About a dozen major dams were built after World War II and were designed for 0.1 W lateral loads. Some of the other major dams need attention. Because of the potential hazard to downstream populations, an on-going dam safety evaluation program is being conducted. It utilizes both pseudostatic and dynamic analysis methods to check seismic safety. The program has revealed some deficiencies which the Company has corrected. Thus far, a major dam has been replaced, a reservoir has been lowered, and a half-dozen major strengthening projects have been completed.

ABILITY TO RECOVER.

It would be too much to expect a power system to come through an

earthquake unscathed. Economic considerations require that the defenses against seismic hazards be prudently high but when prevention of such possible damage becomes significantly expensive, some damage must be accepted. Therefore, it is essential to be ready to spring into action quickly and efficiently as soon as the shaking has stopped. An assessment of damage must be made, damaged circuits must be isolated and undamaged areas restored to service immediately. Available crews must be dispatched, reserve forces must be mobilized, material needs must be identified and supplies located. The rapidly changing situation must be kept under continuous observation so that personnel and materials can be redeployed if necessary. To accomplish all of this, a communications and control system is essential.

PG&E has a mobile radio system, with 250 base stations at service centers throughout the area controlling 3400 maintenance and supervisory vehicles. Power control signals can be transmitted directly over the power lines. Also available are microwave transmission stations and intra-company telephone lines.

Each of the 13 operating divisions of the Company has one or more switching centers, each of which is continuously staffed. The operators monitor the status of all transmission circuits and take immediate action on emergency situations as they develop. At the energy control center, the dispatcher coordinates actions which are outside the control of the switching center operators and reports to management any situation which cannot readily be taken care of.

The communications system is capable of operating on batteries and emergency generators for 72 hours. Communication racks and battery racks have been surveyed for resistance to earthquake loads and have been provided with bracing and anchorage sufficient for 0.5g horizontal and 0.30g vertical acceleration in all critical relay stations. 73

Substation and switching center storage battery racks are currently being surveyed to identify and strengthen those which need improvements to withstand possible seismic loads.

Line crews would not be able to accomplish much if their trucks were wrecked by the earthquake or if the gas tanks were empty. Most trucks are parked outdoors, so there is little danger of their being trapped by collapsed buildings. In several division areas, resupply of gasoline is carried out by tanker trucks with on-board pumps. The tanker goes to where the trucks are parked and fills the gas tanks. There is little danger, therefore, that the crews would be crippled by running out of gasoline just when they need it most. In all divisions, either the gasoline tanks are above ground or an emergency generator is available to run the pumps in case of power failure.

#### SUMMARY AND RECOMMENDATIONS

PG&E is not unique in the way in which it has addressed the earthquake problem. Probably all of the West Coast utility systems are similarly ready and able to cope with seismic events. However,

there should be no relaxation of efforts to search out ways to improve the seismic withstandability of critical components of the system. Also, redundancy should be developed in all parts of the system so that alternate paths are available for routing of power in an earthquake disrupted system.

Utilities should exchange among themselves detailed reports of earthquake damage. Development of seismically resistant critical electrical equipment for substations and switchyards should be undertaken cooperatively.

Rapid restoration of electric service in an earthquake damaged area is achievable if foresight is applied.

#### ACKNOWLEDGMENTS

Arle Schuurman and many others in the engineering and electric operations department of PG&E were very helpful in providing information and suggestions for this paper. Jamie Chin typed the manuscript. M. Callejas, H. Filter, and R. Fogliasso did the graphics.

#### REFERENCES

1. ASCE Special Committee, "Effects of Earthquakes on Engineering Structures," unpublished manuscript in Engineering Societies Library, New York, N. Y., 1923; Microfilm 9808 TH in UC Berkeley Library.
2. Shibusawa, M., "Description of the Damage Done by the Great Earthquake of 9/1/23 to Electrical Installations in Japan," Japanese Electrotechnical Committee, April 1925.
3. Binder, R. W., "Engineering Aspects of the 1933 Long Beach Earthquake," Proceedings of Conference on Earthquake and Blast Effects on Structures, EERI, June 1952.
4. ---, "Earthquakes in Kern County, California, During 1952," California Division of Mines and Geology, Bulletin No. 171, 1955.
5. Vivian, J. H., "Earthquake Damage in California," Minutes of Electric Equipment Committee, EEI, October 1952.
6. Kawasumi, H., "General Report of Niigata Earthquake of 1964," Tokyo Electrical Engineering College Press, 1968.
7. ---, "Wracked Alaska has Power," Reclamation ERA, v. 50, n. 4, November 1964.
8. Scott, H. P., "Electrical Damage and Restoration in Alaska," Electrical Construction and Maintenance, v. 63, n. 6, June 1964.
9. Novoa, F., "Earthquake Analysis and Specification of High Voltage Electrical Equipment," Proceedings of 5th WCEE, Rome, 1973, Session 2B.
10. ---, "San Fernando Earthquake of 2/9/71, Effects on Power System Operation and Facilities," L. A. Dept. of Water and Power, 1973 (Design and Construction Division, unpublished manuscript).
11. ---, "The San Fernando, California, Earthquake of 2/9/71 -- Utility Systems," NOAA, 1973, Vol. 2.
12. Berg, G., Degenkolb, H., Ferver, G., "The Managua Earthquake of 12/23/72," AISI, 1973.
13. ---, "Managua, Nicaragua, Earthquake of 12/23/72 -- Reconnaissance Report," EERI, May 1973.
14. Chieruzzi, R., "Summary of Observations and Comments Regarding Guatemala Earthquake Damage," EERI, March 1976.

ADVANCES IN MITIGATING SEISMIC EFFECTS ON POWER SYSTEMS

by

Anshel J. Schiff<sup>1</sup>, M. ASCE

ABSTRACT

The history of earthquake damage and facility specifications for electrical power systems is reviewed. A bibliography of power system damage reports is given. Current practices for mitigating earthquake effects in different parts of the country with high risk are discussed. Research to mitigate earthquake effects is reviewed and problem areas are discussed.

INTRODUCTION

This paper is one of a series written in conjunction with the Technical Council on Lifeline Earthquake Engineering to review the state of the art of lifeline earthquake engineering -- in this case, the electric power industry. The paper will review the history of earthquake damage suffered by power facilities, and concurrently, it will follow the evolution of seismic specifications for power equipment and facilities to address the lessons gained from damage experiences. Current engineering practice for mitigating earthquake effects in high and moderate seismic risk areas with both high and low awareness of the earthquake problem will be reviewed. Current research to mitigate earthquake effects is reviewed and problem areas are discussed. Finally, the paper gives conclusions and recommendations.

HISTORY OF EARTHQUAKE DAMAGE AND SEISMIC SPECIFICATIONS

This section will review reported earthquake damage to power systems and the attendant changes in design practice adopted by utilities to improve earthquake resistance of power system facilities.

Japan experienced its most damaging earthquake and post-earthquake fire in 1923. The earthquake and fire took 150,000 lives, destroying 500,000 dwellings. The earthquake magnitude is estimated at 8.2 and affected Tokyo and Yokohama. Seven different systems serviced the damage area, although two of the systems suffered most of the damage, which was extensive. The description of damage reported here will be rather detailed, since many of the failures observed in this earthquake will be reported in subsequent earthquakes. The material has been taken from a

report [12] which probably represents the most complete effort to date to document earthquake damage to power systems. It is unfortunate that it did not serve as a model for future efforts. The paper which is published in English is "an outline from the original (published in Japanese) which was very extensive." [This "outline" has some 51 pages of text and 66 pages of photographs. The coverage is broad, detailed, and concise. The paper was prepared by The Japanese Electrical Committee, consisting of 60 members representing the Institute of Electrical Engineers of Japan, the Joint Electro-Technical Committee, and the Electrical Association of Japan. The original paper was published on December 24, 1923. The English version was published in April, 1925, and at least one U.S. utility had a file copy by March 1927.

The material described below will, of necessity, be brief and fragmentary, as the source material is itself a concise summary. To give one an appreciation of the effort which went into the preparation of the original, one section dealt on the possibility of the power system as a source of fire. In this study, some 36,000 houses (in unburned portions of the city) were inspected for fire damage and sources.

From an overall perspective, there was a total disruption of service with very limited service restoration after two days. It was felt that the disruption of electric power "greatly added to the chaos and turmoil at the time." Table 1 shows the growth of power demand after the earthquake. The practice of not providing system redundancy, particularly for transmission facilities, greatly affected the extent and duration of disruption.

TABLE 1. POST-EARTHQUAKE POWER DEMAND

Date	Power Demand (KW)
9/1/23	0
9/3/23	5
9/10/23	35,000
9/20/23	70,000
10/1/23	90,000
11/1/23	140,000
12/1/23	170,000
12/8/23	203,000
2/1/24	193,000
2/12/24	213,000

Maximum power consumption prior to the earthquake was 203,000 kilowatts

GENERATION

Steam and gas units were, for the most part, on reserve at the time of the earthquake, power being supplied by hydrogeneration. Steam and

75

<sup>1</sup>Assoc. Prof., School of Mech. Engrg., Purdue Univ., W. Lafayette, Indiana 47907.

gas units required from one to several months to resume operation. Most units were on poor sofs. Boilers had no serious problems except for leaks which developed at joints of tubes and drums from external structural failures. Thirteen boilers (21%) had severe damage, 26 (41%) had the sidewall bricks of the combustion chamber damaged, and 24 (38%) had no damage.

Steel pressure piping was undamaged, but cast iron water return pipes had cracked flanges. Prime movers were undamaged, although they were typically on good foundations.

Some hydroelectric generation systems required a month or more to recover, while others were totally destroyed in the most severely shaken area. Earth-filled dams experienced severe cracking, although there were no failures. None, however, were in the severely shaken area.

The transmission system experienced damage primarily from landslides and foundation failures. In some cases, cylindrical footings pulled up, legs failed if diagonal bracing did not start close to the footing, and poor workmanship, such as loose bolts, was observed. Concrete towers responded relatively poorly because their weight aggravated foundation problems. Wood towers experienced broken stays and also failed due to overload. Pin-type insulators fared worse than suspension-type insulators.

Poles on the distribution system -- primarily wood -- behaved well. Many conductors short-circuited because of inadequate separation. Un-anchored pole transformers, which were common, fell. Service wires failed due to building damage.

Direct and conduit-enclosed buried cables (370 miles of transmission and 1025 miles of distribution) had twenty junction box failures and two shorts due to moisture seepage through failed casings. Brick and steel manholes and vaults were damaged. The damage to steel enclosures was caused by the fire. Reinforced concrete enclosures behaved well. Great difficulty was experienced in locating and repairing cable damage due to debris. Extensive damage was experienced at bridge crossings due to fire on wood, steel, and stone bridges. Outside of the fire area, there were no failures.

Substations and similar facilities associated with generating stations were most heavily damaged by falling buildings. Transformers, which were generally on wheels or unattached to pads, moved. Thirty-one units moved and developed leaks, broken bushings and broken control lines. Some foundations, which were often of poor quality, tilted, also causing units to shift. Oil circuit-breakers, disconnect switches, and control boards behaved well if they were in good structures and well-secured. Lightning arresters were extensively damaged. For some utilities, all lightning arresters of a given type failed, emphasizing the importance of design practice. Batteries, in general, (78%) were turned over, short circuited, or completely destroyed. One station had them tied to the floor and experienced no damage.

Communication lines used to control the transmission system were carried on transmission towers or on adjacent, but separate, poles

Tower-supported cables behaved better, but still experienced wrapping, and communications were, in general, disrupted. Public telephones which were operational and messengers provided communication to control the transmission system.

Within buildings, switchgear and accessories failed due to building collapse or improper mounting. Transformers broke power, oil, and water connections due to poor mounting. Batteries overturned and had shorted plates. Lights were heavily damaged (83% in one structure). Motors associated with various building systems failed due to poor mounting. Loss of power stopped all elevators and lack of emergency exits trapped passengers.

An extensive survey (36,000) of the electrical systems within houses indicated that existing interior wiring standards were adequate to avoid fires.

A summary of the various recommendations and conclusions of the report follows:

1. Siting with particular attention to soil conditions and foundations is vital to the earthquake resistance of facilities.
2. The improvement of the earthquake resistance of structures is vital.
3. There should be redundancy in transmission and communication lines between major facilities.
4. Earth-filled dams require further study.
5. Equipment must be adequately secured.
6. Adequate slack of electrical connections between equipment is required.

While present day facilities are physically much larger and the state-of-the-art for analysis and design has made significant advances since 1923, it is interesting to note that most of the recommendations voiced in this, the first comprehensive report of power system earthquake damage, have by and large, been reiterated, in part, after each damaging earthquake. The author does not know to what extent the recommendations in the report were effectively acted upon in Japan. It would appear that U.S. utilities did not respond to the report.

The Long Beach Earthquake of 1933 had a magnitude of 6.3. The reported power system damage was not too significant, consisting of the loss of two 220KV buses (450 broken pillar-type insulators, broken connections to transformers which shifted on their rails, shifted potential transformers, and overturned batteries). While the first building code with seismic requirements was initiated as a result of the Santa Barbara Earthquake of 1923, the Long Beach Earthquake stimulated their wider use in California. Prior to 1933 a .2g static lateral force was used in the design of some utility facilities. After 1933 the .2g specification

was used more widely. Also, flexible bus was adopted for new high voltage facilities and then transformers were secured to their foundations. It was not until after 1945 that the .2g lateral force requirement was formally incorporated into equipment specifications. It should be noted that the decision to adopt seismic specifications rested with individual utilities.[3]

The Olympia Earthquake of 1949, with its epicenter located 15 miles from Olympia and 80 miles from Seattle, was of 7.1 magnitude. Damage was not significant, consisting of a 230KV transformer rolling and breaking insulators and control conduits; wrapping of wires on long spans caused delays in restoration in outlying areas; soil problems caused transformer faults; an insulation string broke and many units tripped; and many service lines were pulled from buildings. A brick stack on a standby unit was also damaged. The Bonneville Power Administration (BPA) experienced some damage and instituted a .2g seismic specification. Also, for new facilities transformers were secured to their foundations. [2]

The Arvin-Jericho earthquake of 1952 with a magnitude of 7.1 caused damage to generation, transmission and distribution facilities. A generator thrust bearing was damaged and a shaft bent but was corrected with a heat soak. Fifty-six cooling fans, four fuel tank roofs, and a boiler feed water pump were also damaged. Transmission facilities experienced two burnt down lines and three towers were lost due to slides. Several transformers shifted but there were no failures. Over 800 pole transformers fell to the ground although none which were secured to their platforms fell. It was felt that relaying of transmission lines prevented burn downs on distribution lines which were wrapped. The lines were difficult to clear. As a result of this earthquake, some California utilities reviewed their facilities and secured older equipment not covered by the practices adopted in 1933.[3,14]

The Niigata, Japan, earthquake of 1964 was of 7.5 magnitude and caused extensive power system damage and disruption of customer service. Eleven of 232 hydroelectric facilities were damaged as were condenser and cooling ducts at a thermoelectric plant. Seven of eight substations were severely damaged, requiring 5 days to restore, during which time approximately 50% of electrical service was disrupted. Portable transformers helped restore service. Underground facilities were extensively damaged and were difficult to repair.[4,13]

The 1964 Alaska earthquake with a magnitude of 8.4 caused damage to the inlet of a hydroelectric facility which maintained service but with numerous problems. Valdez lost the fuel supply and start up power for its diesel generators. Damaged circuit breakers were bypassed enabling the hydroelectric facility to provide service. Extensive damage, which was not reported in detail, was repaired so that service was 90% restored within three days.[7,15]

Power systems were damaged to different degrees by four South America earthquakes of Chile, 1960 and 1965, Nicaragua 1972 and Guatemala 1976. The now common damage of unsecured transformers and topped battery racks was as observed but other types of damage were also observed. Three turbine-generating units were damaged. In one case damage was aggravated when the oil lubrication pump stopped due to the failure of

emergency batteries. Also of note was the failure of high voltage substation equipment from inherent inadequate strength.

The San Fernando earthquake of 1971 of magnitude 6.6 severely damaged power systems and other lifelines. While the magnitude of this earthquake would put it in a moderate class, there was very severe shaking in the area close to the epicenter. As this earthquake was extensively reported [5, 6, 11] the extensive damage will not be reviewed in detail. Because of the extensive damage to high voltage substation facilities, this earthquake triggered the most extensive evaluation of power system equipment done in the U.S. Some of the activities in the post San Fernando period are discussed below.

Caution must be exercised in attempting to summarize and identify patterns and trends from damage reports from earthquakes which span a forty-three year period, occurred in different parts of the world and for equipment and facilities designed in many different countries. The six recommendations from the 1923 Tokyo earthquake are not only applicable to the U.S. today but remain unused outside of California. Recent earthquakes have also indicated that high voltage transmission facilities are inherently more vulnerable to earthquake damage. This could also be said for large fuel storage tanks. Large fossil fuel generating facilities in the 1000+ megawatt class, particularly coal fired units, have not been subjected to strong earthquake motions to date. While the vulnerability of underground transmission lines may be no greater than overhead lines, which have proved to be quite earthquake resistant, when they are damaged the entire line is put out of service for an extended period.

#### POST-SAN FERNANDO DEVELOPMENTS

While the Santa Barbara and Long Beach earthquakes provided the motivation for the development of seismic requirements of building codes, the San Fernando earthquake has stimulated more governmental, professional and industrial activity to mitigate earthquake effects than any other U.S. earthquake. A significant part of this activity has been associated with lifelines. It would be impossible to summarize all of the developments since 1971 related to power systems in this paper, but a few of the developments will be traced and the present situation relative to earthquake mitigation will be reviewed.

Each of the utilities which experienced damage developed damage reports. Also the federal government funded through NSF a study of unprecedented magnitude to study the effects of the earthquake which included a modest effort related to power systems [11]. The utilities in the damaged area also started extensive analysis and test programs. Directed primarily at transmission equipment this work was done by utility personnel in conjunction with consultants or manufacturers at

considerable expense to the utilities. The Bonneville Power Administration (BPA) also funded [ 1 ] detailed studies of the DC converter station. While the Bonneville work has been published, many of the utility studies have not been released. There are several reasons for this situation. In some cases manufacturers have participated in the work or have provided detailed information about their equipment and consider the results as proprietary. In other cases the work was not done with the participation of the manufacturer but the utilities are reluctant to release the information, as to do so may adversely affect their accessibility to information from the manufacturer in the future.

Most of the major California utilities have had seismic risk maps made of their service area which are used to establish excitation levels in seismic specifications for equipment and facilities. The utilities have also developed relatively sophisticated seismic specifications for their equipment and facilities. While specifications differ for the different utilities, important equipment in high risk areas would require dynamic analysis or testing with inputs as high as .5g horizontal and .3g vertical. One difficulty encountered by the utilities is getting manufacturers to meet the specifications. In some cases smaller manufacturers do not have the technical resources to understand and perform the required tests or analysis. Even larger manufacturers who have the resources are unwilling to bid on equipment if all specifications must be satisfied. Also, for some equipment the meeting the specifications is technically or economically impractical. A complicating factor is that some equipment must be mounted on structures which may dominate the dynamic response of the equipment. Some manufacturers are not interested in designing the support structures and will not be responsible for the work of others. As the time from the San Francisco earthquake increases it would appear that some utilities are reluctant to provide the resources for the detailed dynamic analysis for new facilities.

An important aspect of the earthquake resistance of facilities is associated with installation details. The securing of battery racks and transformers to their foundations has now been uniformly adopted, although some utilities have done this since 1933. The connection of buses to equipment is treated in several different ways and somewhat unevenly among the utilities. This factor is becoming increasingly important since the newer tubular structures tend to be more flexible and have lower damping than the older lattice type structures.

California State Government has become more actively involved in earthquake related problems. The Seismic Safety Commission and The Energy Resources Conservation and Development Commission have been established. The latter is now reviewing the need for expanded earthquake specifications for fossil fuel power generating facilities. The California Water and Power Earthquake Engineer Forum has been established to improve communications on earthquake related developments between water and power utilities within the state. The forum meets a few times a year and consists primarily of top civil engineering representatives from each utility.

The practice to mitigate earthquake effects outside of California is markedly different. While BPA has done extensive studies of their DC converter station - a mirror image of which was severely damaged in

the San Fernando earthquake - and they do have seismic specifications requiring dynamic analysis for their important facilities, other utilities in the Northwest have not implemented the simple low cost measures such as securing transformers to their foundations or providing adequate slack in bus-equipment connections.

In other high seismic risk areas of the country (as defined by the Uniform Building Code) generating facilities have in some cases satisfied the .2g horizontal static equivalent load. Not surprisingly, transmission and distribution facilities in these areas have no seismic specifications.

#### CURRENT RESEARCH ACTIVITIES

The following discussion does not include work related to nuclear power generation facilities. As noted earlier, there was extensive research related to power systems being funded by numerous sources. Following the San Fernando earthquake of 1971 most of this activity dealt with the analysis of various power system components such as circuit breakers, switches, etc. At the present time the character of the research effort has shifted to looking at the system as a whole, major facilities such as fossil fuel power plants and underground facilities. The majority of current research is funded by the National Science Foundation (NSF), RANN, Earthquake Engineering Program. Appendix A contains a list of NSF projects related to electrical utilities giving the title, the principal investigator, and a brief abstract of research objectives. While there is extensive research activity on structures which might relate to power systems, this material is not included. Recently the California Energy Resources Conservation and Development Commission has initiated a modest effort related to power generation facilities.

Initial results from one of the above studies are now available. The major objective of the study was to develop a methodology for evaluating the response of an electrical power system in a metropolitan area to a major earthquake [8, 9, 10]. The methodology uses digital computer simulation in which the power system is represented in detail. That is, power sources, transmission lines, transformers, circuit breakers, switches, busses, etc. in the study area are included. For each of a series of hypothesized earthquakes the probability of failure for each piece of equipment in the study area is evaluated taking into account the location of the site relative to the earthquake fault, the soil conditions at the site, the dynamic properties of the equipment and its support structure where appropriate. The operating status of each piece of equipment is then determined so as to be consistent with its probability of failure. The system is then reconfigured to take advantage of its redundancy. Load flows are performed to determine the existence of overloaded equipment. The importance of the various restoration tasks is determined, and available crews are dispatched to restore the system. In this manner system performance, as measured by the extent and duration of service disruption, can be evaluated. In addition, effects on system performance can be evaluated for changes in repair strategies or changes in seismic specifications of equipment at specific sites or of a given class.

For the "typical" power system modeled, it was found that service could be restored from earthquakes of magnitude 7.0 in about two days while a magnitude 6.3 earthquake would require about a week. For a given magnitude, earthquake position alone of that part of the fault which released energy, can have significantly different effects on power system response. Results also indicate that not all equipment is equally important to maintaining system operation. For example, transformers may be more important than circuit breakers used with them. Secondly, the high degree of redundancy in power systems means that extensive damage can be sustained without system disruptions. For example, only about 60% of damaged equipment need be repaired to fully restore service after a major earthquake.

In developing the simulation it was necessary to get fragility data for the various pieces of equipment which constitute the power system. Not only is this information difficult to obtain, but attempts by utilities to determine the cost of increased earthquake resistance of equipment have been frustrated. For example, a request for bid for equipment wanted quotations for specifications of .2, .3, .4, and .5g. All bids had the same price.

#### CONCLUSIONS AND RECOMMENDATIONS

At the present time, major California electric utilities have institutionalized seismic specifications for equipment and facilities. While regional seismic risk maps are used and site conditions are sometimes considered, this should become standard practice for all facilities down through important substations. Dynamic analysis should also be performed on all high voltage equipment and structures so as to minimize deleterious interaction between equipment and support structures. Since most utilities use "standardized" structures which evolve slowly, in time the cost of dynamic analysis per structure would be relatively low.

One of the major impediments to improve seismic resistance of utilities outside of California is that no effective infrastructure exists for the utility industry to insure that minimum earthquake mitigation measures are adopted. There are no parallels for seismic resistance in the power industry such as the boiler code or elevator code which have been formulated primarily by the affected industries and have served the cause of public safety effectively. Trade organizations such as Edison Electric Institute or Electric Power Research Institute consider the earthquake problem as regional in character (exclusive of nuclear safety) and give it so low a priority as to exclude it from consideration. Likewise the Federal Power Commission, the National Reliability Councils, and the Energy Research and Development Administration consider the earthquake problem outside of their charters or of low priority. Thus there is a need for some organization at the national level to insure that at least minimal, cost-effective earthquake mitigation measures are adopted on a national basis.

Professional organizations such as the Institute of Electrical and Electronics Engineering have regional committees addressing some earthquake related problems through the development of seismic design guidelines.

The development of design guidelines for use in high seismic risk areas outside of California may be of limited value unless they are very specific as to things that are to be done. It has only been in the post-San Fernando Earthquake period that the California utilities have developed significant expertise on structure and equipment dynamic behavior. It is highly unlikely that Mid-Western and Eastern utilities will develop the expertise required to effectively utilize seismic design guidelines which only give general procedures. Numerous reasons can be cited for the utilities outside of the West Coast not adopting earthquake mitigation measures. These include the fact that there is no record of earthquake damage to power facilities in these areas; most utilities' experience with seismic requirements is related to nuclear generating facilities and this often has associated with it excessive bureaucratic red tape and high cost; and the uninitiated usually overestimate the cost of implementing earthquake mitigation measures. Guides should also provide information on the cost-effectiveness of recommended actions. With this information, engineering staffs will be in a better position to get the support from management required for implementation.

Where seismic specifications for equipment and facilities have been implemented, a uniform design excitation level, usually expressed as a fraction of the acceleration of gravity, is given for all equipment associated with a given function. Simulation studies show that the importance of different pieces of equipment is different. Thus, the level of seismic specifications should more closely correspond to the importance of equipment function. Closely related to this is the need for incremental costs associated with improved resistance. 79

Since the cost of many of the measures to reduce earthquake hazards on new installations is very low, it would appear that the failure to do so is due to a lack of awareness of the problem or a tendency to resist change in a large organization. The low initial cost and the difficulty in retrofitting facilities speak strongly for ensuring that new facilities have at least minimum earthquake resistance. Also, since the Northwest is aware of the seismic hazard and still has not acted, it would appear that code requirements will be necessary to achieve implementation outside of California.

Investigations since the San Fernando earthquake have confirmed that higher voltage transmission facilities are in general more vulnerable to earthquake damage. The importance of a growing 800KV transmission network and the introduction of 1100KV service in the Midwest suggests that the earthquake resistance of these facilities should be evaluated.

There is a need for better documentation and communication of earthquake induced damage. Substation damage is usually repaired quite rapidly because of the need to restore service. While damage statistics are valuable for the state-of-the-art to continue to progress, more details about the equipment and its installation must be known. Thus, information on damaged equipment, including its age, manufacturer, method of mounting, details on interconnections, and type of failure should be documented. Procedures for obtaining this type of information are probably most important for California because it is the most seismically active area.

A potential problem associated with the communication of damage information is that it might be restricted because of litigation associated with equipment damage or disruption of service. Historically, this has not been a problem after disruptions due to natural disasters. However, the national attitude towards product liability and the general recourse to the courts in recent years hold the potential of denying access to information which is vital for improving the earthquake resistance of equipment and facilities. As the procedures for obtaining damage information are most important in California, the problem of litigation is also most critical there. Fortunately, there would appear to be an administrative way around the problem. California courts have held that safety studies conducted by the Department of Industrial Safety are confidential and thus cannot be subpoenaed for purposes of litigation. Thus, if damage reports can be so classified, access of vital information will be assured without jeopardizing anyone's legal position.

#### ACKNOWLEDGEMENTS

The support of the National Science Foundation is gratefully acknowledged.

#### REFERENCES

1. Assessment of Earthquake Resistant Design of AC-DC Converter Stations, HV-DC Pacific Inter tie, Agbabian-Jackson Associates, R-7119-1984, August 1971.
2. Crawford, M. T., "The Puget Sound Area Earthquake and its Effects on Transmission and Distribution Facilities; minutes of 15th meeting, Transmission and Distribution Committee, EEI 1949.
3. "Effects of Earthquakes on Power System Design," EEI, Electrical Systems and Equipment Committee, 1965.
4. Kawasumi, M., Editor, "General Report of the Niigata Earthquake of 1964;" published by Tokyo Electrical Engineering College Press, 1968, pp. 517-524.
5. Paul C. Jennings, Editor, Engineering Features of the San Fernando Earthquake, February 9, 1971, California Institute of Technology, Earthquake Engineering Research Laboratory, EERL 71-02, June 1971.
6. San Fernando, California Earthquake of February 9, 1971, U.S. Department of Commerce, National Oceanic and Atmospheric Administration, Washington, D.C. 1973 (in three volumes) Vol. II, pp. 27-38.
7. Scheffer, J. A., "Miracle in Alaska," Qualified Contractor, Vol. 29, No. 5, May 1964.
8. Schiff, A., Newsom, D., Fink, R., "Lifeline Simulation Methods of Modeling Local Seismic Environment and Equipment Damage," U.S. National Conference on Earthquake Engineering, June 18-20, 1975, University of Michigan, Ann Arbor, Michigan.
9. Schiff, A. J., Feil, P. J., and Newsom, D. E., "Evaluating Power System Response to Earthquakes with Simulation," Joint US-Japan Seminar for Earthquake Engineering with Emphasis on Life Lines. Nov. 8-12, 1976, Tokyo, Japan.
10. Schiff, P. J., Feil, Peter J., Newsom, Donald E., "Computer Simulation of Lifeline Response to Earthquakes," VI WCEE, New Delhi, India, January 10-14, 1977.
11. Schiff, A. J. and Yao, J.T.P., "Response of Power Systems to the San Fernando Valley Earthquake of 9 February 1971," Report 72-1,

Purdue University, Center for Large-Scale Systems, Lafayette, Ind., Jan., 1972.

12. Shibusawa, M., "A Description of the Damage Done by the Great Earthquake of 9-1-23 to the Electrical Installations in Japan," Japanese Electrotechnical Committee, April 1925, Tokyo, Japan.
13. Shibata, H. (et al), "Observation of Damages of Industrial Firms in Niigata Earthquake," Proceedings of 4th WCEE, Vol. III, 1969.
14. Vivian, J. H., "Earthquake Damage in California," minutes of EE Committee, EEI, October 1952.
15. "Wrecked Alaska has Power," Reclamation ERA report, Vol. 50, No. 4, November 1964.

#### APPENDIX A: RESEARCH ACTIVITIES

National Science Foundation supported research projects relative to power systems as reported in NSF Summary of Awards.

1. Seismic Safety of Electrical Power Equipment, Anshel J. Schiff; Purdue University, School of Mechanical-Engineering, West Lafayette, Indiana 47907; \$193,800 for 24 months beginning June 15, 1973.

A methodology will be developed to evaluate the response of power systems to major earthquakes. The methodology will enable the extent and duration of services disruption resulting from earthquakes to be determined. The effects on system performance of changes in equipment specifications, repair strategies and system configuration can be evaluated. Efficient methods for vibration testing of power equipment in the field will be developed.

2. Seismic Resistance of Fossil-Fuel Power Plants; John L. Bogdanoff, Purdue University, Lafayette, Indiana; \$372,100 for 24 months beginning January 1, 1974.

This project will concentrate upon the determination of the dynamic behavior of large fossil-fuel steam power generating plants when subjected to earthquake forces. The results of the research will be used to establish design guidelines and procedures for the principal components of a power plant for earthquake resistance. These guidelines and procedures will form the basis for the development of seismic code provisions and recommendations for the design and construction of fossil-fuel steam power generating plants.

This research will study, as a start, the behavior of the principal components such as the furnace-boiler, steam and feedwater piping system, coal handling equipment and conveyor system, cooling towers, and stack.

3. Earthquake Response of Dams Including Hydrodynamic and Foundation Interaction; A.K. Chopra; University of California, Berkeley, California 94720; \$89,400 for 24 months beginning August 30, 1974.

The research program will: (1) develop reliable and effective techniques for analysis of response of dams to earthquake motions including effects of hydrodynamic and foundation interaction; and (2) understanding the effects of interaction and the significance in the dynamic response of dams. The research will include studies on concrete gravity dams, arch dams, and earth dams.

4. Optimal Earthquake Design of Energy Production, Storage, and Distribution Systems; Alfred M. Freudenthal; The George Washington University, Washington, D.C. 20006; \$140,400 for 24 months beginning February 1, 1976.

This project focuses on the elements of risk, cost, and loss associated with earthquakes as important design parameters in developing structural design methods. Specifically, the objectives of this project are to: 1) establish a new structural design concept on the basis of maintaining a proper balance between the cost of providing a protective measure and the expected cost of earthquake damage; 2) develop procedures of optimal design for ultimate seismic load carrying capacity and functional reliability of structures; 3) apply these procedures in the design of important industrial facilities; and 4) make the results of the study available to user groups, and prepare guidelines for making the optimal design and planning decision.

5. Analysis of the Seismic Stability of Earth Dams; H. R. Seed; University of California, Berkeley, California 94720; \$173,500 for 24 months beginning February 15, 1976.

As part of this project, a study will be made of the significant differences between earth dams known to have performed well and dams known to have performed poorly during strong earthquake shaking to determine the factors responsible for the differences in behavior. Specific objectives of the project are to: 1) establish a data base concerning the field behavior of earth dams during earthquakes so that adequate and inadequate types of construction can be identified; 2) investigate the adequacy of dynamic analysis methods in predicting satisfactory and unsatisfactory performance of earth dams during earthquakes; and 3) develop simplified but rational procedures for evaluating the earthquake shaking. The results of this project will contribute significantly to both improved safety and economy in the design of these critical earth dam structures.

6. Vulnerability of Transportation and Water Systems to Seismic Hazards; Irving Oppenheim; Carnegie-Mellon University, Schenley Park, Pittsburgh, Pennsylvania 15213; \$187,000 for 24 months beginning May 1, 1976.

This project focuses on the general transportation system and associated water systems in order to determine a lifeline model which can be used to measure the performance and the principal causes of failure or decreased performance in these systems. The model will recognize the effects of redundancies in the system, the geographical features of the total system, and will contain the principal seismic failure criteria.

7. Underground Lifelines in a Seismic Environment; M.L. Baron; Weidinger Associates, 110 East 59th Street, New York, New York 10022; \$407,430 for 24 months beginning June 1, 1976.

Research will concentrate on underground water distribution lifelines. The specific tasks include: 1) a survey of underground water lifelines; 2) the development of appropriate seismic input; 3) methodology development for modeling and analysis; 4) methodology application to real systems; and 5) risk and cost-benefit studies of lifeline systems. The results of the research will be presented in the form of design aids, guides, and specifications.

## ASEISMIC DESIGN OF 500KV AIR CIRCUIT BREAKER WITH FRICTION DAMPERS

by Taro Shimogoe<sup>1)</sup> and Shigeru Fujimoto<sup>2)</sup>

## Abstract

Statistical properties of the response of a 500KV air circuit breaker under nonstationary seismic excitation are studied by using a simplified mathematical model of the top-heavy tall structure and it is shown that the analytical results are in fairly good agreement with the experimental results.

## Notation

The following symbols are used in this paper:

- $a_1, b_1$  ( $i=1,2,3$ ) = x-, y-coordinates of the lower end position of each stay;  
 $f$  = frequency;  
 $g$  = acceleration of gravity;  
 $K$  = stiffness of the support column (ratio of the restoring moment to the inclination angle);  
 $k, k'$  = stiffnesses of the damper;  
 $L$  = length of the support column;  
 $l_0$  = initial length of the stay;  
 $M_1 = m_1 \cdot m_2 / (3 + m_3)$  = mass related to the inertia;  
 $M_2 = m_1 \cdot m_2 / 2$  = mass related to the gravity;  
 $m_1$  = mass of the mounted body;  
 $m_2$  = mass of the support column;  
 $m_3$  = mass of the stay;  
 $P_0$  = frictional force of the damper;  
 $R$  = radius of the circle, on which the lower ends of the stays are arranged;  
 $t$  = time;  
 $T_0$  = initial tension of the stay;  
 $u$  = input acceleration in the horizontal direction;  
 $x, y, z$  = coordinate system (the z-axis is vertical);  
 $\gamma$  = angle of the input direction making with the x-axis;

## 1. Introduction

A 500KV air circuit breaker is constructed with a heavy interrupting chamber installed on the top of a long support column, the bottom of which is connected with a rigid foundation rack. Three stays are stretched from the interrupting chamber to the foundation rack to increase the aseismic performance and additionally friction dampers are provided for the stays to absorb the vibration energy as roughly illustrated in Fig.1. This kind of construction can be available not only for the circuit breaker but also for any top-heavy tall structures to increase the

aseismic performance. The friction dampers such as ring springs are usually used in practice for these constructions, because the friction damper can be made compact and absorbs relatively big vibration energy. However, it is somewhat difficult to estimate the seismic response of these structures by an analytical method owing to the nonlinearity of the friction damper. Although the 500KV air circuit breaker is commonly designed to withstand an horizontal earthquake shock of 0.3G sinusoidal wave for three cycles at resonance frequency in Japanese electric power industry<sup>(1)</sup>, it is an important

matter for establishing an anti-earthquake design principle of the top-heavy tall structure equipped with the stays and friction dampers that the dynamic characteristics are examined under nonstationary random excitation corresponding to a horizontal earthquake input. In this paper the effects of structural parameters such as frictional force of the damper upon the statistical properties of the response are especially examined by using a simplified mathematical model and these results are compared with the experimental results.

## 2. Mathematical Model of the Structure

A mathematical model of the structure is simplified under the following assumptions ( see Fig.3 ):

(1) The coupling effects caused by the attachments such as cables, stays, rack and so on are not taken into account.

(2) The body mounted on the top of the support column such as the interrupting chamber is assumed to be a single mass point and the support column is assumed to be a uniform straight rigid bar, the bottom of which is replaced by a flexible joint. Accordingly the whole structure is expressed as a two-degrees-of-freedom system under the horizontal excitation.

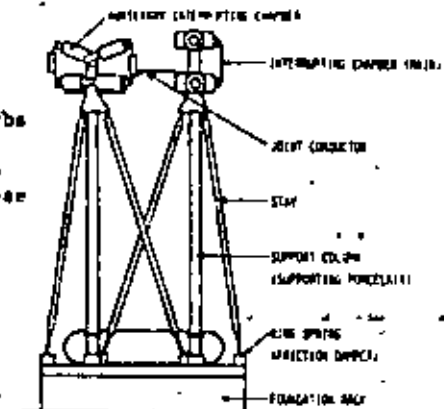


Fig. 1 The scheme of the 500KV AB-type air circuit breaker (1/2 phase)

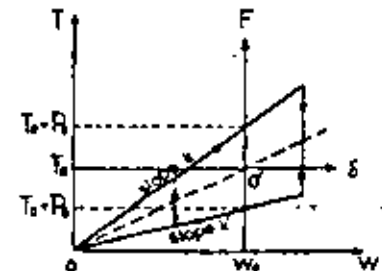


Fig. 2 The load-deflection diagram of the friction damper ( the ring spring )

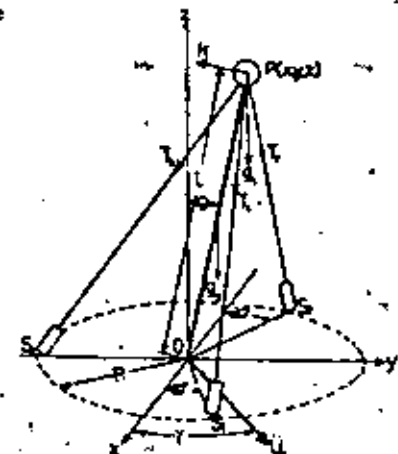


Fig. 3 The dynamic model of the circuit breaker structure

1) Professor of Mechanical Engineering, Keio University, Japan

2) Graduate Student, Keio University, Japan

(3) The effects of the material and geometrical nonlinearities are neglected with the exception of the friction dampers. When the friction damper is constructed with a ring spring, the load-deflection characteristics of the damper is represented by a bilinear hysteresis as illustrated in Fig. 2. In this case the frictional force  $P_0$  at the equilibrium point is proportional to the initial tension  $T_0$  of the stay ( $P_0 = T_0(1-r)/(1+r)$ ,  $r = k'/k < 1$ ).

From the above-mentioned assumptions the equations of motion are derived as follows (3):

$$\begin{cases} \delta^2 \theta \dot{c}^2 + A\epsilon + C\eta + A_0 = -u_g \cos \gamma \\ \delta^2 \eta \dot{c}^2 + C\epsilon + B\eta + B_0 = -u_g \sin \gamma \end{cases} \quad (1)$$

where

$$\epsilon = x/L, \quad \eta = y/L, \quad \tau = \omega_0 t \quad (\omega_0 = \sqrt{g/L}), \quad u_g = \dot{u}/g \quad (2)$$

$$\begin{cases} A = \kappa - \mu - \tau_0 \lambda^2 \xi \alpha_i^2 - \lambda^2 \xi \alpha_i^2 \eta_i + \lambda^2 \xi \alpha_i^2 \kappa_i \\ B = \kappa - \mu - \tau_0 \lambda^2 \xi \beta_i^2 - \lambda^2 \xi \beta_i^2 \eta_i + \lambda^2 \xi \beta_i^2 \kappa_i \\ C = -\tau_0 \lambda^2 \xi \alpha_i \beta_i - \lambda^2 \xi \alpha_i \beta_i \eta_i + \lambda^2 \xi \alpha_i \beta_i \kappa_i \end{cases} \quad (3)$$

$$\begin{cases} A_i = -\tau_0 \lambda \xi \alpha_i - \lambda \xi \alpha_i \eta_i \\ B_i = -\tau_0 \lambda \xi \beta_i - \lambda \xi \beta_i \eta_i \\ \kappa = K/M_1 g, \quad \mu = M_2/M_1, \quad \tau_0 = T_0/M_1 g, \quad \lambda = L/L_0 \\ \alpha_i = a_i/L, \quad \beta_i = b_i/L \quad (i=1, 2, 3) \end{cases} \quad (4)$$

$$\begin{cases} \eta_i = P_0/M_1 g, \quad \kappa_i = kL/M_1 g \quad \text{for } \alpha_i \frac{d\epsilon}{dt} + \beta_i \frac{d\eta}{dt} < 0 \\ = 0, \quad = (\lambda + k')L/(2M_1 g) \quad + \quad = 0 \\ = -P_0/M_1 g, \quad = k'L/M_1 g \quad + \quad > 0 \end{cases} \quad (5)$$

When the input acceleration occurs in the y-direction ( $\gamma = \pi/2$ ), the equation of motion is reduced to a simple form

$$\delta^2 \eta \dot{c}^2 + B\eta + B_0 = -u_g \quad (6)$$

because the structure is symmetric about the y-z plane.

From the above equation the approximate value of the resonance circular frequency  $\omega_n$  is estimated by using the mean values of frictional force and stiffness of the damper, that is, by putting  $\eta_i = 0$ ,  $\kappa_i = (\lambda + k')L/(2M_1 g)$  as follows:

$$\begin{aligned} (\omega_n/\omega_0)^2 &= B = \kappa - \mu - \tau_0 \lambda^2 \xi \beta_i^2 + \lambda^2 \xi \beta_i^2 \kappa_m \\ &= \kappa - \mu - \frac{1}{2} \tau_0 \lambda^2 \rho^2 + \frac{1}{2} \lambda^2 \rho^2 \kappa_m = \Omega_n^2 \end{aligned} \quad (7)$$

where  $\rho = R/L, \quad \kappa_m = (K + k')L/(2M_1 g) \quad (8)$

3. Nonstationary Seismic Input

An approximate value of the mean squared response of a nonlinear system excited by a nonstationary random input is obtained by solving statistical moment equations which are introduced from the Fokker-Planck

equation. In this case the input is assumed to be a Gaussian white noise having nonstationary characteristics, that is

$$\ddot{u}(t) = \Omega(t)\zeta(t) \quad (9)$$

where  $\Omega(t)$  expresses an envelope of the input acceleration and  $\zeta(t)$  is a stationary random function with zero mean. Although  $\zeta(t)$  has generally the dominant frequencies,  $\zeta(t)$  is approximated to a Gaussian white noise in order to derive the Fokker-Planck equation. Then the power spectral density function of  $\ddot{u}(t)$  is given by the expression

$$S_{\ddot{u}}(f, t) = S_{\zeta}(f)D^2(t), \quad -\infty < f < \infty \quad (10)$$

where  $S_{\zeta}(f) = 1/(4\pi f^2)$  (power spectral density of  $\zeta(t)$ ).

For example, the envelope of the El Centro seismic wave (N-S component, the maximum acceleration  $\dot{u}_{max} = 0.3g$ ), is obtained by a lag window and normalized so that the maximum value is unity as shown in Fig. 4. The power spectral density of the stationary wave, which is obtained from the El Centro seismic wave divided by its normalized envelope function, is represented in Fig. 5. On the other hand, the approximate value of the resonance frequency of the circuit breaker calculated by Eq. (7) is  $\omega_n/\omega_0 = \Omega_n = 7.54$  ( $f_n/\omega_0 = 1.20$ ), in the case when the dimensionless structural parameters are  $\kappa = 8.69$ ,  $\mu = 0.996$ ,  $\tau_0 = 0.896$ ,  $\lambda = 0.96$ ,  $\rho = 0.287$ ,  $\kappa_m = 589$  as a typical numerical example. It may be assumed that the response of the circuit breaker mainly depends on the resonance frequency components of the input over the appropriate range, say,  $\pm 30\%$  of the resonance frequency, if the damping ratio is approximated to 15%. This range is indicated with the shadowed portion in Fig. 5.

Therefore the input seismic wave may be replaced by an equivalent white noise whose power spectral

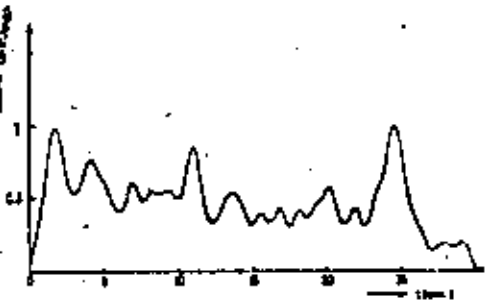


Fig. 4 The normalized envelope function of the El Centro seismic wave

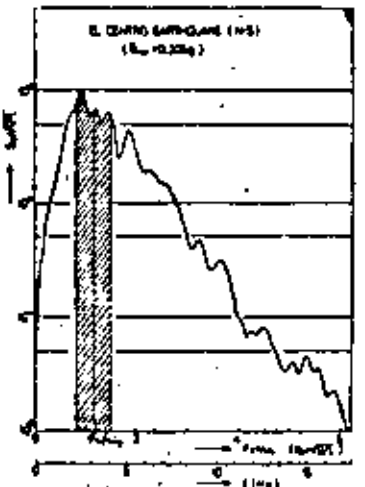


Fig. 5 The dimensionless power spectral density of the stationary wave corresponding to the El Centro seismic wave

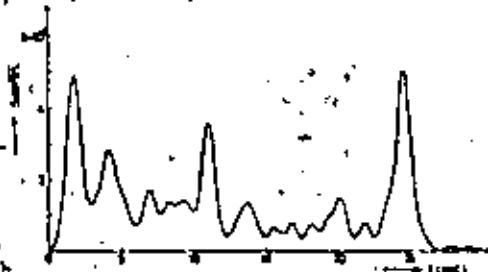


Fig. 6 The dimensionless power spectral density of the nonstationary white noise approximating to the El Centro seismic wave

density has the same value as the average level of the input power spectral density over the above-mentioned frequency range. In this example, the value of the dimensionless power spectral density of the equivalent white noise is about  $5 \times 10^{-3}$ . Since this value corresponds to the maximum value of the power spectral density of the nonstationary input, the time history of the dimensionless power spectral density  $S_{ij}(t)/\sqrt{g^3 L} = S_{ij}(t)/\sqrt{g^3 L}$  is given as the squared value of the normalized envelope function multiplied by  $5 \times 10^{-3}$  (see Fig. 6).

4. The r.m.s. value of the Acceleration Response

The Fokker-Planck equation governing the joint probability density function of the responses is derived with the aid of the equation of motion, and further the equations relating to the second order moments of the responses are obtained from the Fokker-Planck equation on the assumption that the responses are Gaussian random processes with zero mean. When  $\gamma = \pi/2$ , the moment equations are reduced to (2)

$$\begin{aligned} dM_{11}/dt &= 2M_{12} \\ dM_{12}/dt &= M_{22} - \Omega^2 M_{12} - 2\sqrt{2/\pi} \rho \lambda \pi_0 M_{12} / \sqrt{M_{22}} \end{aligned} \quad (11)$$

$$dM_{22}/dt = -2\Omega^2 M_{12} - 4\sqrt{2/\pi} \rho \lambda \pi_0 \sqrt{M_{22}} + S_{ij}(t)/\sqrt{g^3 L}$$

where  $M_{ij} = E[\eta_i \eta_j]$  ( $i, j = 1, 2$ ),  $\eta_1 = \eta = y/L$ ,  $\eta_2 = d\eta/dt$  (12)

$$\pi_0 = P_0/M_1 g = \pi_0(1-r)/(1+r), \quad r = k'/k < 1 \quad (13)$$

The moment equations (11) are numerically solved by using the input power spectral density  $S_{ij}(t)/\sqrt{g^3 L}$  indicated in Fig. 6 and putting  $\pi_0 = 0.2125$  ( $r = 0.616$ ), and the r.m.s. value of the acceleration response is obtained from the values of  $M_{ij}$  (see broken line in Fig. 7).

The solid line in Fig. 7 represents an experimental result. In the experimental study, a physical model of the circuit breaker was excited by a vibration testing machine under the El Centro seismic wave input and the r.m.s. response was investigated from the envelope of the squared value of the acceleration picked up at the top of the support column.

A similarity of the dynamical properties between the physical model and the full-size structure of circuit breaker was taken into consideration by using the preceding mathematical model (3). In this physical model,  $L = 1.250m$  ( $\omega_0 = 2.8rad/sec$ ),  $L_0 = 1.30m$ ,  $K = 0.357m$ ,  $k = 51.3kgf-m$ ,  $M_{1g} = 4.07kgf$ ,  $M_{2g} = 4.05kgf$ ,  $T_0 = 4.23kgf$ ,  $P_0 = 1.00kgf$ .

From Fig. 7 it is seen that the approximate value of the response obtained from the moment equations are in good agreement with the experimental result with the exception of the peak values.

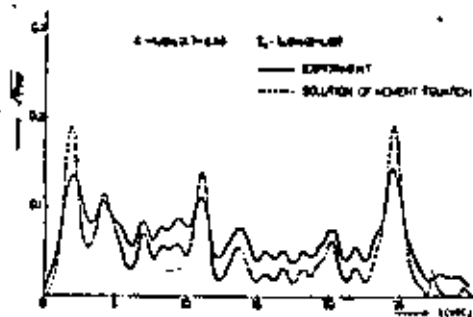


Fig. 7 The dimensionless r.m.s. values of the acceleration response (theoretical and experimental values)

The fact that the peak values of the theoretical result are overestimated may be originated in the variation of the dominant frequency of the El Centro seismic wave. The dominant frequency of the El Centro seismic wave becomes somewhat low and gets away from the resonance frequency of the structure at the time of the intense acceleration, thus the peak values of the response are relatively low in comparison with the theoretical result. However, if only the time history of the input power spectral density at the resonance frequency of the system can be estimated as the ensemble average of the actual seismic waves, then the analytical method described in this paper is available to estimate the r.m.s. value of the response.

5. Effect of the Nonlinearity of the Friction Dampers

The response of the structure was assumed to be a Gaussian process in preceding theoretical treatment notwithstanding a nonlinear problem. In order to examine how the probability density of the response deviates from the Gaussian distribution, a digital simulation is carried out by using a stationary Gaussian white noise as an input at the mathematical model. The level of this white noise is chosen to be equal to that of the equivalent white noise described in section 3, whose probability density is shown in Fig. 8. The value of Chi-square for testing a fitness with the Gaussian distribution is also indicated in this figure. In the simulation, the characteristics of the friction damper is approximated to be parallel bilinear by putting  $k = k' = (k+k')/2$  as a matter of convenience. The probability densities of the response obtained by the simulation are shown in Fig. 9 and 10 for  $\kappa = 8.69$ ,  $\tau_0 = 0.896$  and  $\tau_0 = 1.144$ , respectively. From these figures it

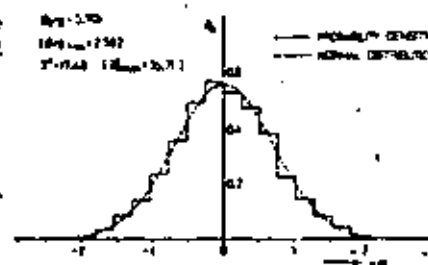


Fig. 8 The probability density of the input white noise for a digital simulation

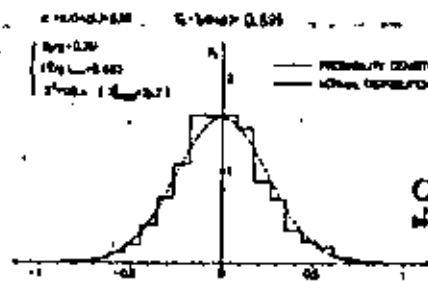


Fig. 9 The probability density of the response to the input white noise at the digital simulation (the case of lower initial tension at the stays or lower frictional force at the dampers)

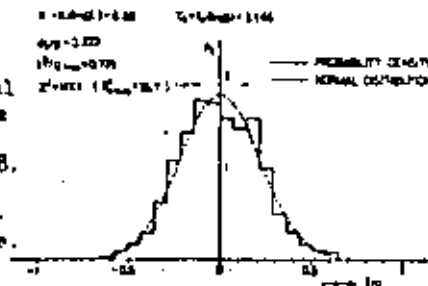


Fig. 10 The probability density of the response to the input white noise at the digital simulation (the case of higher initial tension at the stays or higher frictional force at the dampers)

From these figures it

is seen that the value of Chi-square increases and the fitness with the Gaussian distribution becomes poor, when the initial tension in the stays or the frictional force of the dampers become large. However, the shapes of the probability densities are not so largely different from the Gaussian distribution within the range of the initial tension or the frictional force at the circuit breaker and accordingly the error caused by the assumption of the Gaussian process in the preceding theory is not so big.

Although it is seen in these numerical examples that the r.m.s. value of the acceleration response decreases for the higher initial tension in the stays, the acceleration response may rather increase for the extremely high initial tension, because the relative displacement in the friction damper becomes small.

#### 6. Conclusion

The optimal requirements of the parameters of the top-heavy tall structure, for example, the initial tension in the stays, the frictional force of the dampers, the stiffness of the support column, may be investigated by using the simplified mathematical model and the method of statistical approach described in this paper.

#### Acknowledgment

The authors are grateful to the associates of Tokyo Shibaura Electric Co. Ltd. for valuable discussion from the engineering point of view and for supporting experiment and computation.

#### References

- (1) Shinogo, T. and Fujimoto, S., "Response Analysis of 500KV Circuit Breaker with Nonlinear Damping Devices under Seismic Excitation," U.S.-Japan Seminar on Earthquake Engineering Research with Emphasis on Lifeline System, Nov. 1976.
- (2) Fujimoto, S., Shinogo, T. and Arai, K., The 1975 Joint JSME-ASME Applied Mechanics Western Conference, 75-AM, JSME C-7.

UNDERGROUND PIPES

85



**DIVISION DE EDUCACION CONTINUA  
FACULTAD DE INGENIERIA U.N.A.M.**

VII CURSO INTERNACIONAL DE INGENIERIA SISMICA

DISEÑO SISMICO DE ESTRUCTURAS ESPECIALES

DISEÑO SISMICO DE PLANTAS  
INDUSTRIALES

M en C Enrique Martínez Romero

Agosto, 1981

**CURSO INTERNACIONAL DE INGENIERIA SISMICA  
DISEÑO SISMICO DE PLANTAS INDUSTRIALES**

Las presentes notas para diseño sísmico, pretenden establecer normas para definir el criterio de diseño sísmico a seguir, con el objeto de que las estructuras de plantas industriales tengan un comportamiento adecuado ante un sismo de mediana intensidad, después del cual la operación de la planta sea normal y que además para un sismo de gran intensidad no se produzca el colapso parcial o total de las estructuras y que los daños ocasionados puedan repararse en un período de tiempo relativamente corto.

Estas recomendaciones se aplican a la estructura completa y a todas sus partes, incluyendo la estructura en sí, pisos, muros y sistemas de techo, así como partes específicas de equipo y maquinaria de la planta.

NOTACION

Cada símbolo empleado en el presente capítulo se define donde se emplea por primera vez. Los más importantes son:

- a (adimensional) = coeficiente empleado en análisis dinámico modal.
- B (m) = base de un panel de vidrio.
- C (adimensional) = coeficiente basal (sin reducir por ductilidad).
- c (adimensional) =  $0.95 CD/Q$
- D (adimensional) = Factor reductivo por flexibilidad.
- H (m) = altura de un panel de vidrio o espesor de estratos de suelo.

- h (m) = altura de un tablero de muro entre pisos consecutivos.
- J (adimensional) = factor de amortiguamiento.
- L (m) = longitud de un tablero de muro o mitad de la longitud de un tanque rectangular.
- D (adimensional) = factor reductivo por ductilidad.
- T (seg) = período natural de vibración.
- V (ton) = fuerza constante horizontal en la base de la construcción.
- W (ton) = peso de la construcción.
- y (cm) = desplazamiento del centro de gravedad de la estructura descontando el que proviene de las deformaciones locales del terreno.
- Y<sub>s</sub> (cm) = desplazamiento del centro de gravedad de la estructura que se debe a deformaciones locales del terreno.

ZONAS

Para fines de diseño sísmico se considerará que las construcciones pueden desplazarse en las Zonas I ó II, atendiendo a la estratigrafía local del terreno.

Se consideran como pertenecientes a la zona I todos aquellos sitios donde

exista evidencia de que no se encuentran a profundidades mayores de 20 m, suelos con módulos de rigidez menores de  $50,000 \text{ ton/m}^2$ , o para los que el número de golpes por cada 30 cm, en la prueba de penetración están en sea inferior a 50, y en que además se satisfaga la condición.

$$\sum H_i \sqrt{\gamma_i V_i G_i} < 0.45$$

En donde  $H_i$  es el espesor, en metros, del  $i$ -ésimo estrato de suelo que se encuentra sobre el material con módulo de rigidez mayor o igual que  $50,000 \text{ ton/m}^2$ .  $\gamma_i$  es su peso volumétrico en  $\text{ton/m}^3$  y  $G_i$  es su módulo de rigidez en  $\text{ton/m}^2$ . La suma deberá incluir los términos correspondientes a todas las capas que se encuentren sobre el material con módulo de rigidez mayor o igual que  $50,000 \text{ ton/m}^2$ .

Para fines de esta clasificación se tomarán en cuenta todos los suelos que se encuentren debajo del nivel en que las aceleraciones horizontales del terreno se transmiten a la construcción.

Se considerarán pertenecientes a la zona II aquellos sitios que no satisfagan los requisitos de los párrafos anteriores.

#### CLASIFICACION DE LAS CONSTRUCCIONES SEGUN SU IMPORTANCIA Y LAS CONSECUENCIAS QUE TENDRA SU FALLA

De acuerdo con este criterio las estructuras se clasifican en los siguientes grupos:

GRUPO A.- Estructuras muy importantes para el funcionamiento de la planta como son, la planta de fuerza, los soportes de tuberías, las chimeneas, los edificios de procesos, los soportes de reactores, etc.

GRUPO B.- Estructuras importantes para el funcionamiento de la planta que no queden comprendidas dentro del Grupo A, y todas aquellas estructuras cuya falla por movimientos sísmicos puedan poner en peligro otras construcciones de este grupo o del grupo A.

GRUPO C.- Estructuras que no intervienen en el proceso de la planta cuya falla no cause daños a construcciones de los dos primeros grupos.

GRUPO D.- Estructuras de poca importancia, cuya falla no cause daños a construcciones de los tres primeros grupos. No necesitan diseñarse por sísmo.

#### CLASIFICACION DE LAS CONSTRUCCIONES SEGUN SU ESTRUCTURACION

De acuerdo con su estructuración, las construcciones a que se refieren estas recomendaciones se clasifican en los siguientes TIPOS:

1. Edificios de cortante, incluyendo marcos de soportes de cubiertas para naves industriales.
2. Edificios de flexión
3. Chimeneas y construcciones tipo torre
4. Péndulos invertidos

5. Tanques
6. Muros de retención
7. Otras estructuras
8. Estructuras principales

#### TIPO 1. Edificio de Contante

Se considerarán como edificios de contante, las construcciones cuyas deformaciones ante fuerzas laterales se deben esencialmente a las fuerzas contantes entre pisos consecutivos. Incluye el presente tipo, por ejemplo, edificios cuya resistencia a fuerzas laterales es suministrada por muros cuando la relación de altura a base no pasa de 0.8, o por portales o marcos contraventados o no cuya relación de altura a base no es mayor que 2.0 si las rigideces de sus vigas son del mismo orden que las de sus columnas.

#### TIPO 2. Edificios de Flexión

Se considerarán como edificios de flexión aquellos edificios cuyas deformaciones se deben en forma significativa a flexión de conjunto, como es el caso de las estructuras cuya resistencia a fuerzas laterales se debe a la acción combinada de marcos y muros esbeltos, o de marcos con crujeas contraventadas cuya acción sea semejante a la de muros esbeltos, de marcos con relación de altura a base mayor de 2 ó de marcos cuyas vigas son mucho menos rígidas que sus columnas.

#### TIPO 3. Chimeneas y Otras Construcciones Tipo Torre

Se incluye en este tipo las construcciones cuya deformación ante fuerzas laterales sea esencialmente como la de una viga de flexión en voladizo.

#### TIPO 4. Péndulos Invertidos

Se incluyen en este tipo las estructuras en que 50 por ciento o más de su masa se halla en el extremo superior y cuyo elemento de apoyo trabaja como una viga en voladizo.

#### TIPO 5. Tanques

#### TIPO 6. Muros de Retención

#### TIPO 7. Otras Estructuras

#### TIPO 8. Estructuras Principales

En este tipo se incluyen todas las construcciones del Grupo A. En general, tienen una estructuración especial que comprende uno o varios de los tipos ya mencionados y dado su trabajo específico y sus cargas de operación requieren de un estudio detallado.

#### MÉTODOS DE ANÁLISIS SISMICO

El análisis sísmico podrá efectuarse empleando el método de análisis estático, o el método de análisis dinámico.

Se requerirá análisis dinámico en todas las estructuras en las que los efectos de modos superiores de vibración o la amplificación dinámica excesiva pueden afectar significativamente la respuesta de partes importantes de la construcción o de equipo costoso.

Deberán calcularse los efectos de las aceleraciones verticales y los de las aceleraciones horizontales para dos planos ortogonales, según los párrafos que siguen. Se revisará la seguridad de cada elemento estructural para la condición más desfavorable que resulte de considerar la acción de cada una de las componentes horizontal y vertical por separado o la combinación del efecto de cada componente horizontal con 0.7 veces el efecto de la componente vertical.

a) El efecto de las aceleraciones horizontales se tomará en cuenta suponiendo un sistema de fuerzas laterales obtenido de acuerdo con lo especificado más adelante.

b) El efecto de las aceleraciones verticales se considerará equivalente a un sistema de fuerzas verticales (actuando hacia arriba o hacia abajo) obtenido multiplicando por 0.4 las cargas muertas y las vivas. Alternativamente, puede efectuarse un análisis dinámico que tome en cuenta los modos de vibración vertical de la estructura y que considere un espectro de diseño igual a 0.75 veces el correspondiente a aceleraciones horizontales.

#### COEFICIENTE BASAL.

Se entienda por coeficiente basal, "C", el cociente de la fuerza cortante horizontal  $V$ , en la base de la estructura, sin reducir por ductilidad, y el peso  $W$  del mismo sobre dicho nivel.

El peso  $W$ , deberá incluir cargas muertas y cargas vivas. Los porcentajes de carga viva que deben incluirse en el análisis sísmico están definidos adelante.

Para el análisis estático de construcciones clasificadas según las consecuencias de su falla en el Grupo "A" se tomará  $C$  igual a 0.78.

Tratándose de las construcciones clasificadas en el Grupo B, el valor de  $C$  se tomará igual a 0.60.

Para construcciones clasificadas dentro del Grupo "C" el valor de  $C$ , será igual a 0.48.

#### REDUCCIÓN POR DUCTILIDAD

Para el cálculo de fuerzas internas en la estructura el producto  $QW$  se dividirá entre el factor  $Q$  que se especifica en los siguientes párrafos. El valor que adopta  $Q$  depende de la ductilidad de la estructura.

Para el cálculo de las deformaciones en la estructura no se hará reducción por ductilidad.

El factor Q podrá diferir en las dos direcciones ortogonales en que se analiza la estructura, según sea la clasificación y ductilidad de ésta en dichas direcciones.

A continuación, se presenta una relación de los valores del factor de ductilidad (Q) y los requisitos que debe llenar la estructura para poder adoptar éste valor en el diseño.

$$Q = 0$$

Este valor de Q se utilizará en estructuras del Tipo I, cuya resistencia en todos los niveles sea suministrada exclusivamente por marcos continuos no contraventados de concreto reforzado o de acero que tengan zona de fluencia definida y que cumplan con las siguientes condiciones.

a) Las vigas y columnas de acero, poseen secciones compactas según los requisitos del AISC.

Todas las juntas deberán admitir rotaciones importantes antes de fallar. Teniendo en cuenta lo anterior, el proporcionamiento y detalle de las juntas se hará de acuerdo con la parte 2 de la "Specification for the Design, Fabrication and Erection of Structural Steel for Buildings" de la última edición del AISC. Estas especificaciones, deberán adaptarse para tomar en cuenta que se puede producir una inversión de momentos.

Además, todas las conexiones de los miembros que inciden a una junta, se

diseñarán para tener una resistencia de 1.2 veces la capacidad del miembro incidente.

b) No se permitirá la formación de articulaciones plásticas en las zonas donde el área efectiva se reduce, (por ejemplo, por agujeros para remaches) a menos que la relación entre la resistencia última y la resistencia de diseño sea mayor que 1.6.

c) En la determinación de la longitud efectiva, que interviene en el cálculo de la relación de esbeltez de las columnas, se debe ignorar la ayuda proporcionada por contraventados, ya que estos deberán ser diseñados para fallar ante la presencia de un sismo de gran magnitud.

d) En estructuras de concreto, el marco llenará los requisitos que para marcos dúctiles especiales fija el ACI 318 - 71 en su apéndice A y tendrá (por lo menos en la planta baja) columnas de concreto zunchadas.

e) Los factores de seguridad contra: falla en compresión por flexión compresión de columnas de concreto reforzado con estribos; fuerza cortante y torsión, en miembros de concreto reforzado, así como compresión axial y pandeo en todos los miembros, son cuando menos 1.3 veces los que resulten en flexión y en torsión para resistir fuerzas laterales.

f) En todo entrepiso, la estructura debe ser capaz de resistir 0.9 veces las acciones de diseño bajo la condición más desfavorable que resulta de considerar que la capacidad crítica de cualquiera de los miembros

de dicho entrepiso se reduce a 0.8 de su resistencia de diseño.

g) El factor de seguridad para fuerza cortante de entrepisos, debe ser mayor en todos los niveles que 0.8 del promedio de dichos factores de seguridad.

h) La estructuración no sufrirá cambios repentinos en los distintos niveles y en las distintas crujeas.

i) Se podrán usar contraventeos, con el fin de reducir las deflexiones siempre y cuando estos no se consideren como elementos resistentes y se diseñen para que fallen o se desconecten ante la acción de un sismo de gran magnitud.

Q = 4.

Se considerará un factor de ductilidad Q=4 para estructuras Tipo 1, cuya resistencia en todos los niveles sea suministrada exclusivamente por muros de concreto, maderas o acero con o sin zonas de fluencia definidas, sean estos contraventeados o no, si se cumplen las siguientes condiciones:

a) Deberá cumplir con los incisos (a), (b), (e), (f) y (h) del art.

b) El factor de seguridad para fuerza cortante de entrepiso, es mayor en todos los niveles que 0.85 del promedio de dichos factores de seguridad.

c) La capacidad del marco para resistir fuerzas horizontales sin contar con la contribución de los contraventeos sea cuando menos 25% del total.

d) Los elementos de concreto deberán diseñarse, de acuerdo con los requisitos para estructuras en zona sísmica del ACI 318 - 71 ( Apéndice A ).

Q = 3.

Estructuras tipo 1 que reúnan los requisitos del artículo 7.4 y cuya altura sea mayor que 3 veces la dimensión de la base. Para valores de h/b comprendidos entre 2 y 3 el valor de Q, se obtendrá interpolando linealmente entre Q = 3 y Q = 4 donde h es la altura de la estructura y b la dimensión de la base.

Q = 2.

Se usará un coeficiente de ductilidad Q = 2 en estructuras de los tipos 1, 2 y 3, cuya resistencia a fuerzas laterales sea suministrada exclusivamente por muros o columnas de concreto reforzado, maderas o acero o por muros de concreto o mampostería de piezas macizas.

Q = 1.50

El valor del coeficiente de ductilidad Q será igual a 1.5 para estructuras del tipo 4 cuya resistencia a fuerzas laterales sea suministrada por una

columna o hilera de columnas de concreto reforzado, madera o acero. Si la estructura se analiza dinámicamente puede considerarse  $Q = 2$ .

También se usará  $Q = 1.5$  en estructuras de los tipos 1 a 4, cuya resistencia o fuerzas laterales en todos los niveles sea suministrada por elementos que se describen en el párrafo 7.5 y al menos en un nivel por muros de mampostería de piezas huecas.

#### Q = 1.

Para estructuras de cualquier tipo, cuya resistencia a fuerzas laterales sea suministrada al menos parcialmente por elementos hechos de materiales que no sean los arriba indicados, se usará un coeficiente de ductilidad  $Q = 1$ .

Para estructuras principales Tipo 8, el valor de  $Q$ , se proporcionará adelante.

Quando las deformaciones locales del suelo contribuyan significativamente a los desplazamientos de la estructura los valores de  $Q$  que se especifican en los párrafos precedentes serán sustituidos por una nueva  $Q_m$  dada por:  $Q_m = (Q_y + 2y_s) / (y + y_s)$ , donde  $y$  es el desplazamiento en cm. del centro de gravedad de la estructura, calculado sin tener en cuenta las deformaciones locales del terreno;  $y_s$ , en cm, es la parte del desplazamiento del centro de gravedad de la estructura que se debe a las defor-

aciones locales del terreno, y  $Q$  se especifica en los párrafos que anteceden. Para valores de  $Q$  iguales o menores que 2 el valor de  $Q_m$  se tomará igual a  $Q$ .

Las recomendaciones que anteceden, corresponden a estructuras con relación fuerza-deformación sensiblemente elasto-plástica y para las cuales no se realizó un estudio de ductilidades. En otras condiciones, se calculará  $Q$  según otros lineamientos.

Quando la estructuración propuesta sea susceptible de tomar diferentes valores de  $Q$  se adoptará aquel valor de  $Q$  que proporcione la solución más económica.

#### CRITERIOS DE ANALISIS

En el análisis sísmico de toda estructura se supondrá que de manera independiente actúan los movimientos en cada una de dos direcciones horizontales ortogonales. Se verificará que la estructura es capaz de resistir cada una de estas condiciones por separado. Las estructuras de planta irregular o estructuras que son aproximadamente cuadradas en planta pueden requerir análisis en otra dirección. Además, en miembros que son más débiles en direcciones oblicuas que según los ejes de análisis, se revisará la resistencia en aquellas direcciones.

El análisis de los efectos debidos a cada componente del movimiento del terreno debe satisfacer los siguientes requisitos:

a) La influencia de fuerzas laterales se analizará tomando en cuenta los desplazamientos horizontales y verticales y los giros de todos los elementos integrantes de la estructura, así como la continuidad y rigidez de los mismos. En particular se considerarán los efectos de la inercia rotacional en los péndulos invertidos.

b) En cada elemento se tomarán en cuenta todas las deformaciones que afecten seriamente los desplazamientos y esfuerzos de diseño. También se tomarán en cuenta las deformaciones locales del terreno y las debidas a las fuerzas gravitacionales que actúan en la estructura deformada cuando estas tengan efectos significativos en la respuesta.

c) En estructuras metálicas revestidas de concreto reforzado, será factible considerar la acción combinada de estos materiales en el cálculo de esfuerzos de rigideces, debiéndose asegurar el trabajo combinado de las acciones compuestas.

d) Se supondrá que no obran tensiones entre la subestructura y el terreno, debiéndose satisfacer el equilibrio de las fuerzas y momentos totales calculados. Se revisará la seguridad contra los estados límite de la cimentación. Si existan elementos, tales como pilotes o pilas, capaces de tomar tensiones, se les prestará atención en el análisis.

e) El cortante en cualquier plano horizontal, deberá distribuirse entre los elementos resistentes proporcionalmente a su rigidez, conside-

lando la rigidez del sistema de piso, diafragma o contraventeo horizontal.

Se verificará que las deformaciones de los sistemas estructurales, incluyendo las de las losas de piso, sean compatibles entre sí. Se revisará que todos los elementos estructurales, incluso las losas y los arriostramientos de los sistemas de piso o cubiertas, sean capaces de resistir los esfuerzos inducidos por las fuerzas sísmicas.

Como simplificación en el diseño sísmico de construcciones de altura menor o igual que dos pisos o 6 m, con sistemas de piso o cubierta arriostrados mediante sistemas cuya rigidez en su plano sea pequeña en comparación con la rigidez de los elementos que proporcionan la resistencia lateral, podrá considerarse que cada uno de estos elementos resistentes se ve sometido a la parte de fuerza sísmica que corresponde a su área tributaria por piso en cada nivel.

f) En el diseño de marcos que contengan tableros de mampostería se supondrá que las fuerzas cortantes que obran en éstos están equilibradas por fuerzas axiales y cortantes en los miembros que constituyen el marco.

Asimismo, se revisará que las esquinas del marco sean capaces de resistir los esfuerzos causados por los empujes que sobre ellas ejercen los tableros.

## ANÁLISIS ESTÁTICO

Para calcular las fuerzas cortantes de diseño a diferentes niveles de una estructura, se supondrán los dos siguientes estados de carga actuando simultáneamente:

a) Un conjunto de fuerzas horizontales, actuando sobre cada uno de los puntos donde se supongan concentradas las masas de la estructura. Cada una de estas fuerzas se tomará igual al producto del peso de la masa correspondiente por un coeficiente que varía linealmente, desde cero en el desplante de la estructura (o desde el nivel a partir del cual sus deformaciones pueden considerarse despreciables) hasta un máximo en el extremo superior de la misma, de modo que la relación  $V/V$  en la base sea igual a  $0.95 \frac{CDW}{Q}$ , en donde C y Q son los coeficientes definidos, D es un factor reductivo que depende de la flexibilidad de la estructura y que vale  $0.6/T$  para construcciones en la zona I, y  $1.2/T$  para construcciones en la zona II, donde T es el período natural de vibración de la estructura en seg, calculado según se indica más adelante en este artículo. El valor de D no debe tomarse menor que 0.4, ni mayor que 1.0.

J es un factor reductivo que depende del amortiguamiento de la estructura, y que adquiere los siguientes valores:

J = 0.8; Para estructuras de acero remachadas o atornilladas, así como para estructuras de maderas.

J = 0.9; Para estructuras de concreto reforzado o pretensado.

J = 1.0; Para estructuras de acero soldadas o con juntas a base de tornillos de alta resistencia trabajando a fricción.

La fuerza horizontal aplicada en el nivel i estará dada por la siguiente expresión:

$$F_i = 0.95 \frac{CDW}{Q} W \times \frac{W_i H_i}{\sum (W_j H_j + W_2 H_2 + W_3 H_3 + \dots + W_n H_n)}$$

$F_i$  = Fuerza horizontal en el centro de la masa de peso  $W_i$  y altura  $H_i$  sobre el nivel de la base de la estructura,

$H_i$  = Altura sobre el nivel de la base del centro de la masa considerada.

$W = W_1 + W_2 + W_3 + \dots + W_n$  = Peso total de la estructura.

$W_i$  = Peso de la masa i

n = Número total de masas de la estructura

C y Q definidos en los artículos 6. y 7.

D y J definidos en este artículo.

El cálculo del período natural de vibración (T) de las estructuras de la planta que se utilizará en el cálculo del valor de D, se podrá efectuar utilizando la siguiente expresión:

$$T = 0.28 d \left( \frac{1}{g} \sum W_i y_i^2 / \sum P_i y_i \right)^{1/2}$$

donde

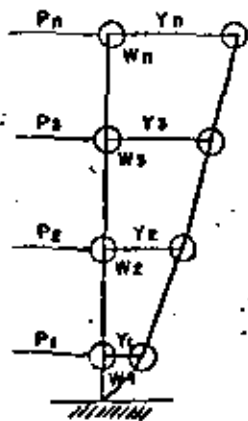
$W_i$  = peso de nivel  $i$

$y_i$  = Desplazamiento horizontal en nivel  $i$

$P_i$  = Fuerza aplicada en el nivel  $i$ , proporcional a  $F_i$

$d$  = Coeficiente para tomar en cuenta las variaciones en el cálculo del periodo natural ( $d = 0.75$ )

En la figura siguiente se muestra esquemáticamente el significado de las variables que intervienen en el cálculo de  $T$ .



b) Una fuerza actuando horizontalmente concentrada en el extremo superior de la estructura, sin incluir tanques, apéndices u otros elementos cuya estructuración difiera radicalmente del resto de la construcción, igual a  $0.05V$ .

La estabilidad de tanques que se hallen sobre las estructuras, así como la de todo otro elemento cuya estructuración difiera radicalmente de la del resto de la construcción no menor que el doble de la que resulta de aplicar la especificación anterior ni menor que la gravedad multiplicada por  $0/2$ . Se incluyen en esta requisito los parapetos, pretilas, arcos, ornamentos, ventanales, muros, revestimientos y su anclaje y otros apéndices.

Se incluyen asimismo, los elementos sujetos a esfuerzos que dependen principalmente de su propia aceleración (no de la fuerza cortante ni del incremento de volteo), como las losas que transmiten fuerzas de inercia de las masas que soportan.

Para fines de diseño se tomará el momento de volteo calculado para cada marco o grupo de elementos resistentes, en el nivel que se analiza, igual al producto de la fuerza cortante que allí obra por su distancia al centro de las masas ubicadas arriba de dicho nivel.

La excentricidad torsional calculada en cada nivel se tomará como la distancia entre el centro de torsión del nivel correspondiente y la posición de la fuerza cortante en dicho nivel.

La excentricidad de diseño se tomará como se describe a continuación:

a) 1.5 veces el valor calculado más 0.05 veces la máxima dimensión del piso que se analiza (excentricidad accidental), medida en la dirección normal a la fuerza cortante, para el diseño de miembros estructurales en que los efectos de la torsión calculada sean aditivos a los de fuerza cortante directa.

b) El valor calculado de la excentricidad menos la excentricidad accidental, para el diseño de los miembros estructurales en que los efectos de torsión calculada y de cortante directo difieran en signo.

Además en ningún caso se tomará la excentricidad de diseño menor que la mitad de la máxima excentricidad de diseño de los niveles que se hallan arriba del que se analiza, ni se tomará la torsión de diseño de entrepisos menor que la mitad de la máxima torsión de diseño calculada para los entrepisos que se hallan arriba del que se analiza.

NOTA: Lo mencionado anteriormente se aplica cuando se garantiza la transmisión de la fuerza cortante sísmica entre marcos adyacentes por medio de sistemas de piso rígidos, contraventados horizontales, u otros sistemas.

#### ANÁLISIS DINAMICO

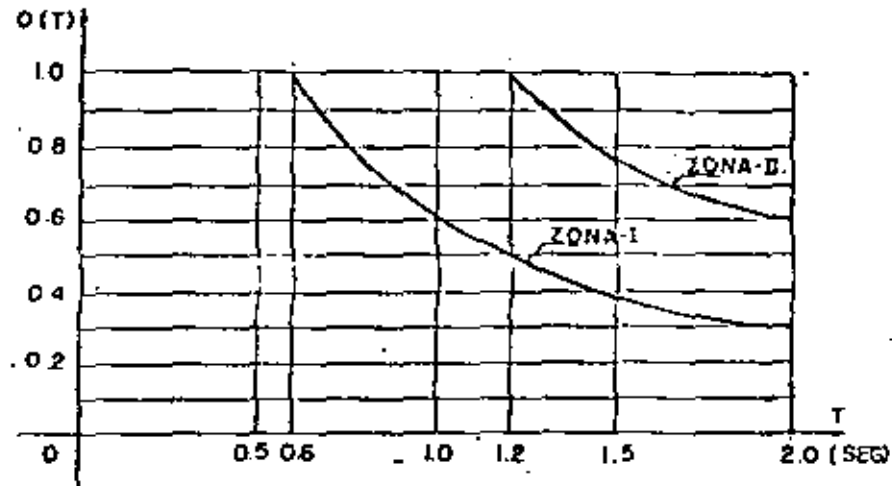
Son admisibles como métodos de análisis dinámico el análisis modal y el cálculo paso a paso de respuestas a temblores específicos.

Si se usa el análisis modal, podrán despreciarse aquellos modos naturales de vibración cuyo efecto combinado no modifique los esfuerzos de diseño sísmico en más de 10 por ciento. Puede también despreciarse el efecto dinámico torsional que resulte de excentricidades, calculadas estáticamente, no mayores de 5 por ciento de la dimensión del piso, medida en la misma dirección que la excentricidad. El efecto de dichas excentricidades y de la excentricidad accidental se calculará como lo especifica el artículo correspondiente del análisis estático.

Cuando sea aplicable el análisis dinámico modal, este se llevará a cabo de acuerdo con las siguientes hipótesis:

a) La estructura se comporta elásticamente.

b) Tratándose de edificios ordinarios, el espectro de aceleraciones para diseño sísmico, expresado como fracción de la gravedad, es igual a  $a(T)C$ , donde  $C$  es el coeficiente basal  $T$  es el período natural de interés y  $a(T)$  está dada por las siguientes expresiones, en las que  $T$  es en segundos:



Zona I

$$a(T) = 1, \text{ si } T < 0.6 \text{ seg.}$$

$$a(T) = 0.6/T, \text{ si } T \geq 0.6 \text{ seg.}$$

Zona II

$$a(T) = 1, \text{ si } T < 1.2 \text{ seg.}$$

$$a(T) = 1.2/T, \text{ si } T \geq 1.2 \text{ seg.}$$

En cualquiera de las zonas (I ó II) la aceleración espectral está dada por la expresión siguiente:  $A(T) = a(T)G$  donde  $g$  es la aceleración de la gravedad.

Las fuerzas y esfuerzos calculados con los espectros citados arriba deberán dividirse entre el valor de  $Q$  aplicable.

Se supondrá que cada periodo natural de vibración puede ser inferior al

calculado hasta en 25 por ciento y se adoptará el valor más desfavorable.

c) Las aceleraciones espectrales especificadas se deberán multiplicar por el coeficiente de amortiguamiento  $J$ , definidos anteriormente.

Si se emplea el método de cálculo paso a paso de respuestas a temblores específicos podrá acudir a registros de temblores reales o de movimientos simulados o a combinaciones de éstos siempre que se usen no menos de cuatro movimientos representativos, independientes entre sí, cuyas intensidades sean compatibles con los demás criterios que consigna el presente reglamento y que se tengan en cuenta el comportamiento no lineal de la estructura y las incertidumbres que haya en cuanto a sus parámetros.

#### CALCULO Y LIMITACION DE DESPLAZAMIENTOS HORIZONTALES

Se deberán revisar los desplazamientos horizontales de la estructura y de partes y equipo que lo ameritan, debidos a las fuerzas producidas por un sismo de intensidad media.

Los desplazamientos se calcularán suponiendo que sobre la estructura o sobre una fuerza cortante total,  $V$ , (que) es  $0.3 D J W$ , si ésta es del grupo A, de  $0.23 D J W$  si es del grupo B y de  $0.18 D J W$  si es del grupo C. Esta fuerza se considerará actuando sobre la estructura con la distribución que se obtiene de aplicar los criterios de los artículos 9 ó 10.

Quando haya peligro de colisión entre estructuras o partes de la misma, debidas a desplazamientos horizontales relativos, así como cuando se requiera revisar la estabilidad del conjunto ante un sismo de gran intensidad, las fuerzas constantes totales,  $V$ , que se considerarán, serán iguales a  $0.78 D W$ ,  $0.60 D W$  y  $0.48 D W$  para estructuras de los grupos A, B y C respectivamente. La fuerza se distribuye igual que en 11.1.

Las deformaciones laterales relativas entre entrepisos o entre niveles de sujeción de acabados o de plazas de equipo se limitarán de acuerdo con lo que se requiere para evitar daños en dichos elementos. Los límites impuestos a deformaciones en cuestión, deberán ser aprobados por el director del proyecto. La limitación puede omitirse cuando los elementos que no forman parte integrantes de la estructura estén ligados a ella en tal forma que no sufran daños por las deformaciones de ésta. En este caso no será necesario limitar los desplazamientos laterales sísmicos salvo para evitar choques entre estructuras contiguas.

En el cálculo de los desplazamientos se tomará en cuenta la rigidez de todo elemento que forme parte integrante de la estructura.

#### PRECAUCIONES EN VENTANAS

En fachadas tanto interiores como exteriores, los vidrios de ventanas se colocarán en los marcos de éstas dejando en todo el alrededor de cada ta-

bierno una holgura por lo menos (igual a la mitad del desplazamiento horizontal relativo entre sus extremos, calculado a partir de la deformación por cortante de entrepiso y dividido entre  $1 + H/B$ , donde  $B$  es la base y  $H$  la altura del tablero de vidrio de que se trata. Podrá omitirse esta precaución cuando los marcos de las ventanas estén ligados a la estructura de tal manera que las deformaciones de ésta no les afecten.

#### PRECAUCIONES CONTRA CHOQUES ENTRE ESTRUCTURAS ADYACENTES :

Las estructuras adyacentes deben separarse entre sí un mínimo de 5 cm, pero no menos que la suma de los valores absolutos de los desplazamientos máximos calculados para ambas construcciones, ni que 0.008 de la altura de la construcción más baja.

Estas separaciones pueden reducirse si se toman precauciones especiales para evitar daños por choques.

#### MUROS DE RETENCION

Los empujes que los rellenos ejercen sobre muros de retención debido a la acción de los sismos de valuarán suponiendo que el muro y la cuña de falla crítica se encuentran en equilibrio límite bajo la acción de las fuerzas debidas a carga vertical, a una aceleración vertical igual a  $0.3 C_g$  (hacia arriba o hacia abajo) y a una aceleración horizontal igual a  $0.5 C_g$ , siendo  $C$  el coeficiente del Art. 6 y  $g$  la aceleración de la gravedad.

A partir de los empujes determinados mediante lo que se especifica arriba, deberán incluirse los siguientes conceptos en el diseño sísmico de todo muro de retención:

a) Diseño estructural del muro

b) Seguridad contra volteo. Incluyendo los efectos de empujes estáticos y de sismo, el factor de seguridad contra volteo, calculado como el cociente de los momentos con respecto al centro potencial de volteo de las fuerzas que tienden a estabilizar el muro entre aquellos que tienden a voltearlo, debe ser cuando menos igual a 1.2.

c) Seguridad contra deslizamiento. Incluyendo los efectos de empujes estáticos y sismo, el factor de seguridad contra deslizamiento, calculado como el cociente de la suma de aquellas fuerzas que tienden a impedir el deslizamiento sobre una superficie crítica entre aquellas que tienden a producirlo, debe ser cuando menos a 1.2.

#### OTRAS ESTRUCTURAS

El análisis y el diseño de estructuras que no puedan clasificarse en alguno de los tipos descritos se harán de manera congruente con lo que marcan las presentes especificaciones, para los tipos aquí tratados.

#### VALUACION DE LA RESISTENCIA ESTRUCTURAL

La valuación de los factores de seguridad y de la capacidad de miembros estructurales de concreto, acero y mampostería, se efectuará según se especifica, respectivamente, en el reglamento vigente del Instituto Americano del Concreto ACI (poniendo especial atención a su apéndice A) y en las especificaciones vigentes para diseño estructural del Instituto Americano de la Construcción en Acero AISC.

Quando se diseña para los efectos combinados de sismo y carga vertical se seguirán los lineamientos de dichos reglamentos, utilizando los valores que se dan a continuación en sustitución de los valores que especifican los reglamentos antes mencionados.

a) En diseño por esfuerzos de trabajo el incremento de esfuerzos permisibles será de 50% para concreto, 50% para acero de refuerzo y 80% para acero estructural.

b) En diseño por resistencia última se usará un factor de carga de 1.1.

Por lo que respecta a mampostería se usará el capítulo correspondiente del reglamento de las construcciones vigente del Distrito Federal u otro código especializado.

No deberá considerarse la acción simultánea de viento y sismo.

### VALORES DE LOS COEFICIENTES SISMICOS

Las construcciones del grupo A, así como aquéllas del grupo B deberán ser capaces de resistir:

a) Un sismo de mediana intensidad, después del cual la operación de la planta no debe interrumpirse. ( Sismo de operación ).

b) Un sismo de gran intensidad en el cual no deberá producirse el colapso de la estructura y en el que los daños sufridos puedan repararse en un período de tiempo relativamente corto. ( Sismo de diseño ).

Las construcciones de los grupos B y C, se diseñarán únicamente para resistir el sismo de diseño según se indica en el párrafo b precedente.

A modo indicativo, la tabla siguiente proporciona los valores del coeficiente basal para construcciones de los grupos B y C.

La tabla es aplicable para estructuras Grupo "B". Para construcciones grupo "C" los valores de la tabla deberán multiplicarse por 0.8 y por las del grupo A por 1.3

Para análisis estático deberá usarse el factor reductivo "D" que toma en cuenta la flexibilidad de la estructura que se definió anteriormente.

### REDUCCIONES DE CARGA VIVA

Para el cálculo de las fuerzas sísmicas al valor del peso "W", deberá incluir las cargas muertas ( cargas que actúan permanentemente sobre la estructura ), más un porcentaje de las cargas vivas utilizadas en el diseño por fuerza vertical. El valor de este porcentaje se da en la tabla siguiente:

<u>DESTINO DEL PISO</u>	<u>PORCIENTO DE LA CARGA VERTICAL.</u>
Oficinas, habitaciones, pasillos	20%
Áreas de almacenamiento	50%
Techos con pendientes mayores de 5%	20%
Techos con pendientes menores de 5%	40%
Contenidos de Tolvas de almacenamiento tuberías y tanques	100%

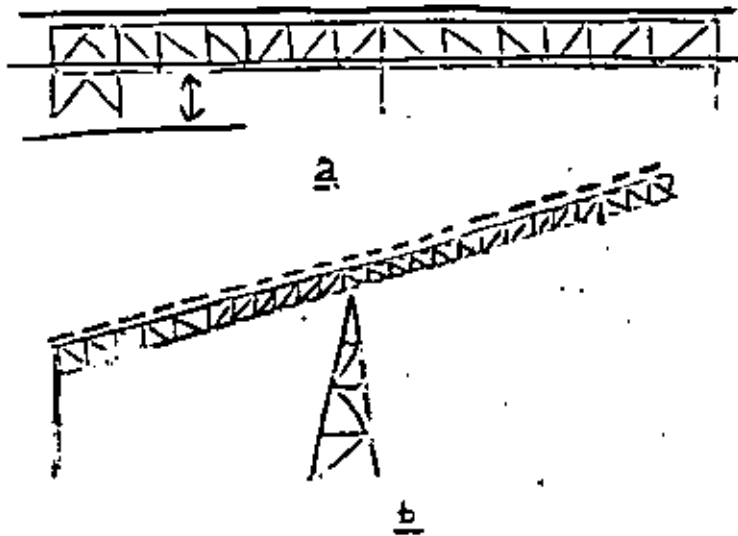
### COMBINACIONES DE CARGA

Las estructuras se analizarán para las siguientes combinaciones de carga:

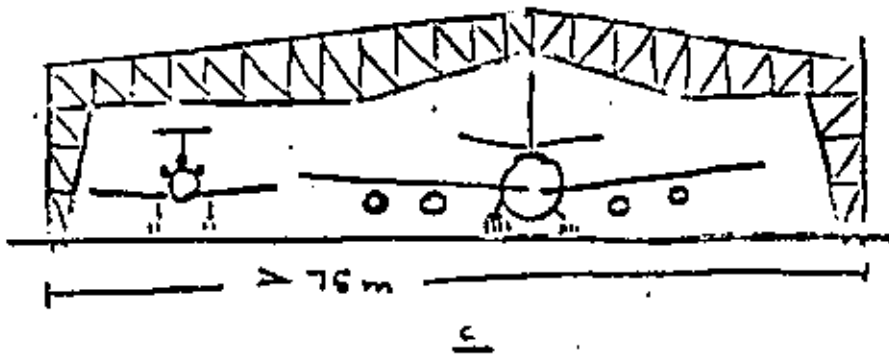
- 1) E.L. ( debido a D.L. + L.L.1 + L.L.2A + C.L. ) + D.L. + L.L.2 + C.L. + T.L.
- 2) E.L. ( debido a D.L. + L.L.1 ) + D.L. + L.L.1 + T.L.
- 3) E.L.H. ( debido a D.L. + L.L.1 + L.L.2A + C.L. ) + 0.7E.L.V. ( debido a D.L. + L.L.1 + L.L.2A + C.L. ) + D.L. + L.L.1 + L.L.2 + C.L. + T.L.



III. Soportes de tuberías y transportadores

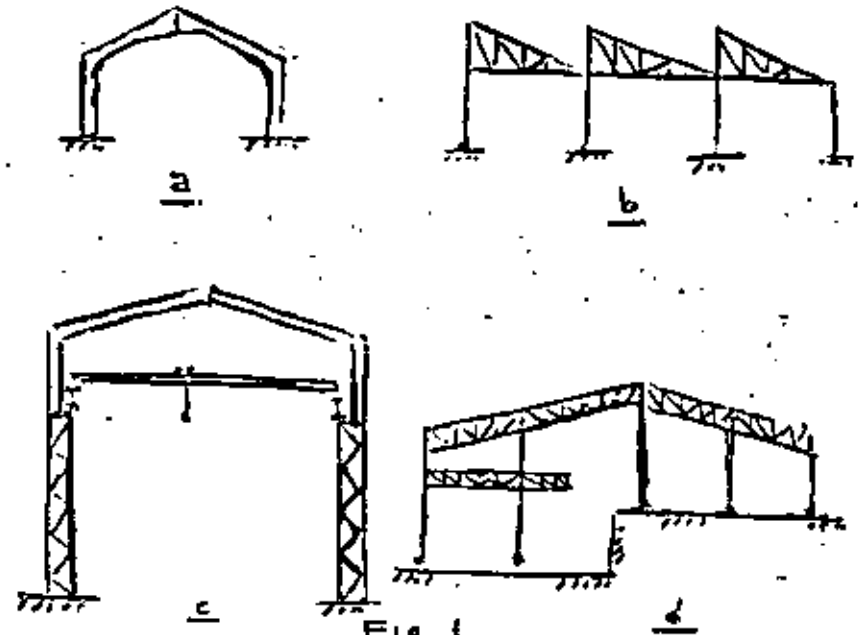


IV. Estructuras de grandes claros...

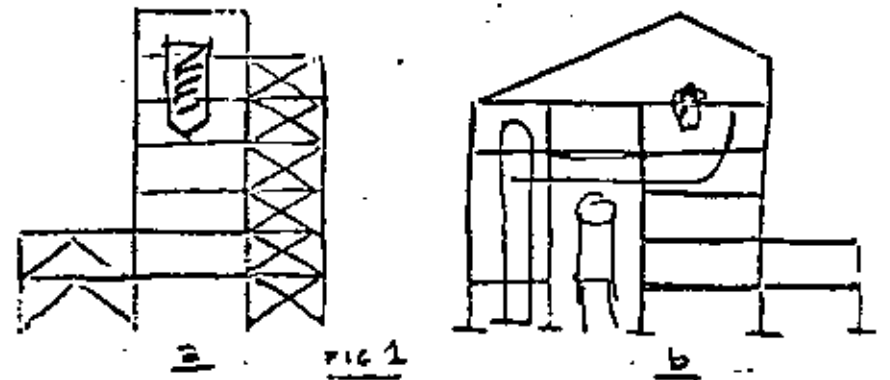


Principales tipos de estructuras industriales:

I. Naves industriales con y sin grúas



II. Estructuras de pilares





**DIVISION DE EDUCACION CONTINUA  
FACULTAD DE INGENIERIA U.N.A.M.**

**DISEÑO SISMICO DE ESTRUCTURAS ESPECIALES**

**DISEÑO SISMICO DE ESTRUCTURAS  
DE TIPO INDUSTRIAL**

**M. en C. MAURICIO NANES**

**Agosto, 1981.**

1. The first part of the document is a list of names and addresses, which appears to be a directory or a list of contacts. The names are written in a cursive hand, and the addresses are listed below them. The list includes names such as "John Doe" and "Jane Smith", and addresses such as "123 Main Street" and "456 Elm Street".

2. The second part of the document is a list of names and addresses, which appears to be a directory or a list of contacts. The names are written in a cursive hand, and the addresses are listed below them. The list includes names such as "John Doe" and "Jane Smith", and addresses such as "123 Main Street" and "456 Elm Street".

3. The third part of the document is a list of names and addresses, which appears to be a directory or a list of contacts. The names are written in a cursive hand, and the addresses are listed below them. The list includes names such as "John Doe" and "Jane Smith", and addresses such as "123 Main Street" and "456 Elm Street".

ANÁLISIS DE ESTRUCTURAS CON SISTEMAS DE PISO  
CONTRAVENTEADOS CONSIDERADOS COMO DIAFRAGMAS FLEXIBLES

Mauricio Nanes G.\*

RESUMEN

Se describe el comportamiento de estructuras con sistemas de piso contraventeados, como afectan la distribución de fuerzas sísmicas y de viento. Se plantean modelos estructurales para el análisis de los sistemas de piso con diafragmas flexibles enfocados a satisfacer la compatibilidad de desplazamientos de los marcos transversales producidos tanto por cargas horizontales como por cargas verticales.

Se discuten dos de las funciones básicas del contraventeo horizontal de piso, que son: concentrar fuerzas laterales uniformes en marcos de mayor rigidez y el distribuir fuerzas laterales concentradas entre varios marcos paralelos. Se describe un estudio paramétrico en el que se aprecia el efecto de tipos de contraventeo, y su geometría en la concentración o distribución de dichas fuerzas laterales. Finalmente se aplican estos conceptos a Naves Industriales.

I N D I C E

1. Introducción.....	1
2. Concepto de diafragma.....	2
3. Modelación y análisis de diafragmas flexibles.....	5
4. Diafragma como elemento concentrador de fuerzas laterales uniformes.....	6
5. Diafragma como elemento distribuidor de fuerzas laterales concentradas.....	11
6. Aplicación a Naves Industriales con grúa.....	14
7. Conclusiones.....	19
8. Referencias.....	20

\* Jefe de Sección Estructural, Bufete Industrial.

El análisis estructural de edificios industriales con sistemas de piso contraventeados presenta una serie de características especiales en lo referente a las condiciones de carga que involucren fuerzas horizontales. El concepto de distribución de cortantes sísmicos del método estático equivalente, no es aplicable tal como se ha planteado (1)\*, ya que tiene implícito que los sistemas de piso son indeformables en su plano, y en general el considerar las cargas estáticas equivalentes de viento, calculadas en base a áreas tributarias, es válido en ciertos casos únicamente.

En realidad los sistemas de piso de edificios industriales de acero, en pocas ocasiones pueden ser considerados como indeformables en su plano; por el contrario, resultan ser bastante flexibles, ya sea por la necesidad funcional de dejar huecos de acceso o para equipo, o por la utilización de pisos tipo rejilla o placa antiderrapante. En ocasiones es necesario contraventear el sistema de piso para aumentar su rigidez para lograr una mejor distribución de cargas entre los diferentes marcos.

Este tipo de estructuras, tradicionalmente son analizadas y diseñadas considerando cada marco en forma independiente (por área tributaria), sin tomar en cuenta el comportamiento del conjunto de marcos y sistemas de piso. En el límite (sistemas de piso sin losa de concreto ni contravientos), los marcos tanto transversales como longitudinales se comportan en forma independiente; sin embargo existe un rango amplio en el que el contraventeo de piso afecta, en menor o mayor grado, la interacción entre marcos paralelos y ortogonales redistribuyendo cargas y alejándose del criterio de considerar las cargas por área tributaria, y sin llegar al caso de diafragmas rígidos.

El objetivo básico es el poder efectuar una serie de análisis de estructuras planas de tal manera que simulen, en la forma más realista posible, el comportamiento tridimensional de la estructura, y lograr de esta manera diseños más económicos.

En este artículo se presentan las herramientas para poder efectuar la distribución de cortantes sísmicos y de viento incluyendo la flexibilidad de los sistemas de piso, se presenta una evaluación cualitativa y cuantitativa del comportamiento de diafragmas flexibles por medio de su modelación y análisis estructurales.

\* Números en paréntesis son referencias enlistadas posteriormente.

Todo entrepiso de un edificio tiene una cierta rigidez a flexión en el plano del sistema de piso en consideración. En el caso de pisos de concreto, estos pueden visualizarse como trabes de concreto muy peraltadas. En el caso de sistemas de piso contraventeados, se pueden considerar como armaduras horizontales. El parámetro importante es la rigidez relativa entre el sistema de piso y la rigidez de los marcos.

En edificios industriales de acero, cuando no existe losa de concreto ni contraventeo horizontal, cada marco se comportará como se estuviera aislado (Fig. 1a); consecuentemente, los desplazamientos laterales, a un cierto nivel de la estructura, de todos los marcos paralelos, serán función de las fuerzas horizontales a que esté sujeto cada marco, consideradas por área tributaria únicamente.

En edificios cuyos sistemas de piso sean de concreto, y cuando la rigidez a flexión en el plano del piso sea grande comparada con las rigideces de entrepiso de los marcos, el sistema de piso puede considerarse como un diafragma rígido, el cual hace que los desplazamientos laterales, a un cierto nivel de la estructura de todos los marcos paralelos, sigan una variación lineal, como se ilustra en la Fig. 1b para el caso que no haya torsión en planta, y en la Fig. 1c cuando sí hay torsión. El diafragma rígido hace que las fuerzas laterales totales se distribuyan a cada marco de acuerdo a sus rigideces de entrepiso relativas.

Los dos tipos de edificios descritos son los casos extremos; sin embargo, existe un gran número de estructuras cuyos sistemas de piso tienen cierta rigidez a flexión, pero no pueden considerarse como diafragmas rígidos. En la Fig. 2 se muestran dos casos de diafragmas flexibles, uno sujeto a cargas simétricas y otro con cargas asimétricas, se muestra también la configuración de desplazamientos laterales, y las fuerzas que absorben cada marco en función de la rigidez de entrepiso  $K$  y del desplazamiento lateral en el nivel en consideración.

En estructuras con diafragmas rígidos o flexibles, las fuerzas que absorben los marcos ya no son en función de

Las cargas laterales calculadas en base a áreas tributarias, pero no son tales que deben satisfacer la compatibilidad de desplazamientos laterales de diafragma.

## 2.2 Funciones del diafragma.

Un diafragma, sea rígido o flexible, hace que las fuerzas horizontales totales en un cierto nivel sean transmitidas a los marcos dependiendo de sus rigideces de entrepiso y de la rigidez del diafragma.

Los dos usos más importantes que se puede hacer del comportamiento de diafragma son:

- Concentración de fuerzas laterales "uniformes" en los marcos más rígidos.
- Distribución de fuerzas laterales concentradas entre varios marcos adyacentes a la localización de la fuerza concentrada.

La primera aplicación sería por ejemplo, en edificios industriales en los que se proporciona contraventeo en el plano vertical en los marcos transversales cabecera o exteriores; esto resulta en una diferencia grande de rigideces de entrepiso entre los marcos transversales intermedios y los cabecera.

Las fuerzas sísmicas y de viento se concentrarán en los marcos cabecera a través de los diafragmas de piso. Este es el comportamiento real de la estructura y deberá tomarse en consideración.

La segunda aplicación sería el considerar el diafragma para que la fuerza horizontal sísmica de grúa aplicada en un marco no solo sea absorbida por dicho marco, sino entre varios marcos paralelos.

## 2.3 Compatibilidad de desplazamientos laterales debidos a cargas verticales.

El comportamiento de diafragma (rígido o flexible) del sistema de piso, forra las condiciones de compatibilidad de desplazamientos laterales de los marcos cuando están sujetos tanto a fuerzas horizontales como a cargas verticales.

El análisis de estructuras compuestas por marcos planos de marcada diferencia perimetrica, sujetos a cargas verticales, produce desplazamientos laterales distintos

en cada marco analizado aisladamente (Fig. 3). En este caso también debe considerarse el comportamiento del diafragma para forrar la compatibilidad de desplazamientos.

Una forma de lograr dicha compatibilidad para el caso particular que se tenga diafragmas rígidos y que no exista torsión en planta, se presenta en el modelo estructural de la Fig. 4. Se modelan todos los marcos paralelos una a continuación de otro unidos con elementos ficticios de rigidez infinita que simulan la acción del diafragma rígido, y forzan a que los desplazamientos horizontales de todos los marcos en cada nivel sean iguales. En este caso las propiedades geométricas y las cargas para el modelo del marco 1Y-5Y y 2Y-4Y deben duplicarse.

Cuando el diafragma no se puede considerar como rígido, y para el caso en que no haya torsión en planta, se puede modelar a la estructura como se indica en la Fig. 5, en la que las barras de unión entre marcos tienen una rigidez finita obtenida a través de un análisis del diafragma flexible.

Un sistema de piso de un edificio industrial diseñado como estructura metálica y que este contraventeado en su plano, será un diafragma flexible. Este diafragma puede considerarse como una armadura en el plano horizontal soportada sobre una serie de soportes elásticos, los cuales simulan las rigideces del entrepiso inmediatamente abajo del piso en consideración.

En la Fig. 6 se muestra el modelo estructural de dicho diafragma. Las barras verticales y horizontales en las líneas de los ejes del edificio, representan las vigas de los marcos. Todas las diagonales y otras barras son parte del contraventeo horizontal del sistema de piso. La rigidez de los resortes mostrados, son las rigideces de entrepiso calculadas como se indica esquemáticamente en la figura.

A este modelo estructural se le aplican las cargas correspondientes al efecto que se quiera analizar, sea concentración o distribución de fuerzas sísmicas o de viento. Se obtiene del análisis las fuerzas en los resortes, que a su vez son las cargas horizontales que se aplican posteriormente a cada marco para ser analizados como estructuras planas. También se obtienen las fuerzas actuantes en el contraventeo para efectuar su diseño por resistencia.

En edificios industriales de acero los sistemas de piso a veces pueden contraventearse uniformemente como se muestra en la Fig. 7, pero muchas veces resultan diafragmas flexibles tan irregulares como el mostrado en la Fig. 8. Para estos dos casos particulares se muestran los porcentajes obtenidos de las fuerzas totales que absorben los resortes y se comparan con los porcentajes que corresponderían al caso particular de diafragma rígido.

En cierto tipo de industrias, los edificios de proceso de concreto reforzado, requieren de huecos grandes en varios niveles para alojar equipo como se indica en la Fig. 9. Existiría la duda si se puede o no considerar a estos pisos como diafragmas rígidos. En la Fig. 10 se muestra el modelo estructural en forma esquemática, como un marco cerrado con tramos de sección variable en forma escalonada, soportado sobre resortes elásticos; el modelo estructural detallado se muestra en la Fig. 11, el cual fué analizado (2) como diafragma flexible y las fuerzas que se obtuvieron en los resortes se aplicaron posteriormente como cargas horizontales a los marcos planos.

Este sistema de piso puede ser modelado y analizado, sea como estructura plana (elementos finitos) o como modelo simplificado.

En ciertas ocasiones es conveniente el acentuar la diferencia de rigidez de las secciones entre marcos para los, para aliviar a los marcos más rígidos de esfuerzos producidos por cargas laterales, y concentrar en los marcos más rígidos mayor porcentaje de la carga lateral total de un cierto nivel.

Una condición óptima sería el disponer a cierto número de marcos intermedios para cargas verticales, y con estas secciones de miembros calcular la intensidad de las fuerzas laterales que dichos marcos resistirían con un sobreesfuerzo del 3%. La diferencia entre la fuerza horizontal total y la absorbida por los marcos intermedios, deberá ser absorbida por los marcos más rígidos en los que se quiere concentrar las fuerzas laterales.

Un caso particular sería el de naves industriales en las que se contraventea los marcos exteriores y se procura que todos los marcos intermedios no sean penalizados por absorber cargas laterales.

Se efectuó un estudio paramétrico (3) de la concentración de carga uniforme lateral en los marcos exteriores a través de varias configuraciones y rigideces de diafragmas flexibles.

Los parámetros que intervienen en este estudio son los siguientes:

- Tipo de contraventeo.- Se consideraron cuatro configuraciones geométricas mostradas en las Figuras 12 y 13.
- Geometría de contraventeo.- Se consideró un rango amplio de propiedades geométricas de las secciones transversales de contraventeo (Área, momento de inercia).
- Rigideces de entrepiso.- La rigidez de entrepiso de los marcos intermedios considerada fué de 42 T/M y 420 T/M. Los marcos exteriores se consideraron cinco y cincuenta veces más rígidos que los intermedios.
- Dimensiones en planta del diafragma.- Tres relaciones de lado largo a corto (A/B) fueron consideradas,  $A/B = 1.5, 2, 3$ .

El modelo estructural utilizado en el análisis fue simplificado de una armadura plana, a un marco cerrado cuyas barras tienen asociadas propiedades geométricas de área y momento de inercia equivalente a las de la armadura. En las Figuras 12 y 13 se muestran los dos modelos superpuestos para los cuatro tipos de contraventeo. Esta equivalencia fue hecha con el objeto de reducir el número de nudos y miembros en el modelo de análisis para reducir tiempo de computadora (2).

Las cargas a las que se sujetó el modelo fueron fuerzas concentradas en todos los nudos simulando una carga uniforme como sería la de sismo o viento.

En las Figuras 14 a 16 se muestra como afectan los diferentes parámetros al porcentaje de la fuerza horizontal total que absorben los marcos exteriores o cabecera (%CA). Se entiende por geometría (abscisas) en estas curvas, los valores relativos de áreas y momentos de Inercia del contraventeo, tomando como valor unitario o punto de partida los mostrados en la Figura 17.

Se observa en estas curvas que a medida que se robustece el contraventeo (aumento de geometría), aumenta el porcentaje de fuerza (%CA) que absorbe el marco transversal exterior contraventeado. A mayor rigidez de entrepiso de los marcos intermedios  $K_{mi}$ , se requiere mayor geometría de contraventeo para alcanzar el mismo % CA.

También se observa que para mayores relaciones de rigideces de entrepiso de marco exterior a interior ( $K_{me}/K_{mi}$ ), se logra una mayor concentración de fuerza en los marcos cabecera (%CA), o bien si dicha relación  $K_{me}/K_{mi}$  es baja, o sea que las rigideces de entrepiso de todos los marcos es más uniforme, habrá menos concentración de fuerza en los marcos cabecera (% CA).

La condición de diafragma rígido es el límite superior de estas curvas. Se observa que este límite es alcanzado más rápidamente cuando los marcos intermedios tienen menor rigidez; o sea, un diafragma menos rígido (menor geometría) es suficiente para lograr la condición de diafragma rígido. A medida que aumenta la rigidez de los marcos intermedios ( $K_{mi}$ ), se requiere de una mayor geometría (diafragma más robusto) para alcanzar la condición límite de diafragma rígido.

El tipo de contraventeo no es muy importante para diafragmas con A/B bajos y con marcos intermedios de baja rigidez (Fig. 14). Pero a medida que aumenta la relación de dimensiones en planta A/B, y que aumenta la rigidez de los marcos intermedios ( $K_{mi}$ ), los contraventeos tipo 3 y 4 son los más eficientes, como se aprecia en las Figuras 15 y 16.

Es conveniente reducir el número de parámetros que intervienen en las Figuras 14 a 16, para esto se calcularon las rigideces de los diafragmas ( $K_d$ ) en función de la geometría y del tipo de contraventeo. Estas rigideces se muestran en la Fig. 18.

Finalmente, los resultados de este estudio paramétrico se condensan en las Figuras 19 y 20. En la abscisa se tiene la relación adimensional: rigidez de diafragma a rigidez de marco intermedio ( $K_d/K_{mi}$ ), y en las ordenadas el porcentaje de la carga total absorbida por uno de los dos marcos cabecera (%CA). Se muestran dos curvas para diferentes relaciones de rigidez de marcos exteriores o cabecera a marcos intermedios ( $K_{me}/K_{mi}$ ).

#### 4.2 Distribución de fuerzas sísmicas.

Una de las funciones de los diafragmas es el concentrar fuerzas laterales "uniformes", en los marcos de mayor rigidez. Las fuerzas sísmicas son función de la masa la cual, en general, puede considerarse como una fuerza lateral "uniforme", excepto cuando haya pesos concentrados de consideración.

Cuando los sistemas de piso pueden considerarse como diafragmas rígidos, la fuerza sísmica total se distribuye a los marcos únicamente de acuerdo a sus rigideces relativas de entrepiso tal como se indica en la figura 21 (1).

En estructuras cuyos sistemas de piso sean diafragmas flexibles, habrá que efectuar primero un análisis de diafragma en cada nivel aplicándole la fuerza sísmica total en el nivel en consideración como fuerzas concentradas en todos los nudos y cuyas intensidades sean tales que su resultante quede localizada en el centro de masas del nivel. De este análisis se obtienen las fuerzas en los resortes, las cuales se aplican posteriormente a los marcos como cargas para efectuar su análisis como estructuras planas independientes.

#### 4.3 Distribución de fuerzas de viento.

Las cargas estáticas equivalentes de viento también pueden considerarse como fuerzas "uniformes". Los sistemas de piso de los edificios, al comportarse como diafragmas rígidos o flexibles, hacen que las fuerzas de viento también se distribuyan entre los marcos de acuerdo a sus rigideces relativas de entrepiso y dependiendo también de la rigidez del diafragma.

Análogamente a las fuerzas sísmicas, las fuerzas de viento no pueden considerarse por área tributaria, sino se debe tomar en cuenta el comportamiento de diafragma de los sistemas de piso. La excepción sería el caso de diafragmas rígidos y marcos de igual rigidez de entrepiso, en el que sí se puede distribuir las fuerzas de viento por área tributaria.

A continuación se describe la secuela para distribuir las fuerzas de viento:

a. Aplicar las fuerzas laterales totales de viento (P) en cada diafragma calculada en base a área tributaria definida como una franja horizontal a lo ancho del edificio, con una altura igual a la del promedio de los entrepisos adyacentes (Fig. 22).

b. Por medio de un análisis de diafragma flexible, obtener las fuerzas  $F_i$  que absorben los resortes que simulan las rigideces del entrepiso inferior al diafragma. En el caso particular de diafragma rígido sin torsión:

$$F_i = \frac{k_i}{\sum k_i} P$$

c. Calcúlese la fuerza concentrada de nudo en base a área tributaria:

$$F_i \Big|_t = P_{pr.} H S$$

d. Otréngase la diferencia entre estas dos fuerzas concentradas:

$$Q_i = F_i - F_i \Big|_t$$

Esta fuerza diferencial es la que, a través del diafragma, se está distribuyendo hacia otros marcos. Para marcos más rígidos  $Q_i$  será positiva, y para marcos menos rígidos  $Q_i$  será negativa.

e. Efectuar el análisis definitivo de cada marco plano en forma aislada sujeto a presiones calculadas en base a área tributaria como franja vertical, y aplicándole en cada nivel las fuerzas concentradas correctivas como se indica en la Figura 23.

## 5. DIAFRAGMA COMO ELEMENTO DISTRIBUIDOR DE FUERZAS LATERALES CONCENTRADAS.

### 5.1 Estudio Paramétrico

En edificios industriales de proceso hay necesidad de transportar cargas pesadas de un lugar a otro por medio de una grúa viajera, ya sean cargas del producto terminado, o bien de equipo en etapa de instalación y/o mantenimiento.

La fuerza sísmica horizontal de grúas de alta capacidad puede llegar a ser la condición de carga que rija el diseño de los marcos transversales. Esta fuerza concentrada horizontal puede distribuirse entre varios marcos paralelos a través del diafragma de manera que se reduzcan sus efectos en el diseño.

Se efectuó un estudio paramétrico (3) de la distribución de fuerzas laterales concentradas a varios marcos paralelos a través del diafragma. Los parámetros que se hicieron intervenir en este estudio son los mismos que en el estudio de concentración de fuerzas laterales descrito en la sección 4.

El modelo estructural utilizado fué simplificado aún más que el marco cerrado equivalente a la armadura horizontal. Se consideró una viga continua apoyada en soportes elásticos con rigidez lineal únicamente, los cuales simulan las rigideces de entrepiso de los marcos. La rigidez de la viga se igualó a la rigidez del diafragma  $K_d$  que a su vez se correlacionó con el tipo de contraventeo y su geometría (Fig. 18).

En la Figura 24 se muestra el modelo estructural así como la variación de la relación de rigideces de trabe equivalente a diafragma ( $EI/K_d$ ) con respecto a la longitud total de la trabe. Conocida la rigidez del diafragma  $K_d$  y la longitud  $L$ , se puede definir el momento de inercia de la trabe equivalente.

Se consideraron dos condiciones de carga en este estudio paramétrico, la primera aplicando una carga concentrada en el centro de la viga (coincidiendo con un resorte), la segunda aplicando una carga concentrada en el extremo de la viga, simulando la grúa en una posición central y en otra posición extrema.

En la Figura 25 se muestran los resultados de este estudio paramétrico. Las ordenadas son porcentajes de la fuerza concentrada que absorbe el resorte que coincide con el punto de aplicación de la carga; o sea, que del 100% de la fuerza aplicada, el marco absorbería únicamente los porcentajes indicados en la Figura. Las abscisas son valores del momento de inercia de la viga equivalente.

Se observa de la Figura 25, que para un mismo diafragma (valor de la abscisa), el porcentaje de carga que absorbe el marco es mayor entre mayor sea su rigidez de entrepiso. O bien, para poder obtener un mismo porcentaje de carga que absorba un marco (ordenada) se deberá hacer más robusto el diafragma (aumentar  $I$ ) a medida que aumenta la rigidez de entrepiso del marco.

También se observa de la Figura 25 que para diafragmas más rígidos ( $I$  mayor a  $1$ ), cuando la carga concentrada está en el extremo del edificio, el porcentaje de carga  $\%P$  que absorbe el marco en el que coincide la carga, es mayor al porcentaje de carga  $\%P$  que absorbe el marco cuando la carga está aplicada al centro del edificio. Sin embargo para diafragmas muy flexibles ( $I$  menor a  $0.1$ ) el efecto puede llegar a invertirse.

Es conveniente reducir el número de parámetros que intervienen en la Fig. 25 de manera de obtener una gráfica con mayor utilidad práctica. Todas las curvas de la Fig. 25 se transformaron a dos, al graficar en las abscisas el parámetro adimensional  $K_d/K_{pi}$  (relación de la rigidez del diafragma a la rigidez de entrepiso de los marcos). De esta figura, conocidas las rigideces de diafragma y del marco típico, se puede obtener el porcentaje de la fuerza concentrada aplicada ( $\%P$ ) que absorbe el marco en consideración. Este porcentaje para diafragmas medianamente contraventeados es menor del 30% para carga al centro del edificio, y menor de 40% para carga en el extremo del edificio.

### 5.2 Distribución de fuerzas concentradas.

Este estudio paramétrico descrito en la sección anterior puede utilizarse para determinar el porcentaje de la fuerza concentrada horizontal  $P$  que absorbe el marco que coincide con la posición de la carga. Este marco es el de interés, ya que otros paralelos absorben un porcentaje

de carga menor, y siendo la carga concentrada la producida por grúa, al cambiar la posición de la grúa a otro marco paralelo adyacente, se obtendría prácticamente el mismo valor de %P.

El hecho que el %P que absorbe el marco en el que coincide la carga concentrada horizontal permanece prácticamente constante, independientemente de cual de los marcos centrales es el que se carga, será cierto a partir de un cierto número mínimo de marcos paralelos, y de la rigidez relativa entre diáfragma y marcos; lo cual también puede apreciarse de la configuración de desplazamientos laterales del diáfragma.

En la Figura 27 se muestran dos configuraciones de desplazamientos. En el croquis superior de la Figura se aprecia que el diáfragma es bastante rígido y alcanza a distribuir la fuerza entre todos los marcos. En el croquis inferior el diáfragma es más flexible y distribuye la carga entre menos marcos.

Para diáfragmas más rígidos, a mayor número de marcos entre los que se distribuye la carga, menor será el porcentaje del marco más cargado %P, pero en diáfragmas muy flexibles el valor máximo de %P depende menos del número de marcos.

En el caso límite de diáfragma rígido, cuando las rigideces de todos los marcos son iguales, y para una carga simétrica:

$$\%P = \frac{P}{n}$$

Donde: P = Carga concentrada horizontal.  
n = Número de marcos.

Cuando la carga está aplicada en el extremo de un diáfragma rígido, se puede obtener el porcentaje de dicha carga que absorbe el marco extremo (%P) como la suma de la componente rotacional. En la Fig. 28 se muestran dichos valores para diferente número de marcos (n).

## 6.1 Estructuración.

La estructuración de una nave industrial se muestra en forma esquemática en la Fig. 29. Consta de marcos a dos aguas orientados en la dirección corta o transversal de la nave con claros que pueden ser de 10 o 30 metros o mayores, y cuya separación generalmente está entre 4 a 7 metros o mayor, dependiendo del material de la cubierta y los largueros que la soportan.

Las vigas inclinadas de los marcos soportan a los largueros, que a su vez soportan la cubierta de lámina de asbesto cemento o lámina metálica acanalada. La separación de los largueros es función del material de la lámina de cubierta. Debido a la inclinación de los largueros, se proporcionan tirantes para reducir su flexión en el plano de la cubierta.

Los dos marcos longitudinales se contravientean en crujías discretas, ya que las columnas de sección I están orientadas de manera que el menor momento de inercia coincide con la dirección longitudinal.

En la dirección transversal, los marcos cabecera o exteriores, se consideran en este caso que también están contravienteados.

La cubierta de este tipo de estructuras siempre se contravientea; sin embargo la configuración del contraviento depende de la función que sea necesario que desarrolle. En la Fig. 30 se muestran dos tipos de contraviento. La función básica del contraviento Tipo A es para reducir la longitud libre de pandeo lateral de la viga del marco. La función básica del contraviento Tipo B es el concentrar o distribuir fuerzas horizontales entre los marcos transversales y disminuir los desplazamientos horizontales relativos entre dichos marcos. El diáfragma flexible queda compuesto por todo el sistema de contraviento de la cubierta.

## 6.2 Compatibilidad de desplazamientos laterales.

### 6.2.1 Cargas verticales.

Particularizando al caso de cargas verticales de Grúa, se tendrá una fuerza lineal y un momento a nivel de ménsula o cambio de sección de la columna. La máxima asimetría se logra moviendo el carro de

... óa hasta un extremo del puente. En la Fig. 31 se muestra un marco transversal con las cargas de grúa y desplazamiento lateral  $\Delta_g$ .

El mismo marco se carga con una fuerza horizontal unitaria y se obtiene su desplazamiento lateral  $\Delta_1$  (Fig. 31b), con el objeto de evaluar la fuerza horizontal ( $F_h$ ) a nivel de la cubierta que produciría el mismo desplazamiento horizontal que producen las cargas verticales ( $\Delta_g$ ); o sea:

$$F_h = \frac{\Delta_g}{\Delta_1} \times 1$$

El marco de la Fig. 31a se analizó en forma aislada para obtener el desplazamiento  $\Delta_g$ , sin embargo este desplazamiento se debe reducir ya que el marco no se encuentra aislado, sino a través de la cubierta (diafragma flexible) se hace participar a otros marcos paralelos adyacentes. Por medio de un análisis de diafragma flexible (Fig. 31c) se obtiene el porcentaje de la fuerza  $F_h$  que absorbe el marco en consideración ( $\alpha_i$ ). El análisis definitivo de dicho marco se hará aplicándole las cargas verticales de grúa y una fuerza horizontal de restricción en dirección contraria a la de  $\Delta_g$  con valor  $(1 - \alpha_i)F_h$ . O sea, si el marco en consideración absorbe  $\alpha_i$  de la fuerza horizontal equivalente  $F_h$  todos los otros marcos absorben  $(1 - \alpha_i)F_h$  (Ver Fig. 31d).

En realidad, debido a las dimensiones del puente de la grúa, para una cierta posición del puente, se deben cargar dos o tres marcos adyacentes (Fig. 32a). Por medio de un análisis de diafragma, considerando la posición de cada marco cargado como una condición de carga de fuerza horizontal, se puede obtener líneas de influencia de fuerzas en los resortes. El porcentaje total  $\alpha_i$  se puede obtener por superposición lineal. (Ver Fig. 32b):

$$\alpha_i = \beta_0 \alpha_{i0} + \beta_1 \alpha_{i1} + \beta_2 \alpha_{i2}$$

Donde:  $\beta_1 = P_i / P_{max}$

$$\beta_0 = 1$$

El análisis definitivo del marco se hace como se describe en los párrafos anteriores.

## 2.2 Cargas horizontales debidas a grúa.

Las fuerzas horizontales, en la dirección transversal del edificio, que produce el cabeceo de la grúa o la fuerza sísmica de la grúa, están aplicadas a nivel de la ménsula que soporta la trabe-carril, y en general el diafragma distribuidor se encuentra a nivel de cubierta.

El diafragma, en conjunto con los marcos paralelos adyacentes, funciona como elemento restringente de los desplazamientos laterales del marco; sin embargo la flexión local en las columnas del marco producida por la carga horizontal concentrada existirá a su máxima intensidad, a menos que se proporcione una armadura horizontal a cada lado de la trabe-carril, cuyo paralte sea igual a la distancia entre dicha trabe y los patios exteriores de las columnas.

El efecto de restricción del desplazamiento lateral del marco transversal en consideración puede cuantificarse y tomarse en cuenta en el análisis de la siguiente forma:

Aplíquese la fuerza horizontal debida a grúa  $F_g$  al marco como si estuviera aislado y obténgase el desplazamiento lateral a nivel de cubierta  $\Delta_g$  (Fig. 33a). Aplíquese una carga unitaria al mismo marco a nivel de cubierta y el desplazamiento que produce en dicho nivel  $\Delta_1$  (Fig. 33b).

La fuerza horizontal  $F_h$  aplicada a nivel de cubierta que produciría el mismo desplazamiento horizontal en la cubierta que el desplazamiento de la fuerza de grúa es:

$$F_h = \frac{\Delta_g}{\Delta_1} \times 1$$

Esta fuerza  $F_h$  es la que se aplica al modelo del diafragma para obtener el porcentaje de fuerza que absorbe el marco en consideración  $\alpha_i$  (Análogo a la sección 6.2.1). Para la obtención de  $\alpha_i$  se puede hacer uso de la Fig. 26, (Fig. 33c).

El análisis definitivo del marco se hace aplicando las fuerzas actuantes  $F_g$ , y una fuerza horizontal de restricción en dirección contraria a la del desplazamiento  $\Delta_g$ , con valor  $(1 - \alpha_i)F_h$ . Esta última fuerza es la que todos los otros marcos paralelos al marco en consideración absorben.

## Procedimiento para el análisis de naves industriales.

A continuación se describe un procedimiento racional y pseudooptimizado de naves industriales. La filosofía básica consiste en considerar y hacer uso del comportamiento tridimensional de la estructura por medio de artificios que permiten reducir el análisis tridimensional a una serie de análisis de estructuras planas. El análisis de la cubierta considerada como diafragma flexible, permite que se efectúe el análisis de los marcos transversales como parte integral de la estructura y no en forma independiente como se ha hecho tradicionalmente.

El objetivo básico es el diseñar todos los marcos transversales para los elementos mecánicos producidos por las cargas gravitacionales únicamente, y permitir que absorban una carga lateral tal que únicamente produzca un sobre-esfuerzo del 33%. La diferencia entre la carga lateral total y la que absorben todos los marcos intermedios con el criterio descrito, se considera que es la carga que deben absorber los dos marcos exteriores o cabecera.

La transmisión del exceso de carga lateral de los marcos transversales intermedios a los dos cabecera se hace por medio del diafragma en la cubierta. Los marcos cabecera deberán estar contraventeados para forzar su diferencia de rigidez lateral con respecto a los marcos intermedios, y al mismo tiempo, para que puedan absorber dicha carga lateral mayor.

A continuación se describe la secuela de análisis y diseño del procedimiento propuesto:

- Proponer un contraventeo preliminar en la cubierta, determinar la rigidez de la cubierta como diafragma flexible ( $K_d$ ).
- Efectuar el estudio de compatibilidad de desplazamientos laterales producidos por grúa como se describe en las secciones 6.2.1 y 6.2.2 para definir las fuerzas de restricción correctivas.
- Analizar y diseñar los marcos intermedios transversales para cargas gravitacionales y de grúa, así como determinar su rigidez lateral ( $K_{mi}$ ). Las cargas de grúa que se deben considerar son las propias más las correctivas de restricción descritas en el paso b.

- Evaluar la carga horizontal total debida a sismo y la debida a viento ( $P_t$ ).
- Calcular la carga horizontal en los marcos transversales intermedios que produciría un sobre-esfuerzo del 33% en sus elementos ( $P_{33}$ ).
- Evaluar la carga horizontal que deben resistir los marcos exteriores o cabecera ( $P_e$ ) se tendrá:

$$M_i P_{33} + 2P_e = P_t$$

despejando  $P_e$ :

$$P_e = \frac{P_t - M_i P_{33}}{2}$$

donde:

$$M_i = \text{Número de marcos intermedios.}$$

Entonces, cada marco exterior deberá absorber:

$$\%CA = \frac{P_e}{P_t}$$

- Hacer el análisis y diseño preliminar de los marcos cabecera, incluyendo su contraventeo, necesarios para absorber  $P_e$ , así como su rigidez lateral  $K_{me}$ .
- Revisar el contraventeo de la cubierta de manera que se garantice la transmisión de  $\%CA$  a los marcos cabecera.

Con relación  $K_{me}/K_{mi}$  conocida, y para el  $\%CA$  necesario, determinar  $K_d/K_{mi}$  de las Figuras 19 & 20, o su interpolación. Conocido  $K_{mi}$  se puede determinar la rigidez del diafragma a partir de la relación  $K_d/K_{mi}$  obtenida.

Si dicha rigidez  $K_d$  difiere de la supuesta inicialmente repetir el ciclo una vez.

7. CONCLUSIONES.

El considerar los sistemas de piso de estructuras tipo industrial como diafragmas flexibles conduce a una utilización más racional de los elementos estructurales, y consecuentemente a diseños más económicos.

El proceso de análisis requiere de ciertos pasos adicionales, que incluye el análisis de los sistemas de piso como estructuras planas, y el forzar la compatibilidad de desplazamientos laterales de los marcos al analizarlos también como estructuras planas. Este trabajo adicional resulta rutinario con el uso de las computadoras, y a pesar del ligero incremento del costo de análisis, se logran ahorros importantes en el costo de la estructura.

AGRADECIMIENTO

El autor quiere agradecer al Ingeniero Alejandro Villicaña por la elaboración numérica de los estudios paramétricos, y en especial al Doctor Fernando Rozado por su estímulo en la elaboración de este artículo así como por su revisión crítica.

8. REFERENCIAS.

1. E. Rosenblueth, L. Esteva "Folleto Complementario, Diseño Sísmico de Edificios", Ediciones Ingeniería, 1962.
2. M. Nanes, "Análisis de Marcos, Planos de Sección Constante o Variable", Programa de Computadora, Bufete Industrial.
3. A. Villicaña, "Análisis Estructural de Naves Industriales Considerando el Efecto de Diafragma Flexible", Tesis Profesional, Facultad de Ingeniería, UNAM, 1977.

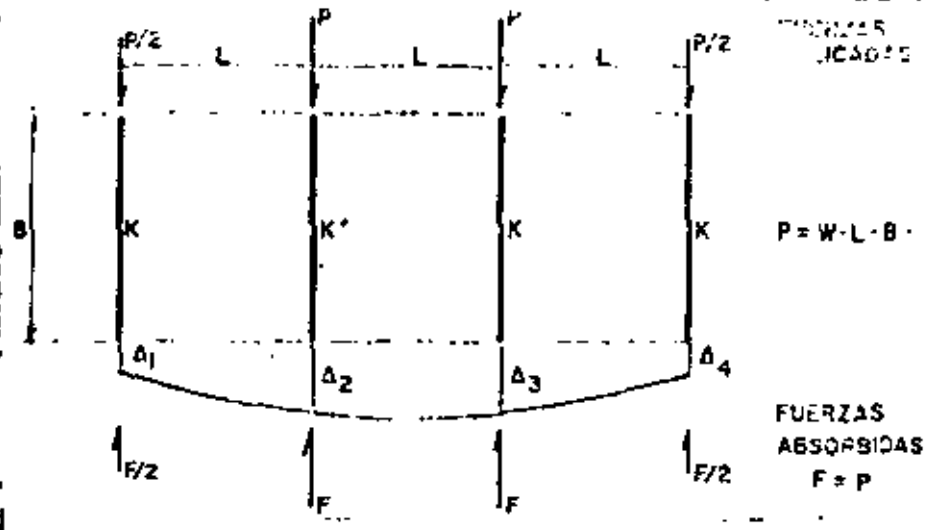


FIG. 1a — NIVEL SIN LOSA DE PISO SIN DIAFRAGMA.

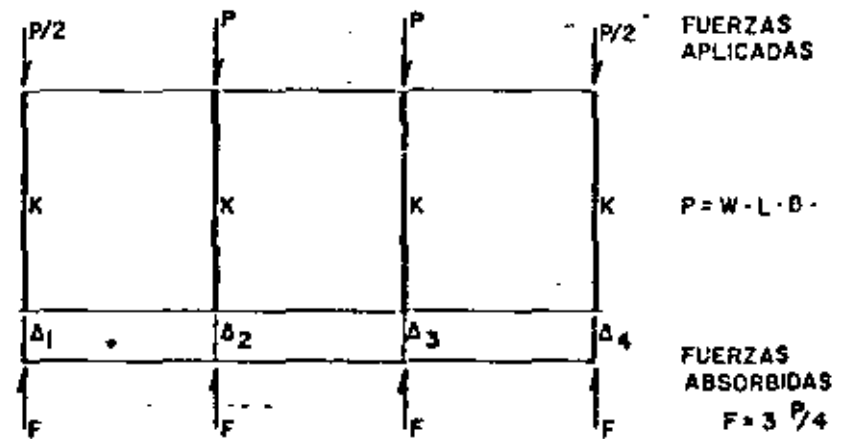


FIG. 1b — NIVEL CON DIAFRAGMA INFINITAMENTE RIGIDO SIN TORSION.

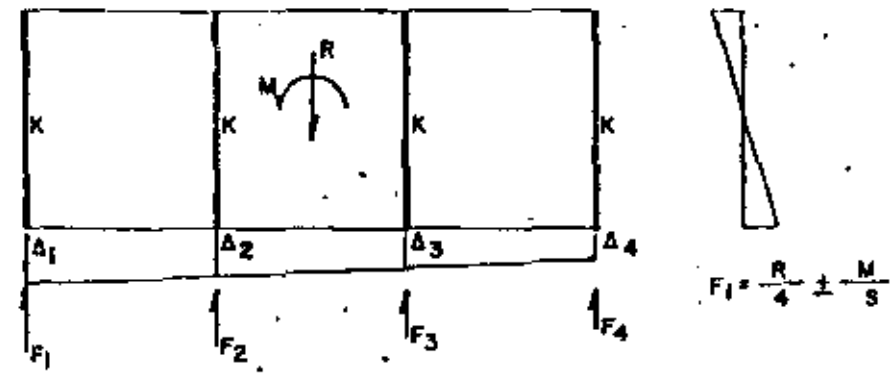
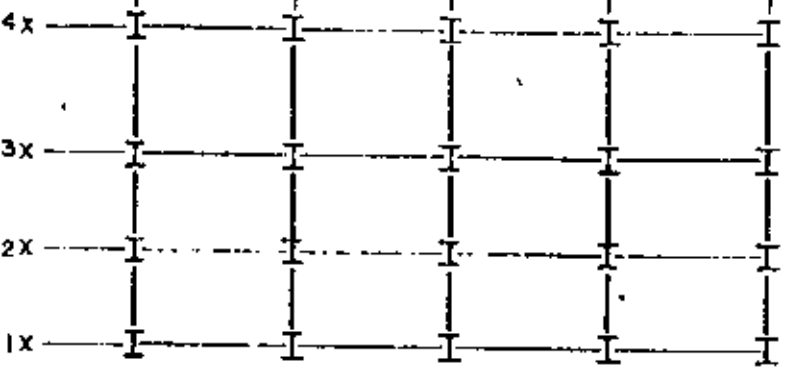
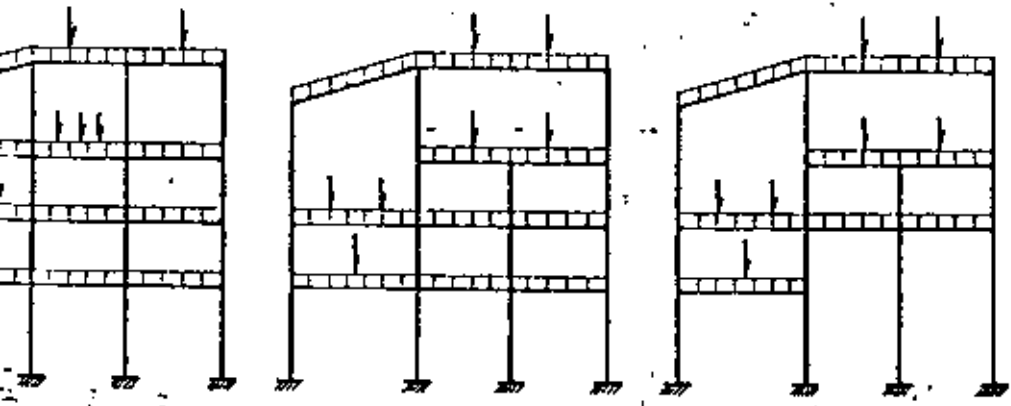


FIG. 1c — NIVEL CON DIAFRAGMA INFINITAMENTE RIGIDO CON TORSION.

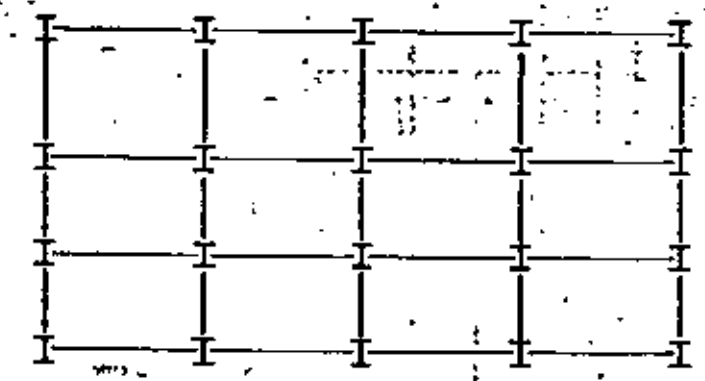


CASO.  
SIMETRIA DE  
CARGAS, SIN  
TORSION CON  
DIAFRAGMA RIGI-  
-DO.

PLANTA



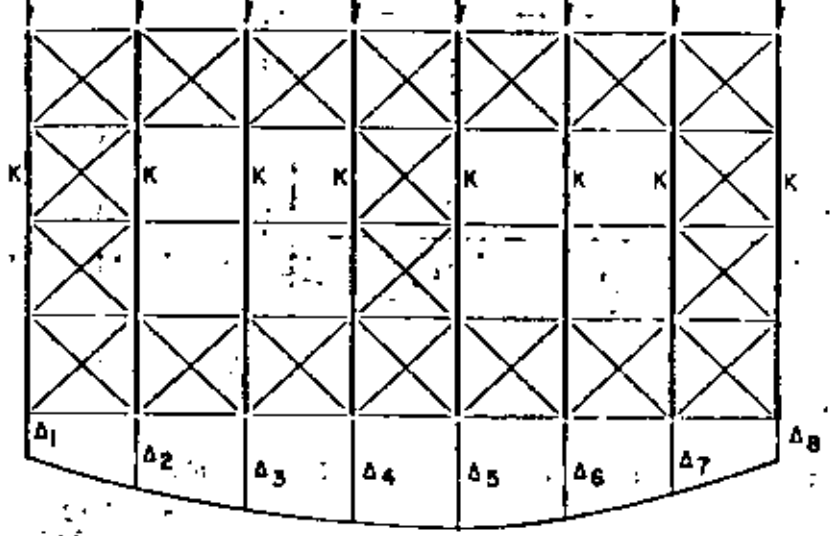
ELEVACIONES DE MARCOS



REAL  
DE ANALISIS  
MARCOS PLANO  
AISLADOS

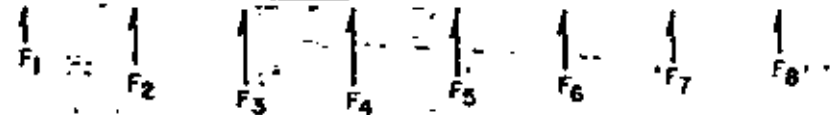
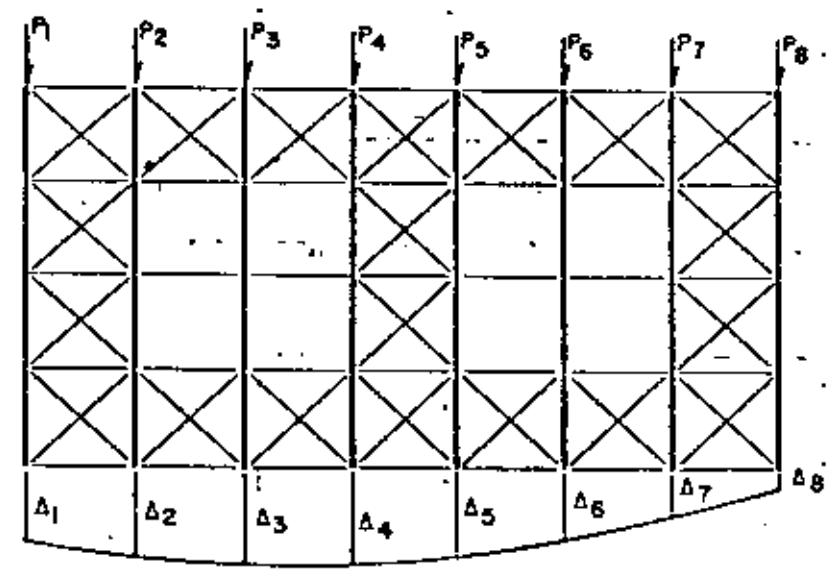
DESPLAZAMIENTOS LATERALES POR CARGAS VERTICALES.

FIG. 3



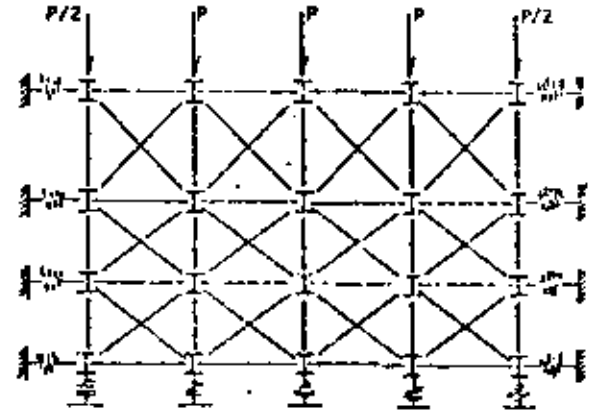
FUERZAS  
ABSORBIDAS  
 $F_i = K \cdot \Delta_i$

DIAFRAGMA FLEXIBLE CARGAS SIMETRICAS.

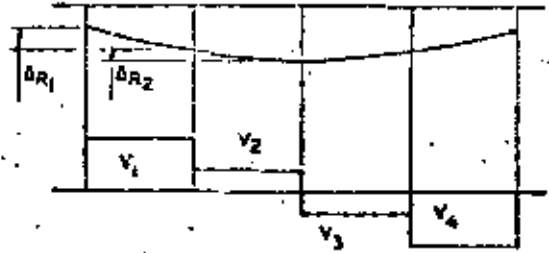


DIAFRAGMA FLEXIBLE CARGAS ASIMETRICAS

FIG. 2



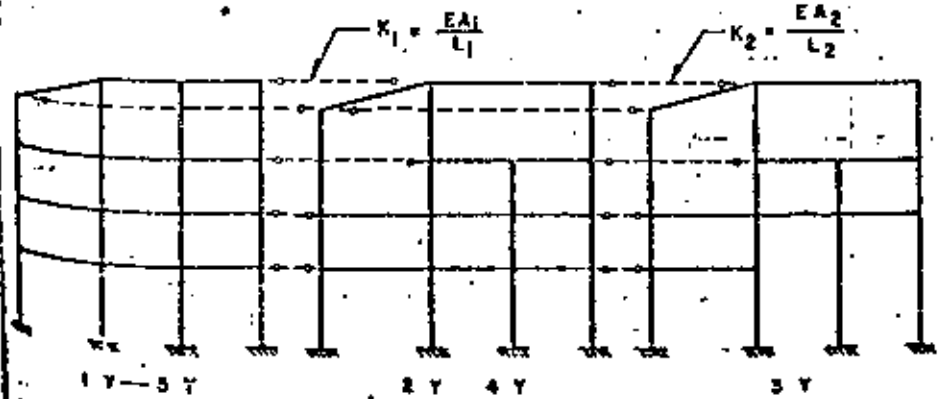
CASO:  
 DIAFRAGMA FLEXIBLE EN  
 CUBIERTA, SIN TORSION,  
 SIMETRIA DE CARGAS Y  
 GEOMETRIA.



DESPLAZAMIENTOS.  
 CUBIERTA.

CORTANTES.  
 CUBIERTA.

$$K_1 = \frac{V_1}{\Delta R_1} \quad K_2 = \frac{V_2}{\Delta R_2}$$

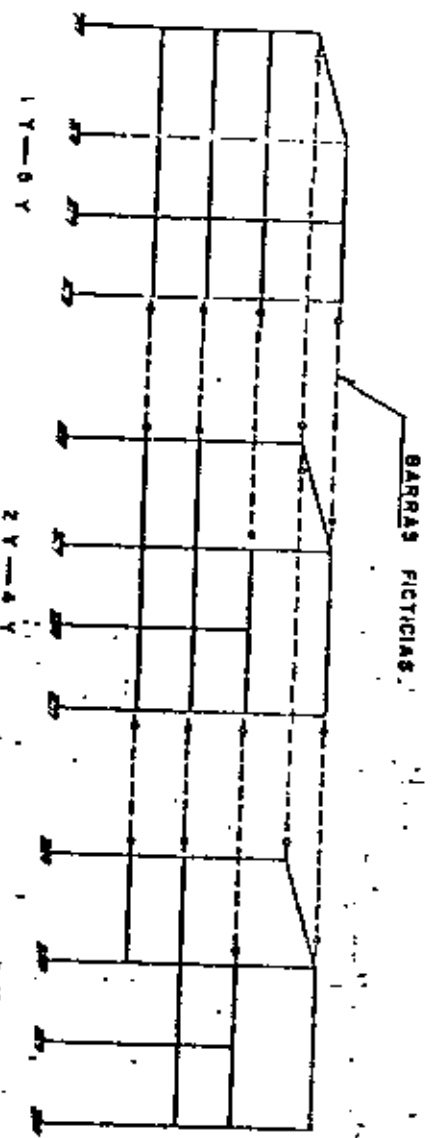


TIPOS DE MARCOS.  
 MODELO ESTRUCTURAL.

PARA LOGRAR COMPATIBILIDAD DE DESPLAZAMIENTO HORIZONTALES  
 DEBIDOS A CARGAS VERTICALES Y CARGAS HORIZONTALES.

FIG. 5

FIG. 4



BARRAS FICTICIAS:

SIMULAN EL DIAFRAGMA RIGIDO

$$\left[ \frac{EA}{L} \right] = 2 \text{ 100 VECES EL } \frac{EA}{L} \text{ DE LAS VIGAS}$$

DE

DEL NIVEL EN CONSIDERACION

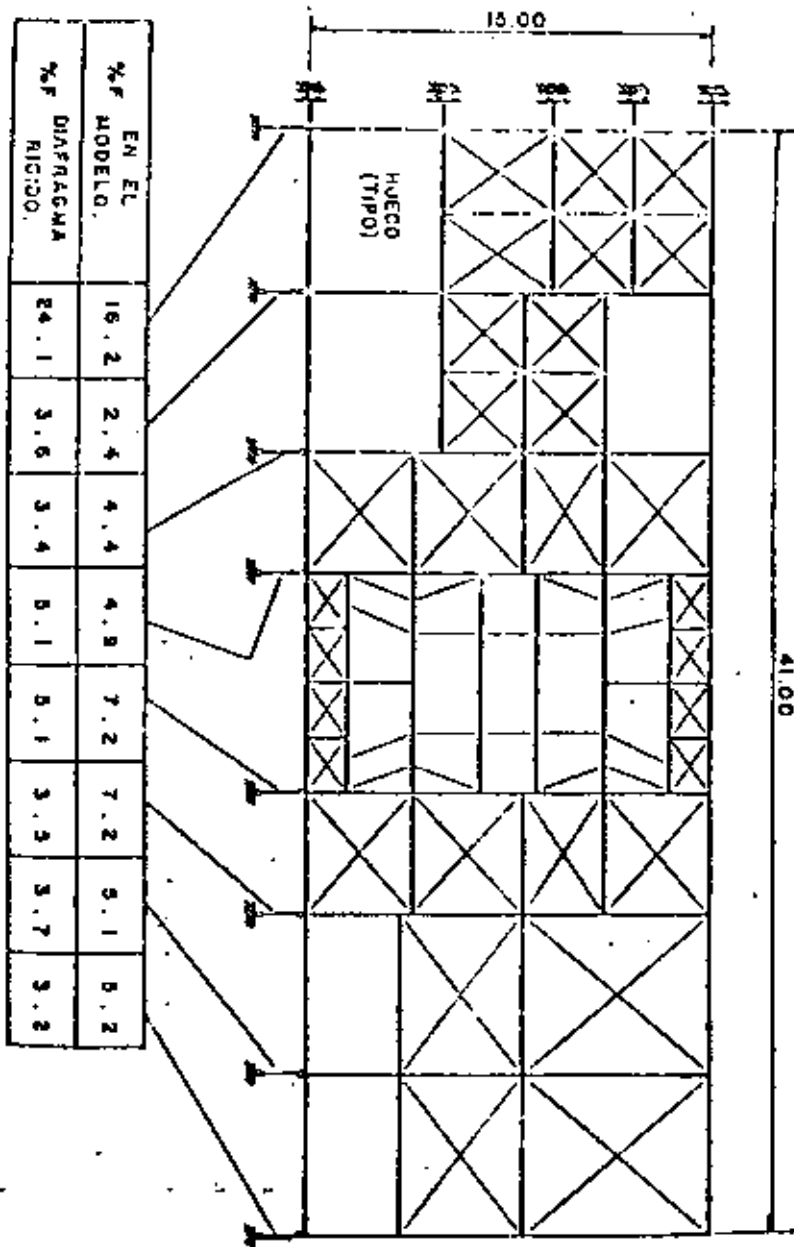
MODELO ESTRUCTURAL

PARA LOGRAR COMPATIBILIDAD DE DESPLAZAMIENTO HORIZONTALES,  
 DEBIDOS A CARGAS VERTICALES Y CARGAS HORIZONTALES

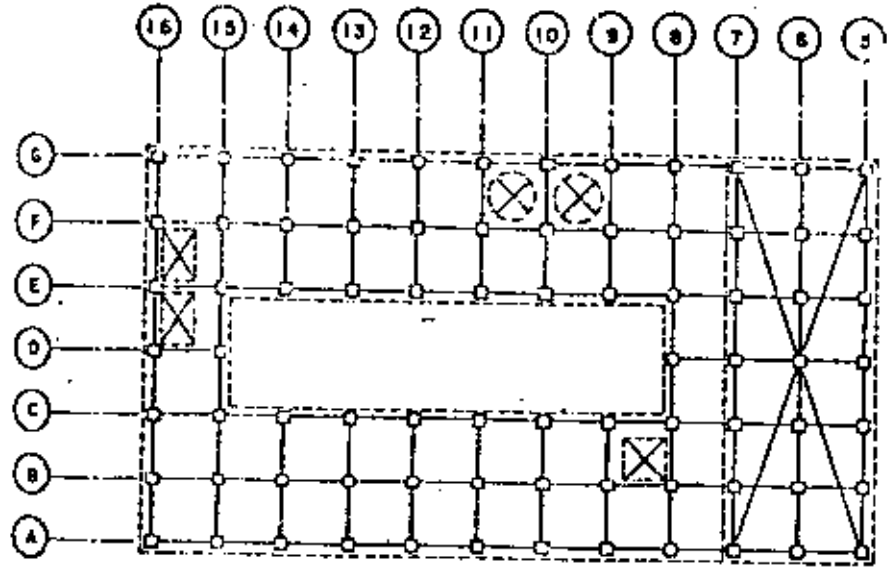
FIG. 4

CASO:  
 DIAFRAGMA RIGIDO EN CADA  
 NIVEL Y SIN TORSION,  
 SIMETRIA DE CARGAS Y GEOMETRICA.

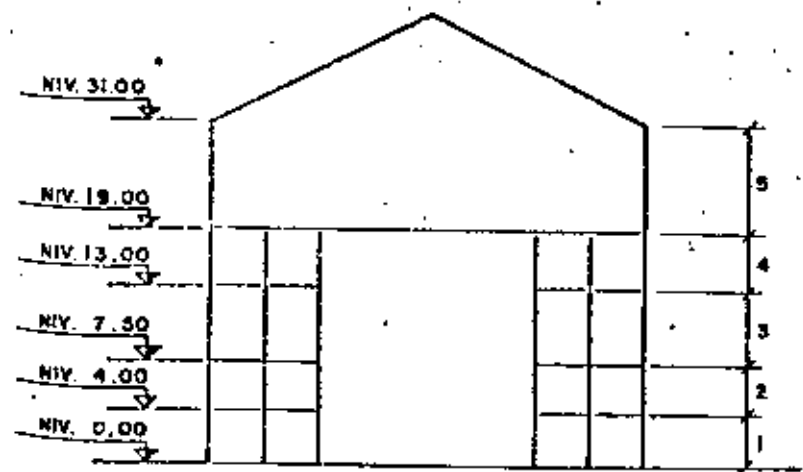




ANALISIS DE DIAFRAGMA NIV. B  
FIG. B



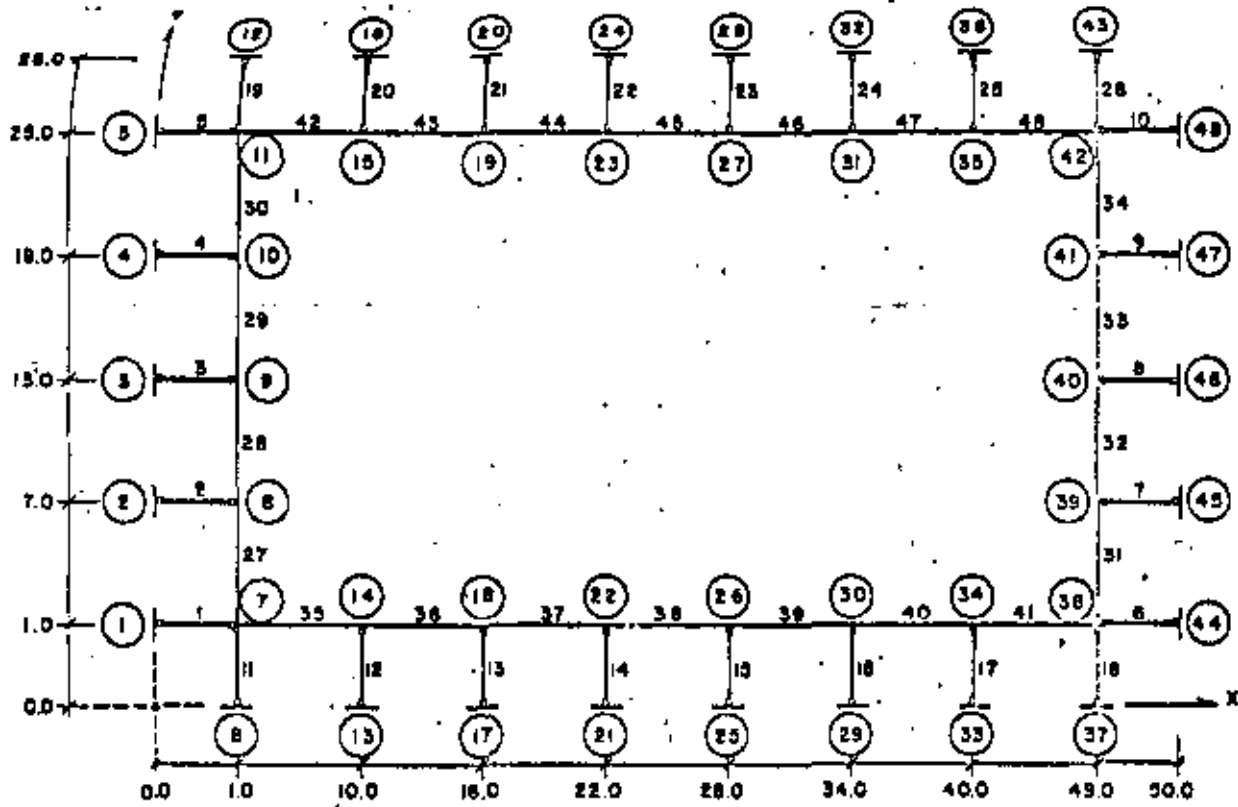
PLANTA



ELEVACION TRANSVERSAL.

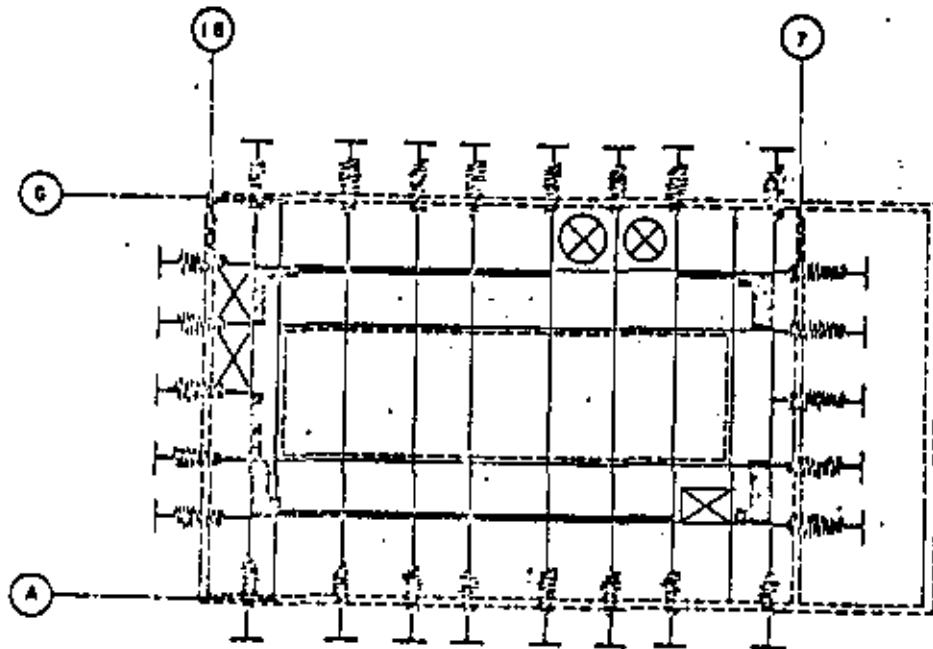
FIG. 9

105

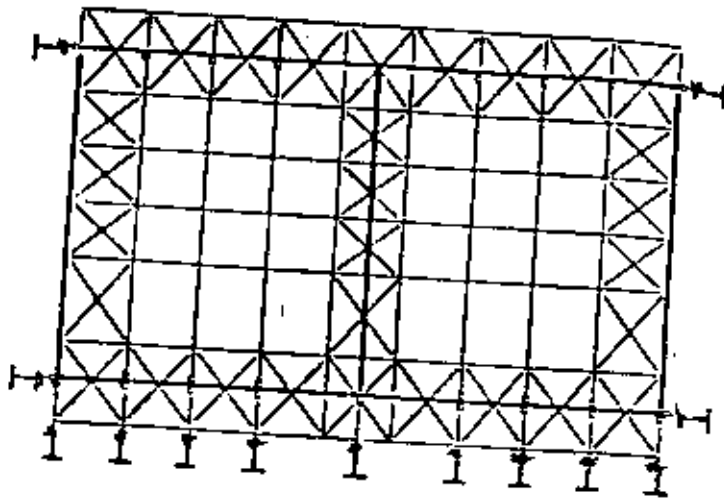


MODELO DE ANALISIS.  
FIG. II

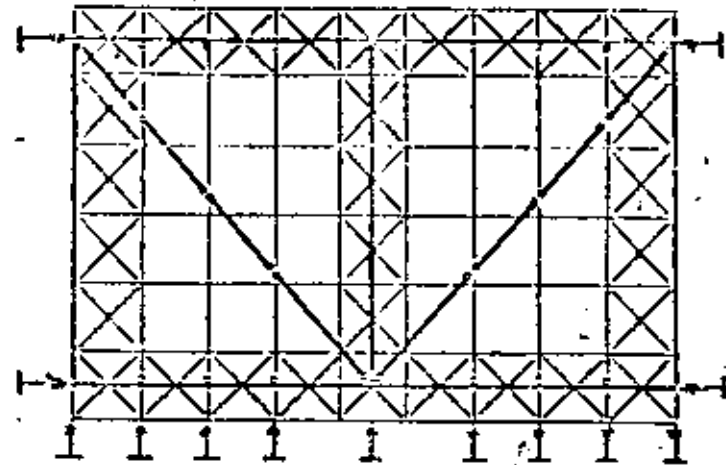
055



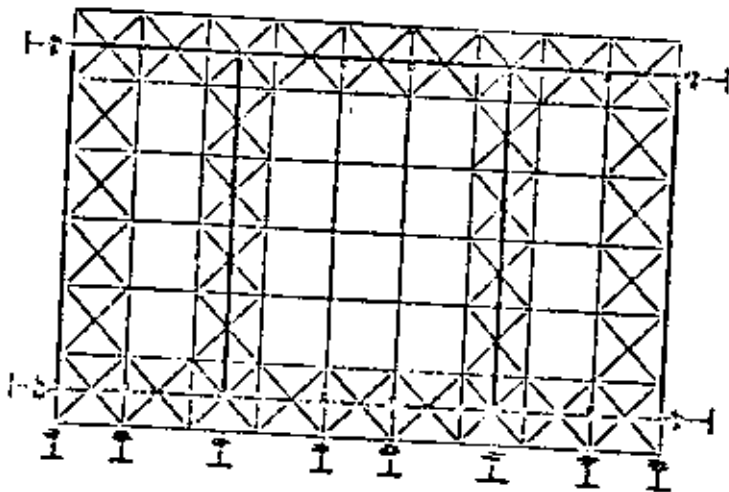
MODELO ESQUEMATICO  
FIG. 10



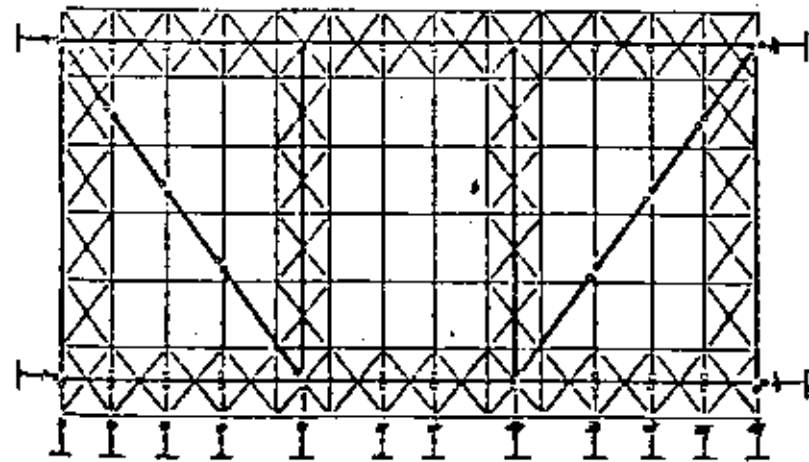
CONTRAVENTED TIPO 1



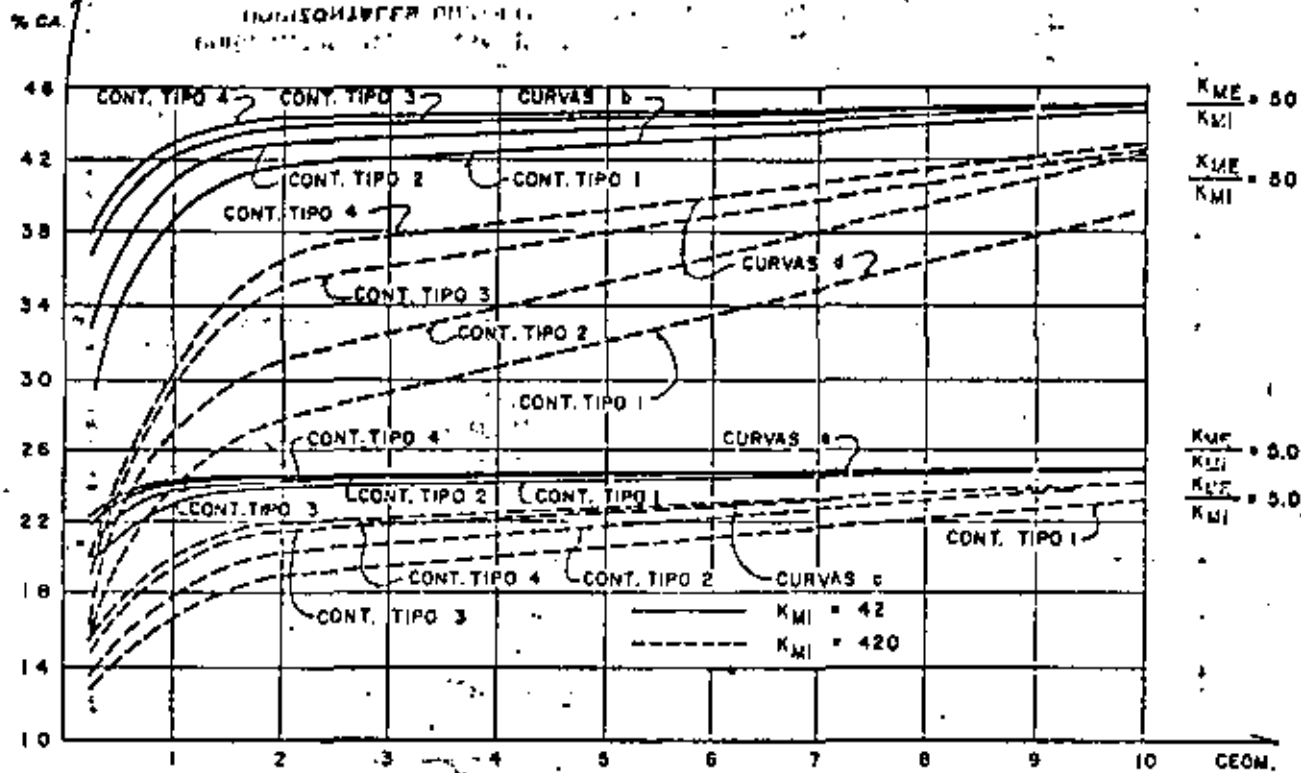
CONTRAVENTED TIPO 3



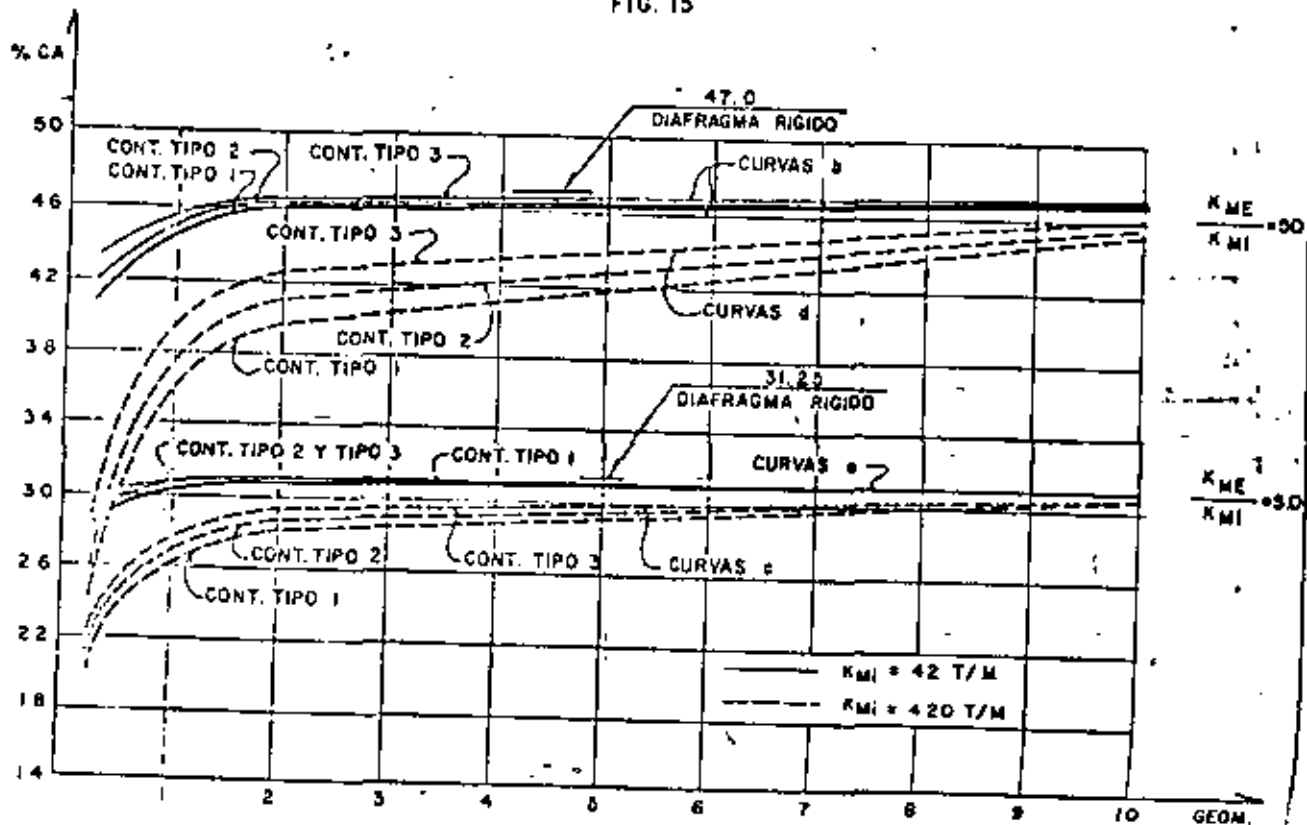
CONTRAVENTED TIPO 2  
TIPOS DE CONTRAVENTEOS  
FIG. 12



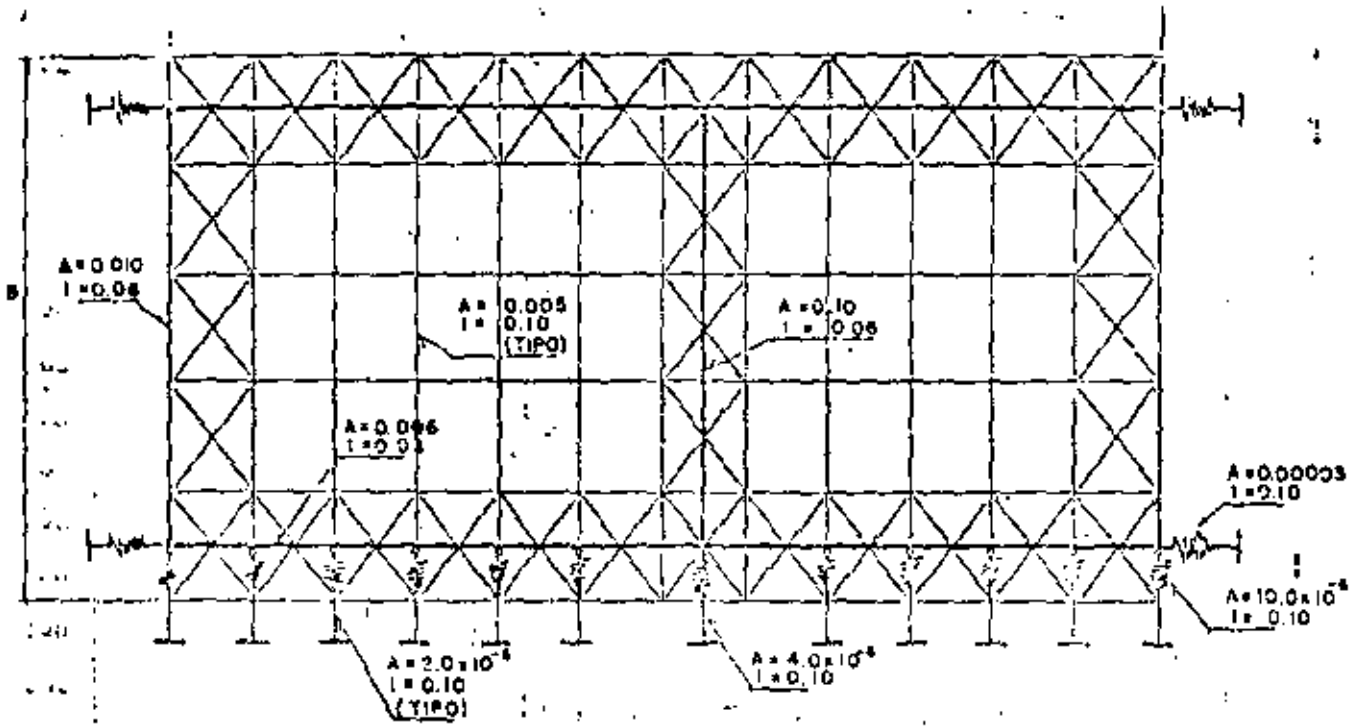
CONTRAVENTED TIPO 4  
TIPOS DE CONTRAVENTEOS  
FIG. 13



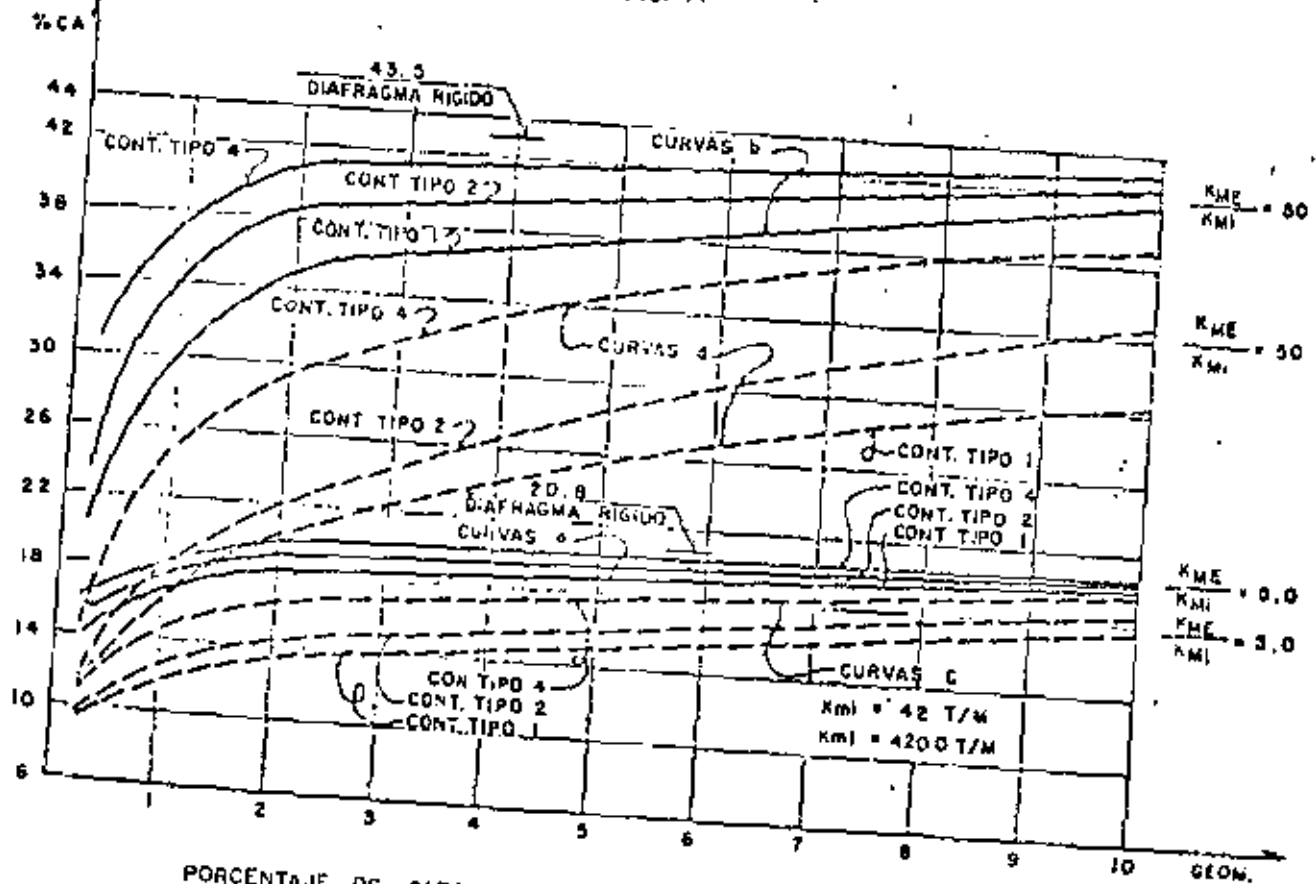
PORCENTAJE DE CARGA QUE ABSORBE EL MARCO CABECERA DEBIDO A FUERZAS HORIZONTALES UNIFORMES PARA UNA RELACION A/B=2.2  
FIG. 15



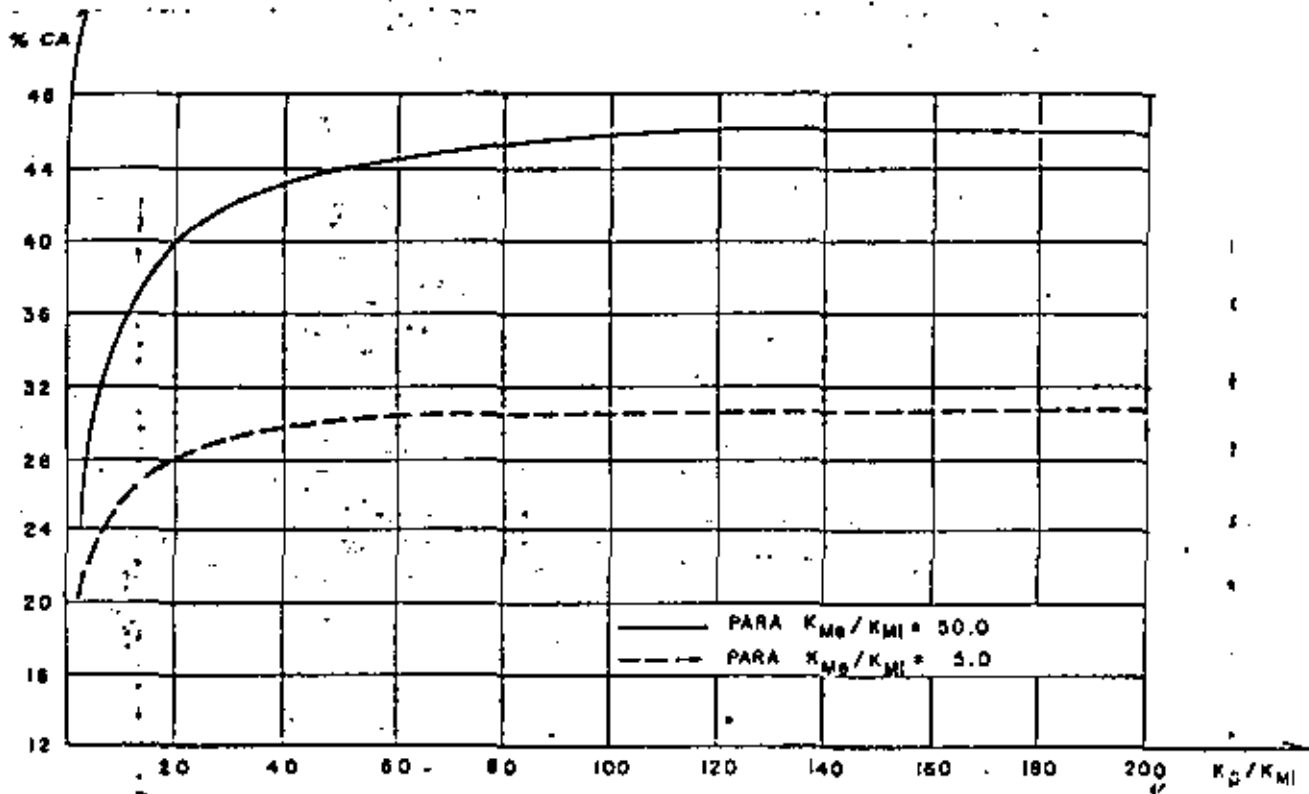
PORCENTAJE DE CARGA EN MARCO CABECERA DEBIDO A FUERZAS HORIZONTALES UNIFORMES PARA UNA RELACION A/B = 1.0  
FIG. 14



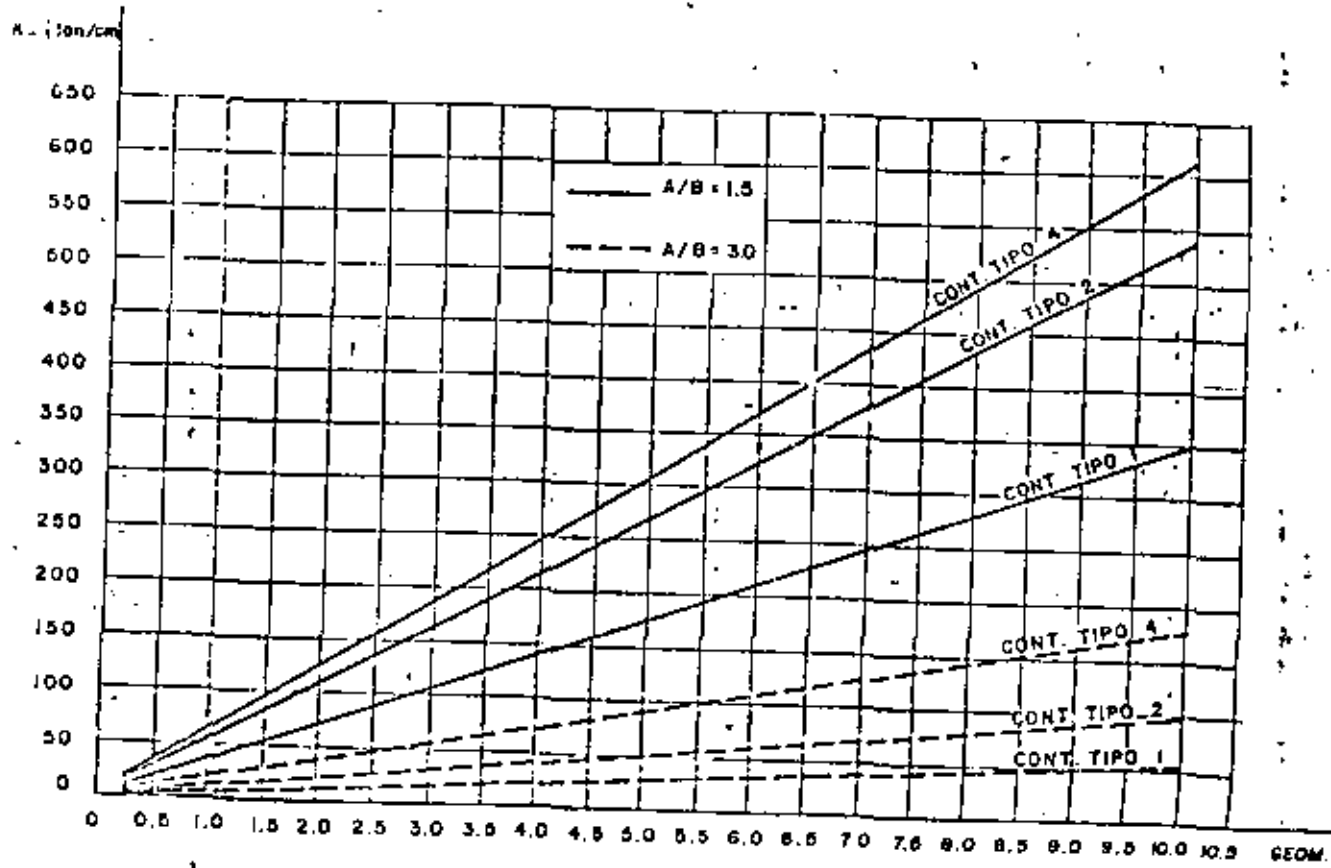
PROPIEDADES GEOMETRICAS DE PARTIDA DEL ESTUDIO PARAMETRICO.  
FIG. 17



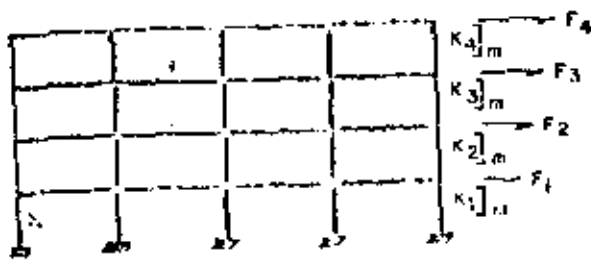
PORCENTAJE DE CARGA EN MARCO CABECERA DEBIDO A FUERZAS  
HORIZONTALES UNIFORMES PARA UNA RELACION A/B = 3.0  
FIG. 16



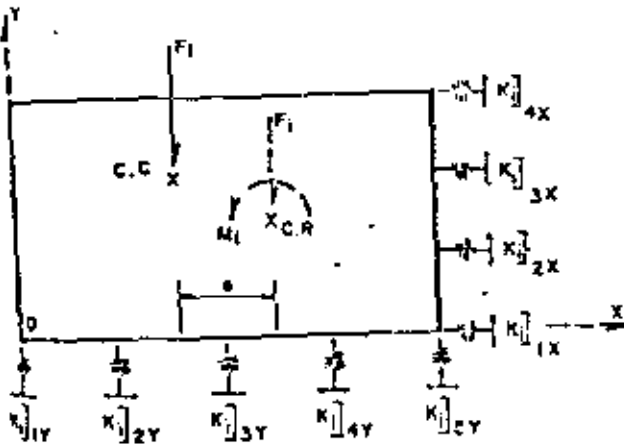
PORCENTAJE DE CARGA EN MARCO CABECERA PARA UNA RELACION  $A/B=1.5$  SEGUN RELACION DE RIGIDEZES, FIG. 19



VARIACION DE LA RIGIDEZ DE DIAFRAGMA CON RESPECTO A LA GEOMETRIA Y TIPO DE CONTRAVIENTO FIG. 20



$$F_i = CWT \frac{W_i h_i}{\sum W_i h_i}$$

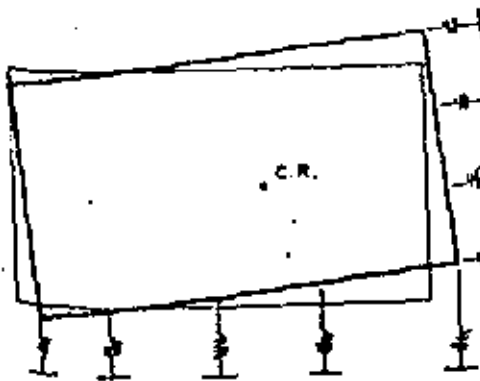


$$X_{CR} = \frac{\sum K_{ij}^y \cdot X_m}{\sum K_{ij}^y}$$

$$Y_{CR} = \frac{\sum K_{ij}^x \cdot Y_m}{\sum K_{ij}^x}$$

$$X_{CC} = \frac{\sum F_{ij}^y \cdot X}{V_x}$$

$$Y_{CC} = \frac{\sum F_{ij}^x \cdot Y}{V_y}$$

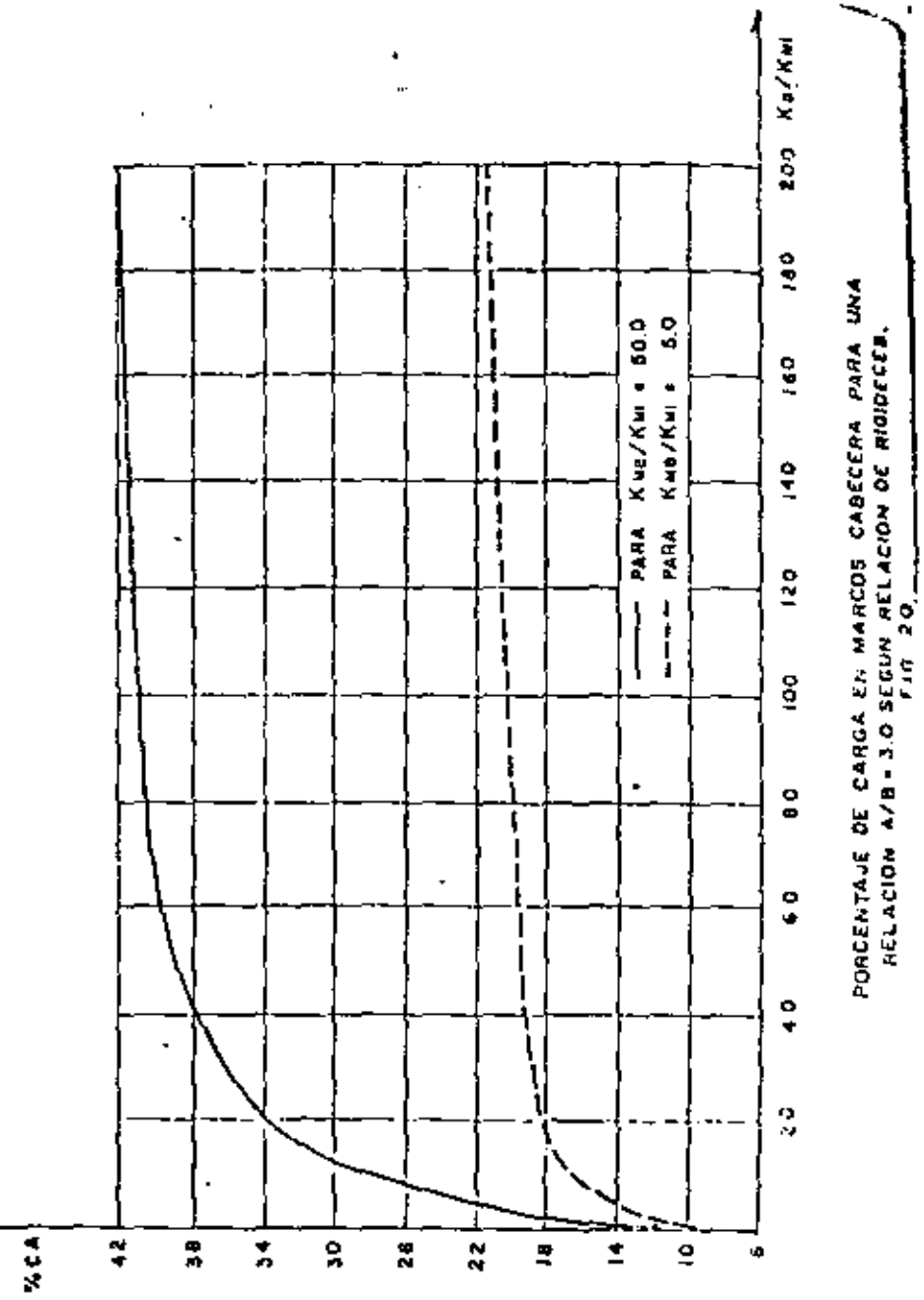


$$F_{Mx} = \frac{K_{ix} \cdot Y_{ij} + \dots}{\sum K_{ix}}$$

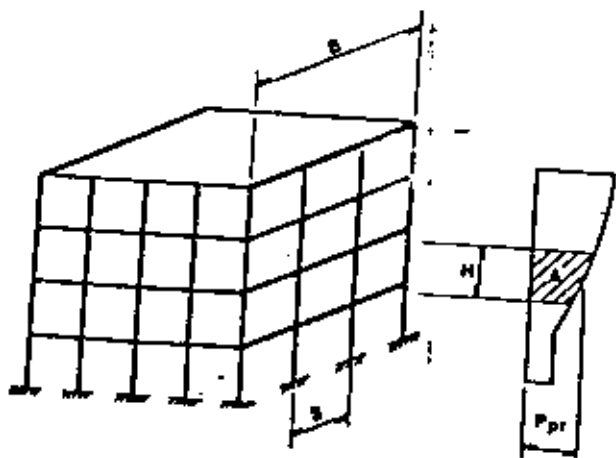
$$\frac{K_{ix} \cdot Y_{ij} \cdot M_T}{\sum K_{ix} Y_{ij} + K_{iy} \cdot X_{ij}}$$

DISTRIBUCION DE FUERZAS SISMICAS CON DIAFRAGMA RIGIDO.

FIG. 21

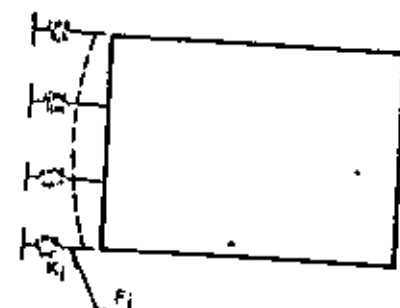


PORCENTAJE DE CARGA EN MARCOS CABECERA PARA UNA RELACION A/B = 3.0 SEGUN RELACION DE RIGIDEZ. FIG. 20

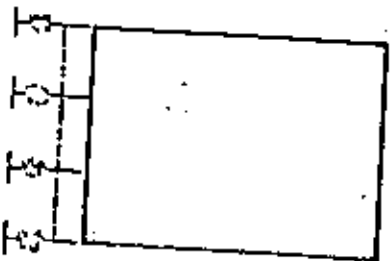


$$P = P_{pr} \cdot H \cdot B$$

$$P = A \cdot q$$



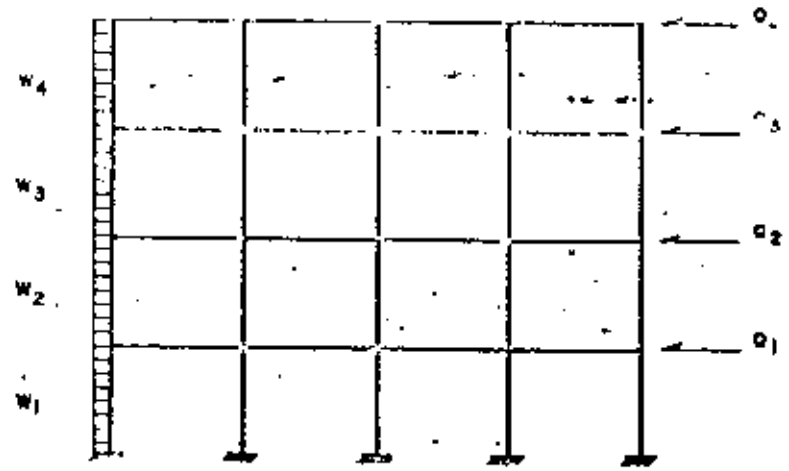
DIAFRAGMA FLEXIBLE



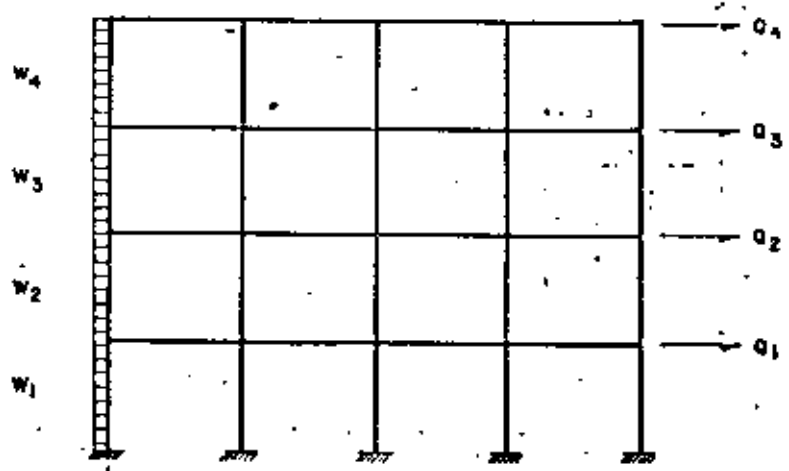
DIAFRAGMA RIGIDO.

$$F_i = \frac{K_i}{\sum K_i} P$$

DISTRIBUCION DE FUERZAS DE VIENTO.  
ANALISIS DE DIAFRAGMAS.  
FIG. 22

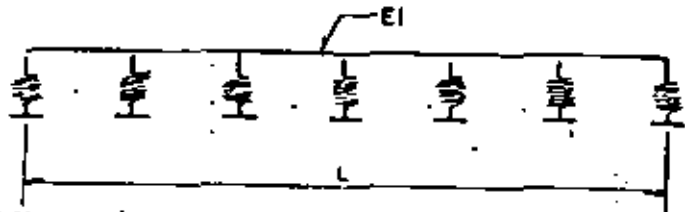


MARCO FLEXIBLE

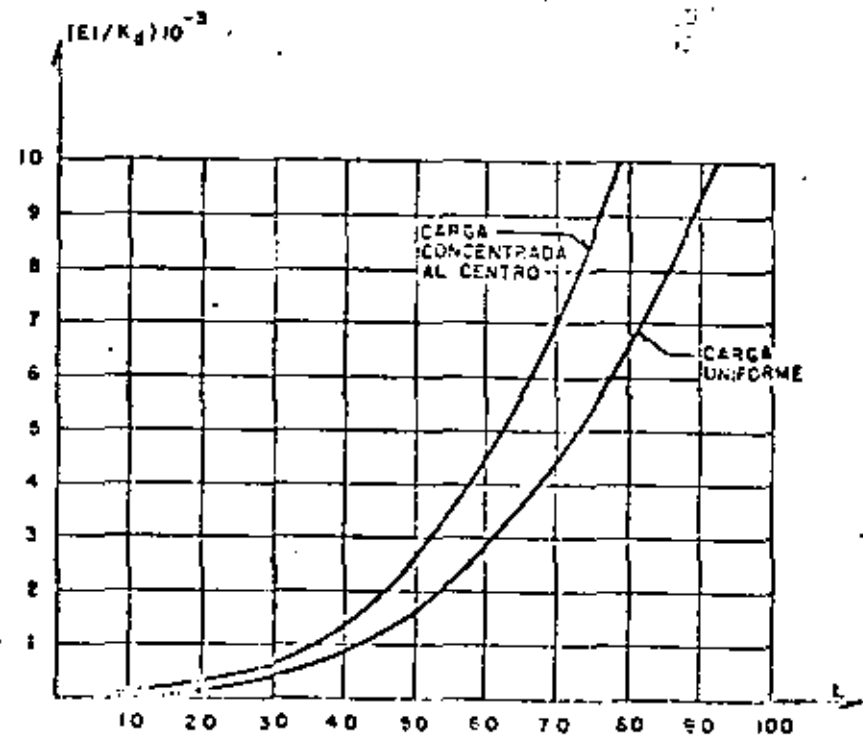


MARCO RIGIDO

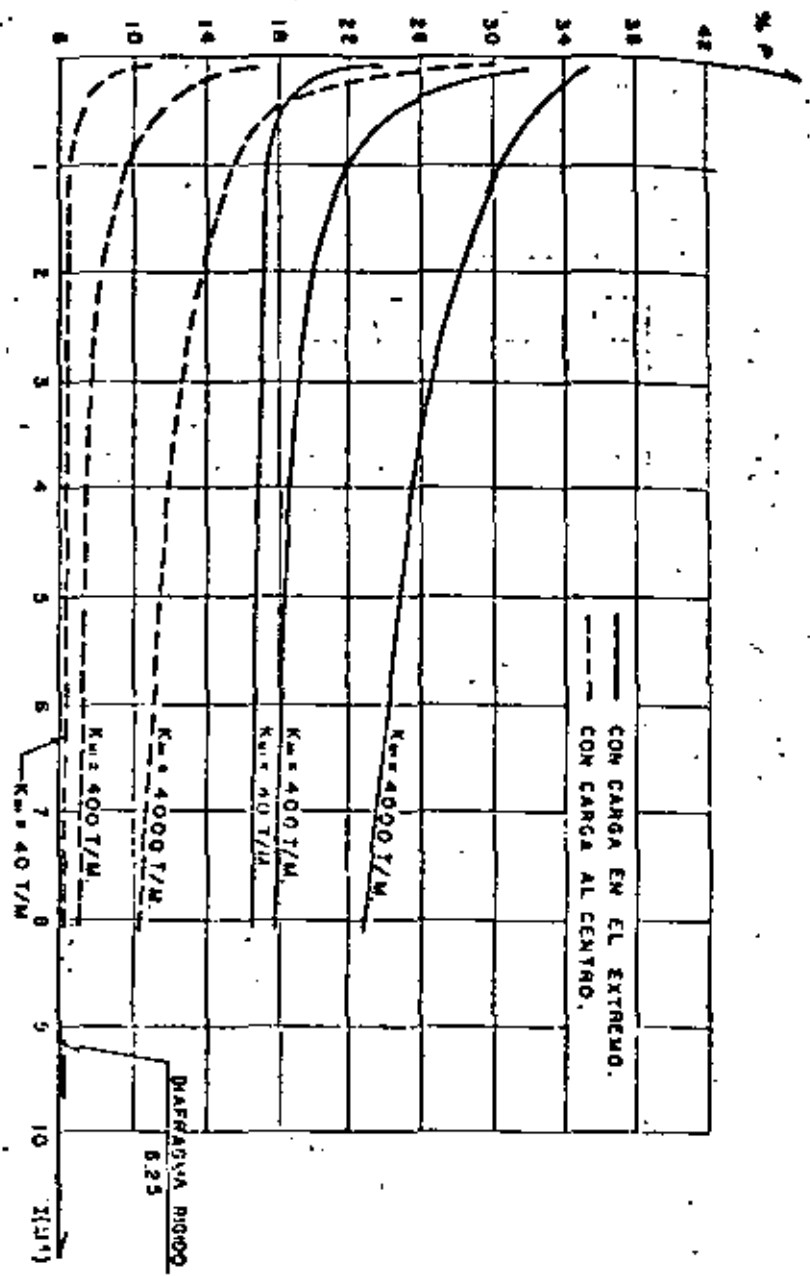
DISTRIBUCION DE FUERZAS DE VIENTO  
ANALISIS DE MARCOS  
FIG. 23



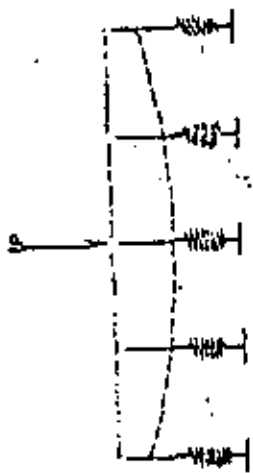
MODELO ESTRUCTURAL.



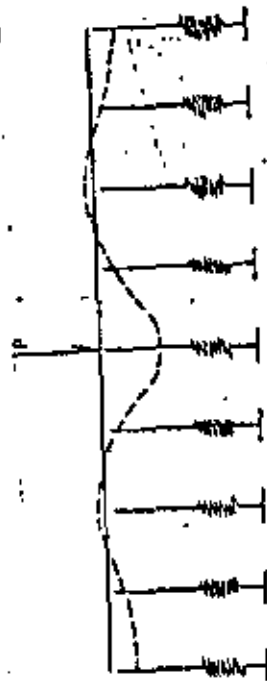
RELACION DE RIGIDEZES VIGA EQUIVALENTE A DIAFRAGMA.  
FIG. 24



PORCENTAJE DE LA CARGA CONCENTRADA QUE ABSORBE EL MARCO CARGADO.  
FIG. 25

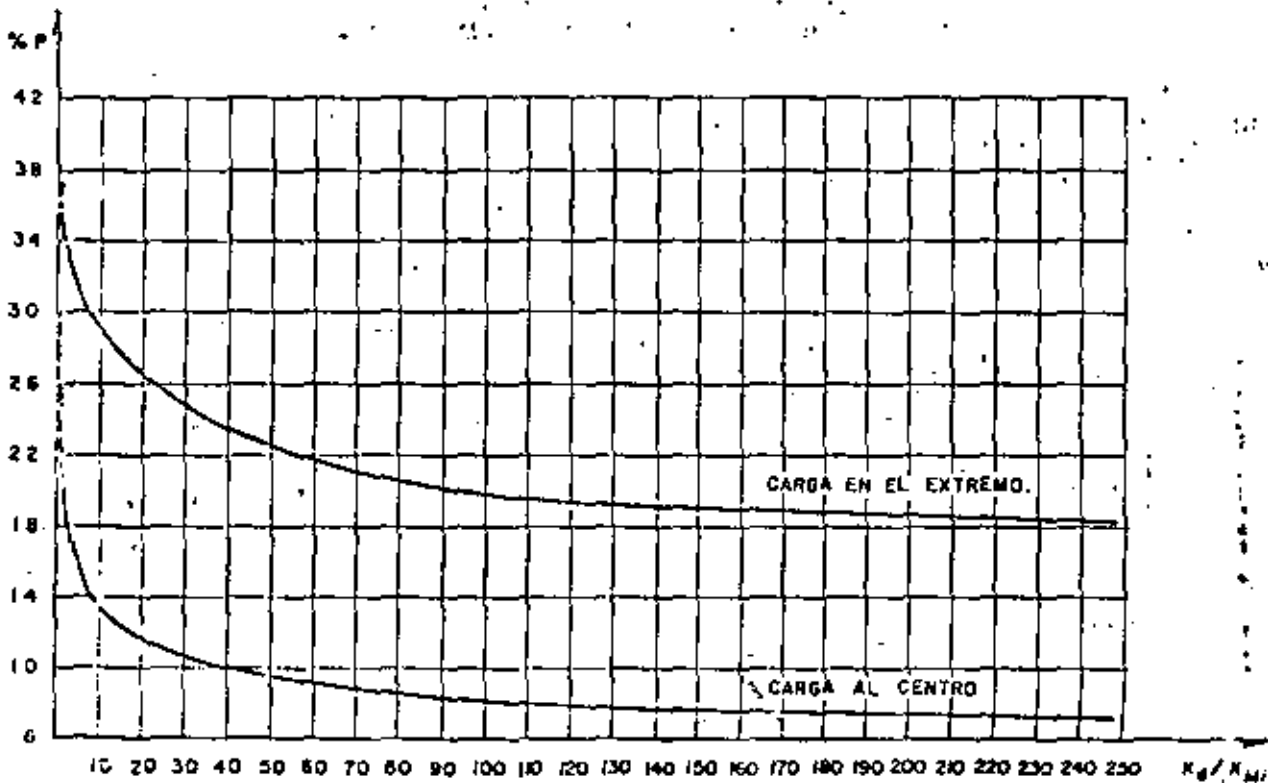


DIAPHRAGMA SEMI-RIGIDO \* FLEXIBLE  
CON POCOS MARCOS



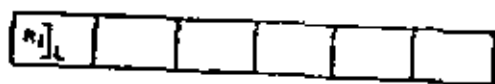
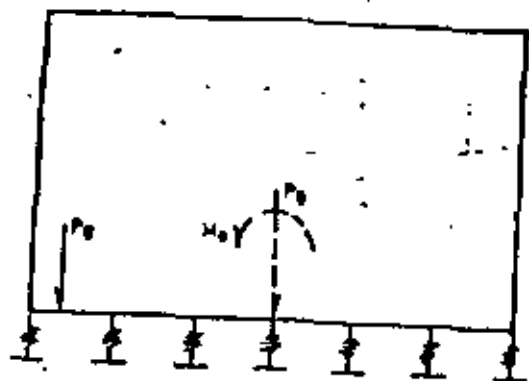
DIAPHRAGMA FLEXIBLE

CONFIGURACION DE DESPLAZAMIENTOS  
LATERALES DEL DIAPHRAGMA  
FIG. 27



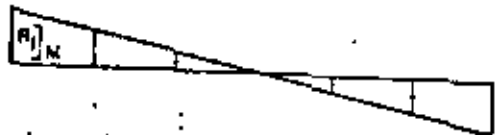
PORCENTAJE DE LA CARGA CONCENTRADA QUE ABSORBE  
EL MARCO CARGADO FINAL

FIG. 28



EFFECTO LINEAL DE  $P_0$

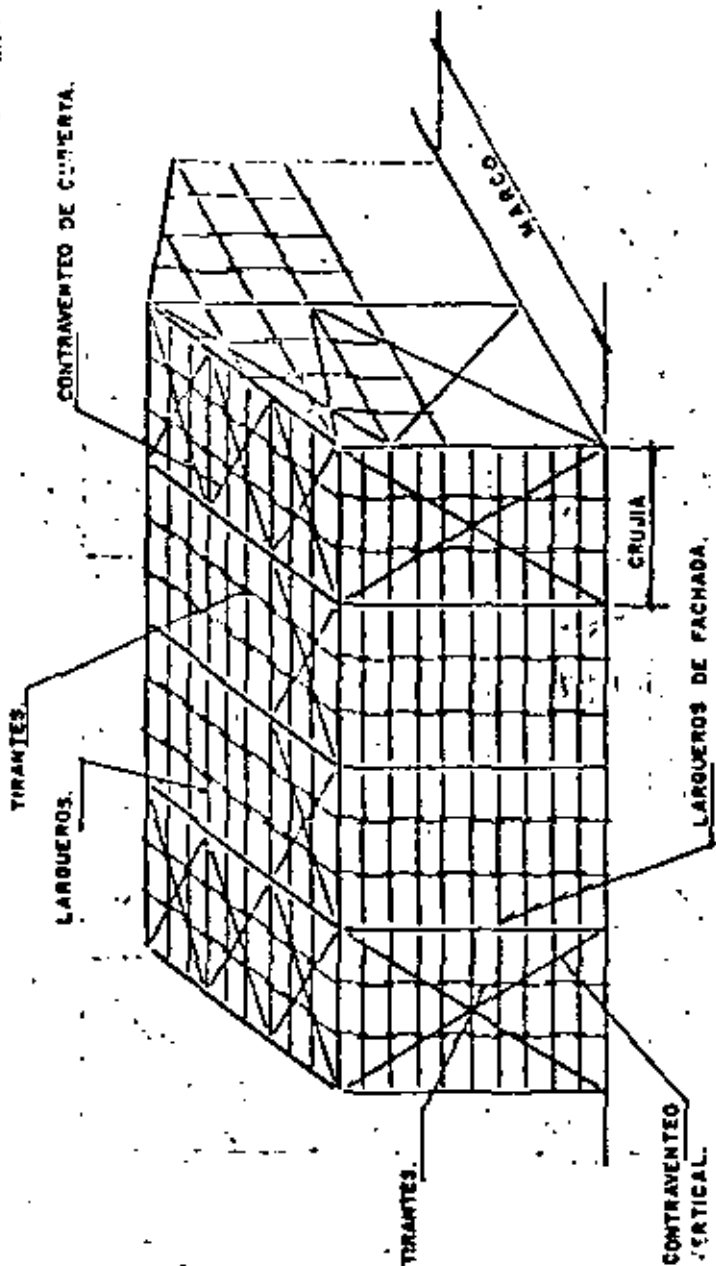
$$R_i = \frac{P_0}{5}$$



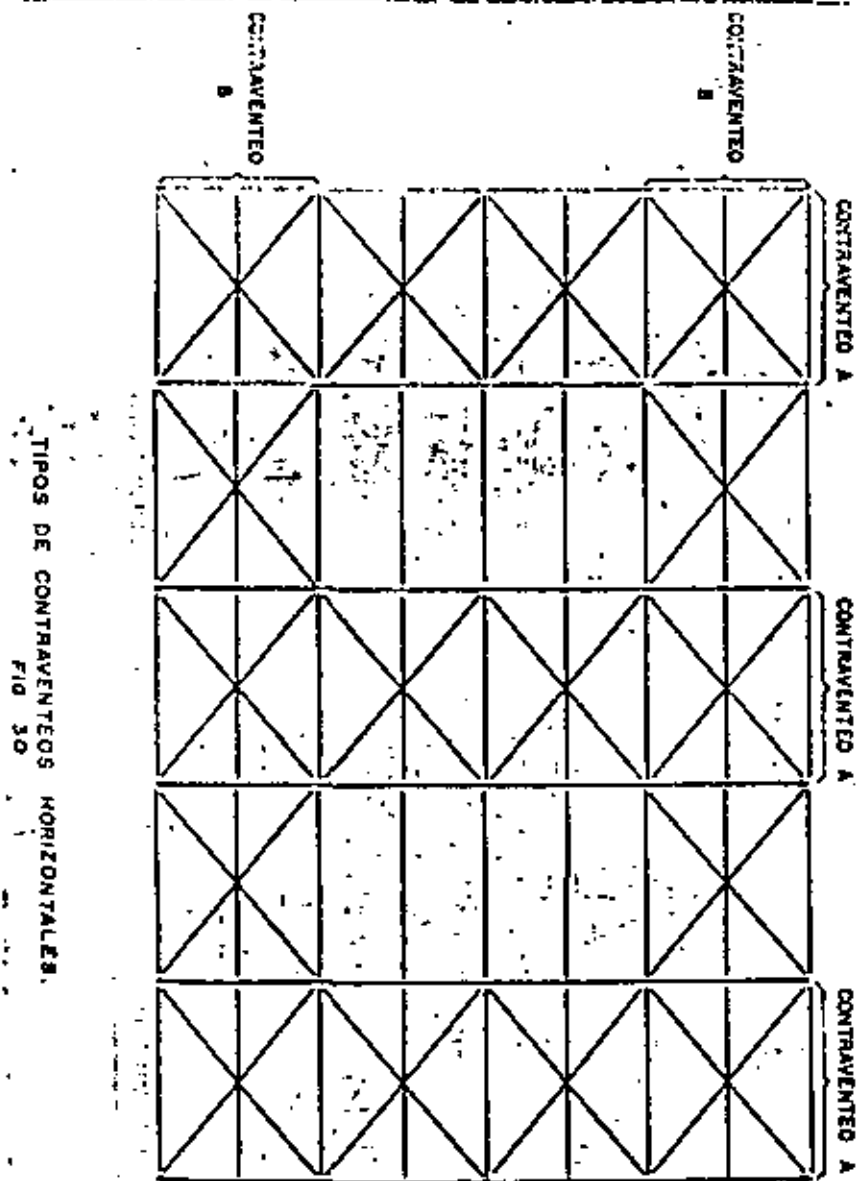
EFFECTO DE  $M_0$

VALORES DE % P EN MARCO EXTREMO			
Nº.	EFFECTOS DE M	EFFECTOS DE P	TOTAL
2	0.8 P	0.5 P	1.0 P
3	0.4 P	0.33 P	0.73 P
4	0.32 P	0.25 P	0.57 P
5	0.27 P	0.20 P	0.47 P

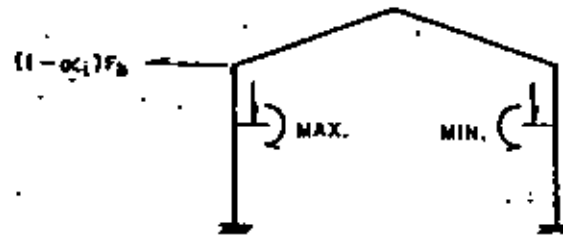
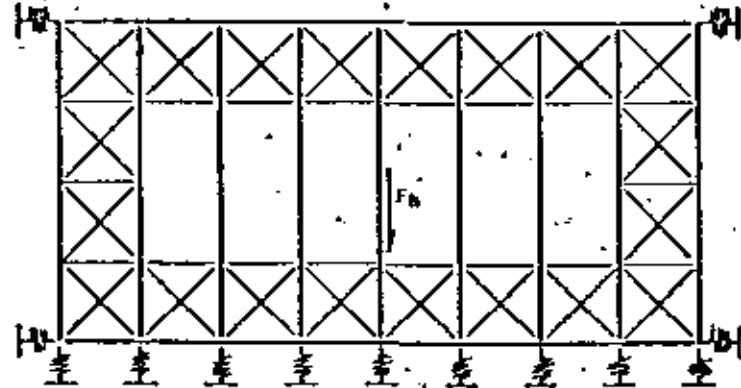
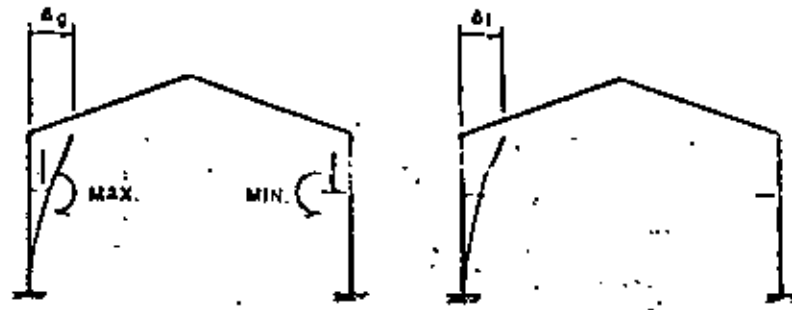
DISTRIBUCION DE FUERZA DE GRUA  
 DIAFRAGMA RIGIDO  
 FIG. 28



ESTRUCTURACION DE UNA NAVE INDUSTRIAL  
 FIG. 29

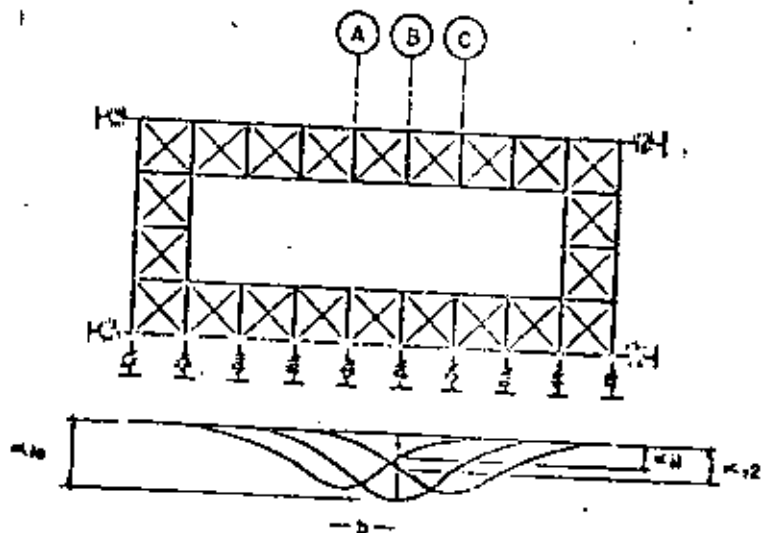
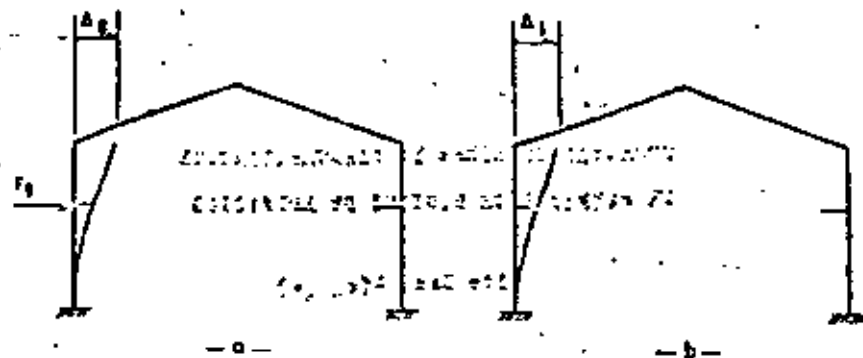
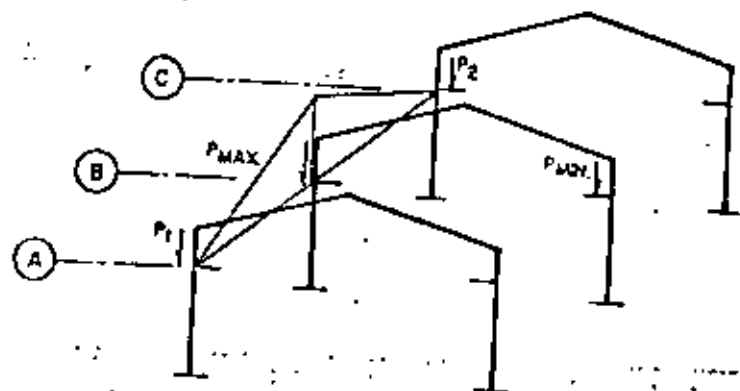


TIPOS DE CONTRAVIENTOS HORIZONTALES.  
FIG. 30



COMPATIBILIDAD DE DESPLAMIENTOS LATERALES.  
DEBIDO A CARGAS VERTICALES.

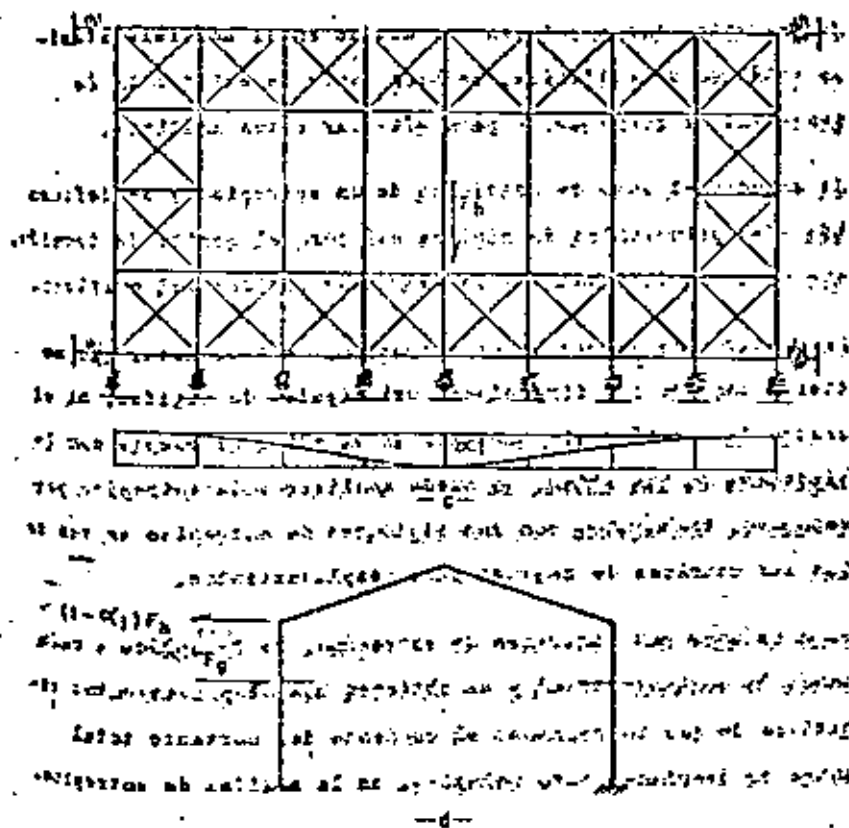
FIG. 31



$$\beta_1 = P_1 / P_{1MAX}$$

$$\alpha_1 = \alpha_{10} + \beta_1 \alpha_{11} + \beta_2 \alpha_{12}$$

EFFECTOS DE LAS DIMENSIONES REALES  
DEL PUENTE DE ERUA  
FIG. 32



COMPATIBILIDAD DE DESPLAZAMIENTOS LATERALES  
DEBIDO A CARGAS HORIZONTALES.

FIG. 33





**DIVISION DE EDUCACION CONTINUA  
FACULTAD DE INGENIERIA U.N.A.M.**

VII CURSO INTERNACIONAL DE INGENIERIA SISMICA

DISEÑO SISMICO DE ESTRUCTURAS ESPECIALES

TUBERIAS

Dr Francisco C Aguilar López de  
Nava

Agosto, 1981

## MÉTODOS ANALÍTICOS

En la Tabla I, se muestran las cargas, propiedades de los materiales y tipo de análisis estructural que es necesario considerar en el diseño de tubería y sus componentes para fallas de formaciones y cargas sobre el equipo que interconectan.

Los objetivos de llevar a cabo el análisis de flexibilidad de un Sistema de tubería son:

1. Verificar que ninguna de las componentes del sistema esté sobre esforzada en ninguna de las condiciones de carga que es posible esperar durante la vida útil del sistema.
2. Revisar que los elementos mecánicos, impuestos por la expansión de la tubería a las boquillas del equipo interconectado no sean mayores a las permisibles.

Las cargas que normalmente se consideran son:

- a) Peso propio de los componentes, líquido que conduce y aislamiento.
- b) Cambios de longitud de la tubería, debidas a cambios de temperatura.
- c) Movimientos del equipo interconectado.
- d) Viento y/o sismo.
- e) Excitaciones inducidas por el equipo interconectado.

El análisis de un sistema de tubería depende tanto de su trazo geométrico, como del tipo y localización de los soportes; sin embargo, a su vez la información para el diseño de estos elementos se obtiene como resultado del análisis, por lo que en general el procedimiento es de tipo interactivo.

Tradicionalmente el análisis estructural de sistemas de tuberías se ha denominado "Análisis de Flexibilidad de Tuberías", sin embargo, debe hacerse notar que esto se debe a que originalmente solo se utilizó el método de las flexibilidades por este tipo de cálculos; mientras que en la actualidad el método de las rigideces es la más popular.

En la referencia de J.E. Brock, se encuentra una revisión amplia sobre el análisis de sistema de tubería, incluyendo 263 referencias al respecto. En la misma referencia se presenta la historia del desarrollo de los programas de computadora en existencia, hasta 1966.

Hasta 1970, la mayoría de este tipo de análisis se hacía en comportamiento elástico lineal, considerando al sistema de tubería como un conjunto de vigas rectas y curvas, incluyendo factores de Intensificación de esfuerzos y flexibilidad para los tramos curvos.

Por lo general, no se consideraba factores de incremento de flexibilidad de otras componentes que en algunos casos pueden alterar las deformaciones de todo el sistema.

La solución analítica del problema general del análisis estructural en tres dimensiones, considerando restricciones intermedias impuestas por los diferentes tipos de apoyos, aunque básicamente es sencilla, involucra una gran cantidad de cálculos, efectuados de acuerdo a una secuencia cuidadosa, aún para configuraciones simples.

Esto motivó que se desarrollaran diversos métodos simplificados para hacer práctico el análisis de tuberías. El uso extensivo de las computadoras digitales y el desarrollo explosivo de los métodos matriciales, ha venido a facilitar el análisis elástico lineal de sistemas de tuberías, eliminando la necesidad de soluciones simplificadas.

En la actualidad, existen principalmente en Estados Unidos una multitud de programas para este fin, variando en detalles menores, tales como: máximo número de ramales, número de "loops", tipo de restricciones intermedias, etc.

Uno de los más ampliamente usados es el desarrollado por la Marina de los Estados Unidos, que se designa como M.F.C./21. El tamaño máximo de problema que puede manejar es de 99 ramales y/o 899 puntos nodales.

El tiempo de máquina empleado por elemento en una computadora IBM-7094, es de 0.05 minutos. El reporte de Griffin describe la aplicación del programa y sirve como manual del usuario. Este programa es manejado por "Los Alamos Scientific Laboratory", Los Alamos New Mexico.

Otro programa bastante utilizado es el PIPE que distribuye Argonne National Laboratory, cuyas limitaciones son 100 nodos, 20 "loops", 25 cargas externas y 10 conjuntos de propiedades de material.

El "Service Bureau Corporation" es otro organismo que proporciona servicio de análisis de flexibilidad de tuberías, el programa que ofrecen tiene la ventaja de permitir una codificación sencilla, aún para configuraciones complejas de tubería.

La mayor parte de las compañías de Ingeniería Norteamericanas, tales como Bechtel Co., C.F. Braun Co., Electric Boat Division of General Dynamics, ESSO Research and Engineering, Fluor Corporation, M.W. Dilling Co., Arthur D. Little, etc.; que se dedican a realizar Ingeniería de proyecto, tiene sus propios programas de computadora que, por lo general, utilizan únicamente en forma interna.

TABLA I

Factores involucrados en el diseño de componentes de tubería

Requerimientos de Diseño - Evitar Fallas por:

A) Ruptura debida a:

1. Carga única de corto tiempo (incluyendo fallas frágil)
2. Cargas repetidas (fatiga)
3. Carga prolongada a alta temperatura (ruptura por creep)
4. Combinaciones de las cargas anteriores

B) Deformación excesiva que conduzca a:

1. Fugas en asientos de válvulas
2. Atascamiento de mecanismos de válvulas
3. Fugas en juntas bridadas

C) Cargas excesivas en equipo conectado que produzcan:

1. Ruptura del equipo
2. Sobrecarga en chumaceras de equipo rotatorio
3. Desalineamiento y modificaciones a los ejes libres de partes rotatorias con posible daño a ellas.

Cargas

1. Presiones internas (operación y prueba)
2. Fuerzas de expansión térmica
3. Peso propio y del fluido
4. Gradientes térmicos
5. Vibración forzada (viento, sismo o equipo rotatorio)
6. Cargas en juntas bridadas
7. Cargas concentradas (válvulas)
8. Golpe de ariete

Cont. Tabla I

Propiedades de material

1. Módulo de elasticidad
2. Relación de Poisson
3. Resistencia última
4. Esfuerzo de fluencia
5. Esfuerzo de "creep"
6. Resistencia por fatiga
7. Ductilidad
8. Resistencia a la ruptura bajo cargas de larga duración

## EFFECTOS DINAMICOS EN SISTEMAS DE TUBERIA

### Introducción

La intención de este capítulo es presentar un resumen de las bases de la teoría de vibraciones aplicables a sistemas de tubería para auxiliar al diseñador a lograr prácticas de diseño que minimicen la aparición de vibraciones objetables o dañinas en condiciones de operación.

Los efectos dañinos de las vibraciones normalmente no son interpretados adecuadamente, ya que han ocurrido fallas debidas a vibración que se han atribuido a otras causas; mientras que por el contrario, oscilaciones de amplitud perceptible, pero no dañinas, han dado lugar a alarmas excesivas.

Entre los efectos indeseables que debe considerar el diseñador de tubería están:

- a) Las pulsaciones de flujo que pueden producir una operación ruidosa y una turbulencia excesiva que a su vez genera mayor transferencia de calor.
- b) Daño o fuga de juntas críticas y sellos
- c) Efectos perjudiciales en equipo interconectado
- d) Corrosión, erosión
- e) Efectos psicológicos en las personas
- f) Falla por fatiga
- g) Propagación de grietas a partir de defectos en la tubería
- h) Transmisión de vibraciones a estructuras de soporte

Se ha publicado relativamente poco sobre vibración de tubería, sin embargo, hay una gama muy amplia de material general sobre vibraciones mecánicas que es directamente aplicable a las oscilaciones estructurales de tubería.

Los libros de texto de S. Timoshenko "Vibration Problems in Engineering" y de J. Den Hartog "Mechanical Vibrations" son los más conocidos por su tratamiento ingenieril de los fundamentos de las vibraciones mecánicas y estructurales.

### Definiciones

1. Período de vibración,  $T$ , (en segundos) es el tiempo que tarda un sistema en efectuar una oscilación completa.
2. Frecuencia de oscilación,  $f$ , (en ciclos por segundo) es igual al recíproco del período de vibración.
3. La frecuencia angular,  $\omega$ , (en radianes por segundo) es la frecuencia en radianes.
4. Grados de libertad es el número de cantidades independientes que definen la posición de un sistema.
5. Modo principal de vibración es la "forma" o configuración que adopta un sistema al vibrar a una frecuencia definida. El número de modos es igual al número de grados de libertad.
6. Frecuencia natural es la frecuencia menor, se conoce como fundamental.
7. Amortiguamiento es una fuerza proporcional a la velocidad de vibración que tiende a reducir las amplitudes de vibración.
8. Resonancia es la amplificación de la amplitud de vibración producida por una coincidencia entre alguna frecuencia natural  $\omega$ , y la frecuencia de excitación externa.
9. Factor de amplificación es la relación entre la máxima amplitud de vibración y la deflexión estática y es función del cociente de la frecuencia de excitación y la natural, así como del amortiguamiento.

### Fuentes de excitación

Debe distinguirse cuidadosamente entre los tres tipos de vibración existente:

- a) libre
- b) forzada
- c) autoexcitada

En vibración libre un sistema vibra sin fuerzas externas, la excitación está proporcionada por condiciones iniciales de des-

plazamiento y/o velocidad.

En vibración forzada un sistema oscila bajo la acción externa de una fuerza perturbadora periódica. Una fuente primaria de excitación puede ser el desbalanceo de maquinaria rotatoria (motores eléctricos, turbinas, compresores, bombas, etc.)

Otras fuentes de vibraciones forzadas de tubería son la variación periódica de presiones en el fluido o "pulsaciones" y la aceleración de masas en un mecanismo reciprocante.

Las vibraciones autoexcitadas son un fenómeno algo complejo, ya que el sistema vibra aún sin fuerzas externas periódicas y la vibración persiste aún en presencia de amortiguamiento, ya que su origen proviene de fuentes de energía interna.

En sistemas de tubería, la vibración de este tipo, normalmente se ha encontrado asociada a inestabilidades de flujo que, por lo general, se deben a una mala operación de equipos rotatorios interconectados.

La maquinaria rotatoria constituye la mayor fuente de vibración mecánica, debido al inevitable desbalanceo de masa que existe en las partes rotatorias del equipo, por lo que a menos que el equipo se balancee muy cuidadosamente o se apoye sobre una cimentación provista de aisladores de vibración, cabe esperar la existencia de vibraciones forzadas con frecuencia igual a la de rotación del equipo en la tubería interconectada y las estructuras cercanas.

Si la velocidad de rotación está en la cercanía de alguna frecuencia natural de la tubería, las amplitudes de vibración pueden llegar a ser muy considerables y producir fallas de la tubería o sus componentes, por lo general, a mediano y largo plazo.

Un compresor del tipo reciprocante es una fuente de variación periódica de la presión a una frecuencia igual a la velocidad de rotación, multiplicada por el número de cilindros de acción simple o por el doble del número de cilindros para acción doble.

Si esta frecuencia está cercana a la frecuencia acústica del sis-

tema de tubería conectado, aparecerán variaciones periódicas grandes de la presión, ésto se conoce como resonancia acústica, la cual puede tener efectos adversos sobre la maquinaria y la tubería.

Otra fuente de excitación periódica es la producida por el viento. Si éste incide perpendicular al eje de un cilindro de diámetro  $D$  (en pies) a una velocidad constante  $U$  (pies/seg), se producen fuerzas periódicas de excitación a una frecuencia  $f$  (en ciclos/seg)

$$f = SU/D$$

en donde  $S$  es el número de Strouhal, que vale aproximadamente -- 0.18 para un cilindro.

Estas fuerzas aerodinámicas son debidas a los movimientos de los vórtices de Von Karman alrededor del cilindro y actúan a 90° de la dirección del viento.

Su magnitud, por lo general, es pequeña, pero si alguna frecuencia natural se encuentra en la cercanía de esta frecuencia perturbadora, se puede producir una resonancia de la tubería.

La eliminación de las fuentes de vibración es indudablemente el método más deseable de solución de un problema de vibración, sin embargo, ésto no siempre es posible en la práctica; por lo que frecuentemente se recurre únicamente a aislar y a controlar la vibración.

Debido al número tan grande de variables y condiciones que hay que tomar en cuenta para determinar un trazo de tubería, no se recomienda que en todos los casos se efectúe un análisis dinámico detallado.

Sin embargo, se justifica emplear algún tiempo en estimar la frecuencia fundamental de una tubería o tramo de tubería en aquellos casos que la fuerza de excitación es evidente.

Una adecuada selección y espaciamento de soportes, guías y restricciones puede permitir alejar la frecuencia natural de un sis-

tema de la frecuencia de excitación, llegándose en casos en que esto no sea posible a la utilización de dispositivos especiales que amortiguen las vibraciones forzadas. Para predecir la respuesta mecánica de un sistema de tuberías se tiene que en la realidad se presentan algunas condiciones que difieren considerablemente de lo que se supone la teoría, por ejemplo:

- a) Los extremos de la tubería no están ni completamente fijos ni simplemente apoyados, sino en una condición intermedia.
- b) El diámetro de la tubería no es uniforme a lo largo de todo el desarrollo.
- c) Por lo general la tubería es continua sobre varios apoyos.
- d) Existen masas concentradas que en realidad son distribuidas porque su longitud es considerable.

Sin embargo a pesar de estas limitaciones es necesario tener conocimiento de las características de vibración de vigas de sección uniforme y definidas condiciones de apoyo en sus extremos para utilizar estos resultados como punto de partida.

En la Tabla 1 se muestra las frecuencias naturales para tuberías ideales con varias condiciones de frontera.

En la Tabla 2 se muestra como conseguir esos resultados en el caso de cargas concentradas adicionales.

CONSIDERACIONES SOBRE TÉCNICAS ANALÍTICAS Y EXPERIMENTALES

A este respecto mencionaremos que las técnicas analíticas por sí solas, aunque representan una herramienta muy valiosa tienen ciertas limitaciones

los instrumentos deben estar perfectamente calibrados, esta operación en condiciones de laboratorio es perfectamente lógica y normal, pero cuando los instrumentos tienen que viajar al campo durante su transporte pueden resultar afectados y quedar descalibrados y en campo es difícil calibrar. Por otra parte la temperatura que es el enemigo mayor de las componentes electrónicas no es controlable en el lugar donde se efectúan las mediciones o sea donde ocurren los problemas.

Suponiendo que las dificultades anteriores logren vencerse aún queda el problema de determinar qué variables medir y bajo qué condiciones hacerlo, esta consideración es muy importante ya que el análisis de los datos tiene que hacerse en laboratorio y sino se obtuvo toda la información necesaria hay que regresar al campo a obtenerla con los consiguientes retrasos de tiempo, habiendo incluso ocasiones en que no es posible repetir las condiciones en que se efectuó la primera medición con lo que crece la complejidad de la interpretación de resultados.

Es en este punto en el que las técnicas analíticas complementan a las experimentales en el sentido de que si se tiene una idea del comportamiento dinámico de una componente o sistema, las determinaciones experimentales pueden enfocarse hacia la verificación del modelo analítico o bien los puntos de medición pueden determinarse a partir de los resultados analíticos y en general puede concentrarse más el esfuerzo de la obtención de datos hacia los puntos más relevantes.

TABLA 1.- FRECUENCIAS NATURALES DE VIGAS ELASTICAS DE ACERO

tipo de viga	Factor de frecuencia	
	$\lambda_1$	$\lambda_2$
Cantiliver	3.52	22.0
Simplemente apoyada	9.87	39.5
empotrada-apoyada	15.8	50.0
empotrada-apoyada libre-libre	22.4	61.7
libre-libre	22.4	61.7

$$f_c = 223 \lambda_c (k/L^2) L$$

$k$ : radio de giro, pulgs.

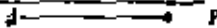
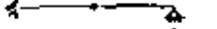
$L$ : longitud, pies

$$E = 30 \times 10^6 \text{ lb/pulg}^2 \quad J' = 0.283 \text{ lb/ pulg}^3$$

	Fuera del plano	En el plano
*L* de piernas iguales	3.74	15.4
*U* de piernas iguales	2.0	3.1



TABLA 2.- CORRECCIONES PARA CALCULO DE FRECUENCIAS NATURALES CUANDO EXISTEN CONCENTRACIONES

Tipo de viga	Factor "C"	Figura
Cantiliver	3.9	
Simplemente apoyada	2.0	
empotrada apoyada	2.3	
empotrada doble	2.7	

$$f_c = f / \sqrt{1 + c \frac{P}{W}}$$

$p$ : carga concentrada, en lb.

$W$ : peso de la viga, en lb.

$f$ : frecuencia de la viga sin carga concentrada, en  $H_z$

### CONSIDERACIONES TEORICAS

La mayor parte de los programas de computadora para análisis dinámico de sistemas de tubería, están basados en el método del elemento finito. A continuación se presenta una breve descripción de la teoría en que están basadas este tipo de herramientas.

Las ecuaciones de equilibrio dinámico para el modelo de elemento finito, pueden expresarse en forma matricial como se indica en la ecuación 1 en donde  $[M]$  es la matriz de masas,  $[C]$  es la matriz de amortiguamiento - viscoso,  $[K]$  es la matriz de rigidez,  $\{u\}$  son los desplazamientos nodales y  $F(t)$  es el vector de fuerzas externas.

En muchos programas de elemento finito, se utilizan matrices de masas concentradas mientras que en otros se utiliza la denominada matriz de masa consistente. La matriz de masas concentradas es diagonal, de manera que se despreja la inercia rotacional. La matriz de masa consistente se evalúa por un procedimiento similar al utilizado en la formulación de la matriz de rigidez. Esta matriz es simétrica no diagonal y se toma en cuenta los grados de libertad de rotación. Las características de amortiguamiento de una estructura son generalmente más difíciles de determinar que su masa o rigidez.

En la mayor parte de los casos se supone que el amortiguamiento es del tipo viscoso o sea dependiente de la velocidad, como se indica en la ecuación 1.

La matriz de rigidez puede tener distintas formas, dependiendo del tipo de análisis que se vaya a realizar. Para análisis elástico es una matriz simétrica y contiene gran cantidad de ceros.

### ANALISIS LINEAL

En este caso sólo se consideran deformaciones pequeñas y las matrices  $[M]$ ,  $[C]$ ,  $[K]$  son simétricas y poco pobladas. Estas propiedades se utilizan en la implementación de los programas de computadora para reducir los requerimientos de almacenaje.

Como en estructuras con gran número de grados de libertad se requiere demasiado tiempo de computadora para resolver problemas dinámicos, se acostumbra utilizar métodos de condensación para reducir los grados de libertad dinámico del modelo.

Los dos métodos más usados son:

- 1.- Condensación estática
- 2.- Reducción de Guyan

En el primer método se eliminan los grados de libertad asociados a masa nula de la matriz de rigidez, y se supone que no hay amortiguamiento asociado. En el segundo que se discute más en detalle, se supone que algunos grados de libertad están "esclavizados a otros" la ecuación general de movimiento puede describirse en forma particionada como se muestra en la ecuación 2, en donde  $U_1$  representa el vector de desplazamiento - nodales que se desea retener y  $U_2$  es el vector de desplazamiento correspondiente a ser eliminado. El superíndice T denota la traspuesta de la matriz o vector. El método de Guyan parte de la hipótesis de que la ecuación 2 se resuelve en conjunto o sujeta a la restricción indicada en la ecuación 3, que también se puede escribir como se indica en la ecuación 3' en donde el superíndice -1 denota la inversa de la matriz. Esto conduce al sistema de ecuaciones 4 que tiene menos grados de libertad que el original.

Los métodos de condensación generalmente trabajan adecuadamente, siempre que las masas más grandes se mantengan incluidas en el modelo reducido y los grados de libertad estén uniformemente distribuidos en toda la estructura. Para el análisis transitorio de sistemas estructurales, los métodos más utilizados son:

- 1.- Integración directa
- 2.- Super posición modal

### INTEGRACION DIRECTA

Los métodos de integración directa están basados en la integración paso a paso de las ecuaciones acopladas de movimiento, representados por las ecuaciones 1 ó 4. Generalmente estos métodos utilizan fórmulas de diferencias para expresar los desplazamientos, las velocidades y las aceleraciones nodales. Los dos grupos de métodos que se utilizan para la integración en el tiempo de las ecuaciones dinámicas, son integración implícita e integración explícita, aunque la mayor parte de los programas de elemento finito utilizan al primero. Existen gran cantidad de fórmulas para la integración de ecuaciones dinámicas, siendo las más utilizadas el método  $\beta$  de Newmark, el método  $D$  de Wilson y el método de Houbolt.

A continuación describiremos brevemente el método  $\beta$  de Newmark.

En este método los vectores de velocidad y desplazamiento en el tiempo  $t_{n+1}$  se expresan como se indican en las ecuaciones 8, en donde  $u_n$ ,  $\dot{u}_n$  y  $\ddot{u}_n$  son los vectores de desplazamiento, velocidad y aceleración respectivamente al final del  $n$ -ésimo intervalo de tiempo,  $\Delta t$  es el intervalo de tiempo,  $\beta$  es un parámetro. El valor de ese parámetro puede variar entre 1/8 y 1/4 y su selección afecta la estabilidad del método. Combinando la ecuación 1 en los tiempos  $t_{n-1}$ ,  $t_n$  y  $t_{n+1}$  con la ecuación 5 se puede obtener la ecuación 6.

Esta ecuación representa un conjunto de ecuaciones diferenciales simultáneas, que permiten obtener estados sucesivos en el tiempo a partir de un conjunto de condiciones iniciales. Una vez conocidos los desplazamientos mediante la ecuación 6, los vectores de velocidad y aceleración se obtienen mediante las ecuaciones 5. Este método es muy útil cuando se tiene comportamiento no lineal del material y/o deformaciones grandes, pero generalmente toma bastante tiempo de computadora.

#### SUPER POSICION MODAL

En este método los grados de libertad físicos del modelo estructural original, se reemplazan por sus coordenadas normales. Para lograr esto, se deben determinar primeramente las frecuencias naturales y las formas modales del modal no amortiguado, lo cual se logra extrayendo las raíces  $\lambda$  de la ecuación 7, mismas que representan los cuadrados de las frecuencias naturales. Una vez encontrados los valores característicos, la misma ecuación 7 permite obtener los vectores característicos que en este caso, representan las formas modales. Existen muchos métodos para efectuar estos cálculos, tales como: el de Givens, Householder, potencias inversas, etc.,... varios de estos métodos permiten obtener todos los valores característicos del sistema y en problemas con muchos grados de libertad, se acostumbra utilizar en combinación con procedimientos de con derivación. Otros métodos son adecuados para obtener sólo un número limitado de valores característicos. Otro procedimiento comúnmente utilizado para determinar frecuencias naturales y formas modales, es el método de matrices de transferencia o tracción, que son más adecuados para analizar estructuras tipo cadena o de conectividad simple. La base de este método consiste en encontrar la relación entre el vector de estado en el nodo  $i$  con el vector de estado en un nodo contiguo  $j$ . La relación entre ambos vectores expresada en la ecuación 8, define a la matriz de tracción  $T_j$ .

Utilizando en forma sucesiva expresiones del tipo de la ecuación 8 para todos los miembros o elementos del sistema de tubería y eliminando los vectores de estado intermedios mediante multiplicaciones matriciales, es posible expresar la relación entre el vector de estado en el primer nodo del sistema que se muestra en la ecuación 9. Aplicando las condiciones de frontera a esta ecuación, se llega a un polinomio cuya solución son los cuadrados de las frecuencias naturales del sistema. La aplicación repetida de la ecuación 9 para cada una de las estaciones una vez conocidas las frecuencias naturales, conduce a las formas y fuerzas modales.

Una vez conocidos valores y vectores de un sistema, las ecuaciones de movimiento se pueden desacoplar para lo cual, se utiliza la matriz de modos ecuación 10, en donde cada columna corresponde al vector característico  $i$ .

Como en algunos casos el número de grados de libertad retenidos en la ecuación 10, es menor que el número total de grados de libertad del sistema, es necesario introducir la transformación indicada en la ecuación 11 en donde el vector  $\{q\}$  contiene los desplazamientos generalizados denominados coordenadas normales. Sustituyendo la ecuación 11 en las ecuaciones 1 ó 4 se llega a las ecuaciones 12 y 13.

#### TRATAMIENTO DEL AMORTIGUAMIENTO

Debido a la ortogonalidad de los vectores característicos las matrices  $[M]$  y  $[K]$  son diagonales, lo que ha conducido también a que se suponga que  $[C]$  es también diagonal. Esta hipótesis es cierta si la matriz de amortiguamiento es una combinación lineal de las ecuaciones de masa y rigidez, como se indica en la ecuación 14. En este caso la ecuación 12 se puede escribir como un sistema desacoplado de  $m$  ecuaciones de tipo indicado en la ecuación 15. La solución de esta ecuación conduce a las coordenadas normales, que mediante la ecuación 11 pueden conducir a la obtención de los desplazamientos  $\{u\}$ .

Cuando la respuesta dinámica puede representarse por un número limitado de modos, es obvio que el método de superposición modal es el más económico. Esto depende del contenido de frecuencia en el vector de excitación y en las características dinámicas de estructuras, debiendo notarse que la mayor parte de tiempo de computadora se ocupa en la solución de problemas de valores característicos.

#### ANÁLISIS SISMICO

En este caso la excitación dinámica consiste en aceleraciones transmiti-

das a la estructura a través de sus puntos de apoyo, siendo usual expresar las aceleraciones absolutas como lo indica la ecuación 22 en donde  $\{a_g\}$  es el vector de aceleraciones nodales del terreno y  $\{a_r\}$  es el vector de aceleraciones nodales relativas al terreno.

Componiendo la ecuación 22 con la ecuación 1, se obtiene la ecuación 23. El vector del lado derecho de esta ecuación, representa las fuerzas de excitación inducidas por el movimiento del terreno. Esta formulación tiene la desventaja de que sólo se puede aplicar la misma aceleración del terreno, y todos los apoyos de la estructura. En cada caso de tuberías de plantas nucleares, los códigos requieren que se apliquen distintas excitaciones del terreno en cada uno de los apoyos, o también en el caso de un sistema de tuberías que este unido o apoyado en uno o varios puntos de una o más estructuras, que también están sujetas a la misma aceleración del terreno en cuyo caso, los puntos de apoyo de la tubería estarán sujetos a diferentes aceleraciones. Para esos casos las ecuaciones de movimiento se expresan más convenientemente en términos de los desplazamientos absolutos como se muestra en la ecuación 24.

La mayor parte de los programas de computadora disponibles, están basados en la formulación indicada en la ecuación 23 en parte por que es la que se utiliza en el análisis de edificios, que es de donde han derivado muchos de los programas y por ser más sencilla de programar que la ecuación 24. Además en general los movimientos del terreno se tienen en forma de aceleración, no de desplazamiento velocidad como se requiere en la ecuación 24.

En el análisis sísmico de sistemas de tuberías, se utilizan 2 métodos:

- 1).- Respuesta transitoria que consiste en obtener la historia de la respuesta de la estructura en el tiempo. Este tipo de análisis puede hacerse por superposición modal o por integración directa en el tiempo.
- 2).- Método del espectro de respuesta que utiliza los modos normales del modelo estructural, por lo tanto, restringido a comportamiento elástico lineal.

#### METODO DEL ESPECTRO DE RESPUESTA

En este método primeramente se determinan las frecuencias naturales y formas modales. Mediante las formas modales, se desacoplan las ecuaciones de movimiento y se obtienen ecuaciones de amplitud similares a las ecuaciones 15, y que pueden expresarse como se indica en la ecuación 25 en donde  $d$  es el vector de dirección nodal del sismo, cuyos componentes son números enteros que varían entre 0 y 1 y  $\{a_g\}$  es la aceleración

del terreno producido por el sismo.

La solución de las ecuaciones 25 pueden escribirse en términos de la denominada Integral Duhamel, como se indica en la ecuación 26. Esta ecuación indica que la respuesta del  $n$ -ésimo modo depende de la frecuencia natural no amortiguada, del porcentaje de amortiguamiento crítico y la aceleración del terreno.

El valor máximo de la Integral de la ecuación 26 se le llama valor espectral de la velocidad relativa al terreno, mientras que los pseudovalores de desplazamiento y aceleración relativos al suelo se definen como se indica en la ecuación 28.

Se denomina espectro de respuesta a una gráfica que muestra la respuesta máxima de desplazamiento, velocidad o aceleración, para una aceleración del terreno y un factor de amortiguamiento dados en función de la frecuencia natural de vibración. En la figura 1 se muestra un espectro de respuesta típico, obtenido de una aceleración horizontal del terreno de 1.0G (aceleración de la gravedad) se muestra en la figura 1.

De acuerdo a las ecuaciones 23 y 27 el valor máximo de la coordenada normal de desplazamiento del  $n$ -ésimo modo, esta dada por la ecuación 29.

Los valores máximos de los desplazamientos naturales reales correspondientes, se obtienen mediante la ecuación 30.

#### ESTIMACION DE LA RESPUESTA MAXIMA

Para estimar la respuesta máxima de estructura una vez encontrados los valores máximos para cada modo, pueden calcularse mediante cualquiera de los tres métodos siguientes:

- 1).- Suma de valores absolutos de los valores máximos. Este valor es conservador ya que los máximos en general, no ocurren al mismo tiempo.
- 2).- Raíz cuadrática media, en donde la respuesta máxima se obtiene como lo indica la ecuación 31, en donde  $N$  es el número de grados de libertad del sistema. Los esfuerzos y otros valores de respuesta se obtienen también mediante expresiones de raíz cuadrática media (RMS).
- 3).- Método de la Naval Research Laboratories (NRL) en el cual la respuesta pico en el nodo  $n$  se define mediante la ecuación 33, en donde el primer término es el máximo de la contribución modal  $u_{jn}$  en el nodo  $n$  y  $u_{jn}$  no se incluye en la suma del segundo término. Este método da resultados intermedios entre los 2 métodos anteriores.

$$[M]\{\ddot{u}\} + [C]\{\dot{u}\} + [K]\{u\} = \{f(t)\} \quad (1)$$

$$\begin{bmatrix} M_{11} & M_{12} \\ M_{12}^T & M_{22} \end{bmatrix} \begin{Bmatrix} \ddot{u}_1 \\ \ddot{u}_2 \end{Bmatrix} + \begin{bmatrix} C_{11} & C_{12} \\ C_{12}^T & C_{22} \end{bmatrix} \begin{Bmatrix} \dot{u}_1 \\ \dot{u}_2 \end{Bmatrix} + \begin{bmatrix} K_{11} & K_{12} \\ K_{12}^T & K_{22} \end{bmatrix} \begin{Bmatrix} u_1 \\ u_2 \end{Bmatrix} = \begin{Bmatrix} f_1(t) \\ f_2(t) \end{Bmatrix} \quad (2)$$

$$[K_{22}]\{u_2\} = [K_{12}]^T\{u_1\} \quad (3)$$

$$\{u_2\} = -[K_{22}]^{-1}[K_{12}]^T\{u_1\} = [H_{12}]\{u_1\} \quad (3')$$

$$[M_c]\{\ddot{u}\} + [C_c]\{\dot{u}\} + [K_c]\{u\} = \{f_c\} \quad (4)$$

$$[M_c] = [M_{11} + M_{12}H_{12} + H_{12}^T M_{12}^T + H_{12}^T M_{22} H_{12}]$$

$$[C_c] = [C_{11} + C_{12}H_{12} + H_{12}^T C_{12}^T + H_{12}^T C_{22} H_{12}]$$

$$[K_c] = [K_{11} + K_{12}H_{12}]$$

$$\{f_c\} = \{f_1(t)\} + [H_{12}]^T\{f_2(t)\}$$

Integracion Directa:

$$\{\ddot{u}_{n+1}\} = \{\ddot{u}\}_n + \frac{\Delta t}{2}\{\ddot{u}_n\} + \frac{\Delta t}{2}\{\ddot{u}_{n+1}\} \quad (5)$$

$$\{u_{n+1}\} = \{u_n\} + \Delta t\{\dot{u}_n\} + (1-\rho)\Delta t^2\ddot{u}_n + \rho\Delta t^2\{\ddot{u}_{n+1}\}$$

$$\begin{aligned} \left[\frac{1}{\Delta t^2}M + \frac{1}{2\Delta t}C + \rho K\right]\{u_{n+1}\} &= \rho\{f_{n+1}\} + (1-2\rho)\{f_n\} + \rho\{f_{n-1}\} \\ &+ \left[\frac{2}{\Delta t^2}M - (1-2\rho)K\right]\{u_n\} - \left[\frac{M}{\Delta t^2} - \frac{1}{2\Delta t}C + \rho K\right]\{u_{n-1}\} \end{aligned} \quad (6)$$

$$[M]\{u\} + [C]\{\dot{u}\} + [K]\{u\} = \{f(t)\} \quad (1)$$

$$\begin{bmatrix} M_{11} & M_{12} \\ M_{12}^T & M_{22} \end{bmatrix} \begin{bmatrix} u_1 \\ u_2 \end{bmatrix} + \begin{bmatrix} C_{11} & C_{12} \\ C_{12}^T & C_{22} \end{bmatrix} \begin{bmatrix} \dot{u}_1 \\ \dot{u}_2 \end{bmatrix} + \begin{bmatrix} K_{11} & K_{12} \\ K_{12}^T & K_{22} \end{bmatrix} \begin{bmatrix} u_1 \\ u_2 \end{bmatrix} = \begin{bmatrix} f_1(t) \\ f_2(t) \end{bmatrix} \quad (2)$$

$$[K_{22}]\{u_2\} = [K_{12}]^T\{u_1\} \quad (3)$$

$$\{u_2\} = -[K_{22}]^{-1} [K_{12}]^T \{u_1\} = [H_{12}]\{u_1\} \quad (3')$$

$$[M_c]\{\dot{u}\} + [C_c]\{\dot{u}\} + [K_c]\{u\} = \{f_c\} \quad (4)$$

$$[M_c] = [M_{11} + M_{12}H_{12} + H_{12}^T M_{12}^T + H_{12}^T M_{22}H_{12}]$$

$$[C_c] = [C_{11} + C_{12}H_{12} + H_{12}^T C_{12}^T + H_{12}^T C_{22}H_{12}]$$

$$[K_c] = [K_{11} + K_{12}H_{12}]$$

$$\{f_c\} = \{f_1(t)\} + [H_{12}]^T \{f_2(t)\}$$

Integración Directa:

$$\{\ddot{u}_{n+1}\} = \{\ddot{u}\}_n + \frac{\Delta t}{2} \{\dot{u}_n\} + \frac{\Delta t}{2} \{\ddot{u}_{n+1}\} \quad (5)$$

$$\{u_{n+1}\} = \{u_n\} + \Delta t \{\dot{u}_n\} + (1-\beta) \Delta t^2 \{\ddot{u}_n\} + \beta \Delta t^2 \{\ddot{u}_{n+1}\}$$

$$\begin{aligned} \left[ \frac{1}{\Delta t^2} M + \frac{1}{2\Delta t} C + \beta K \right] \{u_{n+1}\} &= \beta \{f_{n+1}\} + (1-2\beta) \{f_n\} + \beta \{f_{n-1}\} \\ &+ \left[ \frac{2}{\Delta t^2} M - (1-2\beta) K \right] \{u_n\} - \left[ \frac{M}{\Delta t^2} - \frac{1}{2\Delta t} C + \beta K \right] \{u_{n-1}\} \end{aligned} \quad (6)$$

Superposición Modal:

$$[K - \lambda M] \{u\} = \{0\} \quad (7)$$

$$\left\{ \frac{u_1}{l a_1} \right\} = [T_1] \left\{ \frac{u_1}{l a_1} \right\} \quad (8)$$

$$\left\{ \frac{u_m}{l a_m} \right\} = [T_m] \cdots [T_2] [T_1] \left\{ \frac{u_2}{l a_2} \right\} \quad (9)$$

$$[\phi] = \{ \{ \phi_1 \} \{ \phi_2 \} \cdots \{ \phi_m \} \} \quad (10)$$

$$\{u\} = [\phi] \{q\} \quad (11)$$

$$[\bar{M}] \{\ddot{q}\} + [\bar{C}] \{\dot{q}\} + [\bar{K}] \{q\} = \{\bar{f}(t)\} \quad (12)$$

$$[\bar{M}] = [\phi]^T [M] [\phi]$$

$$[\bar{C}] = [\phi]^T [C] [\phi]$$

$$[\bar{K}] = [\phi]^T [K] [\phi]$$

$$\{\bar{f}(t)\} = [\phi]^T \{f(t)\}$$

(13)

Tratamiento del Amortiguamiento

$$[C] = a_1 [M] + a_2 [K] \quad (14)$$

$$m_i \ddot{q}_i + c_i \dot{q}_i + k_i q_i = f_i(t), \quad i=1,2,\dots,m \quad (15)$$

$$\ddot{q}_i + 2\xi_i \omega_i \dot{q}_i + \omega_i^2 q_i = \frac{1}{m_i} f_i(t)$$

en donde  $\xi_i = \frac{c_i}{2m_i \omega_i}$  es la relación de amortiguamiento

y  $\omega_i$  es la frecuencia natural

## Análisis Sísmico:

$$\{\ddot{u}_a\} = \{\ddot{u}_r\} + \{\ddot{u}_g\} \quad (22)$$

$$[M]\{\ddot{u}_r\} + [C]\{\dot{u}_r\} + [K]\{u_r\} = -[M]\{\ddot{u}_g\} \quad (23)$$

$$[M]\{\ddot{u}_a\} + [C]\{\dot{u}_a\} + [K]\{u_a\} = [C]\{\dot{u}_g\} + [K]\{u_g\} \quad (24)$$

## Método del Espectro de Respuesta:

$$\ddot{q}_1 + 2 \zeta_1 \omega_1 \dot{q}_1 + \omega_1^2 q_1 = \frac{1}{m_1} \{\phi_1\}^T [M] \{\ddot{d}\} \ddot{u}_g \quad (25)$$

$$q_1(t) = \frac{\{\phi_1\}^T [M] \{\ddot{d}\}}{\omega_1 m_1} \int_0^t \ddot{u}_g(\tau) \exp[-\zeta_1 \omega_1 (t-\tau)] \sin \omega_1 (t-\tau) d\tau \quad (26)$$

$$S_{v_1} = \left[ \int_0^t \ddot{u}_g(\tau) \exp[-\zeta_1 \omega_1 (t-\tau)] \sin \omega_1 (t-\tau) d\tau \right]_{\max.} \quad (27)$$

$$S_{\phi_1} = \frac{1}{\omega_1} S_{v_1} \quad (28)$$

$$S_{\phi_1} = \omega_1 S_{v_1}$$

$$q_1 \Big|_{\max.} = \frac{\{\phi_1\} [M] \{\ddot{d}\}}{\omega_1 m_1} S \quad (29)$$

$$\{u\}_i \Big|_{\max.} = \{\phi_i\} q_1 \Big|_{\max.} \quad (30)$$

Estimación de la respuesta máxima

Método 1)

$$\{u\}_{max} = \sum_{i=1}^m \{u\}_i |_{max} \quad (31)$$

Método 2) RMS

$$u_r |_{max} = \left[ \sum_{i=1}^m (u_{ri})^2 \right]^{1/2} \quad r=1, \dots, N \quad (32)$$

Método 3) NRL

$$u_r |_{max} = |u_{r1}|_{max, max} + \left( \sum_{i=1}^n u_{ri} |_{max}^2 \right)^{1/2} \quad (33)$$

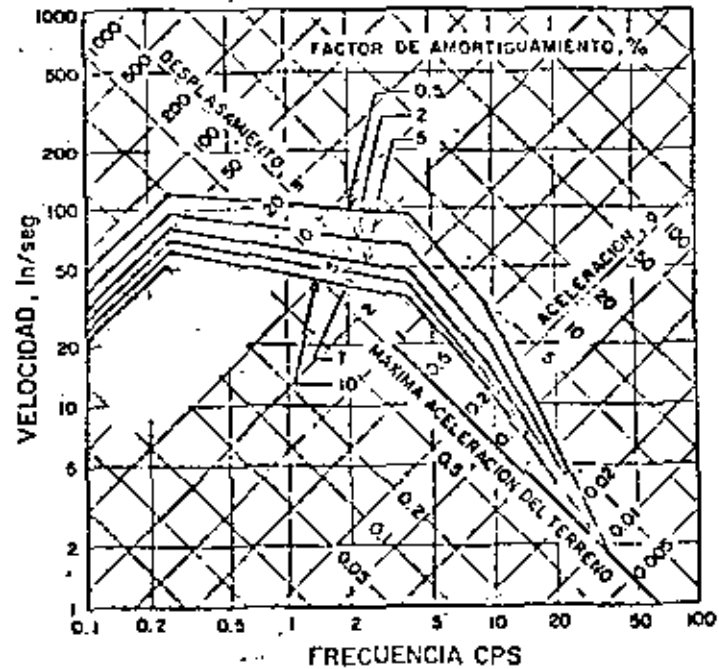


Fig- 1 Espectro de diseño para respuesta vertical escalado a 1g de ocleración horizontal del terreno (USA A.E.C)

Nombre del Programa	Tubería Recta	Reducción Concentrada	Tubo recto con codo	Codos	Tas	Resortes		Elem. "gap"	Elemento de fricción	Vaso		Condición
						Lineal	No-Lineal			Concentr	Consis	
ALUPE	Si	No	Si	Si	Si	Si	No	No	No	Si	No	No
AUSYS	Si	No	Si	Si	No	Si	Si	Si	Si	Si	Si	Si
MARC	Si	Si	Si	Si	No	Si	Si	Si	Si	No	Si	Si
MASTRAN	Si	Si	Si	No	No	Si	Si	Si	Si	Si	Si	Si
PIPE	Si	No	Si	Si	Si	Si	No	No	No	Si	No	No
P-POYN	Si	No	Si	Si	Si	Si	No	No	No	Si	No	No
PIPEPUP	Si	No	Si	Si	Si	Si	No	No	No	Si	No	No
PIPESO	Si	No	No	Si	Si	Si	No	No	No	Si	No	No
SACS/DACS	No	No	Si	Si	Si	Si	No	No	No	Si	No	No
SAP IV	Si	No	Si	Si	No	Si	No	No	No	Si	No	Si
STADYHE	Si	No	Si	Si	Si	Si	Si	Si	No	Si	Si	No
WEGAN	Si	No	Si	Si	No	Si	Si	Si	Si	Si	Si	Si

Análisis de tubería por Elemento finito

Nombre del Programa	Condensación	Model (Modos normales)					Integración directa en el tiempo					
		Frecuencias Naturales	Modos			Espectro de Resp	Lineal	Im. NoLin	Plasticidad	Tal grande	Sismica	
			Lineal	Elem No Lin	Pseudo-Fuerza							
ALUPE	Si	Si	Si	No	Si	Si	Si	No	No	No	No	No
AUSYS	Si	Si	Si	No	Si	Si	Si	Si	Si	Si	Si	Si
MARC	Si	Si	No	No	No	No	Si	Si	Si	Si	Si	No
MASTRAN	Si	Si	Si	Si	No	Si	Si	Si	Si	No	No	Si
P-POYN	Si	Si	Si	No	Si	Si	Si	No	No	No	No	No
PIPESO	Si	Si	No	No	Si	Si	No	No	No	No	No	Si
SACS/DACS	No	Si	Si	No	Si	Si	Si	No	No	No	No	Si
SAP IV	No	Si	Si	Si	Si	Si	Si	Si	Si	No	No	Si
STADYHE	Si	Si	Si	Si	Si	Si	Si	Si	Si	No	No	Si
WEGAN	Si	Si	No	No	No	Si	Si	Si	Si	Si	No	Si

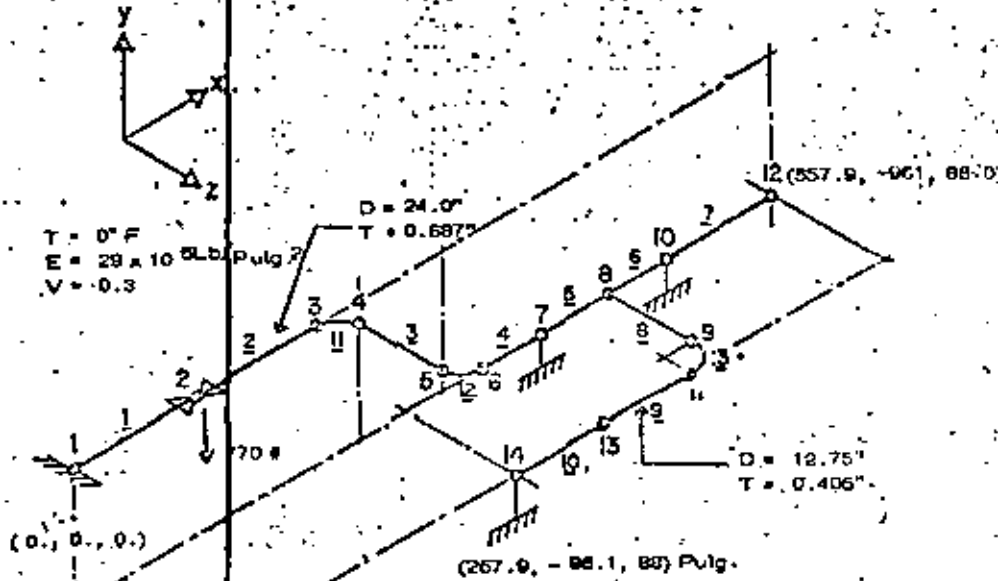
Capacidades de varios programas de computadora para análisis de tuberías

PROBLEMA 12.2 PIPE NETWORK RESPONSE SPECTRUM ANALYSIS

187  
469

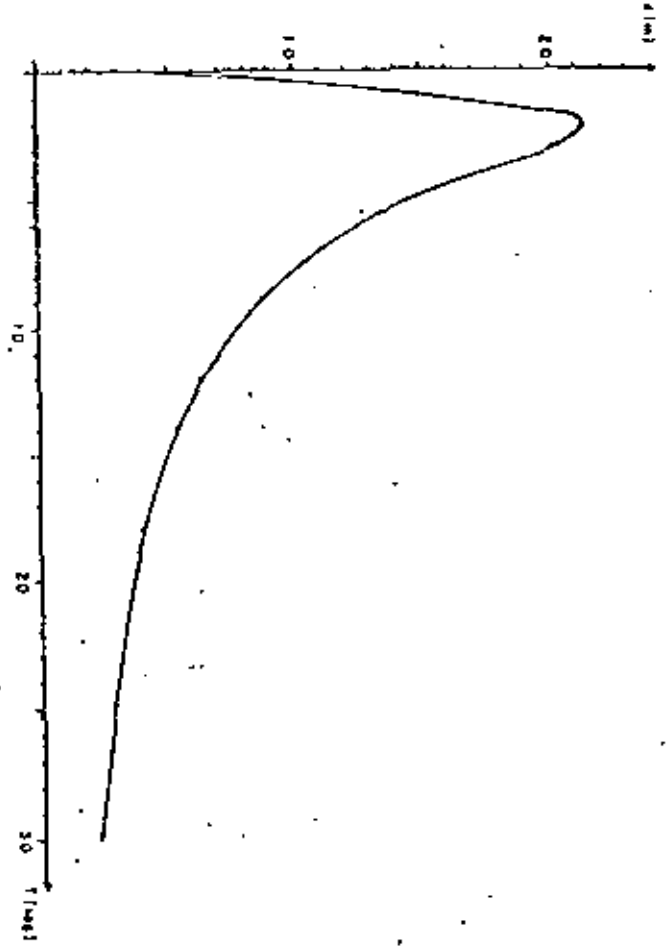
Problem Definition

Ref: SAP IV Manual; problem 4.



MODOS	FREC. CIRCULAR (RAD/SEG)	FRECUENCIA (CPS)	PERIODO (SEG)
1	9.133	1.454	0.6879
2	27.71	4.410	0.2268
3	50.24	7.997	0.1251
4	64.05	10.34	0.0967
5	74.47	11.85	0.0844

ESPECTRO DE DESPLAZAMIENTOS



## REFERENCIAS

USA Standard code for Pressure Piping, Power Piping, -  
ANSI B31.1-1977. Published by the American Society of -  
Mechanical Engineers, 345, East 47th Street, New York, -  
N.Y. 10017.

Pressure Vessel Technology, Part 1, Design and Analysis -  
and Part 2, Materials and Fabrication, First International  
Conference on Pressure Vessel Technology, Delft, Holland, -  
1969. Published by the American Society of Mechanical Eng.  
345 East 47th Street, New York, N.Y. 10017.

Rodabaugh, E.C. and George H.H., "Effect of Internal Pre-  
ssure on Flexibility and Stress-Intensification Factors of Cur-  
ved Pipe or Welding Elbows", Trans. ASME, Vol. 79, p 939  
(1957).

Brock, J.E., "Expansión and Flexibility", Chapter 4 of Piping  
Handbook, 5th edition (1969), Mc Graw-Hill Book Co., New  
York.

ASME Boiler and Pressure Vessel Code, Section III, Divi-  
sion 1, 1980.



CONTROL INFORMATION

NUMBER OF NODAL POINTS = 14  
 NUMBER OF ELEMENT TYPES = 1  
 NUMBER OF LOAD CASES = 1  
 NUMBER OF FREQUENCIES = 5  
 ANALYSIS CODE (MOYN) = 3  
   EC01, STATIC  
   EC02, MODAL EXTRACTION  
   EC03, FORCED RESPONSE  
   EC04, RESPONSE SPECTRUM  
   EC05, DIRECT INTEGRATION  
   EC06, FREQUENCY RESPONSE  
 SOLUTION MODE (MODEX) = 0  
   TC01, EXECUTION  
   TC02, DATA CHECK  
 NUMBER OF SUBSPACE  
 ITERATION VECTORS (MADI) = 0  
 EQUATIONS PER BLOCK = 0  
 TABLE SAVE FLAG (MDSV) = 0  
 GRAVITATIONAL CONSTANT = 386.40  
 TOTAL BLANK COMMON (MTCY)=1550

REQUIRED BLANK COMMON FOR THIS STEP= 141

NODAL POINT INPUT DATA

NODAL POINT NO.	BOUNDARY CONDITION CODES						NODAL POINT COORDINATES				
	X	Y	Z	XX	YY	ZZ	X	Y	Z	T	
1	1	1	1	1	1	1	.000	.000	.000	0	.000
2	0	0	0	0	0	0	100.000	.000	.000	0	.000
3	0	0	0	0	0	0	200.000	.000	.000	0	.000
4	0	0	0	0	0	0	220.456	-10.514	.000	0	.000
5	0	0	0	0	0	0	300.456	-85.514	.000	0	.000
6	0	0	0	0	0	C	320.912	-96.028	.000	0	.000
7	0	0	0	0	0	C	370.912	-96.028	.000	0	.000
8	0	0	0	0	0	0	420.912	-96.028	.000	0	.000
9	0	0	0	0	0	C	420.912	-96.028	70.000	0	.000
10	0	0	0	0	0	0	470.912	-96.028	.000	0	.000
11	0	0	0	0	0	0	427.912	-96.028	87.000	0	.000
12	0	0	0	0	0	0	557.912	-96.028	.000	0	.000
13	0	0	0	0	0	0	337.912	-96.028	87.000	0	.000
14	0	0	0	0	0	0	267.912	-96.028	88.000	0	.000



SECTION PROPERTY TABLE							
SECTION NUMBER	OUTSIDE DIAMETER	WALL THICKNESS	SHAPE FACTOR FOR HEAD	WEIGHT/UNIT LENGTH	MASS/UNIT LENGTH	DESCRIPTION	
1	24.000	.6270	.0000	.2875+00	.7440+01	24	INCH SHD. 40
2	12.750	.4000	.0000	.6500+01	.2200-01	12	INCH SCHD. 40
ELEMENT LOAD CASE MULTIPLIERS							
			CASE A	CASE B	CASE C	CASE D	
X-DIRECTION GRAVITY			.000	.000	.000	.000	
Y-DIRECTION GRAVITY			.000	.000	.000	.000	
Z-DIRECTION GRAVITY			.000	.000	.000	.000	
THERMAL DISTORTION			.000	1.000	.000	.000	
PRESSURE DISTORTION			.000	.000	.000	.000	

PIPE ELEMENT	ELEMENT	HOPE	HOPE	MATL.	SECTION	INTERFACE	INTERNAL	DIRECTION		
NUMBER	TYPE	-I	-J	NUMBER	NUMBER	TEMPERATURE	PRESSURE	AX	AY	AZ
						(BEND	(THICK	(X3-	(Y3-	(Z3-
						RADIUS)	POINT)	ORDINATE)	ORDINATE)	ORDINATE)
1	TANG	T	1	2	1	.00	.00	.0000	.0000	.0000
2	TANG	T	2	3	1	.00	.00	.0000	.0000	.0000
3	TANG	T	4	5	1	.00	.00	.0000	.0000	.0000
4	TANG	T	6	7	1	.00	.00	.0000	.0000	.0000
5	TANG	T	7	8	1	.00	.00	.0000	.0000	.0000
6	TANG	T	8	10	1	.00	.00	.0000	.0000	.0000
7	TANG	T	10	12	1	.00	.00	.0000	.0000	.0000
8	TANG	T	8	9	1	.00	.00	.0000	.0000	.0000
9	TANG	T	11	13	2	.00	.00	.0000	.0000	.0000
10	TANG	T	13	14	2	.00	.00	.0000	.0000	.0000
11	BEND		3	4	1	.00	.00			
						(	(TI)	214.91211	.00011	.00011
12	BEND		5	6	1	.00	.00			
						(	(TI)	311.01011	-96.00011	.00011
13	BEND		9	11	2	.00	.00			
						(	(TI)	425.91211	-96.00011	85.00011

REQUIRED BLANK COMMON FOR THIS STEP= 235

EQUATION PARAMETERS

TOTAL NUMBER OF EQUATIONS	=	75
BANDWIDTH	=	16
NUMBER OF EQUATIONS IN A BLOCK	=	75
NUMBER OF BLOCKS	=	1

EIGENVALUE ANALYSIS

DETERMINANT SEARCH SOLUTION IS CARRIED OUT

CONTROL INFORMATION

FLAG FOR ADDITIONAL PRINTING = 1  
EQ0, SUPPRESS  
EQ1, PRINT

STURM SEQUENCE CHECK FLAG (\*) = 0  
EQ0, PERFORM CHECK  
EQ1, PASS

MAXIMUM ITERATION CYCLES (\*) = 10

CONVERGENCE TOLERANCE (\*) = .1000E-04

CUT-OFF FREQUENCY (CPS) = .1050E+02

NUMBER OF STARTING ITERATION  
VECTORS TO BE READ FROM  
TAPE10 (\*) = 0

(\*) APPLICABLE TO SUBSPACE  
ITERATION SOLUTIONS ONLY

SOLUTION IS SOUGHT FOR FOLLOWING EIGENPROBLEM

NUMBER OF EQUATIONS = 75

HALF BANDWIDTH OF STIFFNESS MATRIX = 18

NUMBER OF EQUATION BLOCKS = 1

NUMBER OF EQUATION BLOCKS = 75

MODAL ANALYSIS

MODE NUMBER 1  
 FREQUENCY= 1.42361 Hz

EIGENVECTORS NORMALIZED TO A UNIT MASS MATRIX

DISPLACEMENTS/ROTATIONS OF UNRESTRAINED NODES

NODE NUMBER	X-TRANSLATION	Y-TRANSLATION	Z-TRANSLATION	X-ROTATION	Y-ROTATION	Z-ROTATION
2	1.56792-006	-5.01805-005	-5.211304-003	4.91351-005	1.07163-004	-7.81116-007
3	2.12561-006	-1.31264-004	-3.20271-002	9.82712-005	2.80455-004	-6.05329-007
4	9.64887-006	-1.03008-004	-6.39151-002	1.28102-004	5.11432-004	1.18552-006
5	1.12913-004	-0.46271-005	-1.27444-001	1.98835-004	5.97558-004	1.20727-006
6	1.02314-004	-6.27080-006	-1.19317-001	2.30013-004	7.04734-004	2.15162-007
7	1.24145-004	0.00110	-1.25117-001	2.23900-004	7.07357-004	1.41075-007
8	1.24926-004	6.39215-006	-1.11652-001	2.32542-004	7.23071-004	-6.02507-007
9	5.11449-002	-1.59045-002	-1.27184-001	2.02442-004	7.21146-004	-4.48275-005
10	1.24928-004	0.40100	-2.23505-001	2.32542-004	7.35079-004	-1.07921-007
11	6.36842-002	-1.22004-002	-1.27937-001	1.28102-004	6.15558-004	-1.09429-004
12	1.24929-004	-8.35434-006	-2.27267-001	2.12146-004	7.41574-004	-1.07457-007
13	6.36861-002	-9.64245-003	-1.28045-001	1.28102-004	6.44072-004	-1.20151-004
14	6.36868-002	0.00000	-2.27826-002	1.56115-004	6.44728-004	-1.40014-004

MODAL ANALYSIS

MODE NUMBER 2  
 FREQUENCY= 4.41568 HZ

EIGENVECTORS NORMALIZED TO A UNIT MASS MATRIX

DISPLACEMENTS/ROTATIONS OF UNRESTRAINED NODES

NODE NUMBER	X- TRANSLATION	Y- TRANSLATION	Z- TRANSLATION	X- ROTATION	Y- ROTATION	Z- ROTATION
2	3.44703-005	-1.14607-003	6.06020-003	-9.80770-005	-9.60012-005	-1.74574-005
3	6.622943-005	-2.91469-003	1.16324-002	-1.97740-004	-9.30025-005	-1.25553-005
4	2.21420-004	-1.76309-003	2.05920-007	-0.87442-004	-1.17009-005	2.72343-005
5	0.61440-002	-4.24051-004	3.46998-002	-0.68077-004	1.12522-004	2.59865-005
6	2.84723-003	-2.00555-005	3.75186-002	-1.75476-004	4.25134-004	0.87285-006
7	0.66354-003	0.00000	7.93523-003	-1.75671-004	5.01633-004	2.44626-007
8	0.67012-003	5.29507-006	-1.65014-002	-1.75770-004	5.90215-004	3.76617-007
9	6.64216-002	1.22425-002	-1.65399-002	-1.76144-004	1.70297-003	3.36410-005
10	0.96053-003	0.00000	-4.07484-002	-1.75770-004	6.13082-004	-1.20074-007
11	1.44287-001	1.43101-002	1.34624-002	-1.51616-004	5.19905-003	1.42162-005
12	2.88106-003	-1.10644-005	-1.09576-001	-1.75770-004	6.01064-004	-1.35132-007
13	1.44326-001	7.65461-003	4.41246-001	-1.51616-004	5.78196-003	1.04072-004
14	1.44319-001	0.00000	6.51877-001	-1.51616-004	5.90767-003	1.11540-004

224667800 1234567800 224667800 1234567800 224667800 1234567800 224667800 1234567800 224667800 1234567800

MODAL PARTICIPATION FACTORS

MODE	X-DIRECTION	Y-DIRECTION	Z-DIRECTION
1	.2743+00	-.5437-01	-.5566+01
2	.6151+00	-.1867-01	.1363+01
3	-.1002+01	.3716+00	-.3601+01
4	.4074+01	-.3277+01	-.1396+01
5	.5617+00	-.2114+01	.2158+01

SPECTRUM TABLE 1 DISPLACEMENT SPECTRUM OF PIPDYL PANEL

NUMBER OF POINTS = 16  
 SCALE FACTOR = .1000+01

INPUT POINT	PERIOD	SPECTRUM VALUE
1	.1000	.4633+00
2	.2000+01	.4633+00
3	.3000+00	.1470+01
4	.4000+00	.2077+01
5	.5000+00	.2116+01
6	.7000+00	.2187+01
7	.8000+00	.2108+01
8	.9000+00	.2008+01
9	.1000+00	.1370+01
10	.7000+00	.1104+01
11	.9000+00	.8609+00
12	.1000+01	.6010+00
13	.1400+01	.5210+00
14	.1800+01	.3970+00
15	.2000+01	.3002+00
16	.3000+01	.2100+00

REQUIRED BLANK COPY FOR THIS STEP = 540

REQUIRED BLANK COPY FOR THIS STEP = 540

RESPONSE SPECTRUM ANALYSIS

RESPONSE FOR POLE 1  
 FREQUENCY= 1.47361 HZ

DISPLACEMENTS/ROTATIONS OF UNRESTRAINED NODES

NODE NUMBER	X-TRANSLATION	Y-TRANSLATION	Z-TRANSLATION	Y-ROTATION	Y-ROTATION	Z-ROTATION
2	6.56403-009	-2.11345-007	-3.71004-005	2.05704-007	6.97634-007	-3.27054-009
3	1.31871-008	-5.45488-017	-1.28001-004	4.11408-007	1.17521-006	-1.58874-009
4	4.03259-008	-9.25895-007	-1.35430-004	7.93400-007	2.17180-006	4.89109-009
5	4.72704-007	-1.03830-007	-4.27004-004	8.32005-007	2.49308-006	5.47054-009
6	5.16456-007	-2.67827-008	-4.09116-004	9.84678-007	2.89034-006	5.00765-010
7	5.18728-007	0.00000	-6.40389-004	9.79014-007	3.05130-006	5.90452-010
8	5.22992-007	2.87005-008	-2.22161-004	9.73551-007	3.07257-006	-1.30047-009
9	5.14116-004	-6.62452-005	-8.71257-004	9.71345-007	3.01808-006	-1.26038-007
10	5.03004-007	0.00000	-9.56671-004	9.73551-007	3.05412-006	-1.51606-010
11	5.06611-004	-7.62505-005	-7.21184-004	7.87704-007	2.74627-006	-4.56102-007
12	5.22011-007	-3.70802-006	-1.20101-007	9.73001-007	3.10457-006	-4.52105-010
13	5.06619-004	-6.03617-005	-5.00754-004	7.87704-007	2.70384-006	-5.57889-007
14	5.66822-004	0.00000	-5.71677-004	7.87704-007	2.68913-006	-1.86104-007

RESPONSE SPECTRUM STRESS COMPONENTS (KIN/CM)

1. NUMBER OF THE MODE WITH THE LARGEST STRESS.  
FOR EACH ELEMENT, THE FOLLOWING INFORMATION IS PRINTED
2. VALUE OF THE STRESS COMPONENT IN THAT MODE.
3. IF REQUESTED; MODE BY MODE STRESSES.
4. RESULTANT OF THE MODAL SUMMATION. (SQUARE ROOT OF THE SUM OF THE SQUARES)

ELEMENT TYPE (3/C	P I P E			ELEMENT NUMBER ( 1 )							
	PX(I)	VY(I)	VZ(I)	TX(I)	PY(I)	MZ(I)	PX(J)	VY(J)	VZ(J)	T	
MAXIMUM	3.654+01	-3.455+01	-9.937+00	3.610+02	1.229+03	-3.761+03	3.694+01	-3.455+01	-9.937+00	3.61	
RESULTANT	3.704+01	3.463+01	1.358+01	4.730+02	1.936+03	3.769+03	3.704+01	3.463+01	1.358+01	4.73	

ELEMENT TYPE (3/C	P I P E			ELEMENT NUMBER ( 2 )						
	PX(I)	VY(I)	VZ(I)	TX(I)	PY(I)	MZ(I)	PX(J)	VY(J)	VZ(J)	T
MAXIMUM	3.686+01	-1.905+01	-4.926+00	3.610+02	5.930+02	-3.010+02	3.686+01	-1.905+01	-4.926+00	3.61
RESULTANT	3.677+01	1.910+01	7.457+00	4.738+02	7.100+02	3.267+02	3.677+01	1.910+01	7.457+00	4.73

ELEMENT TYPE (3/C	P I P E			ELEMENT NUMBER ( 3 )						
	PX(I)	VY(I)	VZ(I)	TX(I)	PY(I)	MZ(I)	PX(J)	VY(J)	VZ(J)	T
MAXIMUM	2.927+01	2.172+01	-1.976+00	3.142+02	3.524+02	1.509+03	2.927+01	2.172+01	-1.976+00	3.14
RESULTANT	2.947+01	2.177+01	3.594+00	4.618+02	5.676+02	1.529+03	2.947+01	2.177+01	3.594+00	4.61

ELEMENT TYPE (3/C	P I P E			ELEMENT NUMBER ( 4 )						
	PX(I)	VY(I)	VZ(I)	TX(I)	PY(I)	MZ(I)	PX(J)	VY(J)	VZ(J)	T
MAXIMUM	2.679+01	-3.453+00	2.921+00	2.630+02	-4.309+02	-1.002+03	2.679+01	-3.453+00	2.921+00	2.60
RESULTANT	2.688+01	3.523+00	3.772+00	2.159+02	5.610+02	1.006+03	2.688+01	3.523+00	3.772+00	2.15

ELEMENT TYPE (3/C	P I P E			ELEMENT NUMBER ( 5 )						
	PX(I)	VY(I)	VZ(I)	TX(I)	PY(I)	MZ(I)	PX(J)	VY(J)	VZ(J)	T



**DIVISION DE EDUCACION CONTINUA  
FACULTAD DE INGENIERIA U.N.A.M.**

**VII CURSO INTERNACIONAL DE INGENIERIA SISMICA**

**DISEÑO SISMICO DE ESTRUCTURAS ESPECIALES**

**DISEÑO SISMICO DE ESTRUCTURAS DE  
TIPO INDUSTRIAL  
( complemento)**

**M en C Mauricio Names**

**Agosto, 1981**

DISTRIBUCION DE FUERZAS SISMICASEN EDIFICIOS CON DIAFRAGMAS FLEXIBLES

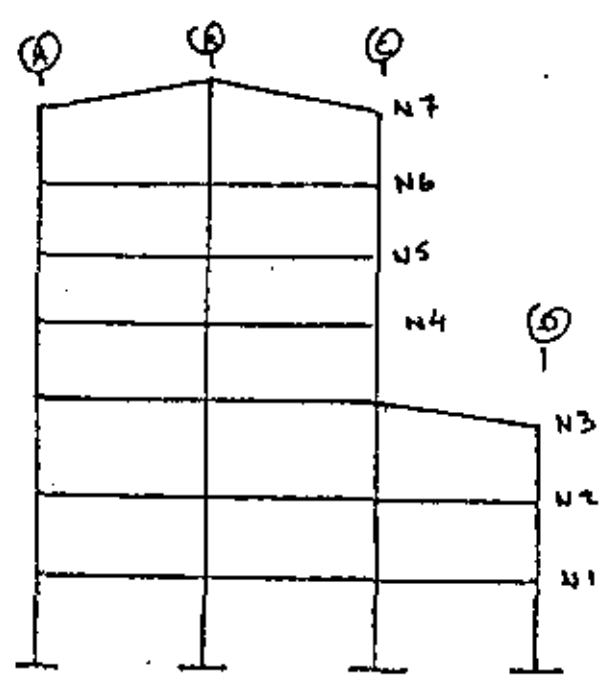
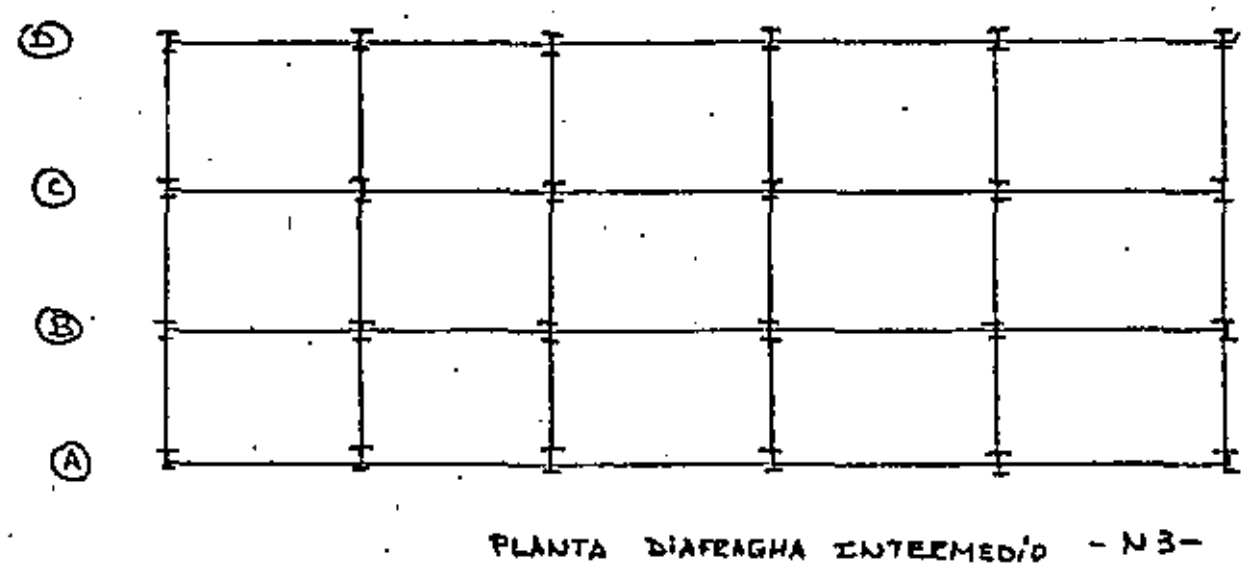
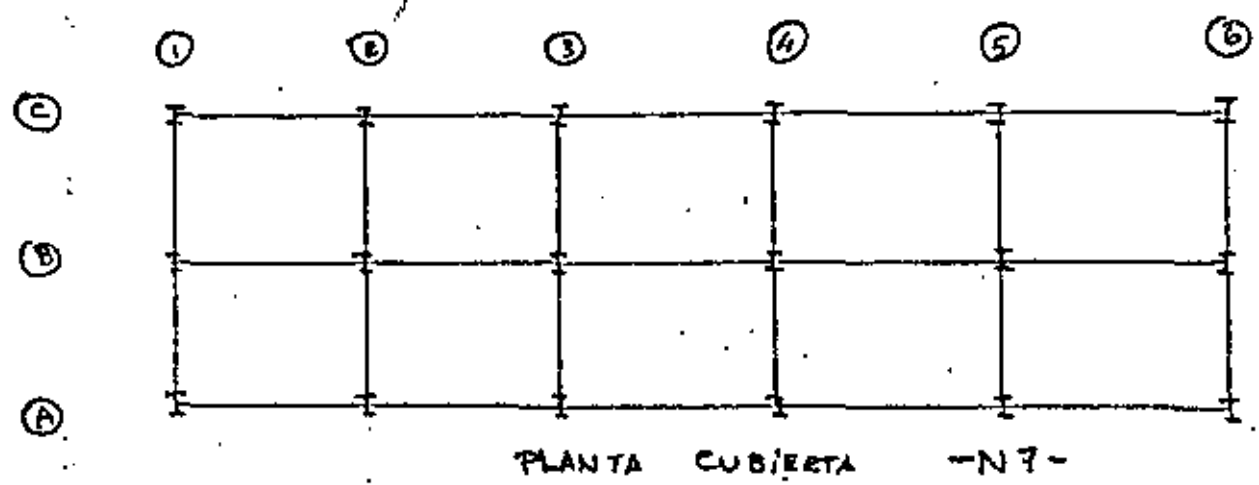
En edificios tipo industrial de elementos de acero, y con sistemas de piso de rejilla, la acción de las fuerzas laterales, generalmente debe tomarse, de manera que cada marco absorba las fuerzas correspondientes al área tributaria.

Sin embargo en edificios donde existan concentraciones fuertes de cargas en ciertas áreas discretas, conviene forzar la presencia de diafragmas de piso flexibles por medio de contraventeo horizontal en ciertos pisos (o niveles) discretos.

La distribución de fuerzas sísmicas según el procedimiento descrito en el folleto complementario, solo es aplicable a edificios que cada nivel sea un diafragma infinitamente rígido.

A continuación se describe el procedimiento para determinar las fuerzas sísmicas que actúan en cada marco cuando hay diafragmas flexibles en niveles discretos:

Para visualizar mas claramente el procedimiento, se plantea a continuación la siguiente estructura:

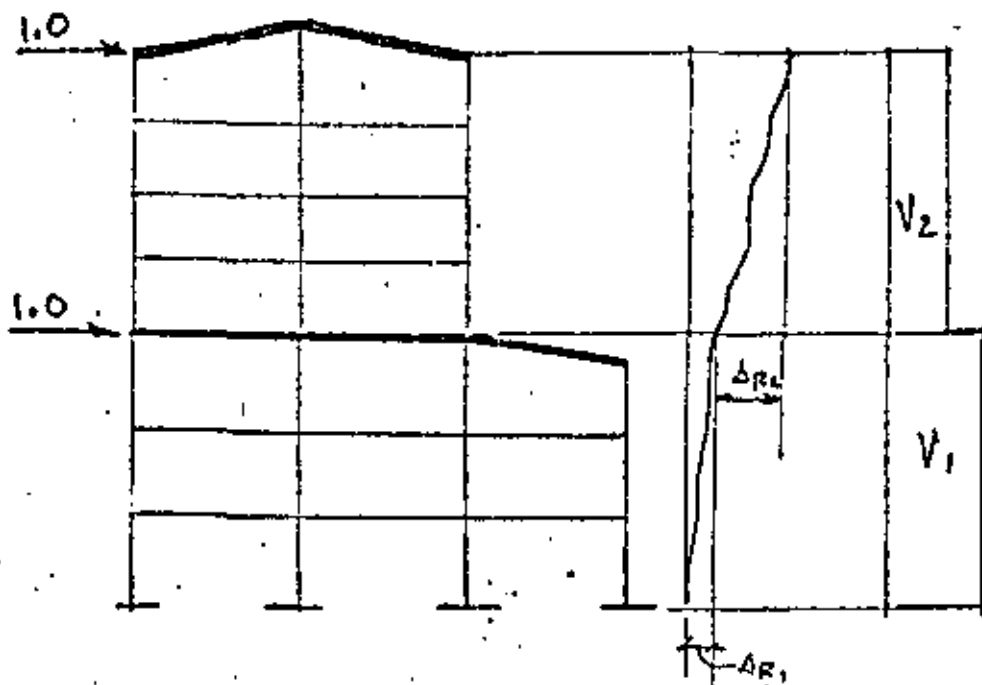


MARCO EJE A - contraventado  
 ✓ EJE D - ✓  
 ✓ EJE C - contraventado de N3 a N7  
 MARCO EJES ① y ⑥ - contrav.

SECUELA:

Determinar rigideces de entrepiso, considerando como "entrepisos" únicamente entre diafragmas flexibles:

Así por ejemplo para el marco transversal mostrado en la hoja anterior:



$$K_{2m} = \frac{\Delta R_2}{V_2}$$

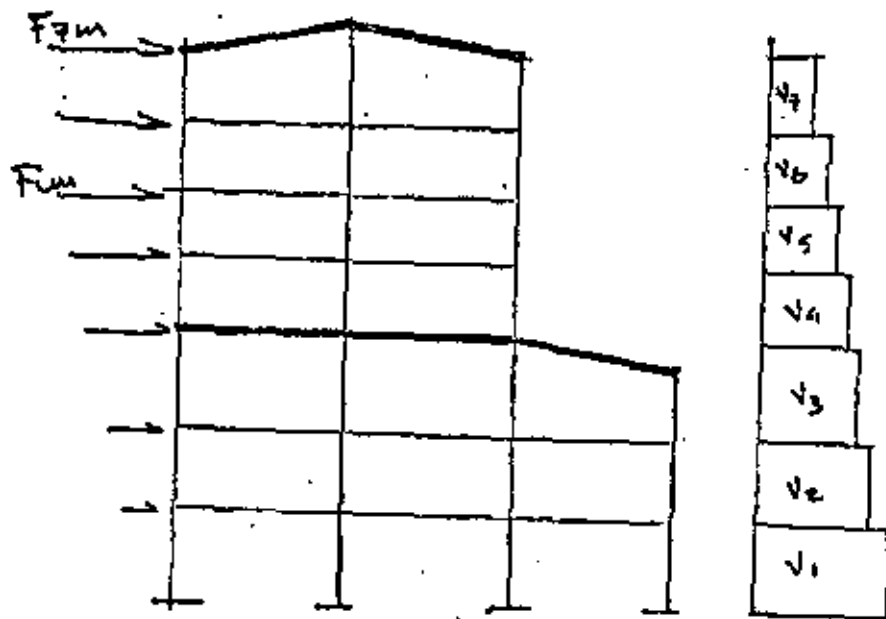
$$K_{1m} = \frac{\Delta R_1}{V_1}$$

m = no de marco

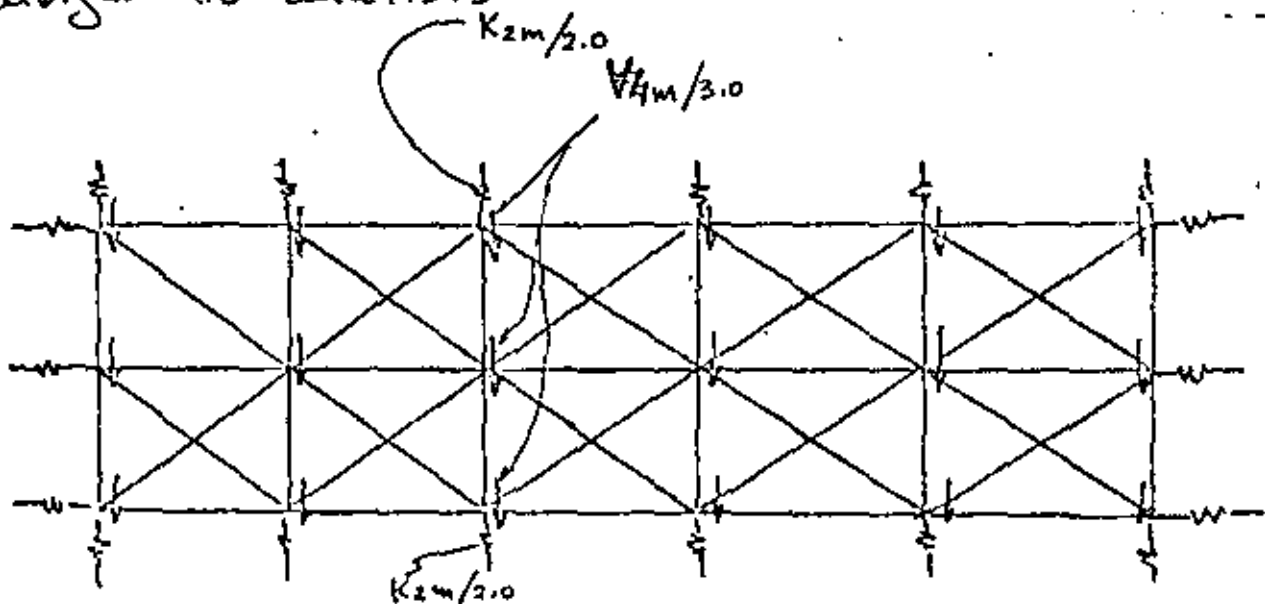
Se determinan así las rigideces de "superentrepisos" de todos los marcos, tanto transversales como longitudinales, por medio de un análisis de marcos planos con las cargas unitarias laterales a nivel de los diafragmas flexibles.

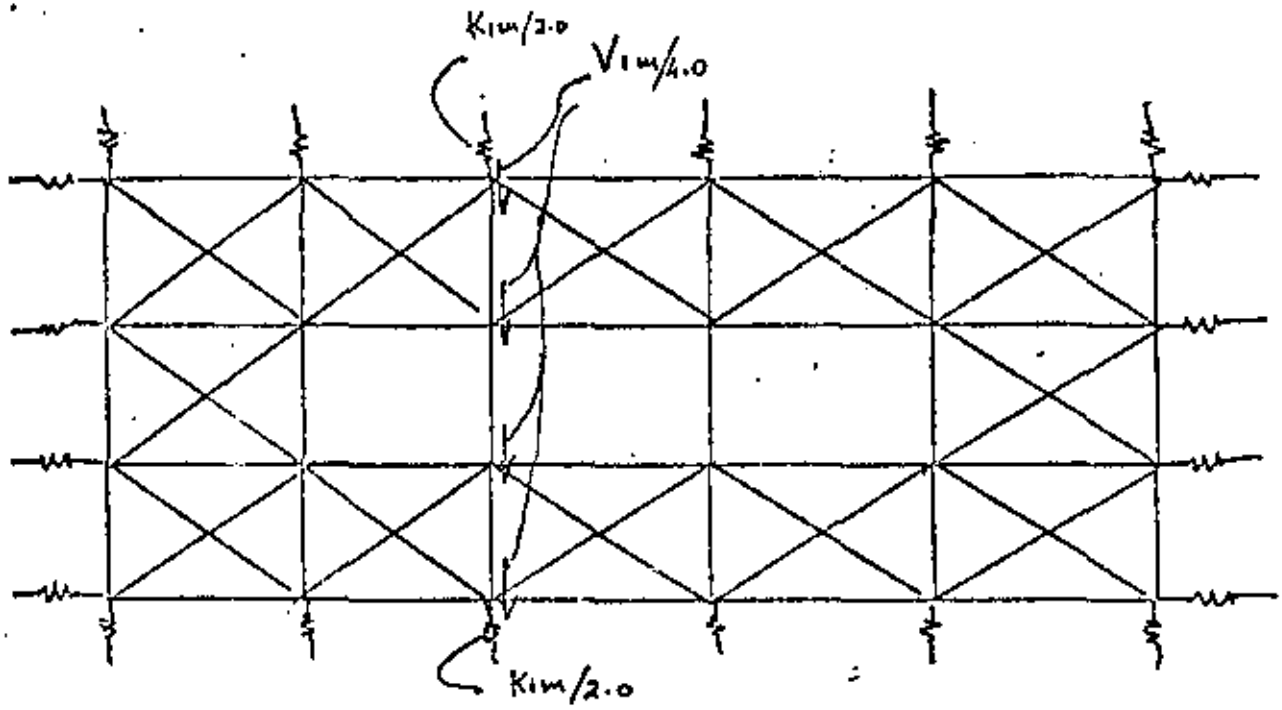
2. Determinar las fuerzas sísmicas laterales de cada marco considerando pesos por área tributaria al marco.

$$F_{im} = C W_T \frac{W_i h_i}{\sum W_i h_i}$$



3. Efectuar el análisis de <sup>cada</sup> diafragma flexible aplicando en cada marco el constante sísmico entre superentrepisos, como fuerzas de análisis





DIAPHRAGMA - N3 -

Del análisis de diafragma se obtienen las fuerzas en los "resortes" (que simulan las rigideces de "superentrepisos") -  $F_{Rm}$

4. Obtener la diferencia de fuerzas cortantes  $Q$  de cada marco a nivel del diafragma (de cada diafragma)

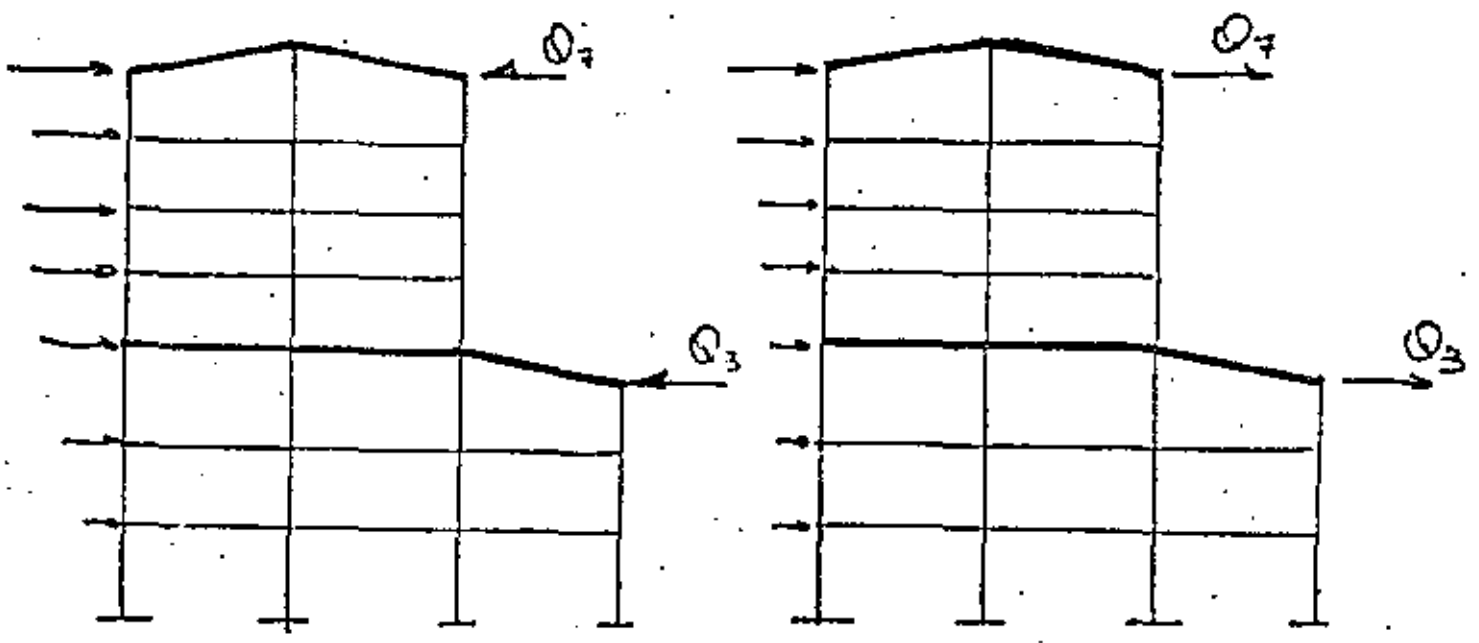
$$Q_{m7} = F_{Rm7} - V_{4m} \quad \text{- para el diafragma N7.}$$

$$Q_{m3} = F_{Rm3} - V_{1m} \quad \text{para el diafragma N3.}$$

donde  $F_{Rm}$  = fza. resultante del análisis de diafragma en el resorte correspondiente al marco  $m$ .

$Q_m$  - será negativa para marcos flexibles (en contra de las fuerzas sísmicas calculadas por una tributaria)

6. Analizar cada marco (vertical) en forma aislada, aplicandole las fuerzas sismicas calculadas en la area tributaria, y ademas dos fuerzas concentradas  $Q$  (una en cada nivel donde existen los diafragmas) como se ilustra a continuacion



MARCO FLEXIBLE

MARCO RIGIDO

Las fuerzas  $Q$  representan el efecto del diafragma sobre el marco; en los marcos flexibles, los diafragmas "detienen" al marco, pero en los marcos rigidos es donde los diafragmas se apoyan e incrementa sus fuerzas laterales.

Utilizar los signos de las  $Q$ 's que resultan de las diferencias de fuerzas anteriores.

6. Se ilustró en los puntos anteriores el análisis de <sup>7/4</sup> diafragmas para sismo paralelo al lado corto. Se debe efectuar un análisis semejante para sismo en la dirección larga (como otra condición de carga del "marco-diafragma").

Las fuerzas que se obtengan en las barras diagonales del análisis de diafragma, se puedan utilizar para ~~el~~ el diseño del contraventeo horizontal.

E.4. Valores de Q en estructuras especiales.

En esta sección se considerarán algunos casos no cubiertos en la sección E.3.

DESCRIPCION	FACTOR DE DUCTILIDAD.
-------------	-----------------------

Chimeneas y torres de proceso de acero (un solo "elemento" resistente), - - - - -	2.0
---	-----

Chimeneas, silos, torres cilíndricas de concreto (un solo "elemento" resistente), - - - - -	2.0
---	-----

Péndulos invertidos cuya estructura de soporte de la masa concentrada superior está compuesta de:

Marcos de acero con o sin contraventeo. - - - - -	4.0
---	-----

Marcos de concreto. - - - - -	4.0
-------------------------------	-----

Cimentación soportante de recipientes horizontales, alargados, hornos rotatorios, etc.

a. Dirección transversal

Muro H/b	≤	7	- - - - -	2.0
Muro H/b	>	7	- - - - -	3.0
Muro con hueco.			- - - - -	4.0
b. Dirección longitudinal			- - - - -	4.0
Pedestales de concreto de turbos			- - - - -	2.0
Muros de piezas macizas confinados por castillos y dalas.			- - - - -	2.0
Muros de piezas huecas confinados o con refuerzo interior.			- - - - -	1.5

F. CLASIFICACION DE LAS ESTRUCTURAS SEGUN SU USO.

En ésta especificación se distinguen estructuras urbanas, y las estructuras de tipo industrial:

La clasificación se basa en la importancia de la estructura en lo que se refiere al evento que quedara inoperable o inhabitable a consecuencia de un sismo de gran intensidad.

GRUPO A.1.

Construcciones urbanas importantes, que en caso de falla por sismo, causarían pérdidas directas o indirectas excepcionalmente altas, tales como:

Centrales, telefónicas, estaciones de bombeo y archivos hospitales, escuelas, estadios, auditorios, templos, salas de espectáculo, estaciones terminales de transporte, monumentos y museos.

GRUPO A.2.

Construcciones industriales, cuya falla por sismo causaría una contaminación ambiental tal que pondría en peligro la vida de los habitantes de la región, tales

como:

Plantas que generan gases tóxicos como cloro, derivados clorados, insecticidas, anhídrido - sulfúrico, etc.

GRUPO A.3.

Construcciones industriales cuya falla por sismo causaría un potencial de explosión y/o incendio, tales como:

Refinerías.

GRUPO A.4.

Construcciones industriales cuya falla por sismo dejaría inoperativas plantas completas y complejos industriales, tales como:

Cuartos o edificios de control, subestaciones eléctricas, casas de fuerza.

GRUPO B.1.

Construcciones urbanas que en caso de falla por sismo ---- causarían pérdidas de magnitud intermedia, tales como:

Comercios, bancos, restaurantes, casas habitación, edificios de departamentos y oficinas.

GRUPO B.2.

Construcciones industriales, no incluidas en los grupos A, cuya falla por sismo causaría una pérdida local, pero que pueden poner en peligro construcciones de los grupos A.2 a A.4.

GRUPO B.3.

Construcciones industriales, no incluidas en los grupos A, cuya falla por sismo causaría una pérdida local únicamente, tales como:

Edificios de proceso, bodegas, casetas de entrada e instalaciones exteriores aisladas.

GRUPO C.

Construcciones cuya falla por sismo implicaría un costo pequeño y no pueda causar daños a construcciones de los grupos A y B, tales como:

Bodegas provisionales, bardas con altura menor a 2.5 m.

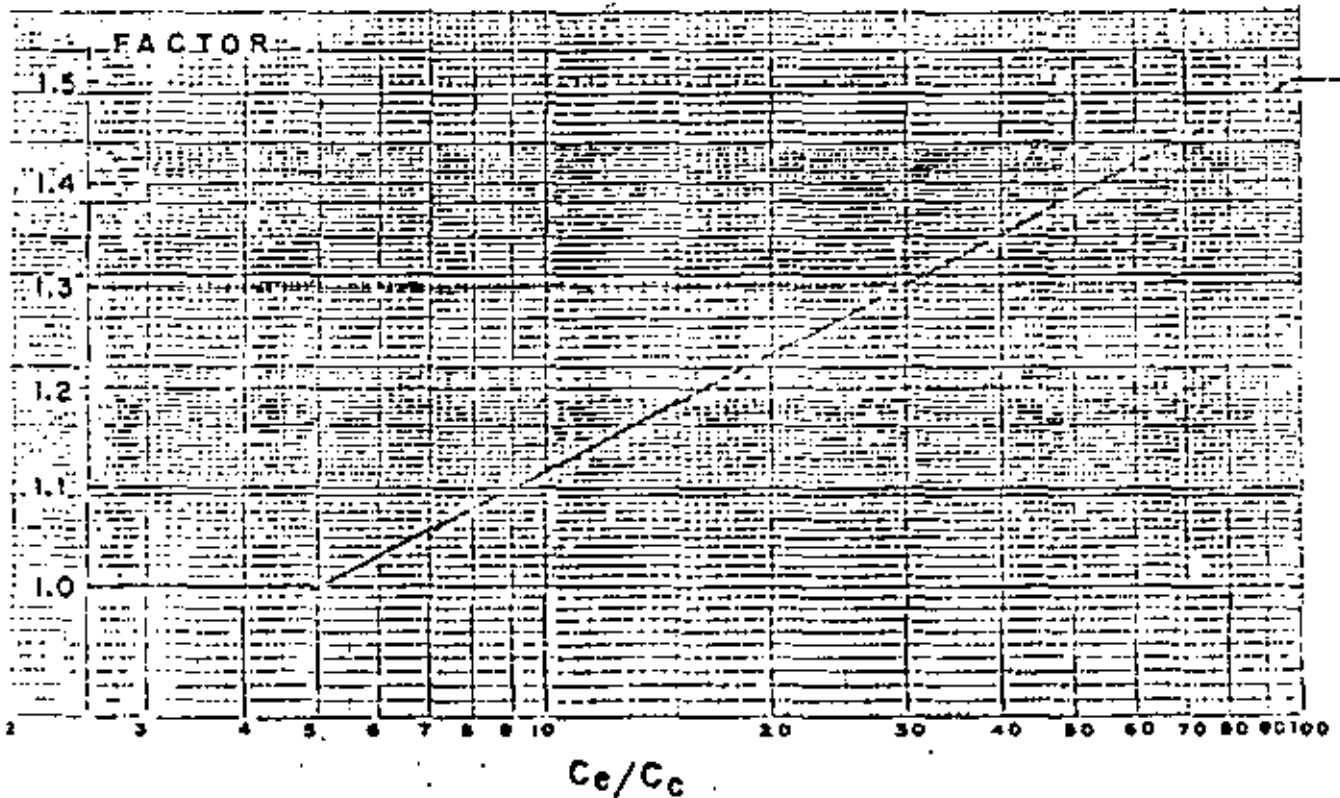
Los coeficientes sísmicos especificados en la Tabla 1 deberán ser multiplicados por los siguientes factores para estructuras de cada uno de los grupos anteriores:

TABLA 2

FACTORES MULTIPLICADORES DE ESPECTROS.

GRUPO	FACTOR
A.1	1.3
A.2	1.5
A.3	1.4
A.4	1.3
B.1	1.0
B.2	1.2
B.3	≥ 1.0*
C	0

\*Para edificios de proceso el "factor" podrá ser mayor que uno (1.0), dependiendo de la relación costo equipo - costo obra civil.





**DIVISION DE EDUCACION CONTINUA  
FACULTAD DE INGENIERIA U.N.A.M.**

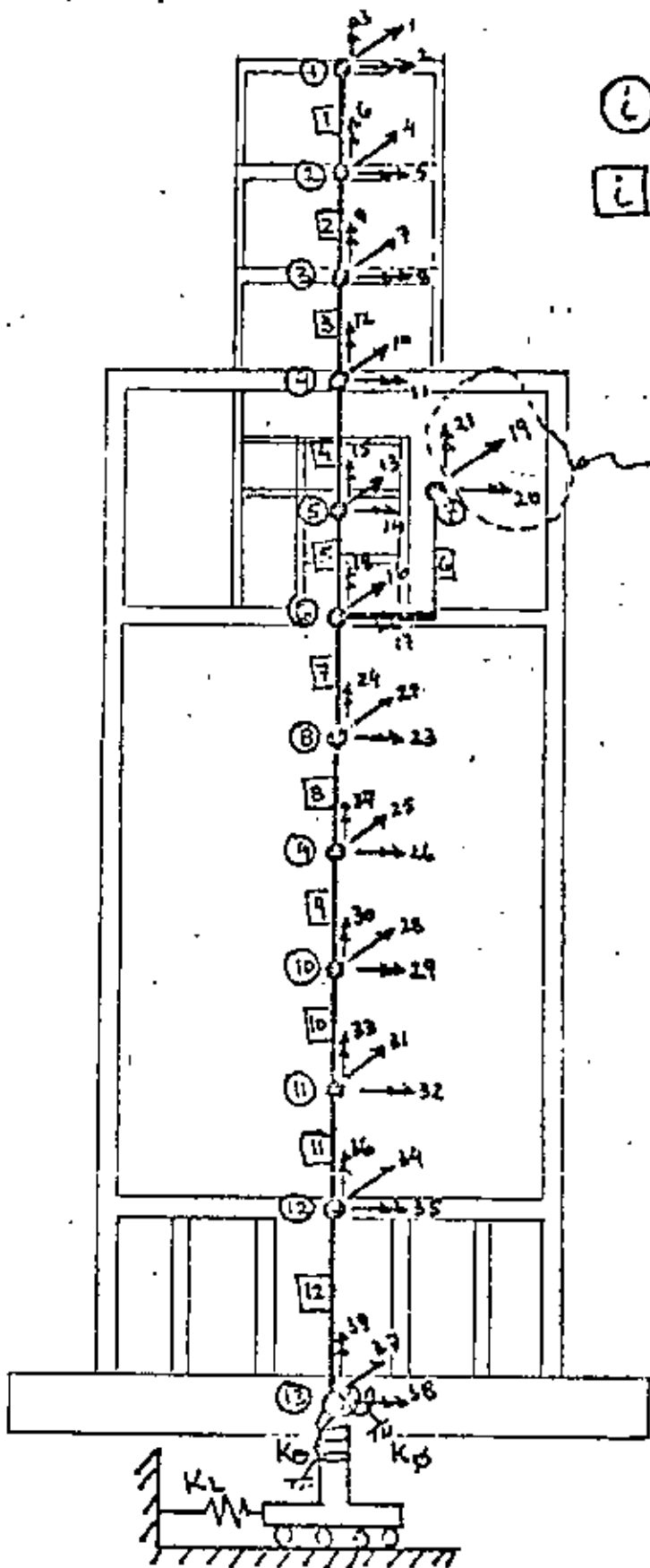
VII CURSO INTERNACIONAL DE INGENIERIA SISMICA

DISEÑO SISMICO DE ESTRUCTURAS ESPECIALES

EFECTOS DE INTERACCION  
SUELO-ESTRUCTURA

M en C Mauricio Names

Agosto, 1981



(i) NUM. DE MASA

[i] NUM. DE MIEMBRO

NUM. DE LOS GRADOS DE LIBERTAD ASIGNADOS INTERNAMENTE POR EL PROGRAMA.

FIG. 2

•

•

•

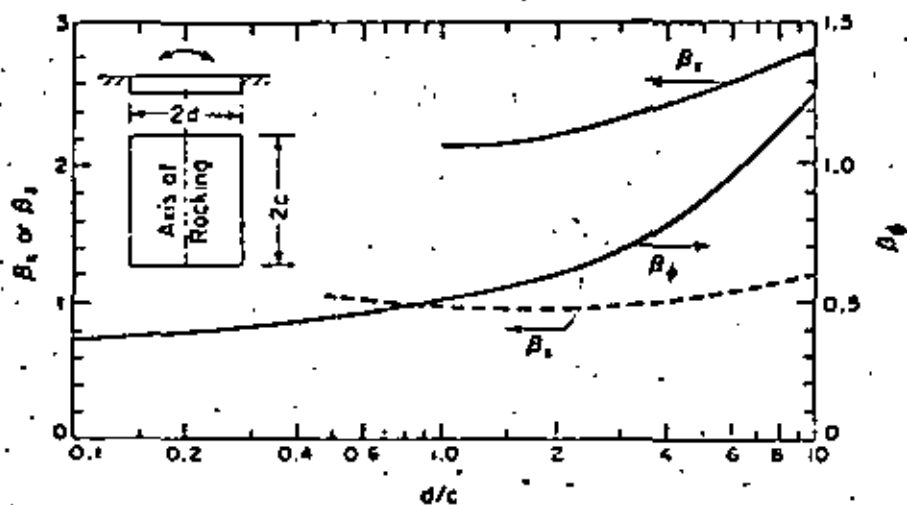
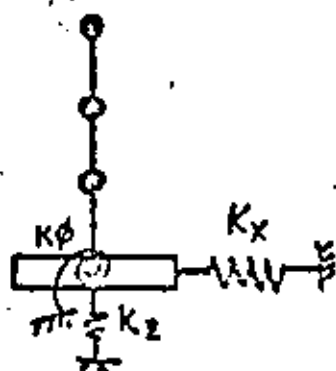


Figure 10-16. Coefficients  $\beta_x$ ,  $\beta_y$ , and  $\beta_\phi$  for rectangular footings (after Whitman and Richert, 1967).



$K_\theta$  - TORSIÓN  
 $K_\phi = K_\psi$  CABECED

$$K_x = 4(1+\mu) G \beta_x \sqrt{c \cdot d}$$

$$K_\phi = \frac{G}{1-\mu} \beta_y 8cd^2$$

$$K_\theta = \frac{16}{3} G r_0^3 ; r_0 = \sqrt[4]{\frac{16cd(c^2+d^2)}{6\pi}}$$

$$K_2 = \frac{G}{1-\mu} \beta_z \sqrt{4cd}$$

$G$  = MÓDULO DE ELASTICIDAD AL CORTANTE DINAMICO

$\mu$  = RELACION DE POISSON

FIG. 3

PARA CIMENTACIONES CIRCULARES

$$K_x = \frac{32(1-\mu)E\Gamma_0}{7-8\mu}$$

HORIZONTAL

$$K_y = \frac{8E\Gamma_0^3}{3(1-\mu)}$$

CABECED

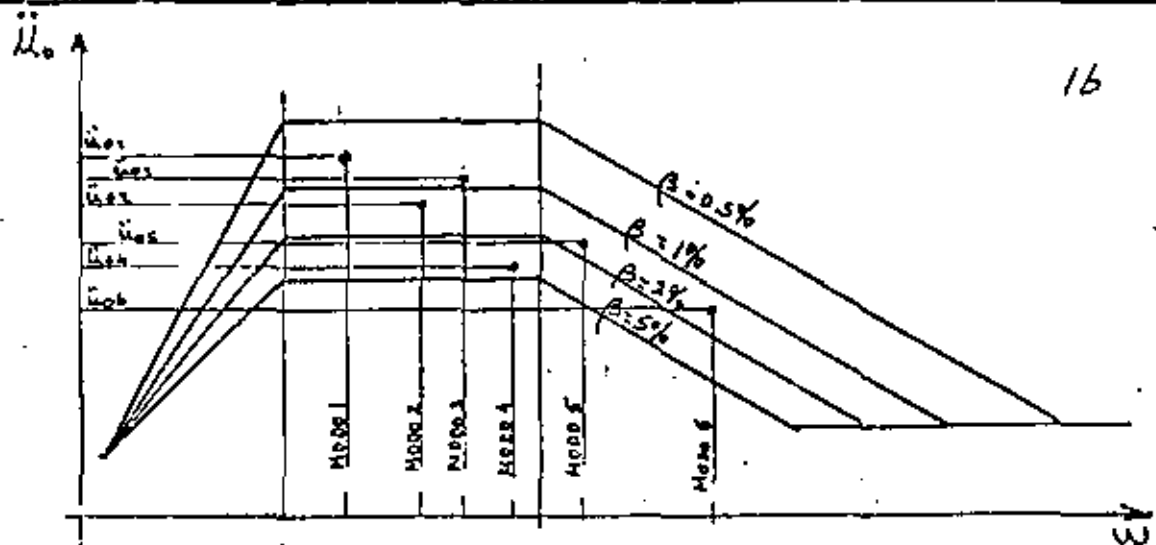
$$K_\theta = \frac{16}{3}E\Gamma_0^3$$

TORSION

$$K_z = \frac{4E\Gamma_0}{1-\mu}$$

VERTICAL

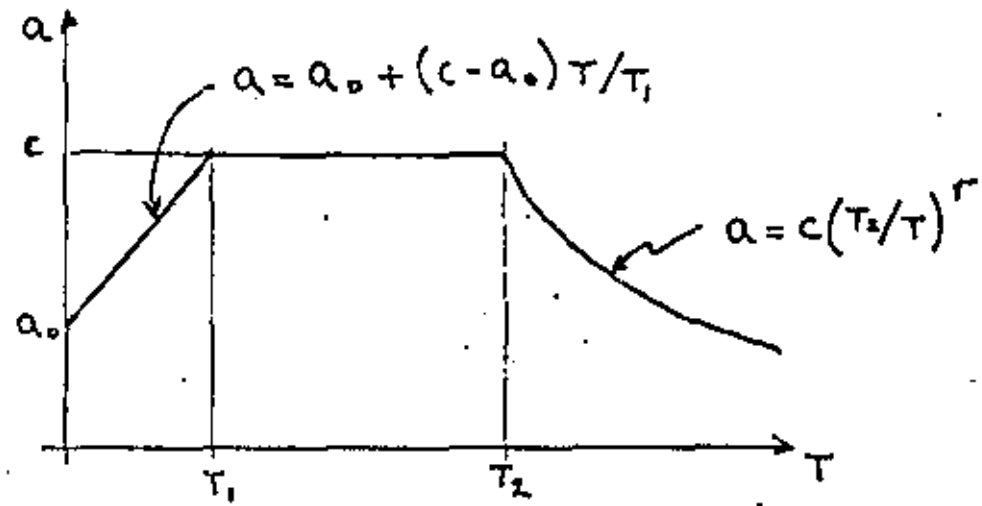
FIG. 4



ACELERACIONES ESPECTRALES MODALES

FIG. 5

Considérese el espectro del RCDF zona B, suelo compresible (tipo III):



$a_0 = 0.06$        $T_1 = 0.8$        $r = 1$   
 $c = 0.24$        $T_2 = 3.3$

La normalización de los factores de amplificación de Newmark se indica a continuación

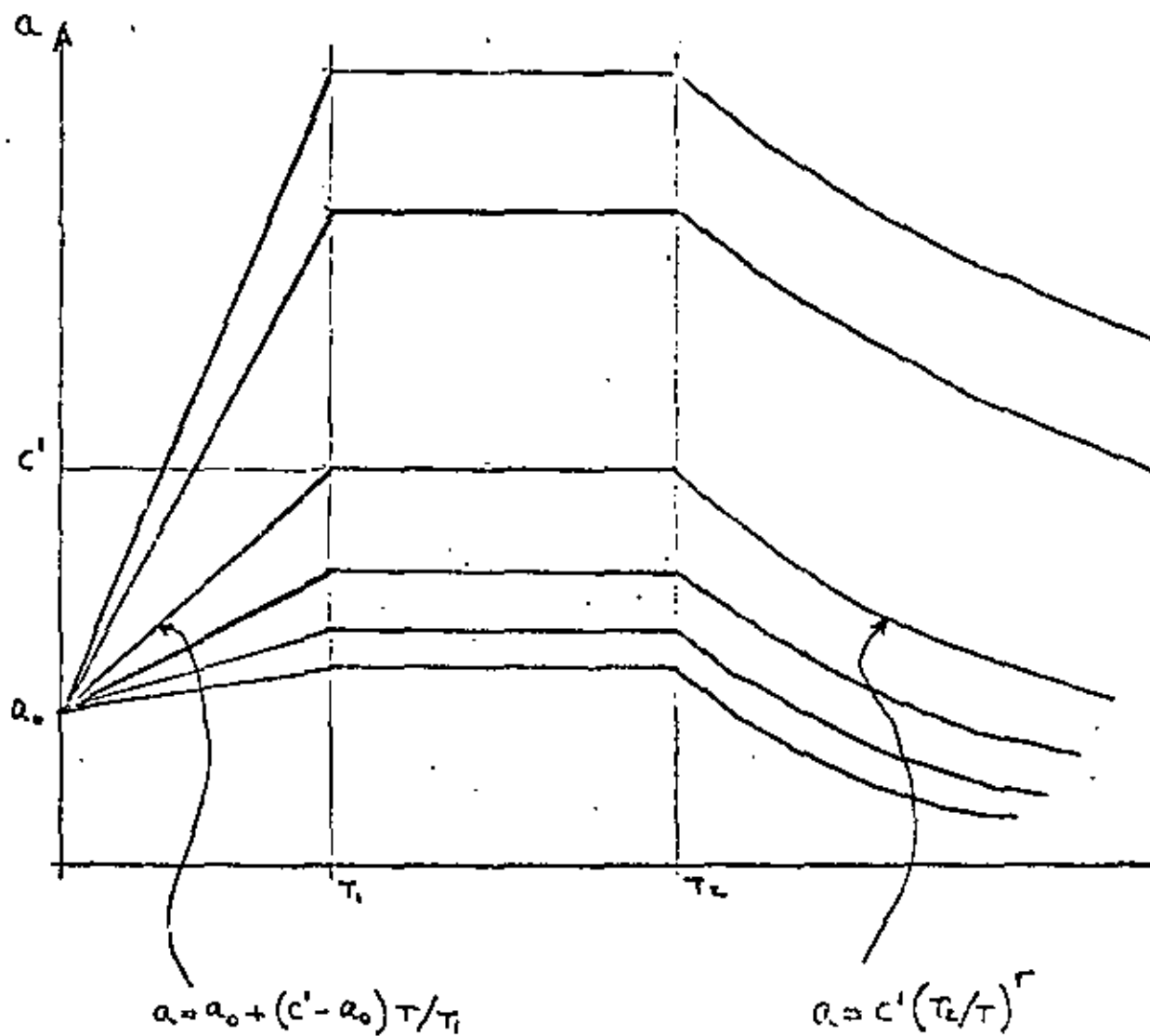
$\xi$ %	FACTOR DE AMPLIFICACION	
	Newmark (F)	Normalizado (f)
0	6.4	2.46
0.5	5.8	2.23
1	5.2	2.00
2	4.3	1.65
5	2.6	1.00
7	1.9	0.73
10	1.5	0.58
20	1.2	0.46

para el espectro correspondiente a un amortiguamiento  $\xi$ , la única variable será la aceleración espectral máxima  $c$ , - que debe mutliplicarse por el factor de amplificación normalizado  $f$ .

$$c' = c \cdot f$$

Se obtiene así la familia de espectros:

18



donde  $c' = c.f.$



## APENDICE IV

CALCULO DEL AMORTIGUAMIENTO PROMEDIO PESADO

Tabla 13.1. Valores típicos de amortiguamiento en las instalaciones de reactores nucleares. Según Newmark y Hall (1969) y Newmark (1969b)

Nivel de esfuerzo	Tipo y condición de la estructura	Porcentaje del amortiguamiento sísmico
1. Bajo, muy por abajo del límite de proporcionalidad, esfuerzos inferiores a $\frac{1}{4}$ del límite de fluencia	Tuberías vitales	0.5
	Acero, concreto reforzado o preforzado, madera; sin grietas; sin deslizamientos en las conexiones	0.5-1.0
2. Esfuerzos de trabajo, no mayores que aproximadamente $\frac{1}{2}$ del límite de fluencia	Tuberías vitales	0.5-1.0
	Acero soldado, concreto preforzado, concreto bien reforzado (sólo pequeños agrietamientos)	2
	Concreto reforzado muy agrietado	3-5
	Acero atornillado y/o remachado, estructuras de madera con juntas clavadas o atornilladas	5-7
3. Al límite de fluencia o justamente abajo de él	Tuberías vitales	2
	Acero soldado, concreto preforzado (sin pérdida total de esfuerzo)	5
	Concreto reforzado y concreto preforzado	7-10
	Acero atornillado y/o remachado, estructuras de madera con juntas atornilladas	10-15
	Estructuras de madera con juntas clavadas	15-20
4. Pasando el punto de fluencia, con deformación permanente mayor que la deformación al límite de fluencia	Tubería	5
	Acero soldado	7-10
	Concreto reforzado y concreto preforzado	10-15
	Acero atornillado y/o remachado, y estructuras de madera	20

#### AMORTIGUAMIENTOS ESTRUCTURALES

FIG. 7

CABECEO (N. Newmark)

DESCRIPCION DEL SUELO	VELOCIDAD ONDAS DE CORTANTE	PORCENTAJE DE AMORTIGUAMIENTO CRITICO
ROCA	$V_s > 1800$ m/seg	2 - 5
SUELO FIRME	$600 \leq V_s \leq 1800$ m/seg	5 - 7
SUELO COMPR.	$V_s < 600$ m/seg	7 - 10

HORIZONTAL Y TORSION (Preliminar)

DESCRIPCION DEL SUELO	PROFUNDIDAD DE LA ROCA (m)	PORCENTAJE DE AMORTIGUAMIENTO CRITICO
ROCA	0.0	5 - 7
SUELO FIRME	$\pm$ 5.0 m	7 - 10
SUELO COMPR.	5.0 m	10 - 20
SUELO COMPR.	10.0 m	20 - 40

## AMORTIGUAMIENTO DEL SUELO

FIG. 8

El amortiguamiento promedio pesado se calcula modo a modo de la siguiente manera:

1. Calcular el vector velocidades

$$v_{ij} = F_j \phi_{ij} \cdot g / \omega_j$$

donde:  $F_j$  = factor de participación del modo  $j$

$\phi_{ij}$  = componente del vector característico en la dirección del grado de libertad  $i$  del modo  $j$ .

$g$  = aceleración de la gravedad

$\omega_j$  = frecuencia natural del modo  $j$ .

las unidades correspondientes son:

$$v_{ij} = F_j \cdot \phi_{ij} \cdot g / \omega_j$$

$$[m/seg] = [1/m] \cdot [m] \cdot [m/seg^2] / [rad/seg]$$

2. Calcular la energía total (cinética):

$$E_T]_j = \sum_{i=1}^n m_i \cdot v_{ij}^2 / 2.0$$

3. Se calcula la energía absorbida por los resortes de interacción:

$$E_{sh}]_j = K_{sh} \cdot \Delta_{sh}]_j^2 / 2.0 \quad (\text{horizontal del modo } j)$$

$$E_{sc}]_j = K_{sc} \cdot \phi_{sc}]_j^2 / 2.0 \quad (\text{cabeceo del modo } j)$$

$$E_{st}]_j = K_{st} \cdot \theta_{st}]_j^2 / 2.0 \quad (\text{torsión del modo } j)$$

donde:  $K_{sh}$ ,  $K_{sc}$ ,  $K_{st}$  son las rigideces de los resortes de interacción.

$\Delta_{sh}$ ,  $\phi_{sc}$ ,  $\theta_{st}$  son los desplazamientos de la masa de la cimentación para el modo  $j$ .

4. La energía absorbida por la estructura es:

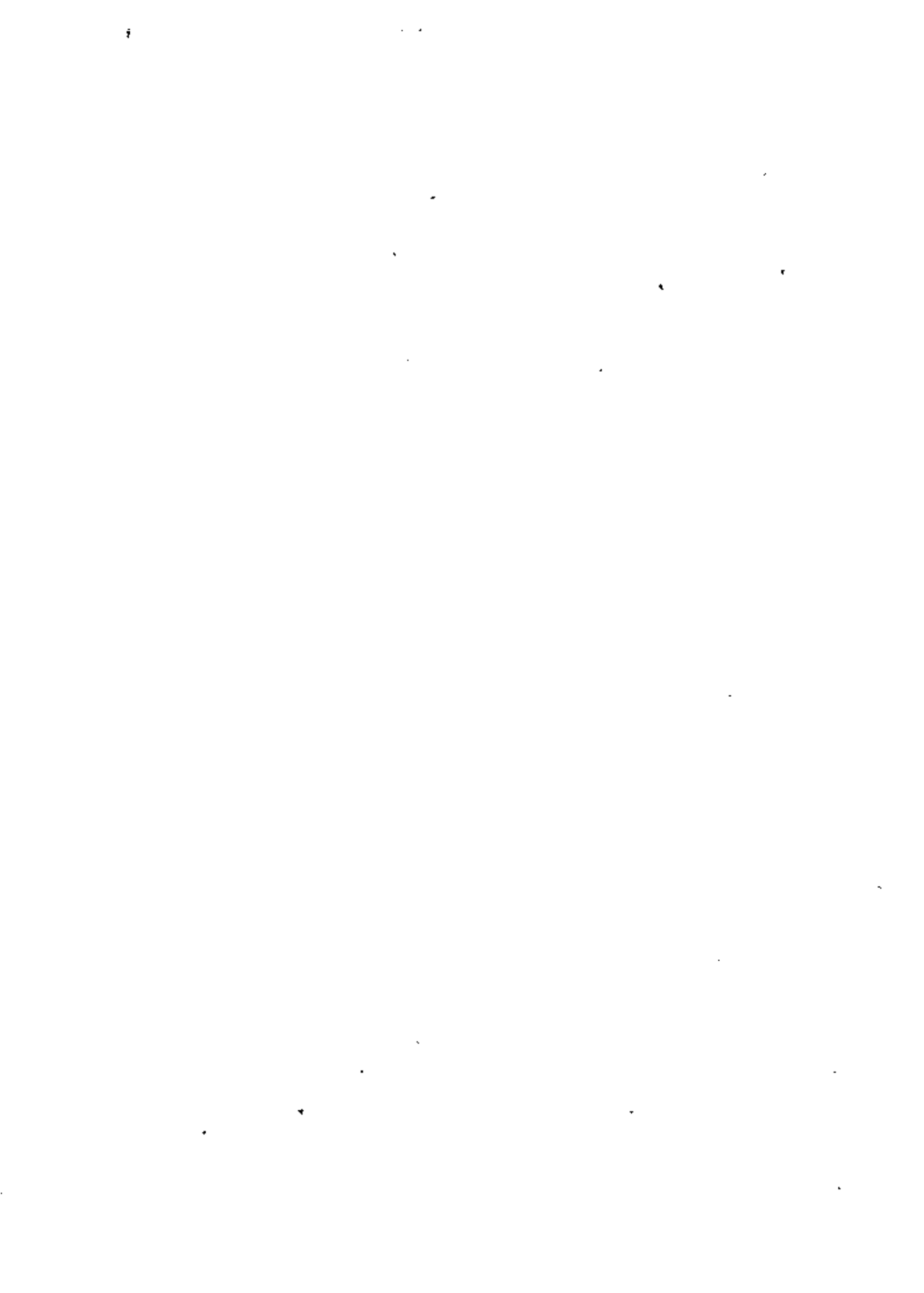
$$E_e]_j = E_T]_j - E_{sh}]_j - E_{sc}]_j - E_{st}]_j$$

5. Se calcula el amortiguamiento promedio pesado como:

$$\xi_p]_j = \frac{\xi_e \cdot E_e]_j + \xi_{sh} \cdot E_{sh}]_j + \xi_{sc} \cdot E_{sc}]_j + \xi_{st} \cdot E_{st}]_j}{E_T]_j}$$

donde:  $\xi$  son amortiguamientos, cuyo subíndice identifica estructura, suelo horizontal, suelo cabeceo, etc.

y  $\xi_p]_j$  es el amortiguamiento promedio pesado del modo  $j$ .



# DISEÑO SISMICO DE ESTRUCTURAS ESPECIALES

1981

## Directorio de Asistentes

1. Jerónimo Aguilar Chávez  
Industria Metálica Integrada, S.A.  
de C.V.  
Av. Constituyentes 1160  
Col. Lomas Altas  
México 10, D.F.  
5 70 38 58  
Av. Lázaro Cárdenas 734-302  
Col. Postal  
México 13, D.F.  
5 79 57 42
2. Ricardo Castellanos Avila  
AIN, S.A. Ingeniería y Construc-  
ción Industrial  
Blvd. Manuel Avila Camacho 6-A  
México 10, D.F.  
Braga 67,  
Col. San Andrés Tetepilco,  
México 13, D.F.  
5 32 05 69
3. Rubén Castillejos Sosa  
Dirección General de Obras  
Marítimas  
Insurgentes Sur 465  
Col. Condesa  
México 11, D.F.  
5 64 51 01  
El Cántaro 33 - C - 106,  
Col. Villa Coapa,  
México 22, D.F.  
5 94 33 65
4. José Luis Castillo Soto  
Secretaría de Agricultura y Recursos  
Hidráulicos  
Reforma No. 20 - 4º piso  
México 1, D.F.  
5 46 75 22  
Av. Universidad No. 491  
Col. Del Valle  
México 12, D.F.  
5 43 91 57
5. Mario Castro Usla  
S A R H Comisión de Aguas del  
Valle de México  
Rancho Guadalupe, Metepec,  
Estado de México.  
Unidad Vallejo Edificio 16-C-304  
Col. Lindavista  
México 14, D.F.  
5 87 79 29
6. Filiberto Cervantes Rodríguez  
C I E P S, S.C.  
Córdoba 127  
Col. Roma  
México 7, D.F.  
5 84 16 99  
Dr. Lucio 103, Edificio A-5  
Departamento 704,  
Col. Doctores,  
México 7, D.F.  
5 84 16 99



7. Juan J. de los Santos Barbosa  
I S T M E  
Legaria 252  
Col. Pensil  
México 17, D.F.  
Av. División del Norte 134-16  
Col. Del Valle  
México 12, D.F.  
5 23 98 54
8. Gonzalo del Valle Lecona  
Diseño de Sistemas Estructurales  
Col. Condesa  
México 11, D.F.  
553 10 85  
Estearina No. 78  
Col. Plenitud  
México 16, D.F.  
5 61 94 75
9. J. Fernando Fournier Montiel  
F E R T I M E X  
Morena  
Col. Narvarte  
México 12, D.F.  
Carpio # 114  
Col. Santa María la Ribera  
México 4, D.F.  
5 47 82 19
10. José Frías Díaz  
Universidad Autónoma del Estado  
de México  
Domicilio Conocido, Cerro de  
Coatepec,  
Toluca, Edo. de México  
Manuel Acuña 306  
Col. Progreso,  
Toluca,  
Estado de México.
11. Néstor Gabriel Gallo Guimil  
Calle 61 No. 890  
La Plata,  
Argentina
12. Moisés Napoleón García Sainz  
Instituto Tecnológico Regional  
de Oaxaca  
Calzada Tecnológico y Wilfrido  
Massieu s/n  
Oaxaca, Oax.  
INFONAVIT, Edificio C,  
Departamento 6,  
Oaxaca, Oax.
13. Angel Garfias Flores  
T E C H I N T, S.A.  
Mariano Escobedo 510-9o. Piso  
Col. Anzures  
México 5, D.F.  
San Francisco 1425 Depto. 4  
Col. del Valle  
México 12, D.F.

14. Tomás Hernández Cruz  
I.M.P.  
Av. 100 Metros # 152  
Col. Atepehuacán  
México 14, D.F.      Prolongación Rubí # 22  
Col. Estrella,  
México 14, D.F.,  
5 17 14 02
15. Marco Antonio Islas Ramírez  
Técnicas Modernas de Ingeniería  
Insurgentes Sur 550-4o. Piso  
Col. Roma Sur  
México 7, D.F.      Soria 89-1  
Col. Alamos  
México 13, D.F.  
5 74 76 55      5 38 72 58
16. Ramón Jiménez Jiménez  
Dirección General de Captacio-  
nes y Conducciones .  
S A R H  
Ignacio Ramírez # 20-1er. piso  
Col. San Rafael  
México 4, D.F.      Ebano # 7 .  
Col. Lomas Quebradas  
México 20, D.F.,  
5 66 49 73      5 95 52 75
17. Ricardo Lara Pedrero  
S A H O P  
Dirección General de Aeropuertos  
Chiapas # 121  
Col. Roma,  
México 13, D.F.      Calle 10-B # 129,  
Col. Vértiz Narvarte.  
México 13, D.F.,  
574-82-55      5 32 19 46
18. Juan León Núñez  
S A R H  
Ignacio Ramírez # 20  
Col. San Rafael  
México 4, D.F.      Niños Héroes # 14,  
Col. San Pedro Xalpa,  
Tlalnepantla,  
Estado de México,  
5 66 49 73      3 82 05 95
19. Arturo López Portillo González  
TECHIN, S.A.  
Mariano Escobedo 510-9o. Piso  
Col. Anzures  
México 5, D.F.      Av. Coyoacán 126-502  
Col. del Valle  
México 12, D.F.  
5 45 72 39      5 43 13 13
20. Saturnino López Reynoso  
Bufete Industrial  
Moras 845  
Col. Mixcoac  
México 7, D.F.  
6 58 35 11

21. Manuel Manricke r Rodríguez  
SICARTSA  
Domicilio Conocido,  
Ciudad Lázaro Cárdenas,  
Michoacán, Domicilio Conocido,  
Col. 1600 Casas,  
Ciudad Lázaro Cárdenas,  
Michoacán,
22. Carlos Martínez García  
Dirección General de Obras  
Marítimas,  
S. C. T.  
Insurgentes Sur # 465,  
Col. Roma,  
México 7, D.F.  
5 61 51 01 Niebla 166  
Col. San Pedro Xalpa,  
Azcapotzalco,  
México 16, D.F.  
3 52 22 90
23. Enrique Mejía Paniagua Tres Picos 73,  
Col. Polanco,  
México 5, D.F.  
5 45 02 11
24. Rafael Méndez Navarro  
Instituto Mexicano del Petróleo  
Avenida Lázaro Cárdenas  
México 14, D.F.  
5 67 66 00 Laurel # 28  
Col. Santa María la Ribera,  
México 4, D.F.  
5 41 24 49
25. Miguel Angel Parra Cabañas  
TECNO-DISEÑO, S.A  
Torres de Mixcoac, edificio A-12  
Departamentos 301 - 304  
Col. Mixcoac,  
México 19, D.F.  
5 93 47 22 Juan Sarabia # 67-2-C  
Col. Nueva Santa María  
México 16, D.F.  
5 47 52 35
26. Mario Plancarte García  
C. F. E.  
Mississippi 71-9o. piso  
Col. Cuauhtémoc  
México 5, D.F.  
553 71 33 Ext. 2649 Apdo. Postal 5-314  
Col. Cuauhtémoc  
México 5, D.F.  
5 38 15 52
27. Horacio Ramírez de Alba  
Universidad Autónoma del Estado  
de México,  
Cd. Universitaria,  
Cerro de Coatepec,  
Apdo. Postal 545,  
4 08 55 Churubusco # 112  
Col. Pensiones  
Toluca,  
Edo. de México,  
5 67 11

28. C. Virgilio Reyes Reyes  
Dirección General de Obras  
Marítimas  
Insurgentes Sur 465  
Col. Condesa,  
México 11, D.F.  
5 64 51 01
29. Fortino Robles García  
Secretaría de Agricultura y  
Recursos Hidráulicos  
Carretera Durango - Torreón,  
KM 5  
Ciudad Industrial,  
Durango,  
1 56 91
30. Armando A. Rodríguez Amigo  
Dirección General de Obras  
Marítimas  
Insurgentes Sur 465,  
Col. Hipódromo Condesa  
México 17, D.F.  
5 64 51 01
31. José Roberto Rosas Piña  
S A R II  
Reforma # 20-4o. Piso  
Centro,  
México 1, D.F.  
5 46 75 22
32. Juan Manuel Sánchez Torres  
ELECTROCONSTRUCTORA, S.A.  
Leibnitz 34-4o. piso  
Col. Anzures  
5 14 19 94
33. Jorge Silva Ballesteros  
ESIA- IPN  
Pabellón # 4 de la Unidad Profesional  
Zacatenco,  
Col. Lindavista  
México 14, D.F.  
5 86 96 44
34. Miguel Trujillo Ferrusquia  
Dirección General de Obras Marítimas  
Insurgentes Sur 465  
Col. Condesa
- Debussy # 81 ,  
Col. Ex-Hipódromo de  
Peralvillo,  
México 2, D.F.:  
5 83 56 15
- 5 de Febrero # 517 - Oriente,  
Centro,  
Ciudad Durango  
2 01 08
- Avenida del Taller, Ret. 38 U-1  
Depto. 520,  
Col. Jardín Balbuena,  
México 9, D.F.:  
5 71 77 32
- Berlioz # 102  
Col. Ex-Hipódromo de Peralvi-  
llo  
México 2, D.F.:  
5 83 16 67
- Estrella 92-44  
Col. Guerrero  
México 3, D.F.
- Marmolería 324  
Col. 20 de Noviembre  
México 2, D.F.  
7 89 89 75
- Calle Norte No. 104  
Col. Olivar del Conde  
Mexico 19, D.F.:

México 11, D.F.  
5 64 51 01

6 51 79 76

35. Juan Valdéz Alvarez  
Instituto Mexicano del Petróleo  
Av. 100 Metros # 152

Calle 7 # 199  
Col. Juárez Pantitlán  
México 9, D.F.:

36. José Ma. Guillermo Valencia  
E S I A - I P N  
Pabellón #4 de la Unidad Profesional  
Zacatenco  
Col. Lindavista  
México 11, D.F.  
5 86 96 44

Villa de Allende 310  
Col. Romero  
Ciudad Nezahualcóyotl  
7 65 27 39

37. Armando Villalobos López  
Proyectos Marinos, S.C.  
Boulevard Manuel Avila Camacho #1  
Col. Polanco  
México 5, D.F.  
3 95 00 88

Guerrero 380- Depto. 1309  
Col. Guerrero  
México 3, D.F.  
5 83 96 31

38. Noel Gabriel Zaragoza Luna  
Instituto Tecnológico Regional de  
Oaxaca  
Calzada Instituto Tecnológico s/n  
Oaxaca, Oax.  
6 17 42

2 de Abril # 109  
Col. Santa María  
Oaxaca, Oax.  
6 32 26

